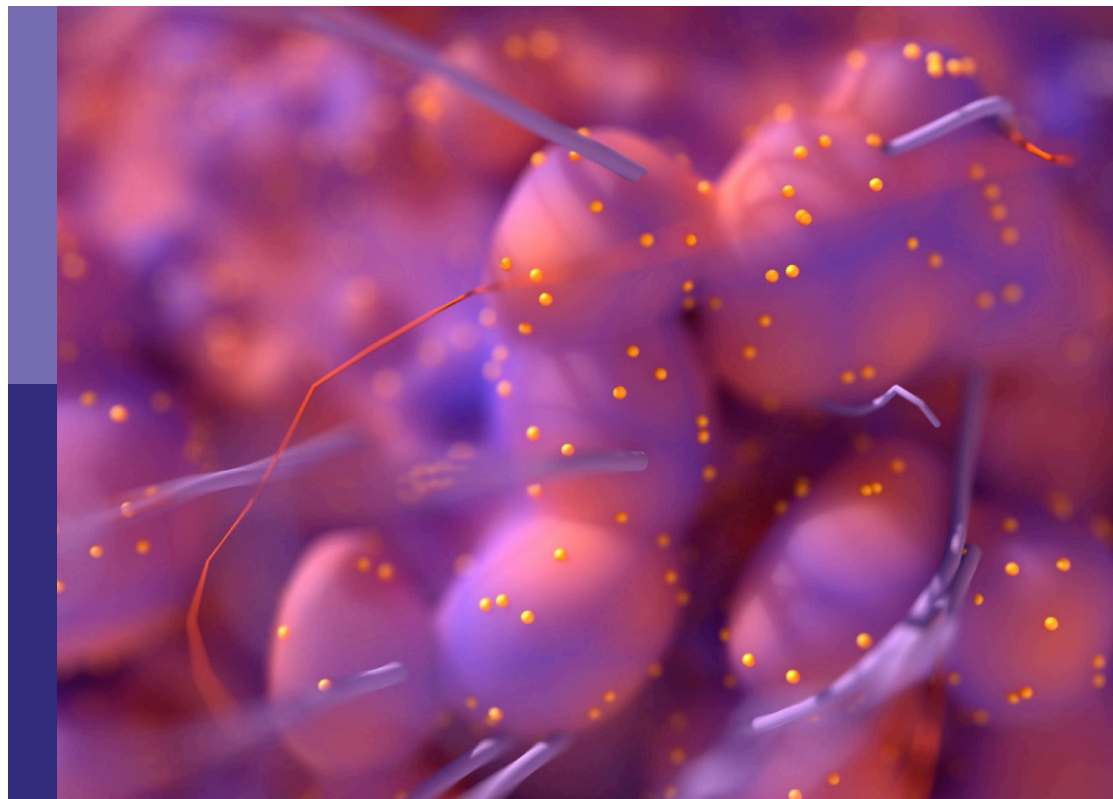


Investigating drugs used off-label in various cancers

Edited by
Benyi Li and Christian Celia

Published in
Frontiers in Oncology



FRONTIERS EBOOK COPYRIGHT STATEMENT

The copyright in the text of individual articles in this ebook is the property of their respective authors or their respective institutions or funders. The copyright in graphics and images within each article may be subject to copyright of other parties. In both cases this is subject to a license granted to Frontiers.

The compilation of articles constituting this ebook is the property of Frontiers.

Each article within this ebook, and the ebook itself, are published under the most recent version of the Creative Commons CC-BY licence. The version current at the date of publication of this ebook is CC-BY 4.0. If the CC-BY licence is updated, the licence granted by Frontiers is automatically updated to the new version.

When exercising any right under the CC-BY licence, Frontiers must be attributed as the original publisher of the article or ebook, as applicable.

Authors have the responsibility of ensuring that any graphics or other materials which are the property of others may be included in the CC-BY licence, but this should be checked before relying on the CC-BY licence to reproduce those materials. Any copyright notices relating to those materials must be complied with.

Copyright and source acknowledgement notices may not be removed and must be displayed in any copy, derivative work or partial copy which includes the elements in question.

All copyright, and all rights therein, are protected by national and international copyright laws. The above represents a summary only. For further information please read Frontiers' Conditions for Website Use and Copyright Statement, and the applicable CC-BY licence.

ISSN 1664-8714
ISBN 978-2-83251-524-2
DOI 10.3389/978-2-83251-524-2

About Frontiers

Frontiers is more than just an open access publisher of scholarly articles: it is a pioneering approach to the world of academia, radically improving the way scholarly research is managed. The grand vision of Frontiers is a world where all people have an equal opportunity to seek, share and generate knowledge. Frontiers provides immediate and permanent online open access to all its publications, but this alone is not enough to realize our grand goals.

Frontiers journal series

The Frontiers journal series is a multi-tier and interdisciplinary set of open-access, online journals, promising a paradigm shift from the current review, selection and dissemination processes in academic publishing. All Frontiers journals are driven by researchers for researchers; therefore, they constitute a service to the scholarly community. At the same time, the *Frontiers journal series* operates on a revolutionary invention, the tiered publishing system, initially addressing specific communities of scholars, and gradually climbing up to broader public understanding, thus serving the interests of the lay society, too.

Dedication to quality

Each Frontiers article is a landmark of the highest quality, thanks to genuinely collaborative interactions between authors and review editors, who include some of the world's best academicians. Research must be certified by peers before entering a stream of knowledge that may eventually reach the public - and shape society; therefore, Frontiers only applies the most rigorous and unbiased reviews. Frontiers revolutionizes research publishing by freely delivering the most outstanding research, evaluated with no bias from both the academic and social point of view. By applying the most advanced information technologies, Frontiers is catapulting scholarly publishing into a new generation.

What are Frontiers Research Topics?

Frontiers Research Topics are very popular trademarks of the *Frontiers journals series*: they are collections of at least ten articles, all centered on a particular subject. With their unique mix of varied contributions from Original Research to Review Articles, Frontiers Research Topics unify the most influential researchers, the latest key findings and historical advances in a hot research area.

Find out more on how to host your own Frontiers Research Topic or contribute to one as an author by contacting the Frontiers editorial office: frontiersin.org/about/contact

Investigating drugs used off-label in various cancers

Topic editors

Benyi Li — University of Kansas Medical Center, United States

Christian Celia — University of Studies G. d'Annunzio Chieti and Pescara, Italy

Citation

Li, B., Celia, C., eds. (2023). *Investigating drugs used off-label in various cancers*.
Lausanne: Frontiers Media SA. doi: 10.3389/978-2-83251-524-2

Table of contents

- 05 **Editorial: Investigating drugs used off-label in various cancers**
Wang Liu and Benyi Li
- 07 **Psychotropic Drugs Show Anticancer Activity by Disrupting Mitochondrial and Lysosomal Function**
Marco Varalda, Annamaria Antona, Valentina Bettio, Konkonika Roy, Ajay Vachamaram, Vaibhav Yellenki, Alberto Massarotti, Gianluca Baldanzi and Daniela Capello
- 26 **Magnesium in Combinatorial With Valproic Acid Suppressed the Proliferation and Migration of Human Bladder Cancer Cells**
Tianye Li, Yang Yu, Hang Shi, Yuhua Cao, Xiangfu Liu, Zhenzhen Hao, Yuping Ren, Gaowu Qin, Yongye Huang and Bing Wang
- 43 **Volatile Anesthetics Regulate Anti-Cancer Relevant Signaling**
Jiaqiang Wang, Chien-shan Cheng, Yan Lu, Shen Sun and Shaoqiang Huang
- 54 **Anticancer Properties of the Antipsychotic Drug Chlorpromazine and Its Synergism With Temozolomide in Restraining Human Glioblastoma Proliferation *In Vitro***
Silvia Matteoni, Paola Matarrese, Barbara Ascione, Mariachiara Buccarelli, Lucia Ricci-Vitiani, Roberto Pallini, Veronica Villani, Andrea Pace, Marco G. Paggi and Claudia Abbruzzese
- 66 **Cyclovirobuxine D Induces Apoptosis and Mitochondrial Damage in Glioblastoma Cells Through ROS-Mediated Mitochondrial Translocation of Cofilin**
Lin Zhang, Ruoqiu Fu, Dongyu Duan, Ziwei Li, Bin Li, Yue Ming, Li Li, Rui Ni and Jianhong Chen
- 80 **Repositioning of Antiparasitic Drugs for Tumor Treatment**
Yan-Qi Li, Zhi Zheng, Quan-Xing Liu, Xiao Lu, Dong Zhou, Jiao Zhang, Hong Zheng and Ji-Gang Dai
- 96 **Vitamin D: Possible Therapeutic Roles in Hepatocellular Carcinoma**
Isaacson B. Adelani, Oluwakemi A. Rotimi, Emmanuel N. Maduagwu and Solomon O. Rotimi
- 106 **Atorvastatin Plus Low-Dose Dexamethasone May Be Effective for Leukemia-Related Chronic Subdural Hematoma but Not for Leukemia Encephalopathy: A Report of Three Cases**
Jiangyuan Yuan, Ying Li, Xuanhui Liu, Meng Nie, Weiwei Jiang, Yibing Fan, Tangtang Xiang, Hanhua Wang, Wei Quan, Chuang Gao, Jinghao Huang, Shuo An, Yongxin Ru, Qiufan Zhou, Jianning Zhang and Rongcai Jiang

- 113 **Epigenetics-Associated Risk Reduction of Hematologic Neoplasms in a Nationwide Cohort Study: The Chemopreventive and Therapeutic Efficacy of Hydralazine**
Bing-Heng Yang, Wei-Zhi Lin, Yu-Ting Chiang, Yeu-Chin Chen, Chi-Hsiang Chung, Wu-Chien Chien and Chia-Yang Shiau
- 127 ***In Vitro* Cell Density Determines the Sensitivity of Hepatocarcinoma Cells to Ascorbate**
Hsiu-Lung Fan, Shu-Ting Liu, Yung-Lung Chang, Yi-Lin Chiu, Shih-Ming Huang and Teng-Wei Chen
- 141 **A bibliometric and visualization-based analysis of temozolomide research hotspots and frontier evolution**
Peng Song, Hui Li, Kuo Xu, Zi-Wei Li, Xia Ren and Xian-Jun Fu



OPEN ACCESS

EDITED AND REVIEWED BY

Olivier Feron,
Université catholique de Louvain, Belgium

*CORRESPONDENCE

Benyi Li
bli@kumc.edu

SPECIALTY SECTION

This article was submitted to
Pharmacology of Anti-Cancer Drugs,
a section of the journal
Frontiers in Oncology

RECEIVED 23 December 2022

ACCEPTED 09 January 2023

PUBLISHED 18 January 2023

CITATION

Liu W and Li B (2023) Editorial:
Investigating drugs used off-label
in various cancers.
Front. Oncol. 13:1130834.
doi: 10.3389/fonc.2023.1130834

COPYRIGHT

© 2023 Liu and Li. This is an open-access
article distributed under the terms of the
[Creative Commons Attribution License](#)
(CC BY). The use, distribution or
reproduction in other forums is permitted,
provided the original author(s) and the
copyright owner(s) are credited and that
the original publication in this journal is
cited, in accordance with accepted
academic practice. No use, distribution or
reproduction is permitted which does not
comply with these terms.

Editorial: Investigating drugs used off-label in various cancers

Wang Liu and Benyi Li*

Department of Urology, University of Kansas Medical Center, Kansas City, KS, United States

KEYWORDS

cancer treatment, drug reposition, drug repurposing, human cancers
anti-cancer medication

Editorial on the Research Topic

Investigating drugs used off-label in various cancers

Cancer drug discovery is a long, expensive, drawn-out process involving the identification and optimization of lead compounds, followed by pre-clinical testing and clinical trials (1). It has been proved that its span varies between 11.4 to 13.5 years, and the costs range from 161 to 1800 million dollars from initial experiments to completed regulatory reviews (2, 3). Currently, more than 10,000 clinical trials investigating drug candidates in cancer are registered at www.clinicaltrials.gov. However, only a limited number of drug candidates progress to the next phase in clinical trials, with reports showing that less than 5% of drug compounds can be approved to enter phase I trials (4). Collectively, there is an urgent need to expand more discovery methods to remedy the growing anti-tumor medication needs gap.

Drug repurposing or repositioning is the application of a drug for another indication than its original application (5). Discovering that already licensed medication readily available in the market affects diseases otherwise not knowingly attributed to these drug molecules avoids this research process. It can bring new, potentially life-saving treatments to patients with a cheaper cost and a faster path. However, repositioning the drug for further indication may accompany side effects not previously reported and will require validation in a new clinical trial. Nevertheless, the safety profile can be referred to as the initial indication, thus, increasing the likelihood of the drug through the trial (1).

Recent clinic reports show that several epidemiological studies reveal lower cancer incidence in individuals receiving long-term psychotropic drug treatment. Varalda et al. investigated psychotropic drugs for their anti-tumor activity and evaluated their cytotoxic activity in colorectal carcinoma, glioblastoma, and breast cancer cell lines. The investigation revealed that penfluridol, ebastine, pimozide, fluoxetine, fluspirilene, and nefazodone have apparent cytotoxicity in all cancer cell lines tested in the low micromoles range. These psychotropic drugs caused mitochondrial membrane depolarization, increased the acidic vesicular compartments, and induced phospholipidosis in breast cancer MCF-7 cells. Varalda et al. showed that psychotropic drugs via dual targeting of lysosomes and mitochondria are a novel promising approach to cancer therapy, especially for cancer cells deficient in apoptotic machinery. Chlorpromazine has been used to treat psychiatric disorders for more than six decades. Clinic reports show that chlorpromazine is a potential anti-tumor medicine, but the mechanism is unclear. Matteoni et al. tested the anti-tumor effect of chlorpromazine in six glioblastoma cell lines. The results showed that chlorpromazine inhibited cancer cell viability in an apoptosis-independent way, induced hyperdiploidy, reduced cloning efficiency, neurosphere formation, and downregulated the expression of stemness genes. Furthermore, combining chlorpromazine with

temozolomide, the first-line therapeutic in GBM patients, significantly inhibited cell growth and cloning efficiency in GBM cell lines.

Volatile anesthetics, such as inhalation anesthetics in clinical anesthesia, were found to regulate cancer-related signaling. Wang et al. systematically summarize the research progress of volatile anesthetics in anti-cancer signaling regulation. It provided good insights for guiding clinical anesthesia procedures and instructing to enhance recovery after surgery. Cyclovirobuxine D (CVBD) is a triterpenoid alkaloid extracted from *Buxus Sinica* and other plants of the same genus used in cardiomyopathy, myocardial infarction, and arrhythmia (6, 7). Accumulating evidence showed that CVBD has a potential anti-tumor effect in multiple tumor cell types. Zhang et al. investigated the anti-cancer effect of CVBD on GBM and showed that CVBD has a significant anti-proliferation effect on the T98G and U251 cell lines. CVBD also induced apoptosis and mitochondrial damage in GBM cells. Mechanistically, CVBD caused cofilin mitochondrial translocation and superoxide species accumulation in mitochondria in a dose-dependent manner. In addition, Li et al. found that both anti-helminthic and anti-protozoal drugs suppressed tumor growth by targeting multiple pathways *via* different mechanisms. They suggested further evaluation of these anti-parasitic drugs for cancer therapy.

Magnesium (Mg^{2+}), the second most predominant intracellular cation, plays an essential role in many physiological functions. Several reports showed that the high intracellular concentration of magnesium contributes to cancer initiation and progression in various cancers. To investigate the effect of magnesium concentration in cancer therapy, Li et al. designed a series of experiments to assess the underlying mechanisms in bladder cancer both *in vitro* and *in vivo*. The results indicated that cancer cell proliferation was inhibited in a high concentration of $MgCl_2$ or $MgSO_4$ treatment. $MgCl_2$ treatment induces apoptosis, G_0/G_1 cell cycle arrest, autophagy, and ER stress but not cell migration. Combinational treatment of $MgCl_2$ and VPA dramatically reduced the proliferation, migration, and *in vivo* tumorigenicity. Vitamin D is a lipid-soluble hormone that promotes skeletal mineralization and maintains calcium homeostasis by binding to the vitamin D receptor. Vitamin D also involves cell proliferation, angiogenesis, apoptosis, inflammation, and cell difference. Adelani et al. had a review article summarizing the functions of vitamin D in Hepatocellular carcinoma (HCC). They discussed the specific therapeutic targets from *in vivo*, *in vitro*, and clinical studies. They elucidated that vitamin D-associated target genes have essential functions in the anti-tumor effect through inflammation, oxidative stress, invasion, and apoptosis pathways.

Combining different chemotherapy medications is also an excellent method to improve the anti-tumor effect and overcomes chemotherapy resistance. Atorvastatin is a popular preventive medicine for cardiovascular diseases. Yuan et al. used Atorvastatin plus dexamethasone in two patients with leukemia-related chronic subdural hematoma. However, this combinational therapy was not effective for a patient with leukemia-related encephalopathy. Fan et al. used Ascorbate plus tyrosine kinase inhibitors (TKIs) in hepatocellular carcinoma cells. They found that Ascorbate enhanced TKI's efficacy in HCC cells by disturbing redox homeostasis. Yang et al. screened the Human Epigenetic Drug Database and tested the positive lead compounds in cytotoxic experiments. Their results showed that the anti-hypertension drug Hydralazine reduced the overall incidence rate in most subgroups of hematologic neoplasms when chronically used at a low dose. Song et al. presented a complete analysis of the historical progression in Temozolomide (TMZ) development and suggested several research directions for future research.

In conclusion, this Research Topic had a thriving collection of 11 articles on repurposing multiple existing medications for anti-cancer treatment. These research results significantly contributed to the development of novel cancer therapies.

Author contributions

WL drafted the manuscript. BL revised and approved the submission.

Conflict of interest

The authors declare that the research was conducted in the absence of any commercial or financial relationships that could be construed as a potential conflict of interest.

Publisher's note

All claims expressed in this article are solely those of the authors and do not necessarily represent those of their affiliated organizations, or those of the publisher, the editors and the reviewers. Any product that may be evaluated in this article, or claim that may be made by its manufacturer, is not guaranteed or endorsed by the publisher.

References

1. Sleire L, Førde HE, Netland IA, Leiss L, Skeie BS, Enger PØ. Checkmate: Drug repurposing in cancer. *Pharmacol Res* (2017) 124:74–91.
2. Paul SM, Mytelka DS, Dunwiddie CT, Persinger CC, Munos BH, Lindborg SR, et al. How to improve R&D productivity: the pharmaceutical industry's grand challenge. *Nat Rev Drug Discovery* (2010) 9(3):203–14.
3. Adams CP, Brantner VV. Estimating the cost of new drug development: is it really 802 million dollars? *Health Aff (Millwood)* (2006) 25(2):420–8.
4. Hay M, Thomas DW, Craighead JL, Economides C, Rosenthal J. Clinical development success rates for investigational drugs. *Nat Biotechnol* (2014) 32(1):40–51.
5. Ashburn TT, Thor KB. Drug repositioning: identifying and developing new uses for existing drugs. *Nat Rev Drug Discovery* (2004) 3(8):673–83.
6. Guo Q, Guo J, Yang R, Peng H, Zhao J, Li L, et al. Cyclovirobuxine d attenuates doxorubicin-induced cardiomyopathy by suppression of oxidative damage and mitochondrial biogenesis impairment. *Oxid Med Cell Longev* 2015:151972.
7. Yu B, Fang T-H, Lü G-H, Xu H-Q, Lu J-F. Beneficial effect of cyclovirobuxine d on heart failure rats following myocardial infarction. *Fitoterapia* (2011) 82(6):868–77.



Psychotropic Drugs Show Anticancer Activity by Disrupting Mitochondrial and Lysosomal Function

Marco Varalda^{1,2†}, Annamaria Antona^{1†}, Valentina Bettio^{1,2}, Konkonika Roy³, Ajay Vachamaram^{1,3}, Vaibhav Yellenki¹, Alberto Massarotti⁴, Gianluca Baldanzi^{1,3} and Daniela Capello^{1,2*}

¹ Department of Translational Medicine, Centre of Excellence in Aging Sciences, University of Piemonte Orientale, Novara, Italy, ² UPO Biobank, University of Piemonte Orientale, Novara, Italy, ³ Center for Translational Research on Allergic and Autoimmune Diseases (CAAD), University of Piemonte Orientale, Novara, Italy, ⁴ Department Pharmaceutical Sciences, University of Piemonte Orientale, Novara, Italy

OPEN ACCESS

Edited by:

Brian Gabrielli,
The University of
Queensland, Australia

Reviewed by:

Vladimir Trajkovic,
University of Belgrade, Serbia
Xiuli Dan,
National Institute on Aging, National
Institutes of Health (NIH),
United States

*Correspondence:

Daniela Capello
daniela.capello@med.uniupo.it

†These authors share first authorship

Specialty section:

This article was submitted to
Pharmacology of Anti-Cancer Drugs,
a section of the journal
Frontiers in Oncology

Received: 14 May 2020

Accepted: 15 September 2020

Published: 19 October 2020

Citation:

Varalda M, Antona A, Bettio V, Roy K, Vachamaram A, Yellenki V, Massarotti A, Baldanzi G and Capello D (2020) Psychotropic Drugs Show Anticancer Activity by Disrupting Mitochondrial and Lysosomal Function. *Front. Oncol.* 10:562196. doi: 10.3389/fonc.2020.562196

Background and Purpose: Drug repositioning is a promising strategy for discovering new therapeutic strategies for cancer therapy. We investigated psychotropic drugs for their antitumor activity because of several epidemiological studies reporting lower cancer incidence in individuals receiving long term drug treatment.

Experimental Approach: We investigated 27 psychotropic drugs for their cytotoxic activity in colorectal carcinoma, glioblastoma and breast cancer cell lines. Consistent with the cationic amphiphilic structure of the most cytotoxic compounds, we investigated their effect on mitochondrial and lysosomal compartments.

Results: Penfluridol, ebastine, pimozide and fluoxetine, fluspirilene and nefazodone showed significant cytotoxicity, in the low micromolar range, in all cell lines tested. In MCF7 cells these drugs caused mitochondrial membrane depolarization, increased the acidic vesicular compartments and induced phospholipidosis. Both penfluridol and spiperone induced AMPK activation and autophagy. Neither caspase nor autophagy inhibitors rescued cells from death induced by ebastine, fluoxetine, fluspirilene and nefazodone. Treatment with 3-methyladenine partially rescued cell death induced by pimozide and spiperone, whereas enhanced the cytotoxic activity of penfluridol. Conversely, inhibition of lysosomal cathepsins significantly reduced cell death induced by ebastine, penfluridol, pimozide, spiperone and mildly in fluoxetine treated cells. Lastly, Spiperone cytotoxicity was restricted to colorectal cancer and breast cancer and caused apoptotic cell death in MCF7 cells.

Conclusions: The cytotoxicity of psychotropic drugs with cationic amphiphilic structures relied on simultaneous mitochondrial and lysosomal disruption and induction of cell death that not necessarily requires apoptosis. Since dual targeting of lysosomes and mitochondria constitutes a new promising therapeutic approach for cancer, particularly those in which the apoptotic machinery is defective, these data further support their clinical development for cancer therapy.

Keywords: lysosomotropism, cationic amphiphilic drugs (CADs), autophagy, psychotropic drug, cancer, repositioning

INTRODUCTION

Cancer represents a major public health problem, with total cure remaining elusive for most cancer types (1, 2). Chemotherapy resistance in patients with recurrent and advanced disease (3) and strong systemic toxicity, especially in elderly (4), have raised concerns over the progress of cancer therapy, making it necessary to change the paradigm in the search for new treatments, more effective and with milder adverse effects. Thus, alternative cell death pathways capable of killing apoptosis- and therapy resistant cancer cells, have gained vast interest among cancer researchers, leading to the identification of autophagy and lysosomal cell death programs as attractive means to circumvent therapy resistance (5–8). Lysosomal activation is common in aggressive cancers, where lysosomes promote disease progression and treatment resistance (9–13). In cancer, cell transformation increases the requirement for new biomass production, and the core function of the lysosomes is to recycle endogenous or exogenous macromolecules to provide energy and metabolic precursors for the synthesis of new cell mass. In response to typical challenges encountered by cancer cells, such as nutrient starvation, growth factor withdrawal, energy depletion, organelle damage, or accumulation of abnormal proteins, autophagy is further enhanced to meet the cellular needs (10, 13). In certain circumstances, however, the prolonged over activation of the autophagosomal/lysosomal pathway can lead to autophagic-dependent cell death a caspase-independent form of programmed cell death (14), that can be evaluated as an alternative cancer treatment modality (15). On the other hand, since many tumors are highly dependent on autophagy for survival and treatment resistance, pharmacological inhibition of lysosomal activity can limit the growth of advanced diseases and improve response to therapy (5, 16). Moreover, the cancer-associated changes in lysosomal composition result in reduced lysosomal membrane stability, thereby sensitizing tumor cells to lysosome-dependent cell death (LDCD) (17). The main feature LDCD is lysosomal membrane permeabilization (LMP) (17, 18) with translocation to the cytoplasm of the lysosomal contents, including cathepsins, which act as the main executors of this cell death modality (19). Mitochondria have a well-recognized role in the production of ATP, metabolic intermediates and also participate in several signaling pathways; accumulating evidence now suggests that mitochondrial bioenergetics, biosynthesis and signaling are required for tumorigenesis. Thus, emerging studies have begun to demonstrate that mitochondrial functions are a potentially fruitful field for cancer therapy (20, 21). Drug repositioning is a strategy for identifying new uses for approved drugs that are outside the scope of the original medical indication (22, 23) and psychotropic medications are promising compounds for cancer treatment. Epidemiological studies have repeatedly reported that individuals who are receiving long term drug treatment with antipsychotics (24, 25), anti-depressant (26–28) or anti-allergic drugs (29) have a lower cancer incidence than the general population, suggesting that these medications might have a direct effect on neoplastic cells. Pre-clinical studies confirmed the direct anti-tumoral activity of these compounds in a wide range of malignancies (30–34). However, despite the large body

of experimental evidence, the mechanisms of actions of these compounds in cancer cells remain poorly defined.

In this study we screened a panel of psychotropic compounds for their cytotoxicity in different tumor cell lines to clarify the pharmacological properties underpinning their clinical application for cancer therapy. We identified a group of drugs characterized by cationic amphiphilic properties impairing both mitochondrial and lysosomal function and reducing cancer cells viability at clinically relevant concentrations.

METHODS

Cell Culture

HCT116, SW620, MCF7, MDA-MB-231, U87 and U251 cell lines were purchased from the American Type Culture Collection (ATCC). HCT116, MCF7, and U251 cells were cultured in Dulbecco's Modified Eagle Medium (DMEM, Gibco; Life Technologies) supplemented with 10% fetal bovine serum (FBS, Euroclone) and 1% antibiotics and antimycotics (Penicillin, Streptomycin, Amphotericin, Sigma). SW620 and MDA-MB-213 cells were cultured in RPMI-1640 (Gibco, Life Technologies) with 10% fetal bovine serum (FBS, Euroclone) and 1% antibiotics and antimycotics (Penicillin, Streptomycin, Amphotericin, Sigma). U87 cells were cultured in Minimum Essential Medium (MEM, Gibco; Life Technologies) with 10% FBS and 1% antibiotics and antimycotics. All the cell lines were maintained in incubator at 37°C with 5% CO₂.

Drugs

Psychotropic drugs used in the screening were purchased from Cayman Chemicals, Sigma, TCI Chemicals and Selleck Chemicals. List of drug used: aripiprazole, brexpiprazole, cetirizine, diphenhydramine, droperidol, ebastine, fluoxetine, fluspirilene, haloperidol, iloperidone, ketanserin, metoclopramide, nefazodone, paliperidone, penfluridol, pimozone, pipamperone, R59022, R59949, risperidone, ritanserin, spiperone, trazodone, urapidil, way-100135, and ziprasidone. All drugs were dissolved in DMSO at a 10 mmol/L concentration and stored, in small aliquots at –20°C.

MTT Viability Assay

For each cell line, 1000 cells/well were plated in a volume of 100 µL in 96 wells plate. Cells were treated with different concentrations of drug (160, 80, 40, 20, and 10 µmol/L) and incubated for 72 h. For each concentration of drug, the same concentration of vehicle (DMSO) was used as control. MTT (thiazolyl blue tetrazolium bromide, Sigma) 0.5 mg/ml was, then, added to each well and incubated for 4 h at 37°C and 5% CO₂. Crystals were dissolved using 100 µL of acidic isopropanol (4 mmol/L HCl) and the absorbance (570 and 650 nm) was read at the spectrophotometer (Victor, PerkinElmer).

To perform viability assay with biogenic amines 4,000 cells/well from MCF7 and HCT116 were plated in 96 wells plate. Cells were treated with different doses of serotonin, dopamine and histamine (Cayman Chemicals) in DMEM 0% FBS and viability was evaluated after 24- and 48-h treatment by MTT assay.

Viability Rescue Assay

To perform viability rescue experiments, 1,500 MCF7 cells were plated in 96 wells plate and treated with 10 $\mu\text{mol/L}$ spiperone, nefazodone, fluoxetine, fluspirilene, ebastine, pimozide or 5 $\mu\text{mol/L}$ penfluridol in combination with vehicle alone (DMSO), or with 5 $\mu\text{mol/L}$ carbobenzoxy-valyl-alanyl-aspartyl-[O-methyl]fluoromethylketone (zVAD-fmk, AdipoGen), 2.5 mmol/L 3-methyladenine (3-MA, AdipoGen), 5 mmol/L N-[(2S,3S)-3-[(propylamino) carbonyl]-2-oxiranyl]carbonyl]-L-isoleucyl-L-proline, methyl ester (CA-074 me, Cayman Chemical), 5 $\mu\text{mol/L}$ cyclosporin A (Cayman Chemical) and 5 $\mu\text{mol/L}$ N-Acetyl-L-cysteine (NAC, Sigma Aldrich). MTT viability assay was performed after 72 h as previously described, except for NAC where, prior to MTT adding, medium was removed and each well was washed with 100 μL of phosphate buffered saline. For biogenic amines viability rescue, 1,500 MCF7 cells were seeded in 96 wells plate and treated with IC_{50} concentration of the following drugs: spiperone, nefazodone, fluoxetine, fluspirilene, ebastine, pimozide, penfluridol in combination with vehicle (DMSO) or 5 $\mu\text{mol/L}$ dopamine, serotonin or histamine. MTT viability assay was performed as described before after 24, 48, and 72 h.

Apoptosis Assay

Fifty thousand MCF7 cells were plated in 24 wells plate and treated for 48 h with 10 $\mu\text{mol/L}$ fluoxetine, ebastine, pimozide, fluspirilene, spiperone, nefazodone, or 5 $\mu\text{mol/L}$ penfluridol.

Cells were then stained following the manufacturer's instruction (AdipoGen). Briefly, cells were incubated for 10 min at room temperature with annexin binding buffer 1X (10 mmol/L HEPES/NaOH, pH 7.4, 140 mmol/L NaCl, 2.5 mmol/L CaCl_2) containing Annexin V-FITC. Lastly, cells were washed and resuspended in annexin binding buffer 1X. Propidium iodide was added to all the samples 5 min before FACS analysis (Attune Nxt, Flow Cytometer, Thermo Fisher Scientific). Data were analyzed with FlowJoTM software (Becton, Dickinson and Company).

Migration Assay

Migration assay was performed using culture-insert 2 well in μ -dish (ibidi GmbH, Martinsried, Germany) as previously described (35). Briefly 30,000 HCT116 cells and 25,000 MCF7 cells were plated in each side of the insert in 24 wells plate. After 24 h, inserts were removed, and cells were treated with respective psychotropic drugs (5 $\mu\text{mol/L}$) or DMSO (0.05%) in complete medium. Images were acquired at 0 and 24 h after treatment, with phase contrast microscope and analyzed through ImageJ software (NIH, USA). Data were shown as % of closure rate relative to time 0.

Vacuolization Assay

MCF7 cells were plated at the concentration of 25,000 cells/well in 48 wells plate and then treated with fluoxetine, ebastine, penfluridol, pimozide, fluspirilene, spiperone, nefazodone at the concentration of 5 $\mu\text{mol/L}$ or rapamycin (10 $\mu\text{mol/L}$). After 2 h treatment one well from each treatment was treated with bafilomycin A1 (50 nmol/L) or 3-MA (1 mmol/L). Pictures

were acquired with a phase contrast microscope 4 and 6 h after treatment, images were analyzed by ImageJ software. Analysis shows the percentage of vacuolization rate for each treatment.

Mitochondrial Membrane Potential Analysis

Mcf7 cells were plated at the concentration of 20,000 cells/well in 48 wells plate and treated with 5 $\mu\text{mol/L}$ fluoxetine, ebastine, fluspirilene, nefazodone penfluridol, pimozide, spiperone. DMSO 0.05% was used as negative control. After treatment, cells were stained with 10 $\mu\text{g/ml}$ JC-1 dye (Adipogen) in PBS for 30 min in the dark at 37°C. FCCP (Cayman chemicals) was added for 15 min after the staining as positive control. Signals were acquired with a fluorescence microscope (FLoid Cell Imaging Station, Life Technology) and images were analyzed by ImageJ software calculating red/green fluorescence ratio.

Lysotracker Assay

MCF7 cells were plated at the concentration of 20,000 cells/well in 48 wells plate and treated with 5 $\mu\text{mol/L}$ fluoxetine, ebastine, fluspirilene, nefazodone penfluridol, pimozide, spiperone or 10 $\mu\text{mol/L}$ rapamycin for 16 h. After the treatment, medium was removed and cells were stained with Lysotracker Deep Red (Invitrogen, 50 nmol/L) and Hoechst 33342 (5 $\mu\text{g/ml}$) for nuclei staining, in the dark at 37°C for 30 min. Signals were acquired with a fluorescence microscope (FLoid Cell Imaging Station, Life Technology). Lysotracker red signal/blue nuclei signal was analyzed by ImageJ software.

Phospholipidosis Assay

MCF7 cells were plated at the concentration of 20,000 cells/well in 48 wells plate and treated with 5 $\mu\text{mol/L}$ ebastine, fluoxetine, fluspirilene, nefazodone penfluridol, pimozide, spiperone or 10 $\mu\text{mol/L}$ rapamycin and stained with 1X LipidTox green (Thermo Fisher Scientific) for 16 h.

Subsequently, nuclei were stained using Hoechst 33342 (5 $\mu\text{g/ml}$) and plate was incubated for 30 min in the dark at 37°C. Afterwards, cells were washed with PBS and fixed with paraformaldehyde 4% for 15 min in the dark. Signals were acquired with a fluorescence microscope (FLoid Cell Imaging Station, Life Technology) and images were analyzed by ImageJ software.

Western Blotting

MCF7 cells were plated at the concentration of 150,000 cells/well in 6 wells plate and treated with 5 $\mu\text{mol/L}$ ebastine, fluoxetine, fluspirilene, nefazodone penfluridol, pimozide, spiperone for 16 h. For experiment of autophagic flux two conditions were carried out for each drug: drug alone and co-treatment of drug and chloroquine 50 $\mu\text{mol/L}$. For experiment to evaluate LC3B expression upon 3-MA treatment, cells were pre-treated with 3-MA 1 mmol/L for 2 h and then cotreated with spiperone and penfluridol 5 $\mu\text{mol/L}$ for 16 h. After treatments, whole cell lysates were prepared using RIPA lysis buffer (25 mmol/L Hepes pH 8, 135 mmol/L NaCl, 5 mmol/L EDTA, 1 mmol/L EGTA, 1 mmol/L ZnCl_2 , 50 mmol/L NaF, 1% Nonidet P40, 10% glycerol) with protease inhibitors (AEBSF, aprotinin, bestatin,

E-64, EDTA, leupeptin, Sigma-Aldrich) and orthovanadate. Lysates were then kept on a wheel for 20 min at 4°C and after centrifuged at 12,500 g for 15 min. Proteins contained in the samples were collected and quantified using Pierce BCA protein assay kit (Thermo Fisher Scientific). Successively, proteins were denatured at 95°C for 5 min in presence of 2% Sodium Dodecyl Sulfate (SDS), 150 mmol/L dithiothreitol (DTT) and 0.01% bromophenol blue. Electrophoresis of the samples was performed using 6, 8, 10, or 15% polyacrylamide gels and proteins were transferred from the gel to a PolyVinylidene DiFluoride membrane (PVDF, Amersham). Lastly, the membrane was saturated using 3% Bovine Serum Albumin (BSA, Sigma) in TBS/Tween-20 0.1% [Tris Buffered Saline 1X containing Trizma base 50 mmol/L, NaCl 120 mmol/L, 0.1% Polyethylene glycol sorbitan monolaurate (Tween-20)] for 1 h and incubated with primary antibody dissolved in the same buffer with sodium azide 0.01%. Primary antibodies were anti-LC3B (Thermo Scientific), anti-P-P70S6K T389 (Cell Signaling Technology), anti-P70S6K (Cell Signaling Technology), anti-P-S6 S235/236 (Cell Signaling Technology), anti-S6 (Cell Signaling Technology) anti-P-AMPK α T172 (Cell Signaling Technology), anti-AMPK (Cell Signaling Technology), anti-GAPDH (Cell Signaling Technology). The day after, primary antibody was removed and the membrane was washed with TBS-Tween-20 0.1% for 15 min three times and then incubated with horseradish peroxidase conjugated secondary anti-mouse or anti-rabbit antibody (Perkin Elmer Life Science) diluted 1:3000 in TBS-Tween-20 0.1% for 45 min. After washing, reading of the membrane was performed using ECL Western Lightning Chemiluminescence Reagent Plus (Perkin Elmer Life Science) and images acquired with the Chemidoc Touch (Bio-Rad).

Immunofluorescence Microscopy Analysis

MCF7 cells at the concentration of 50,000 cells/well were seeded onto glass coverslips and treated with 5 μ mol/L fluoxetine, ebastine, penfluridol, pimozone, fluspirilene, spiperone, nefazodone for 16 h. After the treatment, cells were washed with PBS and fixed with PFA 4% for 10 min at room temperature and washed with PBS. Then cells were permeabilized incubating with cold HEPES-Triton X-100 (20 mM HEPES pH 7.4, 300 mM sucrose, 50 mM NaCl, 3 mM MgCl₂, 0.5% Triton X-100) for 5 min at 4°C. Cells were washed with 0.2% PBS-BSA and saturated using 2% PBS-BSA for 15 min before placing primary antibodies.

Antibodies used in these experiments were anti-mTOR (Cell Signaling Technology), anti-Galectin-1 (Santa Cruz Biotechnology), anti-LAMP1 (Santa Cruz Biotechnology). Cells were incubated with primary antibodies for 30 min, then washed, saturated with 2% PBS-BSA and incubated with secondary antibodies conjugated with Alexa Fluor-488, -536 (Invitrogen) and DAPI for 30 min.

After the incubation, glasses were mounted on glass slides using Mowiol (20% Mowiol 4-88, 2.5% DABCO in PBS, pH 7.4). Images were acquired at confocal microscope Leica TCS SP8 or fluorescence microscope DM5500B (Leica) and analyzed using ImageJ software.

Compounds Chemical Analysis

The properties of the compounds (LogP and basic pKa) were investigated using ACD/ LAB software. As reported in the publication of Muehlbacher (36) there is not a clear CADs classification based on chemical properties. We decided to apply the same parameters based on LogP and pKa applied in the Muehlbacher's manuscript. In particular, compounds were considered CADs when LogP > 3, for the amphiphilic characteristics, and a PKa > 7.4 for the cationic characteristics.

Statistical Analysis

Prism 8.0 software was used for statistical analysis (GraphPad software Inc., San Diego, CA). In viability assays, IC₅₀ was determined using a variable slope model referring to the values obtained during the assay; a semi-logarithmic dose-response curve was created.

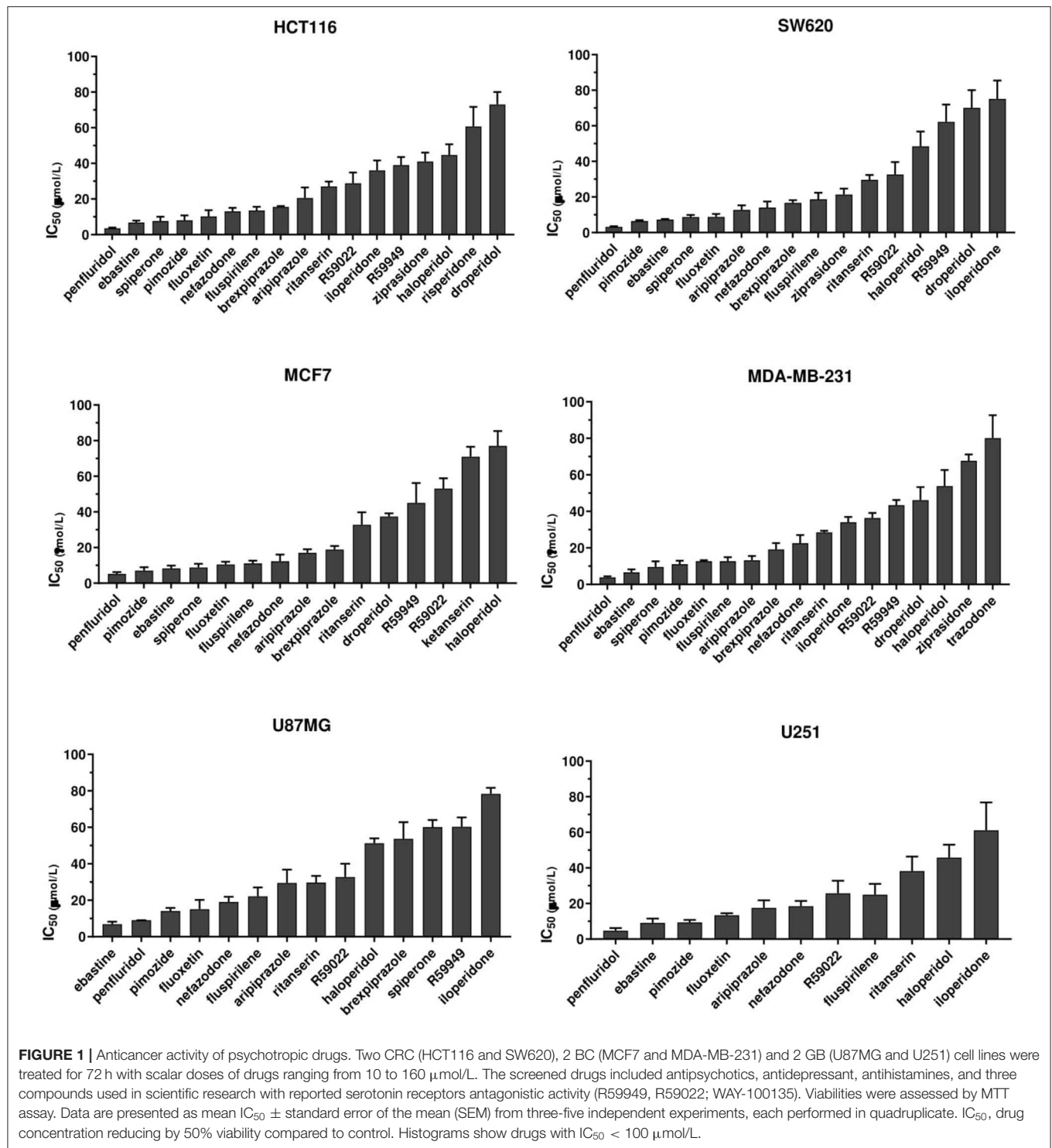
Statistical significance was analyzed using Student's *t*-test with $p < 0.05$ as the criterion of significance when two groups were compared. Analysis of contingency tables were performed using Prism 8.0 software (GraphPad software Inc., San Diego, CA) and statistical significance was evaluated using Fisher exact test with $p < 0.05$.

RESULTS

The Antitumoral Activity of Psychotropic Drugs Transcends the Conventional Therapeutic Classes and Tumor Type

To identify compounds with potential, clinically relevant, anticancer activity we first assessed their effect on six different tumor types represented by two colorectal cancer (CRC; HCT116 and SW620), two breast cancer (BC, MCF7, and MDA-MB-231) and two glioblastoma (GB; U87MG and U251MG) cell lines. Cells were treated for 72 h with scalar doses of drugs ranging from 10 to 160 μ mol/L. The screened drugs ($N = 26$) were represented by antipsychotics ($n = 14$), antidepressant ($n = 2$), antihistamines ($n = 3$) and three compounds used in scientific research with reported serotonin receptors antagonistic activity (**Figure 1**, **Supplementary Figure 1**, **Supplementary Table 1**). For drugs that induced more than 50% cell viability reduction at a concentration lower than 100 μ mol/L, in a dose-dependent manner, the IC₅₀ values were calculated (**Supplementary Figure 2**, **Supplementary Table 1**).

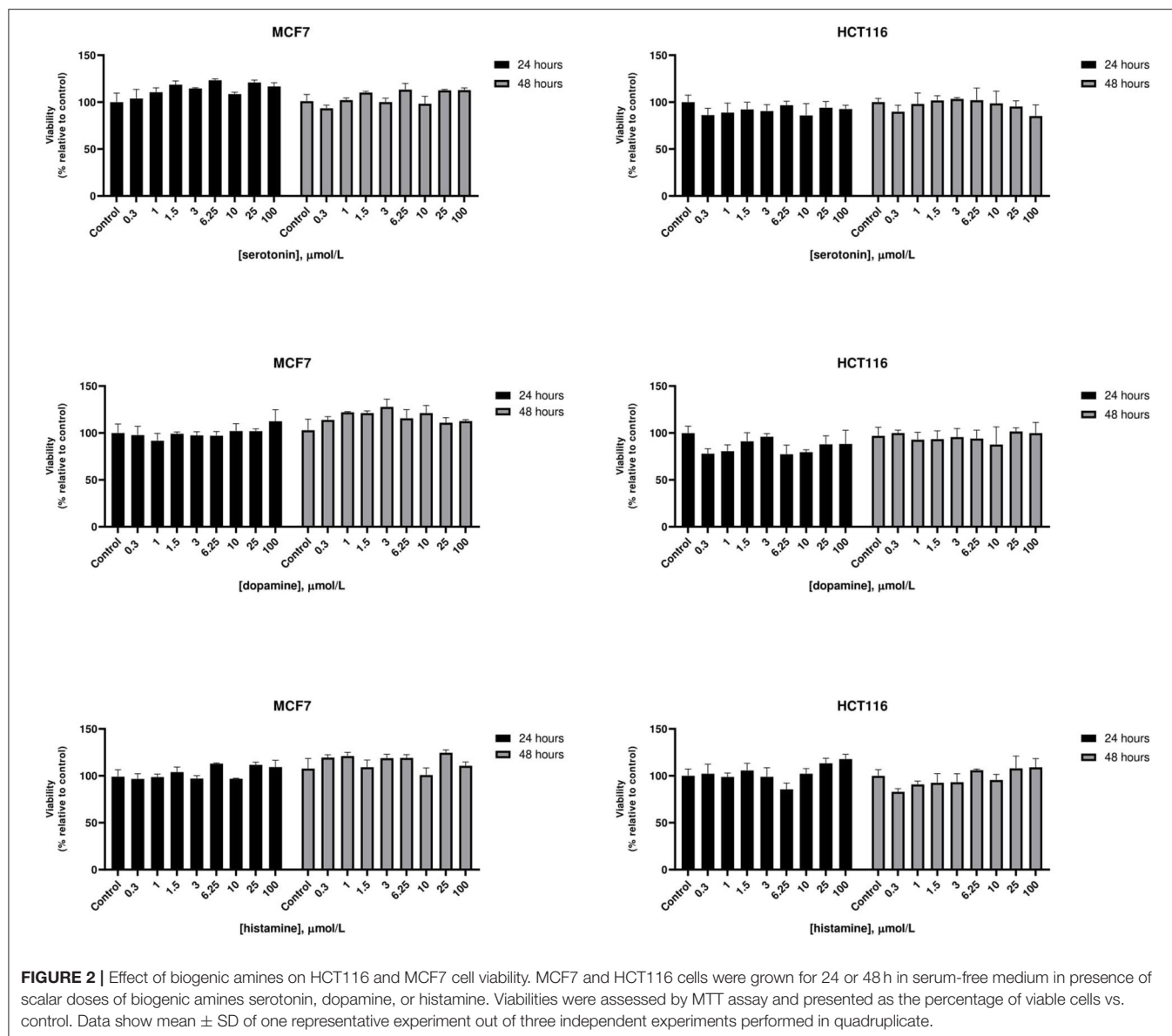
The most effective drugs in all cell lines tested belonged to all three pharmacological classes investigated (antipsychotics, antidepressants, and antihistamines) (**Figure 1**, **Supplementary Figures 1**, **2**, **Supplementary Table 1**). The six most potent drugs induced more than 50% cell viability reduction at a concentration lower than 10 μ mol/L (penfluridol, ebastine), 15 μ mol/L (pimozone and fluoxetine) or 25 μ mol/L (fluspirilene and nefazodone) in all cell lines tested; spiperone and brexpiprazole proved to be highly effective in both CRC and BC (with IC₅₀ < 10 μ mol/L and 10 < IC₅₀ < 20 μ mol/L, respectively) whereas their cytotoxicity was negligible in GB. A tendency for the diphenylbutylpiperidines pimozone, fluspirilene and penfluridol to be more effective in BC and CRC than in



GB was also observed (Supplementary Table 1). Aripiprazole and ritanserin demonstrated a moderate cytotoxicity, whereas droperidol, haloperidol and iloperidone showed a weak effect only in a fraction of cell lines. Notably, in the lower range of concentrations, some compounds induced a moderate increase in cell viability reflecting cell proliferation: haloperidol

in all cell lines tested; ritanserin and the two structurally related compounds R59022 and R5949 in CRC cell lines only, whereas iloperidone in MCF7 and U87MG cell lines (Supplementary Figure 1).

Eight compounds, represented by the antihistamines cetirizine and diphenhydramine, the antipsychotics paliperidone,



pipamperone and risperidone, the antihypertensives ketanserin and urapidil, and the antiemetic metoclopramide showed no cytotoxicity, or caused a reduction of at least 50% of cell viability only at very high concentrations ($>60 \mu\text{mol/L}$) (Supplementary Figure 1, Supplementary Table 1). A few of these drugs i.e., urapidil, cetirizine, diphenhydramine and metoclopramide even induced cell growth in one or more cell lines tested (Supplementary Figure 1). These results clearly suggest that the cytotoxic effect of these compounds in the micromolar range is not associated with their conventional pharmacological properties and clinical use.

Cytotoxicity of Psychotropic Drugs Is Not Mediated by Biogenic Amine Receptors

At therapeutic concentrations, the main pharmacological targets of these compounds are biogenic amines receptors (37, 38). The

precise role of biogenic amines such as histamine, dopamine, and serotonin in cancer is still debated (39–41). To test biogenic amines in our cell lines modes, we treated HCT116 and MCF7 cells with a wide range of concentrations of serotonin, dopamine and histamine and evaluated viabilities after 24 and 48 h. In our assay conditions we observed no significant effect on cell proliferation even at very high doses (Figure 2). Long term treatment of MCF7 cells with the strongest cytotoxic compounds penfluridol, ebastine, pimozone or fluoxetine at clinically significant concentrations determined only a modest increase of drugs efficacy, with IC_{50} values that remained above $3 \mu\text{mol/L}$ even after 6 days of treatment (Supplementary Figure 3).

Notably, neither dopamine, nor serotonin and histamine, added to the culture media, were able to rescue the cytotoxic effect of these drugs (Figure 3).

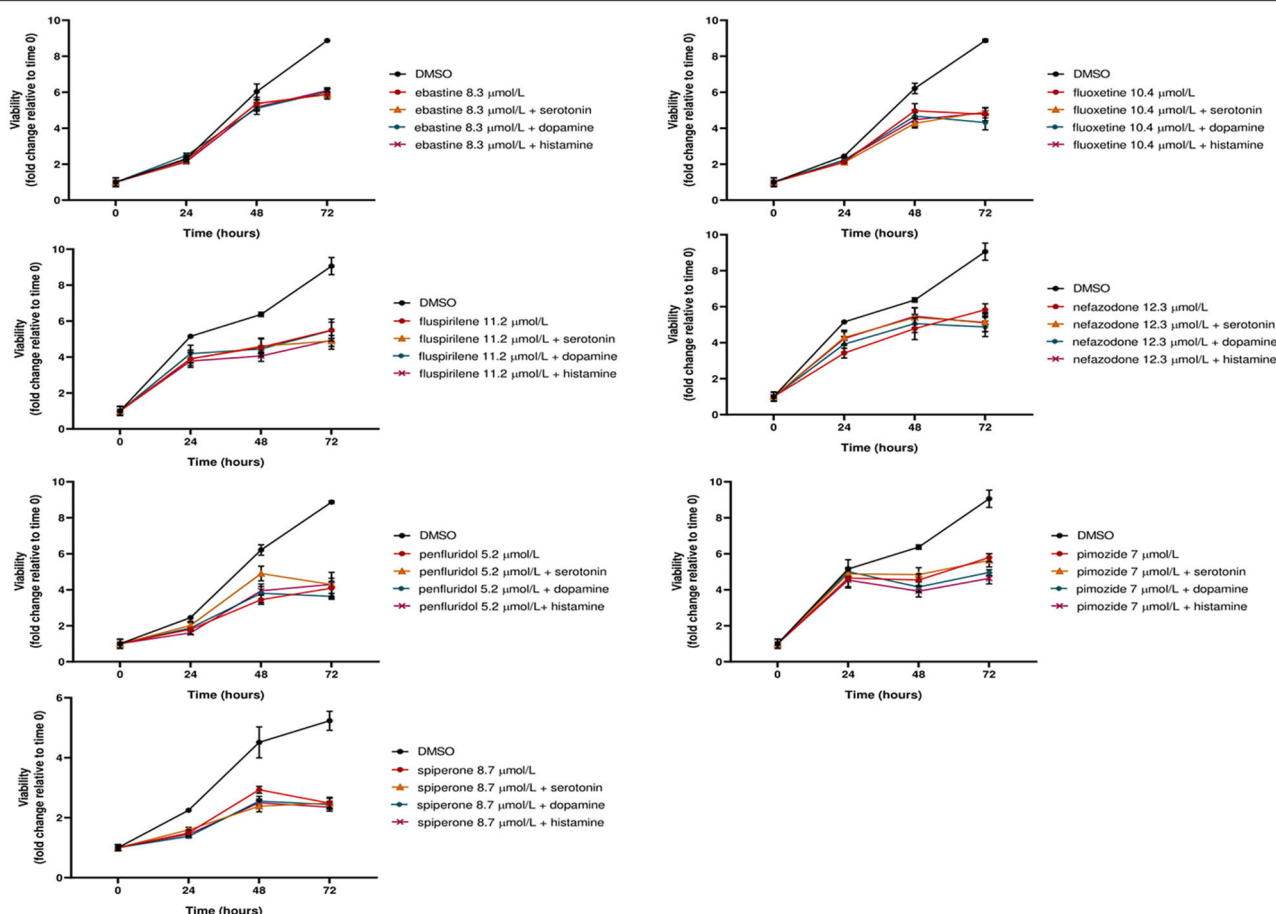


FIGURE 3 | The cytotoxic effect of psychotropic drugs is not reduced by co-treatment with biogenic amines. MCF7 cells were treated with psychotropic drugs alone (at a concentration equivalent to IC_{50}) or in presence of 5 $\mu\text{mol/L}$ biogenic amines serotonin, dopamine or histamine. Viabilities were assessed by MTT assay at different time points and presented as fold change relative to control cells treated with vehicle only. Data show mean \pm SD of one representative experiment out of three independent experiments performed in quadruplicate.

These data further support the hypothesis that these compounds affect tumor cell viability through a mechanism that is not mediated by the major neuroreceptor systems implicated in their psychotropic effects.

Psychotropic Drugs Affect Tumor Cell Migration

To determine the effect of psychotropic drugs on the motility of cancer cells, we assessed MCF7 and HCT116 cells migration by the wound-healing assay (**Figure 4**). All active drugs caused a reduction in the motility of MCF7 cells with the strongest effects observed with penfluridol, spiperone, urapidil and brexpiprazole (**Figure 4A**). On the contrary, the migration rate of HCT116 cells was unexpectedly increased by the cytotoxic compounds ebastine and penfluridol, as well as by different other compounds such as urapidil, diphenhydramine, ritanserin, R59022 and R59949; spiperone, and to a lesser extent, ketanserin and trazodone, reduced HCT116 cells motility (**Figure 4B**). Overall, these results show that: (i) the impact of the different compounds on the migration rate is not strictly associated with their cytotoxic effect

or their conventional pharmacological properties and clinical use; (ii) the effect of the compounds on cell motility is cell line specific.

Psychotropic Drugs With Significant Antitumoral Activity Display a Cationic Amphiphilic Structure

Cationic amphiphilic drugs (CADs) are defined as chemical compounds with the ability to passively diffuse through lipid bilayers stacking in acid organelles such as lysosomes (42). These compounds contain both a hydrophobic and a hydrophilic domain; the hydrophobic domain contains one or more aromatic rings whereas the hydrophilic part contains a functional amine group that can be ionized (43). CADs family comprises a broad spectrum of compound classes, including dozens of approved drugs that are used to treat a wide range of diseases including allergies, heart diseases, and psychiatric disorders (44, 45). Since the antitumoral activity of compounds investigated in this study is not apparently related to their conventional pharmacological

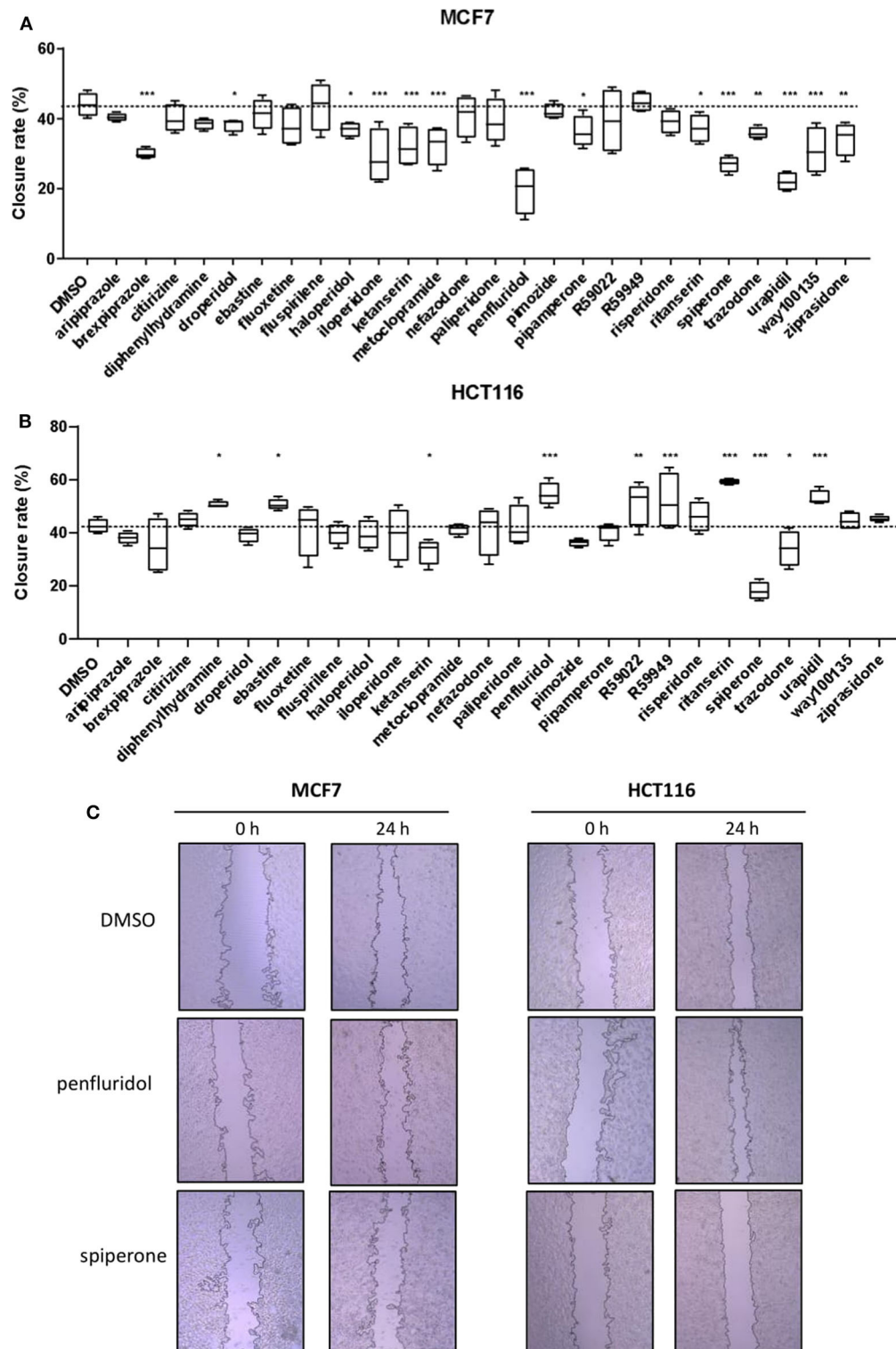
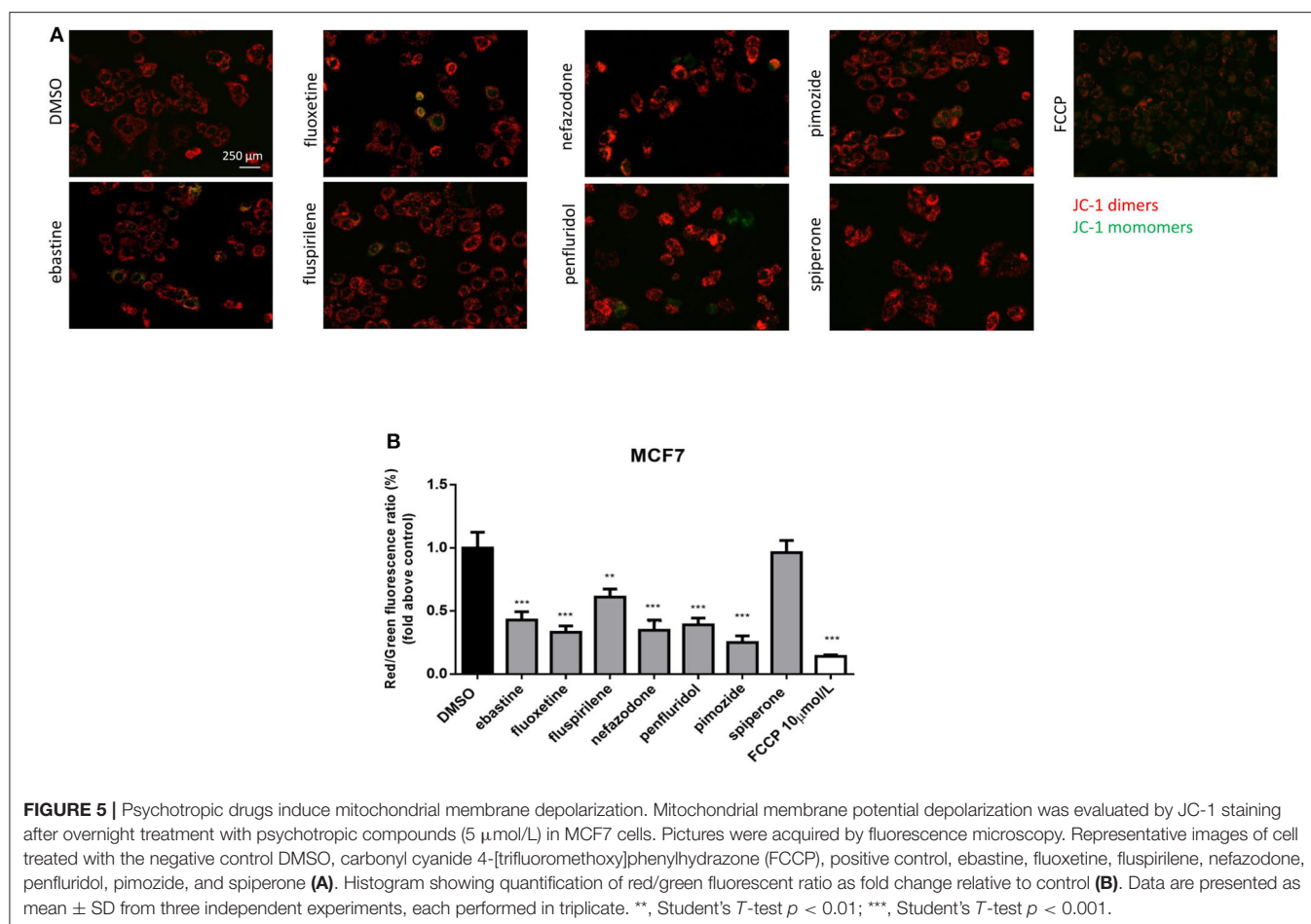


FIGURE 4 | Effect of psychotropic drugs on cancer cells migration. Cell motility was evaluated by wound healing assay. MCF7 (A) and HCT116 (B) cells were plated in 2 wells IBIDI chambers. After removing the insert, cells were treated with drugs (5 μ mol/L) in DMEM 10% FBS. The widths of wounds were measured at 0 and 24 h. Graphs show the closure rate. Data are presented as mean \pm SD from three independent experiments, each performed in triplicate. *, Student's *T*-test $p < 0.05$; **, Student's *T*-test $p < 0.01$; ***, Student's *T*-test $p < 0.001$. Representative images of MCF7 and HCT116 wounds after treatment with penfluridol, spiperone, and DMSO (C).



properties and clinical use, we investigated the CADs properties of psychotropic drugs used in our screening evaluating their chemical structure, logP and pKa in comparison to the well-known CADs compounds amiodarone, chlorpromazine and chloroquine (Supplementary Table 2) (46, 47). Since there is not a clear CADs classification based on chemical properties, we set LogP and pKa cut off as suggested by Muehlbacher (36). Overall, 14 psychotropic drugs out of 26 were classified as CADs. Five out of seven most cytotoxic drugs in MCF7 ($\text{IC}_{50} < 15 \mu\text{mol/L}$) were CADs, whereas spiperone and nefazodone, were excluded from CAD classification just because of a LogP or pKa value below the selected cut off (Supplementary Figure 4, Supplementary Table 2). Since CADs were represented also among drugs without cytotoxic activity (e.g., haloperidol, iloperidone, or ritanserin), cationic amphiphilic characteristics contribute strongly, but are not sufficient to confer significant antitumoral activity to psychotropic compounds.

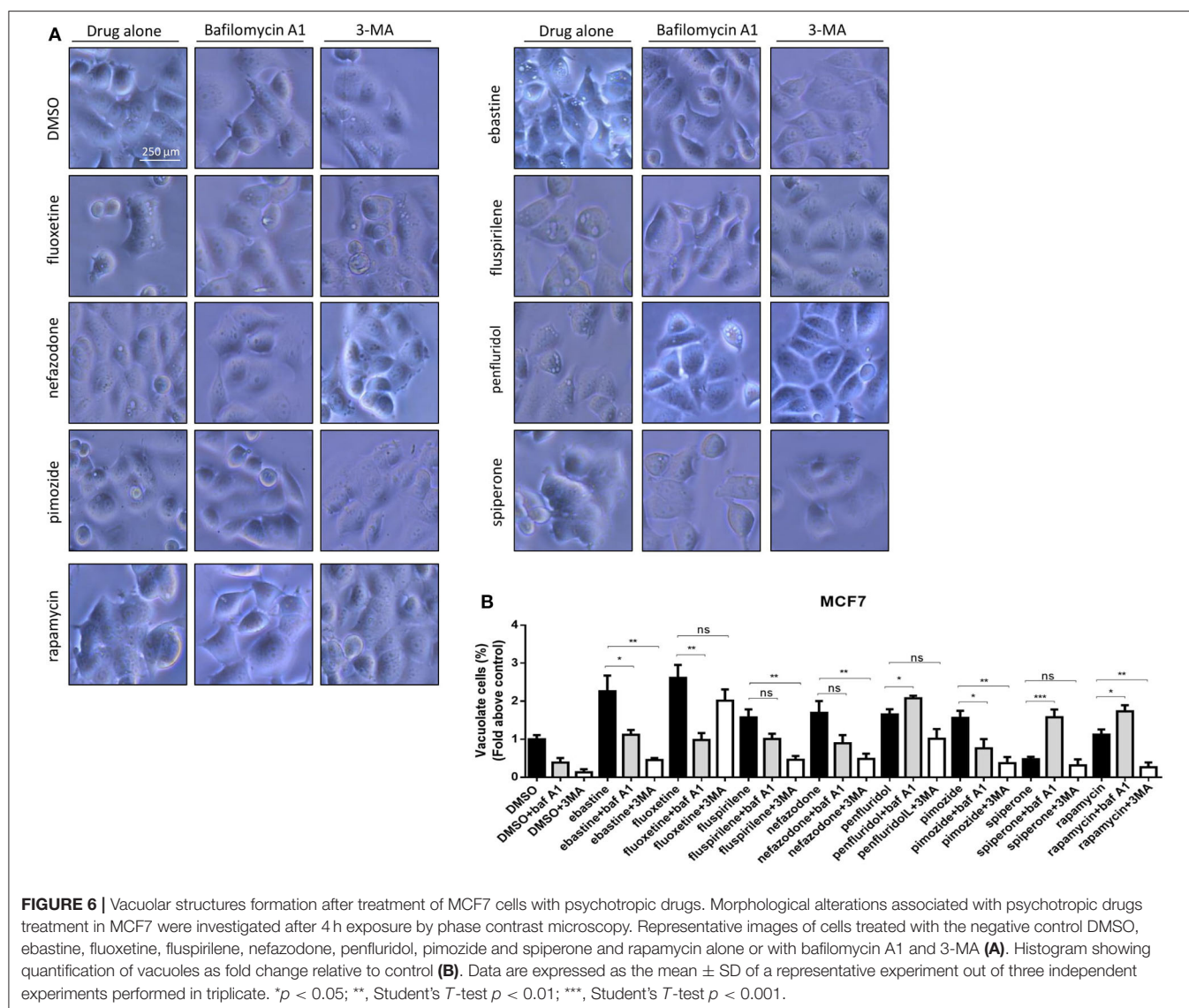
Psychotropic Drugs Cause Mitochondrial Membrane Depolarization

CADs can readily pass through phospholipids bilayers, particularly through membranes with a large transmembrane potential such as the mitochondrial inner membrane. They

readily accumulate in the mitochondrial matrix, causing mitochondrial membrane depolarization (45, 48, 49). Therefore, we evaluated the alteration in mitochondrial membrane potential ($\Delta\psi\text{m}$) as a function of drug treatment, using the lipophilic cationic dye JC-1 (50). MCF7 cells were treated, for 16 h, with 5 $\mu\text{mol/L}$ of each drug or with FCCP, used as positive control. A significant reduction in $\Delta\psi\text{m}$ was observed after treatment with ebastine, fluoxetine, penfluridol, pimozone, nefazodone and fluspirilene, but not with spiperone (Figure 5).

Psychotropics Drugs Induce Vacuolization and Increase Acidic Compartments

CADs are known to concentrate in acidic cell compartments because the retro-diffusion of the protonated form is inefficient (mechanism known as ion-trapping or pH partitioning). If sufficiently intense, this sequestration results in the osmotic formation of numerous large, fluid-filled vacuoles already after short term exposure to drugs (46). These molecules are collectively referred to as lysosomotropic agents, for their propensity to concentrate into lysosomes (51). To test the hypothesis that cytotoxic psychotropic drugs concentrate in MCF7 cells by this mechanism, MCF7 were cultured in the presence of 10% FBS and treated with

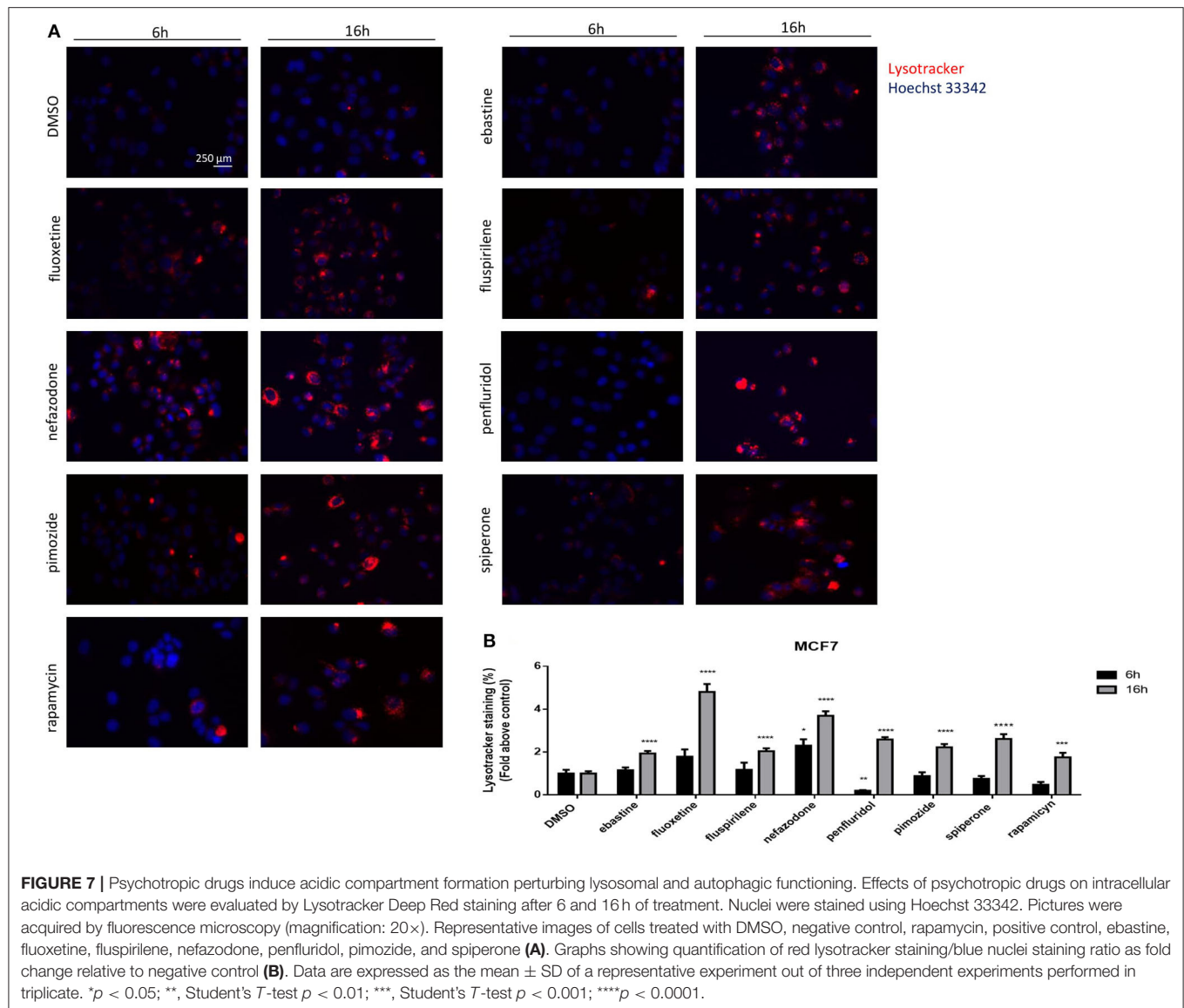


drugs alone or in the presence of the V-ATPase inhibitor bafilomycin A1 or class III PI3K inhibitor 3-MA (Figure 6, Supplementary Figure 5). Fluoxetine induced a strong vacuolar morphology already 6 h after treatment as previously reported (46) (Supplementary Figure 5A); a less prominent, but still significant increase of vacuolar structures was also observed after treatment with fluspirilene, ebastine, pimozide, penfluridol and nefazodone, whereas increase of vacuoles was not observed with spiperone (Supplementary Figure 5). The mTOR inhibitor rapamycin used as a positive control of autophagy induced a mild vacuolar morphology.

In the presence of bafilomycin A1, a significant reduction of vacuoles formation was observed with fluoxetine, ebastine, fluspirilene, pimozide, and nefazodone, suggesting that these drugs require an acidic environment to accumulate and induce vesicles formation; on the contrary, a higher number of vesicles was observed after treatment with penfluridol and spiperone,

suggesting that these drugs do not require pre-existing acidic compartments to induce vacuolization although they can cause the formation of autophagosome structures that accumulate after inhibition of autophagosome-lysosome fusion and autolysosome acidification by bafilomycin A1 (Figure 6). The autophagosome nature of vacuoles induced by all these compounds was supported by the reduction of the number of vesicles in the presence of the class III PI3K inhibitor 3-MA (Figure 6).

The nature of the vacuoles induced by psychotropic drugs was further investigated by staining MCF7 cells with the LysoTracker dye, which is a highly soluble small molecule that is retained in acidic subcellular compartments, such as late endosomes and lysosomes, whose presence is an indirect indication for autophagic activity (52). Although a transient increase of pH in autophagosome-lysosome structures was observed after short term treatment with penfluridol (Figure 6B), LysoTracker dye staining clearly shows a strong increase of acidic compartments



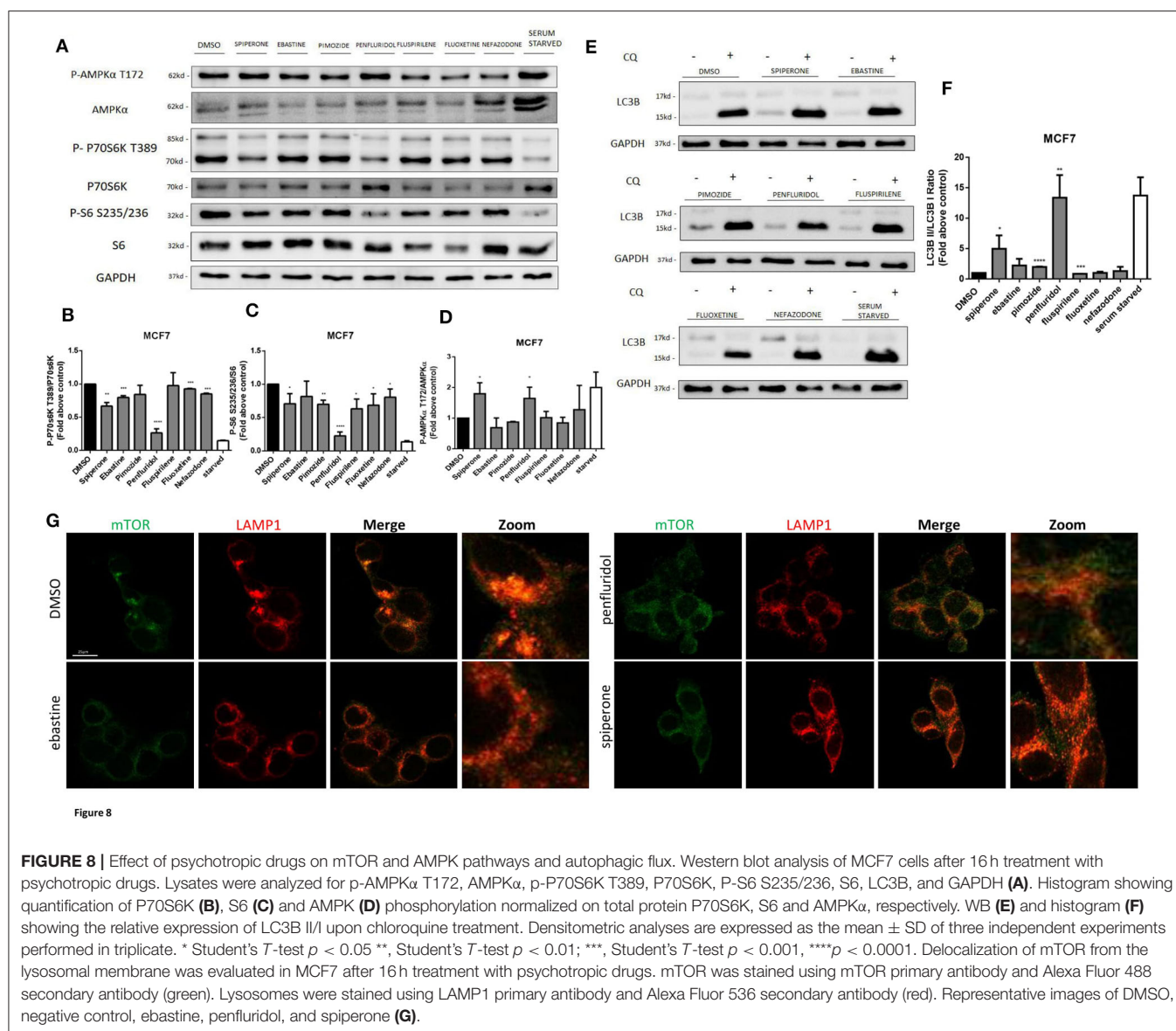
after overnight treatment with all drugs tested, consistent with increased autophagosome-lysosome acidic structures (Figure 7, Supplementary Figure 6).

Spiperone and Penfluridol Induce Autophagy by Modulating mTOR and AMPK Pathways

The increase of acidic structures can be a consequence of both autophagy induction and reduced turnover in the autophagosomal compartment caused by impaired autophagosome-lysosome fusion and/or lysosomal function. In order to clarify this issue, we investigated the main regulators of autophagy: mTOR pathway (represented by phosphorylations in 70S6K T389 and ribosomal protein S6 S235/236) and AMPK activation (Figure 8). Starvation, a strong inducer of autophagy, was used as positive control.

A strong inhibition of mTOR pathway, comparable to that obtained with starvation, was observed after treatment with penfluridol, whereas a milder but significant downregulation of the pathway was detected with spiperone and, to a lesser extent, with the other compounds (Figures 8A–C), since S6 Ser 235/236 phosphorylation might also be modulated by kinases different from P70S6K (53). Notably, a partial delocalization of mTOR from the lysosomal membrane, further supporting mTOR inhibition, was observed after treatment with both penfluridol and spiperone (Figure 8G, Supplementary Figure 7).

In agreement with mTOR dislocation, a significant increase of AMPK phosphorylation in the activation site T172, comparable to that induced by starvation, was observed after treatment with penfluridol and spiperone. On the contrary, AMPK phosphorylation was unaffected or slightly reduced after treatment with all other compounds (Figures 8A,D).



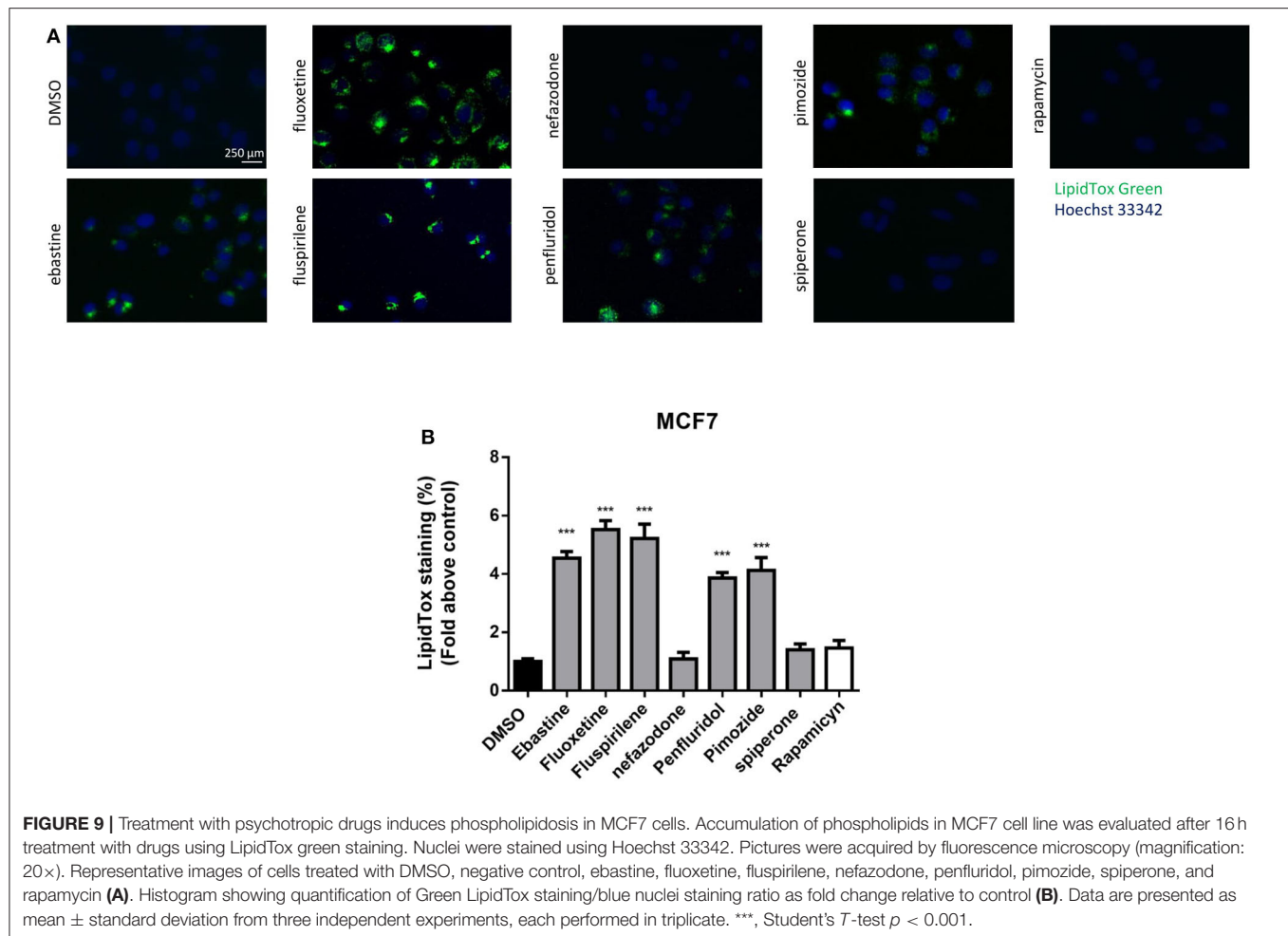
The conversion of the cytosolic LC3B form, LC3B-I, into the faster migrating, phosphatidylethanolamine-conjugated, LC3B-II form, a marker of autophagy induction (54) was significantly enhanced in cells treated with penfluridol, spiperone and pimoziide (Figures 8E,F).

Psychotropic Drugs With Cationic Amphiphilic Properties Cause Lysosomal Disruption

CADs can accumulate into lysosomes and impair lysosomal enzymatic activities (44, 55). It has also been shown that several antipsychotic and antidepressant drugs extensively accumulate in lysosomes and inhibit acid sphingomyelinase and phospholipases (36, 56). Lysosomes are a major site of cellular membranes degradation and complex lipids metabolism, therefore the

hallmark of drug-induced lysosomal impairment is accumulation of phospholipids (42, 57). Therefore, we investigated whether the antitumoral activity of psychotropic drugs was associated with lysosomal impairment by incubating cells in the presence of phospholipids conjugated to fluorescent dye. After incubation for 24 h with LipidTOX, MCF7 cells treated with ebastine, fluspirilene, fluoxetine, pimoziide and penfluridol showed a strong increase of phospholipids aggregates; on the contrary, this phenotype was not observed after treatment with non-CADs spiperone and nefazodone and with the inducer of autophagy rapamycin (Figures 9A,B).

Drugs with cationic amphiphilic properties accumulating into lysosomes can also induce LMP. This phenomenon can lead to the release of lysosomal enzymes inside the cytoplasm and possibly cell death (17). Galectin-1 is a small protein normally located in the cytoplasm and in the nucleus, that



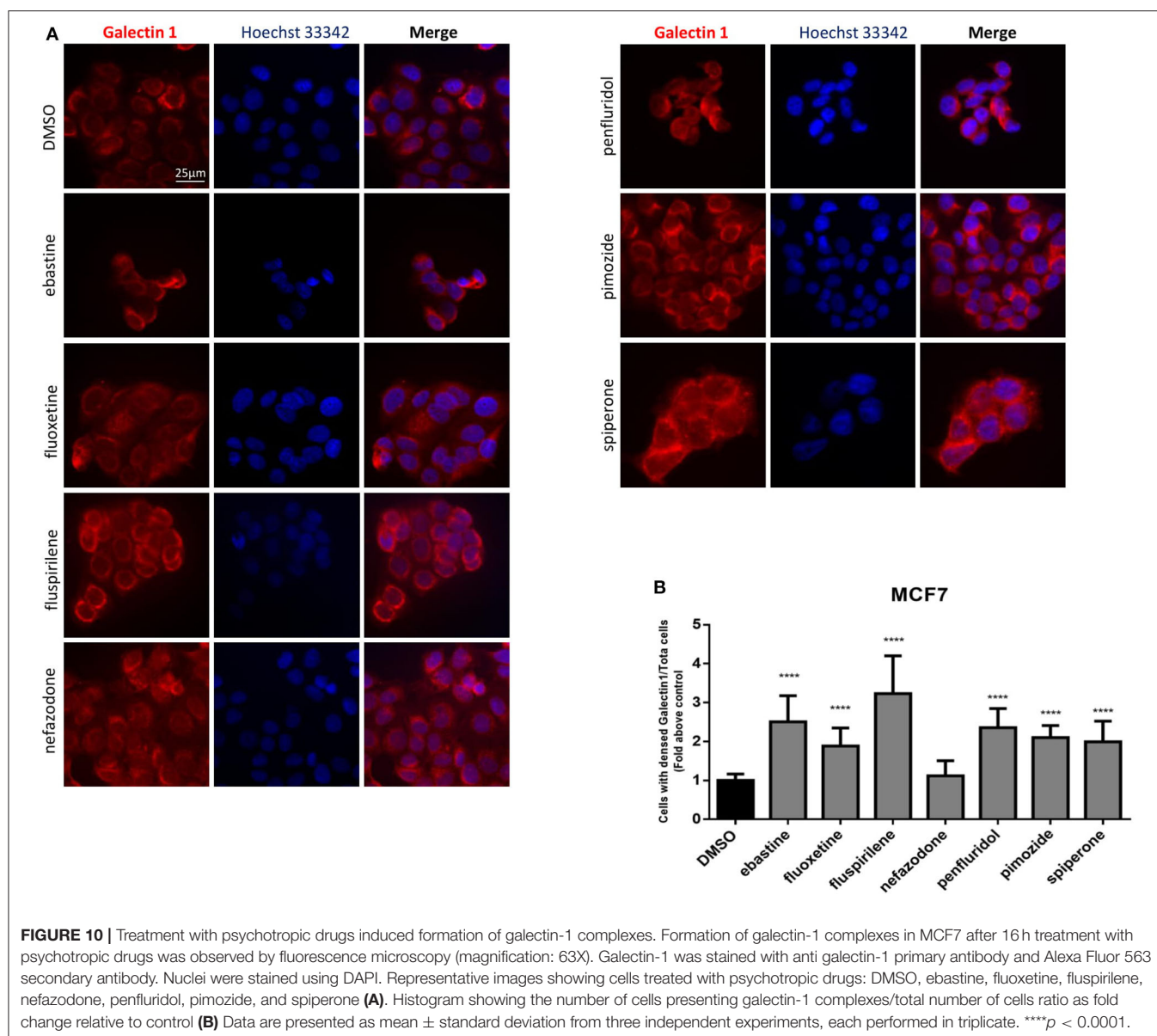
accumulates and forms complexes to the lysosomal membrane in case of lysosomal membrane damage and LMP (58). To evaluate lysosomal membrane damage in response to psychotropic drug treatment we investigated galectin-1 complex formation by immunofluorescence. The formation of galectin-1 complexes was observed with all the drugs tested, apart from nefazodone, indicating that cytotoxic psychotropic drugs can induce lysosomal membrane damage (Figures 10A,B).

Psychotropic Drugs Induce Different Types of Cell Death

To assess if apoptosis is involved in psychotropic drugs-induced cell death we performed PI/Annexin V staining in MCF7 cells. FACS analysis at different time points showed an increase in necrosis cells with all the drugs but a significant induction of apoptosis after 48 h of treatment with the sole spiperone (Supplementary Figure 8). These data were further confirmed by viability rescue experiments with a pan caspase inhibitor zVAD-fmk. As shown in Figure 11A, zVAD-fmk significantly rescued cell death only in cells treated with spiperone and staurosporine, whereas it was ineffective with the other drugs.

Since apoptosis is not the primary mechanism of death elicited by cytotoxic psychotropic drugs, except for spiperone, we investigated the role of autophagy by treating cells with the autophagy inhibitor 3-MA (59). As shown in Figure 11B, 3-MA co-treatment significantly rescued cell viability in cells treated with rapamycin and in cells treated with spiperone and pimozone. Conversely, 3-MA enhanced penfluridol cytotoxicity, whereas it did not show any effect in combination with ebastine, fluoxetine, nefazodone and fluspirilene. However, since it was reported that in particular conditions 3-MA could induce autophagy (59) we performed western blot analysis to investigate the conversion of the cytosolic LC3 I to II form in MCF7 cells treated with spiperone and penfluridol alone or in combination with 3-MA (Supplementary Figure 9). Our data indicate that in our experimental set-up 3-MA does not induce autophagy, on the contrary it is effective in suppressing LC3 II conversion.

To further investigate the mechanism of the observed cytotoxicity we assessed whether inhibition of lysosomal cathepsins B and L rescued cell viability in MCF7 cells, for this purpose we performed experiments with the inhibitor CA-074 me (60). As displayed in Figure 11C CA-074 me significantly

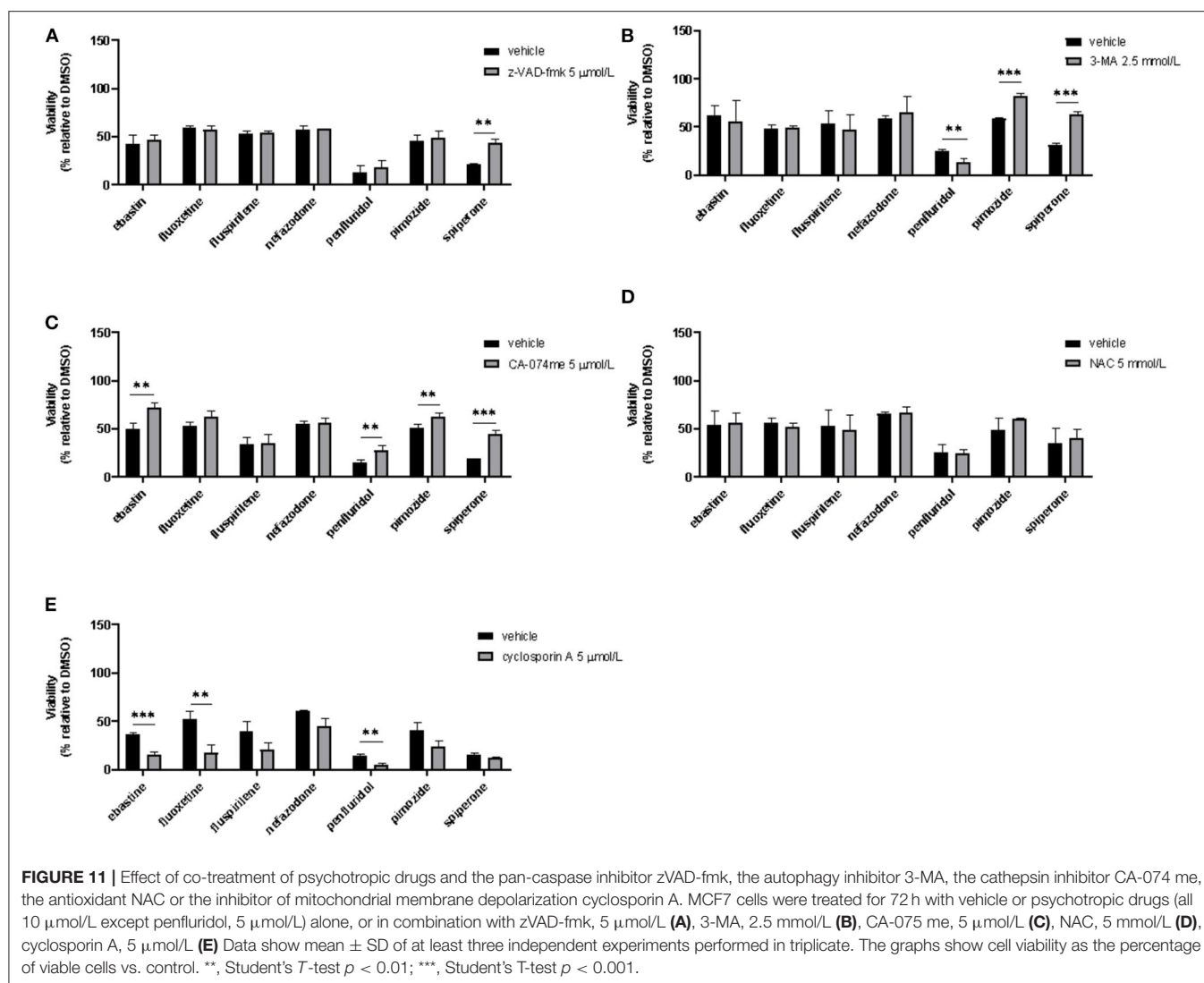


rescued cell death induced by ebastine, penfluridol, pimozone and spiperone, while a mild but not significant effect was observed in cells co-treated with fluoxetine.

Additionally, in order to clarify if oxidative stress was involved in psychotropic drugs-induced cell death, we co-treated MCF7 cells with the antioxidant NAC, however no significant effect was observed in terms of viability rescue (**Figure 11D**). With cyclosporin A, an inhibitor of the mitochondrial permeability transition pore (mPTP), an additive cytotoxic effect was observed with all drugs tested (**Figure 11E**). Cyclosporin A has been reported to be a broad-spectrum multidrug resistance modulator (61) and this activity possibly induces psychotropic drugs retention resulting in a boost of cytotoxicity.

DISCUSSION

Although cancer treatment has witnessed remarkable progress over the past few decades, cancer remains a major threat to humans, with total cure remaining elusive. Repurposing of well-characterized and well-tolerated drugs for cancer therapy has emerged as an attractive alternative for a long and costly process of drug development (23). Psychotropic drugs are revealing promising candidates for drug repositioning in cancer. Although several *in vitro* and *in vivo* models reported the efficacy of this family of drugs in reducing cancer cell viability and tumor growth (30, 32, 62), the pharmacological properties underpinning the possible clinical application of psychotropic drugs for cancer therapy remain poorly understood. In this study we investigated



a large panel of psychotropic drugs for their potential anti-tumoral activity evaluating their cytotoxic effect in six cell lines derived from three different tumor types. By using stringent screening conditions, we identified only a few compounds that significantly reduced cell viability at clinically relevant concentrations. These were represented by the antipsychotics penfluridol, pimoziide, fluspirilene, nefazodone, and spiperone, the antidepressant fluoxetine and the antihistamine ebastine. Except for spiperone, whose cytotoxicity was negligible in GB, all the other compounds showed cytotoxic activity in all cell lines tested.

The comparable efficacy, in three different tumor types, of compounds with clinically different indications allows us to speculate a common mechanism of action independent from the phenotypic and molecular profile of the tumor and not associated with the conventional pharmacological properties and clinical use of these compounds. This hypothesis is corroborated by the negligible cytotoxicity observed with other drugs with superimposable biogenic amine receptors targeting, by the lack

of rescue of cell viability after co-treatment with biogenic amines and by the drug concentration necessary to observe a biologic effect, that it is at least one order of magnitude higher than that needed for their conventional pharmacological targets (63).

Based on the analysis of structure and chemical-physical properties, most psychotropic compounds with a significant cytotoxic activity can be classified as CADs (36, 43). It is well-demonstrated the formation of cytoplasmic vesicles in cells exposed to CADs results from extensive ion-trapping-based accumulation of lysosomotropic weak bases in acidic compartments (36, 55). Vacuoles formation, inhibited by the disruption of the lysosomal V-ATPase, was observed after short term exposure of MCF7 cells to CADs fluoxetine, ebastine, fluspirilene, pimoziide but also to nefazodone, that is not formally a CADs but might display some of their features. Accumulation of vacuoles in the presence of bafilomycin A1 was instead observed after treatment with penfluridol and spiperone, suggesting that the formation of vesicles by these drugs does not necessarily depend on ion-trapping in acidic compartments,

but is favored by the block of lysosomal activity. The acidic autophagosome nature of these vesicles was confirmed by the requirement of class III PI3K for their formation and by the positive staining with the lysosomotropic dye LysoTracker. Notably, both spiperone and penfluridol, that induced the formation of autophagosome structures independently from the ion-trapping mechanism are likely true activator of autophagy, as demonstrated by stimulation of AMPK and LC3B conversion and downregulation of mTOR pathway observed in MCF7 cells.

Although lysosomotropic CADs can increase lysosomal pH after compound sequestration which could lead to suboptimal conditions for lysosomal digestion (64, 65), lysosomal pH increase may be a transient change and pH could be restored after extended exposure to lysosomotropic compounds (47, 66, 67). The increased LysoTracker dye staining we observed after overnight treatment with drugs indicates a pH recovery after compound sequestration and reflects the increased lysosomal volume, suggestive of the occurrence of lysosome biogenesis induced by lysosomotropic drugs (47, 68). Moreover, drug interactions with the lysosomal lipid bilayer and membrane proteins could influence the dynamics of membrane fusion and/or fission, thereby affecting trafficking steps and lysosomal egress (67), causing a reduction in autophagic flux and lysosomal enlargement.

Due to their chemical structure, CADs can accumulate in acidic lysosomes (46) and incorporate to luminal membranes where they function as effective inhibitors of acid sphingomyelinase and other lysosomal lipases (36, 44). At therapeutically relevant concentrations, CADs have been shown to cause the lysosomal accumulation of various lipid species, including sphingomyelin, phosphatidylethanolamine, phosphatidylserine, phosphatidylcholine, lysophosphatidic acid, and cholesterol, with induction of phospholipidosis (42, 57). In our experimental model, CADs ebastine, fluspirilene, fluoxetine and pimozone, that very rapidly accumulated in cells by ion-trapping, caused a strong increase of phospholipids aggregates. Our observations are supported by papers reporting the capacity of these compounds to induce phospholipidosis. Gonzalez-Rothi in 1995 first described the complication of pulmonary phospholipidosis in a patient with manic-depressive illness after treatment with fluoxetine (69); penfluridol, pimozone, and fluspirilene have been reported in a screening of drugs capable to inhibit sphingomyelinase and were found to induce phospholipidosis in neuroglioma H4 cells (36, 44), whereas ebastine was identified by electron microscope screening to evaluate chemicals for drug-induced phospholipidosis (70). Our results demonstrate that, also in cancer cells, ebastine, fluspirilene, fluoxetine and pimozone act as typical CADs, impairing lysosomal activity.

Some compounds investigated in this study, including the antipsychotics diphenylbutylpiperidines fluspirilene, penfluridol, and pimozone and antidepressants such as fluoxetine have been previously reported as autophagy inducers in neurons and in different cancer cell types such as BC and GB by affecting a variety of targets (31, 71–73). Our study shows that the cytotoxic activity of most of these compounds is essentially based on their common cationic amphiphilic properties and

their capacity to perturb acidic intracellular compartments. Moreover, although all investigated drugs caused the formation of acidic structures, apparently inducing the autophagic flux, only spiperone, penfluridol and, potentially, pimozone can be considered true autophagy activators. Overall, these data raise a critical issue related to clinical use of these compounds as autophagy enhancers, but they also reveal interesting therapeutic implications for compounds that transiently increase upstream autophagic flow while compromising downstream lysosomal function.

The lysosome is emerging as a driving force in the progression of numerous human cancers, in which enhanced function of the autophagy–lysosome system enables efficient nutrient scavenging and growth in nutrient-poor microenvironments, promote the metastatic potential and treatment resistance (11). But lysosomal activation in aggressive cancers can lead to alterations in lysosomal structure and function, which, paradoxically, renders cancer cells more sensitive to lysosomal destabilization (5, 74). This frailty can be targeted by lysosomotropic compound that may have an antitumor effect preferentially killing the more sensitive cancer cells by inducing dysregulation of lysosomal lipid metabolism and LMP with release into the cytosol of cathepsins, potent inducers of cell death (17, 75, 76). In our study, we observed increased LysoTracker staining, suggestive of lysosomal swelling that is considered a typical condition preceding LMP (17, 77–79) and galectin-1 complexes, a surrogate marker of lysosomal membrane damage (58), suggesting a possible role of lysosomes in cancer cell death. This was confirmed for ebastine, penfluridol, pimozone, and fluoxetine, whose cytotoxic activity was partially rescued by inhibitor of cathepsins B and L but not by treatment with both apoptosis or autophagy inhibitors.

Inhibition of apoptosis and autophagy were also ineffective in reducing cell death induced by nefazodone and fluspirilene and further experiments are required to clarify the mechanisms of cell death induced by these drugs.

Notably, while inhibition of autophagy significantly rescued pimozone and spiperone cytotoxicity, it further increased cell death induced by penfluridol, the compound that demonstrated the highest cytotoxicity in all cell lines tested. The strong antitumoral activity of penfluridol may be due to its ability to induce both ADCD and LMP. Most of the known compounds that affect autophagy in neoplastic cells are either inducers or inhibitors of this process (80, 81). However, molecules that can modulate autophagy in a dual mode, by both inducing and inhibiting the process, seem to represent a novel and effective strategy for anticancer therapy (82, 83).

Finally, all psychotropic compounds with cationic amphiphilic properties caused a significant reduction in $\Delta\psi_m$. Since oncogenic activation leads to increased mitochondrial metabolism and higher $\Delta\psi_m$ compared to that of non-cancer cells (20) and experimental evidence demonstrates that irreversible mitochondrial membrane depolarization can induce cell death also in apoptotic resistant cells (84), CADs appear excellent candidates for mitochondrial targeting in cancer, as they can easily diffuse in tumor tissues and interact with negatively charged mitochondrial membranes

(20, 45, 49). Since in our cell line model cytotoxicity of psychotropic drugs was not mediated by ROS and thiols oxidation whereas apoptosis has been demonstrated only in cells treated with spiperone, studies are underway to explore the molecular mechanisms underlying CADs induced mitochondrial membrane depolarization and its role in inducing cancer cell death.

In addition to acute cytotoxicity, observed, *in vitro*, at lower micromolar concentrations, *in vivo* psychotropic drugs with cationic amphiphilic properties can also impair cancer cell metabolism and sensitize tumors to chemotherapy at plasma concentrations achieved with standard therapeutic regimens (85, 86). Suggestive of their efficacy in human clinical setting, epidemiologic studies have reported a reduced incidence of glioma and CRC among users of tricyclic antidepressants (27), a lower CRC risk under therapy with fluoxetine (26, 87) and an association between post-diagnostic use of cationic amphiphilic antihistamines and reduced cancer mortality as compared with similar use of antihistamines that do not classify as CADs (88).

In conclusion, the data presented above identify a subset of psychotropic drugs as putative anticancer agents and open a feasible, safe, and economically sound possibility to test the clinical anticancer efficacy of this therapeutic class of compounds. In particular, the cytotoxicity of psychotropic drugs with cationic amphiphilic structures relied on simultaneous mitochondrial and lysosomal disruption and induction of cell death that not necessarily requires apoptosis. Since dual targeting of lysosomes and mitochondria constitutes a new promising therapeutic approach for cancer, particularly those in which the apoptotic machinery is defective, these data further support their clinical development.

REFERENCES

1. Ferlay J, Colombet M, Soerjomataram I, Mathers C, Parkin DM, Pineros M, et al. Estimating the global cancer incidence and mortality in 2018: GLOBOCAN sources and methods. *Int J Cancer*. (2019) 144:1941–53. doi: 10.1002/ijc.31937
2. Bray F, Ferlay J, Soerjomataram I, Siegel RL, Torre LA, Jemal A. Global cancer statistics 2018: GLOBOCAN estimates of incidence and mortality worldwide for 36 cancers in 185 countries. *CA Cancer J Clin*. (2018) 68:394–424. doi: 10.3322/caac.21492
3. Robey RW, Pluchino KM, Hall MD, Fojo AT, Bates SE, Gottesman MM. Revisiting the role of ABC transporters in multidrug-resistant cancer. *Nat Rev Cancer*. (2018) 18:452–64. doi: 10.1038/s41568-018-0005-8
4. Dale W, Chow S, Sajid S. Socioeconomic considerations and shared-care models of cancer care for older adults. *Clin Geriatr Med*. (2016) 32:35–44. doi: 10.1016/j.cger.2015.08.007
5. Piao S, Amaravadi RK. Targeting the lysosome in cancer. *Ann N Y Acad Sci*. (2016) 1371:45–54. doi: 10.1111/nyas.12953
6. Mulcahy Levy JM, Thorburn A. Autophagy in cancer: moving from understanding mechanism to improving therapy responses in patients. *Cell Death Differ*. (2020) 27:843–57. doi: 10.1038/s41418-019-0474-7
7. Chang A. Chemotherapy, chemoresistance and the changing treatment landscape for NSCLC. *Lung Cancer*. (2011) 71:3–10. doi: 10.1016/j.lungcan.2010.08.022

DATA AVAILABILITY STATEMENT

The raw data supporting the conclusions of this article will be made available by the authors, without undue reservation.

AUTHOR CONTRIBUTIONS

MV and AA equally contributed in study design, conducting experiments, acquiring data, analyzing data, and writing the manuscript. VB contributed in data analysis and revising the manuscript. KR, VY, and AV contributed in conducting experiments. AM and GB contributed in data interpretation and manuscript editing. DC contributed in study design, data interpretation, manuscript writing, and the final approval of the manuscript. All authors critically reviewed and agreed on the final version of the manuscript.

FUNDING

This study was (partially) funded by the Università del Piemonte Orientale–FAR 2016 e FAR 2017 (DC), by the Italian Ministry of Education, University and Research (MIUR) program Departments of Excellence 2018–2022, AGING Project—Department of Translational Medicine, Università del Piemonte Orientale (DC), by Consorzio Interuniversitario di Biotecnologie (CIB) call Network-CIB: Catalisi dell’Innovazione nelle Biotecnologie (PRIN 201799WCRH, GB).

SUPPLEMENTARY MATERIAL

The Supplementary Material for this article can be found online at: <https://www.frontiersin.org/articles/10.3389/fonc.2020.562196/full#supplementary-material>

8. Domagala A, Fidyk K, Bobrowicz M, Stachura J, Szczygiel K, Firczuk M. Typical and atypical inducers of lysosomal cell death: a promising anticancer strategy. *Int J Mol Sci*. (2018) 19:2256. doi: 10.3390/ijms19082256
9. Mosesson Y, Mills GB, Yarden Y. Derailed endocytosis: an emerging feature of cancer. *Nat Rev Cancer*. (2008) 8:835–50. doi: 10.1038/nrc2521
10. Galluzzi L, Pietrocola F, Bravo-San Pedro JM, Amaravadi RK, Baehrecke EH, Cecconi F, et al. Autophagy in malignant transformation and cancer progression. *EMBO J*. (2015) 34:856–80. doi: 10.15252/embj.201490784
11. Davidson SM, Vander Heiden MG. Critical functions of the lysosome in cancer biology. *Annu Rev Pharmacol Toxicol*. (2017) 57:481–507. doi: 10.1146/annurev-pharmtox-010715-103101
12. Lawrence RE, Zoncu R. The lysosome as a cellular centre for signalling, metabolism and quality control. *Nat Cell Biol*. (2019) 21:133–42. doi: 10.1038/s41556-018-0244-7
13. Russell RC, Yuan HX, Guan KL. Autophagy regulation by nutrient signaling. *Cell Res*. (2014) 24:42–57. doi: 10.1038/cr.2013.166
14. Liu Y, Levine B. Autosis and autophagic cell death: the dark side of autophagy. *Cell Death Differ*. (2015) 22:367–76. doi: 10.1038/cdd.2014.143
15. Denton D, Kumar S. Autophagy-dependent cell death. *Cell Death Differ*. (2019) 26:605–16. doi: 10.1038/s41418-018-0252-y
16. Ho CJ, Gorski SM. Molecular mechanisms underlying autophagy-mediated treatment resistance in cancer. *Cancers*. (2019) 11:1775. doi: 10.3390/cancers11111775
17. Wang F, Gomez-Sintes R, Boya P. Lysosomal membrane permeabilization and cell death. *Traffic*. (2018) 19:918–31. doi: 10.1111/tra.12613

18. Serrano-Puebla A, Boya P. Lysosomal membrane permeabilization as a cell death mechanism in cancer cells. *Biochem Soc Trans.* (2018) 46:207–15. doi: 10.1042/BST20170130
19. Repnik U, Borg Distefano M, Speth MT, Ng MYW, Progida C, Hoflack B, et al. L-leucyl-L-leucine methyl ester does not release cysteine cathepsins to the cytosol but inactivates them in transiently permeabilized lysosomes. *J Cell Sci.* (2017) 130:3124–40. doi: 10.1242/jcs.204529
20. Weinberg SE, Chandel NS. Targeting mitochondria metabolism for cancer therapy. *Nat Chem Biol.* (2015) 11:9–15. doi: 10.1038/nchembio.1712
21. Zong WX, Rabinowitz JD, White E. Mitochondria and cancer. *Mol Cell.* (2016) 61:667–76. doi: 10.1016/j.molcel.2016.02.011
22. Ashburn TT, Thor KB. Drug repositioning: identifying and developing new uses for existing drugs. *Nat Rev Drug Discov.* (2004) 3:673–83. doi: 10.1038/nrd1468
23. Sleire L, Forde HE, Netland IA, Leiss L, Skeie BS, Enger PO. Drug repurposing in cancer. *Pharmacol Res.* (2017) 124:74–91. doi: 10.1016/j.phrs.2017.07.013
24. Chou FH, Tsai KY, Su CY, Lee CC. The incidence and relative risk factors for developing cancer among patients with schizophrenia: a nine-year follow-up study. *Schizophr Res.* (2011) 129:97–103. doi: 10.1016/j.schres.2011.02.018
25. Li H, Li J, Yu X, Zheng H, Sun X, Lu Y, et al. The incidence rate of cancer in patients with schizophrenia: a meta-analysis of cohort studies. *Schizophr Res.* (2018) 195:519–28. doi: 10.1016/j.schres.2017.08.065
26. Coogan PF, Strom BL, Rosenberg L. Antidepressant use and colorectal cancer risk. *Pharmacoepidemiol Drug Saf.* (2009) 18:1111–4. doi: 10.1002/pds.1808
27. Walker AJ, Grainge M, Bates TE, Card TR. Survival of glioma and colorectal cancer patients using tricyclic antidepressants post-diagnosis. *Cancer Causes Control.* (2012) 23:1959–64. doi: 10.1007/s10552-012-0073-0
28. Chan HL, Chiu WC, Chen VC, Huang KY, Wang TN, Lee Y, et al. SSRIs associated with decreased risk of hepatocellular carcinoma: a population-based case-control study. *Psychooncology.* (2018) 27:187–92. doi: 10.1002/pon.4493
29. Faustino-Rocha AI, Ferreira R, Gama A, Oliveira PA, Ginja M. Antihistamines as promising drugs in cancer therapy. *Life Sci.* (2017) 172:27–41. doi: 10.1016/j.lfs.2016.12.008
30. Huang J, Zhao D, Liu Z, Liu F. Repurposing psychiatric drugs as anti-cancer agents. *Cancer Lett.* (2018) 419:257–65. doi: 10.1016/j.canlet.2018.01.058
31. Shaw V, Srivastava S, Srivastava SK. Repurposing antipsychotics of the diphenylbutylpiperidine class for cancer therapy. *Semin Cancer Biol.* (2019). doi: 10.1016/j.semcancer.2019.10.007. [Epub ahead of print].
32. Zhuo C, Xun Z, Hou W, Ji F, Lin X, Tian H, et al. Surprising anticancer activities of psychiatric medications: old drugs offer new hope for patients with brain cancer. *Front Pharmacol.* (2019) 10:1262. doi: 10.3389/fphar.2019.01262
33. Garcia-Quiroz J, Camacho J. Astemizole: an old anti-histamine as a new promising anti-cancer drug. *Anticancer Agents Med Chem.* (2011) 11:307–14. doi: 10.2174/187152011795347513
34. Frick LR, Rapanelli M. Antidepressants: influence on cancer and immunity? *Life Sci.* (2013) 92:525–32. doi: 10.1016/j.lfs.2013.01.020
35. Velati S, Massarotti A, Antona A, Talmon M, Fresu LG, Galetto AS, et al. Structure activity relationship studies on Amb639752: toward the identification of a common pharmacophoric structure for DGKalpha inhibitors. *J Enzyme Inhib Med Chem.* (2020) 35:96–108. doi: 10.1080/14756366.2019.1684911
36. Muehlbacher M, Tripal P, Roas F, Kornhuber J. Identification of drugs inducing phospholipidosis by novel *in vitro* data. *ChemMedChem.* (2012) 7:1925–34. doi: 10.1002/cmdc.201200306
37. Ostad Haji E, Hiemke C, Pfuhlmann B. Therapeutic drug monitoring for antidepressant drug treatment. *Curr Pharm Des.* (2012) 18:5818–27. doi: 10.2174/138161212803523699
38. Church MK, Church DS. Pharmacology of antihistamines. *Indian J Dermatol.* (2013) 58:219–24. doi: 10.4103/0019-5154.110832
39. Medina VA, Rivera ES. Histamine receptors and cancer pharmacology. *Br J Pharmacol.* (2010) 161:755–67. doi: 10.1111/j.1476-5381.2010.00961.x
40. Sarrouilhe D, Clarhaut J, Defamie N, Mesnil M. Serotonin and cancer: what is the link? *Curr Mol Med.* (2015) 15:62–77. doi: 10.2174/1566524015666150114113411
41. Sarrouilhe D, Mesnil M. Serotonin and human cancer: a critical view. *Biochimie.* (2019) 161:46–50. doi: 10.1016/j.biochi.2018.06.016
42. Reasor MJ, Hastings KL, Ulrich RG. Drug-induced phospholipidosis: issues and future directions. *Expert Opin Drug Saf.* (2006) 5:567–83. doi: 10.1517/14740338.5.4.567
43. Halliwell WH. Cationic amphiphilic drug-induced phospholipidosis. *Toxicol Pathol.* (1997) 25:53–60. doi: 10.1177/019262339702500111
44. Kornhuber J, Tripal P, Reichel M, Muhle C, Rhein C, Muehlbacher M, et al. Functional inhibitors of acid sphingomyelinase (FIASMs): a novel pharmacological group of drugs with broad clinical applications. *Cell Physiol Biochem.* (2010) 26:9–20. doi: 10.1159/000315101
45. Vater M, Mockl L, Gormanns V, Schultz Fademrecht C, Mallmann AM, Ziegart-Sadowska K, et al. New insights into the intracellular distribution pattern of cationic amphiphilic drugs. *Sci Rep.* (2017) 7:44277. doi: 10.1038/srep44277
46. Marceau F, Bawolak MT, Lodge R, Bouthillier J, Gagne-Henley A, Gaudreault RC, et al. Cation trapping by cellular acidic compartments: beyond the concept of lysosomotropic drugs. *Toxicol Appl Pharmacol.* (2012) 259:1–12. doi: 10.1016/j.taap.2011.12.004
47. Lu S, Sung T, Lin N, Abraham RT, Jessen BA. Lysosomal adaptation: how cells respond to lysosomotropic compounds. *PLoS ONE.* (2017) 12:e0173771. doi: 10.1371/journal.pone.0173771
48. Caccia S, Garattini S. Formation of active metabolites of psychotropic drugs. An updated review of their significance. *Clin Pharmacokinet.* (1990) 18:434–59. doi: 10.2165/00003088-199018060-00002
49. Modica-Napolitano JS, Aprille JR. Delocalized lipophilic cations selectively target the mitochondria of carcinoma cells. *Adv Drug Deliv Rev.* (2001) 49:63–70. doi: 10.1016/S0169-409X(01)00125-9
50. Sivandzade F, Bhalerao A, Cucullo L. Analysis of the mitochondrial membrane potential using the cationic JC-1 dye as a sensitive fluorescent probe. *Bio Protoc.* (2019) 9:e3128. doi: 10.21769/BioProtoc.3128
51. de Duve C, de Barsey T, Poole B, Trouet A, Tulkens P, Van Hoof F. Commentary. Lysosomotropic agents. *Biochem Pharmacol.* (1974) 23:2495–531. doi: 10.1016/0006-2952(74)90174-9
52. Rodriguez-Enriquez S, Kim I, Currin RT, Lemasters JJ. Tracker dyes to probe mitochondrial autophagy (mitophagy) in rat hepatocytes. *Autophagy.* (2006) 2:39–46. doi: 10.4161/auto.2229
53. Biever A, Valjent E, Puighermanal E. Ribosomal protein S6 phosphorylation in the nervous system: from regulation to function. *Front Mol Neurosci.* (2015) 8:75. doi: 10.3389/fnmol.2015.00075
54. Mizushima N, Yoshimori T, Levine B. Methods in mammalian autophagy research. *Cell.* (2010) 140:313–26. doi: 10.1016/j.cell.2010.01.028
55. Goldman SD, Funk RS, Rajewski RA, Krise JP. Mechanisms of amine accumulation in, and egress from, lysosomes. *Bioanalysis.* (2009) 1:1445–59. doi: 10.4155/bio.09.128
56. Kornhuber J, Tripal P, Reichel M, Terfloth L, Bleich S, Wiltfang J, et al. Identification of new functional inhibitors of acid sphingomyelinase using a structure-property-activity relation model. *J Med Chem.* (2008) 51:219–37. doi: 10.1021/jm070524a
57. Anderson N, Borlak J. Drug-induced phospholipidosis. *FEBS Lett.* (2006) 580:5533–40. doi: 10.1016/j.febslet.2006.08.061
58. Aits S, Krickler J, Liu B, Ellegaard AM, Hamalisto S, Tvingsholm S, et al. Sensitive detection of lysosomal membrane permeabilization by lysosomal galectin puncta assay. *Autophagy.* (2015) 11:1408–24. doi: 10.1080/15548627.2015.1063871
59. Wu YT, Tan HL, Shui G, Bauvy C, Huang Q, Wenk MR, et al. Dual role of 3-methyladenine in modulation of autophagy via different temporal patterns of inhibition on class I and III phosphoinositide 3-kinase. *J Biol Chem.* (2010) 285:10850–61. doi: 10.1074/jbc.M109.080796
60. Montaser M, Lalmanach G, Mach L. CA-074, but not its methyl ester CA-074Me, is a selective inhibitor of cathepsin B within living cells. *Biol Chem.* (2002) 383:1305–1308. doi: 10.1515/BC.2002.147
61. Qadir M, O'Loughlin KL, Fricke SM, Williamson NA, Greco WR, Minderman H. Cyclosporin A is a broad-spectrum multidrug resistance modulator. *Clin Cancer Res.* (2005) 11:2320–6. doi: 10.1158/1078-0432.CCR-04-1725
62. Hendouei N, Saghaei F, Shadfar F, Hosseinimehr SJ. Molecular mechanisms of anti-psychotic drugs for improvement of cancer treatment. *Eur J Pharmacol.* (2019) 856:172402. doi: 10.1016/j.ejphar.2019.05.031
63. Schulz M, Schmoldt A. Therapeutic and toxic blood concentrations of more than 800 drugs and other xenobiotics. *Pharmazie.* (2003) 58:447–74.

64. Hollemans M, Elferink RO, De Groot PG, Strijland A, Tager JM. Accumulation of weak bases in relation to intralysosomal pH in cultured human skin fibroblasts. *Biochim Biophys Acta*. (1981) 643:140–51. doi: 10.1016/0005-2736(81)90226-1
65. Nadanaciva S, Lu S, Gebhard DF, Jessen BA, Pennie WD, Will Y. A high content screening assay for identifying lysosomotropic compounds. *Toxicol In Vitro*. (2011) 25:715–23. doi: 10.1016/j.tiv.2010.12.010
66. Lu S, Jessen B, Strock C, Will Y. The contribution of physicochemical properties to multiple *in vitro* cytotoxicity endpoints. *Toxicol In Vitro*. (2012) 26:613–20. doi: 10.1016/j.tiv.2012.01.025
67. Logan R, Kong AC, Axcell E, Krise JP. Amine-containing molecules and the induction of an expanded lysosomal volume phenotype: a structure-activity relationship study. *J Pharm Sci*. (2014) 103:1572–80. doi: 10.1002/jps.23949
68. Zhitomirsky B, Yunaev A, Kreiserman R, Kaplan A, Stark M, Assaraf YG. Lysosomotropic drugs activate TFEB via lysosomal membrane fluidization and consequent inhibition of mTORC1 activity. *Cell Death Dis*. (2018) 9:1191. doi: 10.1038/s41419-018-1227-0
69. Gonzalez-Rothi RJ, Zander DS, Ros PR. Fluoxetine hydrochloride (Prozac)-induced pulmonary disease. *Chest*. (1995) 107:1763–5. doi: 10.1378/chest.107.6.1763
70. Shahane SA, Huang R, Gerhold D, Baxa U, Austin CP, Xia M. Detection of phospholipidosis induction: a cell-based assay in high-throughput and high-content format. *J Biomol Screen*. (2014) 19:66–76. doi: 10.1177/1087057113502851
71. Ranjan A, Srivastava SK. Penfluridol suppresses pancreatic tumor growth by autophagy-mediated apoptosis. *Sci Rep*. (2016) 6:26165. doi: 10.1038/srep26165
72. Vucicevic L, Misirkic-Marjanovic M, Harhaji-Trajkovic L, Maric N, Trajkovic V. Mechanisms and therapeutic significance of autophagy modulation by antipsychotic drugs. *Cell Stress*. (2018) 2:282–291. doi: 10.15698/cst2018.11.161
73. Gassen NC, Rein T. Is there a role of autophagy in depression and antidepressant action? *Front Psychiatry*. (2019) 10:337. doi: 10.3389/fpsy.2019.00337
74. Petersen NH, Olsen OD, Groth-Pedersen L, Ellegaard AM, Bilgin M, Redmer S, et al. Transformation-associated changes in sphingolipid metabolism sensitize cells to lysosomal cell death induced by inhibitors of acid sphingomyelinase. *Cancer Cell*. (2013) 24:379–93. doi: 10.1016/j.ccr.2013.08.003
75. Breiden B, Sandhoff K. Emerging mechanisms of drug-induced phospholipidosis. *Biol Chem*. (2019) 401:31–46. doi: 10.1515/hsz-2019-0270
76. Boya P, Kroemer G. Lysosomal membrane permeabilization in cell death. *Oncogene*. (2008) 27:6434–51. doi: 10.1038/onc.2008.310
77. Ono K, Kim SO, Han J. Susceptibility of lysosomes to rupture is a determinant for plasma membrane disruption in tumor necrosis factor alpha-induced cell death. *Mol Cell Biol*. (2003) 23:665–76. doi: 10.1128/MCB.23.2.665-676.2003
78. Wang F, Salvati A, Boya P. Lysosome-dependent cell death and deregulated autophagy induced by amine-modified polystyrene nanoparticles. *Open Biol*. (2018) 8:170271. doi: 10.1098/rsob.170271
79. Repnik U, Hafner Cesen M, Turk B. Lysosomal membrane permeabilization in cell death: concepts and challenges. *Mitochondrion*. (2014) 19(Pt A):49–57. doi: 10.1016/j.mito.2014.06.006
80. Santi M, Baldelli G, Diotallevi A, Galluzzi L, Schiavano GF, Brandi G. Metformin prevents cell tumorigenesis through autophagy-related cell death. *Sci Rep*. (2019) 9:66. doi: 10.1038/s41598-018-37247-6
81. Chude CI, Amaravadi RK. Targeting autophagy in cancer: update on clinical trials and novel inhibitors. *Int J Mol Sci*. (2017) 18:1279. doi: 10.3390/ijms18061279
82. Kucharewicz K, Dudkowska M, Zawadzka A, Ogrodnik M, Szczepankiewicz AA, Czarnocki Z, et al. Simultaneous induction and blockade of autophagy by a single agent. *Cell Death Dis*. (2018) 9:353. doi: 10.1038/s41419-018-0383-6
83. Cirone M, Gilardini Montani MS, Granato M, Garufi A, Faggioni A, D'Orazi G. Autophagy manipulation as a strategy for efficient anticancer therapies: possible consequences. *J Exp Clin Cancer Res*. (2019) 38:262. doi: 10.1186/s13046-019-1275-z
84. Kroemer G, Galluzzi L, Brenner C. Mitochondrial membrane permeabilization in cell death. *Physiol Rev*. (2007) 87:99–163. doi: 10.1152/physrev.00013.2006
85. del Cuvillo A, Mullol J, Bartra J, Davila I, Jauregui I, Montoro J, et al. Comparative pharmacology of the H1 antihistamines. *J Investig Allergol Clin Immunol*. (2006) 16(Suppl. 1):3–12.
86. Mauri MC, Paletta S, Maffini M, Colasanti A, Dragogna F, Di Pace C, et al. Clinical pharmacology of atypical antipsychotics: an update. *EXCLI J*. (2014) 13:1163–91.
87. Chubak J, Boudreau DM, Rulyak SJ, Mandelson MT. Colorectal cancer risk in relation to antidepressant medication use. *Int J Cancer*. (2011) 128:227–32. doi: 10.1002/ijc.25322
88. Ellegaard AM, Dehlendorff C, Vind AC, Anand A, Cederkvist L, Petersen NHT, et al. Repurposing cationic amphiphilic antihistamines for cancer treatment. *EBioMedicine*. (2016) 9:130–9. doi: 10.1016/j.ebiom.2016.06.013

Conflict of Interest: The authors declare that the research was conducted in the absence of any commercial or financial relationships that could be construed as a potential conflict of interest.

Copyright © 2020 Valalda, Antona, Bettio, Roy, Vachamaram, Yellenki, Massarotti, Baldanzi and Capello. This is an open-access article distributed under the terms of the Creative Commons Attribution License (CC BY). The use, distribution or reproduction in other forums is permitted, provided the original author(s) and the copyright owner(s) are credited and that the original publication in this journal is cited, in accordance with accepted academic practice. No use, distribution or reproduction is permitted which does not comply with these terms.



Magnesium in Combinatorial With Valproic Acid Suppressed the Proliferation and Migration of Human Bladder Cancer Cells

Tianye Li¹, Yang Yu¹, Hang Shi¹, Yuhua Cao¹, Xiangfu Liu¹, Zhenzhen Hao¹, Yuping Ren², Gaowu Qin², Yongye Huang^{1*} and Bing Wang^{1*}

¹ College of Life and Health Sciences, Northeastern University, Shenyang, China, ² Key Laboratory for Anisotropy and Texture of Materials (Ministry of Education), School of Materials Science and Engineering, Northeastern University, Shenyang, China

OPEN ACCESS

Edited by:

Benyi Li,
University of Kansas Medical Center,
United States

Reviewed by:

Changlin Li,
Jining Medical University, China
Wang Liu,
University of Kansas Medical Center,
United States

*Correspondence:

Yongye Huang
huangyongye88@163.com
Bing Wang
wangbing@mail.neu.edu.cn

Specialty section:

This article was submitted to
Pharmacology of Anti-Cancer Drugs,
a section of the journal
Frontiers in Oncology

Received: 30 July 2020

Accepted: 05 November 2020

Published: 11 December 2020

Citation:

Li T, Yu Y, Shi H, Cao Y, Liu X, Hao Z,
Ren Y, Qin G, Huang Y and Wang B
(2020) Magnesium in Combinatorial
With Valproic Acid Suppressed the
Proliferation and Migration of Human
Bladder Cancer Cells.
Front. Oncol. 10:589112.
doi: 10.3389/fonc.2020.589112

Magnesium, the second most predominant intracellular cation, plays a crucial role in many physiological functions; magnesium-based biomaterials have been widely used in clinical application. In a variety of cancer types, the high intracellular concentration of magnesium contributes to cancer initiation and progression. Therefore, we initiated this study to investigate the likelihood of confounding magnesium with cancer therapy. In this study, the anti-tumor activity of magnesium and underlying mechanisms were assessed in bladder cancer both *in vitro* and *in vivo*. The results indicated that the proliferation of bladder cancer cells was inhibited by treatment with a high concentration of MgCl₂ or MgSO₄. The apoptosis, G0/G1 cell cycle arrest, autophagy, and ER stress were promoted following treatment with MgCl₂. However, the migratory ability of MgCl₂ treated cells was similar to that of control cells, as revealed by the trans-well assay. Besides, no significant difference was observed in the proportion of CD44 or CD133 positive cells between the control and MgCl₂ treated cells. Thus, to improve the therapeutic effect of magnesium, VPA was used to treat cancer cells in combination with MgCl₂. As expected, combination treatment with MgCl₂ and VPA could markedly reduce proliferation, migration, and *in vivo* tumorigenicity of UC3 cells. Moreover, the Wnt signaling was down-regulated, and ERK signaling was activated in the cells treated with combination treatment. In conclusion, the accurate utilization of MgCl₂ in targeting autophagy might be beneficial in cancer therapy. Although further studies are warranted, the combination treatment of MgCl₂ with VPA is an effective strategy to improve the outcome of chemotherapy.

Keywords: magnesium, apoptosis, autophagy, valproic acid, combinatorial treatment

INTRODUCTION

Bladder cancer ranks the second most frequent urological malignancy worldwide, with an estimated 549,393 newly diagnosed and approximately 199,922 deaths each year (1). Owing to high recurrence rates, periodic cystoscopic tumor surveillance strategies, and high treatment expenses, the lifetime

management of bladder cancer remains very expensive (2). Chemotherapy continues to be the standard of care in patients with unresectable and metastatic bladder cancer (3, 4). Notably, cisplatin-based chemotherapy, a standard first-line treatment of choice based on studies demonstrating improved survival outcomes, has been the mainstay for bladder cancer for decades (5, 6). However, patients who receive traditional chemotherapeutic regimens might suffer from the significant risk of off-target toxicity and the development of resistance to drugs. To overcome these limitations, in recent years, many alternative strategies, including nanotechnology, have been developed to improve the therapeutic outcome of chemotherapy (7). Nanotherapy with the favorable characteristics of improved circulation and reduced toxicity has been implicated as one of the most promising strategies in clinical settings. Of note, the application of a yolk-shell $\text{Fe}_3\text{O}_4@\text{MgSiO}_3$ nanoplateform with the polymerpoly (ethylene glycol) and folic acid modifications has been shown to effectively circumvent multidrug resistance in cancer cells (8). In bladder cancer, a combination of Mg^{2+} -Catechin nanocomposite particles and siRNA has been suggested to be a promising therapeutic modality of combining chemotherapy with gene therapy to acquire higher therapeutic efficacy (9). Recently, nanocomposite particles have received significant attention as useful drug carriers for cancer therapy. However, whether the component of the nanocomposite particle itself plays a role in cancer therapy remains elusive. Magnesium ions (Mg^{2+}), one of the most common components used in the fabrication of nanocomposites. Therefore, in this study, we made an attempt to determine the anti-tumor effect of magnesium in bladder cancer.

Magnesium (Mg^{2+}) is an essential mineral micronutrient that functions as a cofactor for the activation of a variety of transporters and enzymes, and required for the physiologic functions of various organs. Green vegetables, including beans, broccoli, have a high content of magnesium; besides, almonds, bananas, cashews, egg yolk, flaxseed, including other nuts, oatmeal, pumpkin seeds, sesame seeds, soybeans, and whole grains are rich in magnesium (10). Intracellular Mg^{2+} may also act as a secondary messenger and regulate the activities of a vast array of enzymes and participate in the metabolism of various nutrients (11, 12). In humans, the total serum magnesium ranges 0.70 to 1.10 mmol/L (13). Magnesium represents the second most abundant intracellular cation and the fourth most common cation in the human body. Furthermore, magnesium is predominantly involved in many physiologic pathways, energy production, and it also exhibits structural functions. Moreover, magnesium and its alloys have been identified as promising implant materials; besides, the treatment with magnesium implants benefited almost all patients, including patients with cancer (14). In 1904, Payr suggested the use of magnesium for the treatment of cavernous haemangioma and large-vessel aneurysms therapy (14). Subsequent studies also indicated that magnesium alloys exhibit an inhibitory effect on tumor growth (15–17). Accumulative pieces of evidence have indicated the complex relationship between magnesium and cancer. Both

epidemiological and clinical studies suggested that magnesium deficiency is associated with an increased risk of tumorigenesis (18, 19). In breast cancer, the cancer cells promote the expression of magnesium transport channels to enhance the intracellular concentration of the mineral, thereby meeting the increasing energy demand of cancer cells (20). Furthermore, reduced serum levels of Mg^{2+} is frequently associated in patients with solid tumors and is frequently correlated with the advanced malignancy. Moreover, several cycles of chemotherapy may also lead to reduced serum levels of Mg^{2+} in patients with cancer. In addition, in magnesium-deficient mice, tumor growth was inhibited at its primary site; however, it was increased in metastatic colonization (10). All these pieces of evidence indicated that the role of magnesium in tumorigenesis remains elusive and complex. Thus, it becomes imperative better to understand the vital function of magnesium in tumor development. Therefore, the present study investigated the anti-tumor activity of magnesium and assessed the underlying mechanisms in bladder cancer both *in vitro* and *in vivo*.

It appears that magnesium plays a protective role at the early stage of carcinogenesis, but contributes to the proliferation of existing tumors at the later stages (19). Combination therapy has been considered as the standard first-line treatment to improve the clinical outcome in several malignancies. Combination therapy with anticancer drugs has been shown to be effective in inducing the synergistic drug actions, prolonging the onset of chemoresistance, and enhancing the immunogenicity of cancer cells (21, 22). Histone deacetylase (HDAC) inhibitors represent a group of potent epigenetic modulators that are known to exhibit significant potential effects in cancer treatment. Valproic acid (VPA), an HDAC inhibitor, has emerged as a potent drug for cancer therapy in recent years and has shown promising antitumor effects in a variety of *in vitro* and *in vivo* systems. In early clinical trials, VPA alone or in combination with other agents has revealed encouraging results (23). Furthermore, many *in vitro* and *in vivo* studies suggest that VPA exhibits the characteristic of high effectiveness and relatively low toxicity profile. Considering these benefits of VPA, the present study also examined the synergistic effect of the combination of VPA and magnesium in cancer therapy.

Considering these evidences, we initiated this study to investigate the possibility of confounding magnesium with cancer therapy. In this study, the anti-tumor activity of magnesium and/or in combination with VPA and underlying mechanisms were assessed in bladder cancer both *in vitro* and *in vivo*.

MATERIALS AND METHODS

Cell Cultures and Chemicals

Human bladder cancer cell lines (UM-UC3 and UM-UC5), immortalized normal gastric cell line (Ges1), gastric cancer cell line (MKN1), and HEK-293 cells were cultured in Dulbecco's modified Eagle's medium (DMEM) supplemented with 10% fetal bovine serum (FBS), 1% nonessential amino acid, 1% Glutamine,

100 U/ml streptomycin, and 100 U/ml penicillin in a humidified atmosphere of 5% CO₂ at 37°C. Unless otherwise specified, all the chemicals were purchased from Sigma-Aldrich (St. Louis, MO, USA). For ERK inhibition, cells were pre-treated with U0126 (Selleck Chemicals, Houston, TX, USA) for 2 h followed by treatment with MgCl₂ for 24 h. For IRE1α inhibition, cells were treated with STF083010 (Selleck Chemicals, Houston, TX, USA) for 24 h.

Cell Viability Assay

In brief, cancer cells were seeded into 6-well plates at a density of 1.2×10^5 cells/well and then treated with different concentrations of magnesium for 24 h. Subsequently, cells were rinsed with PBS and digested with trypsin containing EDTA. Cell suspensions were centrifuged by at 100 g for 5 min and then resuspended in 1 ml PBS. Cell number in 100 μl PBS was counted using a BD Accuri C6 flow cytometer (BD Biosciences, San Diego, CA, USA). Finally, the IC₅₀ was calculated as the concentration of MgCl₂ that inhibited cell growth by 50%.

Viability of cells with MgCl₂ or VPA alone and in combination was assessed with Cell Counting Kit-8 (CCK8; Bimake, Houston, TX, USA) assay. Briefly, cells were seeded into 96-well plates at a density of 2,000 cells/well and incubated in a humidified incubator of 5% CO₂ at 37 °C. Then, a 200 μl culture medium containing MgCl₂ and/or VPA was added to each well of the treatment group for 24 h. Following different treatments, 10 μl CCK-8 solution was added to each well, and cells were incubated for 2 h at 37°C. The cell viability was revealed by the absorbance (OD), which was measured at 450 nm using a microplate reader.

Flow Cytometric Analyses

For cell cycle distribution analysis, cells were seeded at a density of 3×10^5 cells/well in a 6 cm dish and cultured for 12 h to adhere to cells. Then, the cells were treated with MgCl₂ and/or VPA for 24 h. They were then harvested by centrifugation at 100 g for 5 min, washed twice with PBS, fixed with ice-cold 70% ethanol (in PBS) at -20°C overnight. The fixed cells were stained in propidium iodide (1 mg/ml) and ribonuclease-A (10 g/ml) (PI/RNase; BD Biosciences) for 30 min at room temperature in the dark. Cell cycle distribution was assessed by flow cytometry (BD LSRFortessa, BD Biosciences). Data were analyzed by ModFit software, and the distribution of cells in different phases of the cell cycle was determined as a ratio of the fluorescent area of the appropriate peaks to the total fluorescent area.

Apoptosis was determined using Annexin V/PI assay. Cells were seeded in a 6 cm dish (3×10^5 cells/well). After 12 h, the cells were treated with MgCl₂ and/or VPA for 24 h. Cells were digested with trypsin and harvested by centrifugation at 100 g for 5 min. The cells were resuspended with 100 μl of 1× binding buffer containing 5 μl of Annexin V-FITC/PI for 15 min in the dark at room temperature. The fluorescence of the cells was quantified by flow cytometry (BD Biosciences, Franklin Lakes, NJ, USA) using a FITC signal detector and a PI signal detector.

For the detection of cancer stem cells, the expression profiles of CD133 and CD44 in cultured cells were analyzed by flow cytometry. Briefly, cancer cells were treated with or without

MgCl₂ for 24 h and cells were then digested by trypsin. Following incubation, the suspension was centrifuged, and cells were suspended in PBS. The cell suspension was incubated with FITC-conjugated anti-CD44 or PE-conjugated anti-CD133 at 4°C for 30 min in the dark. Labeled cells were resuspended in PBS and analyzed by flow cytometer (BD Biotechnology).

RNA Extraction and Quantitative Real-Time Polymerase Chain Reaction (qRT-PCR)

The total RNA from cancer cells was extracted with TRIzol reagent (Tiangen Biotech, Beijing, China) according to the manufacture's protocol. One μg of total RNA was reverse transcribed into complementary DNA (cDNA) using All-in-One cDNA synthesis SuperMix (Bimake, Houston, TX, USA) kit according to the manufacturer's instructions. Quantitative real-time PCR (qRT-PCR) was performed with 2× SYBR Green qPCR Master Mix (Bimake, Houston, TX, USA) following the manufacturer's protocol on a CFX96 real-time PCR detection system. The amplification program was as follows: initial denaturation at 95°C for 15 min, followed by 45 cycles of denaturation at 95°C for 10 s, annealing at 60°C for 30 s and extension at 72°C for 20 s; final extension at 72°C for 10 min. Primer sequences were listed in **Table S1**. Glyceraldehyde phosphatedehydrogenase (GAPDH) or β-actin was used as an internal control for the normalization of gene expression data. The relative expression was calculated using the $2^{-\Delta\Delta Ct}$ method.

Western Blotting

Cells treated with MgCl₂ and/or VPA were collected and lysed with RIPA lysis buffer supplemented with protease inhibitor cocktail. Cell suspensions were then centrifuged to collect clear lysates in the supernatant and stored at -20°C. The protein contents were quantitated using the bicinchoninic acid (BCA) protein assay kit (Beyotime, Shanghai, China). Equal amounts (20 μg) of cell extracts were resolved by SDS-PAGE, and transferred to a PVDF membrane, blocked with a 5% non-fat milk solution for 1 h at room temperature, and incubated with primary monoclonal antibodies (as listed in **Table S2**) overnight at 4°C. The membranes were then incubated with the appropriate HRP-conjugated secondary antibodies at room temperature for 1 h; the immunoblots were visualized with an enhanced chemiluminescence detection system (Millipore, Boston, USA).

Wound Healing and Migration Assay

The migration of the cells was assessed using a wound-healing assay. Briefly, cells with or without MgCl₂ treatment were cultured in 6-well plates and cultured to form a tight monolayer. The monolayers were scratched with a 200 μl sterile pipette tip and washed with PBS. Subsequently, the cells were then cultured in serum-free media. After 0, 24, and 48 h, cellular migration toward the scratched area was photographed using an inverted microscope.

For the migration assay, a 24-well Transwell (8-μm pore size) was used. Briefly, 2×10^4 cells suspended in 200 μl serum-free DMEM were seeded to the upper chamber of each well, 600 μl of

FBS-containing medium was added to the bottom chamber. After incubation for 24 h, cells that migrated to the lower membrane of the chamber were fixed with methanol for 30 min at room temperature and stained with 0.2% crystal violet for 20 min. Cells were then counted in five randomly selected fields (at $\times 200$ magnification) under an inverted microscope, and the average cell number per view was calculated. All experiments were performed in triplicate.

Colony Formation Assay

Following treatment with MgCl_2 , cells following treatment with MgCl_2 were seeded into six-well plates at 1,000 cells/well and cultured for 20 days in a humidified atmosphere of 5% CO_2 at 37°C to allow for colony growth. At the assay endpoint, the cells were washed gently with PBS and then fixed with paraformaldehyde for 30 min and stained with 0.1% crystal violet solution for 15 min. Stained colonies with a diameter larger than 50 μm were counted and photographed under microscope.

Subcutaneous Tumorigenesis in Nude Mice

The animals were cared for in accordance with the Guide for the care and use of laboratory animals in China. All experimental procedures were approved by the Animal Care and Use Committee of the Northeastern University Committee, China.

Four-week-old male BALB/c nude mice were procured from Charles River (Beijing, China). The mice were grouped-housed under specific pathogen-free conditions, at a temperature of 24°C with a relative humidity of 50–60%, under a 12-h-light/12-h-dark schedule. Animals were provided ad libitum access to standard food and drinking water. All the mice were healthy and had no infection during the experimental period. All surgical procedures were performed under aseptic conditions. UC3 cells (2×10^7 cells/ml) were injected into the right super lateral subcutaneous tissue of the nude mice. Tumor growth was measured with calipers every 4 days, and tumor volume was calculated according to the following equation: tumor volume (mm^3) = $0.5 \times$ the longest diameter \times the shortest diameter². When the mean tumor volume reached approximately 100 mm^3 , mice were randomized into the vehicle control group (received 100 μl physiological saline solution/2 days), MgCl_2 treated group (50 mg/kg/2 days), VPA treated group (100 mg/kg/2 days), and combination treatment group (50 mg MgCl_2 /kg/2 days + 100 mg VPA/kg/2 days). The drug was administered by intraperitoneal injection. At the termination of the experiment, the mice were euthanized by cervical dislocation, and tumors were harvested and weighed.

Statistical Analysis

Data were expressed as means \pm Standard Error of the Mean (SEM). The differences between the two groups were assessed using the unpaired Student's *t*-test. Analysis of variance (ANOVA) was performed for multiple comparisons. Statistical analyses were performed using the SPSS 16.0 software (SPSS Inc., Chicago, IL, USA). A *p*-value of <0.05 was considered to be

statistically significant. Each experiment was conducted in triplicate and repeated three times.

RESULTS

Magnesium Inhibited the Growth of Bladder Cancer Cells UC3 and UC5

To determine the effects of magnesium on the bladder cancer cell viability *in vitro*, we analyzed the impact of different concentrations of magnesium on the bladder cancer cell lines. It has been reported that a human normal serum reference range for magnesium level is 0.70 to 1.10 mmol/L (13). Thus, we used 0.70 mmol/L magnesium as the lower concentration, defined as $1\times$. As illustrated in **Figure 1A**, the survival rate of UC3 cells was markedly decreased by MgCl_2 in a dose-dependent manner. The IC_{50} of MgCl_2 in UC3 cells was approximately 42.5 mM. The inhibitory effect on the viability of UC5 was also assessed. Results showed that the IC_{50} of MgCl_2 in UC5 cells was about 28.3 mM (**Figure 1B**), indicating that UC5 cells were more sensitive to treatment with MgCl_2 . To further investigate the functions of magnesium in bladder cancer cells, the survival rate of UC3 cells with MgSO_4 exposure was evaluated. The IC_{50} of MgSO_4 in UC3 cells was about 56.6 mM (**Figure 1C**), possibly suggesting that magnesium played an essential role in tumor growth. To better illustrate the cytotoxicity of magnesium, a nontumorigenic HEK-293 (kidney) cell line was applied. The IC_{50} of MgCl_2 in HEK-293 cells was about 60.22 mM which was higher than that in UC3 and UC5 cells (**Figure S1**). Based on these results, the subsequent experiments were performed using 42.5 mM MgCl_2 in UC3 cells.

Effect of MgCl_2 on Canonical Cell Death Modes

Inhibition of cell proliferation is often associated with cell cycle arrest during chemotherapy. Many genes related to cyclin were investigated. To further characterize the impact of MgCl_2 treatment, detailed analyses of cell-cycle distribution were performed. As anticipated, both qRT-PCR and Western blot assay results revealed that p21 expression was markedly increased following treatment with MgCl_2 (**Figures 1D–F and S2A**). Surprisingly, there was no significant differences in the expression of p16, CDK1, and cyclin B1 between the control and MgCl_2 treated cells, indicating that the cell cycle distribution remains mostly unaffected by treatment with MgCl_2 .

To further explore the roles of MgCl_2 in bladder cancer, detailed analyses of canonical cell death modes, including apoptosis, necrosis, and autophagic cell death were performed. Flow cytometry was performed to analyze the apoptosis of cells treated with MgCl_2 . The results demonstrated that the apoptotic rate in the control cells was 4.2% and in the MgCl_2 treated cells were augmented to 12.8% (**Figure 1G**). The results of qRT-PCR assay revealed that the expression of HRK, FAS, TNFRSF10A, and TNFRSF10B was up-regulated in MgCl_2 treated cells (**Figure 2A**). Western blot assay also further confirmed the increased expression of apoptosis-related genes. The expression of Bak and Bax was slightly enhanced in the cells treated with MgCl_2 (**Figure**

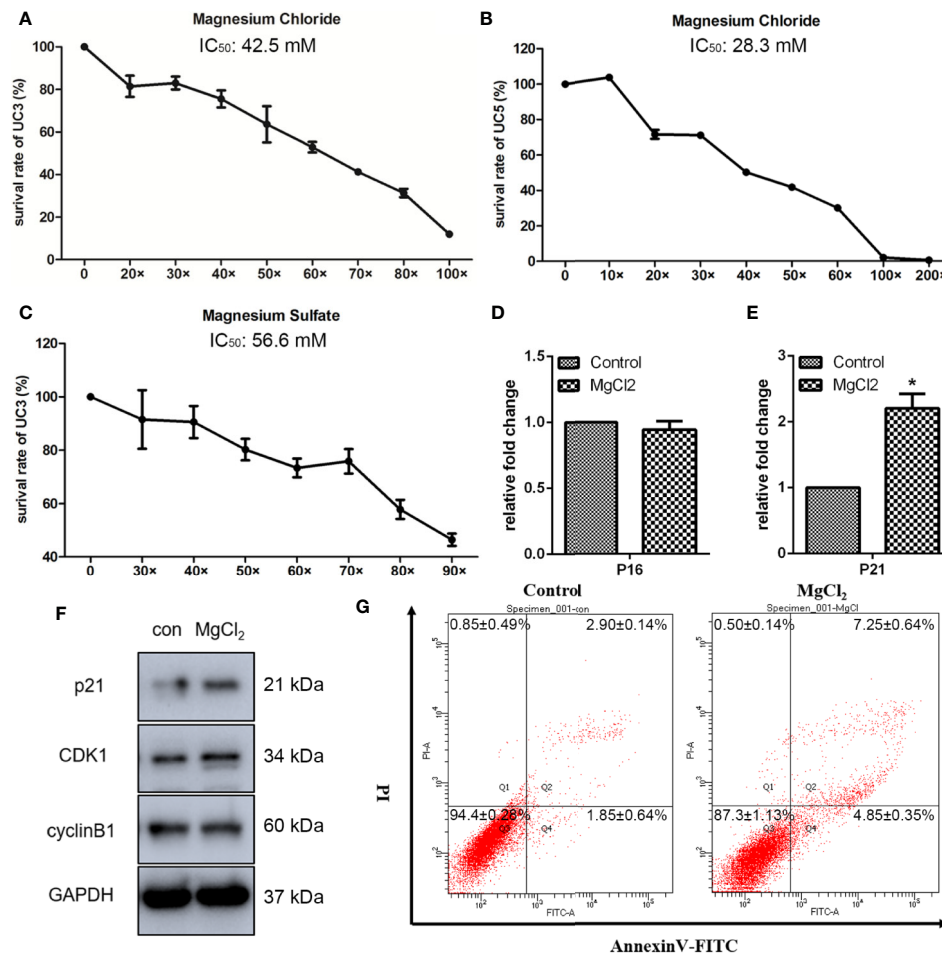


FIGURE 1 | Magnesium inhibited the proliferation of bladder cancer cells. **(A)** The survival rate of UC3 cells at different concentrations of MgCl₂ for 24 h. **(B)** The survival rate of UC5 cells at different concentrations of MgCl₂ for 24 h. **(C)** The survival rate of UC3 cells at different concentrations of MgSO₄ for 24 h. **(D, E)** mRNA expression of P16 and P21 as determined by qRT-PCR. Data were expressed as mean ± SEM of duplicate experiments. The differences between the two groups were assessed using the unpaired Student's t-test. **p* < 0.05 versus control. **(F)** Protein expression as revealed by Western blot analysis. **(G)** Apoptosis was evaluated by flow cytometry using double staining with Annexin V (Annexin V, horizontal line) and propidium iodide (PI, vertical line).

2C and S2B). Western blot analysis of cytosolic vs. mitochondrial extracts revealed that Bax and Bak accumulated in mitochondria (Figure S3), further confirming that apoptosis was triggered by a high concentration of MgCl₂.

Furthermore, a close relationship exists between apoptotic cell death and ER stress. To confirm our hypothesis that MgCl₂ induces apoptosis through ER stress, the expression of ER stress-related genes (ATRC1, Bip, IRE1α, TRAF2, eIF, ERdj4, EDEM1, and P58IPK) was analyzed. As revealed by qRT-PCR, increased expression of Bip, IRE1α, eIF, ERdj4, and EDEM1 were found in MgCl₂ treated cells (Figure 2B). To further confirm whether MgCl₂ can induce ER stress, a Western blot assay was performed to detect the expression of CHOP, Bip, and BAP31. As presented in Figure 2D, treatment with MgCl₂ enhanced the expression of CHOP remarkably. These results indicated that MgCl₂ could induce ER stress, which might play a crucial role in MgCl₂-induced apoptosis of UC3 cells.

Autophagy plays a protective role in the resistance to apoptosis under various apoptotic conditions (24). Autophagy can function as an alternative cell death mechanism defined as programmed cell death type II. Besides, during the progression of autophagy, the cleavage of LC3 is increased. As determined by Western blot assay, the expression of LC3-II was up-regulated in MgCl₂ treated cells (Figure 3B and S2C). However, the expression of other autophagy marker p62/SQSTM1 was down-regulated following treatment with MgCl₂. These results indicated that autophagy was induced by MgCl₂ therapy. Furthermore, additional autophagy-associated genes were also analyzed. Results showed that the expression of ATG3, ATG5 and VDAC were increased following treatment with MgCl₂ (Figures 3A, B), further confirming the role of autophagy in MgCl₂ therapy. However, both qRT-PCR and Western blot assay revealed that the BECN was decreased in the cells treated with MgCl₂, indicating that MgCl₂ mediated autophagy was

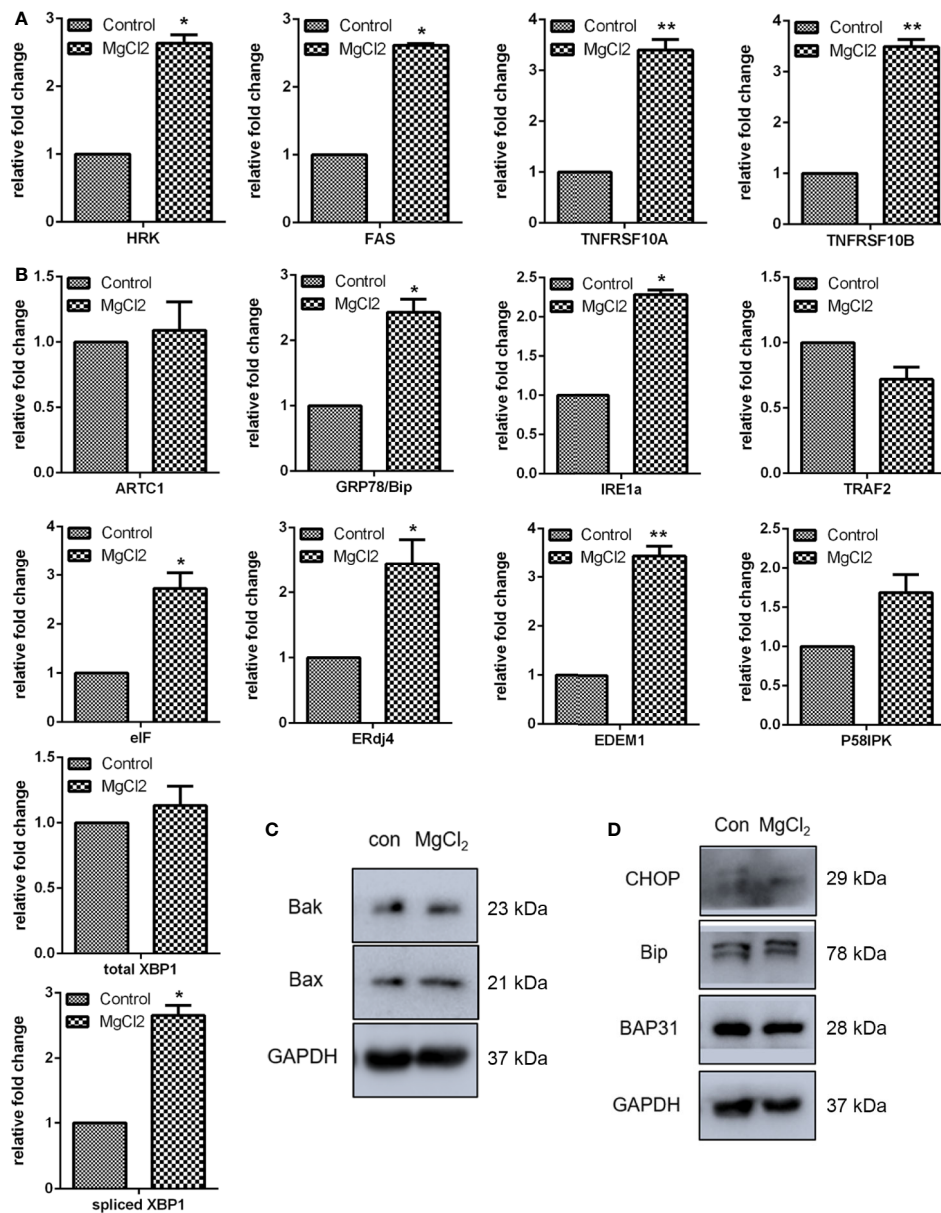


FIGURE 2 | MgCl₂ affected apoptosis and ER stress in bladder cancer cells UC3. **(A)** Expression of apoptosis-related genes as determined by qRT-PCR. **(B)** ER stress-related gene expression as revealed via qRT-PCR. **(C)** Protein expression of apoptosis-related genes as revealed via western analysis. **(D)** Protein expression of ER stress-related genes as determined by Western blot analysis. Data were expressed as mean \pm SEM of duplicate experiments. The differences between the two groups were assessed using the unpaired Student's t-test. * $p < 0.05$ versus control, and ** $p < 0.01$ versus control.

independent of BECN expression. Akt-mTOR pathway is essential for the induction of autophagy, and the results of Western blot analysis revealed that both p-Akt and mTOR was attenuated following treatment with MgCl₂ (Figure 3C). Taken together, the results implicated that MgCl₂ triggered BECN independent autophagy via Akt-mTOR signaling.

The present study also analyzed the expression of necroptosis related genes RIPK1, PARP1, and MLKL. Results of qRT-PCR

indicated that there were no significant differences in the expression of RIPK1 and PARP1 between the control and MgCl₂ treated cells (Figure 3E). However, MLKL mRNA level was decreased in the cells treated with MgCl₂. Western blot assay further confirmed the decreased expression of MLKL in the MgCl₂ treated cells (Figure 3D). Collectively, the results indicated that necroptosis was inhibited with MgCl₂ treatment in bladder cancer cells.

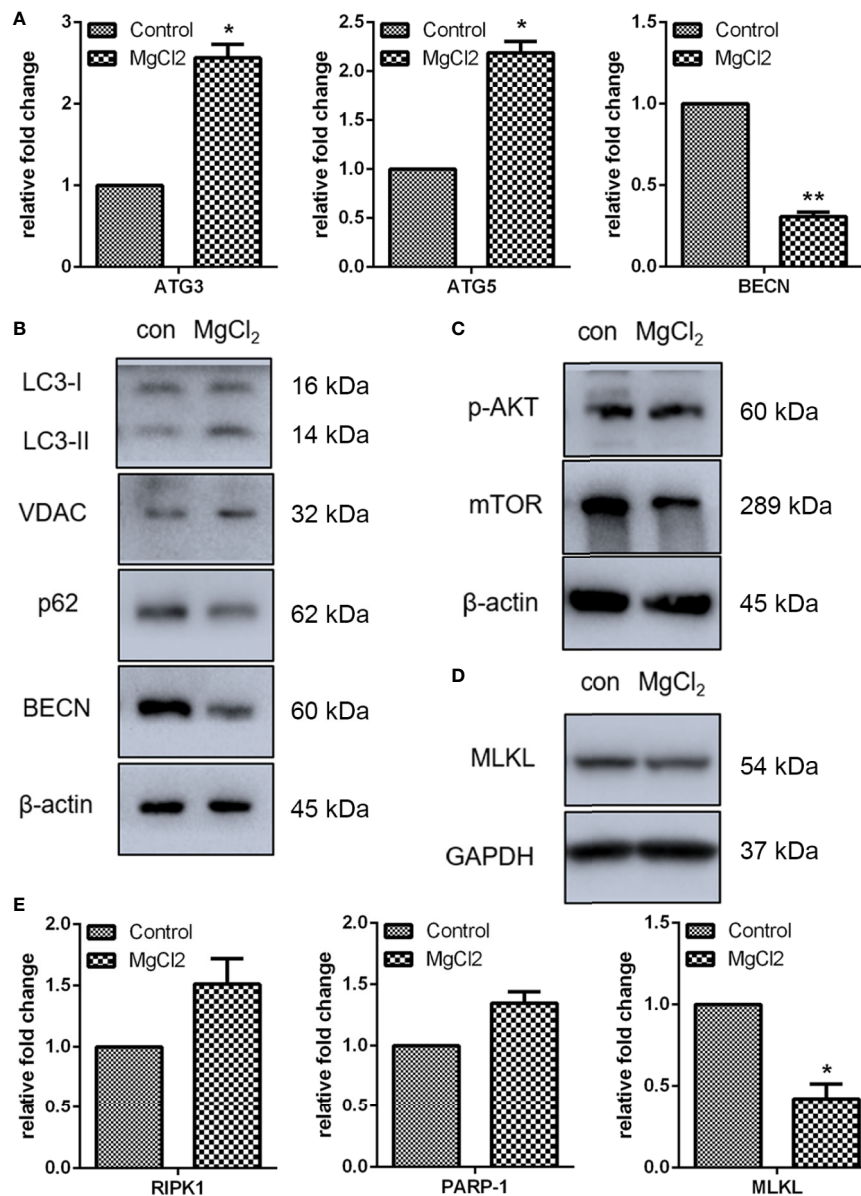


FIGURE 3 | MgCl₂ affected autophagy and necroptosis in UC3 cells. **(A)** mRNA expression of autophagy-associated genes as revealed by qRT-PCR. **(B)** Protein expression of autophagy marker genes as determined by Western blot analysis. **(C)** Evaluation of Akt phosphorylation (p-Akt) and mTOR as determined by Western blot analysis. **(D)** Expression of MLKL as determined by Western blot analysis. **(E)** Gene expression related to necroptosis, as revealed by qRT-PCR. The differences between the two groups were assessed using the unpaired Student's t-test. Data were expressed as mean ± SEM of duplicate experiments. **p* < 0.05 versus control, and ***p* < 0.01 versus control.

Effect of MgCl₂ on Wnt and Ras/Raf/MEK/ERK Signaling

The Wnt signaling pathway has been implicated in tumorigenesis and tumor recurrence, and clinical trial of drugs targeting the Wnt pathway has shown promising results. Therefore, in the present study, we analyzed the expression of Wnt signaling in bladder cancer cells *in vitro*. Using qRT-PCR, we analyzed the expression of SFRP2, WIF-1, Wnt3a, Wnt5a, APC, LEF1, and c-Myc. The results indicated that the expression of SFRP2, Wnt5a, LEF1, and c-Myc

was down-regulated following treatment with MgCl₂ (Figure 4A). While the treatment with MgCl₂ up-regulated the expression of WIF-1. However, there was no significant difference in the expression of Wnt3a and APC between the control and MgCl₂ treated group. Possibly, the Wnt signaling pathway was inhibited by MgCl₂. To support this hypothesis, we performed a Western blot assay to evaluate the expression of β-catenin, which is a pivotal component of the Wnt/β-catenin signaling pathway. The results indicated that the expression of β-catenin was down-regulated following treatment with MgCl₂ (Figure 4C).

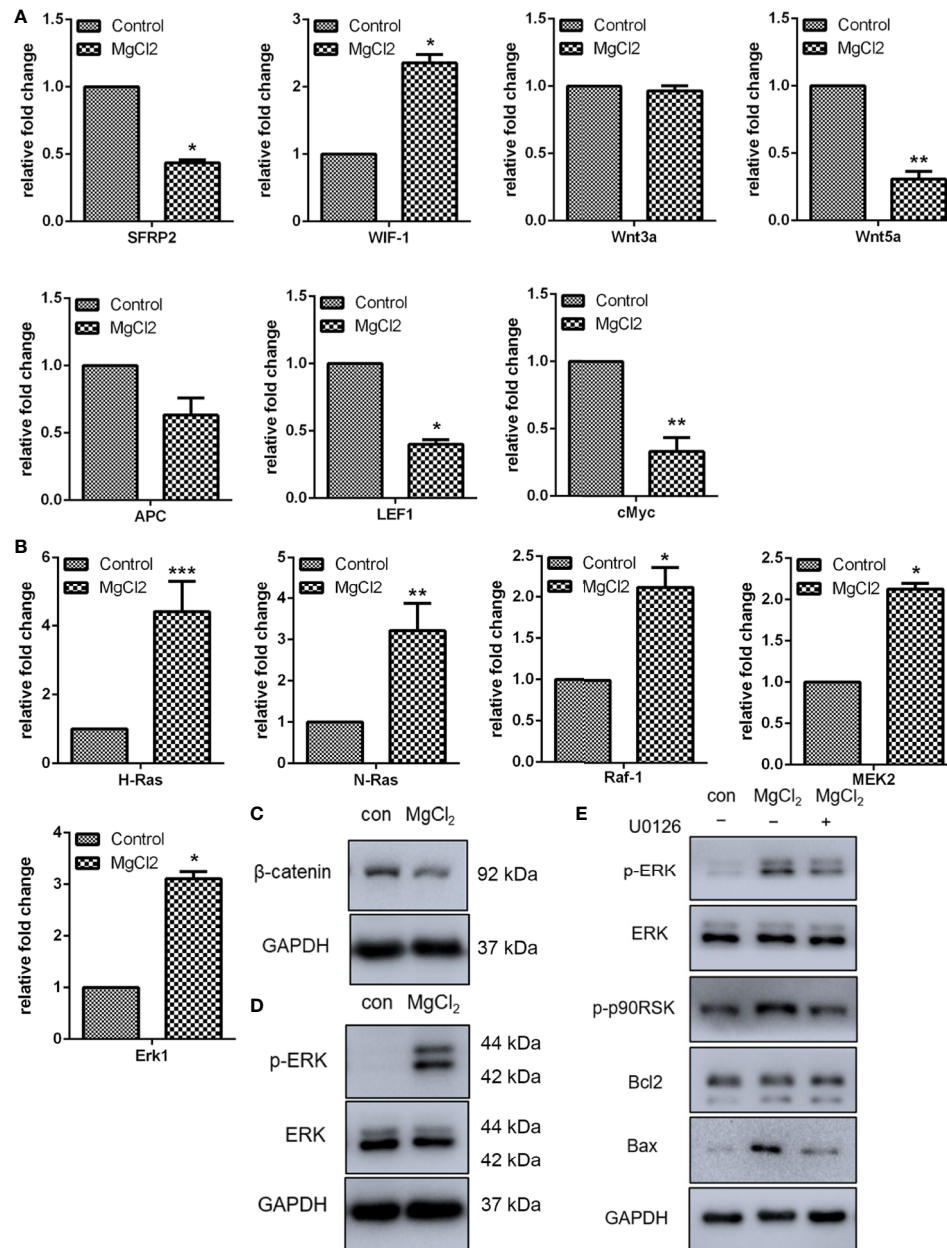


FIGURE 4 | MgCl₂ regulated Wnt and ERK signaling pathways in UC3 cells. **(A)** Wnt signaling genes expression analysis by qRT-PCR. **(B)** mRNA expression of ERK signaling genes was determined by qRT-PCR. **(C)** Protein expression of β-catenin as determined by Western blot analysis. **(D)** Protein expression of ERK and ERK phosphorylation (p-ERK) as determined by Western blot analysis. **(E)** Protein expression as determined by Western blot analysis in cells treated with U0126. Data were expressed as mean ± SEM of duplicate experiments. The differences between the two groups were assessed using the unpaired Student's t-test. **p* < 0.05 versus control, ***p* < 0.01 versus control, and ****p* < 0.001 versus control.

The Ras/Raf/MEK/ERK signaling is yet another important signaling pathway involved in carcinogenesis and progression. Thus, the expression of H-Ras, N-Ras, Raf-1, and MEK2 was analyzed using qRT-PCR, and results showed that all these genes were activated following treatment with MgCl₂ (**Figure 4B**). The expression of ERK was then examined using Western blot assay. As represented in **Figure 4D**, there was no significant difference in the expression of ERK between the control and MgCl₂ treated group.

However, ERK phosphorylation was enhanced in the MgCl₂ treated cells. To further investigate the effect of MgCl₂ on Ras/Raf/MEK/ERK signaling, the pretreatment with mitogen-activation protein kinase kinase inhibitor, U0126, was performed. As anticipated, pretreatment with U0126 suppressed the enhanced effect of MgCl₂ on ERK phosphorylation (**Figure 4E**). Furthermore, the upregulation of Bax and LC3-II induced by MgCl₂ treatment was also inhibited in cells pre-treated with U0126 (**Figure 4E** and **S3**),

possibly indicating that MgCl_2 induced apoptosis and autophagy could be prevented through the inhibition of Ras/Raf/MEK/ERK signaling.

MgCl_2 Exerted Minor Effects on the Migration and Stemness

The epithelial-to-mesenchymal transition (EMT), together with its reverse process mesenchymal-epithelial transition (MET), plays an important role in cancer progression and metastasis. In this study, E-cadherin was found to be up-regulated in the MgCl_2 treated cells (**Figure 5A**). However, the expression of epithelial gene ZO-1 was downregulated following treatment with MgCl_2 . Furthermore, we performed a Western blot assay to analyze the expression of mesenchymal genes. MgCl_2 suppressed the expression of Zeb1 and Slug; however, it enhanced the expression of Vimentin and α -SMA. It was found that the EMT process was disrupted by treatment with MgCl_2 . MMPs have been known to degrade the extracellular matrix, thus promoting migration and invasion of cancer cells. The results of Western blot analysis revealed that MgCl_2 reduced the expression of MMP2 and MMP9. However, treatment with

MgCl_2 was shown to exert no significant effects on colony formation, migration, and invasion (**Figures 6A–C**).

The EMT process is suggested to be closely associated with the acquisition of cancer stemness properties. Therefore, we examined the expression of genes related to cancer stemness. Surprisingly, the expression of CD44 and CD133 was promoted by treatment with MgCl_2 (**Figure 5B**). Next, we analyzed whether prolonged treatment duration would have an impact on the expression profile of these genes. At 48 h post-treatment with MgCl_2 , there were no significant differences in the expression profiles of ABCG2, CD44, and CD133 between the control and MgCl_2 treated cells (**Figure 5C**). To better illustrate the effect of MgCl_2 on the cancer stemness, we performed flow cytometry to analyze the expression of cancer stem cells markers CD44 and CD133 in immortalized normal gastric cells Ges1 and gastric cancer cells MKN1. In both Ges1 and MKN1 cells, treatment with MgCl_2 did not markedly alter the expression of CD44 and CD133 (**Figure 6D**). Considering the gene expression profile and cell biology experiments, it was apparent that the migration and cancer stemness was not significantly inhibited by treatment with MgCl_2 .

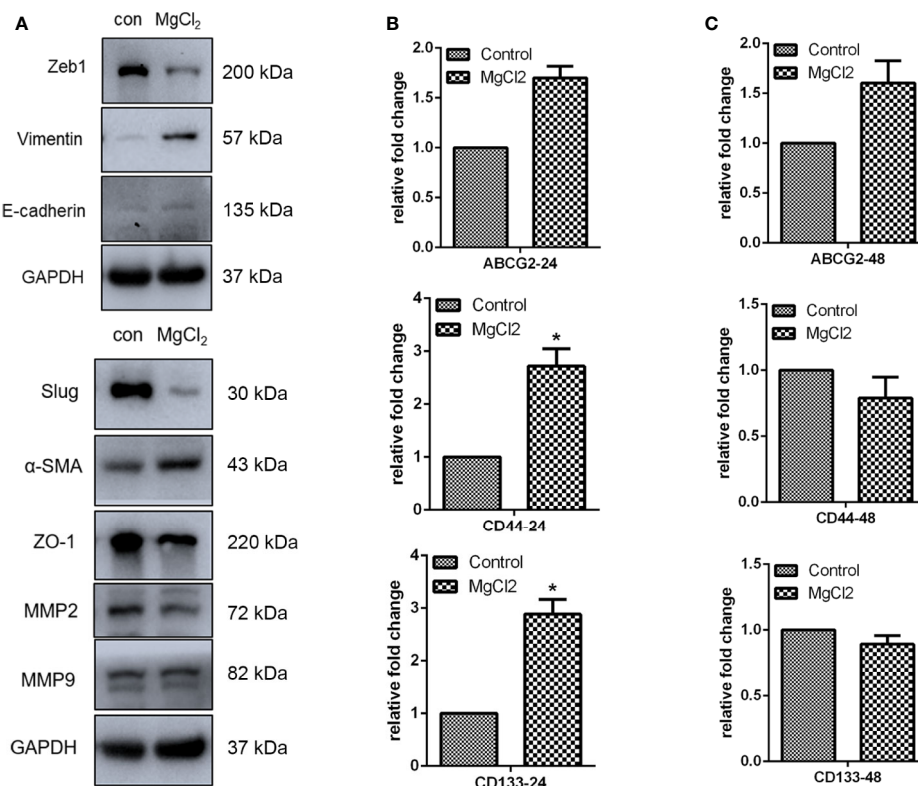


FIGURE 5 | MgCl_2 affected the migration of UC3 cells. **(A)** Protein expression of EMT related genes as evaluated by Western blot analysis. **(B)** mRNA expression of cancer stem cell marker genes was determined by qRT-PCR in the cells treated with MgCl_2 for 24 h. **(C)** mRNA expression of cancer stem cell marker genes was determined by qRT-PCR in the cells treated with MgCl_2 for 48 h. Data were expressed as mean \pm SEM of duplicate experiments. The differences between the two groups were assessed using the unpaired Student's t-test. * $p < 0.05$ versus control.

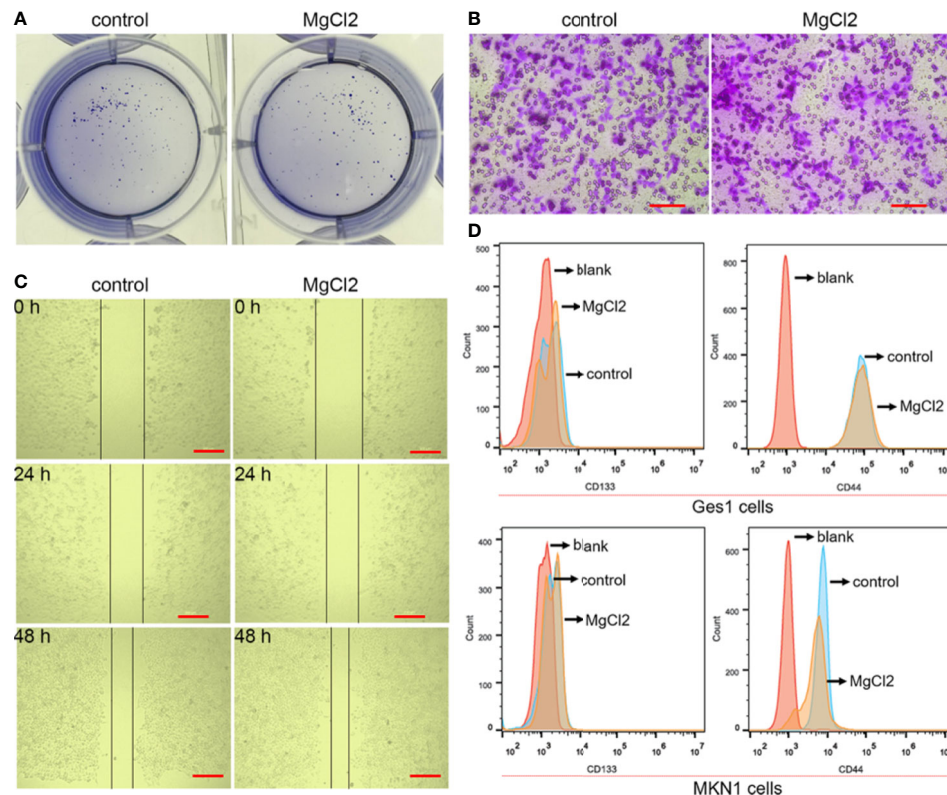


FIGURE 6 | Effect of MgCl_2 on the proliferation, migration, and stemness in the bladder cancer cells. **(A)** Colony formation in the UC3 cells treated with MgCl_2 . **(B)** Trans-well assay of the UC3 cells treated with MgCl_2 . Scale bars indicate 100 μm . **(C)** Results of the wound healing assay of the UC3 cells treated with MgCl_2 . Scale bars indicate 200 μm . **(D)** The proportion of CD44 and CD133 positive cells in MKN1 or Ges1 cells treated with MgCl_2 by flow cytometry.

VPA Enhanced the Anti-Tumor Effect of MgCl_2

Results indicated that MgCl_2 treatment reduced the acH4K5 abundance in UC3 cells (Figure S2E). Many literatures have documented that enhancing acetylation could be useful in the prevention of cancer cell proliferation and metastasis. Therefore, to strengthen the anti-tumor function of MgCl_2 , cancer cells were subjected to combination treatment with MgCl_2 and VPA (5 mM). As illustrated in Figure 7A, cells with combined treatment of MgCl_2 and VPA developed considerably lower numbers of colonies compared to control cells. Furthermore, the number of cells with combined treatment that migrated through the trans-well membrane was also markedly lower than that of control cells (Figure 7B). These results confirmed that VPA could effectively contribute to reinforce the anti-tumor function of MgCl_2 .

Next, we performed CCK8 assay to determine the inhibitory effect of combined treatment on cell proliferation, and results indicated that a considerably lower survival rate was observed in the cells with combination treatment (Figure 8A and S4A). Furthermore, the suppressive effect of MgCl_2 and/or VPA on *in vivo* tumorigenicity was also evaluated in UC3 cells tumor-bearing mice. The results revealed that MgCl_2 and VPA in combination significantly reduced the tumor volume compared

with control ($216.95 \pm 77.21 \text{ mm}^3$ vs. $361.87 \pm 113.21 \text{ mm}^3$, $p = 0.035$; Figures 8H, I). Consistent with the above results, the tumor weight of UC3 cells tumor-bearing mice receiving combined treatment was also significantly lower than the control group ($0.25 \pm 0.07 \text{ g}$ vs. $0.39 \pm 0.12 \text{ g}$, $p = 0.016$; Figures 8H, J).

Then, we further investigated the molecular mechanism underlying combination treatment was then investigated, and as revealed by flow cytometry, G0/G1 cell cycle arrest was most severe in the cells receiving combination treatment (Figure 7C). Consistent with the results of cell cycle analysis, cells with combination treatment exhibited increased expression of CDK1, cyclin B1, cyclin B2, cyclin D1, and p21 (Figure 8 and S4B). Besides, the mRNA level of the apoptotic markers TNFRSF10A, TNFRSF10B, and caspase 9 were also increased in the cells receiving combination treatment (Figure 9A). Results of Western blot assay also indicated that the expression of Bak and Bax was also enhanced following combined treatment with MgCl_2 and VPA (Figure 9B and S4B).

The expression of ER stress-related genes (Bip, CHOP, and BAP31) was also analyzed using qRT-PCR and Western blot assay. The mRNA expression of Bip and CHOP were up-regulated in cell treated with combination treatment (Figure

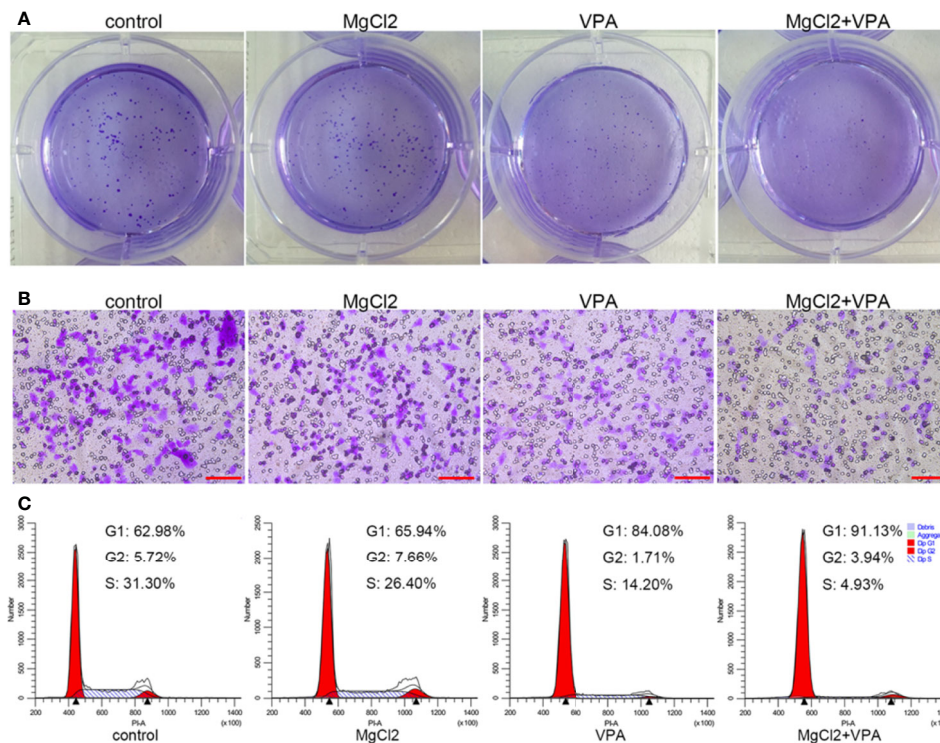


FIGURE 7 | MgCl₂, in combination with VPA, inhibited the proliferation, migration, and cell cycle distribution in UC3 cells. **(A)** Colony formation in the cells following the combination treatment. **(B)** Trans-well assay of the cells with combination treatment. Scale bars indicate 100 μ m. **(C)** Cell cycle distribution was evaluated by flow cytometry based on PI staining.

9D and S4C). The result of Western blot assays further confirmed that the Bip expression was markedly enhanced by combination treatment (Figure 9C). A specific IRE1 α inhibitor STF083010 was applied to uncover the role of ER stress in combination treatment. As shown in Figure S5, the increasement in the expression of spliced XBP1 in the cells with combination treatment was inhibited by STF083010 as expected. Furthermore, the upregulation of TNFRSF10A in the cells with combination treatment was also prevented by STF083010, indicating that ER stress is possible a critical regulator of apoptosis induced by combination treatment.

To demonstrate whether VPA could enhance induced autophagy, the expression of ATG3, ATG5, LC3, VDAC, BECN, and p62 was examined. The expression of ATG3, ATG5, LC3, VDAC1, and BECN at the mRNA level was significantly enhanced with combination treatment (Figure 10A). Western blot analysis also revealed an increased level of LC3-II protein production in cells with combination treatment as compared to the control (Figure 10B and S4D). Results of Western blot analysis also showed that combination treatment promoted the VDAC expression. However, the expression of p62 was suppressed following treatment with MgCl₂ and VPA, as indicated by qRT-PCR and Western blot analysis. In addition, the phosphorylation of mTOR was also up-regulated in the cells receiving combination treatment (Figure 10C), implying that induction of autophagy was reinforced by combination treatment.

Furthermore, we also found that the Ras/Raf/MEK/ERK signaling was activated, and the Wnt signaling was down-regulated following treatment with MgCl₂. Therefore, we next investigated these signaling pathways in cells following combination treatment. The expression of ERK and p38MAPK were similar among the tested groups; however, the phosphorylation of ERK and p38MAPK were predominantly enhanced following combination treatment (Figure 10D). The expression of β -catenin was up-regulated in the cells with VPA treatment but was decreased in the cells with MgCl₂ or combination treatment (Figure 10E). Collectively, these findings suggested that combination treatment inhibited cell proliferation, induced cell cycle arrest, enhanced apoptosis and autophagy, and suppressed migration through activation of ERK signaling and inhibition of the Wnt signaling pathway, thus VPA ameliorated the anti-tumor effect of MgCl₂.

DISCUSSION

The present study demonstrated that treatment with MgCl₂ could affect the proliferation and apoptosis of bladder cancer cells through the regulation of Ras/Raf/MEK/ERK and Wnt signaling pathways. However, the migratory ability and stemness of cancer cells were not markedly disrupted by treatment with MgCl₂. Thus, when

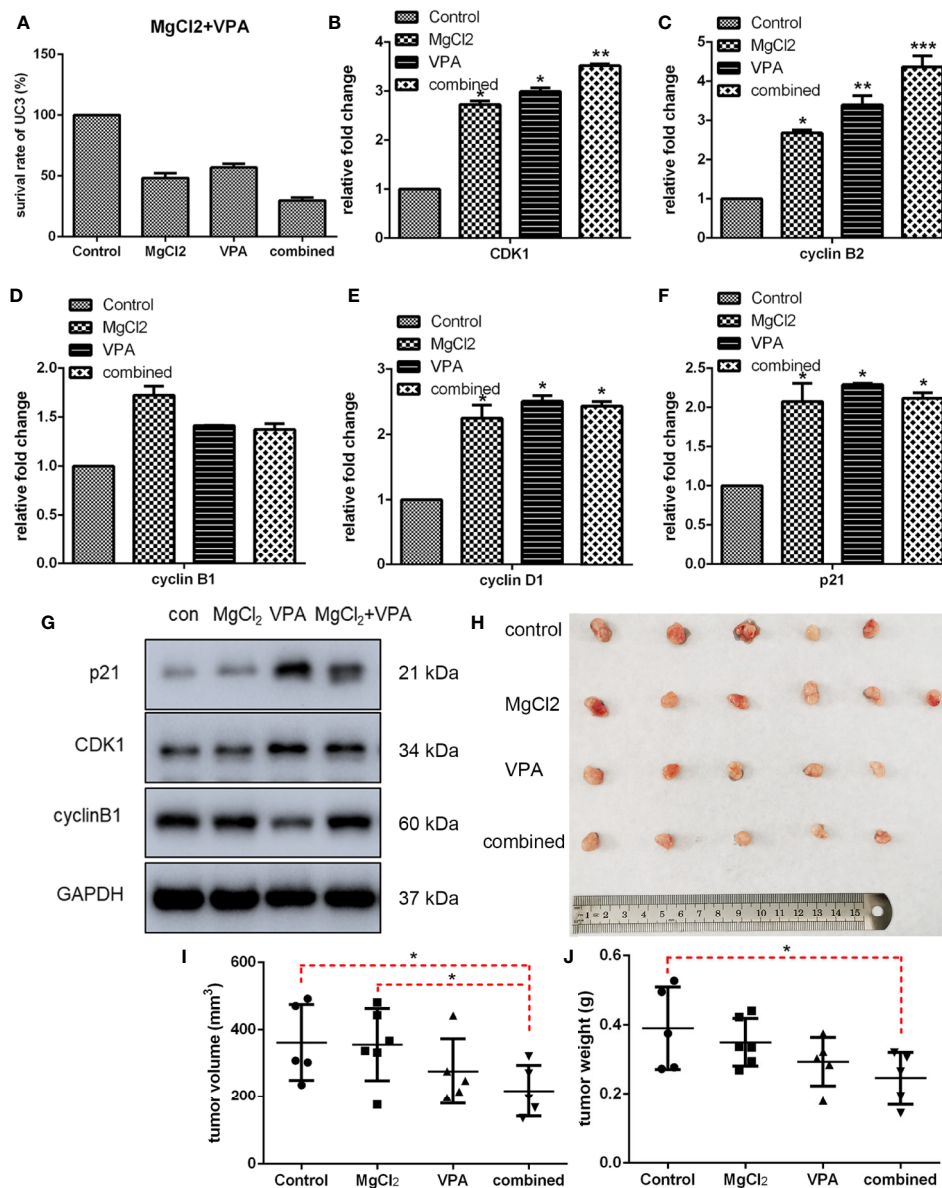


FIGURE 8 | Combination treatment with MgCl₂ and VPA affected cell survival, expression of genes related to cell cycle progression, and *in vivo* tumorigenicity of UC3 cells. **(A)** The survival rate of cells with combination treatment as determined by CCK-8 assay. **(B–F)** mRNA expression of genes related to cell cycle progression was investigated by qRT-PCR. Data were expressed as mean ± SEM of duplicate experiments. **(G)** Western blot analysis of genes related to cell cycle progression. **(H)** UC3 cells were injected into BALB/c nude mice, as indicated. After therapy with MgCl₂ and/or VPA for 14 days, mice were sacrificed to harvest tumors. The tumor volume **(I)** and weight **(J)** were inhibited by combination treatment compared with the control group. The differences among multiple groups were assessed using the Analysis of variance (ANOVA). **p* < 0.05 versus control, ***p* < 0.01 versus control, and ****p* < 0.001 versus control.

MgCl₂ in combination with VPA was used, the migration of cancer cells was severely suppressed.

Accumulating pieces of evidence have reported that magnesium can act as a protective agent in colorectal carcinogenesis by suppressing c-Myc expression and ornithine decarboxylase function in the intestinal mucosa (25). In this study, we also found that the proliferation of bladder cancer cells was inhibited by different concentrations of magnesium. As indicated

by flow cytometry analysis, treatment with MgCl₂ could trigger apoptosis and induce cell cycle arrest. MgCl₂ altered the expression of many genes associated with cell cycle and apoptosis. Notably, p21 was up-regulated following treatment with MgCl₂. The p21 functions as a potent cyclin-dependent kinase inhibitor, up-regulation of which could induce cell cycle arrest (26). Besides, p21 can interact with various molecules, such as p53 and Myc, depending on different stimuli (26). In fact, due

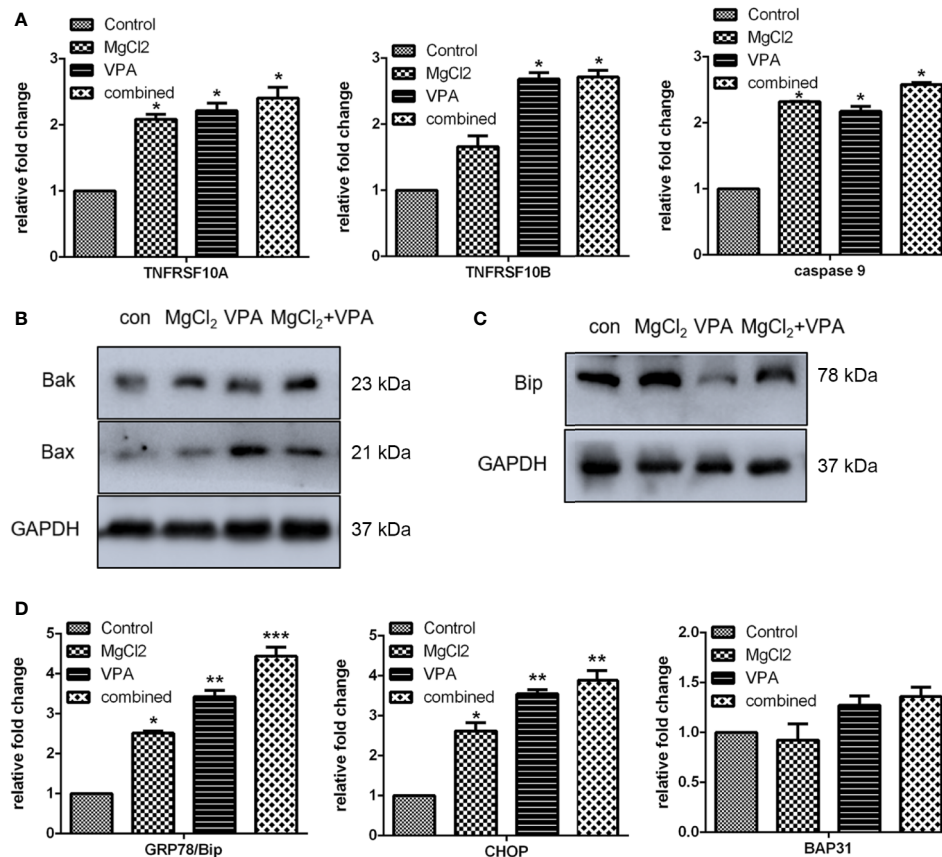


FIGURE 9 | Expression of apoptosis or ER stress-associated genes in UC3 cells with combination treatment. **(A)** mRNA expression of apoptosis-related genes as determined by qRT-PCR. **(B)** Western blotting analysis for the expression of Bax and Bak. **(C)** Western blot analysis for the expression of Bip. **(D)** mRNA expression of genes related to ER stress was investigated by qRT-PCR. Data were expressed as mean \pm SEM of duplicate experiments. The differences among multiple groups were assessed using the Analysis of variance (ANOVA). * $p < 0.05$ versus control, ** $p < 0.01$ versus control, and *** $p < 0.001$ versus control.

to interaction with different units, p21 could also function as an inhibitor of apoptosis, thus contributing to cancer development (26, 27). Therefore, combination therapy is expected to overcome challenges.

Autophagy, a lysosome-dependent cellular degradation program, is an evolutionary conserved catabolic process that provides cellular material to lysosomes for degradation to regulate the cellular homeostasis. A complex interplay between autophagy and apoptosis may contribute to cancer progression and therapeutic outcomes. A growing number of studies indicated that autophagy has a dichotomous role in the regulation of cancer (28, 29). In breast cancer, BECN and ATG7 mediated autophagy is considered as a means of evading apoptosis following DNA damage, thus prolonging cell survival (30). Thus, inhibition of autophagy to improve clinical outcomes in patients with cancer appears to be a favorable strategy. However, several studies have indicated that inhibition of autophagy may not confer benefit in cancer therapy as it may reduce anti-tumor T cell responses (28). In the present study, MgCl₂ triggered autophagy through the

regulation of Akt/mTOR signaling. Indeed, targeting autophagy represents a promising therapeutic strategy to circumvent resistance and improve the outcomes of chemotherapy (31). Therefore, the accurate utilization of MgCl₂ in targeting autophagy might be beneficial in cancer therapy.

ER stress is a typical cellular stress response representing an evolutionarily conserved mechanism for maintaining cellular homeostasis. ER stress is closely associated with the induction of apoptosis and autophagy (32, 33). In this study, the splicing of XBP1 was induced with the MgCl₂ treatment, indicating that the ER stress was triggered following treatment with MgCl₂. Furthermore, treatment with MgCl₂ up-regulated the expression of CHOP, Bip, IRE1 α , eIF, ERdj4, EDEM1, and P58IPK. There are at least three pathways involving sensors of ER stress: (1) pancreatic endoplasmic reticulum kinase (PERK) phosphorylates eukaryotic initiation translation factor 2 α (eIF2 α); (2) translocation of activating transcription factor 6 (ATF6) from the ER to the Golgi and then the nucleus; and (3) inositol-requiring enzyme 1 α (IRE1 α) splices X-box-binding

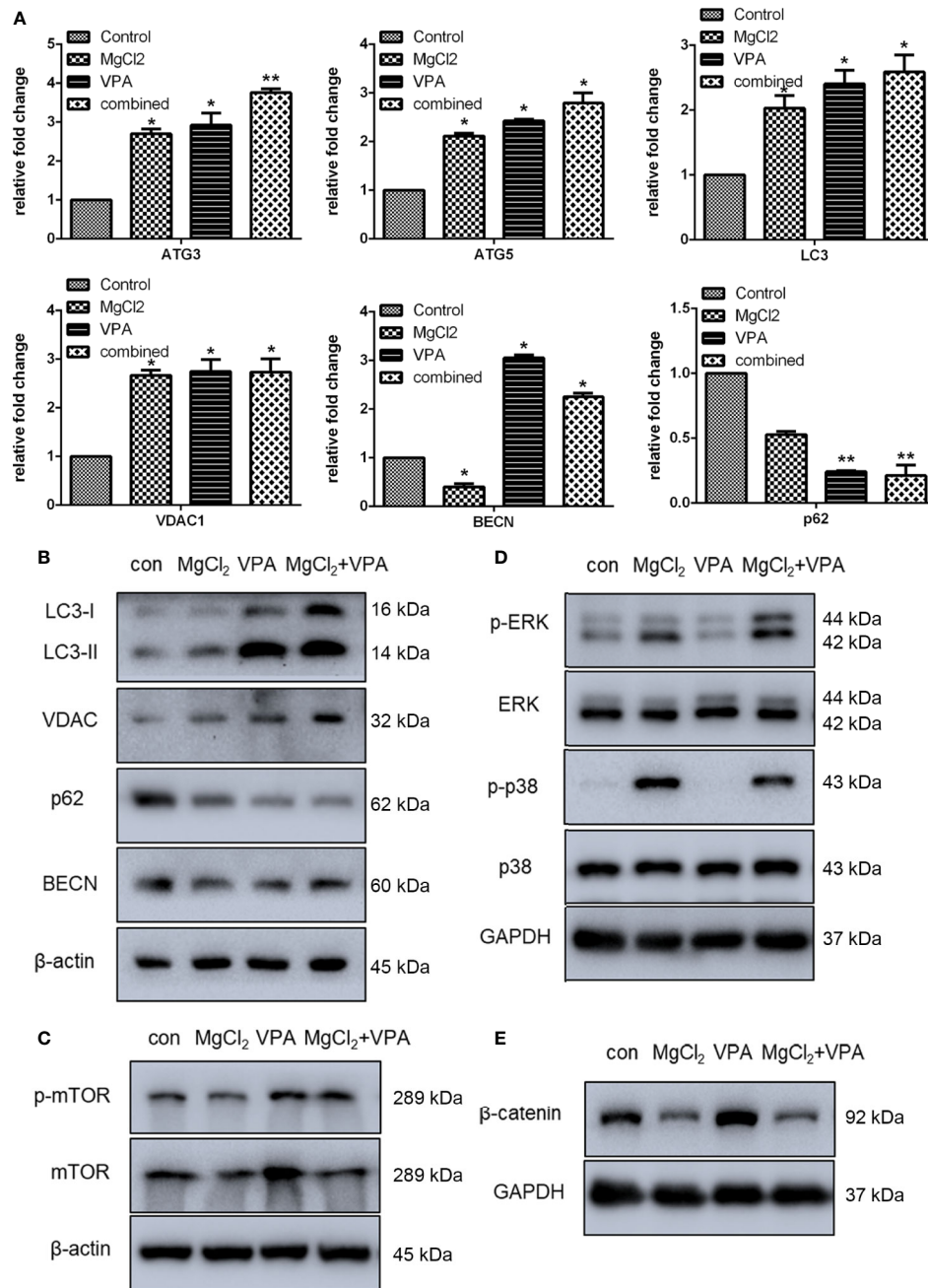


FIGURE 10 | Combination treatment with MgCl₂ and VPA regulated autophagy and many signaling pathways in the UC3 cells. **(A)** mRNA expression of autophagy-related genes as determined by qRT-PCR. **(B)** Western blot analysis for the expression of genes related to autophagy. **(C)** Protein expression of mTOR and phosphorylated mTOR (p-mTOR) as determined by Western blot analysis. **(D)** Protein expression of ERK signaling genes as determined by Western blot analysis. **(E)** Protein expression of β-catenin as determined by Western blot analysis. The differences among multiple groups were assessed using the Analysis of variance (ANOVA). **p* < 0.05 versus control, and ***p* < 0.01 versus control.

protein (XBP1) mRNA (34). Considering the significant upregulation of IRE1α and spliced XBP1 after MgCl₂ treatment, we hypothesized that the IRE1α-XBP1 branch might involve in the treatment. Results of STF083010 treatment confirmed that blocking IRE1α could prevent the splicing of XBP1 and reduce the expression of TNFRSF10A.

IRE1α can activate Jun-N-terminal kinase (JNK) to trigger autophagy or apoptosis (35). JNK mediated Bcl2 phosphorylation lead to the BECN/Bcl2 dissociation and autophagy induction in the early phase of ER stress, and sustained activation of JNK could trigger apoptosis due to prolonged ER stress (32). Conceivably, MgCl₂ mediated the

crosstalk between autophagy and apoptosis by modulating the expression of these genes.

Wnt signaling modulates cancer stem cells, metastasis, and immunity, is tightly associated with cancer (36). Inhibition of Wnt signaling is a universal strategy for cancer therapy, and some of Wnt signaling inhibitors are currently under clinical testing (36, 37). In this study, Wnt signaling was suppressed following treatment, possibly indicating that Wnt signaling was a critical target of the combination therapy. The Ras/RAF/MEK/ERK signaling pathway is another best-defined pathway in cancer biology (38). ERKs belong to the MAPK family of kinases, which also comprise of p38MAPK and JNK (39). ERKs are suggested as a double-edged sword in cancers which can activate pro-survival pathways contributing to cell proliferation and migration, or can function against cancer by regulating apoptosis, differentiation, and senescence (40). Increased ERK phosphorylation emerged in the cells with combination treatment in the present study. To uncover the role of Ras/RAF/MEK/ERK signaling pathway in magnesium treatment, the ERK inhibitor U0126 was applied. The Bax/Bcl2 ratio in MgCl₂ treated cells was decreased by U0126, indicating that the Ras/RAF/MEK/ERK signaling pathway is critical for the apoptotic effect of MgCl₂ treatment. In fact, U0126 has been found to block the apoptosis in many cancer cell types (41, 42). The down-regulation of Bax and cytochrome C in the mitochondrial protein fractions from cells with U0126 exposure further confirmed the role of Ras/RAF/MEK/ERK signaling pathway in MgCl₂ induced apoptosis.

EMT enhances cell migration and metastasis of cancer cells (43, 44). As anticipated, E-cadherin expression was up-regulated following treatment with MgCl₂. However, loss of E-cadherin conveys a poor prognosis in multiple human cancers, including bladder cancer (45). In most experimental models, E-cadherin is evaluated as an indicator of the occurrence of EMT (46). Considering these evidences, we suggested that treatment with MgCl₂ could inhibit the EMT process. However, the expression of some of the marker genes was not apparent after treatment with MgCl₂. Furthermore, the results of the present study also demonstrated that the migratory ability of cancer cells in control and MgCl₂ treated group was similar. It is well recognized that migration is critical for cancer cell invasion and dissemination. Cancer stem cells, a subpopulation of cancers, harbor stemness that is perceived to considerably contribute to cancer metastasis, relapse, and therapy resistance (43). In previous studies, ABCG2, CD44, and CD133 were used to identify and isolate the bladder cancer stem cells (47, 48). In the present study, treatment with MgCl₂ did not show an inhibitory effect on the expression of ABCG2, CD44, and CD133. In contrast, an up-regulation in the expression of CD44 and CD133 were presented in the cells treated with MgCl₂ for 24 h. Possibly, MgCl₂ did not have a favorable effect on the suppression of migration and stemness. Indeed, E-cadherin acts as a pleiotropic molecule that can contribute to either tumor-suppressing or tumor-promoting processes (49).

Combination therapy has been shown to improve clinical efficacy in many reports. VPA, a histone deacetylase inhibitor,

has been widely used as an effective chemotherapeutic drug in a variety of cancers. VPA has been indicated to markedly promote the action of a number of chemotherapy agents in bladder cancer (50). In our previous study, the inhibitory effect on bladder cancer was found to be improved when melatonin was used in combination with VPA (51). In this study, combination treatment with MgCl₂ and VPA revealed a potent ability in the inhibition of cell proliferation, migration, and *in vivo* tumorigenicity. The inhibitory effect of MgCl₂ on proliferation and cell cycle was further strengthened by treatment with VPA. In fact, VPA has been shown to improve the anti-tumor effect of several first-line drugs, including Sorafenib and cisplatin (52, 53). In sum, further studies are warranted to improve the therapeutic effects of magnesium in cancer chemotherapy.

CONCLUSION

Collectively, the findings of the present study indicated that combination treatment of MgCl₂ with VPA inhibited cell proliferation, induced cell cycle arrest, enhanced apoptosis, and autophagy, and suppressed migration through activation of ERK signaling; thus, VPA ameliorated the anti-tumor effect of MgCl₂. Although further studies are warranted, the combination treatment of MgCl₂ with VPA is an effective strategy to improve the outcome of chemotherapy.

DATA AVAILABILITY STATEMENT

The original contributions presented in the study are included in the article/**Supplementary Material**. Further inquiries can be directed to the corresponding authors.

ETHICS STATEMENT

The animal study was reviewed and approved by Animal Care and Use Committee of the Northeastern University Committee, China.

AUTHOR CONTRIBUTIONS

YH, BW, YR, and GQ conceived and designed the experiments. YH, TL, YY, HS, YC, XL, and ZH performed the experiments and analyzed the data. YH wrote the manuscript. TL and BW reviewed the manuscript. All authors contributed to the article and approved the submitted version.

FUNDING

This work was funded by the National Natural Science Foundation of China (Nos.81502582, U1603125, and 31670770). Fund was also provided by the Fundamental

Research Funds for the Central Universities (N182004002 and N141008001-8), the Program for JLU Science and Technology Innovative Research Team (2017TD-28), Liaoning Revitalization Talents Program (XLYC1902063) and Key Research and Development Plan of Liaoning Province (2020JH2/10300080).

REFERENCES

- Bray F, Ferlay J, Soerjomataram I, Siegel RL, Torre LA, Jemal A. Global cancer statistics 2018: GLOBOCAN estimates of incidence and mortality worldwide for 36 cancers in 185 countries. *CA Cancer J Clin* (2018) 68(6):394–424. doi: 10.3322/caac.21492
- Botteman MF, Pashos CL, Redaelli A, Laskin B, Hauser R. The health economics of bladder cancer: a comprehensive review of the published literature. *Pharmacoeconomics* (2003) 21(18):1315–30. doi: 10.1007/BF03262330
- Nagao K, Matsuyama H. Chemotherapy against bladder cancer in geriatric patients. *Nihon Rinsho* (2017) 75(4):615–9.
- Trenta P, Calabro F, Cerbone L, Sternberg CN. Chemotherapy for Muscle-Invasive Bladder Cancer. *Curr Treat Options Oncol* (2016) 17(1):6. doi: 10.1007/s11864-015-0376-y
- Rose TL, Milowsky MI. Improving Systemic Chemotherapy for Bladder Cancer. *Curr Oncol Rep* (2016) 18(5):27. doi: 10.1007/s11912-016-0512-2
- Lobo N, Mount C, Omar K, Nair R, Thurairaja R, Khan MS. Landmarks in the treatment of muscle-invasive bladder cancer. *Nat Rev Urol* (2017) 14(9):565–74. doi: 10.1038/nrurol.2017.82
- Shi J, Kantoff PW, Wooster R, Farokhzad OC. Cancer nanomedicine: progress, challenges and opportunities. *Nat Rev Cancer* (2017) 17(1):20–37. doi: 10.1038/nrc.2016.108
- Wang Y, Zhao R, Wang S, Liu Z, Tang R. In vivo dual-targeted chemotherapy of drug resistant cancer by rationally designed nanocarrier. *Biomaterials* (2016) 75:71–81. doi: 10.1016/j.biomaterials.2015.09.030
- Chen Z, Yu T, Zhou B, Wei J, Fang Y, Lu J, et al. Mg(II)-Catechin nanoparticles delivering siRNA targeting EIF5A2 inhibit bladder cancer cell growth in vitro and in vivo. *Biomaterials* (2016) 81:125–34. doi: 10.1016/j.biomaterials.2015.11.022
- Castiglioni S, Maier JA. Magnesium and cancer: a dangerous liason. *Magn Res* (2011) 24(3):S92–100. doi: 10.1684/mrh.2011.0285
- Wolf FI, Trapani V. Cell (patho)physiology of magnesium. *Clin Sci (Lond)* (2008) 114(1):27–35. doi: 10.1042/CS20070129
- Singh J, Wisdom DM. Second messenger role of magnesium in pancreatic acinar cells of the rat. *Mol Cell Biochem* (1995) 149–150:175–82. doi: 10.1007/BF01076575
- Glasdam SM, Glasdam S, Peters GH. The Importance of Magnesium in the Human Body: A Systematic Literature Review. *Adv Clin Chem* (2016) 73:169–93. doi: 10.1016/bs.acc.2015.10.002
- Witte F. The history of biodegradable magnesium implants: a review. *Acta Biomater* (2010) 6(5):1680–92. doi: 10.1016/j.actbio.2010.02.028
- Li M, Wang W, Zhu Y, Lu Y, Wan P, Yang K, et al. Molecular and cellular mechanisms for zoledronic acid-loaded magnesium-strontium alloys to inhibit giant cell tumors of bone. *Acta Biomater* (2018) 77:365–79. doi: 10.1016/j.actbio.2018.07.028
- Anisimova N, Kiselevskiy M, Martynenko N, Straumal B, Willumeit-Romer R, Dobatkin S, et al. Cytotoxicity of biodegradable magnesium alloy WE43 to tumor cells in vitro: Bioresorbable implants with antitumor activity? *J BioMed Mater Res B Appl Biomater* (2019) 108(1):167–73. doi: 10.1002/jbm.b.34375
- Hakimi O, Ventura Y, Goldman J, Vago R, Aghion E. Porous biodegradable EW62 medical implants resist tumor cell growth. *Mater Sci Eng C Mater Biol Appl* (2016) 61:516–25. doi: 10.1016/j.msec.2015.12.043
- Ismail AAA, Ismail Y, Ismail AA. Chronic magnesium deficiency and human disease; time for reappraisal? *QJM* (2018) 111(11):759–63. doi: 10.1093/qjmed/hcx186
- Anastassopoulou J, Theophanides T. Magnesium-DNA interactions and the possible relation of magnesium to carcinogenesis. Irradiation and free radicals. *Crit Rev Oncol Hematol* (2002) 42(1):79–91. doi: 10.1016/S1040-8428(02)00006-9
- Mendes PMV, Bezerra DLC, Dos Santos LR, de Oliveira Santos R, de Sousa Melo SR, Moraes JBS, et al. Magnesium in Breast Cancer: What Is Its Influence on the Progression of This Disease? *Biol Trace Elem Res* (2018) 184(2):334–9. doi: 10.1007/s12011-017-1207-8
- Vilgelm AE, Johnson DB, Richmond A. Combinatorial approach to cancer immunotherapy: strength in numbers. *J Leukoc Biol* (2016) 100(2):275–90. doi: 10.1189/jlb.5RI0116-013RR
- Al-Lazikani B, Banerji U, Workman P. Combinatorial drug therapy for cancer in the post-genomic era. *Nat Biotechnol* (2012) 30(7):679–92. doi: 10.1038/nbt.2284
- Duenas-Gonzalez A, Candelaria M, Perez-Plascencia C, Perez-Cardenas E, de la Cruz-Hernandez E, Herrera LA. Valproic acid as epigenetic cancer drug: preclinical, clinical and transcriptional effects on solid tumors. *Cancer Treat Rev* (2008) 34(3):206–22. doi: 10.1016/j.ctrv.2007.11.003
- Lee SI, Jeong YJ, Yu AR, Kwak HJ, Cha JY, Kang I, et al. Carfilzomib enhances cisplatin-induced apoptosis in SK-N-BE(2)-M17 human neuroblastoma cells. *Sci Rep* (2019) 9(1):5039. doi: 10.1038/s41598-019-41527-0
- Mori H, Tanaka T, Sugie S, Yoshimi N, Kawamori T, Hirose Y, et al. Chemoprevention by naturally occurring and synthetic agents in oral, liver, and large bowel carcinogenesis. *J Cell Biochem Suppl* (1997) 27:35–41.
- Parveen A, Akash MS, Rehman K, Kyunn WW. Dual Role of p21 in the Progression of Cancer and Its Treatment. *Crit Rev Eukaryot Gene Expr* (2016) 26(1):49–62. doi: 10.1615/CritRevEukaryotGeneExpr.v26.i1.60
- Shamloo B, Usluer S. p21 in Cancer Research. *Cancers (Basel)* (2019) 11(8):1178. doi: 10.3390/cancers11081178
- Levy JMM, Towers CG, Thorburn A. Targeting autophagy in cancer. *Nat Rev Cancer* (2017) 17(9):528–42. doi: 10.1038/nrc.2017.53
- Das CK, Banerjee I, Mandal M. Pro-survival Autophagy: An Emerging Candidate of Tumor Progression through Maintaining Hallmarks of Cancer. *Semin Cancer Biol* (2019) 66:59–74. doi: 10.1016/j.semcancer.2019.08.020
- Abedin MJ, Wang D, McDonnell MA, Lehmann U, Kelekar A. Autophagy delays apoptotic death in breast cancer cells following DNA damage. *Cell Death Differ* (2007) 14(3):500–10. doi: 10.1038/sj.cdd.4402039
- Sui X, Chen R, Wang Z, Huang Z, Kong N, Zhang M, et al. Autophagy and chemotherapy resistance: a promising therapeutic target for cancer treatment. *Cell Death Dis* (2013) 4:e838. doi: 10.1038/cddis.2013.350
- Song S, Tan J, Miao Y, Li M, Zhang Q. Crosstalk of autophagy and apoptosis: Involvement of the dual role of autophagy under ER stress. *J Cell Physiol* (2017) 232(11):2977–84. doi: 10.1002/jcp.25785
- Song S, Tan J, Miao Y, Zhang Q. Crosstalk of ER stress-mediated autophagy and ER-phagy: Involvement of UPR and the core autophagy machinery. *J Cell Physiol* (2018) 233(5):3867–74. doi: 10.1002/jcp.26137
- Corazzari M, Gagliardi M, Fimia GM, Piacentini M. Endoplasmic Reticulum Stress, Unfolded Protein Response, and Cancer Cell Fate. *Front Oncol* (2017) 7:78. doi: 10.3389/fonc.2017.00078
- Ron D, Hubbard SR. How IRE1 reacts to ER stress. *Cell* (2008) 132(1):24–6. doi: 10.1016/j.cell.2007.12.017
- Zhan T, Rindtorff N, Boutros M. Wnt signaling in cancer. *Oncogene* (2017) 36(11):1461–73. doi: 10.1038/onc.2016.304
- Krishnamurthy N, Kurzrock R. Targeting the Wnt/beta-catenin pathway in cancer: Update on effectors and inhibitors. *Cancer Treat Rev* (2018) 62:50–60. doi: 10.1016/j.ctrv.2017.11.002
- Yuan J, Dong X, Yap J, Hu J, The MAPK. and AMPK signalings: interplay and implication in targeted cancer therapy. *J Hematol Oncol* (2020) 13(1):113. doi: 10.1186/s13045-020-00949-4
- Marampon F, Ciccarelli C, Zani BM. Biological Rationale for Targeting MEK/ERK Pathways in Anti-Cancer Therapy and to Potentiate Tumour Responses to Radiation. *Int J Mol Sci* (2019) 20(10):2530. doi: 10.3390/ijms20102530

SUPPLEMENTARY MATERIAL

The Supplementary Material for this article can be found online at: <https://www.frontiersin.org/articles/10.3389/fonc.2020.589112/full#supplementary-material>

40. Salaroglio IC, Mungo E, Gazzano E, Kopecka J, Riganti C. ERK is a Pivotal Player of Chemo-Immune-Resistance in Cancer. *Int J Mol Sci* (2019) 20(10):2505. doi: 10.3390/ijms20102505
41. Moore C, Palau VE, Mahboob R, Lightner J, Stone W, Krishnan K. Upregulation of pERK and c-JUN by gamma-tocotrienol and not alpha-tocopherol are essential to the differential effect on apoptosis in prostate cancer cells. *BMC Cancer* (2020) 20(1):428. doi: 10.1186/s12885-020-06947-6
42. Xu Y, Tao Z, Jiang Y, Liu T, Xiang Y. Overexpression of BPIFB1 promotes apoptosis and inhibits proliferation via the MEK/ERK signal pathway in nasopharyngeal carcinoma. *Int J Clin Exp Pathol* (2019) 12(1):356–64.
43. Rodriguez-Aznar E, Wiesmuller L, Sainz B Jr., Hermann PC. EMT and Stemness-Key Players in Pancreatic Cancer Stem Cells. *Cancers (Basel)* (2019) 11(8):1136. doi: 10.3390/cancers11081136
44. Xiang Y, Guo Z, Zhu P, Chen J, Huang Y. Traditional Chinese medicine as a cancer treatment: Modern perspectives of ancient but advanced science. *Cancer Med* (2019) 8(5):1958–75. doi: 10.1002/cam4.2108
45. Xie Y, Li P, Gao Y, Gu L, Chen L, Fan Y, et al. Reduced E-cadherin expression is correlated with poor prognosis in patients with bladder cancer: a systematic review and meta-analysis. *Oncotarget* (2017) 8(37):62489–99. doi: 10.18632/oncotarget.19934
46. Liao TT, Yang MH. Revisiting epithelial-mesenchymal transition in cancer metastasis: the connection between epithelial plasticity and stemness. *Mol Oncol* (2017) 11(7):792–804. doi: 10.1002/1878-0261.12096
47. Li Y, Lin K, Yang Z, Han N, Quan X, Guo X, et al. Bladder cancer stem cells: clonal origin and therapeutic perspectives. *Oncotarget* (2017) 8(39):66668–79. doi: 10.18632/oncotarget.19112
48. Yin B, Zeng Y, Liu G, Wang X, Wang P, Song Y. MAGE-A3 is highly expressed in a cancer stem cell-like side population of bladder cancer cells. *Int J Clin Exp Pathol* (2014) 7(6):2934–41.
49. Venhuizen JH, Jacobs FJC, Span PN, Zegers MM. P120 and E-cadherin: Double-edged swords in tumor metastasis. *Semin Cancer Biol* (2019) 60:107–20. doi: 10.1016/j.semcancer.2019.07.020
50. Wang D, Jing Y, Ouyang S, Liu B, Zhu T, Niu H, et al. Inhibitory effect of valproic acid on bladder cancer in combination with chemotherapeutic agents in vitro and in vivo. *Oncol Lett* (2013) 6(5):1492–8. doi: 10.3892/ol.2013.1565
51. Liu S, Liang B, Jia H, Jiao Y, Pang Z, Huang Y. Evaluation of cell death pathways initiated by antitumor drugs melatonin and valproic acid in bladder cancer cells. *FEBS Open Bio* (2017) 7(6):798–810. doi: 10.1002/2211-5463.12223
52. Yang X, Liu J, Liang Q, Sun G. Valproic acid reverses Sorafenib resistance through inhibiting activated Notch/Akt signaling pathway in HCC. *Fundam Clin Pharmacol* (2020). doi: 10.1111/fcp.12608
53. Iannelli F, Zotti AI, Roca MS, Grumetti L, Lombardi R, Moccia T, et al. Valproic Acid Synergizes With Cisplatin and Cetuximab in vitro and in vivo in Head and Neck Cancer by Targeting the Mechanisms of Resistance. *Front Cell Dev Biol* (2020) 8:732. doi: 10.3389/fcell.2020.00732

Conflict of Interest: The authors declare that the research was conducted in the absence of any commercial or financial relationships that could be construed as a potential conflict of interest.

Copyright © 2020 Li, Yu, Shi, Cao, Liu, Hao, Ren, Qin, Huang and Wang. This is an open-access article distributed under the terms of the Creative Commons Attribution License (CC BY). The use, distribution or reproduction in other forums is permitted, provided the original author(s) and the copyright owner(s) are credited and that the original publication in this journal is cited, in accordance with accepted academic practice. No use, distribution or reproduction is permitted which does not comply with these terms.



Volatile Anesthetics Regulate Anti-Cancer Relevant Signaling

Jiaqiang Wang^{1†}, Chien-shan Cheng^{2,3†}, Yan Lu^{4†}, Shen Sun^{1*} and Shaoqiang Huang^{1*}

¹ Department of Anesthesiology, The Obstetrics and Gynecology Hospital of Fudan University, Shanghai, China,

² Department of Integrative Oncology, Fudan University Shanghai Cancer Center, Shanghai, China, ³ Department of Oncology, Shanghai Medical College, Fudan University, Shanghai, China, ⁴ Department of Anesthesiology, Shanghai First Maternity and Infant Hospital, Tongji University School of Medicine, Shanghai, China

OPEN ACCESS

Edited by:

Jiang-Jiang Qin,
Chinese Academy of Sciences (CAS),
China

Reviewed by:

Cheng Zhou,
Sichuan University, China
Qiyang Shou,
Zhejiang Chinese Medical University,
China

*Correspondence:

Shen Sun
sunshen1980@126.com
Shaoqiang Huang
timrobbins@163.com

[†]These authors have contributed
equally to this work

Specialty section:

This article was submitted to
Pharmacology of Anti-Cancer Drugs,
a section of the journal
Frontiers in Oncology

Received: 26 September 2020

Accepted: 22 January 2021

Published: 26 February 2021

Citation:

Wang J, Cheng C-s, Lu Y, Sun S and
Huang S (2021) Volatile Anesthetics
Regulate Anti-Cancer Relevant Signaling.
Front. Oncol. 11:610514.
doi: 10.3389/fonc.2021.610514

Volatile anesthetics are widely used inhalation anesthetics in clinical anesthesia. In recent years, the regulation of anti-cancer relevant signaling of volatile anesthetics has drawn the attention of investigators. However, their underlying mechanism remains unclear. This review summarizes the research progress on the regulation of anti-cancer relevant signaling of volatile anesthetics, including sevoflurane, desflurane, xenon, isoflurane, and halothane *in vitro*, *in vivo*, and clinical studies. The present review article aims to provide a general overview of regulation of anti-cancer relevant signaling and explore potential underlying molecular mechanisms of volatile anesthetics. It may promote promising insights of guiding clinical anesthesia procedure and instructing enhance recovery after surgery (ERAS) with latent benefits.

Keywords: volatile anesthetics, inhalation anesthesia, anti-cancer, volatile anesthesia, mechanism

INTRODUCTION

Cancer describes diseases characterized by uncontrolled cell division and tissue invasion. Cancer hallmarks include maintaining proliferation signals, evading cell death, resisting treatment, enabling invasion, inducing angiogenesis, and activating metastasis (1). Cancer treatment strategies include traditional methods, such as surgery, chemo- and radio-therapy; and newer methods such as a ligand or receptor-based target therapy, stem cell therapy, and various forms of novel drug delivery systems (2). Until now, cancer is still an insurmountable problem worldwide, leading to high morbidity and mortality (3).

Volatile anesthetics, including sevoflurane, desflurane, xenon, isoflurane, halothane and others, are used for inhalational anesthesia in clinical practice. Volatile anesthetics target specific central nervous system receptors to perform anesthetic functions, such as the neuronal GABA_A receptor, NMDA receptor and glutamate receptor subtypes. Volatile anesthetics can also affect cells by changing transcriptional elements, thereby changing specific characteristics of cell function. Previous studies have shown that volatile anesthetics have organ protection effects (4, 5). Recently, researchers have focused on the regulation of anti-cancer relevant signaling of volatile anesthetics on different kinds of cancer *in vitro*, *in vivo*, and clinical studies, but the specific mechanism remains unclear.

Everything has two sides. Some studies reported that sevoflurane (6–12), isoflurane (7, 10, 11) and halothane (13–15) may play tumor-promoting effects. We compared the articles and found that the controversy may come from different cancer types, cell lines, incubation concentrations and

other conditions. More research on differences should be studied to discover potential conditions for volatile anesthetics and suitable cancer types. Analysis articles aimed at comparing opposite findings are also welcome. More *in vivo* and clinical studies should be conducted to further determine the regulation of anti-cancer relevant signaling of volatile anesthetics to guide clinical anesthesia procedures.

This review summarized the regulation of anti-cancer relevant signaling, including anti-proliferation, anti-migration and invasion, anti-metastasis, apoptosis-inducing effects, and the underlying mechanisms of volatile anesthetics. It may be instructive for future clinical inhalation anesthesia and beneficial for ERAS.

REGULATION OF ANTI-CANCER RELEVANT SIGNALING

Sevoflurane

Sevoflurane ($C_4H_3F_7O$, **Table 1**) is one of the most commonly used volatile anesthetics. It is a colorless and sweet-smelling inhalation anesthetic used to induce and maintain general anesthesia. For induction and maintenance of general anesthesia, sevoflurane concentration ranges from 0.5%–5% and less than 4%, respectively. In the electrophysiological study of neurons and recombinant receptors, sevoflurane is a positive allosteric modulator of the GABA_A receptors (16–18). However, it can also act as a NMDA receptor antagonist (19), enhancing glycine receptor electro-currents (20) and inhibiting nAChR (21) and 5-HT₃ receptor currents (22, 23). Sevoflurane is particularly non-irritating to the respiratory tract, so it is particularly suitable for asthma patients' anesthesia.

SEVOFLURANE AND miRNAs

miRNAs are single-stranded, highly conserved small non-coding RNAs. More and more studies have shown that miRNAs affect cancer proliferation, metastasis, and invasion. In addition, miRNA expression can also determine the pathogenesis, diagnosis, and diseases prognosis of cancer (24). Recently, miRNAs are proposed to function both as oncogenes and tumor suppressors by regulating various target gene expressions (25, 26). Oncogenes are genes that

may cause cancer and are often mutated and expressed at high cancer cell levels. On the other hand, tumor suppressor genes, or anti-oncogenes, are genes that protect cells from malignant transformation (27). Recent studies have found that Sevoflurane can regulate miRNA expression.

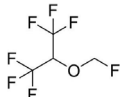
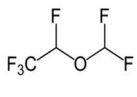

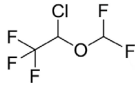
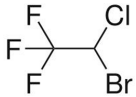
miR-203 has been implicated to play an essential role cancer proliferation regulation and are of potential diagnostic value. It is reported that miR-203 can act both as an oncogene and tumor suppressor gene in the development of different types of cancers (28–30). Fan and colleagues treated colorectal cancer cells (CRC, cell lines: SW620 and HCT116) with 1%, 2%, and 4% sevoflurane for 6 h to investigate the regulation of anti-cancer signaling of sevoflurane in CRC cell lines. The study demonstrated a proliferation suppression effect of sevoflurane, along with its migration and invasion inhibitory effects, by regulating the ERK/MMP-9 pathway through miR-203/Robo1 (31). In another study, MDA-MB-231 and MCF-7 breast cancer cells were exposed to 2% sevoflurane for 6 h. Results demonstrated that clinical concentration of sevoflurane could significantly suppress the proliferation of breast cancer cells *via* up-regulation of miR-203 (32).

miRNA-637 is as a tumor suppressor effect and plays crucial role in carcinogenesis and cancer progression (33–35). Emerging evidence suggested that miRNA-637 regulates the migration and invasion of glioma cells (36). In glioma *in vitro* models, U251 cells were treated with sevoflurane (1.7%, 3.4%, 5.1%) for 6 h. Yi and colleagues reported that sevoflurane inhibited glioma migration and invasion by up-regulating miRNA-637 and suppression of downstream Akt1 expression and activity (37).

In lung cancer, the regulation of anti-cancer signaling of sevoflurane by regulating miRNA has also been investigated (38). A study aimed at elucidating sevoflurane's effect on the miRNA in lung cancer cells showed that A549 cells pretreated with 3% sevoflurane for 0.5 h caused an increase in apoptosis, thereby significantly reduced the risk of cancer cell metastasis and improving patients' postoperative survival rate. Sevoflurane pretreatment up-regulated tumor suppressor miRNA-21, miRNA-221 and down-regulated oncogenic miRNA-34a in A549 cancer cells (39).

miR-124 is widely expressed in the nervous system (40). Rho-associated coiled-coil-containing protein kinase (ROCK1) plays essential roles in regulating tumorigenesis, cell apoptosis, invasion and migration (41). As reported by Cao et al., 4.1% sevoflurane pretreatment for 4 h inhibits glioma proliferation,

TABLE 1 | The volatile anesthetics.

Volatile Anesthetics	Sevoflurane	Desflurane	Xeon	Isoflurane	Halothane
Chemical Formula	$C_4H_3F_7O$	$C_3H_2F_6O$	Xe	$C_3H_2ClF_5O$	$C_2HBrClF_3$
CAS ID	28523-86-6	57041-67-5	20222-53-1	26675-46-7	151-67-7
Molecular Formula					

invasion, and metastasis in U251 and U87 cells through enhancing miR-124-3p level, thereby suppressed tumor malignancy-related ROCK1 signaling pathway (42).

SEVOFLURANE AND MMPs

Matrix metalloproteinases (MMPs) are proteolytic enzymes that contribute to the degradation of extracellular matrix and basement membrane and are associated with cancer cell invasion. Among them, MMP-2 and MMP-9 are remarkably up-regulated in malignant tumors and contribute to cancer invasion (43).

Compared with normal brain tissue, MMP-2 is highly expressed in gliomas. MMP-2 has shown multiple effects in tumor progression, and promoted glioma malignancies (44, 45). Research by Hurmath et al. suggested that 2.5% sevoflurane incubation for 1.5 h suppressed the migration capability of U87MG glioma cells by down-regulation MMP-2 activity (46).

Degrading extracellular matrix is considered first step of tumor cell progression. Prior to tumor invasion into blood vessels or lymph nodes, tumor cells degrade the extracellular matrix, such as MMP-9 (47). Research evidence showed that in an *in vitro* reperfusion injury model, preconditioning with 2.2% sevoflurane for 45 min reduced MMP-9 release from human neutrophils by interfering with its downstream CXCR2 and its upstream PKC. By down-regulating MMP-9, sevoflurane suppressed MC-38 colon cancer cells migration (48).

Sevoflurane also demonstrated growth and invasion inhibitory effects in lung adenocarcinoma A549 cell line (49). The mechanism of its growth inhibition may be related to the synergistic down-regulation of X-linked inhibitor of apoptosis (XIAP) and survivin. Furthermore, its synergistic effect of invasion inhibition may be related to the down-regulation of MMP-2 and MMP-9.

SEVOFLURANE AND CELL CYCLE

Abnormal cell proliferation is most related to the influence of cell cycle regulation (50). 2.5% Sevoflurane treatment for 4 h significantly inhibited A549 cells' proliferation, invasion and induce cellular apoptosis and arrest the cell cycle at the G2/M phase (51). Furthermore, 2% sevoflurane preconditioning for 6 h possessed anti-proliferative and pro-apoptotic effects, possibly related to the down-regulation of XIAP and survivin expression and caspase-3 activation. Cell cycle arrest in the G2/M phase is associated with the down-regulation of cyclin A, cyclin B1, and cdc2 kinase expression. Sevoflurane can significantly inhibit breast cancer cells' proliferation by blocking the cell cycle in the G1 phase (32).

SEVOFLURANE AND CELL APOPTOSIS

In colonic cancer, 3% sevoflurane incubation for 1 or 2 h induced late apoptosis in Caco-2 cells *in vitro* (52). The study reported

that sevoflurane intervention increases CYP2E1, caspase-3, and p53 expression. Furthermore, sevoflurane also facilitates an early increase of *de novo* ceramide synthesis. These results suggested that sevoflurane acts on both signaling pathways and metabolic pathways *in vitro*.

In neck squamous cell carcinoma (HNSCC) cancer, 2% and 4% sevoflurane pretreatment for 2, 4, 6, and 8 h inhibited proliferation, invasion, migration, and induced cellular apoptosis of FaDu and CAL-27 cell lines (53). The anti-proliferation effect of sevoflurane was associated with the downregulation p-Akt expression, and the cell apoptosis effect was associated HIF-1 α activation, which regulated the Fas/FasL signaling pathway.

SEVOFLURANE AND HIF-1 α

The HIF is a family of transcription factors that involved in crucial aspects of cancer biology, such as cell proliferation, angiogenesis, metabolomic adaptation, and metastasis (54). Sevoflurane preconditioning (1.5%, 2.5%, or 3.5% sevoflurane incubation of A549 cells for 4 h) can inhibit the proliferation and invasion of lung cancer A549 cells induced by hypoxia, which may be related to the down-regulation of HIF-1 α and its downstream genes XIAP, survivin, fascin, and HPA (55). Under hypoxia conditions, HIF-1 α activation is dependent on the activation of the p38 MAPK signaling pathway. Also, the study proved that sevoflurane partially reversed the hypoxia induced p38 MAPK activity.

Activation of HIF-1 α by sevoflurane regulates the Fas/FasL signaling pathway to exert cell apoptosis as demonstrated above (43).

SEVOFLURANE AND VEGF

Hypoxia regulates transcriptional factor HIF-1, which regulates hypoxia-inducible angiogenic factor VEGF (56). VEGF is an important survival factor for endothelial and tumor cells. In tongue squamous cell carcinoma cell (TSCC), SCC-4 cells incubated with 4.1% sevoflurane for 24 and 72 h was shown attenuated VEGF level *via* increasing the DNA methylation of the VEGF promoter region *in vitro* (37).

SEVOFLURANE AND Wnt/ β -CATENIN SIGNALING

Sevoflurane was found to significantly inhibited the growth of a panel of chronic myeloid leukemia (CML) cell lines (KCL22, K562, KU812, LAMA84 and KBM-7) (57). It also inhibited proliferation, differentiation and self-renewal capacities of CML CD34 cells. Mechanistically, it is purposed that 2%, 4%, or 8% sevoflurane preconditioning for 24 h dose-dependently decreases β -catenin and c-Myc expressions and activities in K562 and CML CD34 cells. The findings also reveal the Wnt/ β -catenin

pathway may be important targets of volatile anesthetics in cancer treatment.

SEVOFLURANE AND PLATELETS ACTIVATION

It has been demonstrated that activated platelets contribute to tumor cells' metastatic ability and protect circulating tumor cells from immune cells (58, 59). Furthermore, surgery stress potentiates platelets activation. Thus, a promising therapeutic strategy of preventing platelets-induced metastasis during cancer surgery procedure is much needed. Previous study suggested that sevoflurane attenuates platelet activation in lung cancer patients by reducing GPIIb/IIIa, CD62P, and PAR levels and these effects are further validated *in vitro*. It is indicated that sevoflurane at 1 MAC reduces platelets-induced invasive potential of lung cancer A549 cells through decreasing platelets activity (60).

Desflurane

Desflurane ($C_3H_2F_6O$, **Table 1**) is widely used for anesthesia maintenance in contemporary clinical work. Characterized by low blood solubility, it functions as the fastest in acting and revival of volatile anesthetics. Desflurane is prohibited for anesthesia induction in infants and young children due to its potential of causing adverse reactions.

DESFLURANE AND MMPs

In an *in vitro* reperfusion injury model, MC-38 colon cancer cells were incubated with 6% of desflurane for 45 min. It was demonstrated that desflurane could reduce the deliverance of MMP-9 by intervening downstream of the CXCR2 pathway. By down-regulating MMP-9, desflurane reduced the degradation of matrigel and the migration of colorectal cancer cells (48).

DESFLURANE AND DFS

One study conducted a historical cohort study in which all patients received the primary cytoreductive surgery for stage III epithelial ovarian cancer, and the evaluation factor was disease-free survival (DFS). Studies have found that, compared with other volatile anesthetics, desflurane decreased the relative risk of cancer recurrences and is associated with improved DFS after surgery (61).

DESFLURANE AND THE IMMUNE SYSTEM

According to a randomized trial, during the perioperative period, desflurane anesthesia for breast cancer surgery can induce an

adequate immune response in terms of maintaining the ratio of CD4(+)/CD8(+) T cells (62). Regarding leukocytes and NK cells, desflurane anesthesia's adverse immune response is less than that of propofol.

Xenon

Xenon (Xe, **Table 1**), is the most stable gas of noble gas, which targets the glycine binding site of the NMDA receptor and the KATP channel. Xenon gas can dissolve in the fat of cells, causing cell anesthesia and swelling, thereby temporarily stopping the function of nerve endings. Owing to that xenon does not increase the sensitivity of myocardium to catecholamines-induced arrhythmia and it inhibits myocardial contraction but with minimal inhibitory effect on cardiovascular function, xenon is suitable for and widely used in cardiovascular surgery.

XENON AND RANTES

Regulated on activation, normal T cell expressed and secreted (RANTES), also known as CCL5 and functioning on receptor CCR5, is a cytokine that continues to increase in breast cancer subtypes (63) and is associated with promoting breast cancer metastasis and progression (64, 65). Ash et al. investigated the effect of xenon on migration and oncogene expression in human breast adenocarcinoma cells (66). It was demonstrated that 70% xenon incubation for 20 min inhibited the migration of estrogen receptor-positive (MCF-7) and negative (MDA-MB-231) breast cancer cells and reduce the pro-angiogenic factor's release.

XENON AND PMCA

It is reported that xenon, at partial pressures ranging from 0.5 to 1.5 atm (equivalent to 0.5 to 1.6 MAC) for 30 min, can inhibit the pumping of plasma membrane Ca^{2+} -ATPase (PMCA) in synaptic plasma membrane vesicles in rat C6 glioma cells. This mechanism may inhibit the physiological functions of cancer cells (67).

Owning to the inertness of xenon, it can only be extracted and liquefied, but cannot be synthesized artificially. Therefore, it is costly to utilize xenon. However, with the development of novel manufactured techniques, xenon is gradually adopted in various countries. Although it has not been used clinically, it is suggested that xenon may regulate anti-cancer relevant signaling and is worthy of further exploration.

Isoflurane

Isoflurane ($C_3H_2ClF_5O$, **Table 1**) is colorless and of pungent odor. It is used for anesthesia maintenance and has the properties of reducing pain sensitivity and relaxing muscles. Isoflurane may bind to GABA and Glycine receptors, but has different effects. However, the clinical application of isoflurane is gradually

TABLE 2 | Regulation of anti-cancer relevant signaling of volatile anesthetics.

Volatile Anesthetics	Cancer Type	Cell Line	Treatment	Effects	Mechanisms	References
Sevoflurane	Colorectal cancer	SW620; HCT116	Concentration:2.5%; Time: 90 min	Inhibition of cell migration and invasion	Addressing ERK/MMP-9 signaling pathway by regulating miR-203/Robo1 expression	
	Glioma	U87MG	Concentration:2.5%; Time: 24 h	Inhibition of cell migration	MMP-2 activity↓	Hurmath FK et al. (46)
	Lung adenocarcinoma	A549	Concentration:2.5%; Time: 24 h	Inhibition of cell growth and invasion	XIAP↓, survivin↓, MMP-2↓, MMP-9↓	Liang H et al. (49)
	CML	KCL22, K562, KU812, LAMA84 and KBM-7	Concentration:2%, 4%, 8%; Time: 24 h	Inhibition of cell growth, proliferation, differentiation and self-renewal capacities	Inhibiting Wnt/β-catenin in a p38 MAPK-independent manner	Ruan XG et al. (57)
	Lung cancer	A549	Concentration: 1MAC	Suppression of platelets-induced invasion	Decreasing platelets activity <i>via</i> GPIIb/IIIa, CD62P, and PAR levels	Liang H et al (55)
		A549	Concentration: 1.7%, 3.4%, and 5.1%; Time: 2, 4, 6 h	Inhibition of cell proliferation, induction of apoptosis, and block of cell cycle progression	XIAP↓, survivin↓, activating caspase-3, cyclin A↓, cyclin B1↓, cdc2↓	Liang H et al. (51)
		A549	Concentration: 1.5%, 2.5%, 3.5%; Time: 4 h	Suppression of hypoxia-induced growth and metastasis	HIF-1α↓, XIAP↓, survivin↓, fascin↓, HPA↓, p38 MAPK activity↑	Liang H et al. (60)
		A549	Concentration: 3% Time: 30 min	Increase of cell apoptosis	miRNA-155↓ miRNA-146a↑ miRNA-223↑	Wang L et al. (39)
	Glioma	U251; U87	Concentration: 4.1% Time: 4 h	Inhibition of cell proliferation, invasion and migration	miR-124-3p↑ suppression of ROCK1 signaling pathway	Gao C et al. (42)
	HNSCC	CAL-27; FaDu	Concentration: 2%, 4% Time: 2,4,6,8 h	Inhibition of cell proliferation, invasion and migration, and induction of cell apoptosis	Anti-proliferative effect: p-Akt↓ Cell apoptosis: activation of HIF-1α which regulates Fas/FasL signaling pathway	Yang YQ et al. (53)
	TSCC	SCC-4	Concentration: 4.1% Time: 24,72 h	Inhibition of tumor angiogenesis	Attenuate the hypoxia-induced VEGF level <i>via</i> increasing the DNA methylation	Lu Y et al. (37)
	Mouse colon carcinoma	MC-38	Concentration: 2.2% Time:45 min	Reduction in the invasion of CRCs	Impairment of neutrophil MMP-9 release and interference with pathways downstream of CXCR2, but upstream of PKC	Muller-Edenborn, B et al. (48)
	Breast cancer	MDA-MB; MCF-7	Concentration: 2% Time: 6 h	Suppression of cell proliferation	miR-203↑	Liu JY et al. (32)
	Colonic cancer	Caco-2	Concentration: 3% Time: 2 h	Induction of late apoptosis	Induction of p53-dependent apoptosis	S. KVOLIK et al. (52)
Desflurane	Mouse colon carcinoma	MC-38	Concentration: 6% Time: 45 min	Reduction in the invasion of CRCs	Impairment of neutrophil MMP-9 release and interference with pathways downstream of CXCR2, but upstream of PKC	Muller-Edenborn, B et al. (48)
	Epithelial ovarian cancer	Not mentioned	Clinical concentration	Improved DFS	Improved DFS	Elias KM et al. (61)
	Breast cancer	Not mentioned	Concentration: 3%–7%	Keeps the immune system stable	Preservation of CD4(+)/CD8(+) T cell ratio	
Xenon	Rat glioma	C6	Concentration:0.5–1 atm (0.5–1.6 MAC); Time:	Inhibition of physiological functions of the cancer cells	PMCA activity↓	Singh G et al. (67)
	Breast adenocarcinoma	MDA-MB-231; MCF-7	Concentration:70%; Time: 1, 3, 5 h	Inhibited cell migration and secretion of a pro-angiogenesis factor	RANTES↓	Ash SA et al. (66)
Isoflurane	Rat glioma	C6	Concentration:0.5%–4%; Time: 1–24 h	Enhancing glutamate uptake <i>via</i> increasing the expression and activity of EAAT3	Enhancing neurotoxicity in C6 cells <i>via</i> PKC– and PI3K–independent pathways	Huang Y et al. (68)
	Laryngeal papillomas	Laryngeal papillomas cells	Concentration: 1.4%; Time: 0.5 h	Inhibited cell proliferation and apoptosis evasion	Reduces COX2 enhancement and PGE ₂ release by inhibiting the activation of p38 MAPK	Ren HB et al. (70)
	Hepatic carcinoma	Hepatic carcinoma cells	Concentration:2 mg/ml; Time: 48 h	Inhibited cell growth and promoted cell apoptosis, inhibited cancer migration and invasion	Proapoptotic genes expression↑: caspase-3; caspase-8, anti-apoptotic mRNA expression↓: Bcl-2	Hu J et al. (71)

(Continued)

TABLE 2 | Continued

Volatile Anesthetics	Cancer Type	Cell Line	Treatment	Effects	Mechanisms	References
Halothane	Mouse sarcoma	Mouse heteroploid strain; Mouse sarcoma I strain	Concentration: 0%–3.2%; Time: 4 days	Increase of glucose uptake and lactate output and inhibition of oxygen consumption	and Bax; regulation of NF- κ B activity and the PI3K/AKT signaling pathway Mitochondrion	Fink B R et al. (75)
	Rat hepatoma	HTC	Concentration: 0.1%–5.0%; Time: 24 h	Inhibition of cell multiplication and cell growth	Cell replication	Jackson S H, et al. (76)
	Rat hepatoma	HTC	Concentration: 0.1%–5.0%; Time: 24 h	Inhibited the synthesis of DNA and cell replication	DNA synthesis	Jackson S H, et al. (77)
	Mouse neuroblastoma	N2A	Concentration: 100 and 1000 ppm Time: 4, 12, 24 h	Disruption of actin distribution; microspikes lost	Morphology changes	Uemura E, et al. (79)
	Breast cancer		Clinical halothane-nitrogen-oxygen concentration	Halothane anesthesia improved the survival rates of patients	Pituitary- adrenal cortex system; carcinemia development; tumor immunity	Fried I A (80)
	Melanoma	SK-MEL-37	Concentration: 4% Time: 3, 6, 12 or 24 h	Affect the progression of tumor cell metastasis	Tumor cell metastasis; ICAM-1	Azuma K et al. (83)
	Rat Glioma	C6	Concentration: 0.5%, 1%, 2%; Time: 8 min	Inhibited rat glioma cell growth	Morphology changes via RhoA, ERK, and Akt activation	
	Lung carcinoma	A549	Concentration: 1.5 and 2.1 mM; Time: 8 min	Reduction of viability; suppression of mitotic activity; disturbances of nuclear and nucleolar structures	Cellular structure changes	Stephanova, E et al. (81)
	Mouse neuroblastoma	NB2a	Concentration: 0.3%–2.1%; Time: up to 72 h	Inhibited neuroblastoma cell differentiation and neurite extension; abolished microspike formation	Cellular morphological differentiation	HINKLEY R E et al. (82)
	Rat glioma cells; Rat neuroblastoma cells	C6; B104	Concentration: 0.5%–1.75%; Time: 30 min	Might affect physiological functions of cancer cells	Inhibited PMCA activity	Singh, G et al. (67)
	Human colon carcinoma, larynx carcinoma, pancreatic carcinoma cells	Caco-2; HEP-2; MIA PaCa-2; SW-620	Concentration: 1.5%; Time: 2, 4, 6 h	Growth suppression	Decrease in DNA, RNA and protein synthesis; DNA fragmentation	S. Kvolik et al. (78)

replaced by sevoflurane and desflurane due to its potential complication of inducing epileptiform EEG.

ISOFLURANE AND GLUTAMATE

Glutamate is the primary excitatory neurotransmitter and acts as an effective neurotoxin when overexcited. Therefore, the extracellular glutamate concentration must be kept low to carry out neurotransmission and prevent damage effectively. Isoflurane incubation of C6 glioma cells can increase the expression and activity of type 3 excitatory amino acid transporter (EAAT3) through a pathway that depends on PKC and PI3K, thereby exhibiting higher glutamine in a time- and concentration-dependent manner (68). In addition, it has been reported that potential treatments targeting glutamine metabolism can be used to treat many types of cancer (69).

ISOFLURANE AND COX-2

Cyclooxygenase (COX), also known as prostaglandin H₂ (PGH₂) synthase, is an essential enzyme for converting arachidonic acid to PGH₂. Studies have shown that inhibition of COX is related to tumor behavior. A research report pointed out that 1.4% isoflurane treatment for 0.5 h significantly reduced the enhancement of COX-2 and the release of PGE₂ of human laryngeal papilloma cells. By inhibiting the activation of p38 MAPK, isoflurane inhibited cell proliferation and apoptosis evasion (70).

ISOFLURANE AND CELL APOPTOSIS

An *in vitro* and *in vivo* study reported that isoflurane incubation (2 mg/ml, 48 h) could not only inhibited liver cancer growth, but also decreased cell viability in liver cancer patient. The specific

mechanism involves upregulating the expression levels of proapoptotic genes (caspase-3 and caspase-8) and downregulating anti-apoptotic (Bcl-2 and Bax) mRNA expression. Furthermore, isoflurane treatment inhibited migration and invasion of hepatic carcinoma cells. The molecular mechanisms underlying the tumor aggressiveness suppressive role of isoflurane involved regulation of NF- κ B activity, and the PI3K/AKT signaling pathway (71).

Halothane

Halothane (C₂HBrClF₃, **Table 1**) is liquid anesthetic with colorless, clear, volatile and scented properties. It is unstable in nature and can be slowly decomposed by light and heat. Similar to other volatile anesthetics, halothane performs its anesthetic function by activating GABA-A, glycine, and NMDA receptors (72–74).

HALOTHANE AND ENERGY METABOLISM

In the presence of halothane, glucose uptake and lactate output increase and oxygen consumption is inhibited, 0.9% halothane incubation showed 50% inhibition in the heteroploid strain and 0.35% halothane in the mouse sarcoma I strain. Also, population growth and high-energy phosphate production are diminished. A variety of biochemical mechanisms implicating the mitochondrial mechanisms may be involved (75).

HALOTHANE AND DNA OR RNA SYNTHESIS

Jackson et al. reported that halothane treatment varied in 0.1%–5.0% for 24 h was found to inhibit cell multiplication and cell growth in rat hepatoma cells, with 2.5% halothane pretreatment for 6 h being the most significant (76). Another study suggested that 0.1%–5.0% halothane preconditioning for 2 h inhibited the incorporation of extracellular thymidine into DNA, thus inhibiting DNA synthesis on hepatoma HTC cells (77).

Studies on cytotoxicity and anti-proliferative effects indicate that the anti-tumor ability of inhaled anesthetics may be halothane > sevoflurane > isoflurane. In human colon cancer (Caco-2), laryngeal cancer (HEp-2), and poorly differentiated cells from lymph node metastasis of colon carcinoma (SW-620), 1.5% halothane preconditioning for 2, 4, and 6 h showed significantly growth inhibitory effect. Among the cell lines studied, halothane significantly reduced the DNA and RNA synthesis in Caco-2 and Hep-2 cells. Furthermore, decrease in DNA, RNA and protein synthesis were observed in Caco-2 and Hep-2 cells. In SW620 cells, protein synthesis were decreased. A DNA fragmentation was observed in MIA PaCa-2 and Caco-2 cells (78).

HALOTHANE AND MORPHOLOGY

In a study, cultured neuroblastoma cells were incubated of halothane (100 or 1,000 ppm) for 4, 12, or 24 h *in vitro*.

Exposure to halothane resulted in significant changes in the actin distribution pattern of neuroblastoma cells, and the cells exhibited characteristic morphological changes (79).

A clinical study showed that the type of anesthesia influenced the end results of therapy of cancer patients, the survival rates of patients receiving halothane anesthesia were much higher than ether-anaesthetized ones. The mechanism may involve influences of anesthetics on the pituitary-adrenal cortex system and carcinoma development and the role of immunity in tumor cell implantation and growth of metastases (80).

It is reported that 1.5 and 2.21 mM halothane incubation induced genotoxic and cytotoxic effects in lung cancer A549 cells *in vitro*. Consequences of the regulation of anti-cancer relevant effects involved reducing cell viability, inhibiting mitotic activity, and destroying the nucleus and nucleolus structure (81).

Investigations of volatile anesthetics on cellular morphological differentiation unveiled that 0.3%–2.1% halothane preconditioning up to 72 h inhibited neuroblastoma cells (clone NB2a) differentiation, the inhibition of neurite extension dose dependently and virtually abolished microspike formation even at the lowest concentration incubated. The mechanism was demonstrated that halothane inhibited neurite extension and abolished microspike formation (82).

HALOTHANE AND ICAM-1

Intercellular adhesion molecule 1 (ICAM-1) is a cell surface glycoprotein commonly expressed on endothelial cells and immune cells. Recent studies have reported that ICAM-1 is expressed in several tumors, and high expression has been positively correlated with metastatic potential. In human melanoma SK-MEL-37 cells, 4% halothane incubation for 3, 6, 12, or 24 h was demonstrated to perform lower ICAM-1 expression. Thus it was concluded that halothane possessed tumor metastasis inhibiting property by down-regulating ICAM-1 expression *in vitro* (83).

HALOTHANE AND PMCA

The plasma membrane Ca²⁺-ATPase (PMCA), is a ubiquitously expressed Ca²⁺ pump that releases Ca²⁺ from the calcium reservoir to the cytoplasm, regulating physiological functions including cell movement, growth and differentiation. Halothane, at concentration ranging from 0.5% to 1.75% (0.5 to 1.6 MAC), significantly inhibited plasma membrane vesicles Ca²⁺ uptake dose-dependently in rat C6 glioma cells, B104 neuroblastoma cells and PC12 pheochromocytoma cells (67).

DISCUSSION

Recent studies have shown that volatile anesthetics regulate of anti-cancer relevant signaling in human cancers. Specifically,

Anti-cancer Property of Volatile Anesthetics

Sevoflurane	Desflurane	Xenon	Isoflurane	Haloflurane
MMP-9↓;MMP-2↓	MMP-9↓	PMCA activity ↓	COX ₂ ↓	Mitochondrion
XIAP↓;Survivin↓;	DFS↑	RANTES↓	PGE ₂ ↓	Cell replication
fascin ↓; HPA ↓	CD4(+)/CD8(+)		capspase-3↑	DNA synthesis ↓
Wnt/β-catenin↓	T cell ratio ↑		capspase-8↑	RNA synthesis ↓
platelets activity↓			Bcl-2↓	Protein synthesis↓
miRNA-155↓			Bax ↓	DNA fragmentation
miRNA-146a↑			NF-κB	Morphology changes
miRNA-223↑			PI3K/AKT	PMCA activity ↓
miR-124-3p↑				Tumor immunity ↓
miR-203/bcl ↑				ICAM ↓
ROCK1↓				
DNA methylation↓				
miR-203↑				
p53 and Fas/FasL				

FIGURE 1 | Mechanisms of regulation of anti-cancer relevant signaling of volatile anesthetics.

exposure to volatile anesthetics can change the biological response of cancer cells or regulate the gene expression of cancer cells, thereby exerting apoptosis induction, anti-invasion, anti-migration and other anti-cancer properties. There are many studies on the regulate of anti-cancer relevant signaling of sevoflurane, but more research on desflurane, which is also commonly used in clinical practice, is needed. As for the promising new type of inhaled anesthesia xenon, due to the difficulty of production and high price, it has not yet been widely used in clinical practice. The prospect of scientific research is worth exploring. There lacks of research articles concerning the regulation of anti-cancer relevant signaling of enflurane, methoxyhalothane, and ether. These documents are no longer in clinical use, so we did not discuss them in this review.

Although volatile anesthetics are not traditionally regarded as anti-cancer drugs, more and more research have focused on the potential anti-cancer properties. Volatile anesthetics mainly act on NMDA and GABA receptors. Although it is still unclear why anesthetics can regulate of anti-cancer relevant signaling, it has been reported that activated receptors can exert regulate anti-cancer-related signaling in cancer cells (84–87). Therefore, studying the regulation of anti-cancer relevant signaling of volatile anesthetics and their related receptors is a new and enlightening insight with important significance, and therefore may make outstanding contributions to cancer biology. Considering different types of cancer have different sensitivity to volatile anesthetics, this current review may guide the choice of volatile anesthetics to best improve the clinical prognosis of cancer patients and improve their postoperative recovery (ERAS).

The shortcomings of contemporary researches relatively lack of animal studies, clinical trials, genomics analysis and big data

analysis. Volatile anesthetics exert anesthetic functions *via* passing through the respiratory tracts and blood-brain barrier and then acting on the receptors. Do volatile anesthetics demonstrate exceptional sensitivity of anti-cancer relevant signaling in lung cancer and brain tumor? More specific and compelling trials are needed, especially those related to sevoflurane and desflurane which is clinically widely used, to clarify the relationship between anesthetics and tumor prognosis, and to provide more precise guidance for anesthesia management.

CONCLUSION

From the above research and investigation, it can be concluded that volatile anesthetics could regulate anti-cancer relevant signaling (Table 2). The underlying mechanism involves miRNA, transcription factors, apoptotic pathway, MMP, etc. **Figure 1.** Although the current research may shortcomings, more in depth studies, especially clinical research, is warranted to clarify the regulation of anti-cancer relevant signaling of volatile anesthetics.

AUTHOR CONTRIBUTIONS

JW was in charge of the writing. C-sC was responsible for the pictures and editing. YL compiled the table and inserted the references. SS reconstructed and redesigned the work. SH made final agreement and approval of the work to be published. All authors contributed to the article and approved the submitted version.

REFERENCES

- Hanahan D, Weinberg RA. Hallmarks of cancer: the next generation. *Cell* (2011) 144(5):646–74. doi: 10.1016/j.cell.2011.02.013
- Mitra AK, Agrahari V, Mandal A, Cholkar K, Natarajan C, Shah S, et al. Novel delivery approaches for cancer therapeutics. *J Control Release* (2015) 219:248–68. doi: 10.1016/j.jconrel.2015.09.067
- Siegel RL, Miller KD, Jemal A. Cancer statistics, 2019. *CA Cancer J Clin* (2019) 69(1):7–34. doi: 10.3322/caac.21551
- Wu L, Zhao H, Wang T, Pac-Soo C, Ma D. Cellular signaling pathways and molecular mechanisms involving inhalational anesthetics-induced organoprotection. *J Anesth* (2014) 28(5):740–58. doi: 10.1007/s00540-014-1805-y
- Luo Y, Ma D, Jeong E, Sanders RD, Yu B, Hossain M, et al. Xenon and sevoflurane protect against brain injury in a neonatal asphyxia model. *Anesthesiology* (2008) 109(5):782–9. doi: 10.1097/ALN.0b013e3181895f88
- Zhu M, Li M, Zhou Y, Dangelmajer S, Kahlert UD, Xie R, et al. Isoflurane enhances the malignant potential of glioblastoma stem cells by promoting their viability, mobility in vitro and migratory capacity in vivo. *Brit J Anaesth* (2016) 116(6):870–7. doi: 10.1093/bja/aew124
- Zhang W, Shao X. Isoflurane Promotes Non-Small Cell Lung Cancer Malignancy by Activating the Akt-Mammalian Target of Rapamycin (mTOR) Signaling Pathway. *Med Sci Monit* (2016) 22:4644–50. doi: 10.12659/MSM.898434
- Luo X, Zhao H, Hennah L, Ning J, Liu J, Tu H, et al. Impact of isoflurane on malignant capability of ovarian cancer in vitro. *Brit J Anaesth* (2015) 114(5):831–9. doi: 10.1093/bja/aeu408
- Huang H, Benzouana LL, Zhao H, Watts HR, Perry NJS, Bevan C, et al. Prostate cancer cell malignancy via modulation of HIF-1 α pathway with isoflurane and propofol alone and in combination. *Br J Cancer* (2014) 111(7):1338–49. doi: 10.1038/bjc.2014.426
- Benzouana LL, Perry NJ, Watts HR, Yang B, Perry IA, Coombes C, et al. Isoflurane, a commonly used volatile anesthetic, enhances renal cancer growth and malignant potential via the hypoxia-inducible factor cellular signaling pathway in vitro. *Anesthesiology* (2013) 119(3):593–605. doi: 10.1097/ALN.0b013e31829e47fd
- Kawaraguchi Y, Horikawa YT, Murphy AN, Murray F, Miyahara A, Ali SS, et al. Volatile Anesthetics Protect Cancer Cells against Tumor Necrosis Factor-related Apoptosis-inducing Ligand-induced Apoptosis via Caveolins. *Anesthesiology* (2011) 115(3):499–508. doi: 10.1097/ALN.0b013e3182276d42
- Jun R, Gui-he Z, Xing-xing S, Hui Z, Li-xian X. Isoflurane enhances malignancy of head and neck squamous cell carcinoma cell lines: A preliminary study in vitro. *Oral Oncol* (2011) 47(5):329–33. doi: 10.1016/j.oraloncology.2011.03.002
- Moudgil GC, Singal DP. Halothane and isoflurane enhance melanoma tumour metastasis in mice. *Can J Anaesth* (1997) 44(1):90–4. doi: 10.1007/BF03014331
- Melamed R, Bar-Yosef S, Shakhar G, Shakhar K, Ben-Eliyahu S. Suppression of Natural Killer Cell Activity and Promotion of Tumor Metastasis by Ketamine, Thiopental, and Halothane, but Not by Propofol: Mediating Mechanisms and Prophylactic Measures. *Anesth Analg* (2003) 97(5):1331–9. doi: 10.1213/01.ANE.0000082995.44040.07
- Shapiro J, Jersky J, Katzav S, Feldman M, Segal S. Anesthetic Drugs Accelerate the Progression of Postoperative Metastases of Mouse Tumors. *Survey Anesthesiol* (1982) 26(4):231. doi: 10.1097/00132586-198226040-00041
- Jenkins A, Franks NP, Lieb WR. Effects of temperature and volatile anesthetics on GABA(A) receptors. *Anesthesiology* (1999) 90(2):484–91. doi: 10.1097/00005542-199902000-00024
- Wu J, Harata N, Akaike N. Potentiation by sevoflurane of the gamma-aminobutyric acid-induced chloride current in acutely dissociated CA1 pyramidal neurones from rat hippocampus. *Br J Pharmacol* (1996) 119(5):1013–21. doi: 10.1111/j.1476-5381.1996.tb15772.x
- Krasowski MD, Harrison NL. The actions of ether, alcohol and alkane general anaesthetics on GABAA and glycine receptors and the effects of TM2 and TM3 mutations. *Br J Pharmacol* (2000) 129(4):731–43. doi: 10.1038/sj.bjp.0703087
- Brosnan RJ, Thiesen R. Increased NMDA receptor inhibition at an increased Sevoflurane MAC. *BMC Anesthesiol* (2012) 12:9. doi: 10.1186/1471-2253-12-9
- Schüttler J, Schwilden S. *Modern Anesthetics*. Springer-Verlag Berlin Heidelberg, Springer Science & Business Media (2008). 32 p.
- Van Dort CJ. Regulation of Arousal by Adenosine A(1) and A(2A) Receptors in the Prefrontal Cortex of C57BL/6J Mouse. *ProQuest* (2008), 120.
- Hang LH, Shao DH, Wang H, Yang JP. Involvement of 5-hydroxytryptamine type 3 receptors in sevoflurane-induced hypnotic and analgesic effects in mice. *Pharmacol Rep* (2010) 62(4):621–6. doi: 10.1016/s1734-1140(10)70319-4
- Suzuki T, Koyama H, Sugimoto M, Uchida I, Mashimo T. The diverse actions of volatile and gaseous anesthetics on human-cloned 5-hydroxytryptamine3 receptors expressed in Xenopus oocytes. *Anesthesiology* (2002) 96(3):699–704. doi: 10.1097/00005542-200203000-00028
- Hill M, Tran N. MicroRNAs Regulating MicroRNAs in Cancer. *Trends Cancer* (2018) 4(7):465–8. doi: 10.1016/j.trecan.2018.05.002
- Zhang B, Pan X, Cobb GP, Anderson TA. microRNAs as oncogenes and tumor suppressors. *Dev Biol* (2007) 302(1):1–12. doi: 10.1016/j.ydbio.2006.08.028
- Chen CZ. MicroRNAs as oncogenes and tumor suppressors. *N Engl J Med* (2005) 353(17):1768–71. doi: 10.1056/NEJMp058190
- Wang J, Cheng CS, Lu Y, Ding X, Zhu M, Miao C, et al. Novel Findings of Anti-cancer Property of Propofol. *Anticancer Agents Med Chem* (2018) 18(2):156–65. doi: 10.2174/1871520617666170912120327
- Gao G, Ge R, Li Y, Liu S. Luteolin exhibits anti-breast cancer property through up-regulating miR-203. *Artif Cells Nanomed Biotechnol* (2019) 47(1):3265–71. doi: 10.1080/21691401.2019.1646749
- Zhang LS, Ma HG, Sun FH, Zhao WC, Li G. MiR-203 inhibits the malignant behavior of prostate cancer cells by targeting RGS17. *Eur Rev Med Pharmacol Sci* (2019) 23(13):5667–74. doi: 10.26355/eurrev_201907_18303
- Chi Y, Jin Q, Liu X, Xu L, He X, Shen Y, et al. miR-203 inhibits cell proliferation, invasion, and migration of non-small-cell lung cancer by downregulating RGS17. *Cancer Sci* (2017) 108(12):2366–72. doi: 10.1111/cas.13401
- Fan L, Wu Y, Wang J, He J, Han X. Sevoflurane inhibits the migration and invasion of colorectal cancer cells through regulating ERK/MMP-9 pathway by up-regulating miR-203. *Eur J Pharmacol* (2019) 850:43–52. doi: 10.1016/j.ejphar.2019.01.025
- Liu J, Yang L, Guo X, Jin G, Wang Q, Lv D, et al. Sevoflurane suppresses proliferation by upregulating microRNA-203 in breast cancer cells. *Mol Med Rep* (2018) 18(1):455–60. doi: 10.3892/mmr.2018.8949
- Leivonen SK, Sahlberg KK, Makela R, Due EU, Kallioniemi O, Borresen-Dale AL, et al. High-throughput screens identify microRNAs essential for HER2 positive breast cancer cell growth. *Mol Oncol* (2014) 8(1):93–104. doi: 10.1016/j.molonc.2013.10.001
- Stokowy T, Wojtas B, Fajarewicz K, Jarzab B, Eszlinger M, Paschke R. miRNAs with the potential to distinguish follicular thyroid carcinomas from benign follicular thyroid tumors: results of a meta-analysis. *Horm Metab Res* (2014) 46(3):171–80. doi: 10.1055/s-0033-1363264
- Zhang JF, He ML, Fu WM, Wang H, Chen LZ, Zhu X, et al. Primate-specific microRNA-637 inhibits tumorigenesis in hepatocellular carcinoma by disrupting signal transducer and activator of transcription 3 signaling. *Hepatology* (2011) 54(6):2137–48. doi: 10.1002/hep.24595
- Que T, Song Y, Liu Z, Zheng S, Long H, Li Z, et al. Decreased miRNA-637 is an unfavorable prognosis marker and promotes glioma cell growth, migration and invasion via direct targeting Akt1. *Oncogene* (2015) 34(38):4952–63. doi: 10.1038/ncr.2014.419
- Lu Y, Wang J, Yan J, Yang Y, Sun Y, Huang Y, et al. Sevoflurane attenuate hypoxia-induced VEGF level in tongue squamous cell carcinoma cell by upregulating the DNA methylation states of the promoter region. *BioMed Pharmacoth* (2015) 71:139–45. doi: 10.1016/j.biopha.2015.02.032
- Chen X, Hu Z, Wang W, Ba Y, Ma L, Zhang C, et al. Identification of ten serum microRNAs from a genome-wide serum microRNA expression profile as novel noninvasive biomarkers for nonsmall cell lung cancer diagnosis. *Int J Cancer* (2012) 130(7):1620–8. doi: 10.1002/ijc.26177
- Wang L, Wang T, Gu J, Su H. Volatile anesthetic sevoflurane suppresses lung cancer cells and miRNA interference in lung cancer cells. *Oncotarg Ther* (2018) 11:5689–93. doi: 10.2147/OTT.S171672
- An F, Gong G, Wang Y, Bian M, Yu L, Wei C. MiR-124 acts as a target for Alzheimer's disease by regulating BACE1. *Oncotarget* (2017) 8(69):114065–71. doi: 10.18632/oncotarget.23119
- Liu X, Kang J, Sun S, Luo Y, Ji X, Zeng X, et al. iASPP, a microRNA124 target, is aberrantly expressed in astrocytoma and regulates malignant glioma cell migration and viability. *Mol Med Rep* (2018) 17(1):1970–8. doi: 10.3892/mmr.2017.8097
- Gao C, Shen J, Meng Z, He X. Sevoflurane Inhibits Glioma Cells Proliferation and Metastasis through miRNA-124-3p/ROCK1 Axis. *Pathol Oncol Res* (2019) 26:2. doi: 10.1007/s12253-019-00597-1

43. Kessenbrock K, Plaks V, Werb Z. Matrix metalloproteinases: regulators of the tumor microenvironment. *Cell* (2010) 141(1):52–67. doi: 10.1016/j.cell.2010.03.015
44. Choe G, Park JK, Jouben-Steele L, Kremen TJ, Liao LM, Vinters HV, et al. Active matrix metalloproteinase 9 expression is associated with primary glioblastoma subtype. *Clin Cancer Res* (2002) 8(9):2894–901. doi: 10.1159/000063870
45. Forsyth PA, Wong H, Laing TD, Rewcastle NB, Morris DG, Muzik H, et al. Gelatinase-A (MMP-2), gelatinase-B (MMP-9) and membrane type matrix metalloproteinase-1 (MT1-MMP) are involved in different aspects of the pathophysiology of malignant gliomas. *Br J Cancer* (1999) 79(11–12):1828–35. doi: 10.1038/sj.bjc.6690291
46. Hurmath FK, Mittal M, Ramaswamy P, Umamaheswara Rao GS, Dalavaikodihalli Nanjaiah N. Sevoflurane and thiopental preconditioning attenuates the migration and activity of MMP-2 in U87MG glioma cells. *Neurochem Int* (2016) 94:32–8. doi: 10.1016/j.neuint.2016.02.003
47. Nicoud IB, Jones CM, Pierce JM, Earl TM, Matrisian LM, Chari RS, et al. Warm hepatic ischemia-reperfusion promotes growth of colorectal carcinoma micrometastases in mouse liver via matrix metalloproteinase-9 induction. *Cancer Res* (2007) 67(6):2720–8. doi: 10.1158/0008-5472.CAN-06-3923
48. Muller-Edenborn B, Roth-Z'Graggen B, Bartnicka K, Borgeat A, Hoos A, Borsig L, et al. Volatile anesthetics reduce invasion of colorectal cancer cells through down-regulation of matrix metalloproteinase-9. *Anesthesiology* (2012) 117(2):293–301. doi: 10.1097/ALN.0b013e3182605df1
49. Liang H, Wang HB, Liu HZ, Wen XJ, Zhou QL, Yang CX. The effects of combined treatment with sevoflurane and cisplatin on growth and invasion of human adenocarcinoma cell line A549. *BioMed Pharmacoth* (2013) 67(6):503–9. doi: 10.1016/j.biopha.2013.03.005
50. Gerard C, Goldbeter A. The balance between cell cycle arrest and cell proliferation: control by the extracellular matrix and by contact inhibition. *Interface Focus* (2014) 4(3):20130075. doi: 10.1098/rsfs.2013.0075
51. Liang H, Gu MN, Yang CX, Wang HB, Wen XJ, Zhou QL. Sevoflurane inhibits proliferation, induces apoptosis, and blocks cell cycle progression of lung carcinoma cells. *Asian Pac J Cancer Prev* (2011) 12(12):3415–20. doi: 10.1159/000328275
52. Kvolik S, Dobrosevic B, Marci S, Prlc L, Glavas-Obrovac L. Different apoptosis ratios and gene expressions in two human cell lines after sevoflurane anaesthesia. *Acta Anaesth Scand* (2009) 53(9):1192–9. doi: 10.1111/j.1399-6576.2009.02036.x
53. Yang Y, Hu R, Yan J, Chen Z, Lu Y, Jiang J, et al. Sevoflurane inhibits the malignant potential of head and neck squamous cell carcinoma via activating the hypoxia-inducible factor-1 α signaling pathway in vitro. *Int J Mol Med* (2018) 41(2):995–1002. doi: 10.3892/ijmm.2017.3306
54. Semenza GL. Targeting HIF-1 for cancer therapy. *Nat Rev Cancer* (2003) 3(10):721–32. doi: 10.1038/nrc1187
55. Liang H, Yang CX, Zhang B, Wang HB, Liu HZ, Lai XH, et al. Sevoflurane suppresses hypoxia-induced growth and metastasis of lung cancer cells via inhibiting hypoxia-inducible factor-1 α . *J Anesth* (2015) 29(6):821–30. doi: 10.1007/s00540-015-2035-7
56. Guillemin K, Krasnow MA. The hypoxic response: huffing and HIFing. *Cell* (1997) 89(1):9–12. doi: 10.1016/S0092-8674(00)80176-2
57. Ruan X, Jiang W, Cheng P, Huang L, Li X, He Y, et al. Volatile anesthetics sevoflurane targets leukemia stem/progenitor cells via Wnt/ β -catenin inhibition. *BioMed Pharmacoth* (2018) 107:1294–301. doi: 10.1016/j.biopha.2018.08.063
58. Miyashita T, Tajima H, Makino I, Nakagawara H, Kitagawa H, Fushida S, et al. Metastasis-promoting role of extravasated platelet activation in tumor. *J Surg Res* (2015) 193(1):289–94. doi: 10.1016/j.jss.2014.07.037
59. Goubran HA, Stakiw J, Radošević M, Burnouf T. Platelet-cancer interactions. *Semin Thromb Hemost* (2014) 40(3):296–305. doi: 10.1055/s-0034-1370767
60. Liang H, Yang CX, Zhang B, Zhao ZL, Zhong JY, Wen XJ. Sevoflurane attenuates platelets activation of patients undergoing lung cancer surgery and suppresses platelets-induced invasion of lung cancer cells. *J Clin Anesth* (2016) 35:304–12. doi: 10.1016/j.jclinane.2016.08.008
61. Elias KM, Kang S, Liu X, Horowitz NS, Berkowitz RS, Frenzl G. Anesthetic Selection and Disease-Free Survival Following Optimal Primary Cytoreductive Surgery for Stage III Epithelial Ovarian Cancer. *Ann Surg Oncol* (2015) 22(4):1341–8. doi: 10.1245/s10434-014-4112-9
62. Woo JH, Baik HJ, Kim CH, Chung RK, Kim DY, Lee GY, et al. Effect of Propofol and Desflurane on Immune Cell Populations in Breast Cancer Patients: A Randomized Trial. *J Korean Med Sci* (2015) 30(10):1503. doi: 10.3346/jkms.2015.30.10.1503
63. Gonzalez RM, Daly DS, Tan R, Marks JR, Zangar RC. Plasma biomarker profiles differ depending on breast cancer subtype but RANTES is consistently increased. *Cancer Epidemiol Biomarkers Prev* (2011) 20(7):1543–51. doi: 10.1158/1055-9965.EPI-10-1248
64. Lv D, Zhang Y, Kim HJ, Zhang L, Ma X. CCL5 as a potential immunotherapeutic target in triple-negative breast cancer. *Cell Mol Immunol* (2013) 10(4):303–10. doi: 10.1038/cmi.2012.69
65. Zhang Y, Lv D, Kim HJ, Kurt RA, Bu W, Li Y, et al. A novel role of hematopoietic CCL5 in promoting triple-negative mammary tumor progression by regulating generation of myeloid-derived suppressor cells. *Cell Res* (2013) 23(3):394–408. doi: 10.1038/cr.2012.178
66. Ash SA, Valchev GI, Looney M, Ni MA, Crowley PD, Gallagher HC, et al. Xenon decreases cell migration and secretion of a pro-angiogenesis factor in breast adenocarcinoma cells: comparison with sevoflurane. *Br J Anaesth* (2014) 113 Suppl 1:i14–21. doi: 10.1093/bja/aeu191
67. Singh G, Janicki PK, Horn JL, Janson VE, Franks JJ. Inhibition of plasma membrane Ca(2+)-ATPase pump activity in cultured C6 glioma cells by halothane and xenon. *Life Sci* (1995) 56(10):L219–24. doi: 10.1016/0024-3205(95)00011-T
68. Huang Y, Zuo Z. Isoflurane enhances the expression and activity of glutamate transporter type 3 in C6 glioma cells. *Anesthesiology* (2003) 99(6):1346–53. doi: 10.1097/0000542-200312000-00016
69. Choi YK, Park KG. Targeting Glutamine Metabolism for Cancer Treatment. *Biomol Ther (Seoul)* (2018) 26(1):19–28. doi: 10.4062/biomolther.2017.178
70. Ren H, Shi X, Li Y. Reduction of p38 mitogen-activated protein kinase and cyclooxygenase-2 signaling by isoflurane inhibits proliferation and apoptosis evasion in human papillomavirus-infected laryngeal papillomas. *Exp Ther Med* (2016) 12(5):3425–32. doi: 10.3892/etm.2016.3776
71. Hu J, Hu J, Jiao H, Li Q. Anesthetic effects of isoflurane and the molecular mechanism underlying isoflurane-inhibited aggressiveness of hepatic carcinoma. *Mol Med Rep* (2018) 18(1):184–92. doi: 10.3892/mmr.2018.8945
72. Olney JW, Farber NB, Wozniak DF, Jevtovic-Todorovic V, Ikonomidou C. Environmental agents that have the potential to trigger massive apoptotic neurodegeneration in the developing brain. *Environ Health Perspect* (2000) 108 Suppl 3:383–8. doi: 10.1289/ehp.00108s3383
73. Komatsu H, Nogaya J, Ogli K. Volatile anaesthetics as central nervous system excitants. *Ann Acad Med Singapore* (1994) 23(6 Suppl):130–8.
74. Brunner EA, Cheng SC, Berman ML. Effects of anesthesia on intermediary metabolism. *Annu Rev Med* (1975) 26:391–401. doi: 10.1146/annurev.me.26.020175.002135
75. Fink BR, Kenny GE. Metabolic effects of volatile anesthetics in cell culture. *Anesthesiology* (1968) 29(3):505–16. doi: 10.1097/0000542-196805000-00024
76. Jackson SH. The metabolic effects of halothane on mammalian hepatoma cells in vitro. I. Inhibition of cell replication. *Anesthesiology* (1972) 37(5):489–92. doi: 10.1097/0000542-197211000-00005
77. Jackson SH. The metabolic effects of halothane on mammalian hepatoma cells in vitro. II. Inhibition of DNA synthesis. *Anesthesiology* (1973) 39(4):405–9. doi: 10.1097/0000542-197310000-00013
78. Kvolik S, Glavas-Obrovac L, Bares V, Karner I. Effects of inhalation anesthetics halothane, sevoflurane, and isoflurane on human cell lines. *Life Sci* (2005) 77(19):2369–83. doi: 10.1016/j.lfs.2004.12.052
79. Uemura E, Levin ED. The effect of halothane on cultured fibroblasts and neuroblastoma cells. *Neurosci Lett* (1992) 145(1):33–6. doi: 10.1016/0304-3940(92)90196-E
80. Fried IA. The influence of the anaesthetic on survival rates of breast cancer patients after surgery. *Int J Cancer* (1977) 20(2):213–8. doi: 10.1002/ijc.2910200208
81. Stephanova E, Topouzova-Hristova T, Hazarosova R, Moskova V. Halothane-induced alterations in cellular structure and proliferation of A549 cells. *Tissue Cell* (2008) 40(6):397–404. doi: 10.1016/j.tice.2008.04.001
82. Hinkley RE, Telser AG. The effects of halothane on cultured mouse neuroblastoma cells. I. Inhibition of morphological differentiation. *J Cell Biol* (1974) 63(2 Pt 1):531–40. doi: 10.1083/jcb.63.2.531
83. Azuma K, Mike N, Fujiwara Y, Shimada Y, Watanabe T. Effect of halothane on intercellular adhesion molecule-1 (ICAM-1) in melanoma cells. *J Anesth* (1993) 7(4):442–6. doi: 10.1007/s0054030070442
84. Taylor RA, Watt MJ. Unsuspected Protumorigenic Signaling Role for the Oncometabolite GABA in Advanced Prostate Cancer. *Cancer Res* (2019) 79(18):4580–1. doi: 10.1158/0008-5472.CAN-19-2182

85. Chen X, Wu Q, You L, Chen S, Zhu M, Miao C. Propofol attenuates pancreatic cancer malignant potential via inhibition of NMDA receptor. *Eur J Pharmacol* (2017) 795:150–9. doi: 10.1016/j.ejphar.2016.12.017
86. Chen X WQSP. Propofol Disrupts Aerobic Glycolysis in Colorectal Cancer Cells via Inactivation of the NMDAR-CAMKII-ERK Pathway. *Cell Physiol Biochem* (2018) 462(2). doi: 10.1159/000488617
87. Jiang S, Zhu L, Zhang M, Li R, Yang Q, Yan J, et al. GABRP regulates chemokine signalling, macrophage recruitment and tumour progression in pancreatic cancer through tuning KCNN4-mediated Ca²⁺ signalling in a GABA-independent manner. *Gut* (2019) 68(11):1994–2006. doi: 10.1136/gutjnl-2018-317479

Conflict of Interest: The authors declare that the research was conducted in the absence of any commercial or financial relationships that could be construed as a potential conflict of interest.

Copyright © 2021 Wang, Cheng, Lu, Sun and Huang. This is an open-access article distributed under the terms of the Creative Commons Attribution License (CC BY). The use, distribution or reproduction in other forums is permitted, provided the original author(s) and the copyright owner(s) are credited and that the original publication in this journal is cited, in accordance with accepted academic practice. No use, distribution or reproduction is permitted which does not comply with these terms.



Anticancer Properties of the Antipsychotic Drug Chlorpromazine and Its Synergism With Temozolomide in Restraining Human Glioblastoma Proliferation *In Vitro*

OPEN ACCESS

Edited by:

Nor Eddine Sounni,
University of Liège,
Belgium

Reviewed by:

Amin Hajitou,
Imperial College London,
United Kingdom
Caroline Piette,
University of Liège,
Belgium

*Correspondence:

Claudia Abbruzzese
claudia.abbruzzese@iffo.gov.it
Marco G. Paggi
marco.paggi@iffo.gov.it

[†]These authors have contributed
equally to this work

Specialty section:

This article was submitted to
Pharmacology of Anti-Cancer Drugs,
a section of the journal
Frontiers in Oncology

Received: 30 November 2020

Accepted: 14 January 2021

Published: 26 February 2021

Citation:

Matteoni S, Matarrese P, Ascione B,
Buccarelli M, Ricci-Vitiani L, Pallini R,
Villani V, Pace A, Paggi MG and
Abbruzzese C (2021) Anticancer
Properties of the Antipsychotic
Drug Chlorpromazine and Its
Synergism With Temozolomide in
Restraining Human Glioblastoma
Proliferation *In Vitro*.
Front. Oncol. 11:635472.
doi: 10.3389/fonc.2021.635472

Silvia Matteoni^{1†}, Paola Matarrese^{2†}, Barbara Ascione², Mariachiara Buccarelli³,
Lucia Ricci-Vitiani³, Roberto Pallini⁴, Veronica Villani⁵, Andrea Pace⁵, Marco G. Paggi^{1*}
and Claudia Abbruzzese^{1*}

¹ Cellular Networks and Molecular Therapeutic Targets, Proteomics Unit, IRCCS - Regina Elena National Cancer Institute, Rome, Italy, ² Center for Gender Specific Medicine, Oncology Unit, Istituto Superiore di Sanità, Rome, Italy, ³ Department of Oncology and Molecular Medicine, Istituto Superiore di Sanità, Rome, Italy, ⁴ Fondazione Policlinico Universitario A. Gemelli IRCCS, Institute of Neurosurgery, Catholic University School of Medicine, Rome, Italy, ⁵ Neuro-Oncology, IRCCS-Regina Elena National Cancer Institute, Rome, Italy

The extremely poor prognosis of patients affected by glioblastoma (GBM, grade IV glioma) prompts the search for new and more effective therapies. In this regard, drug repurposing or repositioning can represent a safe, swift, and inexpensive way to bring novel pharmacological approaches from bench to bedside. Chlorpromazine, a medication used since six decades for the therapy of psychiatric disorders, shows *in vitro* several features that make it eligible for repositioning in cancer therapy. Using six GBM cell lines, three of which growing as patient-derived neurospheres and displaying stem-like properties, we found that chlorpromazine was able to inhibit viability in an apoptosis-independent way, induce hyperdiploidy, reduce cloning efficiency as well as neurosphere formation and downregulate the expression of stemness genes in all these cell lines. Notably, chlorpromazine synergized with temozolomide, the first-line therapeutic in GBM patients, in hindering GBM cell viability, and both drugs strongly cooperated in reducing cloning efficiency and inducing cell death *in vitro* for all the GBM cell lines assayed. These results prompted us to start a Phase II clinical trial on GBM patients (EudraCT # 2019-001988-75; ClinicalTrials.gov Identifier: NCT04224441) by adding chlorpromazine to temozolomide in the adjuvant phase of the standard first-line therapeutic protocol.

Keywords: glioblastoma, antipsychotic drugs (APDs), drug repurposing and repositioning, cancer stem cells (CSC), neurospheres, drug synergism, clinical trials

Abbreviations: GBM, glioblastoma; CPZ, chlorpromazine; TMZ, temozolomide; DRD2, brain dopamine receptor D2; RPE-1, retinal pigment epithelial cells; AMPA receptor, α -amino-3-hydroxy-5-methyl-4-isoxazolepropionic acid receptor; NMDA receptor, N-methyl-D-aspartate receptor; MGMT, O-6-methylguanine-DNA methyltransferase.

INTRODUCTION

Glioblastoma (GBM, glioblastoma multiforme) is the most frequent and severe adult malignant brain tumor. The best available therapeutic approach toward newly diagnosed GBM patients, *i.e.* surgical ablation followed by radiotherapy plus concomitant and adjuvant chemotherapy with temozolomide (TMZ), is associated with a median survival of 15 months (1). GBM's highly aggressive, chemo-resistant and relapse-prone behavior is mainly attributed to its intra-tumor molecular heterogeneity associated with unpredictable genetic drift under therapeutic pressure (2). Such an adverse scenario prompts for the identification of novel therapeutic approaches even by using repurposed/repositioned drugs that, when supported by robust evidence, represent an attracting alternative to novel drugs, being safer, less expensive, and characterized by a shorter timeframe from laboratory to the clinics.

We focused our attention on chlorpromazine (CPZ, Largactil, Thorazine), the first member of the tricyclic drugs phenothiazines, a medication used since six decades in the treatment of psychiatric disorders. This molecule acts as an antagonist of the brain dopamine receptor D2 (DRD2), thus decreasing post-synaptic dopamine stimulating activity (3, 4). DRD2 is highly expressed in GBM, mainly in glioma-initiating cells, where it regulates homeostasis, enhancing resistance to hypoxia and increasing cellular plasticity (5). Furthermore, several reports show that CPZ can inhibit cancer cell growth through several mechanisms (6–15). In addition, epidemiological data suggest a reduction of cancer risk in psychiatric patients treated with CPZ or related antipsychotic compounds (16, 17), and anecdotal reports of favorable GBM evolution in psychiatric patients treated with neuroleptic medications have been published (16, 18).

We evaluated the ability of CPZ to affect several GBM cellular parameters *in vitro*, using a large number of human GBM cell lines, *i.e.* the anchorage-dependent cell lines T98G, U-87 MG, and U-251 MG as well as three patient-derived, anchorage-independent neurospheres characterized for their ability to display a glioma stem-like cell behavior (19). In addition, hTERT-immortalized retinal pigment epithelial cells (RPE-1) (20), a non-cancer cell line from neuro-ectodermal origin, were also used in selected assays.

Here we investigate, for the first time to our knowledge, the synergistic effect between CPZ and TMZ, the reference drug for first-line GBM clinical treatment, in inhibiting GBM cell growth in either anchorage-dependent or -independent, patient-derived stem-like neurospheres.

MATERIALS AND METHODS

Cell Lines

Anchorage-dependent cell lines T98G, U-251 MG and U-87 MG were cultured as previously reported (21). Anchorage-independent TS#1, TS#83 and TS#163 neurospheres are patient-derived cell lines from surgical samples classified according to WHO 2016 (22), isolated and cultured in order to

enrich them with glioma stem cells, as described (19, 23, 24). Human hTERT-immortalized retinal pigment epithelial cells (RPE-1) (20) were a kind gift from Giulia Guarguaglini, CNR, Rome, Italy.

T98G, U-251 MG and U-87 MG are from the laboratory of one of the authors (L.R.V.). Their authentication was performed by short tandem repeat (STR) profiling, which resulted in $\geq 80\%$ match for eight loci as per interrogation of the ATCC STR profiling database. TS#1, TS#83, and TS#163 neurospheres have been defined as glioma stem-like cells according to established criteria (25, 26). TS#83 grow partially in an anchorage-dependent fashion.

All cell lines were Mycoplasma-free and used for a maximum of 20 passages.

Drugs

CPZ was purchased, as “Largactil”, from Teofarma S.R.L., Valle Salimbene (PV), Italy, as a 25 mg/ml solution (78 mM). TMZ was purchased from Selleckchem (Houston TX, USA) and diluted in DMSO as a 150 mM solution.

Cell Viability Assay

This assay was performed as previously described (27). Briefly, 5×10^3 cells were seeded in a 96-well plate and treated with CPZ for 48 h; then the relative number of viable cells was determined by CellTiter-Glo Luminescent Cell Viability Assay (Promega, Madison, WI), analyzed by means of a GLOMAX 96 Microplate Luminometer (Promega) and dose-response curves were generated (Prism v5, GraphPad Software Inc., San Diego, CA). When synergy between TMZ and CPZ was assayed, cells were initially treated with TMZ for 96 h and then CPZ was added for further 48 h at a fixed dose, approximately corresponding to inhibitory concentration IC₁₀. Control samples were treated with the same final concentration of the respective drug solvent(s) (DMSO for TMZ and PBS for CPZ). A dose-response curve was also calculated using TMZ as a single agent for each GBM cell line; in these experiments, cells were exposed to the drug for 6 d.

Fluorescence Microscopy

For analysis of nuclear morphology by fluorescence microscopy, treated cell lines were exposed to CPZ at the concentrations reported as IC₃₀ in **Figure 1B** for 48 h and control cells to an equal volume of solvent (PBS). Cells were then fixed in 4% paraformaldehyde, stained with Hoechst 33258 (Sigma-Aldrich, St. Louis, MO; 1 mg/ml in PBS) and mounted in glycerol/PBS (ratio 1:1, pH 7.4). Images were acquired by intensified video-microscopy (IVM) with an Olympus fluorescence microscope (Olympus Corporation, Tokyo, Japan), equipped with a Zeiss charge-coupled device camera (Carl Zeiss, Oberkochen, Germany). Control cells were exposed to an equal volume of solvent (PBS).

Colony-Forming Assay

This assay was performed as described (27). Briefly, anchorage-dependent GBM cells were plated at a concentration of $2-3 \times 10^2$ cells/well in 6-well plates and treated with increasing doses of CPZ for 48 h. When synergy between TMZ and CPZ was

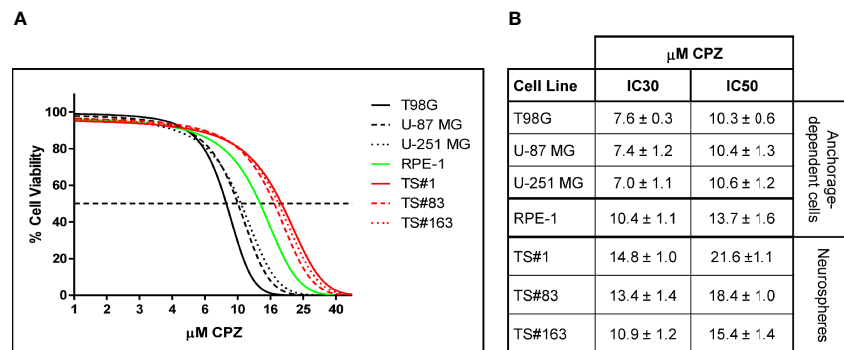


FIGURE 1 | CPZ reduces cell viability in GBM cells. **(A)**. Representative dose-response curves of all cell lines treated with CPZ for 48 h are shown. GBM anchorage-dependent cell lines are represented by black lines, while RPE-1 by a green line and neurospheres by red ones. **(B)**. Table showing μM CPZ concentrations corresponding to the IC30 and IC50 calculated for each cell line. Values are expressed as mean ± SE.

assayed, cells were initially treated with a sub-optimal dose of TMZ for 96 h, then CPZ was added for further 48 h at a sub-optimal dose. Cells were then washed, cultured for additional 12 d and subsequently stained using a 5% crystal violet solution to assess the colony number. Control samples were treated with the same final concentration of the respective drug solvents, PBS for CPZ and DMSO for TMZ.

Neurosphere Formation Assay

This assay was performed as described (27). Briefly, TS#1, TS#83 and TS#163 cells were plated at 2.5×10^5 cells/well in a 6-well plate and treated with increasing doses of CPZ for 48 h. Alternatively, to evaluate the synergy between CPZ and TMZ, cells were treated with the respective drug solvents, PBS for CPZ and DMSO for TMZ, or a fixed dose of TMZ for 96 h and then CPZ was added for further 48 h. Cells were then mechanically dissociated into single cell suspension, counted, diluted at the appropriate concentration and re-seeded in triplicate into new 6-well plates (5×10^2 cells/well) in the absence of drugs. After 20 further days, neurosphere-forming efficiency was examined by inverted microscopy.

RNA Extraction and RT-PCR

Both anchorage-dependent cells and neurospheres were treated with a dose of CPZ corresponding to their respective IC30 for 24 h. Control samples were treated with the same final concentration of PBS. Treated and control cells were harvested, and total RNA was extracted using miRNeasy Extraction Kit (QIAGEN, Hilden, Germany). RNA concentration was determined using the NanoDrop 1000 spectrophotometer, then was reverse-transcribed into cDNA with High Capacity cDNA Reverse Transcription Kit (ThermoFisher Scientific, Waltham, MA). To quantify gene expression, qRT-PCR was performed using SYBR Green in a QuantStudio 6 Flex Real-Time PCR System (ThermoFisher Scientific) and CT values were normalized to GAPDH. All RT-PCR data were analyzed using the $2^{-\Delta\Delta CT}$ method. Values represent the fold changes referred to the respective value for control cells, arbitrarily reported as 1.0.

Flow cytometry—Apoptosis

For apoptosis evaluation, treated cell lines were exposed to TMZ (96 h) and CPZ (48 h), or their combination, at the lowest concentrations considered synergistic based on the viability analysis. Control cells were exposed to an equal volume of solvent(s) (PBS and/or DMSO). Apoptosis was quantified using a fluorescein isothiocyanate (FITC)-conjugated Annexin V (AV) and propidium iodide (PI) detection kit (Marine Biological Laboratory, Woods Hole, MA, USA). This assay enables identifying both early (AV positive/PI negative) and late apoptotic or necrotic (PI positive) cells. Alternatively, cell death was evaluated by incubating cells with 1 μM Calcein-AM (ThermoFisher Scientific) at 37°C for 30 min. In live cells, the non-fluorescent Calcein-AM is converted to a green-fluorescent dye, whereas dead cells, with compromised cell membranes, do not retain Calcein, thus not displaying green fluorescence.

Flow Cytometry—Cell Cycle

For cell cycle analysis, treated cell lines were exposed to CPZ at the concentrations reported as IC30 in Figure 1B for 48 h and control cells to an equal volume of solvent (PBS). Cells were then fixed in cold 70% ethanol for 30 min at 4°C. After washing in PBS, cells were incubated with ribonuclease (50 μl of a 100 μg/ml stock of RNase), to ensure that only DNA, not RNA, was stained, and PI (200 μl from a 50 μg/ml stock solution).

We measured the forward scatter (FS) and side scatter (SS) to identify single cells. Pulse processing (pulse area vs. pulse width) was used to exclude cell doublets from the analysis.

Samples were analyzed by collecting FL2 red fluorescence in a linear scale at 620 nm. Acquisition was performed on a dual-laser FACSCalibur flow cytometer (BD Biosciences, San Jose, CA) and at least 30,000 events/sample were run in low mode and acquired. Data were analyzed using the Cell Quest Pro and ModFit software (BD Biosciences).

Statistical Analysis

Unless otherwise specified, all tests were done in triplicate. Results are expressed as mean ± standard error. Differences between two groups were analyzed using the Student's two-

tailed t test. Asterisks denote statistical significance (* $p < 0.05$; ** $p < 0.01$; *** $p < 0.001$). When statistical analyses were performed among more than two groups, data were analyzed by One-way ANOVA test followed by Tukey's Multiple Comparisons Test (Prism v5).

We used the algorithm described by Fransson et al. (28), to assess if the effect of the combination of CPZ and TMZ was synergistic, additive or antagonist. The effect of either compounds used as single agents compared with that of the drug combination, is expressed as Combination Index (CI). A CI value <0.8 indicates synergism; a CI value between 0.8 and 1.2 indicates an additive effect, while a CI value >1.2 indicates antagonism.

RESULTS

CPZ Reduces GBM Cell Viability

Figure 1A, depicts the effect on viability of a 48 h-exposure to increasing doses of CPZ in six different GBM cell lines cells. The graph refers to the anchorage-dependent cells T98G, U-87 MG, and U-251 MG (solid, dashed, and dotted black lines, respectively) and the TS#1, TS#83, and TS#163 neurospheres (solid, dashed, and dotted red lines, respectively). In addition, the non-cancer RPE-1 cells (20) were also assayed for their susceptibility to CPZ (solid green line).

CPZ markedly affected cell viability in all six GBM cell lines. Drug doses required to achieve IC30 and IC50 (the amount of substance able to inhibit *in vitro* a given biological process by 30 or 50%, respectively) were lower for anchorage-dependent GBM cells and appeared higher in stem-like neurospheres. Interestingly, RPE-1 cells, also growing in an anchorage-dependent fashion, appeared less sensitive to CPZ than anchorage-dependent GBM cells, but more sensitive than neurospheres, which are characterized by slow replication rates and the need of an enriched stem cell culture medium. IC30 and IC50 for all these cell lines are reported in **Figure 1B**.

CPZ Induces Cell Cycle Alterations and causes Hyperdiploidy in GBM Cells

Several reports claim for CPZ the ability of protecting from apoptosis in either normal neural cells exposed to toxic stimuli (29, 30) or malignant glioma cells (10). According to these studies, apoptotic cell death should not be involved in the drug-induced decrease in GBM cell viability and/or proliferation rate. To investigate this topic, we treated GBM cells with CPZ for 48 h before analyzing cell cycle parameters *via* propidium iodide (PI) FACS analysis. As shown in **Figure 2A**, all the anchorage-dependent GBM cells treated with CPZ exhibited a significant increase in the percentage of cells in G2/M phase of the cell cycle, as it has been previously suggested for the sole U-87 MG cell line (10). Furthermore, no increase of the hypodiploid peak, characteristic of apoptosis, was detectable in any of these cell lines after CPZ treatment, where, by contrast, an increased number of hyperdiploid cells were apparent. Of note, RPE-1 cells undergoing the same treatment did not display any hyperdiploid phenotype.

Analysis of nuclear morphology in CPZ-exposed GBM cells confirmed the presence of abnormal nuclei. Also in this case, RPE-1 cells did not show any apparent hyperploidy or alteration of nuclear morphology (**Figure 2B**). The experimental results obtained employing the three neurospheres show that cell cycle modifications and nuclear aberrations after exposure to CPZ were qualitatively comparable with those obtained with anchorage-dependent GBM cells, although at a lesser extent (**Figure 2C, D**).

These data confirm the ability of CPZ to interfere with the G2/M phase of the cell cycle and induce aberrant mitotic segregation in GBM cells, both phenomena able to induce cell death *via* an apoptosis-independent mechanism. The anchorage-dependent T98G cell line displayed a portion of hyperdiploid cells at the baseline, as described (31). Nonetheless, treatment with CPZ significantly increased the number of T98G hyperdiploid cells, as evaluated either *via* cytometry or fluorescence microscopy. Raw data regarding cell cycle analysis are available as **Supplementary Material**.

CPZ Reduces GBM Cell Cloning Efficiency

A distinct hallmark of cancer cells, and especially GBM, is the ability to generate clones from cells seeded *in vitro* at elevated dilutions. We quantified the effect of CPZ in inhibiting cell cloning efficiency in GBM cells by using different methods, according to the capability of these cells to grow in an anchorage-dependent or -independent fashion.

CPZ drastically reduced colony number in T98G, U-251 MG, and U-87 MG anchorage-dependent cell lines. Colony number was also reported in a histogram for each experimental set (**Figure 3A**). In **Figure 3B**, a drastic drop in sphere dimensions and a clear impairment in sphere forming ability were also appreciable in the TS#1, TS#83, and TS#163 neurospheres, according to previous reports concerning other primary GBM cell lines (5, 32). The dose-dependent effect of CPZ in decreasing colony-forming efficiency in anchorage-dependent GBM cells, as well as in reducing the proficiency of neurospheres in forming 3D spheroids, strongly suggests the ability of this compound to inhibit clonogenic power, a common feature of cancer cells.

CPZ Downregulates Stemness Gene Expression in GBM Cells

The sharp effect of CPZ in impairing neurosphere formation drove us to investigate the capability of this compound to reduce the stemness potential in stem-like GBM cells. Thus, we analyzed the relative expression of the stemness genes *OCT 3/4*, *SOX2*, *NANOG*, *Nestin*, *OLIG2* and *ALDH1A3* on TS#1, TS#83, and TS#163 neurospheres by means of qRT-PCR, using the primers listed in **Table 1**.

Cells were exposed to CPZ for 24 h at the concentrations reported as IC30 in **Figure 1B**, or to an equal volume of solvent for the respective controls. As shown in **Figure 4A**, we observed a significant CPZ-induced reduction of the expression of selected stemness markers in neurospheres, showing a behavior peculiar for each cell line.

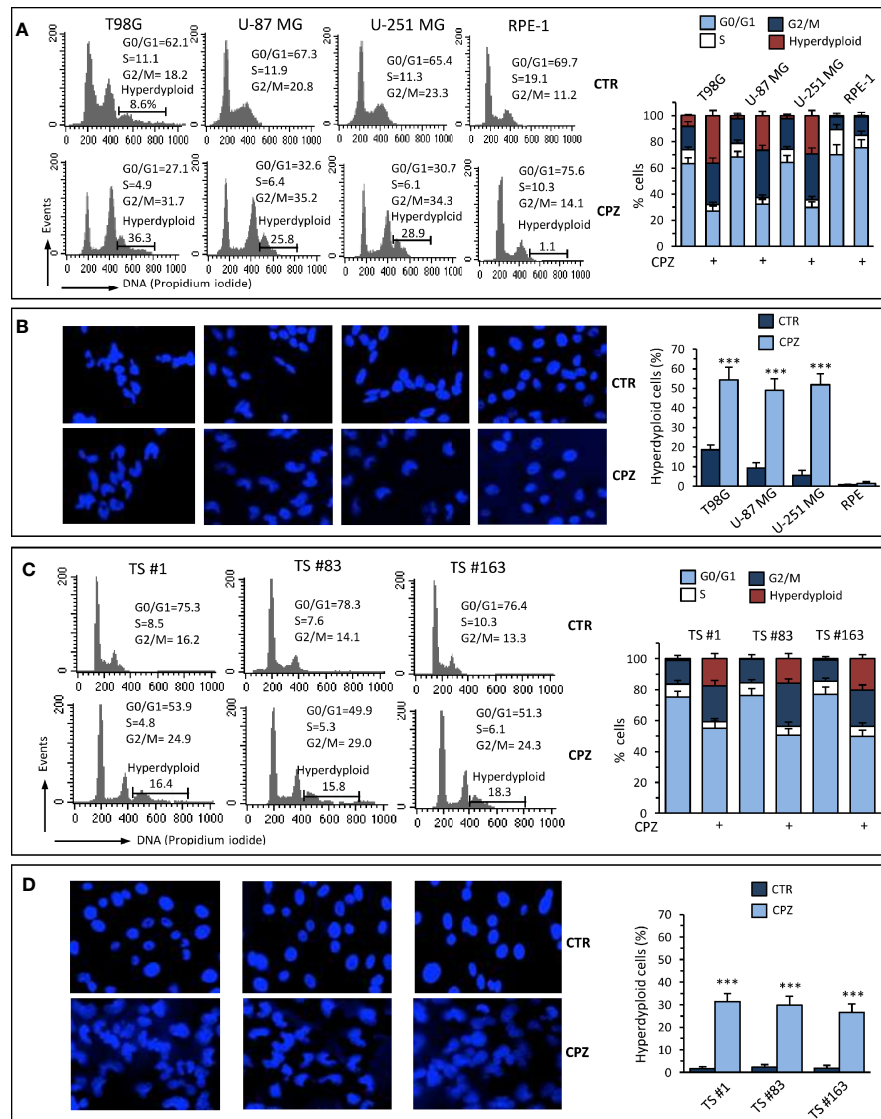


FIGURE 2 | CPZ induces alterations of the cell cycle and hyperdiploidy in GBM cells. Anchorage-dependent GBM cell lines [panels (A) and (B)] or neurospheres [panels (C) and (D)] underwent treatment with CPZ at the calculated IC₅₀ for 48 h. Flow cytometry analysis of the cell cycle. Left panels (A), (C). Histograms obtained in a representative experiment. Numbers represent the percentage of cells in the different phases of the cell cycle or hyperdiploid cells. Right panels (A), (C). Bar graphs showing mean \pm SE of data obtained from three independent experiments. Left panels (B), (D). Representative micrographs of the analysis of nuclear morphology performed after cell staining with Hoechst 33258. Right panels (B), (D). Bar graphs showing the quantification of hyperdiploid cells performed by counting at least 50 cells from 10 different fields observed with a 40 \times objective. Data are reported as mean \pm SE of data obtained from three independent experiments. Statistical significance is referred toward the Control (***) $p < 0.001$.

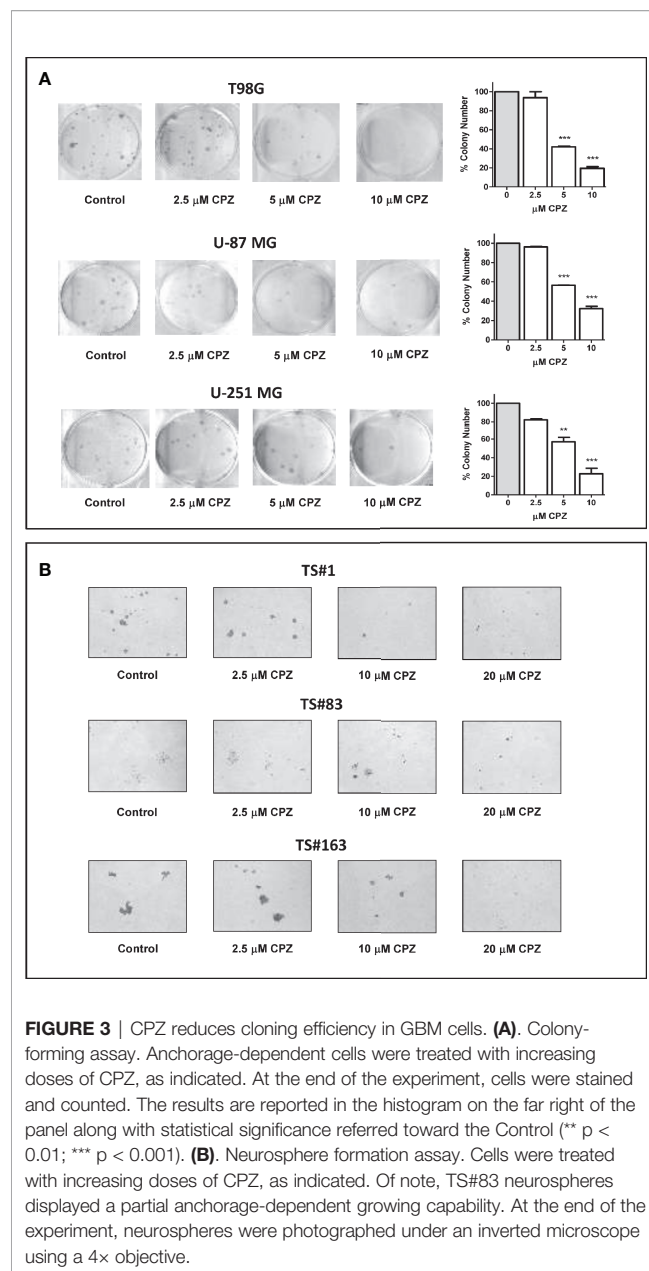
For the sake of completeness, we carried out the same assay also on the T98G, U-251 MG, and U-87 MG anchorage-dependent GBM cell lines, where the influence of CPZ on the expression of these stemness genes was clearly appreciable, especially in the U-251 MG cell line (Figure 4B).

It is worth noting that *ALDH* is a stem cell marker whose activity promotes tumorigenesis and progression in different solid tumors (33). In particular, the isoform *ALDH1A3* analyzed here promotes stemness, triggers mesenchymal transition in GBM and increases resistance to TMZ (34). CPZ

significantly inhibited *ALDH1A3* gene expression in TS#1 TS#163, U-87 MG, and U-251 MG cell lines. *GAPDH* determination was employed for normalization purposes. Raw data regarding RT-PCR analysis are available as **Supplementary Material**.

CPZ Synergizes With TMZ in Reducing GBM Cell Viability

Since CPZ restrained cell growth in all the GBM cell lines examined, we assayed its effect when administered in



combination with TMZ, the first-line drug for GBM treatment. In **Figure 5**, the effects of CPZ alone (blue lines in graphs, blue columns in histograms) and TMZ alone (green lines in graphs, green columns in histograms) on cell viability are shown for the anchorage-dependent GBM cell lines and neurospheres (**Figure 5A, B**, respectively). In order to check for the effect of the combination of the two drugs, we exposed GBM cells to increasing doses of TMZ, ranging from 4 to 1,000 μ M for 96 h prior the addition of CPZ, which was administered at a fixed concentration. CPZ doses were chosen in accordance with the individual sensitivity of each cell line to this compound and corresponded approximately to the IC₁₀ (the amount of substance able to inhibit *in vitro* a given biological process by

TABLE 1 | Primers used for assaying the relative expression of the indicated stemness genes *via* qRT-PCR.

Primers	Sequence
OCT 3/4 FWD	5'-TGGAGAAGGAGAAGCTGGAGCAAAA-3'
OCT 3/4 REV	5'-GGCAGATGGTCGTTTGGCTGAATA-3'
SOX2 FWD	5'-CGATGCCGACAAGAAAACCTT-3'
SOX2 REV	5'-CAAATCTCTGCAAGCTCC-3'
Nanog FWD	5'-CAAAGGCAAACACCCACTT-3'
Nanog REV	5'-ATTGTTCCAGGTCTGGTTGC-3'
Nestin FWD	5'-CAGCGTTGGAACAGAGGTTGG-3'
Nestin REV	5'-TGGCACAGGTGTCTCAAGGGTAG-3'
OLIG2 FWD	5'-CCAGAGCCCGATGACCTTTT-3'
OLIG2 REV	5'-CACTGCCTCTAGCTTGTCC-3'
ALDH1A3 FWD	5'-TGAATGGCACGAATCCAAGAG-3'
ALDH1A3 REV	5'-CACGTCGGGCTTATCTCCT-3'
GAPDH FWD	5'-TCCTGAGCTGAACGGGAAG-3'
GAPDH REV	5'-GGAGGAGTGGGTGCTGCTGT-3'

10%) (see **Figure 5**). After 48 h of further incubation, cell viability was assessed. The effect of the drug combination is indicated for all the GBM cells assayed (red lines in graphs, red columns in histograms).

By using the algorithm described by Fransson et al. (28), we analyzed the outcome of the compounds used as single agents compared with the one of the drug combination, and expressed it as Combination Index (CI), whose value is reported on the top of the red columns. When the addition of CPZ to TMZ yielded a decrease in cell viability attributable to a synergistic effect of the two drugs (CI value < 0.8), the respective CI value was reported in red. The combined effect of the two compounds was especially evident in the anchorage-dependent GBM cell lines and in TS#1 neurospheres, where drugs synergistically cooperated to reduce GBM cell viability. Raw data regarding cell viability analysis are available as **Supplementary Material**.

CPZ Cooperates With TMZ in Inducing Cell Death

With the aim of understanding the mechanisms elicited by TMZ, CPZ or their combination on GBM cells, we analyzed their effect on cell viability. Cytofluorimetric assay with Calcein-AM, coupled with Annexin V/PI analysis, allowed us quantifying cell death and apoptosis in the same experimental setup. The data reported in **Figure 6A**, for anchorage-dependent GBM cells indicate that cells treated with TMZ became positive to Annexin V, thus suggesting an apoptotic cell death, as previously described (35, 36). By contrast, CPZ appeared to induce toxicity *via* its ability to generate aberrant mitoses that cause nuclear fragmentation and cell death. Indeed, CPZ-treated cells were almost completely negative to Annexin V, but positive to PI.

We found similar results in neurospheres (**Figure 6B**) that, despite their positivity to Annexin V after treatment with TMZ, were resistant to classical caspase-mediated apoptosis, but died by ferroptosis, as we demonstrated earlier (37). Importantly, CPZ acted in cooperation with TMZ also in inducing death in neurospheres.

Analysis of cell death by Calcein-AM, a non-fluorescent dye converted to green-fluorescent calcein after acetoxymethyl ester hydrolysis by intracellular esterases in living cells, substantially confirmed data obtained by Annexin V/PI evaluation. Raw data

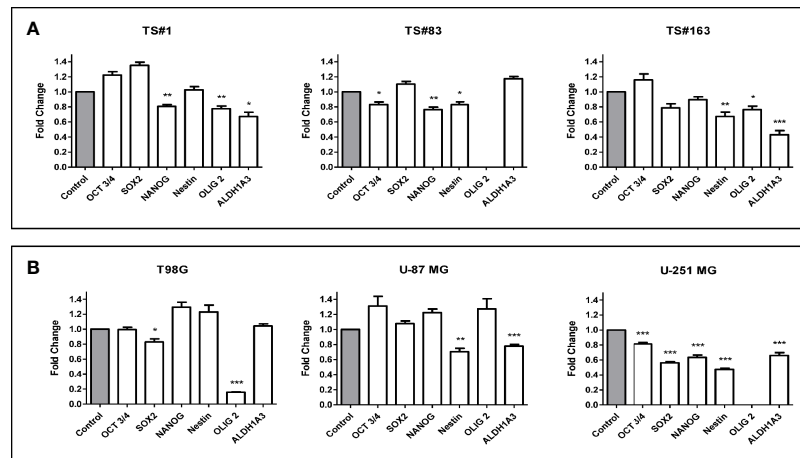


FIGURE 4 | CPZ downregulates stemness gene expression in GBM cells. **(A).** Expression of stemness genes in the three stem-like cell lines (neurospheres). **(B).** Expression of stemness genes in the three anchorage-dependent cell lines. In all cases, determinations were performed via qRT-PCR after 24 h of exposure to CPZ. Histogram values represent the fold-changes referred to the respective value for untreated cells (Control), arbitrarily reported as 1.0 (gray columns on the left of each graph). Statistical significance is referred toward the Control (* $p < 0.05$; ** $p < 0.01$; *** $p < 0.001$). In TS#83 cells and U-251 MG cells, in panel A and in panel B respectively, the amount of OLIG2 mRNA was undetectable in Control as well in CPZ-treated cells.

regarding Annexin V and Calcein-AM analysis are available as **Supplementary Material**.

CPZ Cooperates With TMZ in Reducing GBM Cell Cloning Efficiency

Anchorage-dependent GBM cell lines exposed to a combination of TMZ and CPZ drastically reduced their cloning efficiency. Colony number, quantification of the experimental results and their statistical significance are represented in the histogram on the right of each experimental set (**Figure 7A**).

Then, we analyzed the sphere-forming efficiency in neurospheres treated with sub-optimal doses of TMZ and/or CPZ. While administration of these drugs as a single compound did not reach a noticeable effect, the same doses, administered in combination, produced a marked decrease in both sphere number and volume (**Figure 7B**). This last feature was particularly evident in the right panels (enlarged), where a scale bar allowed the comparison of the size between representative control and TMZ plus CPZ-treated neurospheres.

Colony- and sphere-forming ability assays demonstrate that CPZ cooperated with TMZ in reducing GBM cell cloning efficiency, a distinctive signature of malignancy in cancer cells.

DISCUSSION

The current therapeutic protocol for newly diagnosed GBM results in suboptimal clinical outcomes. In this urgent need for novel therapeutic strategies, scientifically supported drug repurposing represents an appealing alternative, since it involves the use of compounds with shorter development timelines and lower risks for the patients, allowing faster and less expensive delivery from bench to bedside of potentially effective drugs. In the oncology field, several

non-cancer drugs have been proposed and employed in clinical trials for GBM patients (38). Among these, CPZ has been shown effective in hindering key biological features of cancer cells *in vitro*, also in the case of malignant gliomas (15).

Here we confirm the ability of CPZ in restraining key cancer cell features, adding further information concerning the effect of the drug on six human GBM cell lines, either anchorage-dependent or patient-derived neurospheres. In all these cell lines, CPZ generated nuclear aberrations that, associated with its ability to protect from apoptosis, drove cells toward anomalous mitoses, possibly *via* the described inhibition of the mitotic kinesin KSP/Eg5 (8), with subsequent death to be expected *via* mitotic catastrophe. In the same experimental setting, the RPE-1 non-cancer cell line resulted less sensitive to the drug, when compared with the anchorage-dependent GBM cells and, remarkably, refractory to the induction of nuclear aberrations elicited by the drug, as detected in all the GBM cells assayed. These last results need to be validated using other non-cancer model systems; indeed, while the reasons for this selectivity have not been identified yet, such evidence could be of considerable interest in GBM therapy.

In addition, CPZ was able to downregulate the expression of *OCT 3/4*, *SOX2*, *NANOG*, *Nestin*, *OLIG2* and *ALDH1A3*, universal cancer stem cells genes for GBM (39). In particular, *ALDH1A3* expression is related to resistance to TMZ (34). Specifically, stemness characteristics in GBM appear related to the expression of updated gene sets, especially when validated in detailed culture conditions (organoids) and/or *in vivo* (40). It is also worth mentioning that CPZ strongly affected GBM cloning efficiency and neurosphere-forming capability, two features of remarkable therapeutic relevance, since stem cells are considered responsible for GBM drug resistance and clinical relapse (41, 42).

Noteworthy, the first described and most investigated feature of CPZ is the inhibition of the dopamine receptor DRD2 [see (43) for a

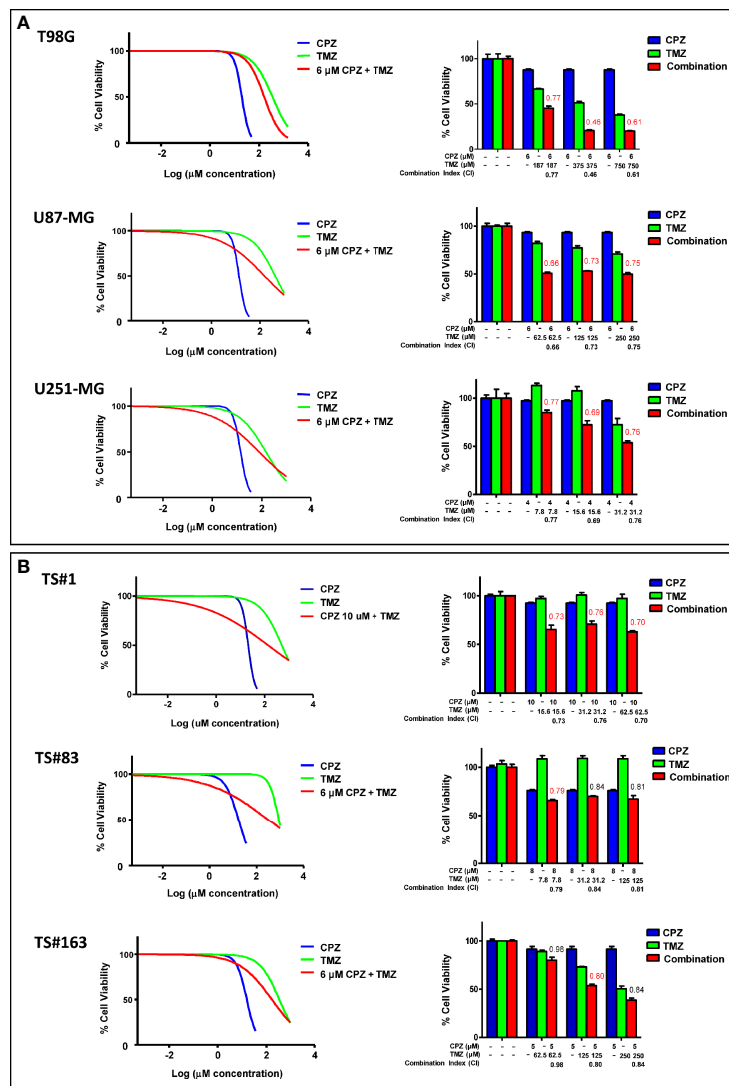


FIGURE 5 | CPZ synergizes with TMZ in reducing GBM cell viability. Anchorage-dependent GBM cell lines **(A)** and neurospheres **(B)**. Dose-response effects of CPZ (blue), TMZ (green) and TMZ plus a constant (k) CPZ concentration, indicated for each cell line (red) on percent cell viability (left panels). Histograms show cell viability at selected drug concentrations, as indicated, to highlight the effect of the association of the two drugs (right panels). The effects of TMZ and CPZ combination were considered synergistic when the CI was <0.8 (in red). CPZ k values were 6.0, 6.0, 4.0, 10.0, 8.0 and 5.0 μM for T98G, U-87 MG, U-251 MG, TS#1, TS#83 and TS163 GBM cells, respectively.

review]. More recently, this compound has also been identified, together with some homologs, as an inhibitor of AMPA and NMDA glutamate receptor channels (44). Dopamine, glutamate and their receptors are vital for physiological neuronal synaptic signaling, and the recent identification of neuron-glioma synapses is giving high relevance to the role of these neuromediators and their post-synaptic receptors in brain cancer proliferation and progression (45, 46). Therefore, the pharmacological effects of CPZ on these receptors might play a major role in brain cancer therapy.

The state of the art of GBM chemotherapy relies on TMZ, a drug proficient in inhibiting GBM growth *in vitro*, even if the doses required to reach the IC₅₀ in these cells result quite high (19) and not comparable at all with those reachable *in vivo*. TMZ, as an

alkylating agent, damages guanine residues of DNA. These damages are partly recovered in cells expressing adequate levels of the O-6-methylguanine-DNA methyltransferase (*MGMT*) gene. Since expression, and thus activity, of the related protein is prevented in some GBM cells by methylation of the promoter of this gene, GBM cells displaying hypo- or non-methylated *MGMT* gene express more *MGMT* protein, thus being less sensitive to TMZ, causing an intrinsic or acquired resistance to this drug.

In order to provide a rationale for a clinical trial for GBM patients, we evaluated the effect of the combination of CPZ plus TMZ on selected cellular parameters, demonstrating a clear synergism between these two drugs in reducing cell viability and a sharp cooperation in restraining cloning efficiency and neurosphere formation. Moreover,

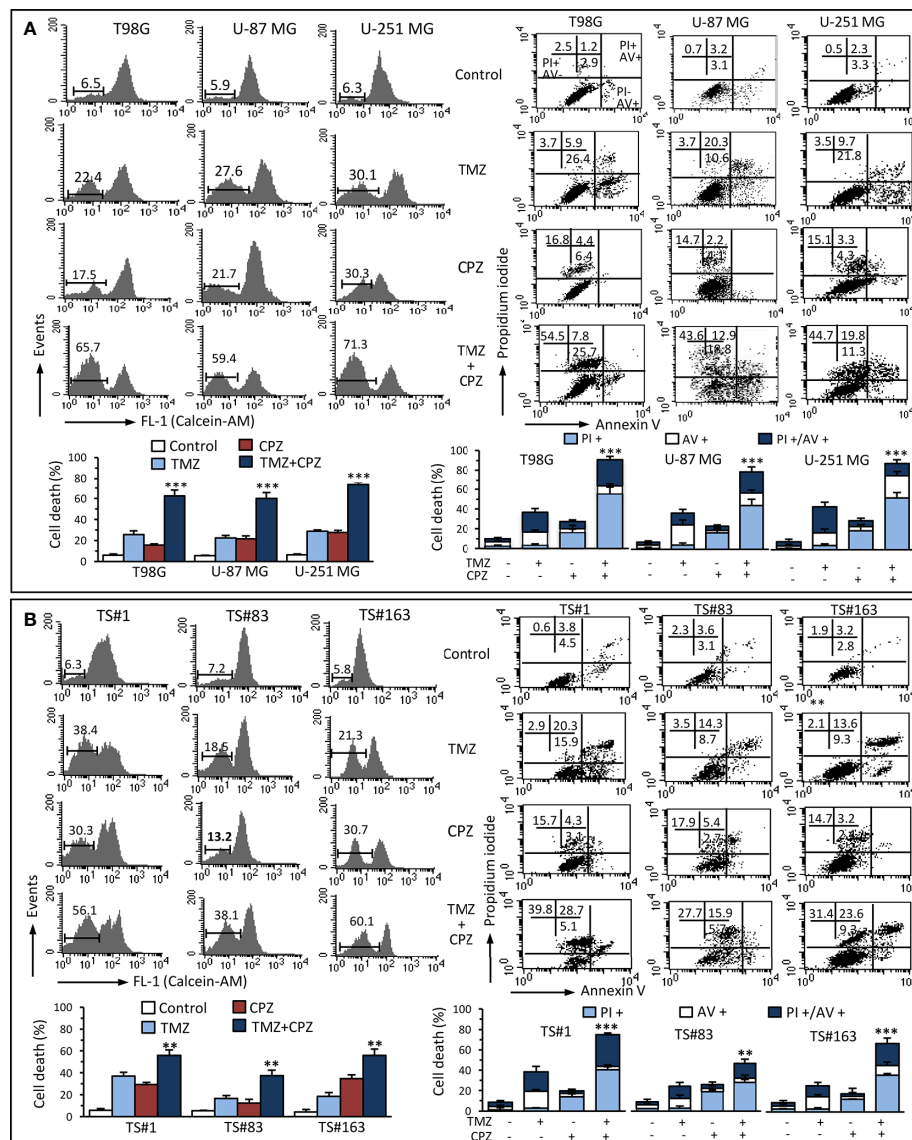


FIGURE 6 | CPZ cooperates with TMZ in inducing cell death. Anchorage-dependent GBM cell lines (A) and neurospheres (B) were analyzed after treatment with TMZ (96 h) and CPZ (48 h), or their combination, at the lowest concentrations considered synergistic on the basis of the viability analysis. Left panels. FACS analysis after staining with Calcein-AM (which is retained in the cytoplasm of live cells). Numbers represent the percentage of Calcein-negative cells (dead cells). One representative experiment is shown. Bar graphs below show the results obtained from four independent experiments, reported as means \pm SE. Right panels. FACS analysis after double staining with Annexin V/PI. Dot plots from a representative experiment are shown. Numbers represent the percentages of Annexin V-positive cells (bottom right quadrant), Annexin V/PI double positive cells (upper right quadrant), or PI-positive cells (upper left quadrant). Note the high percentage of cells positive for PI in CPZ treated cells. Bar graphs below show results obtained from four independent experiments, reported as means \pm SE. ** $p < 0.01$ and *** $p < 0.001$ indicate significant differences vs single drug treatments (TMZ or CPZ).

by combining two different quantitative assays, Calcein-AM and Annexin V/PI, we highlighted how these drugs induced cell death *via* distinct mechanisms. The different mode of action exerted by these drugs might explain their ability to cooperate in inducing cell death and thus restraining GBM growth in both anchorage-dependent cells and neurospheres. Indeed, while TMZ is known to block the DNA replication fork, thus arresting the cell cycle in the G2/M phase, [see **Figure 2** and refs. (35, 36)], CPZ, besides its ability to hinder GBM cells at the G2/M boundary (see **Figure 2**), appears capable of

protecting aberrant or defective cells from apoptosis. Such a feature would drive these cells towards a mitosis with very little chances of being completed, eliciting, on the contrary, the generation of daughter cells with abnormal chromosomal makeup [see **Figure 2** and ref (8)] and death by mitotic catastrophe. It has been demonstrated that autophagic cell death contributes to CPZ-induced cytotoxicity in GBM cells (10). On these bases, the combination of TMZ plus CPZ would simultaneously trigger apoptosis, ferroptosis (especially in neurospheres), mitotic catastrophe, and autophagic death in GBM

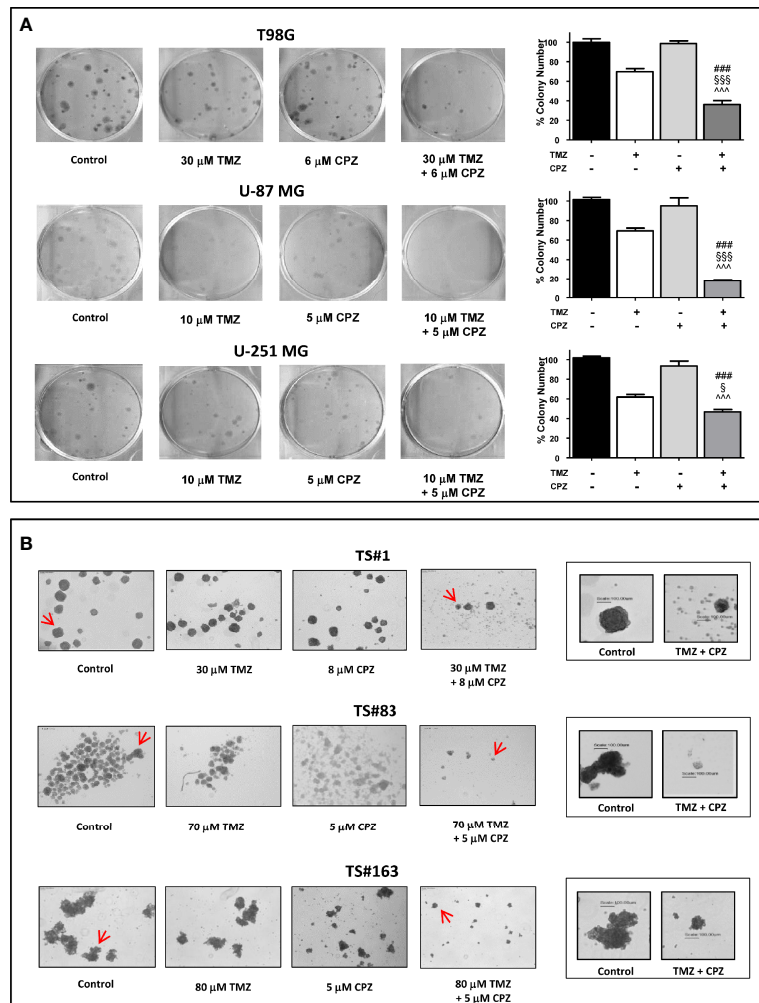


FIGURE 7 | CPZ cooperates with TMZ in reducing GBM cell cloning efficiency. **(A)** Anchorage-dependent cells T98G, U-87 MG and U-251 MG were exposed to solvent(s) (Control), TMZ, CPZ or their association at the doses indicated, then rinsed and allowed to grow in the absence of drugs for the subsequent 12 d. Cell colonies, after staining with crystal violet (left), were counted, and the values reported as percent colony number in the histogram (right). In these panels, variance among groups was assessed via the Bartlett's test for equal variances. Statistical analysis among groups was done using the One-way ANOVA test followed by the Tukey's Multiple Comparison Test (### significance <0.001 vs. Control; ^^ significance <0.001 vs. CPZ; \$\$\$ significance <0.001 vs. TMZ; \$ significance <0.05 vs. TMZ). **(B)** Neurospheres TS#1, TS#83, and TS#163 were treated as described and allowed to grow and form spheres for the subsequent 20 d. For each cell line, the four left images illustrate the effect of TMZ, CPZ or both drugs on neurosphere number and size, observed using a 4 \times objective. The two framed images on the right are enlarged pictures of the respective neurospheres indicated by the red arrows; these neurospheres were randomly chosen due to their dimensions, in order to appreciate their decrease in volume due to the treatment with the drug combo. This suggests a reduced sphere-forming ability in TMZ + CPZ-treated cells. In this panel, no histograms with values and statistical significance are reported, due to the intrinsic difficulty of objectively counting floating neurospheres.

cells, synergistically increasing the cytotoxic effect in GBM and contributing to overcome drug resistance.

GBM is a disease characterized by profound intra-tumor heterogeneity (47) and hierarchically dependent upon pre-existing cancer stem cells that undergo selection under therapeutic pressure (48), with a consequent unpredictable genetic drift (2). Such a scenario implies an intrinsic challenge in the choice of a suitable targeted therapy. From the scientific literature and our results, CPZ appears as a drug with multifaceted effects on cancer cells, being able to affect major signal transduction pathways, spindle assembly and apoptosis, all processes conceivably essential for the survival of the different clones that characterize the marked GBM heterogeneity.

CPZ is the progenitor of the DRD2 inhibitors phenothiazines and is used since the 50s in the therapy of several psychiatric disorders, *e.g.* acute and chronic psychosis, and provides relief from severe vomiting and untreatable hiccups. When necessary, CPZ can be administered for long periods, with doses ranging from 50 to 400 mg/day. Its main side effects are a dose-dependent sedation and, at higher doses, the occurrence of an extrapyramidal syndrome, both reversible when the drug is suspended. Presently, second and third generation neuroleptic drugs acting as DRD2 inhibitors are available, but we focused on CPZ since it is included in the 2019 World Health Organization Model List of Essential Medicines (49). The adverse reactions elicited by CPZ should not impede the

treatment of GBM patients, also considering the poor prognosis attainable, especially in subjects carrying a GBM with a hypo- or non-methylated *MGMT* gene. In addition, CPZ crosses easily the blood-brain barrier.

In the light of these considerations, we submitted a Phase II clinical trial to our Institutional Ethical Committee (Comitato Etico Centrale IRCCS-Sezione IFO-Fondazione Bietti, Rome, Italy), which was approved on September 6, 2019 (EudraCT # 2019-001988-75; ClinicalTrials.gov Identifier: NCT04224441). The schedule consists in the addition of CPZ to the standard GBM treatment in patients carrying hypo- or un-methylated *MGMT* gene, *i.e.* those more resistant to TMZ. CPZ is administered orally at the dose of 50 mg/day, in concomitance with the adjuvant treatment with TMZ.

We are currently investigating, *via* high-throughput methodologies, the effects of CPZ on GBM cell signaling and energy metabolism, as well as identifying, *via* mass spectrometry, other relevant cellular factors directly targeted by the drug.

We expect that our *in vitro* results on the effectiveness of CPZ in restraining GBM cell growth, as well as its synergism with TMZ, could be replicated in the ongoing clinical setting. In addition to such a desirable outcome, which remains the main goal of our efforts, the use of a repurposed medication would allow reducing both development expenses and time predictable for a new drug to travel from the experimental laboratory to the clinics.

DATA AVAILABILITY STATEMENT

The datasets presented in this study can be found in online repositories. The names of the repository/repositories and accession number(s) can be found in the article/**Supplementary Material**.

REFERENCES

- Stupp R, Mason WP, van den Bent MJ, Weller M, Fisher B, Taphoorn MJ, et al. Radiotherapy plus concomitant and adjuvant temozolomide for glioblastoma. *N Engl J Med* (2005) 352(10):987–96. doi: 10.1056/NEJMoa043330
- Korber V, Yang J, Barah P, Wu Y, Stichel D, Gu Z, et al. Evolutionary Trajectories of IDH(WT) Glioblastomas Reveal a Common Path of Early Tumorigenesis Instigated Years ahead of Initial Diagnosis. *Cancer Cell* (2019) 35(4):692–704.e12. doi: 10.1016/j.ccell.2019.02.007
- Horn AS, Snyder SH. Chlorpromazine and dopamine: conformational similarities that correlate with the antischizophrenic activity of phenothiazine drugs. *Proc Natl Acad Sci USA* (1971) 68(10):2325–8. doi: 10.1073/pnas.68.10.2325
- Boyd-Kimball D, Gonczy K, Lewis B, Mason T, Siliko N, Wolfe J, et al. Classics in Chemical Neuroscience: Chlorpromazine. *ACS Chem Neurosci* (2019) 10(1):79–88. doi: 10.1021/acschemneuro.8b00258
- Caragher SP, Shireman JM, Huang M, Miska J, Atashi F, Baisiwal S, et al. Activation of Dopamine Receptor 2 Prompts Transcriptomic and Metabolic Plasticity in Glioblastoma. *J Neurosci* (2019) 39(11):1982–93. doi: 10.1523/JNEUROSCI.1589-18.2018
- Motohashi N, Sakagami H, Kamata K, Yamamoto Y. Cytotoxicity and differentiation-inducing activity of phenothiazine and benzo[a] phenothiazine derivatives. *Anticancer Res* (1991) 11(5):1933–7.

AUTHOR CONTRIBUTIONS

CA, MGP, PM, AP and SM designed the study; CA, SM, PM, BA, LRV and MB applied specific methodologies; CA, SM, PM and BA validated the data; formal analysis, CA, SM, PM and BA; investigation, CA, SM, PM and BA; resources, CA, SM, PM, BA LRV, MB, RP, VV and AP; data curation, CA, SM, PM and BA; writing—original draft preparation, MGP, CA, SM and PM; writing—review and editing, MGP, CA, SM, PM, AP and VV; supervision, CA and MGP; funding acquisition, PM, RP and MGP. All authors contributed to the article and approved the submitted version.

FUNDING

This work has been partially funded by Associazione Italiana per la Ricerca sul Cancro (IG 18526 to PM and 23154 to RP), Arcobaleno Onlus and Peretti Foundation (NaEPF 2019-042) to PM; Ricerca Corrente IRE 2018-2019 to MP.

ACKNOWLEDGMENTS

Editorial assistance was provided by Luca Giacomelli, PhD, Massimiliano Pianta and Aashni Shah (Polistudium SRL, Milan, Italy). This assistance was supported by internal funds.

SUPPLEMENTARY MATERIAL

All Supplementary Material can be found as raw data at the link below: <https://gbox.garr.it/garrbox/index.php/s/ipOLBxGQDns2qMs>.

- Nordenberg J, Fenig E, Landau M, Weizman R, Weizman A. Effects of psychotropic drugs on cell proliferation and differentiation. *Biochem Pharmacol* (1999) 58(8):1229–36. doi: 10.1016/s0006-2952(99)00156-2
- Lee MS, Johansen L, Zhang Y, Wilson A, Keegan M, Avery W, et al. The novel combination of chlorpromazine and pentamidine exerts synergistic antiproliferative effects through dual mitotic action. *Cancer Res* (2007) 67(23):11359–67. doi: 10.1158/0008-5472.CAN-07-2235
- Shin SY, Kim CG, Kim SH, Kim YS, Lim Y, Lee YH. Chlorpromazine activates p21Waf1/Cip1 gene transcription via early growth response-1 (Egr-1) in C6 glioma cells. *Exp Mol Med* (2010) 42(5):395–405. doi: 10.3858/emmm.2010.42.5.041
- Shin SY, Lee KS, Choi YK, Lim HJ, Lee HG, Lim Y, et al. The antipsychotic agent chlorpromazine induces autophagic cell death by inhibiting the Akt/mTOR pathway in human U-87MG glioma cells. *Carcinogenesis* (2013) 34(9):2080–9. doi: 10.1093/carcin/bgt169
- Pinheiro T, Otrocka M, Seashore-Ludlow B, Rrakli V, Holmberg J, Forsberg-Nilsson K, et al. A chemical screen identifies trifluoperazine as an inhibitor of glioblastoma growth. *Biochem Biophys Res Commun* (2017) 494(3–4):477–83. doi: 10.1016/j.bbrc.2017.10.106
- Oliva CR, Zhang W, Langford C, Suto MJ, Griguer CE. Repositioning chlorpromazine for treating chemoresistant glioma through the inhibition of cytochrome c oxidase bearing the COX4-1 regulatory subunit. *Oncotarget* (2017) 8(23):37568–83. doi: 10.18632/oncotarget.17247
- Wiklund ED, Catts VS, Catts SV, Ng TF, Whitaker NJ, Brown AJ, et al. Cytotoxic effects of antipsychotic drugs implicate cholesterol homeostasis as a

- novel chemotherapeutic target. *Int J Cancer* (2010) 126(1):28–40. doi: 10.1002/ijc.24813
14. Yang CE, Lee WY, Cheng HW, Chung CH, Mi FL, Lin CW, et al. The antipsychotic chlorpromazine suppresses YAP signaling, stemness properties, and drug resistance in breast cancer cells. *Chem Biol Interact* (2019) 302:28–35. doi: 10.1016/j.cbi.2019.01.033
 15. Abbruzzese C, Matteoni S, Persico M, Villani V, Paggi MG. Repurposing chlorpromazine in the treatment of glioblastoma multiforme: analysis of literature and forthcoming steps. *J Exp Clin Cancer Res* (2020) 39(1):26. doi: 10.1186/s13046-020-1534-z
 16. Csatory LK. Chlorpromazines and cancer. *Lancet* (1972) 2(7772):338–9. doi: 10.1016/s0140-6736(72)92955-8
 17. Huang J, Zhao D, Liu Z, Liu F. Repurposing psychiatric drugs as anti-cancer agents. *Cancer Lett* (2018) 419:257–65. doi: 10.1016/j.canlet.2018.01.058
 18. Faraz S, Pannullo S, Rosenblum M, Smith A, Wernicke AG, et al. Long-term survival in a patient with glioblastoma on antipsychotic therapy for schizophrenia: a case report and literature review. *Ther Adv Med Oncol* (2016) 8(6):421–8. doi: 10.1177/1758834016659791
 19. D'Alessandris QG, Biffoni M, Martini M, Runci D, et al. The clinical value of patient-derived glioblastoma tumorspheres in predicting treatment response. *Neuro Oncol* (2017) 19(8):1097–108. doi: 10.1093/neuonc/now304
 20. McKinley KL, Cheeseman IM. Large-Scale Analysis of CRISPR/Cas9 Cell-Cycle Knockouts Reveals the Diversity of p53-Dependent Responses to Cell-Cycle Defects. *Dev Cell* (2017) 40(4):405–20.e2. doi: 10.1016/j.devcel.2017.01.012
 21. Abbruzzese C, Catalogna G, Gallo E, di Martino S, Mileo AM, Carosi M, et al. The small molecule SI113 synergizes with mitotic spindle poisons in arresting the growth of human glioblastoma multiforme. *Oncotarget* (2017) 8(67):110743–55. doi: 10.18632/oncotarget.22500
 22. Louis DN, Perry A, Reifenberger G, von Deimling A, Figarella-Branger D, Cavenee WK, et al. The 2016 World Health Organization Classification of Tumors of the Central Nervous System: a summary. *Acta Neuropathol* (2016) 131(6):803–20. doi: 10.1007/s00401-016-1545-1
 23. Pallini R, Ricci-Vitiani L, Banna GL, Signore M, Lombardi D, Todaro M, et al. Cancer stem cell analysis and clinical outcome in patients with glioblastoma multiforme. *Clin Cancer Res* (2008) 14(24):8205–12. doi: 10.1158/1078-0432.CCR-08-0644
 24. Lulli V, Buccarelli M, Ilari R, Castellani G, De Dominicis C, Di Giamberardino A, et al. Mir-370-3p Impairs Glioblastoma Stem-Like Cell Malignancy Regulating a Complex Interplay between HMGA2/HIF1A and the Oncogenic Long Non-Coding RNA (lncRNA) NEAT1. *Int J Mol Sci* (2020) 21(10):3610. doi: 10.3390/ijms21103610
 25. Galli R, Binda E, Orfanelli U, Cipelletti B, Gritti A, De Vitis S, et al. Isolation and characterization of tumorigenic, stem-like neural precursors from human glioblastoma. *Cancer Res* (2004) 64(19):7011–21. doi: 10.1158/0008-5472.CAN-04-1364
 26. Singh SK, Hawkins C, Clarke ID, Squire JA, Bayani J, Hide T, et al. Identification of human brain tumour initiating cells. *Nature* (2004) 432(7015):396–401. doi: 10.1038/nature03128
 27. Matteoni S, Abbruzzese C, Matarrese P, De Luca G, Mileo AM, Miccadei S, et al. The kinase inhibitor SI113 induces autophagy and synergizes with quinacrine in hindering the growth of human glioblastoma multiforme cells. *J Exp Clin Cancer Res* (2019) 38(1):202. doi: 10.1186/s13046-019-1212-1
 28. Fransson A, Glaessgen D, Alfredsson J, Wiman KG, Bajalica-Lagercrantz S, Mohell N, et al. Strong synergy with APR-246 and DNA-damaging drugs in primary cancer cells from patients with TP53 mutant High-Grade Serous ovarian cancer. *J Ovarian Res* (2016) 9(1):27. doi: 10.1186/s13048-016-0239-6
 29. Wu J, Song R, Song W, Li Y, Zhang Q, Chen Y, et al. Chlorpromazine protects against apoptosis induced by exogenous stimuli in the developing rat brain. *PLoS One* (2011) 6(7):e21966. doi: 10.1371/journal.pone.0021966
 30. Wu J, Li A, Li Y, Li X, Zhang Q, Song W, et al. Chlorpromazine inhibits mitochondrial apoptotic pathway via increasing expression of tissue factor. *Int J Biochem Cell Biol* (2016) 70:82–91. doi: 10.1016/j.biocel.2015.11.008
 31. Stein GH. T98G: an anchorage-independent human tumor cell line that exhibits stationary phase G1 arrest in vitro. *J Cell Physiol* (1979) 99(1):43–54. doi: 10.1002/jcp.1040990107
 32. Cheng HW, Liang YH, Kuo YL, Chu CP, Lin CY, Lee MH, et al. Identification of thioridazine, an antipsychotic drug, as an antiglioblastoma and anticancer stem cell agent using public gene expression data. *Cell Death Dis* (2015) 6:e1753. doi: 10.1038/cddis.2015.77
 33. Toledo-Guzman ME, Hernandez MI, Gomez-Gallegos AA, Ortiz-Sanchez E. ALDH as a Stem Cell Marker in Solid Tumors. *Curr Stem Cell Res Ther* (2019) 14(5):375–88. doi: 10.2174/1574888X13666180810120012
 34. Li G, Li Y, Liu X, Wang Z, Zhang C, Wu F, et al. ALDH1A3 induces mesenchymal differentiation and serves as a predictor for survival in glioblastoma. *Cell Death Dis* (2018) 9(12):1190. doi: 10.1038/s41419-018-1232-3
 35. Lee CAA, Banerjee P, Wilson BJ, Wu S, Guo Q, Berg G, et al. Targeting the ABC transporter ABCB5 sensitizes glioblastoma to temozolomide-induced apoptosis through a cell-cycle checkpoint regulation mechanism. *J Biol Chem* (2020) 295(22):7774–88. doi: 10.1074/jbc.RA120.013778
 36. D'Atri S, Tentori L, Lacal PM, Graziani G, Pagani E, Benincasa E, et al. Involvement of the mismatch repair system in temozolomide-induced apoptosis. *Mol Pharmacol* (1998) 54(2):334–41. doi: 10.1124/mol.54.2.334
 37. Buccarelli M, Marconi M, Pacioni S, De Pasqualis I, D'Alessandris QG, Martini M, et al. Inhibition of autophagy increases susceptibility of glioblastoma stem cells to temozolomide by igniting ferroptosis. *Cell Death Dis* (2018) 9(8):841. doi: 10.1038/s41419-018-0864-7
 38. Abbruzzese C, Matteoni S, Signore M, Cardone L, Nath K, Glickson JD, et al. Drug repurposing for the treatment of glioblastoma multiforme. *J Exp Clin Cancer Res* (2017) 36(1):169. doi: 10.1186/s13046-017-0642-x
 39. Schonberger DL, Lubelski D, Miller TE, Rich JN. Brain tumor stem cells: Molecular characteristics and their impact on therapy. *Mol Asp Med* (2014) 39:82–101. doi: 10.1016/j.mam.2013.06.004
 40. Gimple RC, Bhargava S, Dixit D, Rich JN. Glioblastoma stem cells: lessons from the tumor hierarchy in a lethal cancer. *Genes Dev* (2019) 33(11-12):591–609. doi: 10.1101/gad.324301.119
 41. Cheng L, Bao S, Rich JN. Potential therapeutic implications of cancer stem cells in glioblastoma. *Biochem Pharmacol* (2010) 80(5):654–65. doi: 10.1016/j.bcp.2010.04.035
 42. Couturier CP, Ayyadury S, Le PU, Nadaf J, Monlong J, Riva G, et al. Single-cell RNA-seq reveals that glioblastoma recapitulates a normal neurodevelopmental hierarchy. *Nat Commun* (2020) 11(1):3406. doi: 10.1038/s41467-020-17186-5
 43. Beaulieu JM, Gainetdinov RR. The physiology, signaling, and pharmacology of dopamine receptors. *Pharmacol Rev* (2011) 63(1):182–217. doi: 10.1124/pr.110.002642
 44. Barygin OI, Nagaeva EI, Tikhonov DB, Belinskaya DA, Vanchakova NP, Shestakova NN, et al. Inhibition of the NMDA and AMPA receptor channels by antidepressants and antipsychotics. *Brain Res* (2017) 1660:58–66. doi: 10.1016/j.brainres.2017.01.028
 45. Venkatesh HS, Morishita W, Geraghty AC, Silverbush D, Gillespie SM, Arzt M, et al. Electrical and synaptic integration of glioma into neural circuits. *Nature* (2019) 573(7775):539–45. doi: 10.1038/s41586-019-1563-y
 46. Venkataramani V, Tanev DI, Strahle C, Studier-Fischer A, Fankhauser L, Kessler T, et al. Glutamatergic synaptic input to glioma cells drives brain tumour progression. *Nature* (2019) 573(7775):532–8. doi: 10.1038/s41586-019-1564-x
 47. Meyer M, Reimand J, Lan X, Head R, Zhu X, Kushida M, et al. Single cell-derived clonal analysis of human glioblastoma links functional and genomic heterogeneity. *Proc Natl Acad Sci U S A* (2015) 112(3):851–6. doi: 10.1073/pnas.1320611111
 48. Lan X, Jorg DJ, Cavalli FMG, Richards LM, Nguyen LV, Vanner RJ, et al. Fate mapping of human glioblastoma reveals an invariant stem cell hierarchy. *Nature* (2017) 549(7671):227–32. doi: 10.1038/nature23666
 49. World Health Organization Model List of Essential Medicines, 21st List. Geneva: World Health Organization (2019).

Conflict of Interest: The authors declare that the research was conducted in the absence of any commercial or financial relationships that could be construed as a potential conflict of interest.

Copyright © 2021 Matteoni, Matarrese, Ascione, Buccarelli, Ricci-Vitiani, Pallini, Villani, Pace, Paggi and Abbruzzese. This is an open-access article distributed under the terms of the Creative Commons Attribution License (CC BY). The use, distribution or reproduction in other forums is permitted, provided the original author(s) and the copyright owner(s) are credited and that the original publication in this journal is cited, in accordance with accepted academic practice. No use, distribution or reproduction is permitted which does not comply with these terms.



Cyclovirobuxine D Induces Apoptosis and Mitochondrial Damage in Glioblastoma Cells Through ROS-Mediated Mitochondrial Translocation of Cofilin

Lin Zhang[†], Ruoqiu Fu[†], Dongyu Duan, Ziwei Li, Bin Li, Yue Ming, Li Li, Rui Ni and Jianhong Chen^{*}

OPEN ACCESS

Edited by:

Patricia Sancho,
Universidad de Zaragoza, Spain

Reviewed by:

Lala Caja,
Uppsala University, Sweden
Roberta Manuela Moretti,
University of Milan, Italy

*Correspondence:

Jianhong Chen
Chenj_h_110@263.net

[†]These authors have contributed
equally to this work and share
first authorship

Specialty section:

This article was submitted to
Pharmacology of Anti-Cancer Drugs,
a section of the journal
Frontiers in Oncology

Received: 20 January 2021

Accepted: 26 February 2021

Published: 19 March 2021

Citation:

Zhang L, Fu R, Duan D, Li Z, Li B,
Ming Y, Li L, Ni R and Chen J (2021)
Cyclovirobuxine D Induces Apoptosis
and Mitochondrial Damage in
Glioblastoma Cells Through
ROS-Mediated Mitochondrial
Translocation of Cofilin.
Front. Oncol. 11:656184.
doi: 10.3389/fonc.2021.656184

Department of Pharmacy, Daping Hospital, Army Medical University, Chongqing, China

Background: Cyclovirobuxine D (CVBD), a steroidal alkaloid, has multiple pharmacological activities, including anti-cancer activity. However, the anti-cancer effect of CVBD on glioblastoma (GBM) has seldom been investigated. This study explores the activity of CVBD in inducing apoptosis of GBM cells, and examines the related mechanism in depth.

Methods: GBM cell lines (T98G, U251) and normal human astrocytes (HA) were treated with CVBD. Cell viability was examined by CCK-8 assay, and cell proliferation was evaluated by cell colony formation counts. Apoptosis and mitochondrial superoxide were measured by flow cytometry. All protein expression levels were determined by Western blotting. JC-1 and CM-H₂DCFDA probes were used to evaluate the mitochondrial membrane potential (MMP) change and intracellular ROS generation, respectively. The cell ultrastructure was observed by transmission electron microscope (TEM). Colocalization of cofilin and mitochondria were determined by immunofluorescence assay.

Results: CVBD showed a greater anti-proliferation effect on the GBM cell lines, T98G and U251, than normal human astrocytes in dose- and time-dependent manners. CVBD induced apoptosis and mitochondrial damage in GBM cells. We found that CVBD led to mitochondrial translocation of cofilin. Knockdown of cofilin attenuated CVBD-induced apoptosis and mitochondrial damage. Additionally, the generation of ROS and mitochondrial superoxide was also induced by CVBD in a dose-dependent manner. N-acetyl-L-cysteine (NAC) and mitoquinone (MitoQ) pre-treatment reverted CVBD-induced apoptosis and mitochondrial damage. MitoQ pretreatment was able to block the mitochondrial translocation of cofilin caused by CVBD.

Conclusions: Our data revealed that CVBD induced apoptosis and mitochondrial damage in GBM cells. The underlying mechanism is related to mitochondrial translocation of cofilin caused by mitochondrial oxidant stress.

Keywords: cyclovirobuxine D (CVBD), glioblastoma (GBM), apoptosis, mitochondrial damage, oxidative stress

INTRODUCTION

Glioma, which is the most common central nervous system cancer, accounts for about 40% to 50% of all intracranial tumors (1). Glioblastoma (GBM), classified as grade IV by the World Health Organization (WHO), is the most fatal and malignant type of glioma (2). The median survival time of GBM patients is about 18 months, and only about 30% of patients achieve 2-year survival (3, 4). At present, the standard therapy for GBM is surgical resection combined with local radiotherapy, and adjuvant chemotherapy with the alkylating agent temozolomide (TMZ) (5). Although patients treated with TMZ have a significantly higher survival than those treated with radiotherapy alone, the overall prognosis is still poor, and the resistance of GBM cells to TMZ is often to blame (6, 7). Therefore, there is an urgent need to find a novel and effective anti-GBM agent.

Accumulated evidence has revealed that natural products have marvelous anti-cancer effects, such as inhibiting cell proliferation, inducing apoptosis and mitochondrial damage, and promoting oxidative-stress (8–12). Cyclovirobuxine D (CVBD) is an alkaloid derived from *Buxus sinica* and other plants of the same genus (13). Published studies suggest that CVBD has an effect on various cancer cells. For instance, CVBD inhibits colorectal cancer tumorigenesis *via* the CTHRC1-AKT/ERK-Snail signaling pathway (14), and exerts anticancer effects by suppressing the EGFR-FAK-AKT/ERK1/2-Slug signaling pathway in human hepatocellular carcinoma (15). Moreover, CVBD inhibits cell proliferation and induces mitochondria-mediated apoptosis in human gastric cancer cells (16), and induces autophagy-associated cell death *via* the Akt/mTOR pathway in MCF-7 human breast cancer cells (17). However, the anticancer effects and detailed mechanism of CVBD action against GBM have rarely been investigated.

Cofilin is from the actin-depolymerizing factor (ADF) family, which is best known as a key regulator of actin filament dynamics (18). Recent discoveries have increased our knowledge of cofilin beyond its well-characterized roles. Cofilin has a pivotal role in cancer progression, invasion, and apoptosis (19). Increasing evidence indicates that the function of cofilin is strongly associated with apoptosis mediated by mitochondrial functioning and dynamics (20). After induction of apoptosis, dephosphorylated cofilin is translocated from the cytosol into the mitochondria before the release of cytochrome c (21). The excessive generation of reactive oxygen species (ROS) can be harmful to cells, and cancer cells are more vulnerable to damage by increased oxidative stress caused by exogenous agents (22). ROS play a key role in cell growth, progression, differentiation, and death, especially the increased ROS involved in the fate of

cancer cells (23, 24). Several studies have revealed that ROS participate in the activation of the classic apoptosis pathway and mitochondrial damage, through molecules and proteins associated with either mitochondrial function or cell death (25–28). Mitochondria are the main cellular organelles for bioenergetics, metabolism, biosynthesis, and cell death (29). Several reports have shown that the over-generation of mitochondrial superoxide could promote GBM cell death *via* phosphorylation of JNK (30). Mitochondrial superoxide accumulation could activate the intrinsic apoptosis pathway in multiple myeloma cells (31).

In our present study, the mechanism of CVBD for inducing mitochondrial damage and apoptosis in GBM cells was revealed. This work generates fresh insight into the association of CVBD-induced GBM cell apoptosis with the mitochondrial superoxide-mediated translocation of cofilin.

MATERIALS AND METHODS

Chemicals and Antibodies

Cyclovirobuxine D (Cat.no. A0075) was purchased from CHENGDU MUST BIO-TECHNOLOGY CO., LTD (Chengdu, China); Z-VAD-FMK (Cat.no. HY-16658), Mitoquinone (Cat.no. HY-100116A) and CCCP (Cat.no. HY-100941) were purchased from MedChemExpress (Monmouth Junction, NJ, USA); N-acetyl-L-cysteine (NAC) (Cat.no. ST1546) was purchased from Beyotime (Shanghai, China); DMSO (Cat.no. D8418) was purchased from Sigma-Aldrich Chemical Co. (St. Louis, MO, USA); antibodies against C-Caspase3 (Cat.no. 9116S), GAPDH (Cat.no. 2118), phospho-AKT (Cat.no. 4060S) were purchased from Cell Signaling Technology (Beverly, MA, USA); cofilin (Cat.no. ab42824), phospho-Cofilin (S3, Cat.no. ab12866), VDAC1 (Cat.no. ab14734), phospho-ERK (Cat.no. ab50011), AKT (Cat.no. ab200195) and ERK (Cat.no. ab17942) were obtained from Abcam (Cambridge, UK); PARP (Cat.no. 13371-1-AP), and cytochrome c (Cat.no. 10993-1-AP) were purchased from Proteintech (Rosemont, IL, USA).

Cell Lines and Cell Culture

The GBM cell lines, T98G and U251, were obtained from the American Type Culture Collection (ATCC, Manassas, VA, USA). Human astrocytes (HA) and growth medium were obtained from Scien Cell Research Laboratories (Carlsbad, CA, USA). DMEM medium (Cat.no. SH30022.01, Hyclone Laboratories, Inc. Logan, UT, USA) and 10% fetal bovine serum (Cat.no. 10099141C, Gibco, Carlsbad, CA, USA) were used for culturing the T98G and U251 cells. All cell lines were cultured in a humidified atmosphere at 37 °C in 5% CO₂.

CCK-8 Cell Viability Assay

Cells were seeded in 96-well plates with 5×10^3 cells/well and incubated for 24 h, followed by treatment with CVBD (0, 40, 80, 120, 160 μM) for different periods of time (0, 12, 24, 36, 48 h). Additionally, the cells were treated with CVBD (120 μM) for 24 h after being pre-treated with NAC (20 μM) for 2 h or MitoQ (0.5 μM) for 30 min. Subsequently, a 10 μL Cell Counting Kit-8 (CCK-8, MCE, Cat.no. HY-K0301, Monmouth Junction, NJ, USA) was added to each well and incubated at 37 °C and 5% CO_2 for 2 h before the absorbance at 450 nm was measured with a microplate reader (Agilent Technologies, CA, USA). The cell viabilities are expressed as a percentage.

Cell Colony-Forming Assay

Cells were seeded in six-well plates with 500 cells/well and then incubated for 24 h, followed by treatment with different doses of CVBD (0, 40, 80, 120, 160 μM) for 24 h. The medium containing CVBD was then replaced with fresh complete medium and the cells were incubated at 37 °C and 5% CO_2 , changing the culture medium every three days. After 15 days, the colonies were fixed for 10 min with 4% paraformaldehyde (PFA) (Cat.no. C0121, Beyotime, Shanghai, China), followed by staining for 15 min with crystal violet staining solution (Cat.no. P0099, Beyotime, Shanghai, China). The colonies were scanned with CanoScan Lide (Canon, Japan).

Apoptosis Assay

Cells were stained with Annexin V/FITC and PI (Cat.no. 556547, BD Biosciences, Franklin Lakes, NJ, USA) following the manufacturer's specifications. Briefly, 2×10^5 cells/well were collected and centrifuged at 600 g for 5 min. Cell pellets were resuspended with 1 mL PBS. Centrifugation and resuspension were repeated twice. Then, cells were stained with 2 μL Annexin V/FITC and 5 μL PI in $1 \times$ binding buffer for 15 min at room temperature in the dark. Quantitative analysis of apoptotic cells was undertaken by flow cytometry (Accuri C6, BD Biosciences, Franklin Lakes, NJ, USA).

Measurement of Mitochondrial Membrane Potential (MMP)

Cells were seeded in six-well plates with 2×10^5 cells/well and cultured for 24 h. Cells were stained with a JC-1 probe (Cat.no. C2006, Beyotime, Shanghai, China) according to the manufacturer's instructions. After staining, cells were washed twice and 2 mL/well of medium was added. The green and red fluorescence were observed by fluorescence microscope (Thermo Fisher Scientific, Waltham, MA, USA). The level of mitochondrial membrane potential (MMP) is expressed as the relative ratio of red (J-aggregates) and green (monomer) fluorescence. Quantification of fluorescence intensity was obtained through analysis using Image J software (National Institutes of Health, Bethesda, MD, USA).

Transmission Electronic Microscopy (TEM)

Cells were treated according to the previous method, and the collected cell pellets were fixed at 4 °C overnight in 2.5%

glutaraldehyde, then were fixed at room temperature for 1.5 h in 2% osmium tetroxide using uranyl acetate/lead citrate to embed and stain the cells after fixation. The cell sections were carried out using a transmission electron microscope at 60 kV.

RNA Interference Assay

The target shRNA sequence was constructed by Gene Chem Co. Ltd. (Shanghai, China). The sequence of the cofilin shRNA was as follows: 5'-CCGGAAGGTGTTCAATGACATGAAAC TCGAGTTTCATGTCATTGAACACCTTTTTTTTG-3'. The control shRNA plasmid was purchased from Santa Cruz Biotechnology, Inc. (Cat.no. sc-108060, Dallas, TX, USA). 293FT cells were co-transfected with the lentiviral packing vectors pLP1, pLP2, and pLP/VSVG (Invitrogen, Carlsbad, CA, USA), along with the shCofilin or shCon plasmid, using Lipofectamine 3000 (Invitrogen, Carlsbad, CA, USA) for 48 h. The supernatant containing the lentivirus was harvested and used for infection of T98G and U251 cells. Subsequently, selected stable cell lines were treated with 4 $\mu\text{g}/\text{mL}$ puromycin (Cat.no. P9620, Sigma-Aldrich, St. Louis, MO, USA).

Measurement of Intracellular ROS Generation

Cells were seeded in six-well plates with 2×10^5 cells/well and incubated for 24 h. They were treated with the indicated concentrations of CVBD for 24 h, or pre-treated with NAC for 2 h before being treated with CVBD. Following replacement of the cell medium, we incubated the cells with 10 μM CM-H₂DCFDA serum-free culture medium for 30 min at 37 °C (Cat.no. C6827, Molecular Probes, Thermo Fisher Scientific, Waltham, MA, USA). Subsequently, the cells were washed twice with PBS. The green fluorescence change of intracellular ROS was observed using a fluorescent microscope (Thermo Fisher Scientific, Waltham, MA, USA), and Image J software (National Institutes of Health, Bethesda, MD, USA) was used to quantify the ROS fluorescence intensity.

Measurement of Mitochondrial Superoxide Generation

Cells were seeded in six-well plates with 2×10^5 cells/well and cultured for 24 h. The cells were treated with the indicated concentrations of CVBD for 24 h, or were pre-treated with Mito Q for 30 min before being treated with CVBD. After the drug treatments, cells were incubated with MitoSOXTM Red (Invitrogen, Carlsbad, CA, USA) for 30 min at 37 °C. Quantification of mitochondrial superoxide was by flow cytometry (Accuri C6, BD Biosciences, Franklin Lakes, NJ, USA).

Immunofluorescence

Cells were seeded on coverslips and cultured for 24 h. According to the manufacturer's protocol, mitochondria were stained with MitoTracker (Deep Red FM) (Cat.no. M22426, Invitrogen, Carlsbad, CA, USA) for 30 min at 37 °C. Cells were fixed with 4% paraformaldehyde (PFA) for 30 min in the dark, and permeated with 0.1% Triton 100 (Cat.no. ST795, Beyotime,

Shanghai, China) for 5 min. After being blocked in normal goat serum for 30 min at room temperature, cells were incubated with antibody overnight at 4 °C, followed by washing and incubating with the appropriate secondary antibodies. After immunostaining, cells were stained for 3–5 min with DAPI nuclear stain. Cells were observed using confocal microscopy (Cat.no. LSM 780NLO, Carl Zeiss, Germany).

Extraction of Cell Mitochondria

Cells were seeded in 100mm cell culture dish and cultured for 24 h. Cell mitochondria isolation as performed using the Cell Mitochondria Isolation Kit (Cat.no. C3601, Beyotime, Shanghai, China) according to the manufacture's protocol. Cells were collected and suspended with mitochondrial extraction agent. After being centrifugating, the precipitate was followed by washing twice with mitochondrial lysate agent. After being centrifugating again, the supernatant was collected as mitochondrial protein. Finally, the concentration of mitochondrial protein sample was quantified by BCA assay.

Western Blotting

Cells were collected for lysis with RIPA buffer (Cat.no. P0013, Beyotime, Shanghai, China), and the concentration of each protein sample was quantified by BCA assay. The protein samples (15–30 µg) were separated by 10–12% SDS-PAGE and transferred to PVDF membranes (Cat.no. ISEQ00010, Millipore, Billerica, MA, USA). The membranes were incubated overnight with primary antibodies at 4 °C after being blocked with 5% milk for 1 h. Subsequently, the membranes were incubated with horseradish peroxidase (HRP)-conjugated antibodies for 2 h and visualized using an enhanced chemiluminescence (ECL) substrate (Cat.no. 1705060, Bio-Rad, Hercules, CA, USA). We used the Image J software (National Institutes of Health, Bethesda, MD, USA) to determine the gray density of the protein bands.

Statistical Analysis

Colocalization correlation coefficients were determined using Image J software. All experimental data are represented as the mean ± SD from three independent experiments. The comparisons were performed using a one-way analysis of variance (ANOVA) or t-test by SPSS 19.0 (IBM Corporation, Armonk, NY, USA). * $P < 0.05$, ** $P < 0.01$ or *** $P < 0.001$ was considered statistically significant.

RESULTS

CVBD Inhibits Cell Proliferation in Human GBM Cells

The chemical structure of cyclovirobuxine D (CVBD) indicated in **Figure 1A**. To study the effect of CVBD on the growth of human GBM cells and normal human astrocytes (HA), the cell viabilities were determined by CCK-8 assay. We found that the cell viabilities were decreased in a dose-dependent manner in T98G and U251 cells treated with CVBD. The cell viability of

normal human astrocytes (HA) was affected only rarely (**Figure 1B**). In addition, we also evaluated the effect of CVBD on cell clone formation in T98G and U251 cells. As shown in **Figures 1C, D**, treating T98G and U251 cells with CVBD clearly reduced cell clone formation in a dose-dependent manner. These results suggest that CVBD could inhibit GBM cell proliferation.

CVBD Induces Apoptosis in Human GBM Cells

To determine whether CVBD causes GBM cell death, the apoptosis of T98G and U251 cells was detected by flow cytometry. Treatment of cells with CVBD for 24 h noticeably induced apoptosis of T98G and U251 cells in a dose-dependent manner (**Figures 2A, B**). Consistent with these findings, CVBD treatment caused activation of cleaved-caspase3 and degradation of PARP with formation of cleaved-PARP (**Figures 2C, D**). Furthermore, T98G and U251 cells were pre-treated with Z-VAD-FMK, a pan-caspase inhibitor, and this significantly attenuated the apoptotic rate induced by CVBD (**Figures 2E, F**). Western blotting results showed that pre-treatment with Z-VAD-FMK could markedly attenuate the upregulation of C-PARP and C-Caspase3 induced by CVBD, and inhibit the degradation of PARP induced by CVBD (**Figures 2G, H**). Overall, these results indicated that CVBD may induce caspase-dependent apoptosis of T98G and U251 cells.

CVBD Induces Mitochondrial Damage in Human GBM Cells

Several studies have suggested that cell apoptosis can be caused by mitochondrial damage. To determine the effect of CVBD on mitochondrial damage in T98G and U251 cells, the mitochondrial membrane potential (MMP) was detected using a fluorescent probe JC-1, and CCCP as a classical mitochondrial proton carrier uncoupling agent, which can increase the proton permeability of the mitochondrial membrane and destroy the mitochondrial membrane potential. As shown in **Figures 3A, B**, treatment with CVBD or CCCP enhanced the green fluorescence intensity and weakened the red fluorescence intensity in T98G and U251 cells, which indicates that the mitochondrial membrane potential (MMP) was decreased. Notably, the result of MitoTracker (Deep Red FM) staining showed the average length of mitochondria of cells exposed to CVBD was shorter than those exposed to placebo (control), which indicates that CVBD could lead to marked mitochondrial fragmentation (**Figures 3C, D**). To determine the morphology of mitochondria in T98G and U251 cells treated with CVBD, the ultrastructural changes of cells were examined by transmission electron microscopy (TEM). As shown in **Figure 3E**, the mitochondrial morphology of cells treated with CVBD was shrunken and rounded compared to the control group. The release of cytochrome c (Cyto C) from mitochondria into the cytoplasm indicated the activation of the intrinsic pathway of apoptosis, which mitochondrial dependent. Therefore, we evaluated the expression level of Cyto C in the cytosolic fraction by Western blotting analysis. As shown in **Figures 3F, G**, CVBD significantly increased the expression level of Cyto C in the cytosolic fraction.

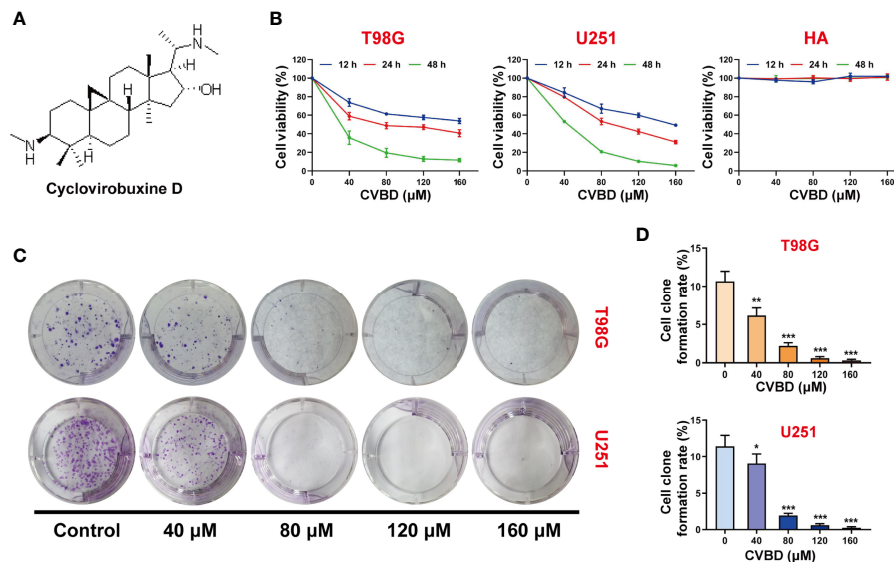


FIGURE 1 | CVBD inhibits cell proliferation and colony formation in glioblastoma (GBM) cells. **(A)** The chemical structure of cyclovirobuxine D (CVBD). **(B)** GBM cells (T98G and U251) and normal human astrocytes (HA) were treated with CVBD (40, 80, 120, 160 μM) for 12, 24, and 48 h. Cell viability was measured by CCK-8 assay, and 0 μM CVBD was used as a control group. **(C, D)** Colony formation was assessed by plate clone formation assay in T98G and U251 cells (mean ± SD of three independent experiments, * $P < 0.05$, ** $P < 0.01$, *** $P < 0.001$ compared with the control group).

Together, these results show that CVBD induces mitochondrial damage in GBM cells.

Mitochondrial Translocation of Cofilin Is Required for CVBD-Induced Mitochondrial Damage and Apoptosis in GBM Cells

We detected the effect of CVBD on de-phosphorylation and mitochondrial translocation of cofilin in T98G and U251 cells. Western blotting showed that CVBD decreased the expression level of phospho-cofilin in whole cell lysate (WCL), but increased the expression level of cofilin in the mitochondria fraction and decreased it in the cytosolic fraction in a dose-dependent manner (Figures 4A, B). To further confirm whether cofilin was translocated to mitochondria, the colocalization of cofilin and MitoTracker (Deep Red FM) was observed in cells treated with CVBD. The colocalization correlation coefficient of CVBD treatment group significantly higher than control group (Figure 4E). Overall, these results suggested that CVBD induced mitochondrial translocation of cofilin in GBM cells.

Based on the above studies, we further investigated whether mitochondrial translocation of cofilin is required for CVBD-induced mitochondrial damage and apoptosis. Therefore, we knocked down the cofilin with shRNA to clarify the role of cofilin in CVBD-induced mitochondrial damage and apoptosis. Western blotting results showed that knockdown of cofilin significantly inhibited the high expression level of cofilin in the mitochondria fraction induced by CVBD (Figures 4F, G). Knockdown of cofilin inhibited the mitochondrial

fragmentation (Figures 4H, I) and attenuated the apoptosis induced by CVBD (Figures 4J, K). Consistent with these findings, knockdown of cofilin reduced the CVBD-mediated upregulation of C-PARP and C-Caspase3 and the release of Cyto C from the mitochondria, and inhibited the degradation of PARP induced by CVBD (Figures 4L, M). Taken together, these results suggest that mitochondrial translocation of cofilin is essential for CVBD-induced mitochondrial damage and apoptosis.

CVBD Induces Accumulation of Reactive Oxygen Species (ROS) in GBM Cells

We explored the effect of CVBD on ROS generation in GBM cells, in which the green fluorescence of the CM-H₂DCFDA probe indicated intracellular ROS generation. As shown in Figures 5A, B, green fluorescence was enhanced in a dose-dependent manner in cells treated with CVBD. Subsequently, cells pre-treated with N-acetyl-L-cysteine (NAC) showed lower green fluorescence intensity than those treated with CVBD alone (Figures 5C, D). In Figure 5E, the cell viability of cells pre-treated with NAC is higher than in those treated with CVBD alone. To further investigate whether ROS were involved in CVBD-induced cell apoptosis, cells were pre-treated with NAC for 2 h, and apoptosis was detected by flow cytometry. As shown in Figures 5F, G, cells pre-treated with NAC significantly decreased the apoptotic rate induced by CVBD. Western blotting results showed that pre-treatment with NAC significantly obstructed the CVBD-induced upregulation of C-PARP and C-Caspase3 and the release of Cyto C, and inhibited the degradation of PARP induced by

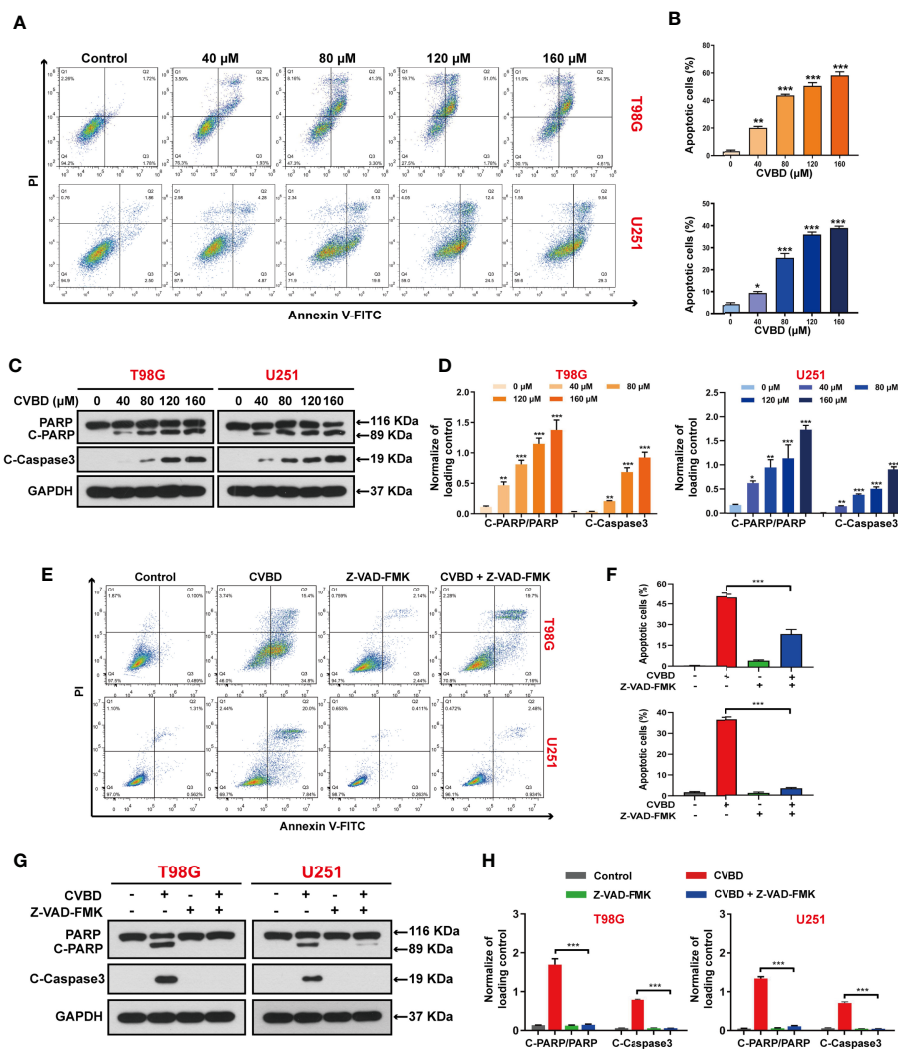


FIGURE 2 | CVBD induces apoptosis in GBM cells. **(A, B)** T98G and U251 cells were exposed to various concentrations of CVBD (80, 120, 160 μM) for 24 h, and 0 μM CVBD was used as the control group. Apoptosis was detected by AnnexinV-FITC/PI staining and flow cytometry. **(C, D)** T98G and U251 cells were treated as indicated in **(A, B)**. The total cellular extracts of T98G and U251 cells were determined by Western blotting using antibodies against total PARP, cleaved PARP (C-PARP), and cleaved-Caspase3 (C-Caspase3) (mean \pm SD of three independent experiments, * $P < 0.05$, ** $P < 0.01$, *** $P < 0.001$ compared with the control group). GAPDH was used as a loading control. **(E, F)** T98G and U251 cells were pre-treated with Z-VAD-FMK (20 μM , 2 h) and post-treated with CVBD (120 μM) for 24 h. Apoptosis was detected by AnnexinV-FITC/PI staining and flow cytometry. **(G, H)** T98G and U251 cells were treated as indicated in **(E)**. The expression level of PARP, C-PARP, and C-Caspase3 were determined by Western blotting analysis. GAPDH was used as a loading control (mean \pm SD of three independent experiments, *** $P < 0.001$ compared with CVBD treatment alone).

CVBD (**Figures 5H, I**). These findings indicated that intracellular ROS accumulation resulted in CVBD-mediated apoptosis in GBM cells.

CVBD Induces Mitochondrial Superoxide Production in GBM Cells

To further clarify the role of mitochondrial oxidative stress in apoptosis induced by CVBD, mitochondrial superoxide production was detected by MitoSOXTM Red staining and flow cytometry. As shown in **Figures 6A, B**, the percentage of mitochondrial superoxide production in GBM cells was

gradually increased after CVBD treatment. Subsequently, cells pre-treated with MitoQ showed a lower percentage of mitochondrial superoxide than those treated with CVBD alone (**Figures 6C, D**). In **Figure 6E**, pretreatment with MitoQ, a mitochondrial superoxide inhibitor, reversed the decrease in cell viability induced by CVBD. To further investigate whether Mito ROS are involved in CVBD-induced cells apoptosis, cells were pre-treated with MitoQ and apoptosis was detected by flow cytometry. As shown in **Figures 6F, G**, pre-treatment with MitoQ significantly decreased the apoptotic rate induced by CVBD. Consistent with the above findings, Western blotting results

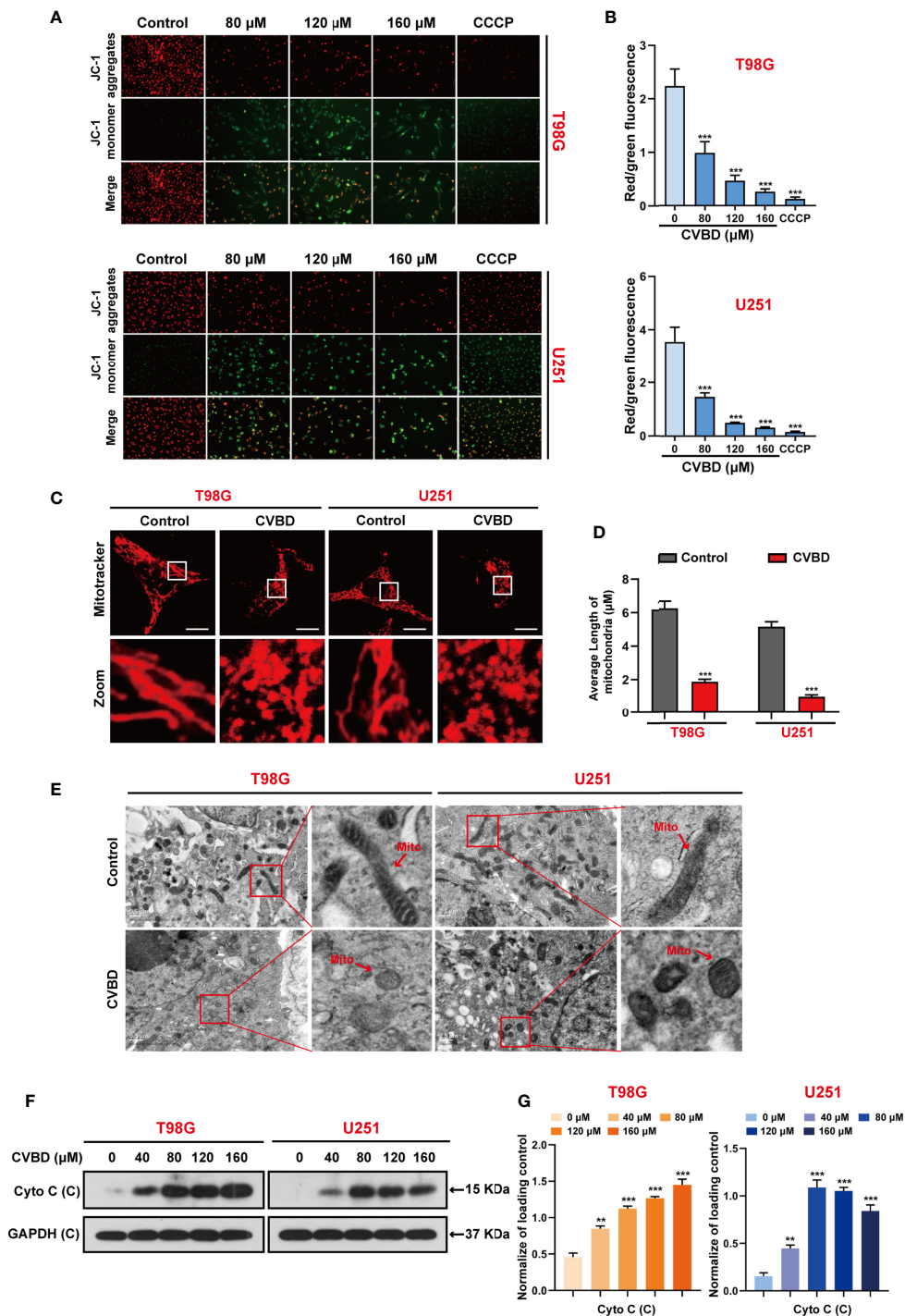


FIGURE 3 | CVBD induces mitochondrial damage in GBM cells. **(A, B)** T98G and U251 cells were exposed to various concentrations of CVBD (80, 120, 160 μ M) for 24 h, and 0 μ M CVBD was used as the control group. CCCP was used as the positive control (50 μ M, 30 min). The mitochondrial membrane potential (MMP) was detected by a fluorescence microscope using JC-1 probe staining (mean \pm SD of three independent experiments, ***P < 0.001 compared with the control group). **(C, D)** T98G and U251 cells were treated with CVBD (120 μ M) for 24 h. Mitochondrial morphology was observed using MitoTracker (Deep Red FM) staining followed by confocal microscopy. Scale bars: 10 μ m. The average length of the mitochondria was measured by Image J software (mean \pm SD of three independent experiments, ***P < 0.001 compared with the control group). **(E)** Representative TEM images of T98G and U251 cells, treated as indicated in **(C)**. Red arrows indicate mitochondria. Scale bars: 0.5 μ m. **(F, G)** T98G and U251 cells were treated with various concentrations of CVBD for 24 h. The expression level of Cyto C in the cytoplasm was detected by Western blotting analysis. GAPDH was used as a loading control (mean \pm SD of three independent experiments, **P < 0.01, ***P < 0.001 compared with the control group).

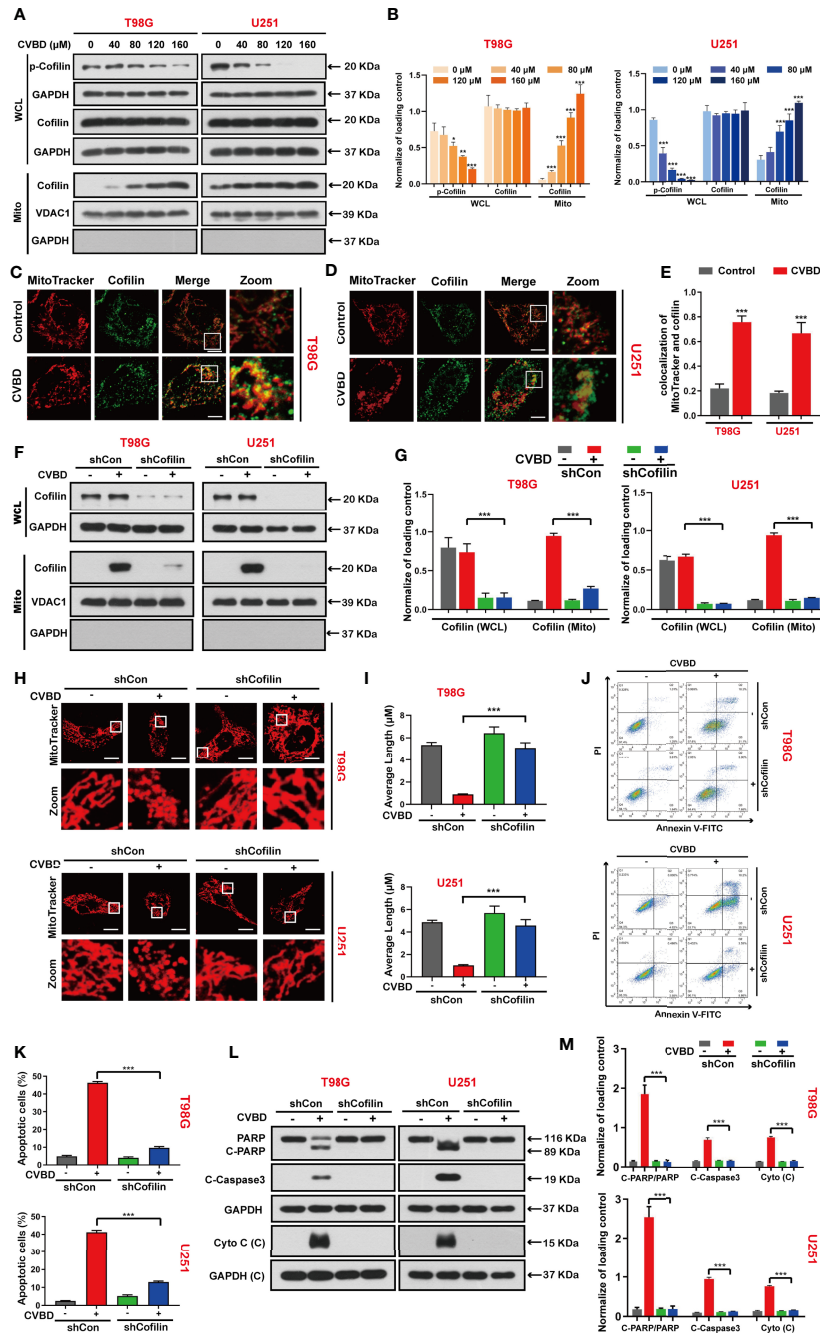


FIGURE 4 | CVBD induces mitochondrial translocation of cofilin, and knockdown of cofilin attenuates CVBD-mediated mitochondrial damage and apoptosis.

(A, B) T98G and U251 cells were exposed to various concentrations of CVBD for 24 h. The expression level of p-cofilin and cofilin in the whole cell lysate (WCL) and cofilin in the mitochondrial fractions was determined by Western blotting analysis. GAPDH and VDAC1 were used as loading controls. GAPDH was also used as cytosolic marker (mean \pm SD of three independent experiments, * $P < 0.05$, ** $P < 0.01$, *** $P < 0.001$ compared with the control group). (C, D) T98G and U251 were treated with CVBD (120 μ M) for 24 h; the colocalization of MitoTracker (red) and cofilin (green) was observed by confocal microscopy. Scale bars: 10 μ M. For (E) Quantitative analysis of colocalization of MitoTracker (red) and cofilin (green). Colocalization correlation coefficients were represented as mean \pm SD (*** $P < 0.001$ compared with the control group). For (F–M), T98G and U251 cells were stably knocked down and exposed to CVBD (120 μ M) for 24 h. (F, G) The expression level of cofilin in the WCL and mitochondrial fractions was determined by Western blotting. GAPDH and VDAC1 were used as loading controls. GAPDH was also used as cytosolic marker. (H, I) The mitochondrial morphology was observed using MitoTracker (Deep Red FM) staining, followed by confocal microscopy. Scale bars: 10 μ M. The mitochondrial average length was measured with Image J software. (J, K) Apoptosis was detected by Annexin V-FITC/PI staining and flow cytometry. (L, M) The expression level of PARP, C-PARP, C-Caspase3, and Cyto C (C) was determined by Western blotting analysis. GAPDH was used as a loading control (mean \pm SD of three independent experiments, *** $P < 0.001$).

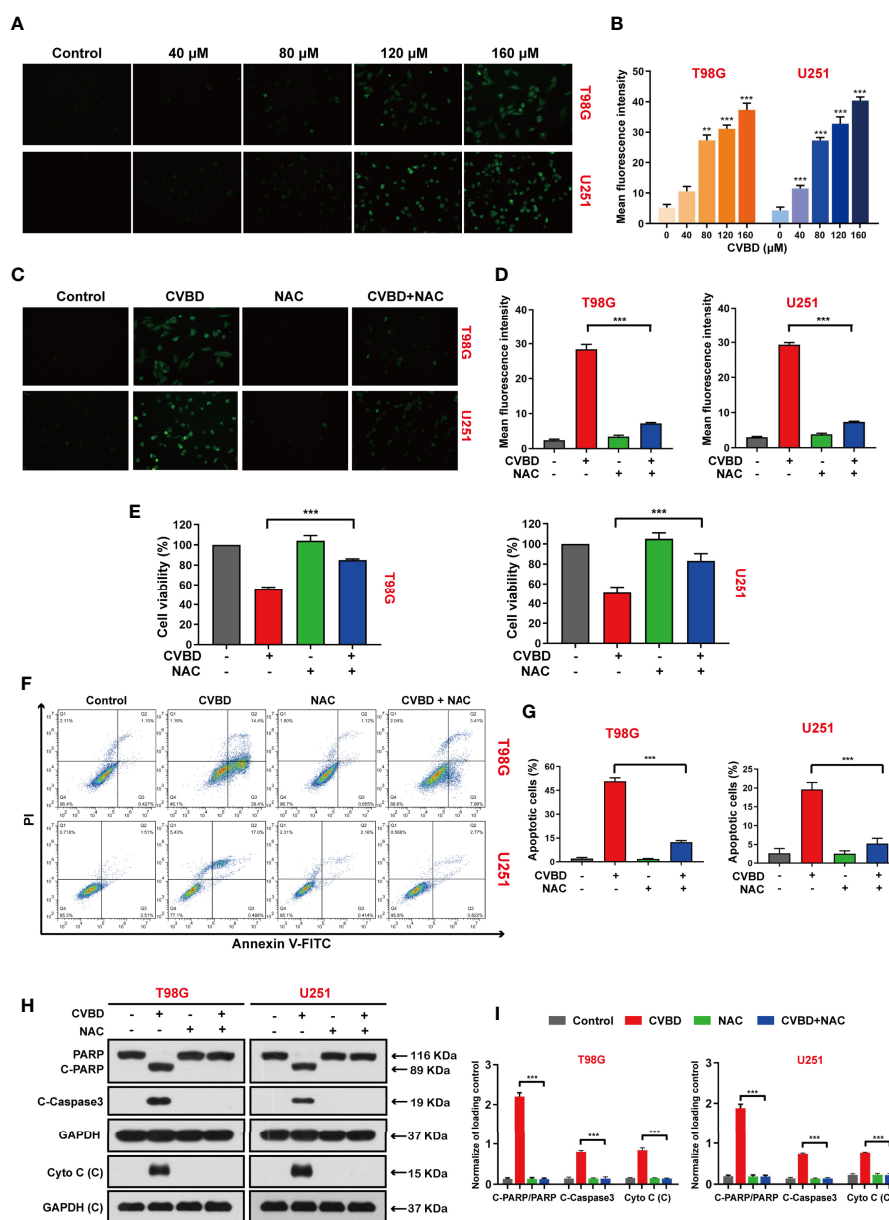


FIGURE 5 | CVBD induces ROS generation and NAC inhibits ROS generation, attenuating CVBD-mediated apoptosis. **(A, B)** T98G and U251 cells were exposed to various concentrations of CVBD for 24 h, and 0 μM CVBD was used as the control group. The ROS generation was observed by fluorescence microscopy using a CM-H₂DCFDA probe (mean \pm SD of three independent experiments, **P < 0.01, ***P < 0.001 compared with the control group). **(C, D)** T98G and U251 cells were pre-treated with NAC (20 μM , 2 h) and post-treated with CVBD (120 μM) for 24 h, and the ROS generation was observed by fluorescence microscopy using CM-H₂DCFDA probe staining. **(E)** T98G and U251 cells were treated as indicated in **(C)**, and the cell viability was examined by CCK-8 assay. **(F, G)** T98G and U251 cells were treated as indicated in **(C)**, and apoptosis was detected by AnnexinV-FITC/PI staining and flow cytometry. **(H, I)** T98G and U251 cells were treated as indicated in **(C)**, and the expression of PARP, C-PARP, C-Caspase3, and Cyto C **(C)** was determined by Western blotting analysis. GAPDH was used as a loading control (mean \pm SD of three independent experiments, ***P < 0.001 compared with CVBD treatment alone).

showed that pre-treatment with MitoQ significantly reduced the upregulation of C-PARP and C-Caspase3 and the release of Cyto C induced by CVBD, and could inhibit the degradation of PARP induced by CVBD (**Figures 6H, I**). These results suggested that apoptosis of T98G and U251 induced by CVBD was caused by mitochondrial superoxide production.

Inhibited Mitochondrial Superoxide Production Blocked CVBD-Meditated Mitochondrial Translocation of Cofilin

To investigate whether the generation of mitochondrial superoxide is related to the mitochondrial translocation of cofilin induced by CVBD, we used Western blotting and an

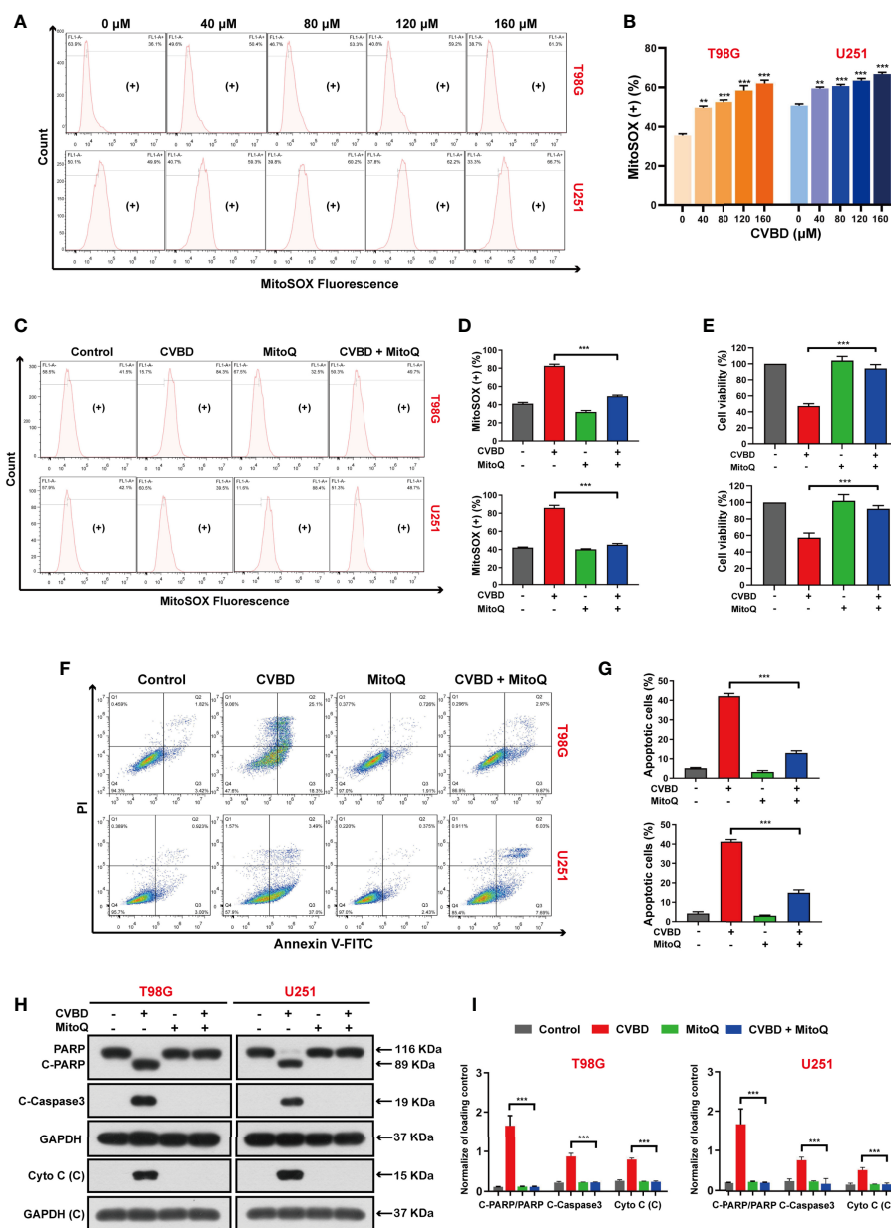


FIGURE 6 | CVBD induces mitochondrial superoxide generation and MitoQ inhibits mitochondrial superoxide production, which attenuates CVBD-mediated apoptosis. **(A, B)** T98G and U251 cells were exposed to various concentrations of CVBD for 24 h, and 0 μ M CVBD was used as the control group. The mitochondrial superoxide generation was detected by flow cytometry using MitoSOXTM Red staining (mean \pm SD of three independent experiments, ** P < 0.01, *** P < 0.001 compared with the control group). **(C, D)** T98G and U251 cells were pre-treated with MitoQ (0.5 μ M, 30 min) and post-treated with CVBD (120 μ M) for 24 h. The mitochondrial superoxide generation was detected by flow cytometry using MitoSOXTM red staining. **(E)** T98G and U251 cells were treated as indicated in **(C)**, and the cell viability was examined by CCK-8 assay. **(F, G)** T98G and U251 cells were treated as indicated in **(C)**, and the apoptosis was detected by AnnexinV-FITC/PI staining and flow cytometry. **(H, I)** T98G and U251 cells were treated as indicated in **(C)**, and the expression of PARP, C-PARP, C-Caspase3, and Cyto C **(C)** was determined by Western blotting analysis. GAPDH was used as a loading control (mean \pm SD of three independent experiments, ** P < 0.01, *** P < 0.001 compared with CVBD treatment alone).

immunofluorescence assay to evaluate the mitochondrial translocation of cofilin. In **Figures 7A, B**, Western blotting results show that pre-treatment with MitoQ markedly decreased the CVBD-induced upregulation of cofilin in the

mitochondria fraction, and reversed the downregulation of p-cofilin in the whole cell lysate (WCL). We subsequently determined the colocalization of cofilin and mitochondria by immunofluorescence assay. As shown in **Figures 7C, D**,

pre-treatment with MitoQ obviously decreased the CVBD-mediated colocalization of cofilin's green puncta and MitoTracker (Deep Red FM). The colocalization correlation coefficient of pre-treatment with MitoQ group significantly lower than CVBD treatment alone (**Figure 7E**). These results indicated that inhibited mitochondrial superoxide generation blocked CVBD-mediated mitochondrial translocation of cofilin.

DISCUSSION

Cyclovirobuxine D (CVBD), a steroidal alkaloid extracted from *Buxus sinica*, has a long history of treating cardiovascular diseases (13). However, studies are increasingly reporting that CVBD shows remarkable suppressive effects in various cancers, such as colorectal cancer, hepatocellular carcinoma, gastric cancers, and breast cancer. In terms of mechanism, several studies have found that CVBD, through the CTHRC1-AKT/ERK-Snail pathway or EGFR-FAK-AKT/ERK1/2-Slug pathway,

inhibit cancer tumorigenesis through CVBD inducing mitochondrial apoptosis in cancer cells. Moreover, CVBD causes cancer cell death of autophagy associated with the AKT/mTOR pathway (14–17). Meanwhile, CVBD could activate AKT/ERK signaling pathway in T98G and U251. In our current study, we found that CVBD inhibited proliferation and induced apoptosis of GBM cells. Mechanistically, we further found that CVBD triggered apoptosis by causing mitochondrial dysfunction, which is primarily attributed to the mitochondria translocation of cofilin *via* the activation of mitochondrial oxidative stress.

As previous published studies have mentioned, cofilin is best known as an actin depolymerizing factor, and it could increase the rate of actin depolymerization through regulating actin dynamics (32, 33). Several studies reveal that cofilin, a member of the cofilin/actin depolymerizing factor (ADF) family, plays a critical role in mitochondrial function and apoptosis. Recently, it was reported that de-phosphorylation and mitochondrial translocation of cofilin are connected with mitochondrial

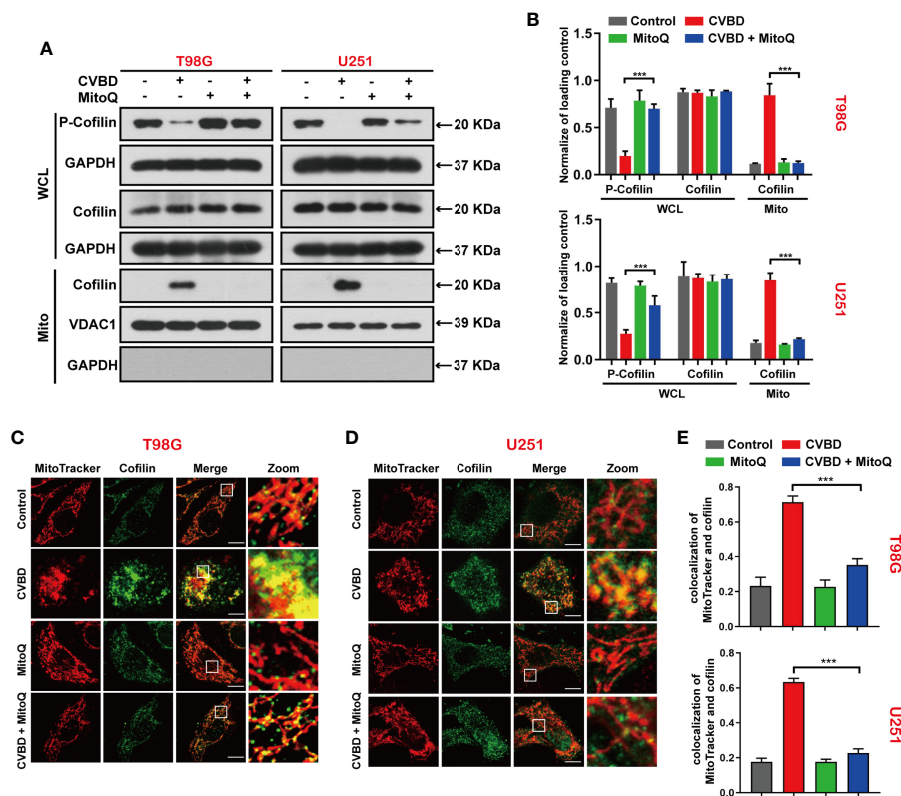


FIGURE 7 | Inhibited Mitochondrial superoxide production attenuates CVBD-induced mitochondrial translocation of cofilin. **(A, B)** T98G and U251 cells were pre-treated with MitoQ (0.5 μ M, 30 min) and post-treated with CVBD (120 μ M) for 24 h. The expression level of p-cofilin and cofilin in the whole cell lysate (WCL), and cofilin in the mitochondrial fractions, was determined by Western blotting analysis. GAPDH and VDAC1 were used as loading controls. GAPDH was also used as cytosolic marker (mean \pm SD of three independent experiments, *** P < 0.001 compared with CVBD treatment alone). **(C, D)** T98G and U251 cells were treated as indicated in **(A)**, and the colocalization of MitoTracker (red) and cofilin (green) was observed by confocal microscopy. Scale bars: 10 μ M. **(E)** Quantitative analysis of colocalization of MitoTracker (red) and cofilin (green). Colocalization correlation coefficients were represented as mean \pm SD (*** P < 0.001 compared with CVBD treatment alone).

damage (34). Cofilin is also involved in the malignant invasion of cancer cells (35), and has been identified as a key protein involved in the initiation phase of oxidative stress-mediated mitochondrial apoptosis (21, 36). Recent research suggested that mitochondrial translocation of cofilin is an early stage in cell apoptosis (21). Mitochondrial translocation of cofilin induced by cyclohexene was found to be the underlying mechanism of anti-leukemia (37). Cofilin was confirmed to translocate to the mitochondria after isoalantolactone-induced apoptosis in GBM (38). These results indicated that mitochondrial translocation of cofilin is pivotal for inducing cell apoptosis. However, only dephosphorylated cofilin could translocate to the mitochondria and lead to mitochondrial damage and cell apoptosis (21). During apoptosis, the dephosphorylated expression level of cofilin is increased, and cofilin is translocated from the cytosol to the mitochondria, resulting in cytochrome c release and activating caspase-dependent apoptosis (39). Consistent with these reports, our study confirmed that cofilin dephosphorylates and translocates to the mitochondria during CVBD-induced apoptosis, leading to mitochondrial damage. CVBD treatment decreased the expression level of phospho-cofilin in the whole cell lysate (WCL) and increased the expression level of cofilin in the mitochondria fraction. Knocking down cofilin reduced the mitochondrial translocation of cofilin induced by CVBD. Third, knocking down cofilin weakened the apoptosis induced by CVBD, reduced the upregulation of cleaved-PARP and cleaved-Caspase3 expression levels, and inhibited the release of cytochrome c from the mitochondria mediated by CVBD. Therefore, these results further support the idea that mitochondrial translocation of cofilin is required for CVBD-induced apoptosis.

It has been demonstrated that ROS play a key role in cell proliferation and differentiation (40, 41), but excessive generation of ROS can lead to oxidative damage of lipids, proteins, and DNA (42). ROS and oxidant stress of cells have been associated with cancer; increased ROS plays an important part in initiation and progression of cancers (23, 43). Previous reports have suggested that excessive production of ROS by exogenous means is more harmful to cancer cells (22). For instance, increasing ROS by exogenous drugs can cause apoptosis, DNA damage, or mitochondrial dysfunction of several cancers, including colorectal cancer, oral cancers, and breast cancer cells (44–46). We found that the effect of CVBD in inducing GBM cell apoptosis is related to the increase of intracellular ROS. First, CVBD increased the level of intracellular ROS in a dose-dependent manner. Second, NAC, as a ROS inhibitor, exhibited clear effects by decreasing the level of intracellular ROS induced by CVBD. Third, NAC pre-treatment significantly attenuated the CVBD-induced apoptosis in T98G and U251 cells. Thus, we explicated that CVBD-induced apoptosis of GBM occurs by upregulating the level of intracellular ROS.

Mitochondria play a pivotal role in cellular energy metabolism and cell apoptosis (29, 47). In the literature we found that

approximately 90% of intracellular ROS is produced by the mitochondria, which are the main source of superoxide radicals (48, 49). Excessive mitochondrial oxidant stress could lead to cytochrome c release from the mitochondria to the cytosol, and activate caspase-apoptosis and DNA damage in cancer cells (50). Mitochondrial superoxide production results in caspase activation and pancreatic cancer cell apoptosis (51, 52). Scavenging MitoSOX could effectively attenuate the mitochondria impairment and apoptosis induced by DOX (53, 54). Consistent with these findings, in our study we found that the effect of CVBD in inducing GBM cell apoptosis is related to the increase of mitochondrial superoxide. First, the level of mitochondrial superoxide was increased by CVBD treatment in a concentration-dependent manner. Second, MitoQ, as a mitochondrial-targeted antioxidant, inhibited the generation of mitochondrial superoxide aroused by CVBD. Third, pre-treatment with MitoQ also significantly weakened the apoptosis caused by CVBD in T98G and U251 cells. These results could be explained by the fact that inhibition of the production of mitochondrial superoxide can largely suppress the apoptosis-inducing effect of CVBD. We also clarified the relationship between the generation of ROS and mitochondrial superoxide with apoptosis induced by CVBD. In light of this, we speculated whether ROS or mitochondrial superoxide production can give rise to the mitochondrial translocation of cofilin. A recent study demonstrated that methyl antinate A (MAA) activated the generation of ROS in Huh7 cells, and that MAA led to mitochondrial translocation of cofilin. Pre-treatment of Huh7 cells with NAC markedly attenuated the apoptosis and mitochondrial translocation of cofilin induced by MAA (55). However, whether mitochondrial superoxide production is the reason for mitochondrial translocation of cofilin has not yet been studied. Surprisingly, we found that the level of cofilin in the mitochondria in GBM cells was decreased following pre-treatment with MitoQ, compared to CVBD treatment alone. Likewise, pre-treatment with MitoQ led to the colocalization of cofilin and mitochondria being dramatically inhibited. These results indicated that mitochondrial superoxide production could lead to the mitochondrial translocation of cofilin.

DATA AVAILABILITY STATEMENT

The datasets presented in this study can be found in online repositories. The names of the repository/repositories and accession number(s) can be found in the article/**Supplementary Material**.

AUTHOR CONTRIBUTIONS

Conceptualization, RF, BL and JC. Methodology, RF, LZ, BL, DD, LL and ZL. Experiments and data curation, LZ, RF, DD, YM, RN, and ZL. Writing—original draft preparation, LZ and RF. Writing—review and editing, RF, BL and JC. Supervision, ZL and JC. All authors contributed to the article and approved the submitted version.

FUNDING

This research was funded by the project of Science and Health Combined Traditional Chinese Medicine of Chongqing (grant no. ZY201801004).

REFERENCES

- Ostrom QT, Bauchet L, Davis FG, Deltour I, Fisher JL, Langer CE, et al. The epidemiology of glioma in adults: a “state of the science” review. *Neuro-Oncology* (2014) 16(7):896–913. doi: 10.1093/neuonc/nou087
- Louis DN, Perry A, Reifenberger G, von Deimling A, Figarella-Branger D, Cavenee WK, et al. The 2016 World Health Organization Classification of Tumors of the Central Nervous System: a summary. *Acta Neuropathol* (2016) 131(6):803–20. doi: 10.1007/s00401-016-1545-1
- Alexander BM, Cloughesy TF. Adult Glioblastoma. *J Clin Oncol* (2017) 35(21):2402. doi: 10.1200/JCO.2017.73.0119
- Jackson CM, Choi J, Lim M. Mechanisms of immunotherapy resistance: lessons from glioblastoma. *Nat Immunol* (2019) 20(9):1100–9. doi: 10.1038/s41590-019-0433-y
- Xiao AY, Maynard MR, Pieltz CG, Nagel ZD, Alexander JS, Kevil CG, et al. Sodium sulfide selectively induces oxidative stress, DNA damage, and mitochondrial dysfunction and radiosensitizes glioblastoma (GBM) cells. *Redox Biol* (2019) 26:101220. doi: 10.1016/j.redox.2019.101220
- Lee SY. Temozolomide resistance in glioblastoma multiforme. *Genes Dis* (2016) 3(3):198–210. doi: 10.1016/j.gendis.2016.04.007
- Bi Y, Li H, Yi D, Bai Y, Zhong S, Liu Q, et al. Corrigendum to “ β -catenin contributes to cordycepin-induced MGMT inhibition and reduction of temozolomide resistance in glioma cells by increasing intracellular reactive oxygen species”. [Cancer Lett. 435 (2018) 66–79]. *Cancer Lett* (2019) 461:157–8. doi: 10.1016/j.canlet.2019.06.006
- Wei G, Sun J, Hou Z, Luan W, Wang S, Cui S, et al. Novel antitumor compound optimized from natural saponin Albiziabioside A induced caspase-dependent apoptosis and ferroptosis as a p53 activator through the mitochondrial pathway. *Eur J Medicinal Chem* (2018) 157:759–72. doi: 10.1016/j.ejmech.2018.08.036
- Fontana F, Raimondi M, Marzagalli M, Di Domizio A, Limonta P. The emerging role of paraptosis in tumor cell biology: Perspectives for cancer prevention and therapy with natural compounds. *Biochim Biophys Acta (BBA) - Rev Cancer* (2020) 1873(2):188338. doi: 10.1016/j.bbcan.2020.188338
- Lin P-H, Chiang Y-F, Shieh T-M, Chen H-Y, Shih C-K, Wang T-H, et al. Dietary Compound Isoliquiritigenin, an Antioxidant from Licorice, Suppresses Triple-Negative Breast Tumor Growth via Apoptotic Death Program Activation in Cell and Xenograft Animal Models. *Antioxidants* (2020) 9(3):228. doi: 10.3390/antiox9030228
- Liu Y, Yang S, Wang K, Lu J, Bao X, Wang R, et al. Cellular senescence and cancer: Focusing on traditional Chinese medicine and natural products. *Cell Proliferation* (2020) 53(10):e12894. doi: 10.1111/cpr.12894
- Younis NS, Abduldaum MS, Mohamed ME. Protective Effect of Geraniol on Oxidative, Inflammatory and Apoptotic Alterations in Isoproterenol-Induced Cardiotoxicity: Role of the Keap1/Nrf2/HO-1 and PI3K/Akt/mTOR Pathways. *Antioxidants* (2020) 9(10):977. doi: 10.3390/antiox9100977
- Yu B, Fang T-H, Lü G-H, Xu H-Q, Lu J-F. Beneficial effect of Cyclovirobuxine D on heart failure rats following myocardial infarction. *Fitoterapia* (2011) 82(6):868–77. doi: 10.1016/j.fitote.2011.04.016
- Jiang F, Chen Y, Ren S, Li Z, Sun K, Xing Y, et al. Cyclovirobuxine D inhibits colorectal cancer tumorigenesis via the CTHRC1–AKT/ERK–Snail signaling pathway. *Int J Oncol* (2020) 57(1):183–96. doi: 10.3892/ijo.2020.5038
- Zhang J, Chen Y, Lin J, Jia R, An T, Dong T, et al. Cyclovirobuxine D Exerts Anticancer Effects by Suppressing the EGFR-FAK-AKT/ERK1/2-Slug Signaling Pathway in Human Hepatocellular Carcinoma. *DNA Cell Biol* (2020) 39(3):355–67. doi: 10.1089/dna.2019.4990
- Wu J, Tan Z, Chen J, Dong C. Cyclovirobuxine D Inhibits Cell Proliferation and Induces Mitochondria-Mediated Apoptosis in Human Gastric Cancer Cells. *Molecules* (2015) 20(11):20659–68. doi: 10.3390/molecules201119729
- Lu J, Sun D, Gao S, Gao Y, Ye J, Liu P. Cyclovirobuxine D Induces Autophagy-Associated Cell Death via the Akt/mTOR Pathway in MCF-7 Human Breast Cancer Cells. *J Pharmacol Sci* (2014) 125(1):74–82. doi: 10.1254/jphs.14013FP
- Kanellos G, Frame MC. Cellular functions of the ADF/cofilin family at a glance. *J Cell Sci* (2016) 129(17):3211–8. doi: 10.1242/jcs.187849
- Bernstein BW, Bamberg JR. ADF/Cofilin: a functional node in cell biology. *Trends Cell Biol* (2010) 20(4):187–95. doi: 10.1016/j.tcb.2010.01.001
- Li G-B, Zhang H-W, Fu R-Q, Hu X-Y, Liu L, Li Y-N, et al. Mitochondrial fission and mitophagy depend on cofilin-mediated actin depolymerization activity at the mitochondrial fission site. *Oncogene* (2018) 37(11):1485–502. doi: 10.1038/s41388-017-0064-4
- Chua BT, Volbracht C, Tan KO, Li R, Yu VC, Li P. Mitochondrial translocation of cofilin is an early step in apoptosis induction. *Nat Cell Biol* (2003) 5(12):1083–9. doi: 10.1038/ncb1070
- Trachootham D, Alexandre J, Huang P. Targeting cancer cells by ROS-mediated mechanisms: a radical therapeutic approach? *Nat Rev Drug Discovery* (2009) 8(7):579–91. doi: 10.1038/nrd2803
- Schumacker PT. Reactive oxygen species in cancer cells: Live by the sword, die by the sword. *Cancer Cell* (2006) 10(3):175–6. doi: 10.1016/j.ccr.2006.08.015
- Redza-Dutordoir M, Averill-Bates DA. Activation of apoptosis signalling pathways by reactive oxygen species. *Biochim Biophys Acta (BBA) - Mol Cell Res* (2016) 1863(12):2977–92. doi: 10.1016/j.bbamcr.2016.09.012
- Yao N, Li Y-j, Lei Y-h, Hu N, Chen W-M, Yao Z, et al. A piperazine derivative of 23-hydroxy betulinic acid induces a mitochondria-derived ROS burst to trigger apoptotic cell death in hepatocellular carcinoma cells. *J Exp Clin Cancer Res* (2016) 35(1):192. doi: 10.1186/s13046-016-0457-1
- Sharma P, Kumar S. Metformin inhibits human breast cancer cell growth by promoting apoptosis via a ROS-independent pathway involving mitochondrial dysfunction: pivotal role of superoxide dismutase (SOD). *Cell Oncol* (2018) 41(6):637–50. doi: 10.1007/s13402-018-0398-0
- Shen Y-Q, Guerra-Librero A, Fernandez-Gil BI, Florido J, García-López S, Martínez-Ruiz L, et al. Combination of melatonin and rapamycin for head and neck cancer therapy: Suppression of AKT/mTOR pathway activation, and activation of mitophagy and apoptosis via mitochondrial function regulation. *J Pineal Res* (2018) 64(3):e12461. doi: 10.1111/jpi.12461
- Kleih M, Böpple K, Dong M, Gaißler A, Heine S, Olayioye MA, et al. Direct impact of cisplatin on mitochondria induces ROS production that dictates cell fate of ovarian cancer cells. *Cell Death Dis* (2019) 10(11):851. doi: 10.1038/s41419-019-2081-4
- Hu Q, Gao M, Feng G, Liu B. Mitochondria-Targeted Cancer Therapy Using a Light-Up Probe with Aggregation-Induced-Emission Characteristics. *Angewandte Chemie Int Edition* (2014) 53(51):14225–9. doi: 10.1002/anie.201408897
- Zheng L, Wang C, Luo T, Lu B, Ma H, Zhou Z, et al. JNK Activation Contributes to Oxidative Stress-Induced Parthanatos in Glioma Cells via Increase of Intracellular ROS Production. *Mol Neurobiol* (2016) 54(5):3492–505. doi: 10.1007/s12035-016-9926-y
- Shi L, Wu Y, Di L, Feng L. Scutellarein selectively targets multiple myeloma cells by increasing mitochondrial superoxide production and activating intrinsic apoptosis pathway. *Biomed Pharmacother* (2019) 109:2109–18. doi: 10.1016/j.biopha.2018.09.024
- Bravo-Cordero JJ, Magalhaes MAO, Eddy RJ, Hodgson L, Condeelis J. Functions of cofilin in cell locomotion and invasion. *Nat Rev Mol Cell Biol* (2013) 14(7):405–15. doi: 10.1038/nrm3609
- Van Troys M, Huyck L, Leyman S, Dhaese S, Vandekerckhove J, Ampe C. Ins and outs of ADF/cofilin activity and regulation. *Eur J Cell Biol* (2008) 87(8-9):649–67. doi: 10.1016/j.ejcb.2008.04.001
- Hu J, Zhang H, Li J, Jiang X, Zhang Y, Wu Q, et al. ROCK1 activation-mediated mitochondrial translocation of Drp1 and cofilin are required for

SUPPLEMENTARY MATERIAL

The Supplementary Material for this article can be found online at: <https://www.frontiersin.org/articles/10.3389/fonc.2021.656184/full#supplementary-material>

- arnidiol-induced mitochondrial fission and apoptosis. *J Exp Clin Cancer Res* (2020) 39(1):649–67. doi: 10.1186/s13046-020-01545-7
35. Chang C-Y, Leu J-D, Lee Y-J. The Actin Depolymerizing Factor (ADF)/Cofilin Signaling Pathway and DNA Damage Responses in Cancer. *Int J Mol Sci* (2015) 16(2):4095–120. doi: 10.3390/ijms16024095
 36. Bamburg JR, Wiggan ONP. ADF/cofilin and actin dynamics in disease. *Trends Cell Biol* (2002) 12(12):598–605. doi: 10.1016/s0962-8924(02)02404-2
 37. Zheng Y, Ouyang Q, Fu R, Liu L, Zhang H, Hu X, et al. The cyclohexene derivative MC-3129 exhibits antileukemic activity via RhoA/ROCK1/PTEN/PI3K/Akt pathway-mediated mitochondrial translocation of cofilin. *Cell Death Dis* (2018) 9(6):656. doi: 10.1038/s41419-018-0689-4
 38. Xing JS, Wang X, Lan YL, Lou JC, Ma B, Zhu T, et al. Isoalantolactone inhibits IKK β kinase activity to interrupt the NF- κ B/COX-2-mediated signaling cascade and induces apoptosis regulated by the mitochondrial translocation of cofilin in glioblastoma. *Cancer Med* (2019) 8(4):1655–70. doi: 10.1002/cam4.2013
 39. Liao PH, Hsu HH, Chen TS, Chen MC, Day CH, Tu CC, et al. Phosphorylation of cofilin-1 by ERK confers HDAC inhibitor resistance in hepatocellular carcinoma cells via decreased ROS-mediated mitochondria injury. *Oncogene* (2016) 36(14):1978–90. doi: 10.1038/onc.2016.357
 40. Boonstra J, Post JA. Molecular events associated with reactive oxygen species and cell cycle progression in mammalian cells. *Gene* (2004) 337:1–13. doi: 10.1016/j.gene.2004.04.032
 41. Feng Y, Hua X, Niu R, Du Y, Shi C, Zhou R, et al. ROS play an important role in ATPR inducing differentiation and inhibiting proliferation of leukemia cells by regulating the PTEN/PI3K/AKT signaling pathway. *Biol Res* (2019) 52(1):26–9. doi: 10.1186/s40659-019-0232-9
 42. Perry G, Raina AK, Nunomura A, Wataya T, Smith MA. How important is oxidative damage? Lessons from Alzheimer's disease. *Free Radical Biol Med* (2015) 28(5):831–4. doi: 10.1016/s0891-5849(00)00158-1
 43. Pelicano H, Carney D, Huang P. ROS stress in cancer cells and therapeutic implications. *Drug Resist Updates* (2004) 7(2):97–110. doi: 10.1016/j.drug.2004.01.004
 44. Gurunathan S, Jeyaraj M, Kang M-H, Kim J-H. Melatonin Enhances Palladium-Nanoparticle-Induced Cytotoxicity and Apoptosis in Human Lung Epithelial Adenocarcinoma Cells A549 and H1229. *Antioxidants* (2020) 9(4):357. doi: 10.3390/antiox9040357
 45. Tang J-Y, Wu K-H, Wang Y-Y, Farooqi AA, Huang H-W, Yuan S-SF, et al. Methanol Extract of *Usnea barbata* Induces Cell Killing, Apoptosis, and DNA Damage against Oral Cancer Cells through Oxidative Stress. *Antioxidants* (2020) 9(8):694. doi: 10.3390/antiox9080694
 46. Yu T-J, Tang J-Y, Lin L-C, Lien W-J, Cheng Y-B, Chang F-R, et al. Withanolide C Inhibits Proliferation of Breast Cancer Cells via Oxidative Stress-Mediated Apoptosis and DNA Damage. *Antioxidants* (2020) 9(9):873. doi: 10.3390/antiox9090873
 47. Pathania D, Millard M, Neamati N. Opportunities in discovery and delivery of anticancer drugs targeting mitochondria and cancer cell metabolism. *Advanced Drug Delivery Rev* (2009) 61(14):1250–75. doi: 10.1016/j.addr.2009.05.010
 48. Sabharwal SS, Schumacker PT. Mitochondrial ROS in cancer: initiators, amplifiers or an Achilles' heel? *Nat Rev Cancer* (2014) 14(11):709–21. doi: 10.1038/nrc3803
 49. Zhang W, Hu X, Shen Q, Xing D. Mitochondria-specific drug release and reactive oxygen species burst induced by polyprodrug nanoreactors can enhance chemotherapy. *Nat Commun* (2019) 10(1):1704. doi: 10.1038/s41467-019-09566-3
 50. Xu L, Wu T, Lu S, Hao X, Qin J, Wang J, et al. Mitochondrial superoxide contributes to oxidative stress exacerbated by DNA damage response in RAD51-depleted ovarian cancer cells. *Redox Biol* (2020) 36:101604. doi: 10.1016/j.redox.2020.101604
 51. Pati ML, Hornick JR, Niso M, Berardi F, Spitzer D, Abate C, et al. Sigma-2 receptor agonist derivatives of 1-Cyclohexyl-4-[3-(5-methoxy-1,2,3,4-tetrahydronaphthalen-1-yl)propyl]piperazine (PB28) induce cell death via mitochondrial superoxide production and caspase activation in pancreatic cancer. *BMC Cancer* (2017) 17(1):51. doi: 10.1186/s12885-016-3040-4
 52. Semkova S, Zhelev Z, Miller T, Sugaya K, Aoki I, Higashi T, et al. Menadione/Ascorbate Induces Overproduction of Mitochondrial Superoxide and Impairs Mitochondrial Function in Cancer: Comparative Study on Cancer and Normal Cells of the Same Origin. *Anticancer Res* (2020) 40(4):1963–72. doi: 10.21873/anticancer.14151
 53. Luanpitpong S, Chanvorachote P, Nimmannit U, Leonard SS, Stehlik C, Wang L, et al. Mitochondrial superoxide mediates doxorubicin-induced keratinocyte apoptosis through oxidative modification of ERK and Bcl-2 ubiquitination. *Biochem Pharmacol* (2012) 83(12):1643–54. doi: 10.1016/j.bcp.2012.03.010
 54. Yin J, Guo J, Zhang Q, Cui L, Zhang L, Zhang T, et al. Doxorubicin-induced mitophagy and mitochondrial damage is associated with dysregulation of the PINK1/parkin pathway. *Toxicol Vitro* (2018) 51:1–10. doi: 10.1016/j.tiv.2018.05.001
 55. Hsieh YC, Rao YK, Wu CC, Huang CYF, Geethangili M, Hsu SL, et al. Methyl Antcinate A from *Antrodia camphorata* Induces Apoptosis in Human Liver Cancer Cells through Oxidant-Mediated Cofilin- and Bax-Triggered Mitochondrial Pathway. *Chem Res Toxicol* (2010) 23(7):1256–67. doi: 10.1021/tx100116a

Conflict of Interest: The authors declare that the research was conducted in the absence of any commercial or financial relationships that could be construed as a potential conflict of interest.

Copyright © 2021 Zhang, Fu, Duan, Li, Li, Ming, Li, Ni and Chen. This is an open-access article distributed under the terms of the Creative Commons Attribution License (CC BY). The use, distribution or reproduction in other forums is permitted, provided the original author(s) and the copyright owner(s) are credited and that the original publication in this journal is cited, in accordance with accepted academic practice. No use, distribution or reproduction is permitted which does not comply with these terms.



Repositioning of Antiparasitic Drugs for Tumor Treatment

Yan-Qi Li, Zhi Zheng, Quan-Xing Liu, Xiao Lu, Dong Zhou, Jiao Zhang, Hong Zheng* and Ji-Gang Dai*

Department of Thoracic Surgery, Xinqiao Hospital, Army Medical University (Third Military Medical University), Chongqing, China

OPEN ACCESS

Edited by:

Christian Celia,
University of Studies G. d'Annunzio
Chieti and Pescara, Italy

Reviewed by:

Patrícia Peres De Oliveira,
Universidade Federal de
São João del Rei, Brazil
Jianxun Ding,
Changchun Institute of Applied
Chemistry (CAS), China

*Correspondence:

Ji-Gang Dai
daijigang@tmmu.edu.cn
Hong Zheng
ziecoe@tmmu.edu.cn

Specialty section:

This article was submitted to
Pharmacology of Anti-Cancer Drugs,
a section of the journal
Frontiers in Oncology

Received: 22 February 2021

Accepted: 13 April 2021

Published: 29 April 2021

Citation:

Li Y-Q, Zheng Z, Liu Q-X, Lu X,
Zhou D, Zhang J, Zheng H and Dai J-G
(2021) Repositioning of Antiparasitic
Drugs for Tumor Treatment.
Front. Oncol. 11:670804.
doi: 10.3389/fonc.2021.670804

Drug repositioning is a strategy for identifying new antitumor drugs; this strategy allows existing and approved clinical drugs to be innovatively repurposed to treat tumors. Based on the similarities between parasitic diseases and cancer, recent studies aimed to investigate the efficacy of existing antiparasitic drugs in cancer. In this review, we selected two antihelminthic drugs (macrolides and benzimidazoles) and two antiprotozoal drugs (artemisinin and its derivatives, and quinolines) and summarized the research progresses made to date on the role of these drugs in cancer. Overall, these drugs regulate tumor growth via multiple targets, pathways, and modes of action. These antiparasitic drugs are good candidates for comprehensive, in-depth analyses of tumor occurrence and development. In-depth studies may improve the current tumor diagnoses and treatment regimens. However, for clinical application, current investigations are still insufficient, warranting more comprehensive analyses.

Keywords: drug repositioning, antiparasitic drugs, macrolides, benzimidazoles, artemisinin, quinolines, autophagy, ferroptosis

INTRODUCTION

There exists a close connection between parasitic infections and cancer (1–3). Helminth infections are widespread the world over, and the causative parasites are thought to be responsible for causing cancer in humans (4). Thus far, *Schistosoma haematobium*, *Clonorchis sinensis*, and *Opisthorchis viverrini* have been recognized as clear biological carcinogens (1). The specific carcinogenic mechanism is not yet clear, and the metabolites of catechol estrogens and parasite-derived oxysterols may play an important role (5). Unlike worms, protozoa have not been identified as biological carcinogens; however, certain characteristics of protozoa are similar to those of cancer. In a manner similar to the immune evasion strategies employed by cancers, *Trypanosoma cruzi* and *Leishmania* parasites leverage the immune mechanisms to persist in the body and establish a chronic infection (6). Although malaria is the most widespread parasitic disease in the world, it does not seem to be carcinogenic (2). However, the incidence of malaria is positively correlated with mortality in most cancers, with the exception of colorectal, lung, gastric, and several other types of cancer whose mortalities exhibit an inverse correlation with malaria (7, 8). Thus, the relationship between malaria and cancer is worth exploring.

Cancer is the second leading cause of death worldwide and is a major burden of disease (9, 10). However, with proper treatment, many cancers can be cured. Drugs are essential in the treatment of tumors but are often not as effective as required because of drug resistance and low specificity (11). Despite the emergence of highly specific monoclonal antibody drugs, the drugs are unsuitable

for a wide range of clinical applications because they have strict requirements for the target (12). Therefore, the development of new antitumor drugs is still urgently needed. However, owing to the similarities between parasitic diseases and cancer as well as the successful clinical administration of antiparasitic drugs for years, it seems feasible to repurpose existing antiparasitic drugs into antitumor drugs. In fact, some antiparasitic and antitumor drugs share the same target, a variety of drugs targeting CDKs, TGR enzyme, tubulin/microtubule system have been confirmed to have dual effects on anti-parasites and anti-cancer (13).

Research on the repurposing antiparasitic drugs for tumors has gradually gained popularity. However, many studies have reported contradictory results. We selected two well-researched antihelminthic drugs and two antiprotozoal drugs and summarized the corresponding research progress to provide direction for further exploration into the repurposing of antiparasitic drugs as antitumor drugs.

PROGRESS ON THE USE OF MACROLIDE ANTIPARASITIC DRUGS FOR TREATING CANCER

Macrolides are antiparasitic drugs with dual functions *in vitro* and *in vivo*. The mechanism of macrolides is mainly to increase the concentration of the inhibitory transmitter GABA and enhance the permeability of the nerve membrane to chloride

ions, causing neuromuscular paralysis and death (14). Macrolides have long been used to kill nematodes and consist of two main categories: avermectins and milbemycins. Apart from the antiparasitic effects, macrolide drugs also show different levels of anticancer activity (**Figure 1**).

Avermectins

Commonly used avermectins include avermectin (AVM), ivermectin (IVM), doramectin (DRM), eprinomectin (EPM), and selamectin (SLM). Although all these avermectins show anticancer activity, studies on IVM are more comprehensive than those on other drugs. IVM can regulate the natural progression of tumors *via* multiple pathways.

Apoptosis is an important mechanism used by IVMs to kill cancer cells. Eukaryotic translation initiation factor 4A isoform 3 (EIF4A3) is an RNA-binding protein involved in the splicing modulation of BCL2L1/Bcl-X and is considered to be closely associated with apoptosis. SILAC-based quantitative proteomic analysis revealed that IVM inhibited the expression of EIF4A3 and 116 EIF4A3-binding mRNAs (15). In LA795 cells, IVM analogs (IVM, EPM, and SLM) can significantly inhibit currents mediated by the transmembrane member 16A (TMEM16A), an endogenous Ca^{2+} -activated Cl^- channel closely related to tumorigenesis, thereby inducing apoptosis (16). In addition, IVMs utilize the well-studied pathway of mitochondrial apoptosis to exert their anticancer activity. When acting on HeLa cells, IVM can increase the ratio of Bax/Bcl-2 and induce release of mitochondrial cytochrome c into the cytoplasm, thus stimulating caspase-9/-3-mediated apoptosis (17). In chronic

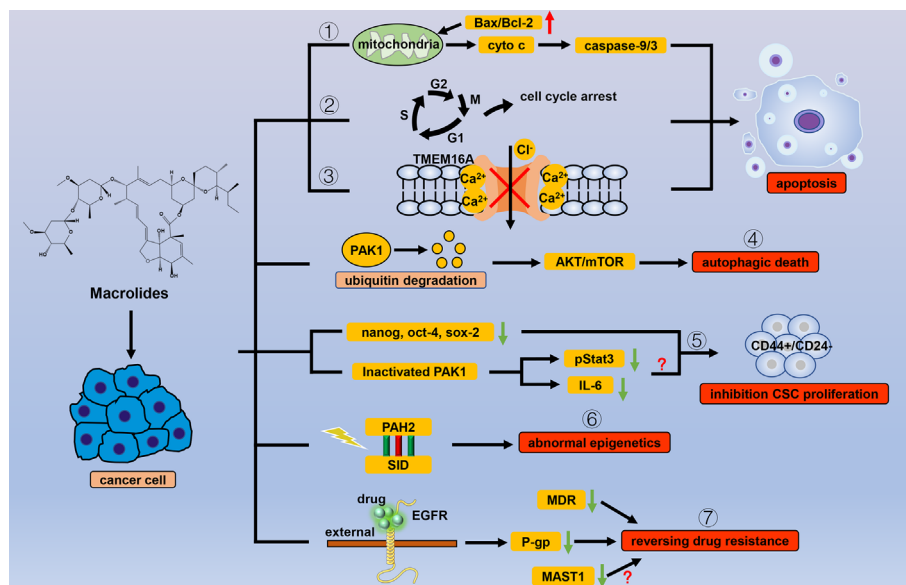


FIGURE 1 | Efficacy of macrolide antiparasitic drugs in cancer. Apoptosis is the chief mechanism used by macrolide drugs to kill cancer cells. Macrolides trigger apoptosis through the (1) mitochondrial pathway, (2) cell cycle arrest, and (3) inhibition of the current of Ca^{2+} ion-activated Cl^- channels. Other than apoptosis, macrolides can cause autophagic death of cancer cells by (4) degrading PAK1. When used for cancer cells, macrolides show selectivity for CSCs by (5) inhibiting stem cell genes and inactivating PAK1. Macrolides also reverse the abnormal epigenetics of tumor cells through (6) the combination of PAH2 and SID domain. By binding to the extracellular segment of EGFR, macrolides can (7) inhibit the transcription of P-gp, thereby reversing tumor resistance in which MDR and MASTA1 are also involved.

myeloid leukemia and renal cell carcinoma cells, IVM can induce apoptosis by inducing mitochondrial dysfunction (18).

Cell cycle arrest can easily lead to apoptosis. Several studies have revealed that in cancer cells, IVM arrests the cell cycle in different phases by regulating the expression of proteins that control the cell cycle, thereby inducing apoptosis (19–22). Especially in epithelial ovarian cancer, IVM induces apoptosis through multiphasic cell cycle arrest, and exhibits KPNB1-dependent antitumor effects (22). The cell cycle is also the target of many chemotherapeutic drugs, and combinatorial treatment with IVM and clinical drugs is worth investigating. In fact, in multiple *in vivo* and *in vitro* experiments, IVM significantly enhanced the efficacy of various drugs, including cisplatin and tamoxifen, but this result still needs clinical verification (20, 23).

Autophagy regulation is another important mechanism underlying IVM action. A study on breast cancer revealed that when IVM was applied to cancer cells, no obvious apoptosis was observed before 24 h of treatment, but the inhibition of growth of these cancer cells during the 24 h was evident. Later in that study, autophagy flux increased during the first 24 h of IVM treatment, and the anticancer effect during this period was reversed when IVM was used to treat cancer cells Beclin 1 or Atg5 knockdown (24). Current studies argue that IVM degrades PAK1 in cancer cells through the ubiquitination pathway, thereby inactivating the AKT-mTOR pathway, which is the key negative regulatory pathway of autophagy (24, 25). Although mechanisms used by IVM require more detailed exploration, it is encouraging that more studies indicate that induction of autophagy may be used as a method of synergistic treatment in clinical tumor chemotherapy, highlighting the potential of IVM as a clinical adjuvant drug (26, 27).

In addition to the anticancer mechanism, the selective functional characteristics of IVMs are also noteworthy. IVMs exhibit more pronounced toxicity toward cancer cells than toward non-cancer cells, which may be related to higher mitochondrial biogenesis in cancer cells (28). More importantly, when acting on cancer cells, IVM still exhibits different levels of cytotoxicity in different cancer cell subgroups. The CD44+/CD24- subpopulation of breast cancer cells have been previously reported to possess stem/progenitor cell properties (29, 30). IVM preferentially inhibits the viability of CD44+/CD24- subpopulation cells (cancer stem cells (CSCs)) and reduces the expression of stemness genes (NANOG, POU5F1, and SOX2) (31). Current research points out that this may be related to the ability of IVMs to inactivate p21-activated kinase (PAK1), thereby reducing the levels of pStat3 and extracellular IL-6 and inhibiting the formation of CSCs (32). Research on the specific effect of IVM on CSCs is still limited, and many other knowledge gaps exist that require further research. In general, the selective nature of IVMs shows that it is almost non-toxic to non-cancer cells but can effectively inhibit the growth of cancer cells, demonstrating its unique potential as an anticancer drug.

IVMs have also shown anticancer capabilities in many fields other than these mentioned above. Although research on these

aspects is rare, it has broadened the scope of exploration of IVMs. The latest research showed that IVMs could reverse tumor resistance. IVM at a low dose that does not produce evident cytotoxicity can bind to the extracellular domain of EGFR, which inhibits the activation of EGFR and its downstream signaling cascade ERK/Akt/NF- κ B, thus inhibiting the transcription factor NF- κ B and leading to reduction in P-glycoprotein (P-gp) transcription (33). Moreover, in triple-negative breast cancer (TNBC), the targeted disruption of the Sin3 (a master transcriptional scaffold and corepressor that plays an essential role in the regulation of gene transcription and maintenance of chromatin structure) complex by introducing a Sin3 interaction domain (SID) decoy that interferes with PAH2 binding by sequestering SID-containing partner proteins reverted the silencing of genes involved in cell growth and differentiation (34–36). Interestingly, IVM and SLM can be used as small molecule inhibitors of SID peptides that play a similar role to that of Sin3 disruption, indicating that AVMs can also exert anticancer effects by regulating the abnormal epigenetics of tumors (37). Furthermore, the activation of WNT-TCF signaling is implicated in multiple diseases, but there are no WNT-TCF antagonists in clinical use. However, SLM and IVM can reduce the expression of target proteins in this pathway by mimicking dnTCF, further demonstrating the application potential of these drugs (38).

Milbemycins

The milbemycin family comprises a series of 16-membered macrolide antibiotics that contain a highly characteristic spiroketal group that can be produced by several *Streptomyces*, these antibiotics have strong biological activities and are used as highly selective and potent broad-spectrum antiparasitic agents (39–41). At present, research on milbemycins in cancer was relatively rare, and milbemycins have been found to play an important role in reversing tumor drug resistance. Milbemycins can restore the sensitivity of cancer cells toward chemotherapy drugs by reducing the expression of MDR1 or P-gp, and its concentration has no obvious cytotoxic effect on cancer cells (42, 43). Cisplatin (DDP) is one of the most widely used chemotherapeutic drugs and is considered the first-line treatment for many cancers, but drug resistance limits its therapeutic potential. A recent study found that serine/threonine kinase 1 (MAST1) was a major driver of DDP resistance in human cancers (44). Encouragingly, in multidrug and cisplatin-resistant human lung adenocarcinoma (A549/DDP) cells, a milbemycin compound isolated from *Streptomyces* sp. FJS31-2, named VM48130, reduced the expression of multiple resistance-related genes, including MAST1, to reverse resistance, which further demonstrated the potential of milbemycin as an adjuvant drug in clinical chemotherapy (45). The anticancer mechanisms of these compounds also include other aspects. For example, moxidectin effectively inhibited the proliferation of rat C6 and human U251 glioma cells. Mitochondria-related apoptotic pathways, cell cycle arrest, and autophagy induced by the AKT/mTOR signaling pathway in cancer cells are all

considered to be involved in this process, but the specific mechanism remains to be explored (46, 47).

PROGRESS ON THE USE OF BENZIMIDAZOLE ANTIPARASITIC DRUGS FOR TREATING CANCER

Benzimidazole is a broad-spectrum antiparasitic drug with a structure similar to that of purines and is mainly used in clinics for nematodes. Benzimidazoles include albendazole (ABZ), flubendazole (FLU), fenbendazole (FBZ), oxibendazole (OBZ), and febantel (FBT). In general, these drugs mainly exert their antiparasitic effects by interfering with sugar metabolism, affecting adenosine triphosphate (ATP) production, and binding to tubulin to affect the cell cycle (48, 49). These biological processes are also critical in cancer, and it seems inevitable that such drugs are effective in tumor treatment. Correspondingly, many studies have shown that benzimidazoles have prominent anticancer activity (Figure 2).

Albendazole

Based on the antiparasitic mechanism, studies have found that ABZ can inhibit glucose uptake through the GLUT1/AMPK/P53 signaling pathway, thereby disrupting sugar metabolism in cancer cells and inducing cell apoptosis (50). ABZ,

a microtubule-targeting agent (MTA), induces apoptosis by disrupting microtubule formation and causes mitotic arrest in tumors (51, 52). ABZ causes bundles of short microtubules to form along the edges of cells rather than covering the entire cell, leading to a series of biological reactions (52). MTAs are a class of drugs currently used in chemotherapy. A synergistic antiproliferative effect is observed upon using combinatorial therapy involving low concentrations of ABZ, colchicine, and ABZ plus 2-methoxyestradiol (2ME) (53). However, recent studies have revealed an interesting mechanism underlying the anticancer activity of ABZs, i.e., targeting the microtubules. In K562 cells, when compared with paclitaxel and other MTAs, ABZ treatment significantly increased the number of cells arrested at the G2/M phase in a short time, and ABZs did not immediately activate apoptosis. Subsequently, ABZs could upregulate SIRT3 expression, which is believed to regulate SOD2 activity to clear mitochondrial reactive oxygen species (ROS). They further speculated that this ability allowed ABZs to protect cancer cells from cytotoxicity in the short-term, but when SIRT3 expression was further reduced, this unique ABZ mechanism was no longer effective (54, 55).

Whether it be inhibiting the glucose metabolism pathway or targeting microtubules to exert anticancer activity, triggering cancer cell apoptosis is the common end result. In fact, ABZs can induce apoptosis in other ways. According to a study on cutaneous squamous cell carcinoma, ABZs increase apoptosis-related signals

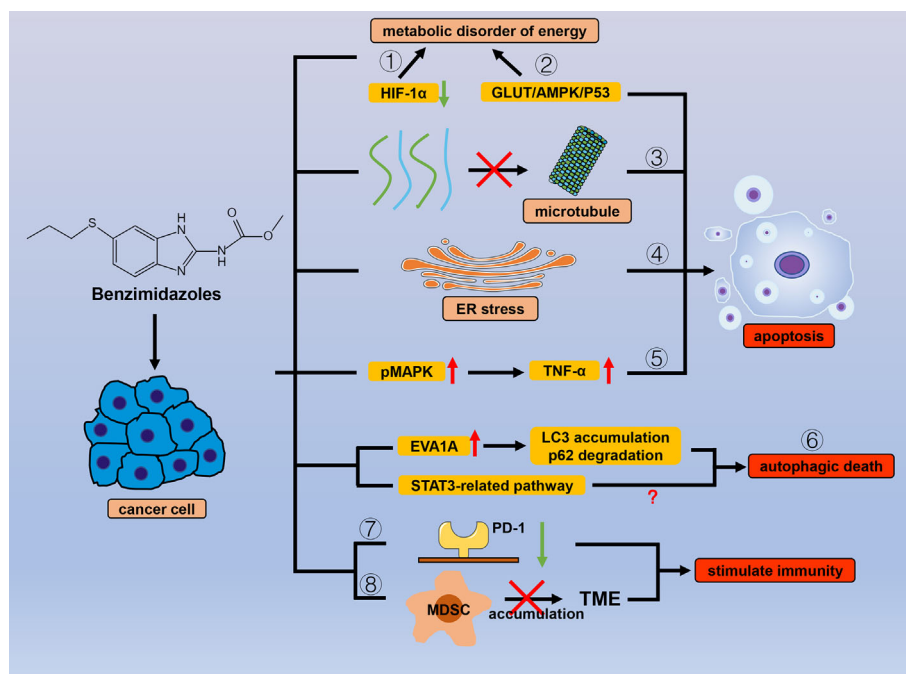


FIGURE 2 | Efficacy of benzimidazole antiparasitic drugs in cancer. Benzimidazoles can cause energy metabolism disorders and reduce cancer cell tolerance to hypoxic environments by (1) inhibiting the expression of HIF-1α and (2) inhibiting sugar intake through the GLUT/AMPK/P53 pathway. Apart from sugar metabolism, benzimidazoles also induce apoptosis by (3) inhibiting microtubule polymerization and (4) ER stress, and (5) promoting MAPK phosphorylation. By affecting numerous autophagy-related proteins (LC3, P62, and EVA1A) and downstream signals related to STAT3, benzimidazole can also cause (6) autophagic cancer cell death. (7) Benzimidazoles reduce the expression of PD-1 and (8) inhibit the accumulation of MDSC in the TME to stimulate antitumor immunity.

by inducing endoplasmic reticulum (ER) stress, and pretreatment with the ER stress inhibitor 4-PBA attenuates ABZ-induced apoptosis (56). Furthermore, in human leukemia U937 cells, ABZs increase MAPK phosphorylation and upregulate TNF- α expression, thus inducing apoptosis. The same pathway is seemingly involved in the ABZ-induced death of HL-60 cells (57).

Moreover, most cancer cells generate ATP using accelerated glycolysis rates, and glucose is converted to lactate instead of being metabolized by oxidative phosphorylation, even when oxygen is abundant (58, 59). Current research indicates that hypoxia-inducible factor-1 α (HIF-1 α) plays a critical role in this process. In general, under hypoxic conditions, HIF-1 α maintains the survival requirements of cancer cells by regulating the expression of a series of glycolytic enzymes and can also bind to the vascular endothelial cell growth factor (VEGF) gene promoter to induce VEGF expression and angiogenesis (60, 61). Therefore, HIF-1 α is becoming an increasingly attractive therapeutic target in the treatment of cancer. It is encouraging that ABZs significantly inhibited the expression of HIF-1 α in non-small cell lung cancer and ovarian cancer; however, ABZ treatment did not affect the HIF-1 α mRNA level, suggesting that other unknown regulatory pathways may be involved in this process (62, 63).

Research institutions have already carried out phase I clinical trials of oral ABZ to treat advanced cancer patients to detect its maximum tolerated dose. Results from the 36 patients with refractory solid tumors enrolled in the study showed that the recommended dose for further study was 1,200 mg twice daily for 14 days in a 21-day cycle, with myelosuppression being the main dose-limiting toxicity (64). Although no patients achieved partial or complete response according to the RECIST study's criteria, 4 out of 24 patients with assessable tumor markers (16%) demonstrated a decrease in tumor markers of more than 50%. In contrast, another patient had a significant decrease in tumor markers and a prolonged period of stable disease. Overall, as research continues to progress, new anticancer drugs based on ABZ can be expected.

Flubendazole

Similar to ABZ, FLU induces monopolar spindle formation by inhibiting tubulin polymerization, inhibiting proliferation and migration, ultimately triggering apoptosis in a variety of cancer cell lines (65–69). However, more distinctive is that autophagy seems to play an important role in the anticancer activity of FLU. Using molecular docking simulation technology to screen numerous small molecule drugs approved by the Food and Drug Administration (FDA), FLU was found to have the highest antitumor activity and the ability to target autophagy-related gene (ATG) 4 B. Molecular dynamics simulation revealed that FLU bound with high affinity to ATG4B protein, and that it could induce autophagy and exhibit an antiproliferative effect on TNBC cancer cells (70). The latest research, however, has proposed another possible mechanism for FLU's anticancer activity on TNBC cells. FLU treatment promotes autophagy by upregulating the expression of Eva-1 homolog A (EVA1A), a protein involved in autophagy and apoptosis-induced cell death (71). EVA1A knockdown, results in the partial inhibition of LC3

puncta accumulation, p62 degradation, and LC3 lipidation in TNBC cells (72). FLU also promotes autophagy in other malignant cell lines, such as A549 and H460 (73), through the regulation of the signal transducer and activator of transcription 3 (STAT3)-related pathway to induce apoptosis in human colorectal cancer cells, but the specific mechanism remains unclear (74).

Moreover, FLU has clinical value because it is potentially involved in tumor immunotherapy and molecular targeted drug resistance. Programmed cell death protein-1 (PD-1) and programmed cell death-ligand 1 (PD-L1) are immune system regulators that play a role in dampening the immune response to cancer cells, and PD-1 inhibitors have already changed the paradigm of cancer treatment in many cancers (75, 76). However, all available PD-1/PD-L1 treatments are antibodies that require intravenous infusion, resulting in exorbitant costs. PD-1/PD-L1 treatments can also have unpredictable and/or poor response in second-line treatment; therefore, finding a small molecule inhibitor is more convenient (77). A study on melanoma showed that FLU could inhibit the expression of PD-1 in cancer cells and the accumulation of myeloid-derived suppressor cells (MDSCs) in the tumor microenvironment, indicating its ability to elicit the host's antitumor immunity, but the specific mechanism remains to be explored (78). In general, this suggests huge potential application of FLU in tumor immunotherapy. Apart from this, trastuzumab provides significant clinical benefit for HER2-positive breast cancers, but nearly 70% of patients experience primary or acquired resistance, which dramatically limits the therapeutic effect (79). Encouragingly, FLU significantly reduced p95HER2 expression and the phosphorylation level of HER2, HER3, and AKT, preventing the hetero-dimerization of HER2/HER3 in trastuzumab-resistant cells (80), which play an important role in trastuzumab resistance (81–83). Combination therapy with FLU seems to be a possible solution to improve the efficacy of trastuzumab.

PROGRESS ON THE USE OF ARTEMISININ AND ITS DERIVATIVES FOR TREATING CANCER

Artemisinin (ARS) is a 1,2,-trioxane from the Chinese medicinal plant Sweet Wormwood, and since its antimalarial effect was discovered, research on ARS has been continuously focused on. A variety of ARS and its derivatives (ARTs), including dihydroartemisinin (DHA), artemether (ARM), artesunate (ART), and artemisitene (ATT), have emerged because of the advancements of drug modification and synthesis technology. ARS-based combination therapies are established standard treatments for malaria worldwide (84–87). It is currently considered that the heme-irons released by *Plasmodium*-attacking red blood cells can cleave the endoperoxide bridge of ARS via a Fe (II) Fenton-type reaction, and that free radical intermediates kill the *Plasmodia* (88, 89). Other pathways are also involved in ARTs antimalarial response (90, 91), but comprehensive research on antimalarial mechanisms remains necessary. Interestingly, as with other natural products,

antimalarial properties are not the only benefits of ARTs, and ARTs have shown application value in many diseases, including cancer (**Figure 3**).

Long-term studies on the anticancer mechanism of ARTs have shown that the endoperoxide moiety is essential for its biological activity, and ARTs without the endoperoxide moiety were inactive (92, 93). In general, ARTs mainly exert anticancer effects in three ways with the endoperoxide moiety. (i) The cleavage of the endoperoxide moiety leads to the formation of ROS and oxidative stress in the tumor. Excessive production of ROS causes death by damaging cellular components, including DNA, proteins, and lipids (94); a notable feature of ARTs is that they can spontaneously generate a large amount of ROS in a heme-dependent manner (95–97). Many studies have indicated that ARTs increase the expression of cleaved caspase-3 and PARP in a variety of cancer cells by producing excessive amounts of ROS, thus inducing apoptosis in cancer cells (98–100). Further, excessive amounts of ROS may trigger an ER stress response in cancer cells (99), but the specific mechanism is not clear. Interestingly, increasing the concentration of ferrous ions and oxygen in the tumor environment to further increase the concentration of ROS has been shown to enhance the anticancer activity of ARTs (101, 102), which provides a possible strategy for the development of new anticancer drugs based on ARTs.

(ii) ARTs rely on excessive amounts of ROS to cause DNA damage in cancer cells. In the alkaline comet assay, both ARS and ART caused significant DNA damage, and the fold changes of OTM and tail DNA significantly increased (103). In addition, molecular docking indicated that various ARTs might induce

DNA damage in cancer cells by inhibiting topoisomerase 1 (104), an enzyme that resolves the topological stress in genomic DNA by preventing double-stranded breaks in the DNA during cell proliferation (105). Subsequent studies involved in-depth exploration of the specific mechanism of ARTs. ATT can increase the expression of E3 ligase NEDD4, resulting in the destabilization of c-Myc protein, thereby inhibiting the expression of DNA topoisomerases. Importantly, neither a decrease in the concentration of NEDD4 protein nor DNA damage has been observed in non-cancer cells (106). DNA damage inducers such as cisplatin and doxorubicin have become the first-line cancer treatment (107, 108). However, these drugs lack strict selectivity, and are toxic to non-cancer cells. The high selectivity of ATT as a DNA damage inducer suggests that ARTs may be a potential alternative to cisplatin and doxorubicin.

(iii) ARTs induce cycle arrest to trigger cancer cell death. This anticancer effect of ARTs is closely related to excessive amounts of ROS and oxidative DNA lesions that affect cell integrity, leading to perturbations in DNA replication and cell division mechanisms. More specifically, CDK4 encodes a cyclin-dependent serine-threonine kinase in response to mitogenic or proliferation-promoting stimuli and interacts with cyclin D1 to phosphorylate the tumor suppressor protein Rb (109, 110). DHA can regulate the cyclin D1-CDK4-Rb pathway by inhibiting the expression of CDK4 to trigger cycle arrest (111). In cisplatin-resistant human breast carcinoma cells, ARS exerts anticancer activity by targeting multiple key cell cycle-related proteins, including cyclin-B1, cyclin D1, and cyclin E, to trigger cycle block (112). In general, with the help of the endoperoxide

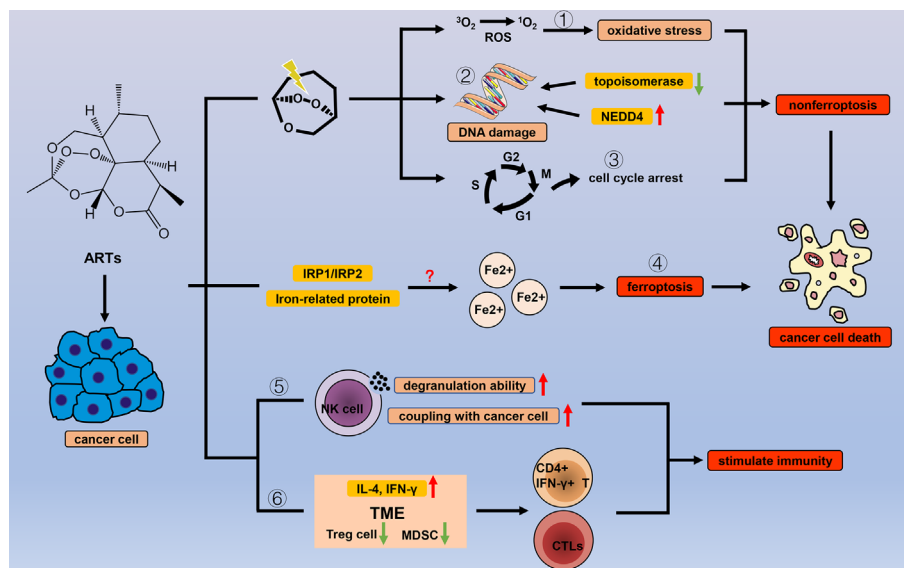


FIGURE 3 | Efficacy of ARTs in cancer. With the help of endogenous peroxides, ARTs can cause oxidative stress by (1) increasing the concentration of ROS, (2) DNA damage, and (3) cell cycle arrest to cause cancer cell death. In addition to the common types of cell death, ARTs increase the concentration of unstable iron ions in cancer cells by (4) regulating a variety of iron-related proteins and IRP1/IRP2, thereby triggering ferroptosis. ARTs strengthen the cancer-killing effect of NK cells by (5) enhancing their degranulation ability and increasing the connection between NK cells and cancer cells. ARTs (6) reduce negative regulation factors (Treg cells and MDSCs) and increase IL-4 and IFN- γ in TME to stimulate T cell immune response.

moiety, ARTs can kill cancer cells in a variety of ways. Moreover, these pathways are closely interconnected.

Ferroptosis, a new type of programmed cell death that is iron-dependent and differs from apoptosis, cell necrosis, and autophagy, has recently become a research hotspot in cancer (113–115). Interestingly, ART anticancer activity is also based on ferroptosis. Current research shows two main mechanisms of ferroptosis. In the first mechanism, the expression of the core enzyme GPX4 in the antioxidant system is reduced or inactivated, depending on the level of intracellular GSH (116). In the second mechanism, unstable iron ions accumulate in cancer cells (100). The accumulation of unstable iron ions may be the main mechanism by which ART-induced ferroptosis. The anticancer effects of ARTs are related to many iron-related proteins, including transferrin (TF), transferrin receptors 1 and 2 (TFR1, TFR2), ceruloplasmin (CP), and lactoferrin (LTF) (117). Furthermore, in DHA-induced ferroptosis, intracellular GSH levels are not affected. However, when DHA is combined with deferoxamine (DFO), an iron chelator, DHA-induced ferroptosis is completely inhibited. Further, DHA may inhibit the translation activity of a series of ferritin-related genes by maintaining the binding of iron regulatory protein-1 (IRP1) and IRP2 to iron-responsive element sequences, thus greatly increasing the concentration of unstable iron ions in cancer cells (118). However, counterintuitively, ARTs also strangely induce a negative feedback pathway in ferroptosis. ARTs can significantly increase the expression of GRP78, an anti-ferroptosis glucose-regulated protein, and knockdown of GRP78-enhanced ART-induced ferroptosis in AsPC-1 and PaTU8988 cells (119). DHA increases the expression of HSPA5, a negative regulator of DHA-induced ferroptosis, by activating GPX4 in glioma cells (120). It is worth considering that the induction of ferroptosis activity by ARTs could be enhanced by inhibiting the negative feedback pathway. In summary, the specific mechanism by

which ARTs induce ferroptosis is still unclear, and more research is warranted. In addition, except for ferroptosis, other types of programmed cell death modes, such as apoptosis and autophagy, are also important for ARTs to kill cancer cells, and many excellent research results have been published (**Table 1**).

The regulation of the immune system seems to be one of the antitumor mechanisms of ARTs. This idea was first supported when ARS was directly applied to natural killer (NK) cells, and the degranulation ability of NK cells was enhanced to effectively kill cancer cells. Combination treatment with the degranulation inhibitor concanamycin A completely reversed these effects of ARS. ARS does not change the expression of activated receptors on the surface of NK cells to enhance their degranulation ability, but it could induce the activation of downstream signaling molecules (134). Subsequently, ARS can also increase the coupling between tumor and NK cells, but the expression of the main ligands of NK receptors is not affected; the specific mechanism needs to be further explored (135). Moreover, except for the innate immune system, ARTs can also regulate specific immune systems. For example, ARM can reduce Treg cells and increase IL-4 and IFN- γ in the tumor microenvironment (136). More directly, treatment with ARS in a 4T1 breast cancer model significantly reduced the number of MDSCs and Treg cells in mice and significantly increased CD4⁺ IFN- γ ⁺ T cells and cytotoxic T lymphocytes (CTLs) (137). Although obvious immune regulation can be observed, few studies have investigated immune system regulation by ARTs, and the exact underlying mechanism remains unclear; however, it is still a promising research direction.

As studies on ARTs in cancer have increased, so too have the number of case reports and related clinical trials that support the potential role of ARTs in cancer treatment. There were two uveal melanoma cases in which compassionate treatment with ART was administered after ineffective standard chemotherapy (138). One patient received fotemustine plus ART and reached a

TABLE 1 | Non-ferroptosis cancer cell death induced by ARTs.

Cell death	Cell line	Drug	Effect	Reference
apoptosis	C4, C4-2 and C4-2B prostate Ca	DHA	miR-34a \uparrow , miR-7 \uparrow , Axl \downarrow	Pacez et al. (121)
Apoptosis	HL-60 and KG1a leukemia	ART	cleaved caspase3 \uparrow , Bax/Bcl-2 \uparrow	Chen et al. (122)
Apoptosis	A549/TAX lung Ca	ART	Inhibit lysosome function and the clearance of dysfunctional mitochondria	Li et al. (123)
Apoptosis	4T1 and MCF-7 breast Ca	ART	HSP70 \downarrow , Bcl-2 \downarrow , cleaved caspase-9 \uparrow	Pirali et al. (124)
Autophagy-related apoptosis	RT4, RT112, T24, and TCCSup bladder Ca	ART	DNA damage \uparrow , LC3B-I \downarrow , LC3B-II \uparrow	Zhao et al. (125)
Apoptosis	HCT116 and DLD-1 colorectal Ca	ART, DHA	P53 \uparrow , DR5 \uparrow , caspase-3/7 \uparrow , cleaved PARP-1 \uparrow	Zhou et al. (126)
Apoptosis	MM.1S and MM.1R multiple myeloma	ARS, DHA	ROS \uparrow , cytochrome C translocation \uparrow	Chen et al. (98)
Apoptosis	HT-29 and HCT-116 colorectal Ca	DHA	endoplasmic reticulum stress	Elhassanny et al. (99)
Autophagy-dependent apoptosis	T24 and EJ bladder Ca	ART	ROS \uparrow , pAMPK \uparrow , pmTOR \downarrow , pULK1 \uparrow	Zhou et al. (127)
Apoptosis	EGFR-mutant and KRAS -mutant lung Ca	DHA	pSTAT3 \downarrow , Mcl-1 \downarrow , Survivin \downarrow , Bcl-2 \downarrow	Yan et al. (128)
Apoptosis	18 types of B-cell lymphoma	ART	endoplasmic reticulum stress	Våtsveen et al. (129)
Apoptosis	CNE-2Z Nasopharyngeal Ca	DHA	CLC-3 chloride channel protein \uparrow , cleaved caspase-3 \uparrow	Zhou et al. (130)
Autophagy	A549 lung Ca	DHA-37	HMGB1 \uparrow , pMAPK \uparrow , LC3-II/LC3-I \uparrow	Liu et al. (131)
Apoptosis	HCT116 colorectal Ca	ART	Inhibit the NF- κ B pathway, ROS \uparrow , Bax/Bcl-2 \uparrow	Chen et al. (132)
Apoptosis	PC3, 22RV1 and LNCaP prostate Ca	ART	Induce oxidative stress, survivin \downarrow , cleaved PARP \uparrow	Nunes et al. (133)

temporary response, although the tumor progressed under prior fotemustine therapy alone, and the patient died 23 months after being diagnosed with stage 4 disease. The second patient reached disease stabilization after administration of dacarbazine and ART, and the survival time of the patient greatly exceeded that of the median survival time for patients with uveal melanoma, which is 2 to 5 months. Furthermore, the results of a phase I clinical study on intravenous ART in patients with advanced solid tumor malignancies were recently published (139). Nineteen patients were enrolled in the study and had various cancers. In the study, dose-limiting toxicities were observed in one of six patients at dose levels of 12 mg/kg (neutropenic fever) and 18 mg/kg (grade 3 hypersensitivity reaction on C1D1); both patients treated with 25 mg/kg experienced dose-limiting toxicities (one patient had grade 3 nausea/vomiting, and the other experienced neutropenic infection, grade 3 ALT elevation, and grade 4 ALT elevation). They also observed a disease control rate of 27% (4 out of 16). In summary, although there are issues to be resolved, ARTs have great potential as anticancer drugs.

PROGRESS ON THE USE OF QUINOLINE ANTIPARASITIC DRUGS FOR TREATING CANCER

Similar to ARTs, the design and synthesis of quinoline drugs, which are characterized by a quinoline ring, has been researched for application as antimalarial drugs. Quinolines exert their

antimalarial effects during the blood or liver stages of the life cycle of the parasite (140), but different drugs have different mechanisms (141, 142). With the progress in research, an increasing number of quinoline drugs have shown therapeutic effects in other diseases, including cancer (Figure 4).

Chloroquine

Chloroquine (CQ), a 4-aminoquinoline, has been used as an antimalarial drug for many years and is often recommended to be co-administered with primaquine to prevent recurrence of *Plasmodium vivax* (143). CQ is currently considered a protonated, weakly basic drug that increases the pH and accumulates in the food vacuole of parasites, thereby interfering with the degradation of host red blood cell hemoglobin, and preventing the growth of malaria parasite (144). The exact mechanism requires further investigation. Similar to other antiparasitic drugs, CQ has also shown potential in the treatment of cancers and other diseases (145, 146).

As lysosomotropic agents, CQ increases the pH of the lysosome from 4.5 to 6, such a change in pH is not conducive for the activity of lysosomal enzymes. This mode of action is known as a lysosomotropic effect (147, 148). Therefore, CQ can affect various biological processes by acting on receptors, enzymes, and transcriptional factors, which would determine the therapeutic effects in cancer (149) (1). Inhibit autophagy to induce anticancer effects. As an autophagy inhibitor approved by the FDA. At present, this particular function has been studied quite thoroughly. CQ blocks the final step of the autophagy process by impeding the degradation of autophagic proteins

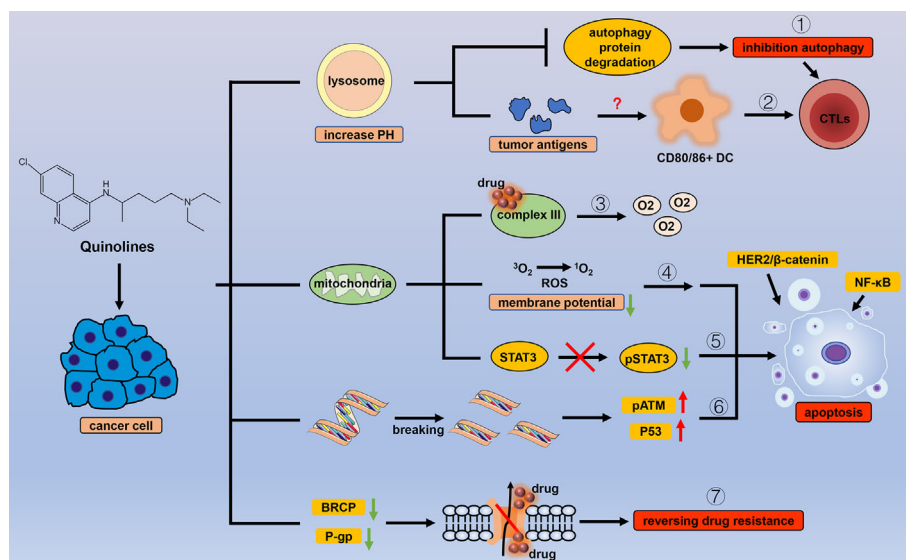


FIGURE 4 | Efficacy of quinoline antiparasitic drugs in cancer. Lysosomes are an important target of quinoline drugs, and quinolines increase the pH of the lysosome, thereby triggering a variety of cascade reactions. Quinolines can (1) inhibit the degradation of autophagy proteins to block autophagy and (2) stimulate antitumor immune responses by increasing tumor antigens. Mitochondria are also a target for quinolines. Quinolines increase the oxygen concentration in cancer cells by (3) inhibiting the related processes of mitochondrial complex III and cause apoptosis by (4) inducing oxidative stress with the change in mitochondrial membrane potential, (5) inhibiting the phosphorylation level of STAT3 in mitochondria, and (6) introducing double-strand breaks in DNA in cancer cells. (7) Quinolines inhibit the drug delivery mediated by P-gp and BRCP.

such as light chain 3B-II (LC3B-II) (150, 151). Thus, CQ prevents the production and recycling of important nutrients and metabolites, causing tumor cell damage and death. Further, the inhibition of the final stage of autophagy increases cytotoxic effects in cancer cells by promoting cell apoptosis and cell cycle arrest (152) (2). Regulate immunity to prevent tumor cells from escaping. Successive studies have shown that when ultra-low concentrations of chemotherapeutics are used on tumor cells, the expression of some genes related to inflammation, immunity, and tumor antigens in the cell increases, thereby increasing the cell's ability to use CTLs to induce immunogenic death of tumor cells (153–157). A recent study reported for the first time the effect of low concentrations of CQ on the immunogenicity of tumor cells (158). In that study, when HCT-116 colon cancer cells were treated with CQ and 5-fluorouracil in combination, their cell lysates significantly induced the maturation of dendritic cells, and the expression of surface markers, including CD80 and CD86, was significantly increased. Additionally, dendritic cells increased the production of CTLs and triggered tumor cell death. Subsequently, they detected an increase in tumor-associated carcinoembryonic antigen family gene expression in the treated cancer cells, but the specific mechanism still needs to be explored, which may be related to the inhibition of autophagy by CQ. CQ has also been found to directly affect the function and differentiation of various immune cells by altering the pH of the lysosome and has been described in detail in this review (149).

CQ also has multiple functions in tumors by regulating a variety of key signaling molecules. Platinum drugs are recognized as the mainstay drugs for the treatment of epithelial ovarian cancer (159). However, drug-resistant cancer cells can survive the DNA damage induced by anticancer drugs through DNA repair pathways or bypassing cell cycle checkpoints (160, 161); however, CQ can upregulate the expression of p21^{WAF1/CIP1} to prevent this phenomenon and reverse the drug resistance of cancer cells. This function seems to depend on autophagy inhibition, but the connection is not yet clear (162). Many other functions of CQ depend on its inhibitory effect on autophagy. However, CQ can reduce the expression of CXC chemokine receptor 4 (CXCR4) by inhibiting STAT3 expression, thereby reducing the stemness of esophageal squamous cell carcinoma cells. This process is independent of autophagy, and the expression of key molecules, ATG7 and BECN1, in the autophagy pathway does not change (163), suggesting that CQ has other effects that do not depend on autophagy inhibition, but these have not yet been elucidated. In addition, CQ can regulate the expression of signaling molecules, including NF- κ B and p53, to exert an anticancer effect (164).

As an autophagy inhibitor approved by the FDA, CQ has received widespread attention, and the possibilities of its clinical application have been extensively studied. To date, many clinical trials using CQ alone or in combination to treat cancer have been conducted (165, 166). Most findings indicate that the combination of CQ with other drugs was well tolerated, and the maximum tolerated dose increases compared with using CQ alone. However, in these trials, no significant differences between the treatment and control group and no significant improvement

in overall survival were observed. This may also be related to the small sample size used in the phase I clinical trials; thus, the efficacy of CQ should be further evaluated and explored in a larger sample.

Atovaquone

Atovaquone (ATV), a hydroxy 1,4-naphthoquinoline, is a homolog of coenzyme Q. Current research shows that ATV's antimalarial site is the mitochondrial complex III (141). Compared with non-cancer cells, cancer cells rely more heavily on mitochondrial functions to generate ATP for growth and survival (167, 168). Naturally, respiratory energy metabolism, especially oxidative phosphorylation, has become a focus of research. ATV, an inhibitor of the mitochondrial complex III, can significantly reduce the oxygen consumption rate and increase the concentration of oxygen in cancer cells (169). In clinical practice, hypoxia is a major problem in cancer treatment (170). The current novel photodynamic therapy technology mainly relies on ROS to kill cancer cells, but the hypoxic tumor environment limits its therapeutic value (171, 172); thus, combinations with ATV may be a solution. Many studies have also revealed that ATV can indeed improve the efficacy of radiotherapy, chemotherapy, and immunotherapy by reducing the rate of oxygen consumption (173, 174).

The reduction in mitochondrial function greatly inhibits the proliferation of CSCs, which mainly rely on mitochondrial respiration rather than glycolysis. The decrease in mitochondrial membrane potential and the increase in ROS levels lead to apoptosis in CSCs; thus, ATV selectively acts on CSCs (175). More specifically, ATV can inhibit the phosphorylation of mitochondrial STAT3 but not of nuclear STAT3. The inhibition of STAT3 phosphorylation is not accompanied by changes in JAK, Src, or MEK, indicating that this function of ATV is independent of JAK/Src/MEK (176). ATV can also reduce the expression of a variety of STAT3 target genes, thereby exerting anticancer effects in tumors (177, 178). There is still much to be discovered regarding mitochondria and related functions, an aspect that has received much attention in the context of cancer treatment (179).

Mitochondrial respiratory function is not the only target of ATVs. ATVs can degrade HER2 and β -catenin in a proteasome-dependent manner, thereby inhibiting the activation of HER2/ β -catenin and triggering apoptosis in cancer cells; however, application of the proteasome inhibitor MG-132 eliminates this effect of ATV (180). In addition, ATV can also introduce double-stranded breaks in DNA, thereby upregulating phosphorylated ATM and p53 to trigger cycle arrest and apoptosis in cancer cells (181). ATV is also an inhibitor of BRCP and P-gp-mediated drug delivery (182), indicating the broader application value of ATV, but its specific mechanism remains to be elucidated.

FUTURE DIRECTIONS

People are increasingly aware of the value of drug repositioning with the urgent clinical situation that large number of new

anticancer drugs have appeared unignorable drug resistance after short-term clinical use (183, 184). Encouragingly, numerous clinically approved non-cancer drugs have shown antitumor activity *in vitro*, *in vivo*, and even clinically, and antiparasitic drugs account for a large portion of these repurposed drugs (185).

Based on the current research, the application of antiparasitic drugs in anticancer therapy is multitargeted and multimodal (Table 2). Macrolide drugs induce cell cycle arrest, apoptosis, and autophagic death in cancer cells by regulating multiple targets and multiple signaling pathways, including WNT-TCF and PAK1-AKT-mTOR, and also play a role in reversing tumor resistance. Benzimidazole drugs induce cancer cell death by inhibiting sugar metabolism and interfering with the formation of microtubules. In particular, benzimidazoles can also inhibit the expression of HIF-1 α protein to inhibit the stress behavior of cancer cells under hypoxic environments, and by changing the tumor microenvironment to stimulate the host's antitumor immunity, benzimidazoles may also exert anticancer effects. Endoperoxide is very important for the anticancer activity of ARTs. Specifically, an endoperoxide moiety can produce a large amount of ROS in tumor cells and trigger a series of biological processes that are lethal to cancer cells. Interestingly, ARTs increase the concentration of unstable iron ions in cancer cells by regulating various ferritin and related pathways to induce ferroptosis, a new programmed cell death mode (115, 186), which may be worthwhile to study further. Similar to clinical antimalarial drugs, quinoline drugs also exert anticancer effects. CQ, a lysosomotropic agent, affects various biological pathways in cancer cells by changing the pH of lysosomes. Autophagy is

currently studied more thoroughly than other mechanisms, but CQ also increases the immunogenicity of cancer cells. In addition, as a competitive inhibitor of the mitochondrial complex III, ATV can significantly affect the oxidative phosphorylation of cancer cells to change the hypoxic environment of tumor cells and greatly improve the efficacy of various clinical treatment methods. At present, the application of antiparasitic drugs in tumor treatment is not only at the stage of theoretical experimentation, but several clinical trials have already been carried out to analyze the feasibility of specific drugs.

In summary, antiparasitic drugs are involved in almost all aspects of tumors, including cell cycle, apoptosis, autophagy, ferroptosis, stress, energy homeostasis, immunity, and drug resistance. Besides, when used in combination with existing clinical tumor drugs, many antiparasitic drugs show significant synergistic effects (187–189). However, according to current research results, antiparasitic drugs are still far from being repurposed into antitumor drugs that can be widely used in clinical practice. The current research on the anticancer mechanisms of antiparasitic drugs is still not comprehensive enough, and more thorough research is needed. In addition, antiparasitic and tumor therapy have two different application environments, and many problems remain to be solved. The first problem is drug delivery; the external microenvironment of the parasite-infected foci is relatively normal, whereas the growth of tumors mainly depends on glycolysis, which leads to an acidic external microenvironment. Whether this microenvironment affects the delivery of drugs needs further exploration. The second problem is drug concentration. Different drug concentrations cause different dominant effects.

TABLE 2 | Antitumor mechanism of antiparasitic drugs.

Category	Drug	Drug action	Effect
Macrolides	Avermectins	Apoptosis	Inhibit Cl ⁻ Channel, Mitochondrial related pathways
		Cell cycle	Cycle-related protein, KPNB1-dependent
		Autophagy	Ubiquitination pathway, PAK1↓, Inactivate AKT-mTOR
		Cell stemness	Inhibit stemness genes, Inactivate PAK1, pStat3↓, IL-6↓
Benzimidazoles	Milbemycins	Drug resistance	MDR1↓, P-gp↓, MAST1↓
	Albendazole	Energy homeostasis	Inhibition GLUT1/AMPK/P53, HIF-1 α ↓
		Cell cycle	Inhibit microtubule formation
		Apoptosis	ER stress, pMAPK↑, TNF- α ↑
	Flubendazole	Cell cycle	Inhibiting tubulin polymerization
		Autophagy	EVA1A↑, LC3 puncta↓, p62 degradation↓, and LC3 lipidation↓, STAT3 related pathways
Artemisinin and derivatives	Artemisinin	Immunity	PD-1↓, accumulation of MDSCs↓
		DNA damage	ROS↑, topoisomerase 1↓
		Cell cycle	Cycle-related protein (cyclin-B1, cyclin D1, cyclin E)
	Artesunate	Immunity	Degranulation of NK cells↑, MDSCs and Treg cells↓, CD4 +IFN- γ + T and CTL↑
		DNA damage	ROS↑
		DNA damage	NEDD4↑, the stability of c-Myc↓, DNA topoisomerases↓
		Dihydroartemisinin	ROS↑, CDK4↓
Quinolines	Artemether	Ferroptosis	Iron-related proteins, Binding of iron IRP1 and IRP2↑, unstable iron ions↑
		Immunity	Treg↓, IL-4 and IFN- γ ↑
		Chloroquine	Impeding the degradation of autophagic proteins
	Atovaquone	tumor-associated carcinoembryonic antigen↑, CD80 and CD86↑	
		Drug resistance	p21WAF1/CIP1↑
		Cell stemness	STAT3↓, CXCR4↓
		Energy homeostasis	Inhibiting mitochondrial complex III, Oxidative phosphorylation↓
		Cell stemness	mitochondrial membrane potential↓, ROS↑, pSTAT3 in mitochondrial↓
		Apoptosis	Degrade HER2 and β -catenin, pATM and p53↑

The concentration that has the best anticancer effect and does not cause side effects in the human body needs to be established. The third problem is that although antiparasitic drugs have many advantages, we cannot rule out they might promote tumor growth. Studies have shown that CQ-induced stress in cancer cells can activate NF- κ B, thereby conferring transcriptional and phenotypic plasticity to cells, resulting in the reprogramming of cells and allows tumor cells to escape cell death induced by either drug therapy or the immune system (190, 191). Fortunately, for the first two issues, many studies have conducted in-depth study. Increasing evidence shows that nanotechnology-based drug delivery methods yield better therapeutic effects at lower concentrations and might be clinically implemented in the near future (192–198). Successive preclinical studies and clinical trials have clarified in detail the therapeutic effects of different drug concentrations and various possible side effects. However, there are very few studies have investigated the cancer-promoting effects of antiparasitic drugs. However, this may be very important for us to fully understand the role of antiparasitic drugs in tumors. After understanding these cancer-promoting effects, with the help of modern drug modification and improvement technologies (199–202), it can greatly accelerate the real application of antiparasitic drugs in

clinical cancer treatment. More problems are likely to be encountered as research and practice progress. Nevertheless, it is undeniable that antiparasitic drugs indeed have great potential for development as broad-spectrum, clinically applicable antitumor drugs.

AUTHOR CONTRIBUTIONS

J-GD and HZ contributed substantially to the design of this review and gave the approval of the final version for publishing. DZ and JZ prepared the table. Q-XL and XL prepared the figures. Y-QL and ZZ wrote the manuscript. All authors contributed to the article and approved the submitted version.

FUNDING

This work was supported by grants from the National Natural Science Foundation of China (No. 81972190), Natural Science Foundation of Chongqing (cstc2018jcyjAX0178) and the Scientific Research Project of Undergraduate, the Army (Third Military) Medical University (2019XBK48).

REFERENCES

- Arora N, Kaur R, Anjum F, Tripathi S, Mishra A, Kumar R, et al. Neglected Agent Eminent Disease: Linking Human Helminthic Infection, Inflammation, and Malignancy. *Front Cell Infect Microbiol* (2019) 9:402. doi: 10.3389/fcimb.2019.00402
- van Tong H, Brindley PJ, Meyer CG, Velavan TP. Parasite Infection, Carcinogenesis and Human Malignancy. *Ebiomedicine* (2017) 15:12–23. doi: 10.1016/j.ebiom.2016.11.034
- Pastille E, Frede A, McSorley HJ, Gräb J, Adamczyk A, Kollenda S, et al. Intestinal Helminth Infection Drives Carcinogenesis in Colitis-Associated Colon Cancer. *PLoS Pathog* (2017) 13(9):e1006649. doi: 10.1371/journal.ppat.1006649
- Moormann AM, Bailey JA. Malaria - How This Parasitic Infection Aids and Abets EBV-associated Burkitt Lymphomagenesis. *Curr Opin Virol* (2016) 20:78–84. doi: 10.1016/j.coviro.2016.09.006
- Brindley PJ, Costa J, Sripa B. Why Does Infection With Some Helminths Cause Cancer? *Trends Cancer* (2015) 1(3):174–82. doi: 10.1016/j.trecan.2015.08.011
- Ouaissi A, Ouaissi M. Molecular Basis of Trypanosoma Cruzi and Leishmania Interaction With Their Host(s): Exploitation of Immune and Defense Mechanisms by the Parasite Leading to Persistence and Chronicity, Features Reminiscent of Immune System Evasion Strategies in Cancer Diseases. *Arch Immunol Ther Exp (Warsz)* (2005) 53(2):102–14.
- Qin L, Chen C, Chen L, Xue R, Ou-Yang M, Zhou C, et al. Worldwide Malaria Incidence and Cancer Mortality are Inversely Associated. *Infect Agent Cancer* (2017) 12:14. doi: 10.1186/s13027-017-0117-x
- Lehrer S. Association Between Malaria Incidence and All Cancer Mortality in Fifty U.S. States and the District of Columbia. *Anticancer Res* (2010) 30(4):1371–3.
- Gao F, Zhang X, Wang T, Xiao J. Quinolone Hybrids and Their Anti-Cancer Activities: An Overview. *Eur J Med Chem* (2019) 165:59–79. doi: 10.1016/j.ejmech.2019.01.017
- Bray F, Ferlay J, Soerjomataram I, Siegel RL, Torre LA, Jemal A. Global Cancer Statistics 2018: GLOBOCAN Estimates of Incidence and Mortality Worldwide for 36 Cancers in 185 Countries. *CA Cancer J Clin* (2018) 68(6):394–424. doi: 10.3322/caac.21492
- Xu Z, Zhao SJ, Liu Y. 1,2,3-Triazole-containing Hybrids as Potential Anticancer Agents: Current Developments, Action Mechanisms and Structure-Activity Relationships. *Eur J Med Chem* (2019) 183:111700. doi: 10.1016/j.ejmech.2019.111700
- Feng M, Xiong G, Cao Z, Yang G, Zheng S, Song X, et al. Pd-1/Pd-L1 and Immunotherapy for Pancreatic Cancer. *Cancer Lett* (2017) 407:57–65. doi: 10.1016/j.canlet.2017.08.006
- Dorosti Z, Yousefi M, Sharafi SM, Darani HY. Mutual Action of Anticancer and Antiparasitic Drugs: Are There Any Shared Targets? *Future Oncol* (2014) 10(15):2529–39. doi: 10.2217/fon.14.65
- Geary TG. Ivermectin 20 Years on: Maturation of a Wonder Drug. *Trends Parasitol* (2005) 21(11):530–2. doi: 10.1016/j.pt.2005.08.014
- Li N, Zhan X. Anti-Parasite Drug Ivermectin can Suppress Ovarian Cancer by Regulating lncRNA-EIF4A3-mRNA Axes. *Epma J* (2020) 11(2):289–309. doi: 10.1007/s13167-020-00209-y
- Zhang X, Zhang G, Zhai W, Zhao Z, Wang S, Yi J. Inhibition of TMEM16A Ca(2+)-Activated Cl(-) Channels by Avermectins is Essential for Their Anticancer Effects. *Pharmacol Res* (2020) 156:104763. doi: 10.1016/j.phrs.2020.104763
- Zhang P, Zhang Y, Liu K, Liu B, Xu W, Gao J, et al. Ivermectin Induces Cell Cycle Arrest and Apoptosis of HeLa Cells Via Mitochondrial Pathway. *Cell Prolif* (2019) 52(2):e12543. doi: 10.1111/cpr.12543
- Wang J, Xu Y, Wan H, Hu J. Antibiotic Ivermectin Selectively Induces Apoptosis in Chronic Myeloid Leukemia Through Inducing Mitochondrial Dysfunction and Oxidative Stress. *Biochem Biophys Res Commun* (2018) 497(1):241–7. doi: 10.1016/j.bbrc.2018.02.063
- Juarez M, Schcolnik-Cabrera A, Dominguez-Gomez G, Chavez-Blanco A, Diaz-Chavez J, Duenas-Gonzalez A. Antitumor Effects of Ivermectin At Clinically Feasible Concentrations Support its Clinical Development as a Repositioned Cancer Drug. *Cancer Chemother Pharmacol* (2020) 85(6):1153–63. doi: 10.1007/s00280-020-04041-z
- Zhang X, Qin T, Zhu Z, Hong F, Xu Y, Zhang X, et al. Ivermectin Augments the In Vitro and In Vivo Efficacy of Cisplatin in Epithelial Ovarian Cancer by Suppressing Akt/mTOR Signaling. *Am J Med Sci* (2020) 359(2):123–9. doi: 10.1016/j.amjms.2019.11.001
- Intuyod K, Hahnvanawong C, Pinlaor P, Pinlaor S. Anti-Parasitic Drug Ivermectin Exhibits Potent Anticancer Activity Against Gemcitabine-

- Resistant Cholangiocarcinoma In Vitro. *Anticancer Res* (2019) 39(9):4837–43. doi: 10.21873/anticancer.13669
22. Kodama M, Kodama T, Newberg JY, Katayama H, Kobayashi M, Hanash SM, et al. In Vivo Loss-of-Function Screens Identify KPNB1 as a New Druggable Oncogene in Epithelial Ovarian Cancer. *Proc Natl Acad Sci USA* (2017) 114(35):E7301–10. doi: 10.1073/pnas.1705441114
 23. Lokich E, Singh RK, Han A, Romano N, Yano N, Kim K, et al. HE4 Expression is Associated With Hormonal Elements and Mediated by Importin-Dependent Nuclear Translocation. *Sci Rep* (2014) 4:5500. doi: 10.1038/srep05500
 24. Dou Q, Chen HN, Wang K, Yuan K, Lei Y, Li K, et al. Ivermectin Induces Cytostatic Autophagy by Blocking the PAK1/Akt Axis in Breast Cancer. *Cancer Res* (2016) 76(15):4457–69. doi: 10.1158/0008-5472.CAN-15-2887
 25. Wang K, Gao W, Dou Q, Chen H, Li Q, Nice EC, et al. Ivermectin Induces PAK1-mediated Cytostatic Autophagy in Breast Cancer. *Autophagy* (2016) 12(12):2498–9. doi: 10.1080/15548627.2016.1231494
 26. Wei W, Hardin H, Luo QY. Targeting Autophagy in Thyroid Cancers. *Endocr Relat Cancer* (2019) 26(4):R181–94. doi: 10.1530/ERC-18-0502
 27. Peng PL, Kuo WH, Tseng HC, Chou FP. Synergistic Tumor-Killing Effect of Radiation and Berberine Combined Treatment in Lung Cancer: The Contribution of Autophagic Cell Death. *Int J Radiat Oncol Biol Phys* (2008) 70(2):529–42. doi: 10.1016/j.ijrobp.2007.08.034
 28. Zhu M, Li Y, Zhou Z. Antibiotic Ivermectin Preferentially Targets Renal Cancer Through Inducing Mitochondrial Dysfunction and Oxidative Damage. *Biochem Biophys Res Commun* (2017) 492(3):373–8. doi: 10.1016/j.bbrc.2017.08.097
 29. Tanaka H, Nakamura M, Kameda C, Kubo M, Sato N, Kuroki S, et al. The Hedgehog Signaling Pathway Plays an Essential Role in Maintaining the CD44+CD24-/low Subpopulation and the Side Population of Breast Cancer Cells. *Anticancer Res* (2009) 29(6):2147–57.
 30. Al-Hajj M, Wicha MS, Benito-Hernandez A, Morrison SJ, Clarke MF. Prospective Identification of Tumorigenic Breast Cancer Cells. *Proc Natl Acad Sci USA* (2003) 100(7):3983–8. doi: 10.1073/pnas.0530291100
 31. Dominguez-Gomez G, Chavez-Blanco A, Medina-Franco JL, Saldivar-Gonzalez F, Flores-Torrontegui Y, Juarez M, et al. Ivermectin as an Inhibitor of Cancer Stem-Like Cells. *Mol Med Rep* (2018) 17(2):3397–403. doi: 10.3892/mmr.2017.8231
 32. Kim JH, Choi HS, Kim SL, Lee DS. The PAK1-Stat3 Signaling Pathway Activates IL-6 Gene Transcription and Human Breast Cancer Stem Cell Formation. *Cancers (Basel)* (2019) 11(10):1527. doi: 10.3390/cancers11101527
 33. Jiang L, Wang P, Sun YJ, Wu YJ. Ivermectin Reverses the Drug Resistance in Cancer Cells Through EGFR/ERK/Akt/NF- κ B Pathway. *J Exp Clin Cancer Res* (2019) 38(1):265. doi: 10.1186/s13046-019-1251-7
 34. Farias EF, Petrie K, Leibovitch B, Murtagh J, Chornet MB, Schenk T, et al. Interference With Sin3 Function Induces Epigenetic Reprogramming and Differentiation in Breast Cancer Cells. *Proc Natl Acad Sci USA* (2010) 107(26):11811–6. doi: 10.1073/pnas.1006737107
 35. Ellison-Zelski SJ, Solodin NM, Alarid ET. Repression of ESR1 Through Actions of Estrogen Receptor Alpha and Sin3A At the Proximal Promoter. *Mol Cell Biol* (2009) 29(18):4949–58. doi: 10.1128/MCB.00383-09
 36. Ellison-Zelski SJ, Alarid ET. Maximum Growth and Survival of Estrogen Receptor-Alpha Positive Breast Cancer Cells Requires the Sin3A Transcriptional Repressor. *Mol Cancer* (2010) 9:263. doi: 10.1186/1476-4598-9-263
 37. Kwon YJ, Petrie K, Leibovitch BA, Zeng L, Mezei M, Howell L, et al. Selective Inhibition of SIN3 Corepressor With Avermectins as a Novel Therapeutic Strategy in Triple-Negative Breast Cancer. *Mol Cancer Ther* (2015) 14(8):1824–36. doi: 10.1158/1535-7163.MCT-14-0980-T
 38. Melotti A, Mas C, Kuciak M, Lorente-Trigos A, Borges I, Ruiz IAA. The River Blindness Drug Ivermectin and Related Macrocytic Lactones Inhibit WNT-TCF Pathway Responses in Human Cancer. *EMBO Mol Med* (2014) 6(10):1263–78. doi: 10.15252/emmm.201404084
 39. Prichard RK. Is Anthelmintic Resistance a Concern for Heartworm Control? What Can We Learn From the Human Filariasis Control Programs? *Vet Parasitol* (2005) 133(2–3):243–53. doi: 10.1016/j.vetpar.2005.04.008
 40. Wang XJ, Wang M, Wang JD, Jiang L, Wang JJ, Xiang WS. Isolation and Identification of Novel Macrocytic Lactones From Streptomyces Avermitilis NEAU1069 With Acaricidal and Nematocidal Activity. *J Agric Food Chem* (2010) 58(5):2710–4. doi: 10.1021/jf902496d
 41. Xiang WS, Wang JD, Wang XJ, Zhang J. Two New Beta-Class Milbemycins From Streptomyces Bingchengensis: Fermentation, Isolation, Structure Elucidation and Biological Properties. *J Antibiot (Tokyo)* (2007) 60(6):351–6. doi: 10.1038/ja.2007.47
 42. Gao A, Liang H, Wang X, Zhang X, Jing M, Zhang J, et al. Reversal Effects of Two New Milbemycin Compounds on Multidrug Resistance in MCF-7/adr Cells In Vitro. *Eur J Pharmacol* (2011) 659(2–3):108–13. doi: 10.1016/j.ejphar.2011.03.023
 43. Xiang W, Gao A, Liang H, Li C, Gao J, Wang Q, et al. Reversal of P-glycoprotein-mediated Multidrug Resistance In Vitro by Milbemycin Compounds in Adriamycin-Resistant Human Breast Carcinoma (MCF-7/adr) Cells. *Toxicol Vitro* (2010) 24(6):1474–81. doi: 10.1016/j.tiv.2010.07.020
 44. Jin L, Chun J, Pan C, Li D, Lin R, Alesi GN, et al. Mast1 Drives Cisplatin Resistance in Human Cancers by Rewiring Craf-Independent MEK Activation. *Cancer Cell* (2018) 34(2):315–30. doi: 10.1016/j.ccell.2018.06.012
 45. Li XQ, Yue CW, Xu WH, Lü YH, Huang YJ, Tian P, et al. A Milbemycin Compound Isolated From Streptomyces Sp. FJS31-2 With Cytotoxicity and Reversal of Cisplatin Resistance Activity in A549/DDP Cells. *BioMed Pharmacother* (2020) 128:110322. doi: 10.1016/j.biopha.2020.110322
 46. Liu J, Liang H, Khilji S, Li H, Song D, Chen C, et al. Moxidectin Induces Cytostatic Autophagic Cell Death of Glioma Cells Through Inhibiting the AKT/mTOR Signalling Pathway. *J Cancer* (2020) 11(19):5802–11. doi: 10.7150/jca.46697
 47. Song D, Liang H, Qu B, Li Y, Liu J, Chen C, et al. Moxidectin Inhibits Glioma Cell Viability by Inducing G0/G1 cell Cycle Arrest and Apoptosis. *Oncol Rep* (2018) 40(3):1348–58. doi: 10.3892/or.2018.6561
 48. Lacey E. The Role of the Cytoskeletal Protein, Tubulin, in the Mode of Action and Mechanism of Drug Resistance to Benzimidazoles. *Int J Parasitol* (1988) 18(7):885–936. doi: 10.1016/0020-7519(88)90175-0
 49. Valdez J, Cedillo R, Hernández-Campos A, Yépez L, Hernández-Luis F, Navarrete-Vázquez G, et al. Synthesis and Antiparasitic Activity of 1H-Benzimidazole Derivatives. *Bioorg Med Chem Lett* (2002) 12(16):2221–4. doi: 10.1016/s0960-894x(02)00346-3
 50. Liu H, Sun H, Zhang B, Liu S, Deng S, Weng Z, et al. (18)F-Fdg PET Imaging for Monitoring the Early Anti-Tumor Effect of Albendazole on Triple-Negative Breast Cancer. *Breast Cancer-Tokyo* (2020) 27(3):372–80. doi: 10.1007/s12282-019-01027-5
 51. Zhang X, Zhao J, Gao X, Pei D, Gao C. Anthelmintic Drug Albendazole Arrests Human Gastric Cancer Cells At the Mitotic Phase and Induces Apoptosis. *Exp Ther Med* (2017) 13(2):595–603. doi: 10.3892/etm.2016.3992
 52. Chu SW, Badar S, Morris DL, Pourgholami MH. Potent Inhibition of Tubulin Polymerisation and Proliferation of Paclitaxel-Resistant 1A9PTX22 Human Ovarian Cancer Cells by Albendazole. *Anticancer Res* (2009) 29(10):3791–6.
 53. Ehteda A, Galettis P, Pillai K, Morris DL. Combination of Albendazole and 2-Methoxyestradiol Significantly Improves the Survival of HCT-116 Tumor-Bearing Nude Mice. *BMC Cancer* (2013) 13:86. doi: 10.1186/1471-2407-13-86
 54. Wang LJ, Liou LR, Shi YJ, Chiou JT, Lee YC, Huang CH, et al. Albendazole-Induced SIRT3 Upregulation Protects Human Leukemia K562 Cells From the Cytotoxicity of MCL1 Suppression. *Int J Mol Sci* (2020) 21(11):3907. doi: 10.3390/ijms21113907
 55. Chen Y, Zhang J, Lin Y, Lei Q, Guan KL, Zhao S, et al. Tumour Suppressor SIRT3 Deacetylates and Activates Manganese Superoxide Dismutase to Scavenge ROS. *EMBO Rep* (2011) 12(6):534–41. doi: 10.1038/embor.2011.65
 56. Zhang QL, Lian DD, Zhu MJ, Li XM, Lee JK, Yoon TJ, et al. Antitumor Effect of Albendazole on Cutaneous Squamous Cell Carcinoma (ScC) Cells. *BioMed Res Int* (2019) 2019:3689517. doi: 10.1155/2019/3689517
 57. Wang LJ, Lee YC, Huang CH, Shi YJ, Chen YJ, Pei SN, et al. Non-Mitotic Effect of Albendazole Triggers Apoptosis of Human Leukemia Cells Via SIRT3/ROS/p38 MAPK/TTP Axis-Mediated TNF- α Upregulation. *Biochem Pharmacol* (2019) 162:154–68. doi: 10.1016/j.bcp.2018.11.003
 58. Kim JW, Dang CV. Cancer's Molecular Sweet Tooth and the Warburg Effect. *Cancer Res* (2006) 66(18):8927–30. doi: 10.1158/0008-5472.CAN-06-1501
 59. Alfaraouk KO, Muddathir AK, Shayoub ME. Tumor Acidity as Evolutionary Spite. *Cancers (Basel)* (2011) 3(1):408–14. doi: 10.3390/cancers3010408

60. Cairns RA, Harris IS, Mak TW. Regulation of Cancer Cell Metabolism. *Nat Rev Cancer* (2011) 11(2):85–95. doi: 10.1038/nrc2981
61. Ahluwalia A, Tarnawski AS. Critical Role of Hypoxia Sensor–HIF-1 α in VEGF Gene Activation. Implications for Angiogenesis and Tissue Injury Healing. *Curr Med Chem* (2012) 19(1):90–7. doi: 10.2174/092986712803413944
62. Zhou F, Du J, Wang J. Albendazole Inhibits HIF-1 α -Dependent Glycolysis and VEGF Expression in non-Small Cell Lung Cancer Cells. *Mol Cell Biochem* (2017) 428(1–2):171–8. doi: 10.1007/s11010-016-2927-3
63. Pourgholami MH, Cai ZY, Badar S, Wangoo K, Poruchynsky MS, Morris DL. Potent Inhibition of Tumoral Hypoxia-Inducible Factor 1 α by Albendazole. *BMC Cancer* (2010) 10:143. doi: 10.1186/1471-2407-10-143
64. Pourgholami MH, Szwajcer M, Chin M, Liauw W, Seef J, Galetti P, et al. Phase I Clinical Trial to Determine Maximum Tolerated Dose of Oral Albendazole in Patients With Advanced Cancer. *Cancer Chemother Pharmacol* (2010) 65(3):597–605. doi: 10.1007/s00280-009-1157-8
65. Hanušová V, Skálová L, Králová V, Matoušková P. The Effect of Flubendazole on Adhesion and Migration in SW480 and SW620 Colon Cancer Cells. *Anticancer Agents Med Chem* (2018) 18(6):837–46. doi: 10.2174/1871520618666171213141911
66. Kralova V, Hanušová V, Caltová K, Špaček P, Hochmalová M, Skálová L, et al. Flubendazole and Mebendazole Impair Migration and Epithelial to Mesenchymal Transition in Oral Cell Lines. *Chem Biol Interact* (2018) 293:124–32. doi: 10.1016/j.cbi.2018.07.026
67. Čáňová K, Rozkydalová L, Vokurková D, Rudolf E. Flubendazole Induces Mitotic Catastrophe and Apoptosis in Melanoma Cells. *Toxicol Vitro* (2018) 46:313–22. doi: 10.1016/j.tiv.2017.10.025
68. Králová V, Hanušová V, Rudolf E, Čáňová K, Skálová L. Flubendazole Induces Mitotic Catastrophe and Senescence in Colon Cancer Cells In Vitro. *J Pharm Pharmacol* (2016) 68(2):208–18. doi: 10.1111/jphp.12503
69. Hou ZJ, Luo X, Zhang W, Peng F, Cui B, Wu SJ, et al. Flubendazole, FDA-approved Anthelmintic, Targets Breast Cancer Stem-Like Cells. *Oncotarget* (2015) 6(8):6326–40. doi: 10.18632/oncotarget.3436
70. Zhang L, Guo M, Li J, Zheng Y, Zhang S, Xie T, et al. Systems Biology-Based Discovery of a Potential Atg4B Agonist (Flubendazole) That Induces Autophagy in Breast Cancer. *Mol Biosyst* (2015) 11(11):2860–6. doi: 10.1039/c5mb00466g
71. Hu J, Li G, Qu L, Li N, Liu W, Xia D, et al. TMEM166/EVA1A Interacts With ATG16L1 and Induces Autophagosome Formation and Cell Death. *Cell Death Dis* (2016) 7(8):e2323. doi: 10.1038/cddis.2016.230
72. Zhen Y, Zhao R, Wang M, Jiang X, Gao F, Fu L, et al. Flubendazole Elicits Anti-Cancer Effects Via Targeting EVA1A-modulated Autophagy and Apoptosis in Triple-negative Breast Cancer. *Theranostics* (2020) 10(18):8080–97. doi: 10.7150/thno.43473
73. Dong T, Lu Z, Li J, Liu Y, Wen J. [Flubendazole Inhibits the Proliferation of A549 and H460 Cells and Promotes Autophagy]. *Zhongguo Fei Ai Za Zhi* (2020) 23(5):306–13. doi: 10.3779/j.issn.1009-3419.2020.104.17
74. Lin S, Yang L, Yao Y, Xu L, Xiang Y, Zhao H, et al. Flubendazole Demonstrates Valid Antitumor Effects by Inhibiting STAT3 and Activating Autophagy. *J Exp Clin Cancer Res* (2019) 38(1):293. doi: 10.1186/s13046-019-1303-z
75. Dolan DE, Gupta S. PD-1 Pathway Inhibitors: Changing the Landscape of Cancer Immunotherapy. *Cancer Control* (2014) 21(3):231–7. doi: 10.1177/107327481402100308
76. Gong J, Chehrizi-Raffle A, Reddi S, Salgia R. Development of PD-1 and PD-L1 Inhibitors as a Form of Cancer Immunotherapy: A Comprehensive Review of Registration Trials and Future Considerations. *J Immunother Cancer* (2018) 6(1):8. doi: 10.1186/s40425-018-0316-z
77. Li K, Tian H. Development of Small-Molecule Immune Checkpoint Inhibitors of PD-1/PD-L1 as a New Therapeutic Strategy for Tumour Immunotherapy. *J Drug Target* (2019) 27(3):244–56. doi: 10.1080/1061186X.2018.1440400
78. Li Y, Acharya G, Elahy M, Xin H, Khachigian LM. The Anthelmintic Flubendazole Blocks Human Melanoma Growth and Metastasis and Suppresses Programmed Cell Death Protein-1 and Myeloid-Derived Suppressor Cell Accumulation. *Cancer Lett* (2019) 459:268–76. doi: 10.1016/j.canlet.2019.05.026
79. Slamon DJ, Leyland-Jones B, Shak S, Fuchs H, Paton V, Bajamonde A, et al. Use of Chemotherapy Plus a Monoclonal Antibody Against HER2 for Metastatic Breast Cancer That Overexpresses HER2. *N Engl J Med* (2001) 344(11):783–92. doi: 10.1056/NEJM200103153441101
80. Kim YJ, Sung D, Oh E, Cho Y, Cho TM, Farrand L, et al. Flubendazole Overcomes Trastuzumab Resistance by Targeting Cancer Stem-Like Properties and HER2 Signaling in HER2-positive Breast Cancer. *Cancer Lett* (2018) 412:118–30. doi: 10.1016/j.canlet.2017.10.020
81. Sáez R, Molina MA, Ramsey EE, Rojo F, Keenan EJ, Albanell J, et al. p95HER-2 Predicts Worse Outcome in Patients With HER-2-positive Breast Cancer. *Clin Cancer Res* (2006) 12(2):424–31. doi: 10.1158/1078-0432.CCR-05-1807
82. Watanabe S, Yonesaka K, Tanizaki J, Nonagase Y, Takegawa N, Haratani K, et al. Targeting of the HER2/HER3 Signaling Axis Overcomes Ligand-Mediated Resistance to Trastuzumab in HER2-positive Breast Cancer. *Cancer Med* (2019) 8(3):1258–68. doi: 10.1002/cam4.1995
83. Parra-Palau JL, Moranchó B, Peg V, Escorihuela M, Scaltriti M, Vicario R, et al. Effect of p95HER2/611CTF on the Response to Trastuzumab and Chemotherapy. *J Natl Cancer Inst* (2014) 106(11):dju291. doi: 10.1093/jnci/dju291
84. Visser BJ, Wieten RW, Kroon D, Nagel IM, Bêlard S, van Vugt M, et al. Efficacy and Safety of Artemisinin Combination Therapy (ACT) for non-Falciparum Malaria: A Systematic Review. *Malar J* (2014) 13:463. doi: 10.1186/1475-2875-13-463
85. Naing C, Whittaker MA, Mak JW, Aung K. A Systematic Review of the Efficacy of a Single Dose Artemisinin-Naphthoquinone in Treating Uncomplicated Malaria. *Malar J* (2015) 14:392. doi: 10.1186/s12936-015-0919-5
86. Dahal P, D'Alessandro U, Dorsey G, Guerin PJ, Nsanabana C, Price RN, et al. Clinical Determinants of Early Parasitological Response to ACTs in African Patients With Uncomplicated Falciparum Malaria: A Literature Review and Meta-Analysis of Individual Patient Data. *BMC Med* (2015) 13:212. doi: 10.1186/s12916-015-0445-x
87. Yakasai AM, Hamza M, Dalhat MM, Bello M, Gadanya MA, Yaqub ZM, et al. Adherence to Artemisinin-Based Combination Therapy for the Treatment of Uncomplicated Malaria: A Systematic Review and Meta-Analysis. *J Trop Med* (2015) 2015:189232. doi: 10.1155/2015/189232
88. Cumming JN, Ploypradith P, Posner GH. Antimalarial Activity of Artemisinin (Qinghaosu) and Related Trioxanes: Mechanism(s) of Action. *Adv Pharmacol* (1997) 37:253–97. doi: 10.1016/s1054-3589(08)60952-7
89. O'Neill PM, Posner GH. A Medicinal Chemistry Perspective on Artemisinin and Related Endoperoxides. *J Med Chem* (2004) 47(12):2945–64. doi: 10.1021/jm030571c
90. Shandilya A, Chacko S, Jayaram B, Ghosh I. A Plausible Mechanism for the Antimalarial Activity of Artemisinin: A Computational Approach. *Sci Rep* (2013) 3:2513. doi: 10.1038/srep02513
91. Lisewski AM, Quiros JP, Ng CL, Adikesavan AK, Miura K, Putluri N, et al. Supergenomic Network Compression and the Discovery of EXP1 as a Glutathione Transferase Inhibited by Artesunate. *Cell* (2014) 158(4):916–28. doi: 10.1016/j.cell.2014.07.011
92. Zheng GQ. Cytotoxic Terpenoids and Flavonoids From *Artemisia Annua*. *Planta Med* (1994) 60(1):54–7. doi: 10.1055/s-2006-959408
93. Beekman AC, Wierenga PK, Woerdenbag HJ, Van Uden W, Pras N, Konings AW, et al. Artemisinin-Derived Sesquiterpene Lactones as Potential Antitumor Compounds: Cytotoxic Action Against Bone Marrow and Tumour Cells. *Planta Med* (1998) 64(7):615–9. doi: 10.1055/s-2006-957533
94. Trachootham D, Alexandre J, Huang P. Targeting Cancer Cells by ROS-mediated Mechanisms: A Radical Therapeutic Approach? *Nat Rev Drug Discovery* (2009) 8(7):579–91. doi: 10.1038/nrd2803
95. Mercer AE, Copple IM, Maggs JL, O'Neill PM, Park BK. The Role of Heme and the Mitochondrion in the Chemical and Molecular Mechanisms of Mammalian Cell Death Induced by the Artemisinin Antimalarials. *J Biol Chem* (2011) 286(2):987–96. doi: 10.1074/jbc.M110.144188
96. Zhang CJ, Wang J, Zhang J, Lee YM, Feng G, Lim TK, et al. Mechanism-Guided Design and Synthesis of a Mitochondria-Targeting Artemisinin Analogue With Enhanced Anticancer Activity. *Angew Chem Int Ed Engl* (2016) 55(44):13770–4. doi: 10.1002/anie.201607303
97. Wang J, Zhang J, Shi Y, Xu C, Zhang C, Wong YK, et al. Mechanistic Investigation of the Specific Anticancer Property of Artemisinin and Its

- Combination With Aminolevulinic Acid for Enhanced Anticorectal Cancer Activity. *ACS Cent Sci* (2017) 3(7):743–50. doi: 10.1021/acscentsci.7b00156
98. Chen Y, Li R, Zhu Y, Zhong S, Qian J, Yang D, et al. Dihydroartemisinin Induces Growth Arrest and Overcomes Dexamethasone Resistance in Multiple Myeloma. *Front Oncol* (2020) 10:767. doi: 10.3389/fonc.2020.00767
 99. Elhassanny A, Soliman E, Marie M, McGuire P, Gul W, ElSohly M, et al. Heme-Dependent ER Stress Apoptosis: A Mechanism for the Selective Toxicity of the Dihydroartemisinin, NSC735847, in Colorectal Cancer Cells. *Front Oncol* (2020) 10:965. doi: 10.3389/fonc.2020.00965
 100. Zhu S, Yu Q, Huo C, Li Y, He L, Ran B, et al. Ferroptosis: A Novel Mechanism of Artemisinin and its Derivatives in Cancer Therapy. *Curr Med Chem* (2020) 28(2):329–45. doi: 10.2174/0929867327666200121124404
 101. Guo S, Yao X, Jiang Q, Wang K, Zhang Y, Peng H, et al. Dihydroartemisinin-Loaded Magnetic Nanoparticles for Enhanced Chemodynamic Therapy. *Front Pharmacol* (2020) 11:226. doi: 10.3389/fphar.2020.00226
 102. Luo Y, Sun X, Huang L, Yan J, Yu BY, Tian J. Artemisinin-Based Smart Nanomedicines With Self-Supply of Ferrous Ion to Enhance Oxidative Stress for Specific and Efficient Cancer Treatment. *ACS Appl Mater Interfaces* (2019) 11(33):29490–7. doi: 10.1021/acsami.9b07390
 103. Li X, Gu S, Sun D, Dai H, Chen H, Zhang Z. The Selectivity of Artemisinin-Based Drugs on Human Lung Normal and Cancer Cells. *Environ Toxicol Pharmacol* (2018) 57:86–94. doi: 10.1016/j.etap.2017.12.004
 104. Kadioglu O, Chan A, Cong LQA, Wong V, Colligs V, Wecklein S, et al. Artemisinin Derivatives Target Topoisomerase 1 and Cause Dna Damage in Silico and In Vitro. *Front Pharmacol* (2017) 8:711. doi: 10.3389/fphar.2017.00711
 105. Bollimpelli VS, Dholaniya PS, Kondapi AK. Topoisomerase I β and its Role in Different Biological Contexts. *Arch Biochem Biophys* (2017) 633:78–84. doi: 10.1016/j.abb.2017.06.021
 106. Chen J, Li W, Cui K, Ji K, Xu S, Xu Y. Artemisitene Suppresses Tumorigenesis by Inducing DNA Damage Through Deregulating c-Myc-topoisomerase Pathway. *Oncogene* (2018) 37(37):5079–87. doi: 10.1038/s41388-018-0331-z
 107. Nitiss JL. Targeting DNA Topoisomerase II in Cancer Chemotherapy. *Nat Rev Cancer* (2009) 9(5):338–50. doi: 10.1038/nrc2607
 108. Zhang P, Wang H, Rowe PS, Hu B, Wang Y. MEPE/OF45 as a New Target for Sensitizing Human Tumour Cells to DNA Damage Inducers. *Br J Cancer* (2010) 102(5):862–6. doi: 10.1038/sj.bjc.6605572
 109. Harbour JW, Luo RX, Dei SA, Postigo AA, Dean DC. Cdk Phosphorylation Triggers Sequential Intramolecular Interactions That Progressively Block Rb Functions as Cells Move Through G1. *Cell* (1999) 98(6):859–69. doi: 10.1016/s0092-8674(00)81519-6
 110. Musgrove EA, Caldon CE, Barraclough J, Stone A, Sutherland RL. Cyclin D as a Therapeutic Target in Cancer. *Nat Rev Cancer* (2011) 11(8):558–72. doi: 10.1038/nrc3090
 111. Fan HN, Zhu MY, Peng SQ, Zhu JS, Zhang J, Qu GQ. Dihydroartemisinin Inhibits the Growth and Invasion of Gastric Cancer Cells by Regulating Cyclin D1-CDK4-Rb Signaling. *Pathol Res Pract* (2020) 216(2):152795. doi: 10.1016/j.prp.2019.152795
 112. Guan X, Guan Y. Artemisinin Induces Selective and Potent Anticancer Effects in Drug Resistant Breast Cancer Cells by Inducing Cellular Apoptosis and Autophagy and G2/M Cell Cycle Arrest. *J Buon* (2020) 25(3):1330–6.
 113. Dixon SJ, Lemberg KM, Lamprecht MR, Skouta R, Zaitsev EM, Gleason CE, et al. Ferroptosis: An Iron-Dependent Form of Nonapoptotic Cell Death. *Cell* (2012) 149(5):1060–72. doi: 10.1016/j.cell.2012.03.042
 114. Gao M, Monian P, Quadri N, Ramasamy R, Jiang X. Glutaminolysis and Transferrin Regulate Ferroptosis. *Mol Cell* (2015) 59(2):298–308. doi: 10.1016/j.molcel.2015.06.011
 115. Stockwell BR, Friedmann AJ, Bayir H, Bush AI, Conrad M, Dixon SJ, et al. Ferroptosis: A Regulated Cell Death Nexus Linking Metabolism, Redox Biology, and Disease. *Cell* (2017) 171(2):273–85. doi: 10.1016/j.cell.2017.09.021
 116. Yang WS, SriRamaratnam R, Welsch ME, Shimada K, Skouta R, Viswanathan VS, et al. Regulation of Ferroptotic Cancer Cell Death by GPX4. *Cell* (2014) 156(1–2):317–31. doi: 10.1016/j.cell.2013.12.010
 117. Ooko E, Saeed ME, Kadioglu O, Sarvi S, Colak M, Elmasaoudi K, et al. Artemisinin Derivatives Induce Iron-Dependent Cell Death (Ferroptosis) in Tumor Cells. *Phytomedicine* (2015) 22(11):1045–54. doi: 10.1016/j.phymed.2015.08.002
 118. Chen GQ, Benthani FA, Wu J, Liang D, Bian ZX, Jiang X. Artemisinin Compounds Sensitize Cancer Cells to Ferroptosis by Regulating Iron Homeostasis. *Cell Death Differ* (2020) 27(1):242–54. doi: 10.1038/s41418-019-0352-3
 119. Wang K, Zhang Z, Wang M, Cao X, Qi J, Wang D, et al. Role of GRP78 Inhibiting Artesunate-Induced Ferroptosis in KRAS Mutant Pancreatic Cancer Cells. *Drug Des Devel Ther* (2019) 13:2135–44. doi: 10.2147/DDDT.S199459
 120. Chen Y, Mi Y, Zhang X, Ma Q, Song Y, Zhang L, et al. Dihydroartemisinin-Induced Unfolded Protein Response Feedback Attenuates Ferroptosis Via PERK/ATF4/HSPA5 Pathway in Glioma Cells. *J Exp Clin Cancer Res* (2019) 38(1):402. doi: 10.1186/s13046-019-1413-7
 121. Paccez JD, Duncan K, Sekar D, Correa RG, Wang Y, Gu X, et al. Dihydroartemisinin Inhibits Prostate Cancer Via JARID2/miR-7/miR-34a-dependent Downregulation of Axl. *Oncogenesis* (2019) 8(3):14. doi: 10.1038/s41389-019-0122-6
 122. Chen S, Gan S, Han L, Li X, Xie X, Zou D, et al. Artesunate Induces Apoptosis and Inhibits the Proliferation, Stemness, and Tumorigenesis of Leukemia. *Ann Transl Med* (2020) 8(12):767. doi: 10.21037/atm-20-4558
 123. Li Z, Zhu YT, Xiang M, Qiu JL, Luo SQ, Lin F. Enhanced Lysosomal Function is Critical for Paclitaxel Resistance in Cancer Cells: Reversed by Artesunate. *Acta Pharmacol Sin* (2020) 42(4):624–32. doi: 10.1038/s41401-020-0445-z
 124. Pirali M, Taheri M, Zarei S, Majidi M, Ghafouri H. Artesunate, as a HSP70 Atpase Activity Inhibitor, Induces Apoptosis in Breast Cancer Cells. *Int J Biol Macromol* (2020) 164:3369–75. doi: 10.1016/j.ijbiomac.2020.08.198
 125. Zhao F, Vakhursheva O, Markowitsch SD, Slade KS, Tsaur I, Cinatl JJ, et al. Artesunate Impairs Growth in Cisplatin-Resistant Bladder Cancer Cells by Cell Cycle Arrest, Apoptosis and Autophagy Induction. *Cells-Basel* (2020) 9(12):2643. doi: 10.3390/cells9122643
 126. Zhou X, Zijlstra SN, Soto-Gamez A, Sotrikromo R, Quax WJ. Artemisinin Derivatives Stimulate DR5-Specific Trail-Induced Apoptosis by Regulating Wildtype P53. *Cancers (Basel)* (2020) 12(9):2514. doi: 10.3390/cancers12092514
 127. Zhou X, Chen Y, Wang F, Wu H, Zhang Y, Liu J, et al. Artesunate Induces Autophagy Dependent Apoptosis Through Upregulating ROS and Activating AMPK-mTOR-ULK1 Axis in Human Bladder Cancer Cells. *Chem Biol Interact* (2020) 331:109273. doi: 10.1016/j.cbi.2020.109273
 128. Yan X, Li P, Zhan Y, Qi M, Liu J, An Z, et al. Dihydroartemisinin Suppresses STAT3 Signaling and Mcl-1 and Survivin Expression to Potentiate ABT-263-induced Apoptosis in Non-small Cell Lung Cancer Cells Harboring EGFR or RAS Mutation. *Biochem Pharmacol* (2018) 150:72–85. doi: 10.1016/j.bcp.2018.01.031
 129. Vatsveen TK, Myhre MR, Steen CB, Wälchli S, Lingjærde OC, Bai B, et al. Artesunate Shows Potent Anti-Tumor Activity in B-cell Lymphoma. *J Hematol Oncol* (2018) 11(1):23. doi: 10.1186/s13045-018-0561-0
 130. Zhou C, Tang X, Xu J, Wang J, Yang Y, Chen Y, et al. Opening of the CLC-3 Chloride Channel Induced by Dihydroartemisinin Contributed to Early Apoptotic Events in Human Poorly Differentiated Nasopharyngeal Carcinoma Cells. *J Cell Biochem* (2018) 119(11):9560–72. doi: 10.1002/jcb.27274
 131. Liu X, Wu J, Fan M, Shen C, Dai W, Bao Y, et al. Novel Dihydroartemisinin Derivative DHA-37 Induces Autophagic Cell Death Through Upregulation of HMGB1 in A549 Cells. *Cell Death Dis* (2018) 9(11):1048. doi: 10.1038/s41419-018-1006-y
 132. Chen X, Wong YK, Lim TK, Lim WH, Lin Q, Wang J, et al. Artesunate Activates the Intrinsic Apoptosis of HCT116 Cells Through the Suppression of Fatty Acid Synthesis and the NF- κ B Pathway. *Molecules* (2017) 22(8):1272. doi: 10.3390/molecules22081272
 133. Nunes JJ, Pandey SK, Yadav A, Goel S, Ateeq B. Targeting NF-Kappa B Signaling by Artesunate Restores Sensitivity of Castrate-Resistant Prostate Cancer Cells to Antiandrogens. *Neoplasia* (2017) 19(4):333–45. doi: 10.1016/j.neo.2017.02.002
 134. Houh YK, Kim KE, Park S, Hur DY, Kim S, Kim D, et al. The Effects of Artemisinin on the Cytolytic Activity of Natural Killer (Nk) Cells. *Int J Mol Sci* (2017) 18(7):1600. doi: 10.3390/ijms18071600

135. Lu Z, Bi J, Wan X. Artemisinin Sensitizes Tumor Cells to NK Cell-Mediated Cytolysis. *Biochem Biophys Res Commun* (2020) 524(2):418–23. doi: 10.1016/j.bbrc.2020.01.094
136. Farsam V, Hassan ZM, Zavarán-Hosseini A, Noori S, Mahdavi M, Ranjbar M. Antitumor and Immunomodulatory Properties of Artemether and its Ability to Reduce CD4+ CD25+ Foxp3+ T Reg Cells In Vivo. *Int Immunopharmacol* (2011) 11(11):1802–8. doi: 10.1016/j.intimp.2011.07.008
137. Cao Y, Feng YH, Gao LW, Li XY, Jin QX, Wang YY, et al. Artemisinin Enhances the Anti-Tumor Immune Response in 4T1 Breast Cancer Cells In Vitro and In Vivo. *Int Immunopharmacol* (2019) 70:110–6. doi: 10.1016/j.intimp.2019.01.041
138. Berger TG, Dieckmann D, Efferth T, Schultz ES, Funk JO, Baur A, et al. Artesunate in the Treatment of Metastatic Uveal Melanoma—First Experiences. *Oncol Rep* (2005) 14(6):1599–603. doi: 10.3892/or.14.6.1599
139. Deeken JF, Wang H, Hartley M, Cheema AK, Smaglo B, Hwang JJ, et al. A Phase I Study of Intravenous Artesunate in Patients With Advanced Solid Tumor Malignancies. *Cancer Chemother Pharmacol* (2018) 81(3):587–96. doi: 10.1007/s00280-018-3533-8
140. Milner DJ. Malaria Pathogenesis. *Cold Spring Harb Perspect Med* (2018) 8(1):a025569. doi: 10.1101/cshperspect.a025569
141. Nixon GL, Moss DM, Shone AE, Laloo DG, Fisher N, O'Neill PM, et al. Antimalarial Pharmacology and Therapeutics of Atovaquone. *J Antimicrob Chemother* (2013) 68(5):977–85. doi: 10.1093/jac/dks504
142. Watkins WM. Pharmacology and Pharmacokinetics of New Antimalarials. *Med Trop (Mars)* (1995) 55(4 Suppl):33–6.
143. Commons RJ, Simpson JA, Thriemer K, Humphreys GS, Abreha T, Alemu SG, et al. The Effect of Chloroquine Dose and Primaquine on Plasmodium Vivax Recurrence: A WorldWide Antimalarial Resistance Network Systematic Review and Individual Patient Pooled Meta-Analysis. *Lancet Infect Dis* (2018) 18(9):1025–34. doi: 10.1016/S1473-3099(18)30348-7
144. Skrzypek R, Callaghan R. The “Pushmi-Pullu” of Resistance to Chloroquine in Malaria. *Essays Biochem* (2017) 61(1):167–75. doi: 10.1042/EBC20160060
145. Thomé R, Lopes SC, Costa FT, Verinaud L. Chloroquine: Modes of Action of an Undervalued Drug. *Immunol Lett* (2013) 153(1–2):50–7. doi: 10.1016/j.imlet.2013.07.004
146. Aguiar A, Murce E, Cortopassi WA, Pimentel AS, Almeida M, Barros D, et al. Chloroquine Analogs as Antimalarial Candidates With Potent In Vitro and In Vivo Activity. *Int J Parasitol Drugs Drug Resist* (2018) 8(3):459–64. doi: 10.1016/j.ijpddr.2018.10.002
147. Pasquier B. Autophagy Inhibitors. *Cell Mol Life Sci* (2016) 73(5):985–1001. doi: 10.1007/s00018-015-2104-y
148. Mindell JA. Lysosomal Acidification Mechanisms. *Annu Rev Physiol* (2012) 74:69–86. doi: 10.1146/annurev-physiol-012110-142317
149. Martinez GP, Zabaleta ME, Di Giulio C, Charris JE, Mijares MR. The Role of Chloroquine and Hydroxychloroquine in Immune Regulation and Diseases. *Curr Pharm Des* (2020) 26(35):4467–85. doi: 10.2174/1381612826666200707132920
150. Amaravadi RK, Lippincott-Schwartz J, Yin XM, Weiss WA, Takebe N, Timmer W, et al. Principles and Current Strategies for Targeting Autophagy for Cancer Treatment. *Clin Cancer Res* (2011) 17(4):654–66. doi: 10.1158/1078-0432.CCR-10-2634
151. Cortegiani A, Ingoglia G, Ippolito M, Giarratano A, Einav S. A Systematic Review on the Efficacy and Safety of Chloroquine for the Treatment of COVID-19. *J Crit Care* (2020) 57:279–83. doi: 10.1016/j.jcrc.2020.03.005
152. Pascolo S. Time to Use a Dose of Chloroquine as an Adjuvant to Anti-Cancer Chemotherapies. *Eur J Pharmacol* (2016) 771:139–44. doi: 10.1016/j.ejphar.2015.12.017
153. Kaneno R, Shurin GV, Kaneno FM, Naiditch H, Luo J, Shurin MR. Chemotherapeutic Agents in Low Noncytotoxic Concentrations Increase Immunogenicity of Human Colon Cancer Cells. *Cell Oncol (Dordr)* (2011) 34(2):97–106. doi: 10.1007/s13402-010-0005-5
154. Zitvogel L, Apetoh L, Ghiringhelli F, Kroemer G. Immunological Aspects of Cancer Chemotherapy. *Nat Rev Immunol* (2008) 8(1):59–73. doi: 10.1038/nri2216
155. Zitvogel L, Kroemer G. Anticancer Immunotherapy Using Adjuvants With Direct Cytotoxic Effects. *J Clin Invest* (2009) 119(8):2127–30. doi: 10.1172/JCI39991
156. Vanmeerbeek I, Sprooten J, De Ruyscher D, Tejpar S, Vandenbergh P, Fucikova J, et al. Trial Watch: Chemotherapy-Induced Immunogenic Cell Death in Immuno-Oncology. *Oncoimmunology* (2020) 9(1):1703449. doi: 10.1080/2162402X.2019.1703449
157. Kaneno R, Shurin GV, Tourkova IL, Shurin MR. Chemomodulation of Human Dendritic Cell Function by Antineoplastic Agents in Low Noncytotoxic Concentrations. *J Transl Med* (2009) 7:58. doi: 10.1186/1479-5876-7-58
158. Zamame RJ, Romagnoli GG, Falasco BF, Gorgulho CM, Sanzochi FC, Dos SD, et al. Blocking Drug-Induced Autophagy With Chloroquine in HCT-116 Colon Cancer Cells Enhances DC Maturation and T Cell Responses Induced by Tumor Cell Lysate. *Int Immunopharmacol* (2020) 84:106495. doi: 10.1016/j.intimp.2020.106495
159. Kim S, Han Y, Kim SI, Kim SJ, Song YS. Tumor Evolution and Chemoresistance in Ovarian Cancer. *NPJ Precis Oncol* (2018) 2:20. doi: 10.1038/s41698-018-0063-0
160. Sakthivel KM, Hariharan S. Regulatory Players of DNA Damage Repair Mechanisms: Role in Cancer Chemoresistance. *BioMed Pharmacother* (2017) 93:1238–45. doi: 10.1016/j.biopha.2017.07.035
161. Nagel ZD, Kitange GJ, Gupta SK, Joughin BA, Chaim IA, Mazzucato P, et al. Dna Repair Capacity in Multiple Pathways Predicts Chemoresistance in Glioblastoma Multiforme. *Cancer Res* (2017) 77(1):198–206. doi: 10.1158/0008-5472.CAN-16-1151
162. Hwang JR, Kim WY, Cho YJ, Ryu JY, Choi JJ, Jeong SY, et al. Chloroquine Reverses Chemoresistance Via Upregulation of p21(WAF1/CIP1) and Autophagy Inhibition in Ovarian Cancer. *Cell Death Dis* (2020) 11(12):1034. doi: 10.1038/s41419-020-03242-x
163. Yue D, Zhang D, Shi X, Liu S, Li A, Wang D, et al. Chloroquine Inhibits Stemness of Esophageal Squamous Cell Carcinoma Cells Through Targeting Cxcr4-STAT3 Pathway. *Front Oncol* (2020) 10:311. doi: 10.3389/fonc.2020.00311
164. Varisli L, Cen O, Vlahopoulos S. Dissecting Pharmacological Effects of Chloroquine in Cancer Treatment: Interference With Inflammatory Signaling Pathways. *Immunology* (2020) 159(3):257–78. doi: 10.1111/imm.13160
165. Compter I, Eekers D, Hoeben A, Rouschop K, Reymen B, Ackermans L, et al. Chloroquine Combined With Concurrent Radiotherapy and Temozolomide for Newly Diagnosed Glioblastoma: A Phase IB Trial. *Autophagy* (2020), 1–9. doi: 10.1080/15548627.2020.1816343
166. Zhou W, Wang H, Yang Y, Chen ZS, Zou C, Zhang J. Chloroquine Against Malaria, Cancers and Viral Diseases. *Drug Discovery Today* (2020) 25(11):2012–22. doi: 10.1016/j.drudis.2020.09.010
167. Lagadinou ED, Sach A, Callahan K, Rossi RM, Neering SJ, Minhajuddin M, et al. BCL-2 Inhibition Targets Oxidative Phosphorylation and Selectively Eradicates Quiescent Human Leukemia Stem Cells. *Cell Stem Cell* (2013) 12(3):329–41. doi: 10.1016/j.stem.2012.12.013
168. Miranda S, Foncea R, Guerrero J, Leighton F. Oxidative Stress and Upregulation of Mitochondrial Biogenesis Genes in Mitochondrial DNA-depleted HeLa Cells. *Biochem Biophys Res Commun* (1999) 258(1):44–9. doi: 10.1006/bbrc.1999.0580
169. Tian S, Chen H, Tan W. Targeting Mitochondrial Respiration as a Therapeutic Strategy for Cervical Cancer. *Biochem Biophys Res Commun* (2018) 499(4):1019–24. doi: 10.1016/j.bbrc.2018.04.042
170. Wang D, Xue B, Ohulchanskyy TY, Liu Y, Yakovlev A, Ziniuk R, et al. Inhibiting Tumor Oxygen Metabolism and Simultaneously Generating Oxygen by Intelligent Upconversion Nanotherapeutics for Enhanced Photodynamic Therapy. *Biomaterials* (2020) 251:120088. doi: 10.1016/j.biomaterials.2020.120088
171. Agostinis P, Berg K, Cengel KA, Foster TH, Girotti AW, Gollnick SO, et al. Photodynamic Therapy of Cancer: An Update. *CA Cancer J Clin* (2011) 61(4):250–81. doi: 10.3322/caac.20114
172. Li XY, Tan LC, Dong LW, Zhang WQ, Shen XX, Lu X, et al. Susceptibility and Resistance Mechanisms During Photodynamic Therapy of Melanoma. *Front Oncol* (2020) 10:597. doi: 10.3389/fonc.2020.00597
173. Chen D, Sun X, Zhang X, Cao J. Targeting Mitochondria by Anthelmintic Drug Atovaquone Sensitizes Renal Cell Carcinoma to Chemotherapy and Immunotherapy. *J Biochem Mol Toxicol* (2018) 32(9):e22195. doi: 10.1002/jbt.22195

174. Ashton TM, Fokas E, Kunz-Schughart LA, Folkes LK, Anbalagan S, Huether M, et al. The Anti-Malarial Atovaquone Increases Radiosensitivity by Alleviating Tumour Hypoxia. *Nat Commun* (2016) 7:12308. doi: 10.1038/ncomms12308
175. Fiorillo M, Lamb R, Tanowitz HB, Mutti L, Krstic-Demonacos M, Cappello AR, et al. Repurposing Atovaquone: Targeting Mitochondrial Complex III and OXPHOS to Eradicate Cancer Stem Cells. *Oncotarget* (2016) 7 (23):34084–99. doi: 10.18632/oncotarget.9122
176. Lv Z, Yan X, Lu L, Su C, He Y. Atovaquone Enhances Doxorubicin's Efficacy Via Inhibiting Mitochondrial Respiration and STAT3 in Aggressive Thyroid Cancer. *J Bioenerg Biomembr* (2018) 50(4):263–70. doi: 10.1007/s10863-018-9755-y
177. Takabe H, Warnken ZN, Zhang Y, Davis DA, Smyth H, Kuhn JG, et al. A Repurposed Drug for Brain Cancer: Enhanced Atovaquone Amorphous Solid Dispersion by Combining a Spontaneously Emulsifying Component With a Polymer Carrier. *Pharmaceutics* (2018) 10(2):60. doi: 10.3390/pharmaceutics10020060
178. Xiang M, Kim H, Ho VT, Walker SR, Bar-Natan M, Anahtar M, et al. Gene Expression-Based Discovery of Atovaquone as a STAT3 Inhibitor and Anticancer Agent. *Blood* (2016) 128(14):1845–53. doi: 10.1182/blood-2015-07-660506
179. Ashton TM, McKenna WG, Kunz-Schughart LA, Higgins GS. Oxidative Phosphorylation as an Emerging Target in Cancer Therapy. *Clin Cancer Res* (2018) 24(11):2482–90. doi: 10.1158/1078-0432.CCR-17-3070
180. Gupta N, Srivastava SK. Atovaquone: An Antiprotozoal Drug Suppresses Primary and Resistant Breast Tumor Growth by Inhibiting Her2/β-Catenin Signaling. *Mol Cancer Ther* (2019) 18(10):1708–20. doi: 10.1158/1535-7163.MCT-18-1286
181. Gao X, Liu X, Shan W, Liu Q, Wang C, Zheng J, et al. Anti-Malarial Atovaquone Exhibits Anti-Tumor Effects by Inducing DNA Damage in Hepatocellular Carcinoma. *Am J Cancer Res* (2018) 8(9):1697–711.
182. Rijpmma SR, van den Heuvel JJ, van der Velden M, Sauerwein RW, Russel FG, Koenderink JB. Atovaquone and Quinine Anti-Malarials Inhibit ATP Binding Cassette Transporter Activity. *Malar J* (2014) 13:359. doi: 10.1186/1475-2875-13-359
183. Ashburn TT, Thor KB. Drug Repositioning: Identifying and Developing New Uses for Existing Drugs. *Nat Rev Drug Discovery* (2004) 3(8):673–83. doi: 10.1038/nrd1468
184. Langedijk J, Mantel-Teeuwisse AK, Slijkerman DS, Schutjens MH. Drug Repositioning and Repurposing: Terminology and Definitions in Literature. *Drug Discovery Today* (2015) 20(8):1027–34. doi: 10.1016/j.drudis.2015.05.001
185. Juarez M, Scholnik-Cabrera A, Dueñas-Gonzalez A. The Multitargeted Drug Ivermectin: From an Antiparasitic Agent to a Repositioned Cancer Drug. *Am J Cancer Res* (2018) 8(2):317–31.
186. Hirschhorn T, Stockwell BR. The Development of the Concept of Ferroptosis. *Free Radic Biol Med* (2019) 133:130–43. doi: 10.1016/j.freeradbiomed.2018.09.043
187. Ayyagari VN, Hsieh TJ, Diaz-Sylvester PL, Brard L. Evaluation of the Cytotoxicity of the Bithionol - Cisplatin Combination in a Panel of Human Ovarian Cancer Cell Lines. *BMC Cancer* (2017) 17(1):49. doi: 10.1186/s12885-016-3034-2
188. Gao A, Wang X, Xiang W, Liang H, Gao J, Yan Y. Reversal of P-glycoprotein-mediated Multidrug Resistance In Vitro by Doramectin and Nemalectin. *J Pharm Pharmacol* (2010) 62(3):393–9. doi: 10.1211/jpp.62.03.0016
189. Wu ZH, Lu MK, Hu LY, Li X. Praziquantel Synergistically Enhances Paclitaxel Efficacy to Inhibit Cancer Cell Growth. *PLoS One* (2012) 7(12):e51721. doi: 10.1371/journal.pone.0051721
190. Moschovi M, Critselis E, Cen O, Adamaki M, Lambrou GI, Chrousos GP, et al. Drugs Acting on Homeostasis: Challenging Cancer Cell Adaptation. *Expert Rev Anticancer Ther* (2015) 15(12):1405–17. doi: 10.1586/14737140.2015.1095095
191. Vlahopoulos SA. Aberrant Control of NF-κB in Cancer Permits Transcriptional and Phenotypic Plasticity, to Curtail Dependence on Host Tissue: Molecular Mode. *Cancer Biol Med* (2017) 14(3):254–70. doi: 10.20892/j.issn.2095-3941.2017.0029
192. Hettiarachchi G, Samanta SK, Falcinelli S, Zhang B, Moncelet D, Isaacs L, et al. Acyclic Cucurbit[n]uril-Type Molecular Container Enables Systemic Delivery of Effective Doses of Albendazole for Treatment of SK-OV-3 Xenograft Tumors. *Mol Pharm* (2016) 13(3):809–18. doi: 10.1021/acs.molpharmaceut.5b00723
193. Akbarian A, Ebtekar M, Pakravan N, Hassan ZM. Folate Receptor Alpha Targeted Delivery of Artemether to Breast Cancer Cells With Folate-Decorated Human Serum Albumin Nanoparticles. *Int J Biol Macromol* (2020) 152:90–101. doi: 10.1016/j.ijbiomac.2020.02.106
194. Yang B, Shi J. Developing New Cancer Nanomedicines by Repurposing Old Drugs. *Angew Chem Int Ed Engl* (2020) 59(49):21829–38. doi: 10.1002/anie.202004317
195. Chen J, Jiang Z, Xu W, Sun T, Zhuang X, Ding J, et al. Spatiotemporally Targeted Nanomedicine Overcomes Hypoxia-Induced Drug Resistance of Tumor Cells After Disrupting Neovasculature. *Nano Lett* (2020) 20(8):6191–8. doi: 10.1021/acs.nanolett.0c02515
196. Wei L, Chen J, Ding J. Sequentially Stimuli-Responsive Anticancer Nanomedicines. *Nanomed (Lond)* (2021) 16(4):261–4. doi: 10.2217/nmm-2021-0019
197. Feng X, Xu W, Xu X, Li G, Ding J, Chen X. Cystine Proportion Regulates Fate of Polypeptide Nanogel as Nanocarrier for Chemotherapeutics. *Sci China Chem* (2021) 64(2):293–301. doi: 10.1007/s11426-020-9884-6
198. Ding J, Chen J, Gao L, Jiang Z, Zhang Y, Li M, et al. Engineered Nanomedicines With Enhanced Tumor Penetration. *Nano Today* (2019) 29:100800. doi: 10.1016/j.nantod.2019.100800
199. Zheng P, Ding B, Jiang Z, Xu W, Li G, Ding J, et al. Ultrasound-Augmented Mitochondrial Calcium Ion Overload by Calcium Nanomodulator to Induce Immunogenic Cell Death. *Nano Lett* (2021) 21(5):2088–93. doi: 10.1021/acs.nanolett.0c04778
200. Ma W, Chen Q, Xu W, Yu M, Yang Y, Zou B, et al. Self-Targeting Visualizable Hyaluronate Nanogel for Synchronized Intracellular Release of Doxorubicin and Cisplatin in Combating Multidrug-Resistant Breast Cancer. *Nano Res* (2021) 14(3):846–57. doi: 10.1007/s12274-020-3124-y
201. Liu J, Li Z, Zhao D, Feng X, Wang C, Li D, et al. Immunogenic Cell Death-Inducing Chemotherapeutic Nanoformulations Potentiate Combination Chemoimmunotherapy. *Mater Design* (2021) 202:109465. doi: 10.1016/j.matdes.2021.109465
202. Feng X, Xu W, Liu J, Li D, Li G, Ding J, et al. Polypeptide Nanoformulation-Induced Immunogenic Cell Death and Remission of Immunosuppression for Enhanced Chemoimmunotherapy. *Sci Bull* (2021) 66(4):362–73. doi: 10.1016/j.scib.2020.07.013

Conflict of Interest: The authors declare that the research was conducted in the absence of any commercial or financial relationships that could be construed as a potential conflict of interest.

Copyright © 2021 Li, Zheng, Liu, Lu, Zhou, Zhang, Zheng and Dai. This is an open-access article distributed under the terms of the Creative Commons Attribution License (CC BY). The use, distribution or reproduction in other forums is permitted, provided the original author(s) and the copyright owner(s) are credited and that the original publication in this journal is cited, in accordance with accepted academic practice. No use, distribution or reproduction is permitted which does not comply with these terms.



Vitamin D: Possible Therapeutic Roles in Hepatocellular Carcinoma

Isaacson B. Adelani^{1*}, Oluwakemi A. Rotimi¹, Emmanuel N. Maduagwu² and Solomon O. Rotimi¹

¹ Department of Biochemistry, Covenant University, Ota, Nigeria, ² Department of Biochemistry, Chrisland University, Abeokuta, Nigeria

OPEN ACCESS

Edited by:

Jiang-Jiang Qin,
Institute of Cancer and Basic
Medicine, Chinese Academy of
Sciences (CAS), China

Reviewed by:

Dandan Lin,
The First Affiliated Hospital of
Soochow University, China
Hung-Wen Tsai,
National Cheng Kung University,
Taiwan
Yan Sun,
Sun Yat-Sen University, China
Claudia Pivonello,
University of Naples Federico II,
Italy

*Correspondence:

Isaacson B. Adelani
isaacson909@gmail.com;
bababode.adelani@
covenantuniversity.edu.ng

Specialty section:

This article was submitted to
Pharmacology of Anti-Cancer Drugs,
a section of the journal
Frontiers in Oncology

Received: 17 December 2020

Accepted: 06 April 2021

Published: 25 May 2021

Citation:

Adelani IB, Rotimi OA, Maduagwu EN
and Rotimi SO (2021) Vitamin D:
Possible Therapeutic Roles in
Hepatocellular Carcinoma.
Front. Oncol. 11:642653.
doi: 10.3389/fonc.2021.642653

Hepatocellular carcinoma (HCC) is a unique type of liver cancer instigated by underlying liver diseases. Pre-clinical evidence suggests that HCC progression, like other cancers, could be aided by vitamin D deficiency. Vitamin D is a lipid-soluble hormone usually obtained through sunlight. Vitamin D elucidates its biological responses by binding the vitamin D receptor; thus, promoting skeletal mineralization, and maintain calcium homeostasis. Other reported Vitamin D functions include specific roles in proliferation, angiogenesis, apoptosis, inflammation, and cell differentiation. This review highlighted studies on vitamin D's functional roles in HCC and discussed the specific therapeutic targets from various *in vivo*, *in vitro* and clinical studies over the years. Furthermore, it described recent advancements in vitamin D's anticancer effects and its metabolizing enzymes' roles in HCC development. In summary, the review elucidated specific vitamin D-associated target genes that play critical functions in the inhibition of tumorigenesis through inflammation, oxidative stress, invasion, and apoptosis in HCC progression.

Keywords: vitamin D, therapeutic, inflammation, apoptosis, differentiation, proliferation, hepatocellular carcinoma

INTRODUCTION

Hepatocellular carcinoma (HCC) is a unique type of liver cancer instigated by underlying liver diseases. In general, liver cancer constitutes a substantial public health problem that ranks as the sixth most commonly diagnosed cancer and the third most common cause of cancer-related mortality in 2020 (1). Although liver cancer occurs in both genders, the incidence and mortality rates in males are 2 to 3 times higher than in females (1). The loss of the liver's regenerative ability exacerbates HCC progression, which subsequently potentiates organ failure (2). This loss of regenerative capacity is further compounded by the disruption of various pathways associated with the pathogenesis and progression of HCC, thereby making HCC an outcome of a complex cascade of events (3). Furthermore, the increasing incidence of HCC is mainly associated with viral infections, including hepatitis B (HBV) and C viruses (HCV), as well as other risk factors like non-alcoholic fatty liver disease (4, 5) and mycotoxin exposure (6–9). Aside from these biotic, lifestyle, and environmental factors, pre-clinical evidence suggests that HCC progression, like many other cancers, could be facilitated by vitamin D (VD) deficiency and germline genetic variants in the Vitamin D receptor (VDR) gene, which has been shown to influence the progression of hepatitis to HCC (10, 11). Also, an epidemiological study showed that increased maternal ultraviolet (UV) exposure is associated with a reduced risk of hepatoblastoma in offspring (12). Additionally, evidence from the SEER data showed

that the incidence of HCC in the United States is associated with ambient UV exposure (13). Hence, this premise supports the VD - cancer hypothesis and further augments the roles of vitamin D metabolism in hepatocellular carcinogenesis (2).

Vitamin D (VD) is a lipid-soluble hormone usually obtained through the exposure of skin to sunlight. Several factors, including skin pigmentation and a modern lifestyle, could limit VD formation, thus causing VD deficiency (14). In VD synthesis, sunlight UV (B) (280–315 nm) exposure on the skin activates 7-dehydrocholesterol to pre-vitamin D₃ and eventually cholecalciferol (VD₃) (2). Similarly, UV (B) exposure to ergosterol in plants and fungi produces another form of vitamin D, ergocalciferol (VD₂) (15). Besides from the endogenous synthesis of VD, VD₃ can also be obtained from diets while VD₂ is principally used during vitamin D fortification. Both forms of VD are naturally inactive and are activated *via* hydroxylation. After synthesis, VD binding protein (DBP) binds VD and transports it to the liver, where hydroxylation at carbon-25 metabolizes VD to 25-hydroxyvitamin D (25(OH)D) through 25-hydroxylase. In this first phase of VD metabolism, hydroxylation occurs predominantly in the hepatic cells although extrahepatic VD hydroxylation reportedly occurs in other tissues with evident 25-hydroxylase activities (16, 17). Most importantly, during this first hydroxylation step, an ubiquitous mitochondrial 25-hydroxylase, CYP27A1 does not hydroxylate VD₂ whereas, CYP2R1 usually located in the liver and testes hydroxylates both forms of VD (15). Equally, Zhu et al. (18) reported CYP2R1 as a major but not the only 25-hydroxylase. After the first hydroxylation, the glomerulus filters 25(OH)D transported into the kidney and converts it to a steroid hormone (the active form of VD), 1 α , 25 (OH)₂D (calcitriol), through 25(OH)D-1 α -hydroxylase (19). This metabolic activity in the kidney signifies the second stage of VD hydroxylation. Although 1 α -hydroxylation occurs predominantly in the kidney, peripheral tissues including the skin and lymph nodes exhibit extra-renal production of the steroid hormone (20). Finally, in a bid to activate VD's biological response to regulate gene expression, calcitriol binds VDR (17) in a binding sequence that allows the effective functioning of retinoid X (RXR). RXR belongs to the nuclear receptor family and a member of the steroid/thyroid hormone, primarily functioning as transcription factors (21). RXR also plays essential roles in metabolism and cell differentiation (21). Hence, VD binding enables the VDR - RXR interaction, leading to VD-related functions through gene transcription (22). Thus, VD's biological action is dependent on VDR, RXR, and the availability of VD (23).

Asides from primary functions, which include promoting skeletal mineralization and maintenance of calcium homeostasis, VD performs pro-apoptotic, pro-differentiation, anti-angiogenic, anti-proliferative, anti-invasive, and anti-metastatic functions (24). Reports show that VD is an indicator of HCC prognosis and could be vital in predicting HCC patients' mortality (25). Meanwhile, VD deficiency is fast becoming a global public health challenge (26), and it is continuously associated with an 'all-cause and cause-specific mortality, despite differences in the VD baseline levels across the world (27, 28). Consequently, there are

pieces of evidence showing connections between VD deficiency and HCC progression. For instance, Gaksch et al. (29) meta-analysis proposed an inverse relationship between serum VD (25(OH)D₃) level and HCC risk; thereby, suggesting VD's prospective therapeutic ability in managing HCC. Moreover, increased bioavailability of circulating 25(OH)D₃ was also associated with HCC survival as against total or free VD level (30). In contrast, Liu et al. (31) reported that increased 25(OH)D level was associated with an increased risk of HCC incidence. However, they observed that genetic variations related to VD metabolism could influence HCC tumor response, survival, and mortality.

Despite the reported association with HCC development, contrasting reports suggest that baseline VD level could play little or no role in cirrhosis-linked HCC (32). Therefore, this review highlights the *in vivo*, *in vitro*, and clinical studies on VD therapeutic targets in HCC. Furthermore, it discussed the significant limitations and possible solutions in using VD as therapeutics.

VD, VDR, AND HCC PATHOLOGICAL CONDITIONS

The progression of HCC and pathological conditions like liver cirrhosis are linked to VD deficiency; hence, suggesting that decreased 25(OH)D is associated with poor liver disease prognosis (33). According to Berkan-Kawińska et al. (34) and Yang et al. (35), patients with liver cirrhosis, HBV, and HCV have decreased 25(OH)D levels and could benefit from VD supplementation. VD deficiency has also been linked with infections in patients with HCV-associated liver cirrhosis (36) and the VD deficiency-associated polymorphisms, like rs1993116, rs10741657, rs2282679, rs7944926, and rs12785878, linked with HCV-related HCC (37). This study by Lange et al. (37) also showed that reduced 25(OH)D₃ levels in HCV-related HCC patients is associated with genetic variations of CYP2R1, GC, and DHCR7. While the circulating form of VD (25(OH)D₃) instigates the hormone's anti-HCV capacity (38), the active form of VD (1 α , 25 (OH)₂D₃) induces CYP24A1 expression in a VDR-dependent manner. However, VDR expression, repressed by HBV transcript upregulation, affects VD's binding to the receptor (39). Also, chronic HBV patients are at a higher risk of increased VD deficiency (40).

HCV and HCV-related HCC patients had lower levels of VD and VDR compared to healthy individuals (41). In the same vein, Falletti et al. (42) reported that VDR polymorphisms are associated with the occurrence of HCC in liver cirrhosis patients, specifically in those with alcoholic etiology. In the study, HCC was linked with the b allele of the BsmI A>G (B/b) polymorphism and the T allele of the TaqI T>C (T/t) polymorphism (42). Several studies have reported relationships between VDR polymorphisms and HCC pathological conditions. In a Chinese population hospital-based case-control study, VDR rs2228570 and DBP rs7041 polymorphisms vary between HBV-related HCC patients and healthy individuals thus, suggesting a relationship with increased risk of HBV-related HCC (11). A meta-analysis strengthened these observations, which

indicated that VDR rs7975232 and rs2228570 polymorphisms are associated with HCC (43).

Although a non-association of VDR polymorphism and risk of HBV infection in Vietnamese HBV patients was reported by Hoan et al. (44), they suggested that ApaI VDR polymorphism (rs7975232) could be associated with clinical outcomes and disease progression. Incidentally, ApaI VDR polymorphism was shown to be associated with HCC in HCV-cirrhotic patients (45). On the contrary, SNPs of VDR at BsmI, ApaI, and TaqI loci showed no difference between HCC and non-HCC patients, according to Yao et al. (46). However, the authors reported a higher frequency of VDR FokI C > T polymorphism in HCC patients. Also, HCC patients showed a higher prevalence of FokI TT genotype, which is a risk factor for HCC development (46). Interestingly, the FokI TT genotype was also associated with HCC clinicopathology characterized by increased serum alpha-fetoprotein (AFP), advanced tumor stage, cirrhosis, and lymph node metastasis (47). Besides, the FokI T allele is linked with a predisposition to reduced VD levels and an increased probability of cancer development in HCV patients (47).

Since there are associations between VD, VDR, and HCC pathological conditions, understanding VD-related mechanisms and therapeutic targets in HCC progression could further substantiate existing evidence and highlight the roles of the hormones in hepatocarcinogenesis.

THERAPEUTIC EFFECTS OF VITAMIN D IN HCC

In Vitro Studies

Over the years, there have been reports of HCC's resistance to many drugs. An example is resistance to Everolimus, which acts as an *mTOR* (mechanistic target of rapamycin) inhibitor. *mTOR* is a serine/threonine-protein kinase found in the PI3K-related kinase (PIKK) family. *mTOR*'s activation plays critical roles in cell metabolism, proliferation, and HCC progression (48). Hence, inhibiting *mTOR* is one of the suggested therapeutic targets used to prevent and manage HCC (49). A recent study reported that calcitriol treatment could restore HCC cell sensitivity, thus becoming less resistant to everolimus (50). The reduced cell resistance modulated through the epithelial-mesenchymal transition pathway increased expression of miRNA-375 and decreased expression of target genes, including Metadherin (*MTDH*), Yes-associated protein-1 (*YAP-1*), and cellular Myc (*c-MYC*) (50).

Likewise, Huang et al. (51) investigated calcitriol's effects on Histone deacetylase 2 (*HDAC2*) and cell cycle markers to explore the senescence and apoptotic pathway involved in HCC. According to Huang et al. (51), silencing the *HDAC2* gene, which is usually highly expressed in HCC tumors, enhances calcitriol's inhibitory effects. Equally, 1,25(OH)₂D₃ treatment decreased the expression of *HDAC2* with a dose-dependent increased expression of cell cycle marker, cyclin-dependent kinase inhibitor (*p21(WAF1/Cip1)*) (51). This result suggests that VD could be a potential therapeutic agent in managing HCC via cell cycle modulation. However, VD₃

treatment significantly increased Thioredoxin Interacting Protein (*TXNIP*); thus, enhancing apoptosis while reducing cell proliferation and thioredoxin activities (52). *TXNIP* is a tumor suppressor gene usually downregulated in HCC; therefore, instigating HCC progression (53). Furthermore, in its hormonal form, VD (1,25(OH)₂D₃) exhibits anti-proliferative ability and increases the apoptotic ratio in HCC cell lines (54). 1000 nM VD treatment also showed potential cell growth ameliorating ability in HCC cell lines according to the study of Xu et al. (51). Although VD reduced cell viability and proliferation while activating apoptosis, the effects were well enhanced when co-administered with Astemizole (a non-sedating antihistamine). In the same study, VD's anti-invasive, anti-tumor, and cell migration inhibitory properties were highlighted (55).

Recently, a combination of VD₂ analog, Doxercalciferol, and Carnosic acid-enhanced Sorafenib induced HCC cell death through blockage of autophagosomes/lysosomes fusion while also activating autophagy and apoptosis (56). To further elucidate the more apparent HCC related mechanisms, Wang et al. (57) showed that 1,25(OH)₂D₃ reversed biological alterations of hepatic progenitor cells caused by Aflatoxin B1 (AFB1) in WB-344 cells. Furthermore, VD₃ attenuated the activation of Protein kinase B (*Akt*) while suppressing the expression of cysteine-rich angiogenic inducer 61 (*CYR61*) and connective tissue growth factor (*CTGF*), thus indicating anti-tumor effects. Calcitriol, also showed inhibitory roles in HCC by suppressing the hepatocyte growth factor (*HGF*) and its receptor, *c-met* (58).

Therefore, it can be deduced from these *in vitro* studies as summarized in **Table 1** that VD acts as an anti-tumor agent in HCC, and it could regulate tumor growth/progression through cell cycle modulation and mTOR inhibition.

In Vivo Studies

VD's anti-inflammatory role in carcinogenesis is now considered an established mechanism of its anti-carcinogenesis property (68). For example, in an activated inflammatory response, dietary VD significantly ameliorated cytokine production observed with diethylnitrosamine (DEN) effects in rats (69). Similarly, a deficient state of 1,25(OH)₂D₃ triggers inflammatory cytokines production through *STAT3* activation (**Figure 1**) (50). Guo et al. (54) also linked the anti-tumor ability of 1,25(OH)₂D₃ with the availability of *p27^{kip1}* in mice (54). *p27^{kip1}* is a cyclin-dependent kinase inhibitor known for its prognostic roles in carcinogenesis. Besides from functioning as a tumor suppressor, *p27^{kip1}* promotes apoptosis, regulates tumor drug resistance, protects against inflammatory effects, and enhance cell differentiation as summarized in **Table 1** (70). Also, the loss of *p27^{kip1}* could negatively affect the anti-tumor ability of 1,25(OH)₂D₃. The ablation of kidney VD metabolic enzyme, 25(OH)D₃-1α-hydroxylase, resulted in tumor formation and increased inflammatory responses in mice (54). However, in the DEN-induced hepatocarcinogenesis mice model, loss of VD₃ upregulated protein 1 (*VDUP1*) promotes carcinogenesis through increased cell proliferation, expression of tumor necrosis factor-α (*TNF-α*) and nuclear factor-kappa B (*NF-κB*) activation, thus suggesting VDUP1 as a potential anti-proliferative therapy target (71).

TABLE 1 | Summary of the effects of vitamin D on HCC targets genes.

Effects of vitamin D on <i>in vitro</i> HCC targets					
S/ N	Vitamin D dosage (duration)	HCC cell lines	Target genes (method)	Summarized findings on vitamin D effects	References
1.	1, 10, 100 or 1000 nM (48 hours)	H22 and Hepa1–6	NA (Colony formation, Annexin V and PI double-staining)	1,25(OH) ₂ D ₃ reduced cell proliferation and induced apoptosis.	(54)
2.	0, 10, 100 or 500 nM (24, 48, 72hrs)	Huh7, HepG2, and Hep3B	<i>TXN</i> <i>CDNK1B</i> <i>CDNK1A</i> <i>TXNIP</i>	VD ₃ had no significant effect on TXN and CDNK1B VD ₃ downregulated the expression of CDNK1A. VD ₃ upregulated the expression of TXNIP.	(52)
3.	10–7 M (12/24 hrs pre-treatment; 21 days co-treatment with Everolimus) 10–7 M for 6 days 12hrs and 6 days of treatment.	PLC/PRF/5 EverR and JHH-6 EverR	NA (Colony formation and cell proliferation) E-cadherin, cytokeratin 18, and vimentin (WB and IF) <i>MTDH</i> , <i>YAP-1</i> , and <i>c-MYC</i> (WB)	1 α , 25 (OH) ₂ D restored everolimus sensitivity to everolimus-resistant (EverR) HCC cell lines 1 α , 25 (OH) ₂ D caused EMT induction through decreased expression of vimentin and increased expression of E-cadherin and cytokeratin-18. While 12hrs of 1 α , 25 (OH) ₂ D treatment upregulated miR-375 expression, 6 days of treatment reduced expression of miR-375 targets <i>MTDH</i> , <i>YAP-1</i> , and <i>c-MYC</i> .	(50)
4.	0, 0.1, 1, 10, 100 or 1000 nM	HpG2	<i>HDAC2</i> , <i>p21(WAF1/Cip1)</i> (Reverse transcription, WB)	1,25(OH) ₂ D ₃ caused a dose-dependent decrease in the HCC growth rate. 1,25(OH) ₂ D ₃ also decreased the mRNA expression and protein level of <i>HDAC2</i> and increased the expression/protein level of <i>p21(WAF1/Cip1)</i> .	(51)
5.	1.0, 10.0 nM (5hrs)	HepG2, Huh-Neo, Huh5-15, and Hep3B	<i>CYP24A1</i> , <i>CYP27B1</i> , and <i>VDR</i> (qRT-PCR, IHC)	1,25(OH) ₂ D ₃ increased the expression of <i>CYP24A1</i>	(59)
6.	0.1, 1, 10, 100 or 1000 nM (24 hours)	HepG2 and SMMC-7221	NA (Cell viability and proliferation)	Astemizole (1–2 μ M) increased VD-induced (>100 nM) cell viability and proliferation reduction, cell invasion, increased pro-apoptotic effects, and upregulated VDR expression-induced anti-tumorigenic effects.	(55)
7.	100nM (14 days)	WB-F344	<i>CD133</i> , <i>EpCAM</i> , <i>HNf4α</i> , <i>CK19</i> (FC, WB, Cell viability) <i>Cyclin D1</i> , <i>p27</i> , <i>lats1</i> , <i>YAP</i> , <i>TAZ</i> , <i>CYR61</i> , <i>CTGF</i> (WB)	1,25(OH) ₂ D ₃ inhibited colony formation, cell viability of WB-334 and promoted apoptosis. 1,25(OH) ₂ D ₃ caused a partial reversal of AKT phosphorylation (at Ser473) and gene alterations of <i>cyclin D</i> and <i>p27kip</i> . 1,25(OH) ₂ D ₃ blocked <i>YAP/TAZ</i> activation and <i>LATS1</i> dephosphorylation.	(57)
8.	0.01–1 μ M (7 days)	HepG2 and Hep3B		VD inhibited cell proliferation. VD also altered cadherin/catenin adhesion through an increased level of β -catenin in Smad3 ^{+/-} MEF cells as well as knockdown of Smad3 and <i>VDR</i> in HepG2 cells	(60)
9.	100 nM Doxercalciferol	Huh7 and HCO2	<i>BIM</i> , <i>Cas 9</i> , <i>Cas 3</i> , <i>Beclin1</i> , <i>Atg3</i> , <i>LC3-II</i>	The combination of Doxercalciferol, Carnosic acid, and sorafenib increases the expression of apoptosis and autophagy-related proteins.	(56)
Effects of vitamin D on <i>in vivo</i> HCC targets					
S/ N	Vitamin D dosage (duration)	Host organism	Target genes (method)	Summarized findings on vitamin D effects	References
10.	0.1 μ g/kg (14 days)	Mice (HCC through orthotopic transplantation)	<i>IL-6</i> , <i>TNF-α</i> (ELISA)	Exogenous supplementation of VD reduced inflammatory cytokines in 1 α (OH)ase knockout mice.	(54)
11.	0.3 μ g/100 μ l (4–20 weeks)	Rats		VD ₃ induced antioxidant defense system	(61)
12.	N/A	Human	<i>VDR</i> , <i>VDUP-1</i> (Reverse transcription)	25(OH)D was reduced in HCC patients with concomitant increased <i>VDR</i> , and <i>VDUP-1</i> mRNA upregulated expression.	(62)
13.	200 IU/kg (daily for 16 weeks)	Rats	<i>Nrf2</i> , <i>TGF-β1</i> , <i>Cas-3</i> (Reverse transcription, ELISA)	VD ₃ triggered hepatoprotective effects while enhancing the anti-tumor effects of 5-fluorouracil. It regulates cancer progression through downregulation of <i>Nrf2</i> , <i>TGF-β1</i> and induces apoptosis by upregulating <i>Cas-3</i> .	(63)
14.		Pig	NA	Administration <i>via</i> hepatic artery rather than intravenous route could allow for an increased dosage of VD	(64)
15.	100nM	Mice	<i>CK19</i> (IHC)	1,25(OH) ₂ D ₃ protected the liver integrity by reducing serum ALT, AST, and <i>CK19</i> cells initially increased with AFB-1 administration.	(57)

(Continued)

TABLE 1 | Continued

Effects of vitamin D on <i>in vitro</i> HCC targets			Summarized findings on vitamin D effects		References
S/	Vitamin D dosage (duration)	HCC cell lines	Target genes (method)		
N					
16.	200 IU/kg and 10000 IU/kg (4 months)	Mice	<i>PDCD4</i> , <i>p21</i> , <i>p27</i> , <i>p53</i> , <i>Akt</i> , <i>c-Myc</i> , <i>mTor</i> , <i>Stat5A</i> , <i>Bcl-XL</i> , <i>PEA15</i> , <i>cyclin D1</i>	Repression of tumor suppressors and induction of oncogenic proteins are associated with VD deficiency.	(60)
Effects of vitamin D in clinical trials					
17.	50, 75, 100 µg (4 weeks)	Human	NA	Co-administration with lipiodol could increase a safe dosage without hypercalcemia complications. Also, the co-administration stabilized HCC patients through the mediation of tumor marker, AFP.	(65)
18.	5 - 20 µg/day seocalcitol	Human	NA	Complete responses in some patients after Seocalcitol treatment showed that the analog could help stabilize HCC patients and may possess the anti-tumorigenic ability.	(66)
19.	50000 IU weekly (26 weeks)	Human	<i>TBR1</i> , <i>TBR2</i> , <i>Smad3</i> , <i>Smad4</i> , and <i>β2SP</i> (IHC)	VD treatment repressed β-catenin expression while inducing the expressions of TBR2, Smad3 in HCC patients. The study showed that VD treatment could restore TGF-β signaling in cirrhosis and liver cancer patients.	(60)
20.	2800 IU daily (8 weeks)	Human		In cirrhotic randomized control trial patients, VD ₃ supplementation significantly increased 25(OH)D serum concentrations. However, the supplementation with VD ₃ had no significant effect on liver function, fibrotic and mineral metabolism parameters.	(67)

EMT, epithelial-mesenchymal transition; TXNIP, thioredoxin interacting protein; HNF4α, hepatocyte nuclear factor 4 alpha; CDNK1, cyclin-dependent kinase inhibitor 1; YAP, Yes-associated protein; TAZ, transcriptional co-activator with PDZ-binding motif; HDAC2, histone deacetylase 2; MTDH, metastherin; EpCAM, epithelial cell adhesion molecule; CYP24A1, cytochrome P450 family 24 subfamily A member 1; CYP27B1, cytochrome P450 family 27 subfamily B member 1; CYP61, cytochrome P450 family 61; CTGF, connective tissue growth factor; FC, flow cytometry; WB, Western blotting; qRT-PCR, quantitative reverse transcription PCR; AFB-1, aflatoxin B-1; Nrf2, TGF-β1, tumor growth factor B-1; IL-6, interleukin 6; TNF-α, tumor necrosis factor-alpha; Cas-3, caspase 3; VDR, vitamin D receptor; VDUP-1, vitamin D3-upregulated protein-1; CK19, cytokeratin 19; IHC, immunohistochemistry.

Generally, inflammation induces oxidative stress by activating neutrophils and Kupffer cells, which subsequently triggers cancer progression (72). Oxidative stress is usually associated with the pathogenesis and progression of HCC. However, reports suggest that VD₃ could be involved in the attenuation of oxidative stress (61, 69). The physiological advantage of this abuts the vital role of inhibiting oxidative stress in managing hepatocarcinogenesis (73, 74). Besides, VD₃ protected against oxidative stress-induced carcinogenesis by reversing different antioxidant enzymes altered in 3' methyl-4-dimethyl-amino-azobenzene-induced hepatocarcinogenesis (61).

Furthermore, increased serum level and gene expression of the M30 apoptotic marker in HCC patients, amongst others, indicates alteration of the apoptotic pathway in carcinogenesis (62). Thus, the co-regulatory interaction between VD signaling and apoptotic pathway in HCC is imperative in the understanding of VD-related mechanisms (62). Besides, VD₃ (cholecalciferol) treatment activates caspase 3 (*Cas-3*) expression while downregulating protein expression of tumor growth factor (*TGF-β*) (63). Likewise, co-administration with 5-fluorouracil alleviated the increased liver function enzymes, alpha-fetoprotein (AFP), and nuclear factor erythroid 2-related factor 2 (*Nrf2*) expression in thioacetamide-induced HCC (63).

Therefore, the *in vivo* studies showed that VD could regulate HCC progression *via* activation of apoptosis, reducing oxidative stress and inflammatory effects (Table 1).

Clinical Studies

Despite promising data from *in vitro* and *in vivo* studies suggesting VD's crucial roles in carcinogenesis, established reports and data from clinical studies are still few and far between. These clinical trials included a phase 1 pilot study on VD administration's effects on serum calcium, hepatic and renal functions by Finlay et al. (75). In the study, HCC patients received up to a 20-fold increased 1,25-(OH)₂D₃ *via* hepatic arterial infusion without hypercalcemic complications. The study also reported 10 µg/day as a safe dosage with no renal or hepatic complications (75).

However, to eliminate hypercalcemia effects of VD administration, Morris et al. (74) reported in a relatively small pilot study that co-administration of 1,25-(OH)₂D₃ with lipiodol in HCC patients could be an excellent therapeutic measure through stabilization of tumor marker, AFP. From this clinical research, the authors suggested that the use of lipiodol could increase permitted 1,25-(OH)₂D₃ dosage about 50 folds (100 µg) without complications of hypercalcemia. Hence, this positive outcome could have resulted from the intra-arterial hepatic administration route used in the study (65). In addition, Dalhoff et al. (66) administered a starting dose of 10 µg/day seocalcitol (VD analog) and reported that seocalcitol could function as an anti-tumorigenic agent in phase 2 clinical trials. The analog can thus stabilize HCC patients due to its cytostatic rather than cytotoxic capacity (66).

VD may also improve HCC by restoring initially lost tumor growth factor-β (*TGF-β*) expression in liver tumor (60). In support of this, Chen et al. (63) reported that dysregulated VD-associated genes, including Foxhead box protein O4

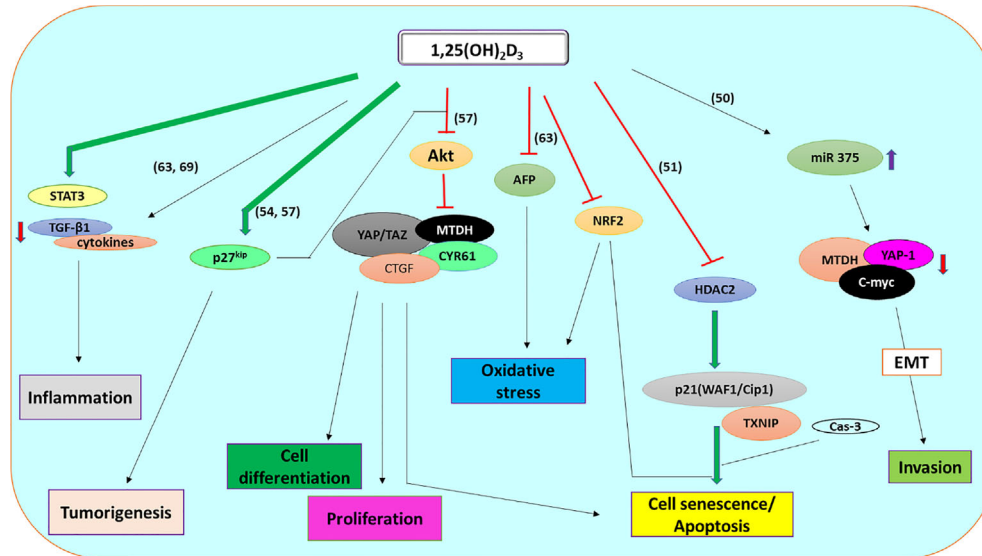


FIGURE 1 | $1,25(\text{OH})_2\text{D}_3$ signaling pathway involved in the regulation of HCC through apoptosis, invasion, proliferation, differentiation, tumorigenesis, oxidative stress, and inflammation.

(FOXO4) and signal transducer and activator of transcription 1 (STAT1), showed a strong correlation with TGF- β , while VD supplementation reduces cell proliferation.

Furthermore, a selected European population Nested Case-Control Study reported that increased concentration of hormonal VD, $1,25(\text{OH})_2\text{D}_3$ decreased the risk of HCC (76). This study informed the idea that $1,25(\text{OH})_2\text{D}_3$ treatment could ameliorate HCC development. Likewise, a randomized controlled trial also showed that $1,25(\text{OH})_2\text{D}_3$ supplementation of daily 2800 IU resulted in increased serum $1,25(\text{OH})_2\text{D}_3$ concentration in cirrhotic patients without significantly altering the mineral metabolism parameters (74).

THE ROLE OF VITAMIN D METABOLIZING ENZYMES

Beyond the modulating roles of circulating VD hitherto described, evidence is emerging that these effects are elicited through its metabolizing genes. In this vein, Horvath et al. (59) reported that $1,25(\text{OH})_2\text{D}_3$ treatment caused a concurrent dose-dependent mRNA increased expression of *CYP24A1* at specific time points in some HCC cell lines. The upregulated expression of *CYP24A1* through $1,25(\text{OH})_2\text{D}_3$ treatment suggests a positive correlation between the enzyme and VD serum concentration. Chiang et al. (77) also reported that $1,25(\text{OH})_2\text{D}_3$ cell line treatment induces upregulation of *CYP24A1* expression. Even though $25(\text{OH})\text{D}-1\alpha$ -hydroxylase, *CYP27B1* further augmented the upregulation of *CYP24A1*, as reported by Bikle et al. (78), its transfection also induced cell arrest at the G0/G1 phase through *p21/p27*; thus, inhibiting tumor cell growth (76). Additionally, single nucleotide polymorphisms of *CYP24A1* are associated with an increased risk of HCV infection in

some high-risk Chinese population (79). Specifically, rs6013897 (T>A) was significantly associated with an increased risk of HCV infection. In contrast, rs6068816 (C>T), rs3787557 (T>C), rs6022999 (A>G), and rs2248359 (C>T) were associated with increased risk of chronic HCV infection. Consequently, combining VD₃ treatment and *CYP24A1* inhibitors could annihilate the increased cytoplasmic expression of *CYP24A1*.

LIMITATIONS OF THE USE OF VITAMIN D AS THERAPEUTICS

VD intoxication, usually characterized by hypercalcemia, is a significant limitation to the therapeutic use of the hormone in alleviating pathological conditions. Consequently, VD analogs have been used in recent years to reduce hypercalcemic effects. For example, a catabolic metabolite of the prodrug, 27 hydroxy BCI-210 (27-OH BCI-210), was reported to inhibit cancer cell growth (80). Although patients take various supplements, including vitamins, to maintain and improve health and prevent disease occurrences (81), there was no observed association between these supplements and HCC patients' survival (81).

The daily intake of 100,000 IU or more could cause VD toxicity (68), while an increased intake of up to 2000 fold against the prescribed dosage could lead to renal failure (82). It has also been reported that an annual treatment of 500,000 IU VD₃ increases fracture risk (83, 84). However, a short-term effect of an accidental overdose of VD₃ was minimal; the long-term effect could be detrimental, as van den Ouweland et al. (83) reported. In the study, a single overdose treatment of 2,000,000 IU VD₃ caused no short-term clinical toxicity. Therefore, terminating VD and reduced the consumption of calcium and phosphorus helps in managing

hypercalcemia. Other interventions integral to controlling hypercalcemia include glucocorticoids, intravenous hydration, diuretics, and calcitonin (85, 86). Equally, to reduce the VD dosage and improve efficacy, combination therapy of VD and its analogs with other chemotherapeutic agents could be explored.

FUTURE PERSPECTIVES

It is important to note that VD as an anticancer therapeutic agent could be associated with the administration route. Aside from the hepatic arterial infusion of this lipophilic vitamin, intravenous administration could determine, to some extent, the therapeutic effects and rate of its effectiveness (64). Also, VD supplementation and CYP27B1 gene transfection therapy are other plausible options of exploration in managing and treating HCC (77). Although dosage limitation exists, it will be beneficial to understand the interaction of the VD signaling pathway and carcinogenesis at the genetic level. The genetic interactions could focus on specific targets; thus, alleviating risks that arise with the limitation.

Another line of thought in VD's therapeutic use could involve understanding the mechanisms in VD's modulatory roles of the tumor microenvironment (TME). Tumor growth, invasion, and metastasis are generally affected by the interactions between the tumors and their respective microenvironments (87). Understanding these bidirectional interactions between the tumor cells and the environment could open up therapeutic targets and regimes in liver cancer treatment (88–90). Although VD influences angiogenesis, metastasis, and cancer progression in TME, the active form of VD, 1, 25 (OH)₂D₃ modulates a couple of stroma cells explicitly, suppresses tumor growth, and act as an anti-inflammatory agent within the TME, leading to cancer reduction (91).

REFERENCES

- Sung H, Ferlay J, Siegel RL, Laversanne M, Soerjomataram I, Jemal A, et al. Global Cancer Statistics 2020 : GLOBOCAN Estimates of Incidence and Mortality Worldwide for 36 Cancers in 185 Countries. *CA Cancer J Clin* (2021) 0:1–41. doi: 10.3322/caac.21660
- Elangovan H, Chahal S, Gunton JE. Vitamin D in Liver Disease: Current Evidence and Potential Directions. *Biochim Biophys Acta Mol Basis Dis* (2017) 1863:907–16. doi: 10.1016/j.bbdis.2017.01.001
- Moeini A, Cornella H, Villanueva A. Emerging Signaling Pathways in Hepatocellular Carcinoma. *Liver Cancer* (2012) 1:83–93. doi: 10.1159/000342405
- Schlageter M, Terracciano LM, D'Angelo S, Sorrentino P. Histopathology of Hepatocellular Carcinoma. *World J Gastroenterol* (2014) 20(43):15955–64. doi: 10.3748/wjg.v20.i43.15955
- Singh AK, Kumar R, Pandey AK. Hepatocellular Carcinoma: Causes, Mechanism of Progression and Biomarkers. *Curr Chem Genomics Transl Med* (2018) 12:9–26. doi: 10.2174/2213988501812010009
- Rotimi OA, Rotimi SO, Duru CU, Ebebeinwe OJ, Abiodun AO, Oyeniyi BO, et al. Acute Aflatoxin B1 – Induced Hepatotoxicity Alters Gene Expression and Disrupts Lipid and Lipoprotein Metabolism in Rats. *Toxicol Rep* (2017) 4:408–14. doi: 10.1016/j.toxrep.2017.07.006
- McGlynn KA, London WT. Epidemiology and Natural History of Hepatocellular Carcinoma. *Best Pract Res Clin Gastroenterol* (2005) 19 (1):3–23. doi: 10.1016/j.bpg.2004.10.004
- Omer RE, Kuijsten A, Kadaru AMY, Kok FJ, Idris MO, El Khidir IM, et al. Population-Attributable Risk of Dietary Aflatoxins and Hepatitis B Virus

CONCLUSION

Despite positive research findings on VD's roles in HCC, resulting limitations hinder its progress as a viable therapeutic agent. Although there might be conflicting reports supporting the roles of serum 1,25-(OH)₂D₃ in HCC, there are ample *in vitro*, *in vivo* data and some randomized clinical control trials suggesting VD-related mechanism is vital in HCC progression. This research gap could be vital in understanding the mechanisms involved in the VD regulation of HCC. Clinical trials on various combination therapies will also help resolve the research deficiencies recorded in standardizing VD dosage. Therefore, it is strongly recommended that more studies should be carried out on combination therapies of various VD analogs and standard therapeutic agents by targeting crucial genes and pathways involved in VD's non-classical functions.

AUTHOR CONTRIBUTIONS

All authors contributed, read, and agreed to the publication of this manuscript. Conceptualization: IA. Supervision: OR, EM, and SR. Roles/writing—original draft: IA. Writing—review and editing: IA, OR, EM, and SR. All authors contributed to the article and approved the submitted version.

ACKNOWLEDGMENTS

The authors acknowledged the Covenant University Centre for Research, Innovation, and Discovery (CUCRID) for publication support.

- Infection With Respect to Hepatocellular Carcinoma. *Nutr Cancer* (2004) 48 (1):15–21. doi: 10.1207/s15327914nc4801_3
- Wild CP, Gong YY. Mycotoxins and Human Disease: A Largely Ignored Global Health Issue. *Carcinogenesis* (2009) 31(1):71–82. doi: 10.1093/carcin/bgp264
- Hung CH, Chiu YC, Hu TH, Chen CH, Lu SN, Huang CM, et al. Significance of Vitamin D Receptor Gene Polymorphisms for Risk of Hepatocellular Carcinoma in Chronic Hepatitis C. *Transl Oncol* (2014) 7(4):503–7. doi: 10.1016/j.tranon.2014.05.001
- Peng Q, Yang S, Lao X, Li R, Chen Z, Wang J, et al. Association of Single Nucleotide Polymorphisms in VDR and DBP Genes With HBV-related Hepatocellular Carcinoma Risk in a Chinese Population. *PLoS One* (2014) 9 (12):e116026. doi: 10.1371/journal.pone.0116026
- Lombardi C, Heck JE, Cockburn M, Ritz B. Solar UV Radiation and Cancer in Young Children. *Cancer Epidemiol Biomarkers Prev* (2013) 22(6):1118–28. doi: 10.1158/1055-9965.EPI-12-1316
- VoPham T, Bertrand KA, Yuan J, Tamimi RM, Hart JE, Laden F. Ambient Ultraviolet Radiation Exposure and Hepatocellular Carcinoma Incidence in the United States. *Environ Heal* (2017) 16:89. doi: 10.1186/s12940-017-0299-0
- O'Connor MY, Thoreson CK, Ramsey NLM, Ricks M, Sumner AE. The Uncertain Significance of Low Vitamin D Levels in African Descent Populations: A Review of the Bone and Cardiometabolic Literature. *Prog Cardiovasc Dis* (2013) 56(3):261–9. doi: 10.1016/j.pcad.2013.10.015
- Bikle DD. Review Vitamin D Metabolism, Mechanism of Action, and Clinical Applications. *Chem Biol* (2014) 21(3):319–29. doi: 10.1016/j.chembiol.2013.12.016

16. Mason SS, Kohles SS, Winn SR, Zelick RD. Extrahepatic 25-Hydroxylation of Vitamin D 3 in an Engineered Osteoblast Precursor Cell Line Exploring the Influence on Cellular Proliferation and Matrix Maturation During Bone Development. *ISRN BioMed Eng* (2013) 2013(956362):1–11. doi: 10.1155/2013/956362
17. Negri M, Gentile A, de Angelis C, Montò T, Patalano R, Colao A, et al. Vitamin D-induced Molecular Mechanisms to Potentiate Cancer Therapy and to Reverse Drug-Resistance in Cancer Cells. *Nutrients* (2020) 12(1798):1–25. doi: 10.3390/nu12061798
18. Zhu JG, Ochalek JT, Kaufmann M, Jones G, DeLuca HF. CYP2R1 is a Major, But Not Exclusive, Contributor to 25-Hydroxyvitamin D Production In Vivo. *Proc Natl Acad Sci* (2013) 110(39):15650–5. doi: 10.1073/pnas.1315006110
19. Christakos S, Dhawan P, Verstuyf A, Verlinden L, Carmeliet G. Vitamin D: Metabolism, Molecular Mechanism of Action, and Pleiotropic Effects Vitamin D Analogs. *Physiol Rev* (2016) 96:365–408. doi: 10.1152/physrev.00014.2015
20. Hewison M, Zehnder D, Bland R, Stewart PM. 1 α -Hydroxylase and the Action of Vitamin D. *J Mol Endocrinol* (2000) 25:141–8. doi: 10.1677/jme.0.0250141
21. Dawson MI, Xia Z. The Retinoid X Receptors and Their Ligands. *Biochim Biophys Acta* (2012) 1821(1):21–56. doi: 10.1016/j.bbali.2011.09.014
22. Bettoun DJ, Burris TP, Houck KA, Buck DW, Stayrook KR, Khalifa B, et al. Retinoid X Receptor Is a Nonsilent Major Contributor to Vitamin D Receptor-Mediated Transcriptional Activation. *Mol Endocrinol* (2003) 17(11):2320–8. doi: 10.1210/me.2003-0148
23. Haussler MR, Whitfield GK, Kaneko I, Haussler CA, Hsieh D, Hsieh JC, et al. Molecular Mechanisms of Vitamin D Action. *Calcif Tissue Int* (2013) 92(2):77–98. doi: 10.1007/s00223-012-9619-0
24. Jeon SM, Shin EA. Exploring Vitamin D Metabolism and Function in Cancer. *Exp Mol Med* (2018) 50(20):1–14. doi: 10.1038/s12276-018-0038-9
25. Finkelmeier F, Kronenberger B, Koberle V, Bojunga J, Zeuzem S, Trojan J, et al. Severe 25-Hydroxyvitamin D Deficiency Identifies a Poor Prognosis in Patients With Hepatocellular Carcinoma – a Prospective Cohort Study. *Aliment Pharmacol Ther* (2014) 39:1204–12. doi: 10.1111/apt.12731
26. Pilz S, Gröbler M, Gaksch M, Schwetz V, Trummer C, Hartaigh BÓ, et al. Vitamin D and Mortality. *Anticancer Res* (2016) 36:1379–87.
27. Schottker B, Jorde R, Peasey A, Thorand B, Jansen EHJM, Groot LD, et al. Vitamin D and Mortality: Meta-Analysis of Individual Participant Data From a Large Consortium of Cohort Studies From Europe and the United States. *Br Med J* (2014) 348:g3656. doi: 10.1136/bmj.g3656
28. Gaksch M, Jorde R, Grimnes G, Joakimsen R, Schirmer H, Wilsgaard T, et al. Vitamin D and Mortality: Individual Participant Data Meta-Analysis of Standardized 25-Hydroxyvitamin D in 26916 Individuals From a European Consortium. *PLoS One* (2017) 12(2):e0170791. doi: 10.1371/journal.pone.0170791
29. Zhang Y, Jiang X, Li X, Găman MA, Kord-Varkaneh H, Rahmani J, et al. Serum Vitamin D Levels and Risk of Liver Cancer: A Systematic Review and Dose-Response Meta-Analysis of Cohort Studies. *Nutr Cancer* (2020) 0:1–9. doi: 10.1080/01635581.2020.1797127
30. Fang AP, Long JA, Zhang YJ, Liu ZY, Li QJ, Zhang DM, et al. Serum Bioavailable, Rather Than Total, 25-Hydroxyvitamin D Levels Are Associated With Hepatocellular Carcinoma Survival. *Hepatology* (2020) 72(1):169–82. doi: 10.1002/hep.31013
31. Liu H, Jiang X, Qiao Q, Chen L, Matsuda K, Jiang G, et al. Association of Circulating 25-Hydroxyvitamin D and its Related Genetic Variations With Hepatocellular Carcinoma Incidence and Survival. *Ann Transl Med* (2020) 8(17):1080. doi: 10.21037/atm-20-1637
32. Saumoy M, Ando Y, Jesudian A, Aden B, Jacobson I, Gambarin-Gelwan M. Vitamin D Deficiency is Not Associated With Increased Risk of Hepatocellular Carcinoma in Patients With Cirrhosis. *Am J Gastroenterol* (2013) 108(Suppl. 1):S108. doi: 10.14309/0000434-201310001-00362
33. Konstantakis C, Tselekouni P, Kalafateli M, Triantos C. Vitamin D Deficiency in Patients With Liver Cirrhosis. *Ann Gastroenterol* (2016) 29(3):297–306. doi: 10.20524/aog.2016.0037
34. Berkan-Kawińska A, Koślińska-Berkan E, Piekarska A. The Prevalence and Severity of 25-(OH)-Vitamin D Insufficiency in HCV Infected and in HBV Infected Patients: A Prospective Study. *Clin Exp Hepatol* (2015) 1:5–11. doi: 10.5114/ceh.2015.51373
35. Yang F, Ren H, Gao Y, Zhu Y, Huang W. The Value of Severe Vitamin D Deficiency in Predicting the Mortality Risk of Patients With Liver Cirrhosis: A Meta-Analysis. *Clin Res Hepatol Gastroenterol* (2019) 43(6):722–9. doi: 10.1016/j.clinre.2019.03.001
36. Buonomo AR, Zappulo E, Scotto R, Pinchera B, Perruolo G, Formisano P, et al. Vitamin D Deficiency is a Risk Factor for Infections in Patients Affected by HCV-related Liver Cirrhosis. *Int J Infect Dis* (2017) 63:23–9. doi: 10.1016/j.ijid.2017.07.026
37. Lange CM, Miki D, Ochi H, Nischalke HD, Bojunga J, Bibert S, et al. Genetic Analyses Reveal a Role for Vitamin D Insufficiency in HCV-Associated Hepatocellular Carcinoma Development. *PLoS One* (2013) 8(5):e64053. doi: 10.1371/journal.pone.0064053
38. Ravid A, Rapaport N, Issachar A, Erman A, Bachmetov L, Tur-Kaspa R, et al. 25-Hydroxyvitamin D Inhibits Hepatitis C Virus Production in Hepatocellular Carcinoma Cell Line by a Vitamin D Receptor-Independent Mechanism. *Int J Mol Sci* (2019) 20:2367. doi: 10.3390/ijms20092367
39. Gotlieb N, Tachlytski I, Lapidot Y, Sultan M, Safran M, Ben-Ari Z. Hepatitis B Virus Downregulates Vitamin D Receptor Levels in Hepatoma Cell Lines, Thereby Preventing Vitamin D-dependent Inhibition of Viral Transcription and Production. *Mol Med* (2018) 24:53. doi: 10.1186/s10020-018-0055-0
40. Farnik H, Bojunga J, Berger A, Allwinn R, Waidmann O, Kronenberger B, et al. Low Vitamin D Serum Concentration is Associated With High Levels of Hepatitis B Virus Replication in Chronically Infected Patients. *Hepatology* (2013) 58(4):1270–6. doi: 10.1002/hep.26488
41. Abdel-Mohsen MA, El-Braky AAA, Ghazal AAER, Shamseya MM. Autophagy, Apoptosis, Vitamin D, and Vitamin D Receptor in Hepatocellular Carcinoma Associated With Hepatitis C Virus. *Med (United States)* (2018) 97(12):1–7. doi: 10.1097/MD.00000000000010172
42. Falletti E, Bitetto D, Fabris C, Cussigh A, Fontanini E, Fornasiere E, et al. Vitamin D Receptor Gene Polymorphisms and Hepatocellular Carcinoma in Alcoholic Cirrhosis. *World J Gastroenterol* (2010) 16(24):3016–24. doi: 10.3748/wjg.v16.i24.3016
43. Quan Y, Yang J, Qin T, Hu Y. Associations Between Twelve Common Gene Polymorphisms and Susceptibility to Hepatocellular Carcinoma : Evidence From a. *World J Surg Oncol* (2019) 17:216. doi: 10.1186/s12957-019-1748-8
44. Hoan NX, Khuyen N, Giang DP, Binh MT, Toan NL, Anh DT, et al. Vitamin D Receptor Apa1 Polymorphism Associated With Progression of Liver Disease in Vietnamese Patients Chronically Infected With Hepatitis B Virus. *BMC Med Genet* (2019) 20:201. doi: 10.1186/s12881-019-0903-y
45. Rowida IR, Eshra KA, El-sharaby RM, Eissa RAE, Saied SM, Amer I, et al. Apa1 (Rs7975232) SNP in the Vitamin D Receptor is Linked to Hepatocellular Carcinoma in Hepatitis C Virus Cirrhosis. *Br J BioMed Sci* (2019) 77(2):53–7. doi: 10.1080/09674845.2019.1680166
46. Yao X, Zeng H, Zhang G, Zhou W, Yan Q, Dai L, et al. The Associated Ion Between the VDR Gene Polymorphisms and Susceptibility to Hepatocellular Carcinoma and the Clinicopathological Features in Subjects Infected With HBV. *BioMed Res Int* (2013) 2013:953974. doi: 10.1155/2013/953974
47. Cusato J, Boglione L, De Nicolò A, Favata F, Ariando A, Mornese Pinna S, et al. Vitamin D Pathway Gene Polymorphisms and Hepatocellular Carcinoma in Chronic Hepatitis C-affected Patients Treated With New Drugs. *Cancer Chemother Pharmacol* (2018) 81(3):615–20. doi: 10.1007/s00280-018-3520-0
48. Ferrin G, Guerrero M, Amado V, Rodríguez-Perálvarez M, De la Mata M. Activation of mTOR Signaling Pathway in Hepatocellular Carcinoma. *Int J Mol Sci* (2020) 21(1266):1–16. doi: 10.3390/ijms21041266
49. Matter MS, Decaens T, Andersen JB, Thorgeirsson SS. Targeting the mTOR Pathway in Hepatocellular Carcinoma: Current State and Future Trends. *J Hepatol* (2014) 60(4):855–65. doi: 10.1016/j.jhep.2013.11.031
50. Provisiero DP, Negri M, de Angelis C, Di Gennaro G, Patalano R, Simeoli C, et al. Vitamin D Reverts Resistance to the mTOR Inhibitor Everolimus in Hepatocellular Carcinoma Through the Activation of a miR-375/oncogenes Circuit. *Sci Rep* (2019) 9(11695):1–13. doi: 10.1038/s41598-019-48081-9
51. Huang J, Yang G, Huang Y, Kong W, Zhang S. 1,25(OH)2D3 Inhibits the Progression of Hepatocellular Carcinoma Via Downregulating HDAC2 and Upregulating P21(WAF1/CIP1). *Mol Med Rep* (2016) 13(2):1373–80. doi: 10.3892/mmr.2015.4676

52. Hamilton JP, Potter JJ, Koganti L, Meltzer SJ, Mezey E. Effects of Vitamin D3 Stimulation of Thioredoxin-Interacting Protein in Hepatocellular Carcinoma. *Hepatol Res* (2014) 44(13):1357–66. doi: 10.1111/hepr.12302
53. Sheth SS, Bodnar JS, Ghazalpour A, Thippavong CK, Tsutsumi S, Tward AD, et al. Hepatocellular Carcinoma in Txnip-deficient Mice. *Oncogene* (2006) 25:3528–36. doi: 10.1038/sj.onc.1209394
54. Guo J, Ma Z, Ma Q, Wu Z, Fan P, Zhou X, et al. 1, 25(OH)₂D₃ Inhibits Hepatocellular Carcinoma Development Through Reducing Secretion of Inflammatory Cytokines From Immunocytes. *Curr Med Chem* (2013) 20 (33):4131–41. doi: 10.2174/09298673113209990248
55. Xu J, Wang Y, Zhang Y, Dang S, He S. Astemizole Promotes the Anti-Tumor Effect of Vitamin D Through Inhibiting miR-125a-5p-mediated Regulation of VDR in HCC. *BioMed Pharmacother* (2018) 107(277):1682–91. doi: 10.1016/j.biopha.2018.08.153
56. Wu Q, Wang X, Pham K, Luna A, Studzinski GP, Liu C. Enhancement of Sorafenib-Mediated Death of Hepatocellular Carcinoma Cells by Carnosic Acid and Vitamin D2 Analog Combination. *J Steroid Biochem Mol Biol* (2020) 197:105524. doi: 10.1016/j.jsbmb.2019.105524
57. Wang J, Chen Y, Mo PL, Wei YJ, Liu KC, Zhang ZG, et al. 1 α ,25-Dihydroxyvitamin D3 Inhibits Aflatoxin B1-induced Proliferation and Dedifferentiation of Hepatic Progenitor Cells by Regulating PI3K/Akt and Hippo Pathways. *J Steroid Biochem Mol Biol* (2018) 183:228–37. doi: 10.1016/j.jsbmb.2018.08.002
58. Wu FS, Zheng SS, Wu LJ, Teng LS, Ma ZM, Zhao WH, et al. Calcitriol Inhibits the Growth of MHCC97 Hepatocellular Cell Lines by Down-Modulating C-Met and ERK Expressions. *Liver Int* (2007) 27(5):700–7. doi: 10.1111/j.1478-3231.2007.01487.x
59. Horvath E, Lakatos P, Balla B, Kósa JP, Tóbiás B, Jozilan H, et al. Marked Increase of CYP24A1 mRNA Level in Hepatocellular Carcinoma Cell Lines Following Vitamin D Administration. *Anticancer Res* (2012) 32(11):4791–6.
60. Chen J, Katz LH, Muñoz NM, Gu S, Shin JH, Jogunoori WS, et al. Vitamin D Deficiency Promotes Liver Tumor Growth in Transforming Growth Factor- β /Smad3-Deficient Mice Through Wnt and Toll-like Receptor 7 Pathway Modulation. *Sci Rep* (2016) 6:30217. doi: 10.1038/srep30217
61. Karmakar R, Banik S, Chatterjee M. Inhibitory Effect of Vitamin D3 on 3' methyl-4-dimethyl-amino-azobenzene-induced Rat Hepatocarcinogenesis: A Study on Antioxidant Defense Enzymes. *J Exp Ther Oncol* (2002) 2(4):193–9. doi: 10.1046/j.1359-4117.2002.01032.x
62. Fingas CD, Altinbas A, Schlattjan M, Beifuss A, Sowa JP, Sydor S, et al. Expression of Apoptosis- and Vitamin D Pathway-Related Genes in Hepatocellular Carcinoma. *Digestion* (2013) 87(3):176–81. doi: 10.1159/000348441
63. Ebrahim AR, El-Mesery M, El-Karef A, Eissa LA. Vitamin D Potentiates Anti-Tumor Activity of 5-Fluorouracil Via Modulating Caspase-3 and Tgf- β 1 Expression in Hepatocellular Carcinoma-Induced in Rats. *Can J Physiol Pharmacol* (2018) 96(12):1218–25. doi: 10.1139/cjpp-2018-0445
64. Finlay IG, Stewart GJ, Shirley P, Woolfe S, Pourgholami MH, Morris DL. Hepatic Arterial and Intravenous Administration of 1,25-Dihydroxyvitamin D3 - Evidence of a Clinically Significant Hepatic First-Pass Effect. *Cancer Chemother Pharmacol* (2001) 48(3):209–14. doi: 10.1007/s002800100333
65. Morris DL, Jourdan JL, Finlay I, Gruenberger T, The MP, Pourgholami MH. Hepatic Intra-Arterial Injection of 1,25-Dihydroxyvitamin D3 in Lipiodol: Pilot Study in Patients With Hepatocellular Carcinoma. *Int J Oncol* (2002) 21 (4):901–6. doi: 10.3892/ijo.21.4.901
66. Dalhoff K, Dancy J, Astrup L, Skovsgaard T, Hamberg KJ, Loft FJ, et al. A Phase II Study of the Vitamin D Analogue Seocalcitol in Patients With Inoperable Hepatocellular Carcinoma. *Br J Cancer* (2003) 89:252–7. doi: 10.1038/sj.bjc.6601104
67. Pilz S, Putz-Bankuti C, Gaksch M, Spindelboeck W, Haselberger M, Rainer F, et al. Effects of Vitamin D Supplementation on Serum 25-Hydroxyvitamin D Concentrations in Cirrhotic Patients: A Randomized Controlled Trial. *Nutrients* (2016) 8:278. doi: 10.3390/nu8050278
68. Liu W, Zhang L, Xu H, Li Y, Hu C, Yang J, et al. The Anti-Inflammatory Effects of Vitamin D in Tumorigenesis. *Int J Mol Sci* (2018) 19:2736. doi: 10.3390/ijms19092736
69. Adelani IB, Ogadi EO, Onuzulu C, Rotimi OA, Maduagwu EN, Rotimi SO. Dietary Vitamin D Ameliorates Hepatic Oxidative Stress and Inflammatory Effects of Diethylnitrosamine in Rats. *Heliyon* (2020) 6(9):e04842. doi: 10.1016/j.heliyon.2020.e04842
70. Lloyd RV, Erickson LA, Jin L, Kulig E, Qian X, Cheville JC, et al. P27kip1: A Multifunctional Cyclin-Dependent Kinase Inhibitor With Prognostic Significance in Human Cancers. *Am J Pathol* (1999) 154(2):313–23. doi: 10.1016/S0002-9440(10)65277-7
71. Kwon H-J, Won Y-S, Suh H-W, Jeon J-H, Shao Y, Yoon S-R, et al. Vitamin D3 Upregulated Protein-1 Suppresses Tnf- α -Induced NF- κ B Activation in Hepatocarcinogenesis. *J Immunol* (2010) 185(7):3980–9. doi: 10.4049/jimmunol.1000990
72. Fu Y, Chung F. Oxidative Stress and Hepatocarcinogenesis. *Hepatoma Res* (2018) 2018(4):1–11. doi: 10.20517/2394-5079.2018.29
73. Glauert HP, Calfee-Mason K, Stemm DN, Tharappel JC, Spear BT. Dietary Antioxidants in the Prevention of Hepatocarcinogenesis: A Review. *Mol Nutr Food Res* (2010) 54(7):875–96. doi: 10.1002/mnfr.200900482
74. Maurya BK, Trigun SK. Fisetin Modulates Antioxidant Enzymes and Inflammatory Factors to Inhibit Aflatoxin-B1 Induced Hepatocellular Carcinoma in Rats. *Oxid Med Cell Longev* (2016) 2016(1972793):1–9. doi: 10.1155/2016/1972793
75. Finlay IG, Stewart GJ, Ahkter J, Morris DL. A Phase One Study of the Hepatic Arterial Administration of 1,25-Dihydroxyvitamin D3 for Liver Cancers. *J Gastroenterol Hepatol* (2001) 16(3):333–7. doi: 10.1046/j.1440-1746.2001.02398.x
76. Fedirko V, Duarte-Salles T, Bamia C, Trichopoulou A, Aleksandrova K, Trichopoulos D, et al. Prediagnostic Circulating Vitamin D Levels and Risk of Hepatocellular Carcinoma in European Populations: A Nested Case-Control Study. *Hepatology* (2014) 60(4):1222–30. doi: 10.1002/hep.27079
77. Chiang K, Yen C, Yeh C, Hsu J, Chen L, Kuo S-F, et al. Hepatocellular Carcinoma Cells Express 25(OH)D-1 α -hydroxylase and are Able to Convert 25(OH)D to 1 α ,25(OH)₂D₃, Leading to the 25(OH)D-Induced Growth Inhibition. *J Steroid Biochem Mol Biol* (2015) 154:47–52. doi: 10.1016/j.jsbmb.2015.06.008
78. Bikle DD, Patzek S, Wang Y. Bone Reports Physiologic and Pathophysiologic Roles of Extra Renal CYP27b1 : Case Report and Review. *Bone Rep* (2018) 8:255–67. doi: 10.1016/j.bonr.2018.02.004
79. Fan Hz, Zhang R, Tian T, Zhong YL, Wu Mp, Xie Cn, et al. CYP24A1 Genetic Variants in the Vitamin D Metabolic Pathway are Involved in the Outcomes of Hepatitis C Virus Infection Among High-Risk Chinese Population. *Int J Infect Dis* (2019) 84:80–8. doi: 10.1016/j.ijid.2019.04.032
80. Wang Y-R, Wigington DP, Strugnelli SA, Knutson JC. Growth Inhibition of Cancer Cells by An Active Metabolite of a Novel Vitamin D Prodrug. *Anticancer Res* (2005) 25:4333–40.
81. Lee V, Goyal A, Hsu CC, Jacobson JS, Rodriguez RD, Siegel AB. Dietary Supplement Use Among Patients With Hepatocellular Carcinoma. *Integr Cancer Ther* (2015) 14(1):35–41. doi: 10.1177/1534735414550038
82. Marins TAp, Galvão TdeFG, Korkes F, Malerbi DA ugust C, Ganc AJos., Korn D, et al. Vitamin D Intoxication: Case Report. *Einstein (Sao Paulo)* (2014) 12 (2):242–4. doi: 10.1590/S1679-45082014RC2860
83. van den Ouweland J, Fleuren H, Drabbe M, Vollaard H. Pharmacokinetics and Safety Issues of an Accidental Overdose of 2,000,000 IU of Vitamin D3 in Two Nursing Home Patients: A Case Report. *BMC Pharmacol Toxicol* (2014) 15(1):1–5. doi: 10.1186/2050-6511-15-57
84. Sanders KM, Stuart AL, Williamson EJ, Simpson JA, Kotowicz MA, Young D, et al. Annual High-Dose Oral Vitamin D and Falls and Fractures in Older Women: A Randomized Controlled Trial. *J Am Med Assoc* (2010) 303 (18):1815–22. doi: 10.1001/jama.2010.594
85. Özkan B, Hatun Ş, Bereket A. Vitamin D Intoxication. *Turk J Pediatr* (2012) 54(2):93–8.
86. Araki T, Holick MF, Alfonso BD, Charlap E, Romero CM, Rizk D, et al. Vitamin D Intoxication With Severe Hypercalcemia Due to Manufacturing and Labeling Errors of Two Dietary Supplements Made in the United States. *J Clin Endocrinol Metab* (2011) 96(12):3603–8. doi: 10.1210/jc.2011-1443
87. Baghban R, Roshangar L, Jahanban-Esfahlan R, Seidi K, Ebrahimi-Kalan A, Jaymand M, et al. Tumor Microenvironment Complexity and Therapeutic Implications At a Glance. *Cell Commun Signal* (2020) 18(59):1–19. doi: 10.1186/s12964-020-0530-4
88. Tsai M-J, Chang W-A, Huang M-S, Kuo P-L. Tumor Microenvironment: A New Treatment Target for Cancer. *ISRN Biochem* (2014) 2014(351959):1–8. doi: 10.1155/2014/351959

89. Benavente S, Sánchez-García A, Naches S, LLeonart ME, Lorente J. Therapy-Induced Modulation of the Tumor Microenvironment: New Opportunities for Cancer Therapies. *Front Oncol* (2020) 10:582884. doi: 10.3389/fonc.2020.582884
90. Murciano-Goroff YR, Warner AB, Wolchok JD. The Future of Cancer Immunotherapy: Microenvironment-Targeting Combinations. *Cell Res* (2020) 30:507–19. doi: 10.1038/s41422-020-0337-2
91. Wu X, Hu W, Lu L, Zhao Y, Zhou Y, Xiao Z, et al. Repurposing Vitamin D for Treatment of Human Malignancies Via Targeting Tumor Microenvironment. *Acta Pharm Sin B* (2019) 9(2):203–19. doi: 10.1016/j.apsb.2018.09.002

Conflict of Interest: The authors declare that the research was conducted in the absence of any commercial or financial relationships that could be construed as a potential conflict of interest.

Copyright © 2021 Adelani, Rotimi, Maduagwu and Rotimi. This is an open-access article distributed under the terms of the Creative Commons Attribution License (CC BY). The use, distribution or reproduction in other forums is permitted, provided the original author(s) and the copyright owner(s) are credited and that the original publication in this journal is cited, in accordance with accepted academic practice. No use, distribution or reproduction is permitted which does not comply with these terms.



OPEN ACCESS

Edited by:

Lanping Xu,
Peking University People's
Hospital, China

Reviewed by:

Francesca Maffei,
University of Bologna, Italy
Inamul Hasan Madar,
Korea University, South Korea

***Correspondence:**

Rongcai Jiang
jiang116216@163.com
Jianning Zhang
jianningzhang@hotmail.com

Specialty section:

This article was submitted to
Pharmacology of
Anti-Cancer Drugs,
a section of the journal
Frontiers in Oncology

Received: 08 March 2021

Accepted: 30 June 2021

Published: 15 July 2021

Citation:

Yuan J, Li Y, Liu X, Nie M,
Jiang W, Fan Y, Xiang T, Wang H,
Quan W, Gao C, Huang J, An S,
Ru Y, Zhou Q, Zhang J and Jiang R
(2021) Atorvastatin Plus
Low-Dose Dexamethasone May
Be Effective for Leukemia-Related
Chronic Subdural Hematoma but
Not for Leukemia Encephalopathy:
A Report of Three Cases.
Front. Oncol. 11:628927.
doi: 10.3389/fonc.2021.628927

Atorvastatin Plus Low-Dose Dexamethasone May Be Effective for Leukemia-Related Chronic Subdural Hematoma but Not for Leukemia Encephalopathy: A Report of Three Cases

Jiangyuan Yuan^{1,2}, Ying Li^{1,2}, Xuanhui Liu^{1,2}, Meng Nie^{1,2}, Weiwei Jiang^{1,2}, Yibing Fan^{1,2}, Tangtang Xiang^{1,2}, Hanhua Wang^{1,2}, Wei Quan^{1,2}, Chuang Gao^{1,2}, Jinghao Huang^{1,2}, Shuo An^{1,2}, Yongxin Ru³, Qiufan Zhou⁴, Jianning Zhang^{1,2*} and Rongcai Jiang^{1,2*}

¹ Department of Neurosurgery, Tianjin Medical University General Hospital, Tianjin, China, ² Tianjin Neurological Institute, Key Laboratory of Post-Neuroinjury Neuro-Repair and Regeneration in Central Nervous System, Tianjin Medical University General Hospital, Ministry of Education, Tianjin, China, ³ Department of Clinical Laboratory, Hospital of Hematology, Chinese Academy of Medical Sciences, Tianjin, China, ⁴ Department of Hematology, Tianjin Medical University General Hospital, Tianjin, China

We are not aware of any reports regarding conservative treatment for leukemia-related chronic subdural hematoma (CSDH). We report our experience with 3 men who were admitted with subdural masses and abnormal leukocyte counts. In two patients, leukemia and CSDH were confirmed on the basis of medical records, mild head trauma, and neuroimaging features. Both patients experienced reduced CSDH and neurological symptoms after receiving atorvastatin (20 mg/day) plus low-dose dexamethasone. However, this combined conservative treatment was ineffective in the third patient, who was diagnosed as having leukemia and showed an increased hematoma volume after two weeks of therapy. Magnetic resonance imaging findings suggested dural metastasis, which prompted a switch from statin-based conservative treatment to chemotherapy. Complete remission of the leukemia and resolution of the subdural mass were observed after chemotherapy, which supported a diagnosis of leukemia encephalopathy. The 5-month follow-ups did not reveal CSDH relapse in all 3 cases. Thus, atorvastatin-based conservative treatment may be effective for leukemia-related CSDH but not for leukemia encephalopathy.

Keywords: chronic subdural hematoma, leukemia, leukemia encephalopathy, atorvastatin, dexamethasone

INTRODUCTION

Chronic subdural hematoma (CSDH) is a common neurological disease that generally develops after a head trauma (1–3). The formation of CSDH is thought to be related to the injury of the bridging vessels that connect the brain to the dural venous sinuses. This allows blood to collect in the subdural space, which induces chronic inflammation, the continuous release of angiogenesis-related cytokines, and the formation of highly permeable capillaries. Blood constantly seeps into the subdural space from these immature vessels, which causes the chronic hematoma (4–6). Cases of CSDH generally involve elderly patients and can co-occur with various neoplasms, including leukemia (7–9). However, there are few reports regarding leukemia-related CSDH, its potential etiology, and conservative treatment.

In this context, if leukemia is effectively treated and the CSDH persists, the underlying mechanisms and treatment strategies would be similar to those in cases of trauma-related CSDH. However, it is also possible that the subdural mass might be directly caused by leukemia encephalopathy, which would suggest that its pathological characteristics and treatment strategies would differ from those of trauma-related CSDH. Burr-hole drainage is the primary treatment for CSDH, although it is associated with unsatisfactory rates of relapse and mortality (10, 11). Furthermore, the current chemotherapeutic protocols for leukemia are still associated with a poor prognosis and abnormal blood parameters, which may motivate patients to select non-surgical conservative therapy if they have CSDH and leukemia (12). Unfortunately, there is no clearly effective conservative treatment for CSDH in patients with leukemia. We confirmed that statin-based conservative treatment is effective for conventional CSDH on the basis of findings from our previous clinical trials (13, 14). In this report, we describe the effectiveness of a statin-based conservative treatment for CSDH in patients with leukemia.

Clinical studies have indicated that atorvastatin, which is a 3-hydroxy-3-methylglutaryl-coenzyme A reductase inhibitor, can effectively treat CSDH by promoting vessel maturation and inhibiting intracapsular inflammation (15–17). Furthermore, preliminary findings from a randomized proof-of-concept clinical trial have indicated that atorvastatin plus low-dose dexamethasone treatment was effective in reducing hematoma and neurological symptoms in patients with CSDH (14). Thus, to save time and achieve better outcomes, it would be reasonable to use atorvastatin plus low-dose dexamethasone to treat leukemia-related CSDH, as this strategy was more effective than atorvastatin monotherapy. We report our experience with 2 patients who had leukemia and trauma-related CSDH and a third patient with leukemia encephalopathy that was diagnosed during hospitalization, who experienced different results from a combination of atorvastatin plus low-dose dexamethasone.

CASE PRESENTATION

Informed consent for the publication of this report was obtained from the patients. All patients received a standard dose of atorvastatin (20 mg/day orally) plus low-dose dexamethasone

(2.25 mg/day for the first 2 weeks, 1.5 mg/day during the third week, and then 0.75 mg/day during the fourth week).

Case 1

A 28-year-old man with acute myeloid leukemia (AML) experienced head trauma during a minor collision while receiving chemotherapy with cytarabine plus decitabine (**Figure 1A**). One month later, the patient developed headache and confusion, and bilateral CSDH was detected during head computed tomography (CT) (**Figure 2A**). Treatment was immediately started using atorvastatin (20 mg/day), the patient's symptoms were significantly relieved after 4 weeks, and magnetic resonance imaging (MRI) revealed slight absorption of the left-side hematoma (**Figure 2B**). Low-dose dexamethasone was added to the conservative treatment at 4 weeks, and CT at the 8-week follow-up revealed substantial absorption of the CSDH (**Figure 2C**). The dexamethasone treatment was subsequently stopped, but atorvastatin treatment was continued until week 12, at which point CT revealed that the hematoma had nearly disappeared (**Figure 2D**). The patient did not experience any adverse drug reactions during the conservative treatment, and no hematoma recurrence has been observed during the 6-month follow-up.

Case 2

A 72-year-old man had a 2-year history of chronic myeloid leukemia (CML) but had not been receiving chemotherapy for approximately 1 year (**Figure 1B**). The patient developed CSDH after experiencing head trauma, which resulted in dizziness, headache, and left-limb weakness (**Figure 3A**). After 2 weeks of conservative treatment using atorvastatin plus dexamethasone, the hematoma was substantially absorbed, and the patient's symptoms were significantly relieved (**Figure 3B**). However, the patient's symptoms worsened during the 4th week of treatment, at which point head MRI revealed new bleeding in the subdural space (**Figure 3C**). Conservative treatment was continued, although dexamethasone was stopped at the 6th week and atorvastatin was stopped after approximately 20 weeks. At 10 weeks, CT revealed that the hematoma had been significantly absorbed (**Figure 3D**), and the hematoma gradually disappeared during the 5-month follow-up, with complete relief of the patient's symptoms (**Figure 3E**). This patient also did not experience any adverse drug reactions or hematoma recurrence.

Case 3

A 68-year-old man with a 1-month history of headache and dizziness was diagnosed as having CSDH (**Figure 4A**). After admission, the patient received conservative treatment using atorvastatin plus low-dose dexamethasone. After 2 weeks of inpatient therapy, head MRI revealed that the subdural mass had grown, with significant enhancement of the dura mater (**Figure 4B**). A substantial leukocyte abnormality was detected during the treatment period, and a diagnosis of AML was made on the basis of bone marrow aspirate examination (**Figure 1C**). Conservative treatment using atorvastatin plus dexamethasone was switched to periodic chemotherapy using cytarabine plus decitabine for over 4 months. Surprisingly, the subdural

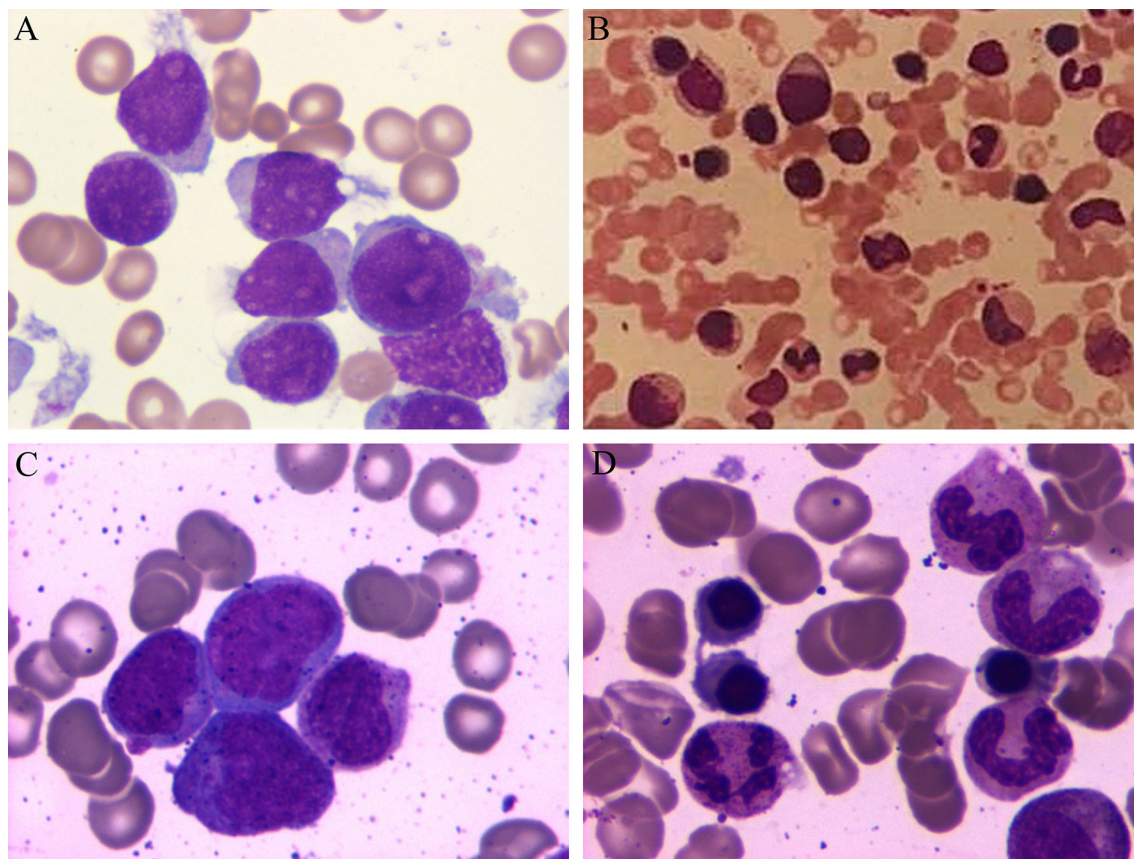


FIGURE 1 | Periodic acid-Schiff staining of bone marrow aspirate from the 3 patients at the time of admission. **(A)** Patient 1 had acute myeloid leukemia, **(B)** Patient 2 had chronic myeloid leukemia, and **(C)** Patient 3 had acute myeloid leukemia. **(D)** Patient 3 experienced complete remission after the chemotherapy.

hematoma was significantly absorbed after completion of chemotherapy (**Figures 4C, D**) and the patient's symptoms disappeared with complete remission of the AML (**Figure 1D**). This course suggested that the patient had CSDH that was related

to leukemia encephalopathy. The 5-month follow-up MRI findings (**Figure 4E**) revealed no subdural hematoma and the patient did not experience any severe side effects during the treatment period.

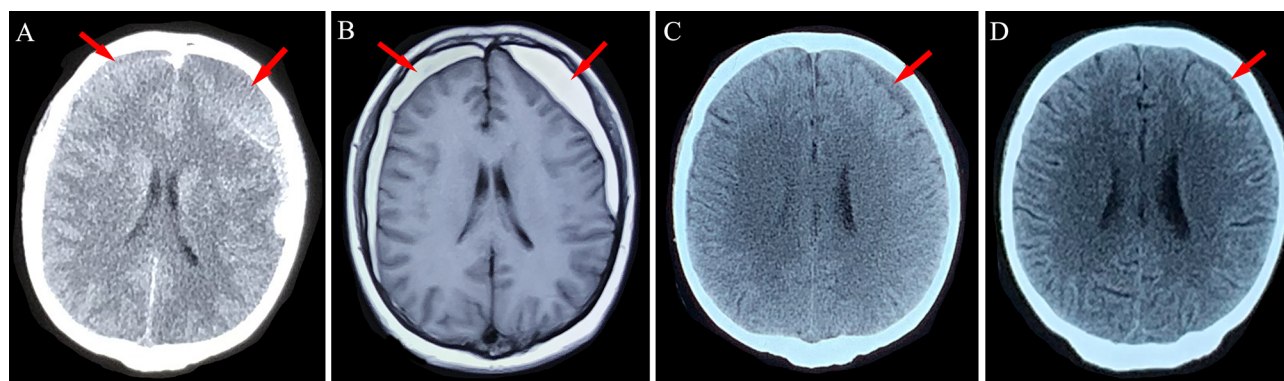


FIGURE 2 | Neuroimaging findings for Patient 1. **(A)** Chronic subdural hematoma (red arrows) was detected in the bilateral frontotemporal lobes after head trauma. **(B)** After 4 weeks of atorvastatin treatment, the left-side hematoma was slightly absorbed. **(C, D)** Absorption of the hematoma after 8 weeks and 12 weeks of conservative treatment using atorvastatin plus low-dose dexamethasone.

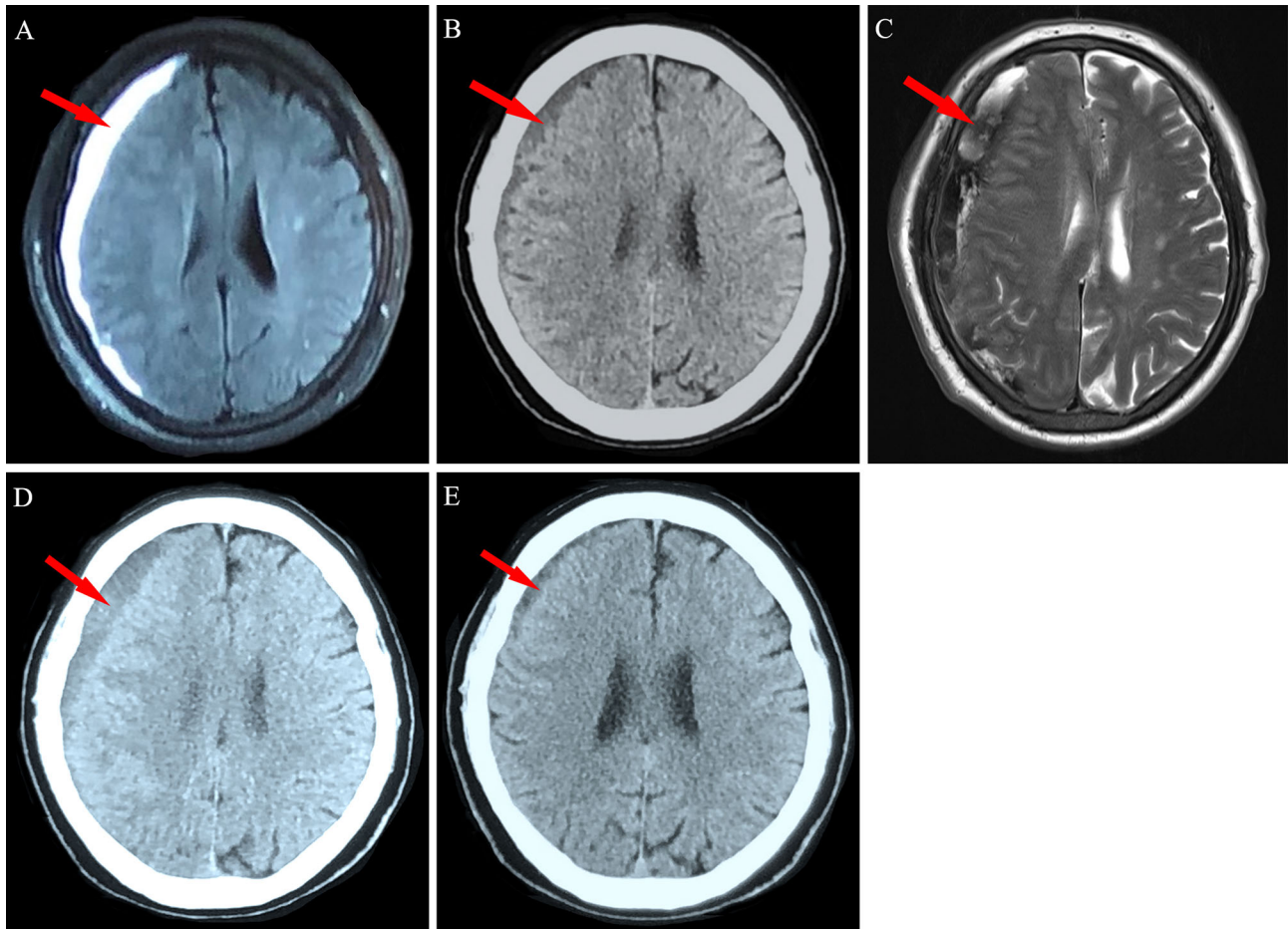


FIGURE 3 | Neuroimaging findings for Patient 2. **(A)** A 72-year-old man with chronic myeloid leukemia was diagnosed as having right frontotemporal chronic subdural hematoma (red arrow). **(B)** The hematoma was significantly absorbed after 2 weeks of conservative treatment. **(C)** New bleeding in the subdural space was detected via magnetic resonance imaging at the 4-week follow-up. **(D)** Obvious absorption was observed after 10 weeks and **(E)** near disappearance was observed after 20 weeks of conservative treatment.

DISCUSSION

The development of CSDH is related to chronic inflammation in the subdural space that induces the formation of highly permeable capillaries, which leads to continuous blood leakage and accumulation in the subdural space (4–6). Among the cases we reported, the CSDH in Patients 1 and 2 might be related to incidental cerebral trauma during leukemia treatment, which could have been accompanied by the inflammation-related formation of immature blood vessels, leading to CSDH. In Patient 3, dural metastasis may have been responsible for the subdural mass, as dural invasion of leukemia can occasionally cause malignant subdural hematoma (8). Our laboratory findings revealed low platelet counts in all 3 patients (**Supplement Table 1**), which is concordant with the relationship between abnormal coagulation function and the development of CSDH (18–20). In Patients 1 and 2, atorvastatin plus low-dose dexamethasone treatment promoted absorption of the CSDH and alleviated the patients' neurological

symptoms with no adverse events occurred and no recurrence during follow-up. Thus, this combination may be a safe and effective treatment for patients with leukemia and conventional CSDH.

Atorvastatin treatment for CSDH is based on the concept that statin treatment is effective for subdural masses (13). The anti-inflammatory effects of statin may play an important role in promoting the absorption of CSDH. For example, our previous studies revealed that atorvastatin treatment of rats with subdural hematoma led to decreased expression of IL-6, IL-8, and TNF- α , which contribute to the development of CSDH, and increased the number of anti-inflammatory regulatory T-cells (15–17). While atorvastatin alone initially improved Patient 1's neurological symptoms, there was no clear CSDH absorption, which was subsequently observed after the addition of dexamethasone. This result agrees with the finding from a phase II randomized proof-of-concept trial, which indicated that atorvastatin plus low-dose dexamethasone was more effective than atorvastatin monotherapy for accelerating CSDH

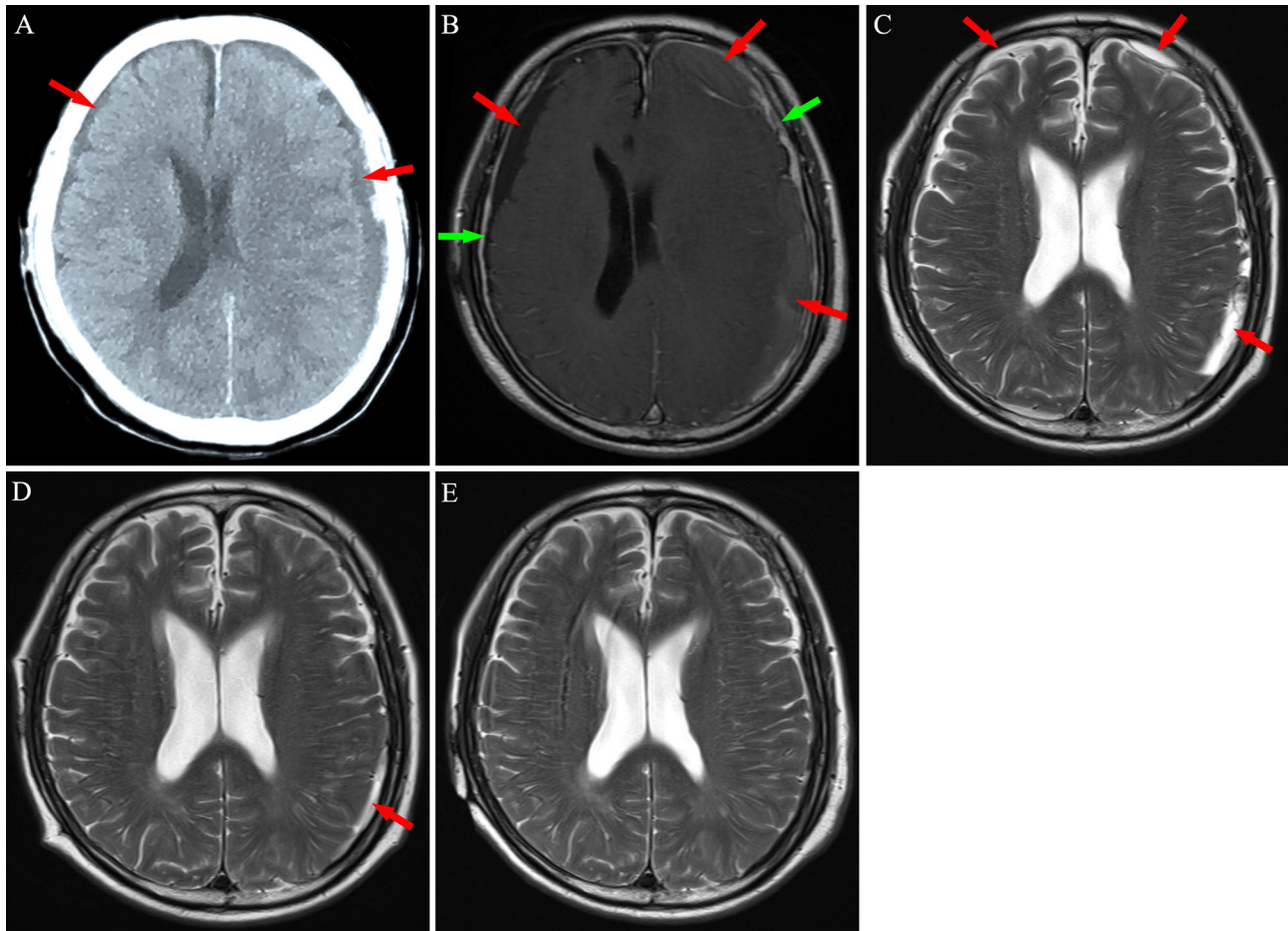


FIGURE 4 | Neuroimaging findings for Patient 3. **(A)** Computed tomography revealed bilateral chronic subdural hematoma (red arrows). **(B)** After 2 weeks of atorvastatin treatment plus low-dose dexamethasone, magnetic resonance imaging revealed an increase in the hematoma, with significant enhancement of the dura mater (green arrows) post-injection of contrast agent. **(C, D)** After chemotherapy, subdural mass was significantly absorbed in 8–14 weeks. **(E)** A 5 months follow-up MRI exhibited no hematoma in the subdural space.

absorption. That study indicated that atorvastatin enhanced the levels of circulating endothelial progenitor cells, which are essential for the formation and maturation of blood vessels, and promoted the maturation of subdural leakage capillaries, whereas dexamethasone strengthened these effects (14). *In vitro* research showed that subdural hematoma could destroy endothelial cell junction by reducing the expression of transcription factor KLF2, while statin could promote the expression of KLF2 to improve endothelial connection. And the effect of statins on promoting the expression of KLF2 was enhanced when combined with low-dose dexamethasone (21).

Patient 3 had an interesting course, as the subdural hematoma was not effectively absorbed during the early stage of treatment using atorvastatin plus dexamethasone. Furthermore, a new subdural hemorrhage during this period led to an increase in the CSDH. However, the patient was immediately switched to chemotherapy after the diagnosis of AML, which resulted in resolution of the leukemia after 6 weeks and rapid absorption of the subdural mass at the same time based on the MRI findings.

Thus, the patient likely had leukemia encephalopathy rather than conventional trauma-related CSDH. Furthermore, enhancement of the dura mater was observed, which confirmed that there was metastasis of the leukemia cells. Although there was no history of trauma in the 3rd patient, dural invasion by leukemic cells may have been the source of subdural masses (8). A recent rat-based study has indicated that the dural lymphatic vessels are an important channel for subdural hematoma drainage to the extracranial space (22). Whereas tumor metastasis can lead to dysfunction of lymphatic drainage (23), leukemia cells invading the patient's dura mater may occlude the meningeal lymphatic drainage pathway, which can reduce the absorption of CSDH. Effective chemotherapy may restore this drainage pathway, with relief from leukemia. Therefore, Patient 3 may not have initially responded to atorvastatin treatment because meningeal metastasis may have caused dural lymphatic drainage dysfunction, which suggests that atorvastatin-based conservative treatment alone may not be effective for patients with subdural masses related to leukemia encephalopathy.

Remission of leukemia by chemotherapy allows hematomas associated with leukemia encephalopathy to be absorbed.

After treatment, subdural hematoma of 3 patients were significantly absorbed, and no recurrence was found in the follow-up. Patients 1 and 2 were satisfied with our statins based treatment, and patient 3 highly appreciated our correct diagnosis and chemotherapy regimen.

CONCLUSION

We encountered 3 men with myeloid leukemia and CSDH, who experienced different responses to conservative treatment using atorvastatin plus low-dose dexamethasone. Two of the patients had conventional trauma-related CSDH, and the conservative treatment promoted subdural hematoma absorption and improved their neurological symptoms with no adverse effects. However, the subdural hematoma in the patient who was diagnosed as having leukemia encephalopathy did not respond to statin-based treatment. After chemotherapy, leukemia resolved and the subdural mass disappeared completely. Thus, atorvastatin plus low-dose dexamethasone may be an effective conservative treatment for conventional trauma-related CSDH in leukemia patients but not for subdural masses caused by leukemia encephalopathy.

DATA AVAILABILITY STATEMENT

The original contributions presented in the study are included in the article/**Supplementary Material**. Further inquiries can be directed to the corresponding authors.

REFERENCES

- Markwalder TM. Chronic Subdural Hematomas: A Review. *J Neurosurg* (1981) 54(5):637–45. doi: 10.3171/jns.1981.54.5.637
- Lee KS, Doh JW, Bae HG, Yun IG. Relations Among Traumatic Subdural Lesions. *J Korean Med Sci* (1996) 11(1):55–63. doi: 10.3346/jkms.1996.11.1.55
- Lee KS. Natural History of Chronic Subdural Haematoma. *Brain Inj* (2004) 18(4):351–8. doi: 10.1080/02699050310001645801
- Edlmann E, Giorgi-Coll S, Whitfield PC, Carpenter KLH, Hutchinson PJ. Pathophysiology of Chronic Subdural Haematoma: Inflammation, Angiogenesis and Implications for Pharmacotherapy. *J Neuroinflamm* (2017) 14(1):108. doi: 10.1186/s12974-017-0881-y
- Frati A, Salvati M, Mainiero F, Ippoliti F, Rocchi G, Raco A, et al. Inflammation Markers and Risk Factors for Recurrence in 35 Patients With a Posttraumatic Chronic Subdural Hematoma: A Prospective Study. *J Neurosurg* (2004) 100(1):24–32. doi: 10.3171/jns.2004.100.1.0024
- Stanisic M, Aasen AO, Pripp AH, Lindegaard KF, Ramm-Petersen J, Lyngstadaas SP, et al. Local and Systemic Pro-Inflammatory and Anti-Inflammatory Cytokine Patterns in Patients With Chronic Subdural Hematoma: A Prospective Study. *Inflamm Res* (2012) 61(8):845–52. doi: 10.1007/s00011-012-0476-0
- Reichman J, Singer S, Navi B, Reiner A, Panageas K, Gutin PH, et al. Subdural Hematoma in Patients With Cancer. *Neurosurgery* (2012) 71(1):74–9. doi: 10.1227/NEU.0b013e3182517938
- Comănescu A, Roșca E, Bota M, Ninulescu G. Chronic Subdural Hematoma in a Patient With Acute Myeloid Leukemia and

ETHICS STATEMENT

Written informed consent was obtained from the individual(s) for the publication of any potentially identifiable images or data included in this article.

AUTHOR CONTRIBUTIONS

JY analyzed dates and wrote article. YL, XL, MN, WJ, YF, HW, and TX collected patients information. WQ, CG, JH, and SA offered writing advices. YR and QZ helped to design figures. JZ and RJ revised papers and provided financial support. All authors contributed to the article and approved the submitted version.

FUNDING

This study was supported by the National Natural Science Foundation of China (No.81671221), the Clinical Study of Tianjin Medical University (No. 2017kylc007) and the Science and Technology Project of Tianjin (No.19YFZCSY00650).

SUPPLEMENTARY MATERIAL

The Supplementary Material for this article can be found online at: <https://www.frontiersin.org/articles/10.3389/fonc.2021.628927/full#supplementary-material>

Dural Metastatic Infiltration. *Rom J Morphol Embryol* (2008) 49(2):259–62.

- Pitner SE, Johnson WW. Chronic Subdural Hematoma in Childhood Acute Leukemia. *Cancer* (1973) 32(1):185–90. doi: 10.1002/1097-0142(197307)32:1<185::AID-CNCR2820320128>3.0.CO;2-O
- Nakaguchi H, Tanishima T, Yoshimasu N. Factors in the Natural History of Chronic Subdural Hematomas That Influence Their Postoperative Recurrence. *J Neurosurg* (2001) 95(2):256–62. doi: 10.3171/jns.2001.95.2.0256
- Nakaguchi H, Tanishima T, Yoshimasu N. Relationship Between Drainage Catheter Location and Postoperative Recurrence of Chronic Subdural Hematoma After Burr-Hole Irrigation and Closed-System Drainage. *J Neurosurg* (2000) 93(5):791–5. doi: 10.3171/jns.2000.93.5.0791
- Kinjo T, Mukawa J, Nakata M, Kinjo N. Chronic Subdural Hematoma Secondary to Coagulopathy. *No Shinkei Geka* (1991) 19(10):991–7. doi: 10.11477/mf.1436900344
- Jiang R, Zhao S, Wang R, Feng H, Zhang J, Li X, et al. Safety and Efficacy of Atorvastatin for Chronic Subdural Hematoma in Chinese Patients: A Randomized Clinicaltrial. *JAMA Neurol* (2018) 75(11):1338–46. doi: 10.1001/jamaneurol.2018.2030
- Wang D, Gao C, Xu X, Chen T, Tian Y, Wei H, et al. Treatment of Chronic Subdural Hematoma With Atorvastatin Combined With Low-Dose Dexamethasone: Phase II Randomized Proof-of-Concept Clinical Trial. *J Neurosurg* (2020) 1–9. doi: 10.3171/2019.11.JNS192020
- Wang D, Li T, Wei H, Wang Y, Yang G, Tian Y, et al. Atorvastatin Enhances Angiogenesis to Reduce Subdural Hematoma in a Rat Model. *J Neurol Sci* (2016) 362:91–9. doi: 10.1016/j.jns.2016.01.017

16. Li T, Wang D, Tian Y, Yu H, Wang Y, Quan W, et al. Effects of Atorvastatin on the Inflammation Regulation and Elimination of Subdural Hematoma in Rats. *J Neurol Sci* (2014) 341(1–2):88–96. doi: 10.1016/j.jns.2014.04.009
17. Quan W, Zhang Z, Li P, Tian Q, Huang J, Qian Y, et al. Role of Regulatory T Cells in Atorvastatin Induced Absorption of Chronic Subdural Hematoma in Rats. *Aging Dis* (2019) 10(5):992–1002. doi: 10.14336/AD.2018.0926
18. Lindvall P, Koskinen LO. Anticoagulants and Antiplatelet Agents and the Risk of Development and Recurrence of Chronic Subdural Haematomas. *J Clin Neurosci* (2009) 16(10):1287–90. doi: 10.1016/j.jocn.2009.01.001
19. Sood P, Sinson GP, Cohen EP. Subdural Hematomas in Chronic Dialysis Patients: Significant and Increasing. *Clin J Am Soc Nephrol* (2007) 2(5):956–9. doi: 10.2215/CJN.03781106
20. Graus F, Saiz A, Sierra J, Arbaiza D, Rovira M, Carreras E, et al. Neurologic Complications of Autologous and Allogeneic Bone Marrow Transplantation in Patients With Leukemia: A Comparative Study. *Neurology* (1996) 46(4):1004–9. doi: 10.1212/WNL.46.4.1004
21. Fan Y, Wang D, Rao C, Li Y, Rong H, Wan Z, et al. Atorvastatin Combined With Low-Dose Dexamethasone Treatment Protects Endothelial Function Impaired by Chronic Subdural Hematoma Via the Transcription Factor Klf-2. *Drug Des Devel Ther* (2020) 14:3291–9. doi: 10.2147/DDDT.S256050
22. Liu X, Gao C, Yuan J, Xiang T, Gong Z, Luo H, et al. Subdural Haematomas Drain Into the Extracranial Lymphatic System Through the Meningeal Lymphatic Vessels. *Acta Neuropathol Commun* (2020) 8(1):16. doi: 10.1186/s40478-020-0888-y
23. Deutsch A, Lubach D, Nissen S, Neukam D. Ultrastructural Studies on the Invasion of Melanomas in Initial Lymphatics of Human Skin. *J Invest Dermatol* (1992) 98(1):64–7. doi: 10.1111/1523-1747.ep12495259

Conflict of Interest: The authors declare that the research was conducted in the absence of any commercial or financial relationships that could be construed as a potential conflict of interest.

Copyright © 2021 Yuan, Li, Liu, Nie, Jiang, Fan, Xiang, Wang, Quan, Gao, Huang, An, Ru, Zhou, Zhang and Jiang. This is an open-access article distributed under the terms of the Creative Commons Attribution License (CC BY). The use, distribution or reproduction in other forums is permitted, provided the original author(s) and the copyright owner(s) are credited and that the original publication in this journal is cited, in accordance with accepted academic practice. No use, distribution or reproduction is permitted which does not comply with these terms.



Epigenetics-Associated Risk Reduction of Hematologic Neoplasms in a Nationwide Cohort Study: The Chemopreventive and Therapeutic Efficacy of Hydralazine

Bing-Heng Yang^{1,2}, Wei-Zhi Lin^{3,4}, Yu-Ting Chiang⁵, Yeu-Chin Chen⁶, Chi-Hsiang Chung^{7,8,9}, Wu-Chien Chien^{7,8,9} and Chia-Yang Shiau^{1,3,4*}

OPEN ACCESS

Edited by:

Benyi Li,
University of Kansas Medical Center,
United States

Reviewed by:

Arjun Singh,
Memorial Sloan Kettering Cancer
Center, United States
Ken Ogasawara,
Bristol Myers Squibb,
United States

*Correspondence:

Chia-Yang Shiau
hehcys1234@gmail.com

Specialty section:

This article was submitted to
Pharmacology of Anti-Cancer Drugs,
a section of the journal
Frontiers in Oncology

Received: 04 November 2021

Accepted: 10 January 2022

Published: 02 February 2022

Citation:

Yang B-H, Lin W-Z, Chiang Y-T,
Chen Y-C, Chung C-H, Chien W-C
and Shiau C-Y (2022)
Epigenetics-Associated Risk
Reduction of Hematologic
Neoplasms in a Nationwide Cohort
Study: The Chemopreventive and
Therapeutic Efficacy of Hydralazine.
Front. Oncol. 12:809014.
doi: 10.3389/fonc.2022.809014

¹ Graduate Institute of Medical Sciences, National Defense Medical Center, Taipei, Taiwan, ² Division of Clinical Pathology, Department of Pathology, Tri-Service General Hospital, Taipei, Taiwan, ³ Graduate Institute of Life Sciences, National Defense Medical Center, Taipei, Taiwan, ⁴ Fidelity Regulation Therapeutics Inc., Taoyuan City, Taiwan, ⁵ Department of Biochemical Science and Technology, National Taiwan University, Taipei, Taiwan, ⁶ Division of Hematology and Oncology, Department of Medicine, Tri-Service General Hospital, National Defense Medical Center, Taipei, Taiwan, ⁷ School of Public Health, National Defense Medical Center, Taipei, Taiwan, ⁸ Department of Medical Research, Tri-Service General Hospital, Taipei, Taiwan, ⁹ Taiwanese Injury Prevention and Safety Promotion Association, Taipei, Taiwan

Background: Although several epigenetic drugs have been reported to have therapeutic efficacy for some hematologic neoplasms (HNs) in clinical trials, few achieved disease-free survival benefit. The traditional drug discovery pathway is costly and time-consuming, and thus, more effective strategies are required. We attempted to facilitate epigenetic drug repositioning for therapy of HNs by screening the Human Epigenetic Drug Database (HEDD) in the web, conducting a bench-work cytotoxicity test and a retrospective nationwide cohort study prior to a clinical trial.

Methods: Four FDA-approved epigenetic drugs with antitumor properties and completion of clinical phase II trials were selected from HEDD. Hydralazine (HDZ) and valproate (VAL) among the four were selected with higher cytotoxicity to HN cells, no matter whether carrying the *JAK2V617F* mutation or not. Both of them were chosen for a cohort study using the Longitudinal Health Insurance Database (LHID) 2000–2015 (N = 1,936,512), a subset of the National Health Insurance Research Database (NHIRD, N = 25.68 millions) in Taiwan.

Results: In the initial cohort, HDZ or VAL exposure subjects (11,049) and matching reference subjects (44,196) were enrolled according to maximal daily consumption (300/2,100 mg per day of HDZ/VAL). The HN incidence in HDZ and VAL exposure groups reduced from 4.97% to 3.90% ($p < .001$) and 4.45% ($p = .075$), respectively. A further cohort study on HDZ at a lower range of the WHO defined daily dose (<34 mg per day) and HN incidence of HDZ exposure subjects (75,612) reduced from 5.01% to 4.16% ($p = 1.725 \times 10^{-18}$) compared to the reference subjects (302,448).

Conclusions: An association of a chronically prescribed HDZ, even prescribed low dose, with reduction of overall incidence rate and in most subgroups of HN was observed in our study. Repositioning HDZ for HN management may be feasible. This is the first nationwide cohort study of the epigenetics-associated risk evaluation of overall HN in the existing literature, showing an effective method with a wider scope to inform contemporary clinical trials of epigenetic drugs in the future.

Keywords: hematologic neoplasms, hydralazine, epigenetic drug, cohort, drug repositioning

INTRODUCTION

Hematologic neoplasms (HNs) including Hodgkin lymphoma, non-Hodgkin lymphoma (NHL), leukemia, and multiple myeloma (1) show high prevalence in many countries. In 2016, there were 1,139,000 newly diagnosed HN cases and 677,000 deaths worldwide. From 2006 to 2016, the incidence of leukemia increased by 26% and that of NHL by 45% (2). Traditionally, chemotherapy is used as the first-line treatment for HN, but its therapeutic efficacy is limited and has various distressing side effects. In addition, long-term treatment with HN can cause significant financial burden on patients and their families, leading to an increased risk of mental illness and impact on life quality that may negatively affect the treatment outcome (3–5).

In cancer cells, genetic instability and epigenetic instability are observed (6). Cell activities such as cell proliferation, apoptosis, invasion, and senescence can be modulated by these modifications, and epigenetic dysregulations led to tumorigenesis (7). Drugs targeting epigenetic regulators have been tried clinically on some HN since 2004 (8). Epigenetic treatment may restore chemosensitivity in relapsed/refractory patients by reversing drug resistance to chemotherapy (9–12), or trigger an innate immune response by alter the function of relevant immune cells to acquired immunity (13).

Drugs, which have epigenetic targets, may be prescribed for indications other than HN. The Taiwan FDA has approved two epigenetic drugs: hydralazine (HDZ), an antihypertension drug shown to act as a DNA methyltransferase inhibitor (DNMTi), and valproate (VAL), an anticonvulsant and established histone deacetylase inhibitor (HDACi). Although clinical trials were conducted on both epigenetic drugs, no cohort study has been conducted prospectively or retrospectively to evaluate the association between HN incidence and the use of two drugs. Here, we carried out a cohort study respectively by analyzing the registries from the National Health Insurance Research Database (NHIRD) in Taiwan during 2000–2015 (14). A highly significant association between a low dose of HDZ and reduction of incidence was found for several subgroups of HN. We observed a significant overall reduction in the incidence of most HN among patients given with HDZ and in dosage-stratified analysis. Our results suggest it may be feasible to reposition HDZ for treating HN. Our cohort study shows a method with a wider scope to inform contemporary clinical trials of epigenetic drugs in the future. We propose that in view of the highly significant association with sufficient subjects, whether

HDZ prescription to HN patients needed to be validated by clinical trial may be reconsidered.

METHODS

Study Design and Drug Selection

Four epigenetic drugs were selected from the 64 listed in the Human Epigenetic Drug Database (HEDD) (15) because they have been reported to have antitumor activity and have passed clinical phase II trials to prove their safety. The four drugs chosen were azacitidine (AZA) and HDZ, both DNMTi, and VAL and suberanilohydroxamic acid (SAHA), both HDACi. These four candidate epigenetic drugs were preliminarily tested for their cytotoxicity. HDZ and VAL showed higher cellular toxicity, no matter whether carrying the *JAK2V617F* mutation or not (Figure 1). They were, therefore, selected for retrospective cohort studies for association with incidence reduction of all subgroups of HN. To study the dose effect, the dose range was stratified according to the defined daily dose (DDD).

Ethics

The personal identification data from NHIRD were encrypted to protect privacy. The protocol of this study was reviewed and approved by the IRB of the Tri-Service General Hospital (No.: 2-108-05-107, B-109-38).

Isolation of Leukocytes From Clinical Waste Blood

Leukocytes were isolated from clinical waste blood of patients who received therapeutic phlebotomy. Briefly, the whole blood was 1-fold diluted with PBS. Tubes (50 ml) containing Ficoll-Paque PLUS solution (10 ml) were prepared beforehand. Diluted blood (25 ml) was slowly added into the tubes without stirring the under-layer solution. Then, the layered solution was centrifuged at $600 \times g$ at room temperature for 40 min. The buffy coat in the middle layer was carefully transferred to a new tube. The cells of the buffy coat were washed with PBS and cultured in RPMI 1640 medium supplied with 10% fetal bovine serum, 2 g/l sodium bicarbonate, 2.5 g/l D-glucose, and 110 mg/l sodium pyruvate.

Cytotoxicity Study

The UT-7 (ACC 137, RRID: CVCL_2233) cell line was purchased from DSMZ (Braunschweig, Germany). The HEL (HEL 92.1.7, RRID: CVCL_2481) cell line was obtained from

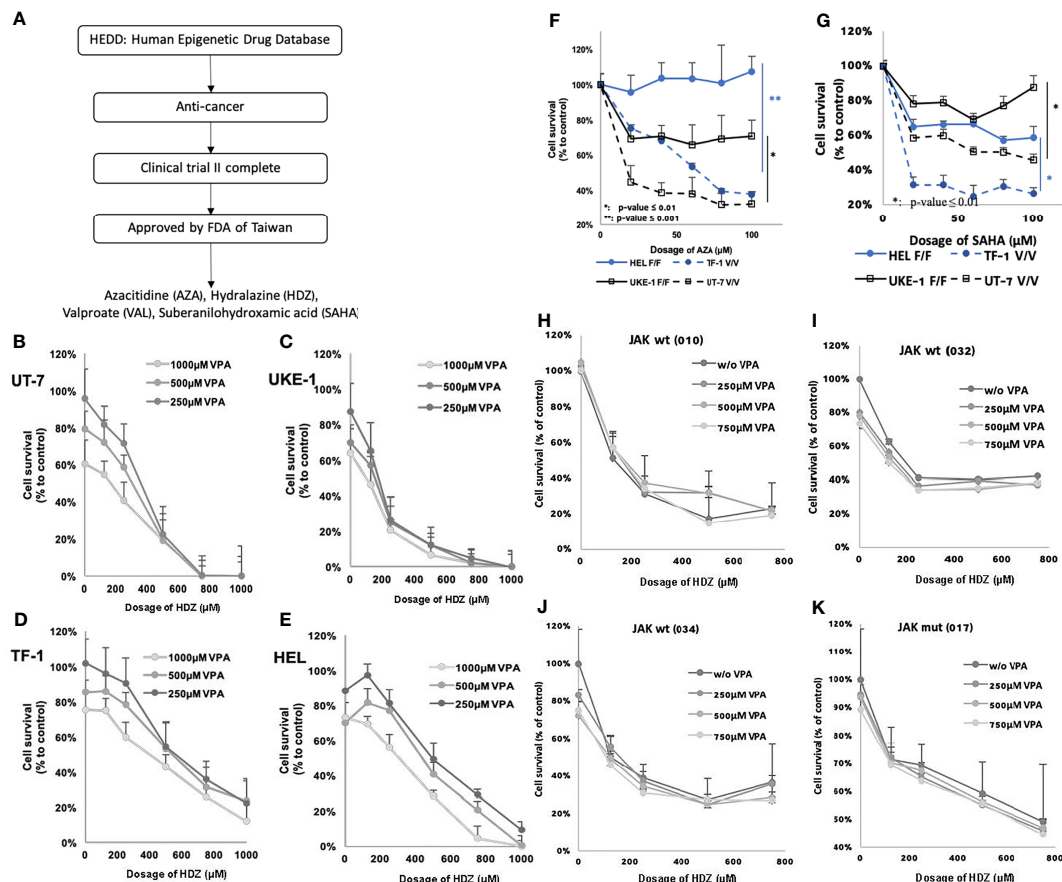


FIGURE 1 | Flowchart showing steps for screening candidate drugs, from *in silico* and *in vitro* to *ex vivo*. (A) *In-silico* screening led to four candidate drugs AZA, HDZ, VAL, and SAHA. (B–E) JAK2V617F mutation may affect the therapeutic efficacy of AZA and SAHA, but not of HDZ-VAL. The cell survival of four MPN cell lines treated with HDZ-VAL combination. (F, G) The cell survival rate of four MPN cell lines treated with AZA or SAHA. (H–K) The inhibitory efficacy of cell survival rate after HDZ-VAL combinational treatment on the leukocytes of PV or ET patients.

American Type Culture Collection (ATCC, VA, USA). The UKE-1 (GM23245 B, RRID: CVCL_0104) cell line was purchased from Coriell Institute (Camden, NJ, USA). The TF-1 (RRID: CVCL_0559) cell line was kindly given by Dr. Jeffrey Jong-Young Yen (Institute of Biomedical Sciences, Academia Sinica, Taipei, Taiwan) and identified as a 100% match with the STR profile recorded in DSMZ (German Collection of Microorganisms and Cell Cultures GmbH, Braunschweig, Germany) (The result of STR profile is not shown).

UT-7, UKE-1, and HEL cells were cultured in RPMI 1640 medium supplied with 10% fetal bovine serum, 2 g/l sodium bicarbonate, 2.5 g/l D-glucose, 110 mg/l sodium pyruvate, and 0.5 µg/ml Mycoplasma Removal Agent (MP Biomedicals, Illkirch, France). TF-1 cells were cultured in RPMI 1640 medium under similar conditions and additionally supplied with 2 ng/ml GM-CSF. Cells were seeded onto 96-well plates at a density of 10,000 per well with/without exposure to candidate drugs. After incubation for 3 days, 10 µl of MTT reagent (1 mg/ml) was added into each well and incubated for 4 h. Then, 37% formaldehyde solution was added (final concentration 4%), and cells were sedimented by using

centrifugation at $1,000 \times g$ for 10 min at room temperature. The medium was removed carefully, and the formazan crystal was dissolved in 50 µl of DMSO. The absorption at 570 nm was read by an ELISA reader. The read was marked as T_i for the test and C for that with no drug. The cell viability was calculated by the following formula:

$$\text{Cell viability} = T_i / C \times 100\% \quad \text{Cell viability} = T_i / C \times 100\%$$

Data Source

The National Health Insurance (NHI) Program was started in Taiwan in 1995 and enrolled more than 99.9% of the Taiwan population, by the end of 2014, according to Liang-Yu Lin (16). NHIRD is a nationally representative cohort that contains detailed registry and claims data from all 23 million residents of Taiwan, including outpatient departments and the inpatient hospital care settings. NHIRD collects basic demographic information, including gender, birthday, insurance premium, prescriptions, operations, investigations, medical encounters, and disease diagnoses according to International Classification

of Diseases, 9th Revision, Clinical Modification (ICD-9-CM) codes. All diagnoses of HNs in Taiwan are made by board-certified clinicians. The Bureau of NHI (a single-payer health insurance system) respectively and randomly reviewed the medical records of 1 in 100 ambulatory care visits and 1 in 20 inpatient claims to verify the accuracy of the diagnoses and appropriate management (see dataset link in section of *Data Availability Statement*). While only a small number of validation studies with small sample sizes have been undertaken, they have generally reported positive predictive values of over 70% for various diagnoses (17, 18). To date, over 2,700 peer-reviewed studies have been published using NHIRD data. Longitudinal Health Insurance Database (LHID) 2000–2015, a subset of the NHIRD (14), was used for this study. LHID 2000–2015 contains all the original claim data of 1,936,512 registries enrolled in year 2005 randomly sampled from the year 2005 Registry for Beneficiaries (ID) of the NHIRD. There are approximately 25.68 million individuals in this registry. There was no significant difference in the age distribution, average insured payroll-related amount, or gender distribution ($\chi^2 = 0.008$, $df = 1$, p value = 0.931) between the patients in the LHID 2000–2015 and the original NHIRD.

Sample Selection

Patients who were treated with either HDZ or VAL continuously for more than 180 days during 2000–2015 were selected and assigned to the exposure group. Enrolling subjects in the exposure group was based on the drug prescriptions presented in medical records or patients' profile. The index date refers to the date that the patient was registered in the database; follow-up began after this date. The inclusion date is defined as day 181 after successive exposure to HDZ or VAL. Subjects, who had been treated with HDZ or VAL before the index date, had been treated with HDZ and VAL simultaneously, had HN before tracking, had lost proper records of their HDZ or VAL dosage and duration, and were younger than 20 years or whose gender was not known were all not included. Exposure groups that were treated with HDZ or VAL were 1:1 matched and referred to as the "HDZ group" and "VAL group", respectively. Subjects without HDZ and VAL exposure were 4:1 matched to HDZ and VAL exposure groups and served as a reference group. All the subjects were matched according to baseline variables such as age, gender, and index date.

To investigate the effect of the dosage of HDZ or VAL on the association with HN incidence, a stratified analysis was applied initially using three levels of dosage: 0%–33%, 34%–66%, 67%–100% of DDD, which is 2,000 mg per day for VAL and 300 mg per day for HDZ, according to maximal daily consumption. In a further HDZ cohort study, a lower level of dose range, 100 mg per day, according to WHO DDD guidance, was analyzed.

Covariates

The covariates included gender, age groups (20–29, 30–39, 40–49, 50–59, and over 60 years old), educational levels (under 12 or over 12 years), marital status (married or unmarried), healthcare insurance premium [$<18,000$, $18,000$ – $34,999$, $\geq 35,000$ New Taiwan Dollars (NT\$)], seasons, location of residence (north, center, south, and east of Taiwan), urbanization level of residence (levels 1 to 4), and level of hospital (medical center, regional

hospital, or local hospital). The urbanization level of residence was defined based on population and several indicators of developmental level. Level 1 was defined in areas containing a population more than 1,250,000 with a specific designation of political, economic, cultural, and metropolitan development. Level 2 was defined as a population in the range of 500,000 to 1,249,999 with an important role in politics, economy, and culture. Level 3 and level 4 were defined as a population in the range 150,000 to 499,999 and under 149,999, respectively.

The comorbidities included hypertension (HTN, ICD-9-CM 401–405), gestational HTN (ICD-9-CM 642.0–642.3, 642.7, 642.9), idiopathic pulmonary artery hypertension (IPAH, ICD-9-CM 416.0), congestive heart failure (CHF, ICD-9-CM 428), affective psychosis (ICD-9-CM 296), epilepsy (ICD-9-CM 345), migraine (ICD-9-CM 346), pulmonary embolism (PE, ICD-9-CM 415.1), gastric ulcer (ICD-9-CM 531), peptic ulcer disease (PUD, ICD-9-CM 533), gastrojejunal ulcer (ICD-9-CM 534), gastrointestinal hemorrhage (ICD-9-CM 578), Budd-Chiari syndrome (ICD-9-CM 453.0), cerebral thrombosis (ICD-9-CM 434.0), ischemic heart disease (IHD, ICD-9-CM 411), vascular insufficiency of intestine (ICD-9-CM 557), obesity (ICD-9-CM 278), and hepatitis B virus (HBV, ICD-9-CM 070.2–070.3). The Charlson Comorbidity Index after removal of the aforementioned comorbidities and malignancies (CCI_R) was used to evaluate the extent of the comorbidities.

Outcome Measure

The HNs described in this study follow the ICD guidelines for hematological disorders: (1) lymphosarcoma and reticulosarcoma and other specified malignant tumors of lymphatic tissue (ICD-9-CM 200); (2) Hodgkin's disease (ICD-9-CM 201); (3) other malignant neoplasms of lymphoid and histiocytic tissue (ICD-9-CM 202); (4) multiple myeloma and immunoproliferative neoplasms (ICD-9-CM 203); (5) lymphoid leukemia (ICD-9-CM 204); (6) myeloid leukemia (ICD-9-CM 205); (7) monocytic leukemia (ICD-9-CM 206); (8) other specified leukemia (ICD-9-CM 207); (9) leukemia of unspecified cell type (ICD-9-CM 208); (10) MPN-like neoplasm (ICD-9-CM 238.4-polycythemia vera; ICD-9-CM 238.5-neoplasm of uncertain behavior of histiocytic and mast cells; ICD-9-CM 238.6-neoplasm of uncertain behavior of plasma cells; ICD-9-CM 238.71-essential thrombocythemia); (11) MDS (ICD-9-CM 238.72-low grade myelodysplastic syndrome lesions; ICD-9-CM 238.73-high grade myelodysplastic syndrome lesions; ICD-9-CM 238.74-myelodysplastic syndrome with 5q deletion; ICD-9-CM 238.75-myelodysplastic syndrome, unspecified; ICD-9-CM 238.76-myelofibrosis with myeloid metaplasia; ICD-9-CM 238.79-other lymphatic and hematopoietic tissues; ICD-9-CM 289.83-myelofibrosis); (12) paraproteinemia (ICD-9-CM 273.1-monoclonal paraproteinemia; ICD-9-CM 273.2-other paraproteinemias; ICD-9-CM 273.3-macroglobulinemia; ICD-9-CM 273.8-other disorders of plasma protein metabolism; ICD-9-CM 273.9-unspecified disorder of plasma protein metabolism); and (13) other polycythemia (ICD-9-CM 289.0-polycythemia, secondary; ICD-9-CM 289.6-familial polycythemia) (**Table S1**).

The 1st endpoint in the cohort was defined as the time to stop follow-up when the diagnosis of any HN was made for a subject;

while the 2nd endpoint was defined as the end of tracking when follow-up of all the subjects was stopped. To prevent multiple counting of HN on each subject, the HR of overall HR was not calculated at the 2nd endpoint.

Statistical Analysis

SPSS software v.22.0 (IBM Corp., Armonk NY, USA) was used for all analysis. The chi-square test was used to compare categorical variables by different treatment type when the categorical outcomes were larger than 5 and Fisher's exact test was used when the categorical outcome was smaller than 5. One-way ANOVA with Scheffe *post-hoc* test was used to compare continuous variables. The Kaplan–Meier method and log-rank test with follow-up time as time scale were used to evaluate the difference of cumulative incidence of HNs between the three groups. Multivariate Cox regression analysis adjusted by covariates mentioned above was used to determine the association of HNs, and the results were presented as a hazard ratio (HR) with a 95% confidence interval (CI). A two-tailed *p* value of less than 0.001 was considered statistically significant (19). We used Schoenfeld's global test to evaluate proportional-hazards assumption (20).

In order to verify the substantial therapeutic potential of the drugs, a sensitivity analysis which excluded the patients earlier diagnosed with HNs after the tracking year was performed. For causal analysis of competing risks, the Fine and Gray competing risk model with all-cause mortality as variant was used to confirm competing risk of mortality (21).

RESULTS

Candidate Drug Selection From the Human Epigenetic Drug Database

A total of 64 epigenetic drugs were listed in the HEDD. Thirty-three of them have been studied for cancer therapy. Listed drugs which were still under development in preclinical or clinical phase I or II trials were excluded (Table S2). Finally, four epigenetic drug candidates were selected from HEDD because they had been reported to have antitumor activity and had passed a phase II clinical trial to prove their safety. The drugs chosen were two DNMTi—AZA and HDZ, and two HDACi—VAL and SAHA (Figure 1A). Furthermore, HDZ and VAL among the above four drugs were found to exert stronger cytotoxicity on HN cell lines and on leukocytes prepared from clinical discarded blood over therapeutic phlebotomy, in comparison with SAHA and AZA which showed much less cytotoxicity (Figures 1B–K). Thus, HDZ and VAL were chosen for the present retrospective cohort study.

Sample Selection Criteria and Flowchart

Among a total of 1,936,512 outpatient and inpatient registries of the NHIRD in Taiwan during 2000–2015, 115,612 subjects were enrolled. Of these, 28,951 subjects were excluded based on the criteria listed in *Material and Methods*. Of the remaining 86,661 subjects, 75,612 subjects were matched to the HDZ exposure

group and 11,049 were matched to the VAL exposure group. Initially, the number of subjects matching the VAL exposure group (11,049) was adopted for both HDZ and VAL exposure group for the purpose of comparing the potential association between their prescription and HN incidence. The 4-fold (44,196) subjects were randomly selected as the reference group from the non-exposure subjects, respectively (Figure 2A). The stratified higher DDD of HDZ (300 mg per day) and VAL (2,100 mg per day), referring to maximal daily consumption, was initially adopted for comparison. Later, a further cohort study focusing on a lower level of dose range of HDZ (100 mg per day) following the WHO DDD guidance was analyzed since HDZ was associated with a much higher reduction of HN incidence than VAL. The dose effect was illustrated by stratification of dose into three levels: high ($\geq 67\%$), intermediate (34%–66%), and low (<34%).

Characteristics of the Study Population

Covariates such as gender, age, marital status, educational level, healthcare insurance premium, comorbidities, season, location of residence, urbanization level of residence, and level of hospital were taken as baseline. Overall, percentage of male subjects was a little higher but not significant than that of female. The proportion of subjects aged 60 years and older is approximately 57%. While about one-third of subjects lived in the north part of Taiwan or high urbanization level of region, the index of hospital level was about equally distributed from medical center to local hospital. Comorbidities such as HTN, affective psychosis, gastrojejunal ulcer, Budd-Chiari syndrome, IHD, and HBV are independent risk factors. Nevertheless, the CCI_R ratio was positively associated with the incidence of HN (Tables S3, S4).

The Association of HN Incidence

In this initial cohort study, the association of HN incidence with HDZ and VAL exposure was compared in contrast to the reference group. At the endpoint of follow-up, 431 subjects (3.90%) in the HDZ exposure group while 492 subjects (4.45%) in the VAL exposure group were diagnosed with HN. However, up to 2,197 subjects (4.97%) were diagnosed with HN in the reference group (Figure 2A). After adjusting for the covariates by the multivariate Cox regression analysis, the adjusted HRs of being diagnosed with HN were recorded and are presented in Table 1. The adjusted HR of the HDZ exposure group to overall HN was significantly lower than that of the reference group ($p < .001$, 95% CI: 0.522–0.840), but the VAL exposure group showed no significant difference ($p = .075$, 95% CI: 0.642–1.032).

The Kaplan–Meier curves of the cumulative incidence of HN over the 15-year follow-up period showed a minor difference but did not reach significance between the HDZ and VAL exposure groups in contrast to the reference group (log-rank test $p = .033$). A lower cumulative incidence in the HDZ group ($p < .001$) in comparison with the reference group was revealed, and it was less significant in the VAL group vs. reference group and HDZ group vs. VAL group (log-rank test $p = .067$ and $.075$, respectively) (Figure 2B).

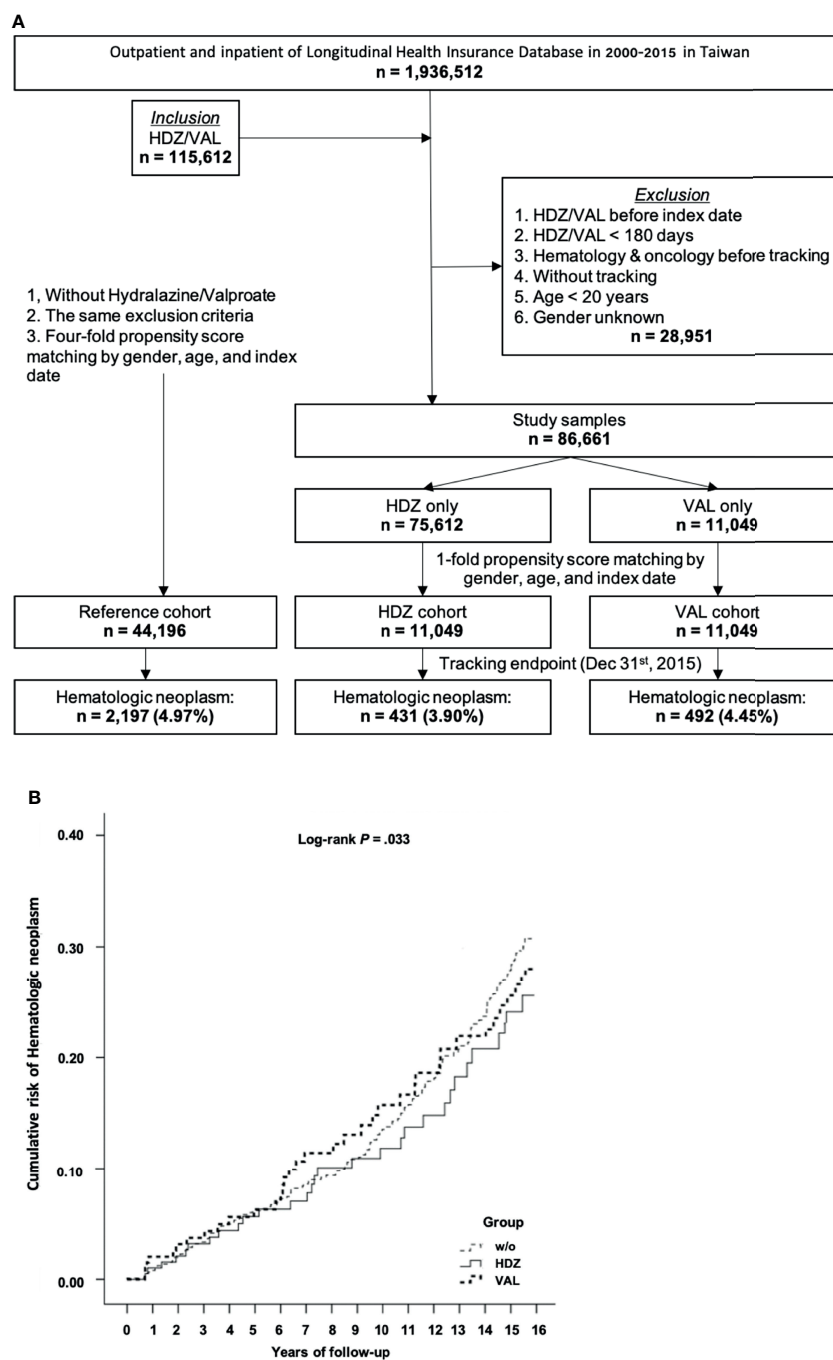


FIGURE 2 | A cohort study for association of HN incidence reduction with HDZ or VAL. **(A)** A flow chart showing the steps for sample-subject selection for the cohort study based on chronic prescription of HDZ and VAL. **(B)** The Kaplan–Meier curve of the cumulative incidence of being diagnosed with HN among the different groups with log-rank test. Log-rank test: without vs. hydralazine, $p < .001$; without vs. valproate, $p = .067$; hydralazine vs. valproate, $p = .075$.

We decided to run a further cohort study focusing on HDZ (100 mg per day) at a stratified and lower level of dose range according to WHO DDD guidance. In this study, the subjects (75,612) matching the inclusion criteria in the HDZ group and 302,448 (four-fold) subjects without exposure of HDZ randomly selected for the reference group were compared (**Figure 3A**).

Among them, 2,910 subjects (3.85%) were diagnosed with HN after exposure with HDZ while 15,151 subjects (5.01%) were diagnosed with HN in the reference group (**Figure 3A**). The Kaplan–Meier curve of the HDZ group demonstrated a much lower cumulative incidence than the reference group from the 9th year of tracking (**Figures 3B, C**). A Schoenfeld’s global test with

TABLE 1 | Adjusted HR of HN according to subgroup stratified by dose level of HDZ and VAL.

Hematologic Neoplasm Subgroup	Drug, Dose (DDD ^b)	1 st Endpoint ^a			2 nd Endpoint ^a				
		Adjusted HR	95% CI		<i>p</i>	Adjusted HR	95% CI		<i>p</i>
Overall	Without	Reference							
	Hydralazine	0.714	0.522	0.840	2.57E-12				
	<34%	0.772	0.565	0.908	2.98E-11				
	34%–66%	0.713	0.522	0.839	3.36E-12				
	≥67%	0.569	0.416	0.669	4.06E-13				
	Valproate	0.877	0.642	1.032	.075				
	<34%	0.909	0.665	1.070	.106				
	34%–66%	0.885	0.648	1.042	.089				
Lymphosarcoma and reticulosarcoma	Without	Reference				Reference			
	Hydralazine	0.728	0.533	0.857	3.57E-6	0.737	0.540	0.868	3.64E-6
	<34%	1.515	0.908	1.782	.202	1.534	0.919	1.804	.225
	34%–66%	0	–	–	.998	0.812	0.597	0.972	5.78E-7
	≥67%	0	–	–	.999	0.675	0.317	0.875	4.03E-8
	Valproate	1.175	0.860	1.382	.187	1.190	0.871	1.399	.208
	<34%	1.631	0.943	1.919	.371	1.651	0.955	1.943	.413
	34%–66%	1.186	0.868	1.395	.190	1.201	0.879	1.412	.211
Hodgkin's disease	Without	Reference				Reference			
	Hydralazine	0.642	0.470	0.756	2.79E-6	0.650	0.476	0.765	4.82E-6
	<34%	0.891	0.652	1.048	.065	0.902	0.660	1.061	.072
	34%–66%	0.649	0.475	0.763	4.50E-7	0.657	0.481	0.772	5.96E-6
	≥67%	0	–	–	.997	0.524	0.311	0.670	8.06E-5
	Valproate	1.152	0.843	1.355	.246	1.166	0.853	1.372	.274
	<34%	1.439	0.953	1.693	.201	1.457	0.965	1.714	.224
	34%–66%	1.395	0.921	1.641	.190	1.412	0.932	1.661	.211
Other malignant neoplasms of lymphoid and histiocytic tissue	Without	Reference				Reference			
	Hydralazine	0.634	0.464	0.746	8.83E-10	0.626	0.458	0.737	2.67E-9
	<34%	0.681	0.498	0.801	6.25E-9	0.673	0.492	0.791	9.33E-9
	34%–66%	0.620	0.453	0.729	5.37E-10	0.612	0.447	0.72	7.82E-10
	≥67%	0.540	0.395	0.635	4.24E-11	0.533	0.390	0.627	6.61E-11
	Valproate	0.858	0.628	1.010	.054	0.848	0.620	0.998	.049
	<34%	0.916	0.670	1.078	.073	0.905	0.662	1.065	.066
	34%–66%	0.866	0.634	1.019	.059	0.855	0.626	1.007	.053
Multiple myeloma and immunoproliferative neoplasms	Without	Reference				Reference			
	Hydralazine	0.578	0.423	0.680	7.86E-8	0.571	0.418	0.672	2.06E-9
	<34%	0.668	0.489	0.786	5.25E-8	0.66	0.483	0.776	1.14E-9
	34%–66%	0.519	0.38	0.611	6.56E-8	0.513	0.375	0.604	1.87E-9
	≥67%	0.452	0.331	0.532	9.25E-8	0.446	0.327	0.526	4.26E-8
	Valproate	0.830	0.607	0.976	.040	0.820	0.600	0.964	.036
	<34%	0.864	0.632	1.016	.168	0.853	0.624	1.004	.151
	34%–66%	0.837	0.612	0.985	.044	0.827	0.605	0.973	.040
Lymphoid leukemia	Without	Reference				Reference			
	Hydralazine	0.420	0.307	0.494	3.37E-5	0.425	0.311	0.500	5.86E-6
	<34%	0	–	–	.985	0.382	0.135	0.491	4.50E-5
	34%–66%	0.849	0.621	0.998	.048	0.859	0.629	1.01	.053
	≥67%	0.740	0.541	0.870	2.65E-6	0.749	0.548	0.881	3.83E-6
	Valproate	0.603	0.441	0.709	4.52E-7	0.610	0.446	0.718	5.58E-7
	<34%	0	–	–	.988	0.284	0.161	0.579	6.86E-5
	34%–66%	1.369	0.991	1.610	.188	1.386	0.978	1.630	.209
Myeloid leukemia	Without	Reference				Reference			
	Hydralazine	0.520	0.38	0.612	7.72E-8	0.526	0.385	0.620	7.98E-8
	<34%	0.866	0.633	1.018	.056	0.877	0.641	1.031	.062
	34%–66%	0	–	–	.993	0.482	0.161	0.597	6.45E-8
	≥67%	0.549	0.402	0.646	6.24E-8	0.556	0.407	0.654	9.03E-8
	Valproate	0.895	0.655	1.053	.176	0.906	0.663	1.066	.196

(Continued)

TABLE 1 | Continued

Hematologic Neoplasm Subgroup	Drug, Dose (DDD ^b)	1 st Endpoint ^a				2 nd Endpoint ^a			
		Adjusted HR	95% CI		<i>p</i>	Adjusted HR	95% CI		<i>p</i>
Leukemia of unspecified cell type	<34%	1.165	0.852	1.370	.287	1.179	0.863	1.387	.319
	34%–66%	0.678	0.496	0.917	.001	0.686	0.502	0.928	.001
	≥67%	0.591	0.432	0.695	8.01E-6	0.598	0.437	0.704	5.29E-7
	Without	Reference				Reference			
	Hydralazine	0.565	0.413	0.665	6.84E-7	0.558	0.408	0.657	7.89E-7
	<34%	0.588	0.43	0.691	8.25E-7	0.581	0.425	0.683	9.22E-7
	34%–66%	0.666	0.487	0.783	5.77E-7	0.658	0.481	0.773	6.03E-7
	≥67%	0.332	0.242	0.390	3.10E-7	0.328	0.239	0.385	3.40E-7
	Valproate	0.878	0.642	1.033	.135	0.867	0.634	1.020	.121
	<34%	0.914	0.669	1.075	.160	0.903	0.661	1.062	.144
MPN-like neoplasm	34%–66%	0.920	0.673	1.083	.175	0.909	0.665	1.070	.157
	≥67%	0.713	0.522	0.929	.012	0.704	0.516	0.918	.011
	Without	Reference				Reference			
	Hydralazine	0.536	0.392	0.631	7.26E-11	0.529	0.387	0.623	5.20E-10
	<34%	0.558	0.408	0.656	8.82E-11	0.551	0.403	0.648	7.26E-10
	34%–66%	0.541	0.396	0.637	7.04E-11	0.534	0.391	0.629	5.58E-10
	≥67%	0.472	0.345	0.555	6.83E-11	0.466	0.341	0.548	1.24E-10
	Valproate	0.841	0.615	0.989	.043	0.831	0.608	0.977	.039
	<34%	0.801	0.586	0.942	.005	0.791	0.579	0.931	.004
	34%–66%	0.946	0.692	1.113	.169	0.934	0.684	1.099	.167
Paraproteinemia	≥67%	0.761	0.557	0.895	7.80E-8	0.752	0.55	0.884	1.04E-9
	Without	Reference				Reference			
	Hydralazine	0.537	0.393	0.632	5.28E-7	0.53	0.388	0.624	6.62E-8
	<34%	0.621	0.454	0.730	3.03E-7	0.613	0.448	0.721	5.04E-8
	34%–66%	0.543	0.397	0.638	5.99E-7	0.536	0.392	0.630	6.88E-8
	≥67%	0.315	0.231	0.371	4.81E-7	0.311	0.228	0.366	4.82E-8
	Valproate	0.771	0.564	0.906	.001	0.762	0.557	0.895	5.54E-6
	<34%	0.802	0.587	0.944	.020	0.792	0.580	0.932	.018
	34%–66%	0.778	0.569	0.915	.007	0.769	0.562	0.904	.006
	≥67%	0.678	0.496	0.798	5.11E-8	0.67	0.490	0.788	4.85E-9
Other polycythemia	Without	Reference				Reference			
	Hydralazine	0.751	0.549	0.883	6.11E-10	0.76	0.556	0.894	7.02E-9
	<34%	0.742	0.542	0.872	6.27E-10	0.751	0.549	0.883	8.11E-9
	34%–66%	0.772	0.564	0.908	5.74E-10	0.782	0.571	0.919	7.34E-9
	≥67%	0.740	0.541	0.870	5.22E-10	0.749	0.548	0.881	6.26E-9
	Valproate	0.849	0.621	1.009	.062	0.859	0.629	1.021	.069
	<34%	0.884	0.647	1.004	.097	0.895	0.655	1.053	.108
	34%–66%	0.871	0.637	1.024	.086	0.882	0.645	1.037	.096
	≥67%	0.723	0.529	0.851	7.80E-9	0.732	0.536	0.862	8.34E-9

^aThe 1st endpoint in the cohort was defined as the date to stop follow-up when the diagnosis of any HN was made for a subject; while the 2nd endpoint was defined as the end of tracking when follow-up of all the subjects was stopped.

^bDDD for HDZ = 300 mg/day, for VAL = 2,100 mg/day. 44,196 subjects who did not receive hydralazine or valproate enrolled in analysis. A total of 11,049 subjects received hydralazine, of which 5,311 received less than 34% DDD, of which 3,646 with 34%–66% DDD, of which 2,092 received more than 67% DDD. A total of 11,049 subjects received valproate, of which 5,307 received less than 34% DDD, of which 3,649 with 34%–66% DDD, of which 2,093 received more than 67% DDD.

Adjusted HR, adjusted hazard ratio; CI, confidence interval.

p value at 0.9014, higher than 0.05, is not against proportional hazards assumption. The Kaplan–Meier curve for cumulative incidence of HN stratified by HDZ dose was disclosed in **Figure 3D**.

Association of Each HN Subgroup Incidence With Stratified Doses

At the 1st endpoint, the adjusted HRs of all the subgroups in the HDZ group without stratification of the DDD were significantly lower. In the group of overall HN, as well as the subgroups of other malignant neoplasms of lymphoid and histiocytic tissue, multiple myeloma and immunoproliferative neoplasms, leukemia of unspecified cell type, MPN-like neoplasm,

paraproteinemia, and other polycythemia, the adjusted HRs of each dose level under defined stratifications were all significantly lower; the adjusted HRs of Hodgkin's disease, lymphoid leukemia, and myeloid leukemia subgroups were significantly lower at median- and/or highest-dose levels (**Table 1**). The association of incidence of each subgroup of HN in the VAL exposure group showed dose-dependent significance (**Table 1**).

Focusing on the association study of HN incidence in the HDZ exposure group, subjects receiving HDZ with a dose lower than 34 mg per day showed significantly lower HR in overall HNs and in several subgroups such as multiple myeloma and immunoproliferative neoplasms, lymphoid leukemia, myeloid leukemia, leukemia of unspecified cell type, MPN-like

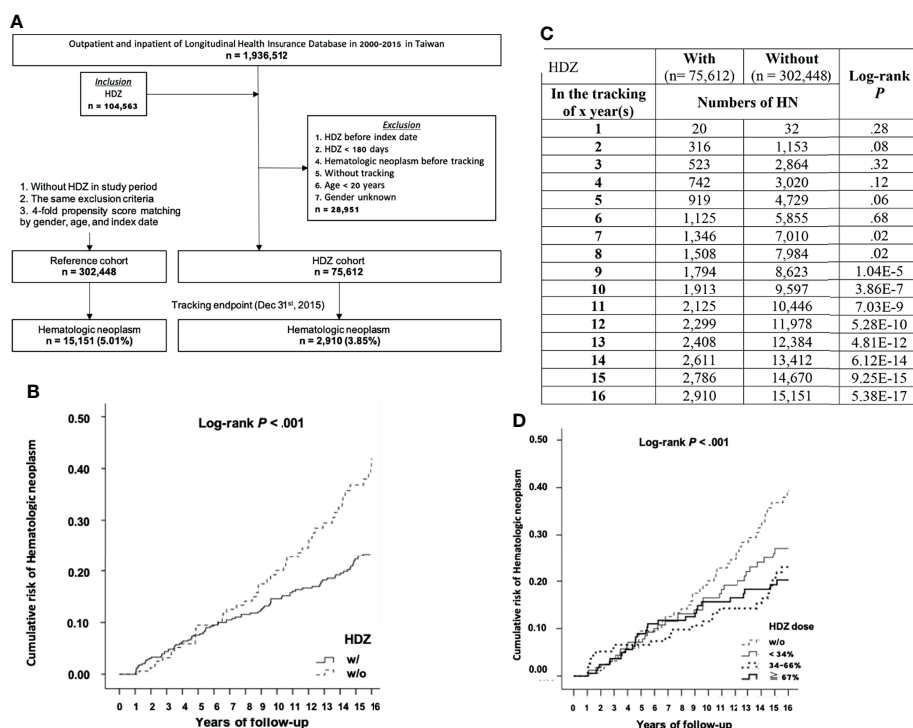


FIGURE 3 | A cohort study focusing on the association of HN incidence reduction with HDZ. **(A)** A flowchart showing sample-subject selection for the cohort study. **(B, C)** The Kaplan-Meier curve for cumulative incidence of HN with log-rank test. **(D)** A Kaplan-Meier curve for cumulative incidence of HN stratified by HDZ dose (% to DDD set as 100 mg per day) with the log-rank test.

neoplasm, MDS, and paraproteinemia ($p < 0.001$ for each subgroup). All the subgroups mentioned above showed a dose-dependent reduction of HR (Table 2).

The associations of HN incidence for each subgroup at the 2nd endpoint are presented in Tables 1, 2. No significant difference of adjusted HR was found between the 1st and 2nd endpoints, showing that subgroups of HN may not compete with each other. Nevertheless, the probability of coincident occurrence of two subgroups of HN in one subject is very few. For the unassociated subgroups of HN even at high doses, the low disease number can be one of the causes. The subject numbers of most subgroups as mentioned above show sufficient number and significance at the 2nd endpoint.

In addition, subjects who had ever been diagnosed with HTN were selected for analysis since HDZ was often prescribed for HTN. However, no significant association was seen (Table S5). The period between start of tracking point and year diagnosed with HN in subjects with HDZ exposure was also significantly longer than those without HDZ ($p = 2.176E-13$, Table S6).

A Sensitivity Analysis for the Association Between the Drugs and HN Incidence

In a cohort study containing VAL, the adjusted HR matching the first endpoint of VAL groups without exclusion, 1st-year exclusion, and 3rd-year exclusion were 0.877, 0.884, and 0.927, respectively. The adjusted HR in the HDZ groups after exclusion of patients diagnosed with HN in the first 1 and 3 years were

0.720 and 0.756, respectively (both $p < 0.001$), in comparison to that without exclusion which was 0.714 ($p < 0.001$) (Table S7). In the further cohort study focusing on HDZ, the adjusted HRs were 0.741 and 0.720 respectively in the HDZ group after exclusion of HN patients in the first 1 and 5 years, in comparison to that without exclusion was 0.730 (Table S8).

In addition, the results obtained from the Fine and Gray competing risk model using all-cause mortality as a competing variable were similar with that obtained from the no competing risk model, indicating that mortality was not a competing variable of HN (Tables S7, S8).

DISCUSSION

Over the last decade, several clinical trials have revealed that a combination of HDZ and VAL is a promising therapy for the several hematological malignancies, including mycosis fungoides (22), MDS (23, 24), CTCL (25, 26), AML (27), chronic myeloid leukemia (CML) (28). However, there has been no integral analysis targeting all the HNs as outcomes based on a large health insurance database.

Once HN is diagnosed, the family incurs a heavy financial burden due to a long period of treatment and a low survival rate within 15 years. Our study revealed that prescription of HDZ or even VAL brought beneficial effects to unforeseen patients of particular subgroups of HN. Our results may indicate inadvertent

TABLE 2 | Adjusted HR of HN according to subgroup stratified by dose level of HDZ.

Hematologic Neoplasm Subgroup	HDZ, dose (DDD ^b)	1 st Endpoint ^a				2 nd Endpoint ^a			
		Adjusted HR	95% CI		p	Adjusted HR	95% CI		p
Overall	Without	Reference							
	With	0.730	0.621	0.793	1.73E-18				
	<34%	0.791	0.578	0.927	3.56E-18				
	34%–66%	0.728	0.530	0.858	2.45E-18				
	≥67%	0.581	0.427	0.684	1.21E-18				
Lymphosarcoma and reticulosarcoma	Without	Reference				Reference			
	With	0.911	0.853	0.973	.027	0.922	0.864	0.985	.030
	<34%	1.031	0.965	1.112	.298	1.044	0.977	1.126	.331
	34%–66%	0.879	0.821	0.940	2.59E-04	0.890	0.831	0.952	.017
	≥67%	0.581	0.543	0.620	6.62E-05	0.588	0.55	0.628	6.83E-05
Hodgkin's disease	Without	Reference				Reference			
	With	0.893	0.837	0.956	.004	0.904	0.847	0.968	.004
	<34%	0.952	0.892	0.972	.027	0.964	0.903	0.984	.030
	34%–66%	0.876	0.824	0.934	1.26E-04	0.887	0.834	0.946	.003
	≥67%	0.752	0.708	0.810	3.31E-05	0.761	0.717	0.820	2.87E-04
Other malignant neoplasms of lymphoid and histiocytic tissue	Without	Reference				Reference			
	With	0.845	0.797	0.906	6.27E-05	0.835	0.787	0.895	3.59E-05
	<34%	0.936	0.878	0.998	.048	0.925	0.867	0.986	.043
	34%–66%	0.761	0.715	0.816	8.00E-07	0.752	0.706	0.806	6.78E-07
	≥67%	0.742	0.698	0.807	4.13E-06	0.733	0.689	0.797	2.18E-06
Multiple myeloma and immunoproliferative neoplasms	Without	Reference				Reference			
	With	0.816	0.763	0.872	6.29E-13	0.806	0.754	0.861	7.89E-13
	<34%	0.825	0.775	0.880	7.89E-12	0.815	0.766	0.869	9.24E-12
	34%–66%	0.820	0.768	0.876	3.12E-13	0.810	0.759	0.865	4.50E-13
	≥67%	0.779	0.724	0.831	4.67E-12	0.770	0.715	0.821	5.98E-12
Lymphoid leukemia	Without	Reference				Reference			
	With	0.698	0.656	0.749	3.58E-17	0.707	0.664	0.758	4.89E-17
	<34%	0.793	0.741	0.848	5.13E-17	0.803	0.750	0.858	7.23E-17
	34%–66%	0.652	0.608	0.698	6.99E-18	0.660	0.616	0.707	7.00E-18
	≥67%	0.494	0.452	0.531	2.79E-20	0.500	0.458	0.538	3.15E-20
Myeloid leukemia	Without	Reference				Reference			
	With	0.759	0.711	0.813	5.56E-17	0.768	0.720	0.823	3.79E-17
	<34%	0.832	0.782	0.898	2.58E-16	0.842	0.792	0.909	5.29E-17
	34%–66%	0.681	0.634	0.735	6.90E-18	0.689	0.642	0.744	7.18E-18
	≥67%	0.666	0.621	0.720	2.01E-19	0.674	0.629	0.729	2.98E-20
Monocytic leukemia	Without	Reference				Reference			
	With	–	–	–	–	0.862	0.625	1.297	.211
	<34%	–	–	–	–	0.975	0.704	1.486	.289
	34%–66%	–	–	–	–	0.813	0.583	1.031	.135
	≥67%	–	–	–	–	0.771	0.492	0.997	.047
Other specified leukemia	Without	Reference				Reference			
	With	1.086	0.303	1.986	.721	1.099	0.307	2.011	.802
	<34%	1.642	0.562	2.111	.521	1.662	0.569	2.137	.580
	34%–66%	0	–	–	.999	1.374	0.289	1.975	.765
	≥67%	0	–	–	.999	1.077	0.161	1.897	.803
Leukemia of unspecified cell type	Without	Reference				Reference			
	With	0.783	0.732	0.839	3.02E-05	0.773	0.723	0.829	2.17E-05
	<34%	0.900	0.848	0.948	2.86E-04	0.889	0.838	0.936	1.01E-04
	34%–66%	0.673	0.634	0.732	3.36E-05	0.665	0.626	0.723	3.15E-05
	≥67%	0.584	0.552	0.637	6.14E-05	0.577	0.545	0.629	5.05E-05
MPN-like neoplasm	Without	Reference				Reference			
	With	0.767	0.718	0.820	6.65E-07	0.758	0.709	0.810	6.26E-07
	<34%	0.817	0.764	0.872	7.80E-07	0.807	0.755	0.861	6.99E-07
	34%–66%	0.781	0.732	0.834	5.46E-07	0.771	0.723	0.824	3.08E-07
	≥67%	0.588	0.551	0.636	2.39E-08	0.581	0.544	0.628	1.09E-08
MDS	Without	Reference				Reference			
	With	0.820	0.764	0.879	6.29E-06	0.810	0.755	0.868	3.19E-06
	<34%	0.871	0.816	0.937	3.86E-05	0.860	0.806	0.926	9.78E-06
	34%–66%	0.860	0.801	0.92	5.48E-05	0.850	0.791	0.909	4.27E-05
	≥67%	0.564	0.522	0.617	3.59E-09	0.557	0.516	0.609	2.85E-09

(Continued)

TABLE 2 | Continued

Hematologic Neoplasm Subgroup	HDZ, dose (DDD ^b)	1 st Endpoint ^a				2 nd Endpoint ^a			
		Adjusted HR	95% CI		p	Adjusted HR	95% CI		p
Paraproteinemia	Without	Reference				Reference			
	With	0.777	0.738	0.849	6.65E-12	0.768	0.729	0.839	5.26E-12
	<34%	0.831	0.775	0.884	5.24E-11	0.821	0.766	0.873	2.73E-11
	34%–66%	0.820	0.762	0.871	6.53E-12	0.810	0.753	0.860	4.01E-12
	≥67%	0.511	0.482	0.555	3.12E-14	0.505	0.476	0.548	1.97E-14
Other polycythemia	Without	Reference				Reference			
	With	0.930	0.871	0.989	.039	0.941	0.882	1.001	.051
	<34%	0.936	0.875	0.996	.047	0.948	0.886	1.008	.059
	34%–66%	0.928	0.866	0.972	.020	0.939	0.877	0.984	.022
	≥67%	0.904	0.852	0.962	.003	0.915	0.863	0.974	.003

^aThe 1st endpoint in the cohort was defined as the date to stop follow-up when the diagnosis of any HN was made for a subject, while the 2nd endpoint was defined as the end of tracking when follow-up of all the subjects was stopped.

^bDDD = 100 mg/day. 302,448 subjects who did not receive hydralazine enrolled in analysis. A total of 75,612 subjects received hydralazine, of which 36,349 received less than 34% DDD, of which 24,952 with 34%–66% DDD, of which 14,311 received more than 67% DDD.

Adjusted HR, adjusted hazard ratio; CI, confidence interval.

prophylactic benefit. Early prescription may block MPN evolving to AML or BP-MPN. Therefore, studies focusing on screening the population at high incidence of HN are desirable in the future. HDZ may be studied on other high-risk populations of HN, including the following. (1) Patients who underwent solid organ transplantation (29). Several subgroups of HNs tend to occur in solid organ transplant recipients, because most of them need lifelong immunosuppression to prevent organ rejection. Hodgkin lymphoma, non-Hodgkin lymphomas, acute and chronic leukemias, and plasma cell neoplasms (multiple myeloma and plasmacytoma) are more common for those patients. (2) Those exposed to 1,3-butadiene (30). (3) Females with less exposure to female sex hormones (31). Tanaka and colleagues reported that an increased risk of lymphoid neoplasms as well as a shorter menstrual cycle was found in parous women and women with later onset of menarche. (4) Patients with immunodeficiency and autoimmune diseases (32, 33).

Lymphoid leukemia has been classified by stage of maturation (acute lymphoblastic leukemia or chronic lymphocytic leukemia) or according to cell type from which the tumor cells differentiate (T-cell leukemia, B-cell leukemia, NK-cell leukemia) (34). In T-cell leukemia, HDZ treatment was reported to induce apoptosis and cause DNA damage (35). Due to the fact that HDZ acting as a DNMTi (36) decreases the mRNA level of DNMT1 and DNMT3a (37), the role of DNMT1 in B cell maturation (38) and its aberration in B-cell leukemia have been reported (39). A therapeutic significance of HDZ on B-cells as suggested in this retrospective cohort study is conceivable. In addition, with the support by the role of DNMT1 in MDS and myeloid leukemia as reported in a previous review (40) and reports indicating a reduction in mRNA level of DNMTs by HDZ (37) and an abnormally high expression level of DNMTs in cell lines of MDS and myeloid leukemia including AML and CML (41), we suggest that HDZ alone may have enough efficacy to inhibit MDS or myeloid leukemia while previous trials selected a combination of HDZ and VAL (23, 24, 27, 28).

For drugs being considered for repositioning for therapy of a group of diseases such as HNs or other malignancies, a retrospective

study like ours could serve as a prior test before a clinical trial protocol is adopted on respective subgroups. We propose that HDZ can be a suitable candidate drug to initiate a phase II clinical trial for treatment of various HNs, instead of starting from a phase I clinical trial. Since epigenetic drugs have a global effect on chromatin, its specific mechanism for a particular disease is not properly defined although several epigenetic drugs have been approved by the FDA. Based on results of our study, chronic prescription of HDZ is significantly associated with reduced HN. However, the adverse effects of repurposing drugs could lead to poor therapeutic compliance and may cause loss-to-follow-up bias in further clinical trials. As a consequence, there should be a reasonable strategy to enhance the therapeutic compliance. Accordingly, we identify that HTN is an independently risk factor for HN (adjusted HR = 1.235, 95% CI = 1.098–1.369, $p = 5.267E-18$, **Table S9**). As HDZ is an established antihypertensive agent, prescribing a higher-dose HDZ (≥ 34 mg/day) for HTN participants would ensure better therapeutic compliance than for non-HTN participants. With regard to hypotension-related adverse effects from HDZ prescription, we suggest that prescribing low-dose HDZ (< 34 mg/day) is feasible for non-HTN participants, owing to causing mild adverse effects but maintaining preventive efficacy for HNs.

However, many repurposing drugs may not be indicated due to the imbalance of its therapeutic benefits and adverse effects (42). For example, aspirin which is an agent for inflammatory management or preventing heart attack or stroke has been repurposed for multiple myeloma (43), but it may also cause adverse effects such as GI hemorrhage or vascular insufficiency of the intestine (44, 45). Valproate, a psychotic drug for epilepsy, migraine, or seizures, has been repurposed for multiple myeloma (46), but its original indications are excluded from independent risk factors of HNs (**Table S9**). Nelfinavir is an antiviral drug, acting as protease inhibitor and repurposed for HNs by its activity to inhibit the Akt/PKB signaling pathway or to activate ER stress (47). As repurposing nelfinavir for HNs, subjects may suffer from adverse effects caused by the activity of protease inhibitor such as cardiovascular risks (48). In summary, whether

a repurposing drug is indicated for HNs depends on the balance of its benefit and harm.

As compared with other drug repurposing for HN therapy, HDZ enables larger potential for repurposing owing to its epigenetics-associated chemopreventive and/or therapeutic efficacy for HNs, as well as its approved indication to manage HTN, an independent risk factor of HNs. In addition to HTN, other independent risk factors of HNs have been identified in **Table S9**, including having gastroduodenal ulcer, Budd-Chiari syndrome, or infection of HBV. If HDZ is prescribed for patients having more risk factors of HNs, it may have better chemopreventive and/or therapeutic efficacy than those having no risk factor of HNs. We suggest that a nationwide retrospective study, as such of this study, could provide evidence for further scientific progress in the medical field.

Limitations

There are several limitations to this study. Firstly, like many previous NHIRD-based studies, our study was a retrospective cohort study using ICD-9-CM codes, rather than the direct medical records. Therefore, the accuracy of the records may be an issue. Secondly, the pathological stages and severity of HN are unclear in the NHIRD. Thirdly, the NHIRD did not include genetic, educational, habitual, and dietary factors, like smoking and drinking frequency, body mass index, lifestyle, and real income. Fourthly, we could only estimate treatment durations of candidate drug medication by dividing the cumulative doses of individual medications by the DDD. Therefore, a prospective cohort study design would be needed to get more convincing results. Fifthly, the NHIRD is a database sampling of an Asian population; the findings may not be directly applied to other racial populations. Finally, the size of the database may be a limitation as the diagnosed cases of some HN subgroups like monocytic leukemia and other specified leukemia were too few to be analyzed.

DATA AVAILABILITY STATEMENT

The data analyzed in this study are subject to the following licenses/restrictions: Data are available from the National Health Insurance Research Database (NHIRD) published by the Taiwan National Health Insurance (NHI) Bureau. Due to legal restrictions imposed by the government of Taiwan in relation to the “Personal Information Protection Act,” data cannot be made publicly available. Requests for data can be sent as a formal proposal to the NHIRD (<http://nhird.nhri.org.tw>). Requests to access these datasets should be directed to https://www.nhi.gov.tw/english/Content_List.aspx?n=A7354F4F704B6377&topn=A7354F4F704B6377 (49).

REFERENCES

- Arber DA, Orazi A, Hasserjian R, Thiele J, Borowitz MJ, Le Beau MM, et al. The 2016 Revision to the World Health Organization Classification of Myeloid Neoplasms and Acute Leukemia. *Blood* (2016) 127:2391–405. doi: 10.1182/blood-2016-03-643544

ETHICS STATEMENT

The studies involving human participants were reviewed and approved by the Institutional Review Board of Tri-Service General Hospital (No. 2-108-05-107, B-109-38). The patients/participants provided their written informed consent to participate in this study.

AUTHOR CONTRIBUTIONS

B-HY: English editing, supervising of this work, interpretation of data, overall direction, project administration, and funding acquisition. W-ZL: conducting of the experiments and data acquisition, and interpretation of the data. Y-TC: interpretation of the data. Y-CC: study conceptualization and supervising of this work. C-HC: conducting the experiments and data acquisition. W-CC: interpretation of the data. C-YS: English editing, supervising of this work, interpretation of data, overall direction, project administration, and funding acquisition. All authors contributed to the article and approved the submitted version.

FUNDING

The study was funded by the Ministry of National Defense Medical Affairs Bureau (MAB106-036, MAB107-023), the Teh-Tzer Study Group for Human Medical Research Foundation of Taiwan (B1081050), and the Tri-Service General Hospital Foundation (TSGH-B-110012 and TSGH-B-111018).

ACKNOWLEDGMENTS

The authors thank the staff of the School of Public Health, National Defense Medical Center and Department of Medical Research, Tri-Service General Hospital, for their comments and assistance in data analysis. The present study was based on the National Health Insurance Research Database provided by the Central Bureau of National Health Insurance, the Department of Health, and managed by the National Health Research Institutes.

SUPPLEMENTARY MATERIAL

The Supplementary Material for this article can be found online at: <https://www.frontiersin.org/articles/10.3389/fonc.2022.809014/full#supplementary-material>

- Fitzmaurice C, Akinyemiju TF, Al Lami FH, Alam T, Alizadeh-Navaei R, Allen C, et al. Global, Regional, and National Cancer Incidence, Mortality, Years of Life Lost, Years Lived With Disability, and Disability-Adjusted Life-Years for 29 Cancer Groups 1990 to 2016: A Systematic Analysis for the Global Burden of Disease Study. *JAMA Oncol* (2018) 4:1553–68. doi: 10.1200/JCO.2018.36.15_suppl.1568

3. Kodama Y, Morozumi R, Matsumura T, Kishi Y, Murashige N, Tanaka Y, et al. Increased Financial Burden Among Patients With Chronic Myelogenous Leukaemia Receiving Imatinib in Japan: A Retrospective Survey. *BMC Cancer* (2012) 12:152. doi: 10.1186/1471-2407-12-152
4. Azzani M, Roslani AC, Su TT. The Perceived Cancer-Related Financial Hardship Among Patients and Their Families: A Systematic Review. *Support Care Cancer* (2015) 23:889–98. doi: 10.1007/s00520-014-2474-y
5. Buzaglo JS, Miller MF, Karten C, Longacre M, Kennedy V, Leblanc TW. Multiple Myeloma Patient Experience With Financial Toxicity: Findings From the Cancer Experience Registry. *Blood* (2015) 126:874–4. doi: 10.1182/blood.V126.23.874.874
6. Holliday R. A New Theory of Carcinogenesis. *Br J Cancer* (1979) 40:513–22. doi: 10.1038/bjc.1979.216
7. Shen H, Laird PW. Interplay Between the Cancer Genome and Epigenome. *Cell* (2013) 153:38–55. doi: 10.1016/j.cell.2013.03.008
8. Cheng Y, He C, Wang M, Ma X, Mo F, Yang S, et al. Targeting Epigenetic Regulators for Cancer Therapy: Mechanisms and Advances in Clinical Trials. *Signal Transduct Target Ther* (2019) 4:62. doi: 10.1038/s41392-019-0095-0
9. Matei D, Fang F, Shen C, Schilder J, Arnold A, Zeng Y, et al. Epigenetic Resensitization to Platinum in Ovarian Cancer. *Cancer Res* (2012) 72:2197–205. doi: 10.1158/0008-5472.CAN-11-3909
10. Lee V, Wang J, Zahurak M, Gootjes E, Verheul HM, Parkinson R, et al. A Phase I Trial of a Guadecitabine (SGI-110) and Irinotecan in Metastatic Colorectal Cancer Patients Previously Exposed to Irinotecan. *Clin Cancer Res* (2018) 24:6160–7. doi: 10.1158/1078-0432.CCR-18-0421
11. Matei D, Ghamande S, Roman L, Alvarez Secord A, Nemunaitis J, Markham MJ, et al. A Phase I Clinical Trial of Guadecitabine and Carboplatin in Platinum-Resistant, Recurrent Ovarian Cancer: Clinical, Pharmacokinetic, and Pharmacodynamic Analyses. *Clin Cancer Res* (2018) 24:2285–93. doi: 10.1158/1078-0432.CCR-17-3055
12. Sun W, Triche T Jr, Malvar J, Gaynon P, Spoto R, Yang X, et al. A Phase I Study of Azacitidine Combined With Chemotherapy in Childhood Leukemia: A Report From the TACL Consortium. *Blood* (2018) 131:1145–8. doi: 10.1182/blood-2017-09-803809
13. Jones PA, Ohtani H, Chakravarthy A, De Carvalho DD. Epigenetic Therapy in Immune-Oncology. *Nat Rev Cancer* (2019) 19:151–61. doi: 10.1038/s41568-019-0109-9
14. Hsieh C-Y, Su C-C, Shao S-C, Sung S-F, Lin S-J, Yang Y-HK, et al. Taiwan's National Health Insurance Research Database: Past and Future. *Clin Epidemiol* (2019) 11:349. doi: 10.2147/CLEP.S196293
15. Qi Y, Wang D, Wang D, Jin T, Yang L, Wu H, et al. HEDD: The Human Epigenetic Drug Database. *Database (Oxf)* (2016) 2016. doi: 10.1093/database/baw159
16. Lin LY, Warren-Gash C, Smeeth L, Chen PC. Data Resource Profile: The National Health Insurance Research Database (NHIRD). *Epidemiol Health* (2018) 40:e2018062. doi: 10.4178/epih.e2018062
17. Cheng CL, Kao YHY, Lin SJ, Lee CH, Lai ML. Validation of the National Health Insurance Research Database With Ischemic Stroke Cases in Taiwan. *Pharmacoepidemiol Drug Saf* (2011) 20:236–42. doi: 10.1002/pds.2087
18. Lee PC, Kao FY, Liang FW, Lee YC, Li ST, Lu TH. Existing Data Sources in Clinical Epidemiology: The Taiwan National Health Insurance Laboratory Databases. *Clin Epidemiol* (2021) 13:175–81. doi: 10.2147/CLEP.S286572
19. Armstrong RA. When to Use the Bonferroni Correction. *Ophthalmic Physiol Opt* (2014) 34:502–8. doi: 10.1111/opo.12131
20. Abeysekera W, Sooriyachchi M. Use of Schoenfeld's Global Test to Test the Proportional Hazards Assumption in the Cox Proportional Hazards Model: An Application to a Clinical Study. *J Natl Sci Found* (2009) 37:41–51. doi: 10.4038/jnsfr.v37i1.456
21. Fine JP, Gray RJ. A Proportional Hazards Model for the Subdistribution of a Competing Risk. *J Am Stat Assoc* (1999) 94:496–509. doi: 10.1080/01621459.1999.10474144
22. Duenas-Gonzalez A, Vega MT, Martinez-Banos D, Garcia-Hidalgo L, Sobrevilla P. Response to Hydralazine-Valproate in a Patient With Mycosis Fungoides. *Case Rep Med* (2010) 2010:657579. doi: 10.1155/2010/657579
23. Candelaria M, Herrera A, Labardini J, Gonzalez-Fierro A, Trejo-Becerril C, Taja-Chayeb L, et al. Hydralazine and Magnesium Valproate as Epigenetic Treatment for Myelodysplastic Syndrome. Preliminary Results of a Phase-II Trial. *Ann Hematol* (2011) 90:379–87. doi: 10.1007/s00277-010-1090-2
24. Candelaria M, Burgos S, Ponce M, Espinoza R, Duenas-Gonzalez A. Encouraging Results With the Compassionate Use of Hydralazine/Valproate (TRANSKRIP) as Epigenetic Treatment for Myelodysplastic Syndrome (MDS). *Ann Hematol* (2017) 96:1825–32. doi: 10.1007/s00277-017-3103-x
25. Espinoza-Zamora JR, Labardini-Mendez J, Sosa-Espinoza A, Lopez-Gonzalez C, Vieyra-Garcia M, Candelaria M, et al. Efficacy of Hydralazine and Valproate in Cutaneous T-Cell Lymphoma, a Phase II Study. *Expert Opin Investig Drugs* (2017) 26:481–7. doi: 10.1080/13543784.2017.1291630
26. Scholnik-Cabrera A, Dominguez-Gomez G, Duenas-Gonzalez A. Comparison of DNA Demethylating and Histone Deacetylase Inhibitors Hydralazine-Valproate Versus Vorinostat-Decitabine In Cutaneous T-Cell Lymphoma in HUT78 Cells. *Am J Blood Res* (2018) 8:5–16.
27. Lubbert M, Grishina O, Schmoor C, Schlenk RF, Jost E, Crysan M, et al. Valproate and Retinoic Acid in Combination With Decitabine in Elderly Nonfit Patients With Acute Myeloid Leukemia: Results of a Multicenter, Randomized, 2 X 2, Phase II Trial. *J Clin Oncol* (2020) 38:257–70. doi: 10.1200/JCO.19.01053
28. Cervera E, Candelaria M, Lopez-Navarro O, Labardini J, Gonzalez-Fierro A, Taja-Chayeb L, et al. Epigenetic Therapy With Hydralazine and Magnesium Valproate Reverses Imatinib Resistance in Patients With Chronic Myeloid Leukemia. *Clin Lymphoma Myeloma Leuk* (2012) 12:207–12. doi: 10.1016/j.clml.2012.01.005
29. Dharnidharka VR. Comprehensive Review of Post-Organ Transplant Hematologic Cancers. *Am J Transplant* (2018) 18:537–49. doi: 10.1111/ajt.14603
30. Sielken RL Jr, Valdez-Flores C. Butadiene Cancer Exposure-Response Modeling: Based on Workers in the Styrene-Butadiene-Rubber Industry: Total Leukemia, Acute Myelogenous Leukemia, Chronic Lymphocytic Leukemia, and Chronic Myelogenous Leukemia. *Regul Toxicol Pharmacol* (2011) 60:332–41. doi: 10.1016/j.yrtph.2011.05.001
31. Tanaka S, Sawada N, Yamaji T, Shimazu T, Goto A, Iwasaki M, et al. Female Reproductive Factors and Risk of Lymphoid Neoplasm: The Japan Public Health Center-Based Prospective Study. *Cancer Sci* (2019) 110:1442–52. doi: 10.1111/cas.13962
32. Roman E, Smith AG. Epidemiology of Lymphomas. *Histopathology* (2011) 58:4–14. doi: 10.1111/j.1365-2559.2010.03696.x
33. Torre LA, Bray F, Siegel RL, Ferlay J, Lortet-Tieulent J, Jemal A. Global Cancer Statistics 2012. *CA Cancer J Clin* (2015) 65:87–108. doi: 10.3322/caac.21262
34. Vardiman JW. The World Health Organization (WHO) Classification of Tumors of the Hematopoietic and Lymphoid Tissues: An Overview With Emphasis on the Myeloid Neoplasms. *Chem Biol Interact* (2010) 184:16–20. doi: 10.1016/j.cbi.2009.10.009
35. Ruiz-Magana MJ, Martinez-Aguilar R, Lucendo E, Campillo-Davo D, Schulze-Osthoff K, Ruiz-Ruiz C. The Antihypertensive Drug Hydralazine Activates the Intrinsic Pathway of Apoptosis and Causes DNA Damage in Leukemic T Cells. *Oncotarget* (2016) 7:21875–86. doi: 10.18632/oncotarget.7871
36. Singh N, Duenas-Gonzalez A, Lyko F, Medina-Franco JL. Molecular Modeling and Molecular Dynamics Studies of Hydralazine With Human DNA Methyltransferase 1. *ChemMedChem* (2009) 4:792–9. doi: 10.1002/cmdc.200900017
37. Deng C, Lu Q, Zhang Z, Rao T, Attwood J, Yung R, et al. Hydralazine May Induce Autoimmunity by Inhibiting Extracellular Signal-Regulated Kinase Pathway Signaling. *Arthritis Rheum* (2003) 48:746–56. doi: 10.1002/art.10833
38. Hoang NM, Rui L. DNA Methyltransferases in Hematological Malignancies. *J Genet Genomics* (2020) 47:361–72. doi: 10.1016/j.jgg.2020.04.006
39. Shakhovich R, Geng H, Johnson NA, Tsikitas L, Cerchietti L, Greal JM, et al. DNA Methylation Signatures Define Molecular Subtypes of Diffuse Large B-Cell Lymphoma. *Blood* (2010) 116:e81–89. doi: 10.1182/blood-2010-05-285320
40. Benetatos L, Vartholomatos G. On the Potential Role of DNMT1 in Acute Myeloid Leukemia and Myelodysplastic Syndromes: Not Another Mutated Epigenetic Driver. *Ann Hematol* (2016) 95:1571–82. doi: 10.1007/s00277-016-2636-8
41. Mizuno S, Chijiwa T, Okamura T, Akashi K, Fukumaki Y, Niho Y, et al. Expression of DNA Methyltransferases DNMT1, 3A, and 3B in Normal

- Hematopoiesis and in Acute and Chronic Myelogenous Leukemia. *Blood* (2001) 97:1172–9. doi: 10.1182/blood.V97.5.1172
42. Kale VP, Habib H, Chitren R, Patel M, Pramanik KC, Jonnalagadda SC, et al. Old Drugs, New Uses: Drug Repurposing in Hematological Malignancies. *Semin Cancer Biol* (2021) 68:242–8. doi: 10.1016/j.semcancer.2020.03.005
 43. Marinac CR, Colditz GA, Rosner B, Ghobrial IM, Birmann BM. Aspirin Use and Survival in Multiple Myeloma Patients. *Blood* (2018) 132:3250. doi: 10.1182/blood-2018-99-113025
 44. Huang ES, Strate LL, Ho WW, Lee SS, Chan AT. Long-Term Use of Aspirin and the Risk of Gastrointestinal Bleeding. *Am J Med* (2011) 124:426–33. doi: 10.1016/j.amjmed.2010.12.022
 45. Birmann BM, Giovannucci EL, Rosner BA, Colditz GA. Regular Aspirin Use and Risk of Multiple Myeloma: A Prospective Analysis in the Health Professionals Follow-Up Study and Nurses' Health Study. *Cancer Prev Res (Phila)* (2014) 7:33–41. doi: 10.1158/1940-6207.CAPR-13-0224
 46. Kikuchi J, Wada T, Shimizu R, Izumi T, Akutsu M, Mitsunaga K, et al. Histone Deacetylases are Critical Targets of Bortezomib-Induced Cytotoxicity in Multiple Myeloma. *Blood* (2010) 116:406–17. doi: 10.1182/blood-2009-07-235663
 47. Koltai T. Nelfinavir and Other Protease Inhibitors in Cancer: Mechanisms Involved in Anticancer Activity. *F1000Res* (2015) 4:9. doi: 10.12688/f1000research.5827.2
 48. Hatleberg CI, Ryom L, Sabin C. Cardiovascular Risks Associated With Protease Inhibitors for the Treatment of HIV. *Expert Opin Drug Saf* (2021) 20:1351–66. doi: 10.1080/14740338.2021.1935863
 49. National Health Insurance Regulations. *National Health Insurance Administration*. Available at: https://www.nhi.gov.tw/english/Content_List.aspx?n=A7354F4F704B6377&topn=A7354F4F704B6377.

Conflict of Interest: Authors W-ZL and C-YS were employed by company Fidelity Regulation Therapeutics Inc.

The remaining authors declare that the research was conducted in the absence of any commercial or financial relationships that could be construed as a potential conflict of interest.

Publisher's Note: All claims expressed in this article are solely those of the authors and do not necessarily represent those of their affiliated organizations, or those of the publisher, the editors and the reviewers. Any product that may be evaluated in this article, or claim that may be made by its manufacturer, is not guaranteed or endorsed by the publisher.

Copyright © 2022 Yang, Lin, Chiang, Chen, Chung, Chien and Shiau. This is an open-access article distributed under the terms of the Creative Commons Attribution License (CC BY). The use, distribution or reproduction in other forums is permitted, provided the original author(s) and the copyright owner(s) are credited and that the original publication in this journal is cited, in accordance with accepted academic practice. No use, distribution or reproduction is permitted which does not comply with these terms.



In Vitro Cell Density Determines the Sensitivity of Hepatocarcinoma Cells to Ascorbate

Hsiu-Lung Fan^{1,2}, Shu-Ting Liu³, Yung-Lung Chang³, Yi-Lin Chiu³, Shih-Ming Huang³ and Teng-Wei Chen^{1,2*}

¹ Graduate Institute of Medical Sciences, National Defense Medical Center, Taipei, Taiwan, ² Division of General Surgery, Department of Surgery, Tri-Service General Hospital, National Defense Medical Center, Taipei, Taiwan, ³ Department of Biochemistry, National Defense Medical Center, Taipei, Taiwan

OPEN ACCESS

Edited by:

Benyi Li,
University of Kansas Medical Center,
United States

Reviewed by:

Leticia Bucio Ortiz,
Autonomous Metropolitan University,
Mexico

Guo-Dong Yao,
Shenyang Pharmaceutical University,
China

*Correspondence:

Teng-Wei Chen
tengweichen@yahoo.com.tw

Specialty section:

This article was submitted to
Pharmacology of Anti-Cancer Drugs,
a section of the journal
Frontiers in Oncology

Received: 26 December 2021

Accepted: 20 April 2022

Published: 23 May 2022

Citation:

Fan H-L, Liu S-T, Chang Y-L, Chiu Y-L,
Huang S-M and Chen T-W (2022) In
Vitro Cell Density Determines the
Sensitivity of Hepatocarcinoma
Cells to Ascorbate.
Front. Oncol. 12:843742.
doi: 10.3389/fonc.2022.843742

Hepatocellular carcinoma (HCC) is the primary histological subtype of liver cancer, and its incidence rates increase with age. Recently, systemic therapies, such as immune checkpoint inhibitors, monoclonal antibodies, and tyrosine kinase inhibitors (TKIs), have been more beneficial than conventional therapies for treating HCC. Nonetheless, the prognosis of late-stage HCC remains dismal because of its high recurrence rates, even with substantial advances in current therapeutic strategies. A new treatment, such as a combination of current systemic therapies, is urgently required. Therefore, we adopted a repurposing strategy and tried to combine ascorbate with TKIs, including lenvatinib and regorafenib, in HepG2 and Hep3B cells. We investigated the potential functional impact of pharmacological concentrations of ascorbate on the cell-cycle profiles, mitochondrial membrane potential, oxidative response, synergistic effects of lenvatinib or regorafenib, and differential responsiveness between HepG2 and Hep3B cells. Our data suggest that the relative level of cell density is an important determinant for ascorbate cytotoxicity in HCC. Furthermore, the data also revealed that the cytotoxic effect of pharmacological concentrations of ascorbate might not be mediated *via* our proposed elevation of ROS generation. Ascorbate might be involved in redox homeostasis to enhance the efficacy of TKIs in HepG2 and Hep3B cells. The synergistic effects of ascorbate with TKIs (lenvatinib and regorafenib) support their potential as an adjuvant for HCC targeted TKI therapy. This research provides a cheap and new combinatory therapy for HCC treatment.

Keywords: hepatocellular carcinoma, ascorbate, reactive oxygen species, tyrosine kinase inhibitors, cell density

Abbreviations: ACTN, α -actinin; L-AA, L-ascorbic acid; CI, combination index; CTLA4, cytotoxic T-lymphocyte-associated protein 4; DCFH-DA, 2',7-dichlorofluorescein diacetate; DMEM, Dulbecco's modified Eagle's medium; DsigDB, Drug SIGNatures DataBase; FAS, fatty acid synthase; FACS, fluorescence-activated cell sorting; FBS, fetal bovine serum; FDA, Food and Drug Administration; FSC-H, forward scatter height; GO, Gene Ontology; GSVA, Gene Set Variation Analysis; HCC, hepatocellular carcinoma; HO-1, heme oxygenase-1; ICIs, immune checkpoint inhibitors; LIHC, liver hepatocellular carcinoma; MTT, thiazolyl blue tetrazolium bromide; PARP, poly-ADP-ribose polymerase; PBS, phosphate-buffered saline; PD-1/PDL-1, programmed death-1/programmed death ligand-1; PI, propidium iodide; ROS, reactive oxidative species; SSC-H, side scatter height; TCGA, The Cancer Genome Atlas; TKIs, tyrosine kinase inhibitors; VEGFR, vascular endothelial growth factor receptor.

INTRODUCTION

Liver cancer is the sixth most frequent cancer and the fourth-leading cause of death worldwide, with 841,000 new cases and 782,000 deaths in 2018, accounting for 7% of all cancers (1–3). Hepatocellular carcinoma (HCC) is the primary histological subtype of liver cancer, and its incidence rates, which peak at around 70 years old, are progressively increasing with age. HCC has a significant male preponderance. The incidence rate of men getting HCC is 2–2.5-fold higher than that of women (1). An already-identified underlying etiology, such as HIV infection, chronic hepatitis virus (HBV and HCV) infections, aflatoxin exposure, cigarette smoking, alcohol intake, and metabolic diseases, resulted in approximately 90% of HCCs. The prognosis of late-stage HCC remains dismal due to its high recurrence rates even with substantial advances in current therapeutic strategies. HCC has a poor 5-year survival rate, resulting from late diagnoses, resistance to anticancer therapies, and a high frequency of recurrences (2). Therefore, for the sake of developing new biomarkers for diagnoses and prognoses, as well as inventing effective treatments and drugs, elucidating the underlying tumorigenesis of HCC is important.

Owing to the significant progress of systemic therapies accompanied by a substantial increase in patients' overall survival rates and 5-year quality of life, applying systemic therapies, such as monoclonal antibodies, immune checkpoint inhibitors (ICIs), and tyrosine kinase inhibitors (TKIs), to HCC patients has recently been more beneficial than traditional therapies (4–7). Sorafenib and lenvatinib are the most effective TKIs and first-line single-drug therapies. Cabozantinib, ramucirumab, and regorafenib have also been recognized to improve survival benefits in second-line therapies after first-line treatment with sorafenib. Many phase III trials have been conducted to investigate the effectiveness of combination therapy, for example, trials investigating the ICI combination of PD-1/PDL-1 (programmed death-1/programmed death ligand-1) axis inhibitors and CTLA4 (cytotoxic T-lymphocyte-associated protein 4) inhibitors or the combination of ICIs and TKIs are ongoing (6). The management of HCC at all stages is expected to be changed by the results of these trials. However, developing resistance is a primary problem for the antitumor effect of first-line and second-line TKIs in HCC (8, 9).

Screening for repurposed drugs is a potential strategy for identifying new cancer therapies (10). It has been hypothesized that the steady-state levels of reactive oxidative species (ROS) stress in cancer cells are higher than in normal cells owing to a defective oxidative metabolism and raised labile iron pool (11, 12). Hence, redox homeostasis plays a significant role in cancer therapy. Recently, L-ascorbic acid (L-AA) at pharmacologic concentrations (>100 μ M) achieved by intravenous administration was redefined as a possible anti-cancer drug acting *via* inducing hydrogen peroxide formation (13–17), in contrast to physiological concentrations that neutralize free radicals/ROS. However, the reason that L-AA kills some tumor cells *via* hydrogen peroxide-related mechanisms but has little effect on normal cells is still under investigation (11, 12). In addition to ROS generation, ascorbate can also serve as a cofactor of

hydroxylases to keep the active site Fe^{2+} in its reduced state (18). Recent advances have shown that the ascorbate-induced cell death of cancer cells involves DNA double-strand breaks and ATP depletion (19, 20). Ferroptosis, necroptosis, and autophagy are involved in caspase-independent pharmacological ascorbate-induced cell death (21).

For *in vitro* toxicity studies, two of the most utilized liver cancer cellular models are the HepG2 and Hep3B cancer cell lines (22, 23). HepG2 has wild-type p53 and is HBV-negative and nontumorigenic, whereas Hep3B is p53-deficient, HBV-positive, and tumorigenic. Many studies have claimed that the differences between HepG2 and Hep3B cell lines cannot merely be determined by p53 or HBx. Moreover, there also exist several differences between HepG2 and Hep3B cell lines, such as differences in gene expression, drug responses, and associated signaling pathways, as described in the literature (24–26). These diverse differences have constantly presented obstacles and led to confusion for many researchers attempting to analyze and interpret the experimental data.

In this study, we investigated the cytotoxic effect of ascorbate (sodium ascorbate or L-AA) on the HepG2 cell line whether mediated through the modulation of ROS status. We further examined the potential functional impact of pharmacological concentrations of ascorbate on the cell-cycle profiles, mitochondrial membrane potential, oxidative response, the synergistic effects of vascular endothelial growth factor receptor (VEGFR)-targeted TKIs, first-line lenvatinib, and second-line regorafenib, and the differential responsiveness between HepG2 and Hep3B cells. Our findings may provide a new direction for combinatory HCC therapy using ascorbate (sodium ascorbate or L-AA), focusing on the management of cellular redox homeostasis.

MATERIALS AND METHODS

GSVA Scoring and Survival Analysis

Sorafenib FDA, lenvatinib FDA, regorafenib FDA, and cabozantinib FDA downloaded from DsigDB (27), and the gene sets associated with ROS downloaded from Gene Ontology (28). About the prognosis of HCC patients, TCGA LIHC whole gene expression and curated survival status were downloaded from the UCSC XENA website (29). In GSVA analysis (in R 4.1.1), *kfcd* was set to “Poisson”, and four TKI gene sets and ROS-related GO gene sets were input for scoring (30). TKI GSVA scores and survival status were entered into the “Evaluate Cutpoints” package (in R 4.1.1) to find the best cut-off point (31), and Kaplan-Meier plots were plotted with GraphPAD software. Log-rank test was used for statistically significant analysis, and $p < 0.05$ was considered a significant difference. The Heatmap showing GSVA scores is drawn with the Morpheus web tool. Violin plots were plotted with GraphPAD software, and Welch's t-test was used for the analysis of statistical significance. ***: $p < 0.001$. For detailed software settings, please refer to the previous article (32, 33).

Cell Culture and Reagents

HepG2 and Hep3B HCC cell lines were obtained from the American Type Culture Collection (ATCC; Manassas, VA). HepG2 and Hep3B cells were cultivated in Dulbecco's modified Eagle's medium (DMEM) supplemented with 10% fetal bovine serum (FBS) and 1% penicillin-streptomycin (Thermo Fisher Scientific, Waltham, MA). Cell lines were regularly tested for mycoplasma infections using Mycoplasma Detection Kit (*In vivo* Gen, San Diego, CA) as well as regularly changed with thawed stocking cell lines. L-AA, sodium ascorbate, 2',7-dichlorofluorescein diacetate (DCFH-DA), lenvatinib, propidium iodide (PI), regorafenib, and thiazolyl blue tetrazolium bromide (MTT) were purchased from Sigma Aldrich (St. Louis, MO).

Cell Metabolic Activity Analysis

Cells were plated into 24-well culture plates and incubated for 1 day, after which fresh DMEM containing the indicated drugs was added to each well. The cells were then incubated with these treatments for the indicated periods. The interaction between L-AA and MTT assay has already been demonstrated (34). Accordingly, to avoid the interference of L-AA with MTT, the L-AA-containing medium was removed before the addition of MTT solution (0.5 mg/mL in phosphate-buffered saline, PBS) to each well. The cells were then incubated with MTT solution for 1 h at 37°C. After adding dimethyl sulfoxide (DMSO; 200 μ L), the absorbances at 570 nm and 650 nm were measured using an ELISA plate reader (Multiskan EX, Thermo, MA). The relative metabolic activity was calculated based on the absorbance ratio between cells cultured with the indicated drugs and the untreated controls, which were assigned a value of 100. The combination index (CI) was calculated utilizing CalcuSyn (Biosoft, Cambridge, UK) to generate the isobolograms. Typically, a CI value <1 denotes a synergistic combination effect, and a CI value >1 denotes an antagonistic combination effect (35).

Fluorescence-Activated Cell Sorting (FACS), Cell-Cycle Profiling, and ROS and Mitochondrial Membrane Potential Analyses

Cell-cycle profiles were measured according to cellular DNA content using FACS. Cells were fixed in 70% ice-cold ethanol, stored at -30°C overnight, washed two times with ice-cold PBS supplemented with 1% FBS, and then stained with PI solution (5 μ g/mL PI in PBS, 0.5% Triton X-100, and 0.5 μ g/mL RNase A) for 30 min at 37°C in the dark.

The intracellular ROS levels were determined using the fluorescent marker DCFH-DA. Cells were exposed to various concentrations of ascorbate for 24 h, stained with DCFH-DA (10 μ M) for 40 min at 37°C, and then harvested. After washing the cells once with PBS, fluorescence was analyzed on channel FL-1 of the FACSCalibur flow cytometer using Cell Quest Pro software (BD Biosciences, Franklin Lakes, NJ). The cell volume gating strategy involved forward scatter height (FSC-H) and side scatter height (SSC-H), and the median fluorescence intensity of the vehicle was used as the starting point for M2 gating.

Mitochondrial depolarization was measured as a function of a decrease in the red/green fluorescence intensity ratio. All dead and viable cells were harvested, washed with PBS, and incubated with 1 \times binding buffer containing the MMP-sensitive fluorescent dye JC-1 for 30 min at 37°C in the dark. After washing the cells once with PBS, JC-1 fluorescence was analyzed on channels FL-1 and FL-2 of the FACSCalibur flow cytometer using Cell Quest Pro software (BD Biosciences, Franklin Lakes, NJ) to detect monomer (green fluorescence) and aggregate (red fluorescence) forms of the dye, respectively. The cell volume gating strategy involved FSC-H and SSC-H, and the median fluorescence intensity of the vehicle was used as the starting point for M2 gating.

Western Blotting

HepG2 and Hep3B cells were lysed in radioimmunoprecipitation assay buffer (100 mM Tris-HCl (pH 8.0), 150 mM NaCl, 0.1% SDS, and 1% Triton X-100) at 4°C. Proteins in the resultant lysates were separated by sodium dodecyl sulfate-polyacrylamide gel electrophoresis and analyzed by immunoblotting with antibodies against α -actinin (ACTN)(H-2), fatty-acid synthase (FAS)(A-5), Nrf2 (A-10), p53 (DO-1), p62 (D-3) (Santa Cruz Biotechnology, Santa Cruz, CA), cleaved poly-ADP-ribose polymerase (PARP) (9546) (Cell Signaling, Danvers, MA), cyclin D1 (ab134175), γ H2A.x (ab81299), p21 (ab109520) (Abcam, Cambridge, UK), and HO-1 (heme oxygenase-1) (ADI-SPA-895-F) (Enzo Life Sciences, Farmingdale, NY).

Statistical Analysis

Values were expressed as the mean \pm SD of at least three independent experiments. All comparisons between groups (vehicle and drug) were conducted using Student's *t*-tests. Statistical significance was set at $p < 0.05$.

RESULTS

The Relationship Between TKIs and ROS in Human Liver Cancer Cells

To evaluate the association of sorafenib and related TKI with ROS response in HCC, we used Gene Set Variation Analysis (GSVA) strategy in combination with four gene sets collected from D1: Food and Drug Administration (FDA) Approved Drug Gene Sets in Drug SIGNatures DataBase (DsigDB) for GSVA scoring. The Evaluate Cutpoints package in the R environment was used to find the best cut-off point for the survival rate of each gene set in The Cancer Genome Atlas (TCGA) Liver Hepatocellular Carcinoma (LIHC) database. **Figure 1A** shows that among the four-drug (sorafenib, lenvatinib, regorafenib, and cabozantinib) gene sets in GSVA scoring, those with higher scores generally had a better prognosis, while those with lower scores generally had a worse prognosis. Considering that the gene set represents genes with increased expression after drug treatment, the poor prognosis of those with lower GSVA scoring implies that lower expression of genes associated with TKI drug treatment in tumors may be associated with poor drug response. Further analysis of the distribution of GSVA scoring and ROS

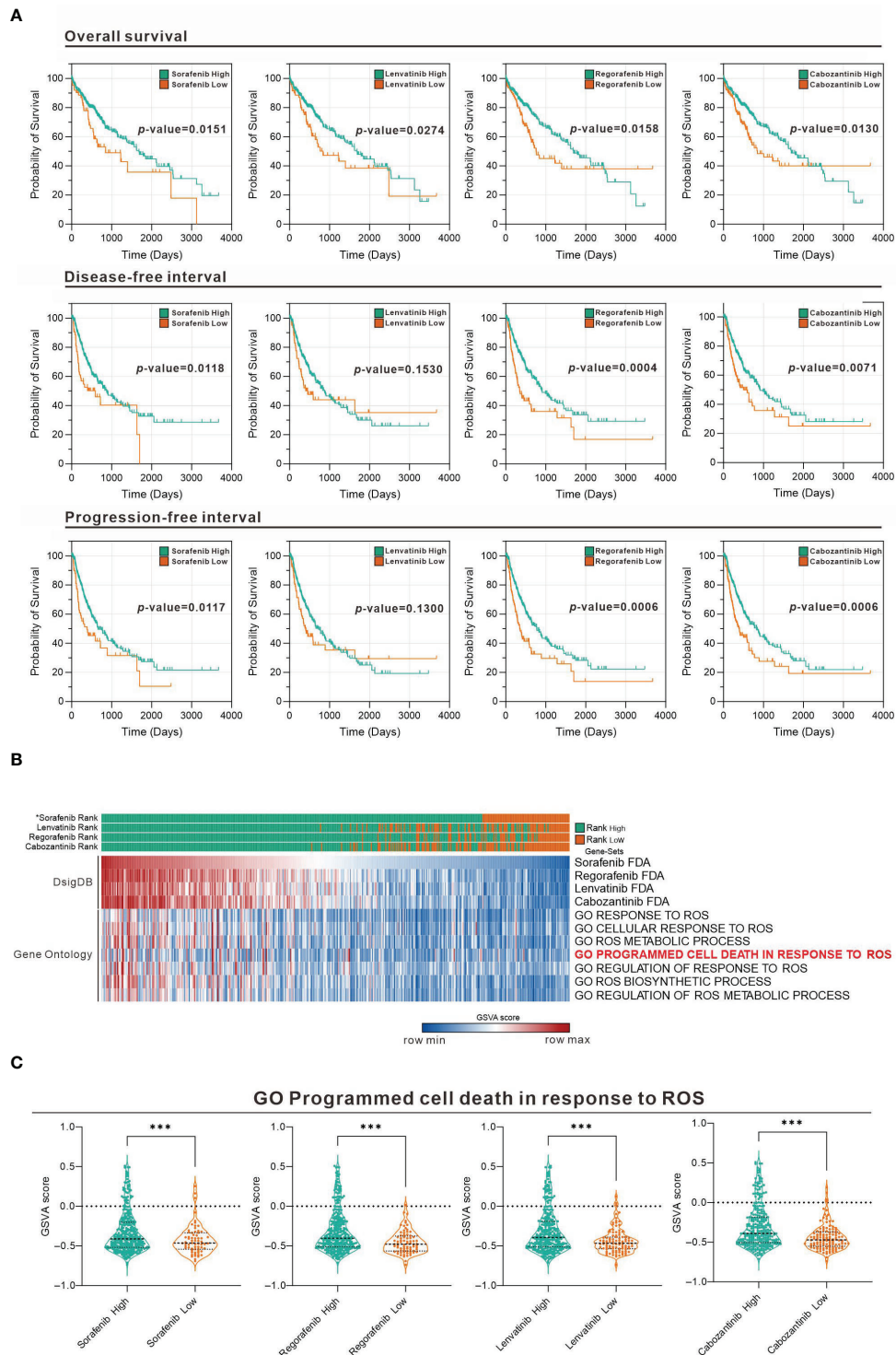


FIGURE 1 | Association between TKI and ROS-responsive gene sets assessed in the TCGA LIHC database. **(A)** Overall survival, disease-free interval, and progression-free interval analysis for high and low GSVAs for the four drugs (sorafenib, lenvatinib, regorafenib, and cabozantinib). **(B)** Heatmap showing the distribution of the four-drug GSVAs high and low and ROS-associated gene sets in TCGA LIHC patients. *: sorted by sorafenib GSVAs from highest to lowest (sorafenib, lenvatinib, regorafenib, and cabozantinib). **(C)** Violin plot showing the difference in GSVAs scores of GO programmed cell death in response to ROS in the high and low GSVAs subgroups of the four drugs. *** $p < 0.001$ (Welch's t-test).

response GSVA scores among the four drugs in the TCGA LIHC patient sample showed that the low GSVA scoring was concentrated in specific patient groups (**Figure 1B**). Similarly, the GSVA scoring of the ROS-associated Gene Ontology (GO) gene-set was also low in this cohort of patients, suggesting that the effect of TKI drugs on tumor suppression by increasing ROS was limited in this cohort. Take “GO Programmed cell death in response to ROS” as an example, we found that all patients with low GSVA scoring of the four drugs had a significantly lower distribution of this gene set (**Figure 1C**). This indicates that the expression of genes related to ROS-induced apoptosis by the four TKI is low in this group of patients, which may be related to the reduced effect of TKI.

The Cytotoxicity of Ascorbate in Human Liver Cancer Cells

Previous studies including ours on human cervical cancer cells have suggested that pharmacologic concentrations of ascorbate (L-AA or sodium ascorbate) may elevate ROS generation and result in cancer cell death (13, 17, 36–38). Based on the conclusion of **Figure 1**, the functional role of ROS generation by ascorbate might be a candidate for HCC treatment. Hence, we applied various concentrations, including pharmacologic concentrations, to HepG2 cells. Our MTT analysis for cell metabolic activity showed that sodium ascorbate treatment for either 24 h or 48 h could cause 50% HepG2 cell death at 15 mM (**Figure 2A**). We further analyzed the effects of sodium ascorbate on cell-cycle progression using Western blotting analysis and on cell-cycle profile using flow cytometry. According to the Western blotting analysis, cyclin D1 and fatty-acid synthase (FAS) were downregulated by sodium ascorbate, whereas the quantitative values of Nrf2 remained constant and the quantitative values of HO-1 and p53 were increased by a dose-dependent manner (**Figure 2B**). According to the cell-cycle profile, the population in the G2/M phase was significantly increased by sodium ascorbate, whereas the populations in the G1 and S phases were decreased (**Figure 2C**). No apparent impact on the subG1 phase of sodium ascorbate was observed, suggesting that the induction of cell death by sodium ascorbate might not be mediated *via* cellular apoptosis. Unexpectedly, we found that the ROS levels did not increase accordingly, indicating that the cell death caused by sodium ascorbate might not be caused by the induction of ROS generation (**Figure 2D**). The declining trend of ROS by sodium ascorbate was a dose-dependent manner.

The Effect of HepG2 Cell Density on the Cytotoxicity of Ascorbate

Our previous study had tested whether the weak acidity of L-AA was responsible for its observed effects by assessing the effects of sodium ascorbate salt and acetic acid in HeLa cells (17). Various sensitivities of ascorbate were previously identified as a function of cell density (39, 40). Therefore, we looked into the potential cell death-inducing effect of L-AA and sodium ascorbate using cell densities ranging from 2.5×10^5 to 5×10^5 . Cell viability analysis using the MTT assay showed that 10 mM L-AA and

sodium ascorbate had dramatically suppressive effects on HepG2 cell growth at lower cell density (**Figure 3A**). To be more specific, the lower the cell density was, the higher the possibility that ascorbate could enter into cells. Therefore, it might result in the accumulation of a higher amount of ascorbate inside HepG2 cells, leading to inducing a more significant cytotoxic effect. The lack of an apparent difference between L-AA and sodium ascorbate suggests the absence of a functional role of weak acidity of L-AA concerning cytotoxicity in HepG2 cells.

There was no apparent cause for the suppression of HepG2 cell growth revealed by the cell-cycle profile and cellular apoptosis. Hence, we checked the impact of L-AA and sodium ascorbate on mitochondria membrane potential at different cell densities using JC-1 dye. Our JC-1 data showed that L-AA and sodium ascorbate potentially disrupted mitochondrial membrane potential in a dose-dependent manner at lower cell density (**Figures 3B–E**).

The Combinatory Effect of Ascorbate With TKIs in HepG2 Cells

Targeted TKI therapy is currently used for HCC treatment (6, 41, 42). The development of resistance is a primary problem for the antitumor effect of first-line and second-line TKIs in HCC (8, 9). Therefore, it is an urgent issue to reduce the recurrence rates by replacing currently targeted monotherapies with combinatory therapies. Lenvatinib is a multiple TKI of the VEGFR1–3 kinases and regorafenib demonstrates an antiangiogenic effect owing to its dual VEGFR2/TIE2 tyrosine kinase inhibition (43, 44). At pharmacologic concentrations, 10 mM L-AA or sodium ascorbate had more suppressive effects on cell metabolic activity than lenvatinib and regorafenib (except 10 μ M) in HepG2 cells independent of cell density (**Figure 4**). HepG2 cells were sensitive to lenvatinib treatment at a lower cell density in a dose-dependent manner (**Figures 4A, B**). The growth of HepG2 cells was almost suppressed by L-AA or sodium ascorbate at a lower (5×10^3) cell density (**Figure 4C**). We observed the combinatory cytotoxic efficiencies of lenvatinib and L-AA or sodium ascorbate at a 10×10^3 cell density (**Figure 4D**). Compared with lenvatinib, HepG2 cells were more sensitive to regorafenib in a cell density-independent manner (**Figures 4E, F**). The combinatory cytotoxic efficiencies of regorafenib with L-AA or sodium ascorbate were dependent on the concentration of ascorbate and the cell density (**Figures 4G, H**).

We further elucidated the potential cytotoxicity mechanism of combination therapy of ascorbate with TKIs. We examined proteins related to cell-cycle progression, ROS response, DNA damage, and apoptosis using Western blotting analysis. We observed that lenvatinib alone induced the expression of cell-cycle progression-related proteins (p53 and p21), a ROS response protein (p62), a DNA damage biomarker (γ H2A.x), and an apoptosis biomarker (cleaved PARP), while it downregulated the expression of an ROS response protein (HO-1) and a cell-cycle progression-related protein (cyclin D1) (**Figure 5A**). Lenvatinib combined with 5 mM L-AA or sodium

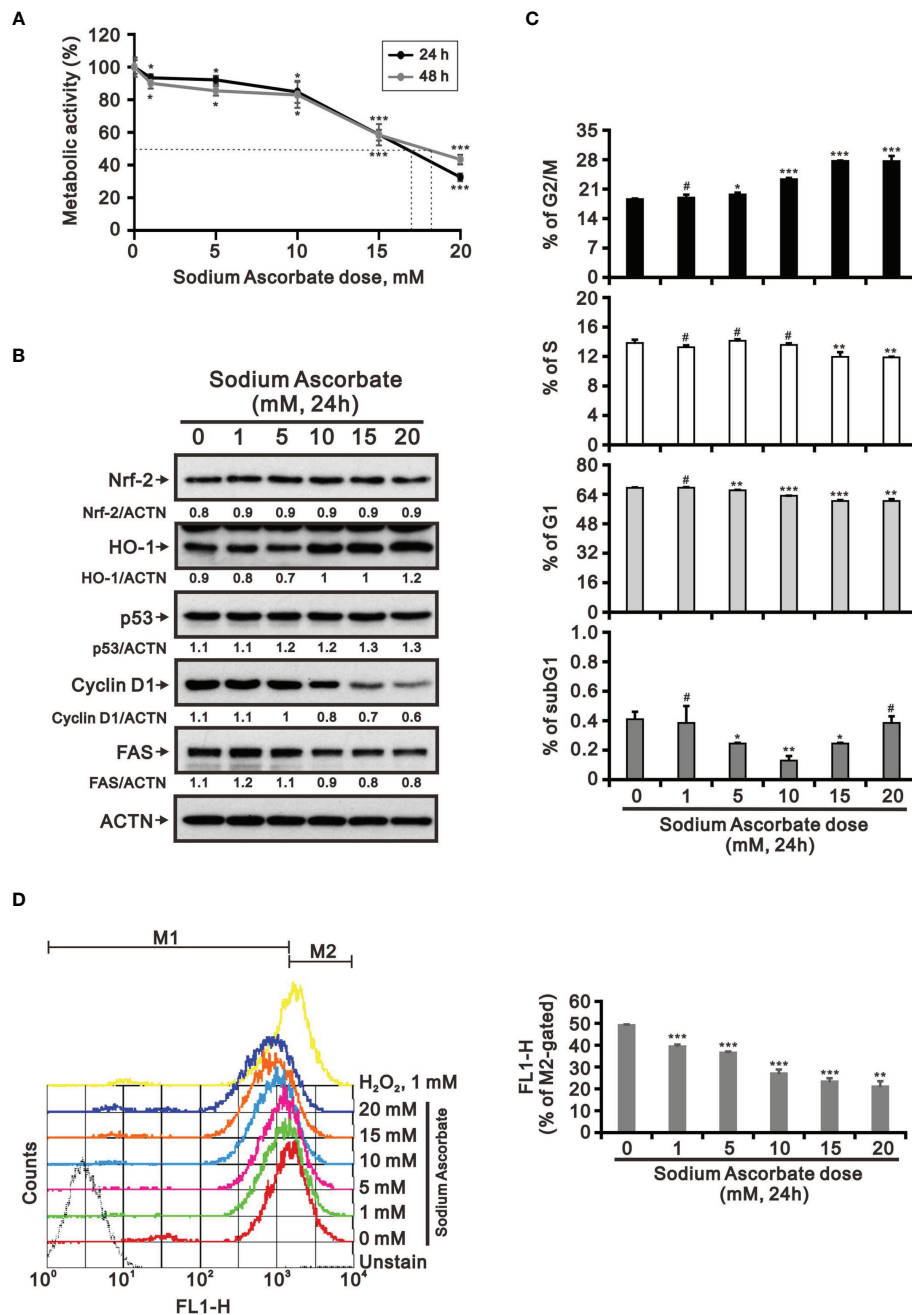


FIGURE 2 | Effects of sodium ascorbate on cell metabolic activity in HepG2 cells. **(A)** HepG2 cells were treated for 24 h or 48 h with the indicated concentrations of sodium ascorbate. Cell metabolic activity was measured using the MTT assay. HepG2 cells were treated with the indicated concentrations of sodium ascorbate for 24 h, after which their cell lysates were subjected to **(B)** Western blot analysis using antibodies against the indicated proteins (ACTN was the protein loading control), **(C)** cell-cycle profiling using flow cytometry analysis, and **(D)** ROS status determination using 10 μ M DCFH-DA. The cell volume gating strategy involved FSC-H and SSC-H, and the median fluorescence intensity of the vehicle was used as the starting point for M2 gating. Protein bands were quantified through pixel density scanning and evaluated using ImageJ, version 1.44a (<http://imagej.nih.gov/ij/>). We show one representative result. Bars depict the mean \pm SD of three independent experiments. $^{\#}p > 0.05$, $^*p < 0.05$, $^{**}p < 0.01$, and $^{***}p < 0.001$ compared with the vehicle (Student's *t*-tests).

ascorbate downregulated the expression of a cell-cycle progression-regulated protein (cyclin D1), a DNA damage biomarker (γ H2A.x), and an apoptosis biomarker (cleaved PARP), whereas it elevated the quantitative values of a cell-

cycle progression-related protein (p21) and ROS response proteins (HO-1 and p62). Regorafenib alone decreased the quantitative values of p53, cyclin D1, p21, and HO-1, while it elevated the quantitative values of p62. Regorafenib combined

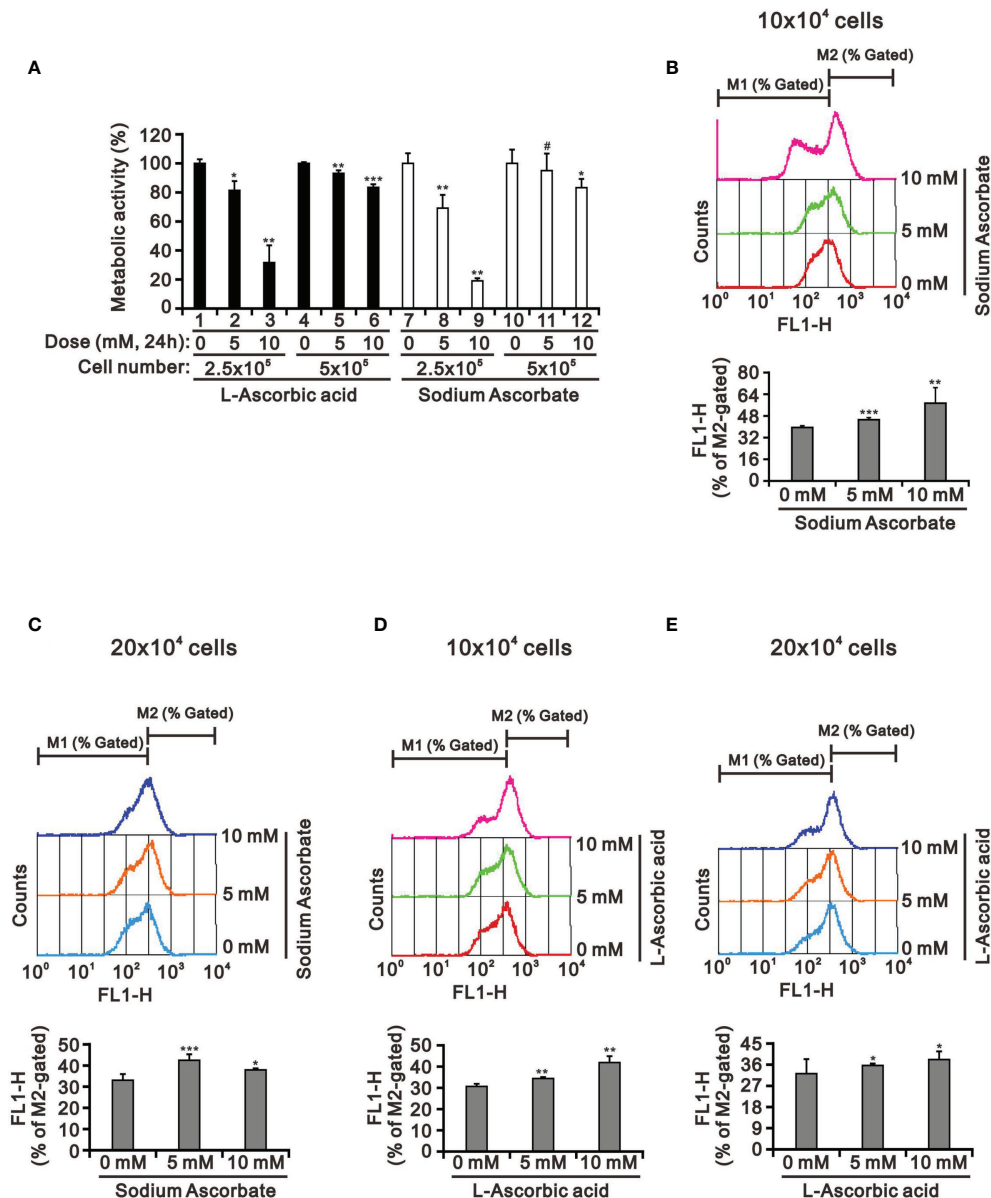


FIGURE 3 | The cell density effect on cell metabolic activity and mitochondrial membrane potential in HepG2 cells. The two indicated cell densities of HepG2 cells were treated with 5 mM or 10 mM L-AA (or sodium ascorbate) for 24 h, after which their cell lysates were investigated for their (A) cell metabolic activity using the MTT assay and (B–E) mitochondrial membrane potential using a flow cytometer. The cell volume gating strategy involved FSC-H and SSC-H, and the median fluorescence intensity of the vehicle was used as the starting point for M2 gating. We show one representative result. Bars depict the mean \pm SD of three independent experiments. # $p > 0.05$, * $p < 0.05$, ** $p < 0.01$, and *** $p < 0.001$ compared with the vehicle (Student's t-tests).

with 10 mM L-AA or sodium ascorbate downregulated the expression of cell-cycle progression-related proteins (p53, cyclin D1, and p21), ROS response proteins (Nrf2 and p62), a DNA damage biomarker (γ H2A.x), and an apoptosis biomarker (cleaved PARP) (Figure 5B). γ H2A.x was the only protein consistent change (decreased) in the combinations of lenvatinib or regorafenib with higher concentrations of ascorbate.

The Cytotoxicity of Sodium Ascorbate in Hep3B Cells

Hep3B and HepG2 are the two most utilized liver cancer cell lines for *in vitro* toxicity studies (23, 25). We wanted to examine the cell context issue and we treated Hep3B with sodium ascorbate and observed the cytotoxicity at 24 h and 48 h (Figure 6A). Sodium ascorbate induced the expression of Nrf2 and HO-1, whereas it downregulated the expression of

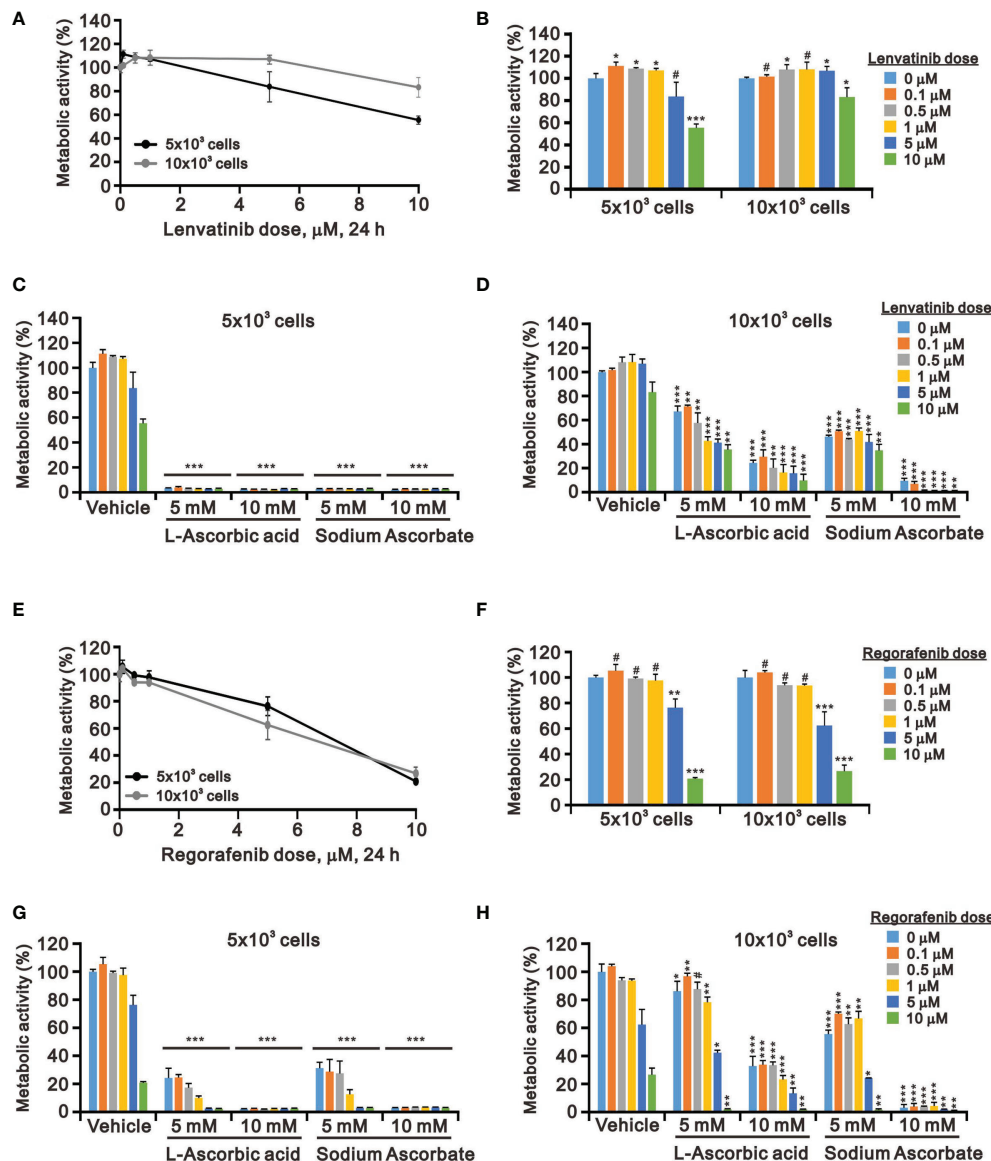


FIGURE 4 | Effects of ascorbate combined with TKIs on cell viability in HepG2 cells. HepG2 cells (5×10^3 and 1×10^4) were treated for 24 h with the indicated concentrations of (A–D) lenvatinib or (E–H) regorafenib in the absence or presence of 5- or 10-mM L-AA or sodium ascorbate. Cell metabolic activity was measured using the MTT assay. We show one representative result. Bars depict the mean \pm SD of three independent experiments. # $p > 0.05$, * $p < 0.05$, ** $p < 0.01$, and *** $p < 0.001$ compared with the vehicle (Student's t-tests).

cyclin D1 and FAS (Figure 6B). No endogenous p53 protein was confirmed. In contrast to HepG2, sodium ascorbate elevated the population in the subG1 phase and decreased the populations in the G1 and G2/M phases in Hep3B cells (Figure 6C). The inductive or suppressive effect of sodium ascorbate on the S phase was dependent on its concentration. Sodium ascorbate significantly suppressed ROS generation in Hep3B (Figure 6D) as did in HepG2 cells (Figure 2D). These findings were consistent in that some differences between HepG2 and Hep3B cell lines were described in the literature (24–26).

The Combination Index of L-AA and TKIs in HepG2 and Hep3B Cells

Our findings revealed that L-AA or sodium ascorbate might play an adjuvant role in the current TKI therapy for HCC patients. Hence, we designed various combinations of concentrations and calculated the combination index (CI) between lenvatinib or regorafenib and L-AA in HepG2 and Hep3B cells as a function of the half-maximal inhibitory concentration (IC_{50}) values, the median effective dose (ED_{50}) values, and classic experimental design (35). A CI value < 1 , which denotes a synergistic effect, was observed in most of the tested combinations of lenvatinib or

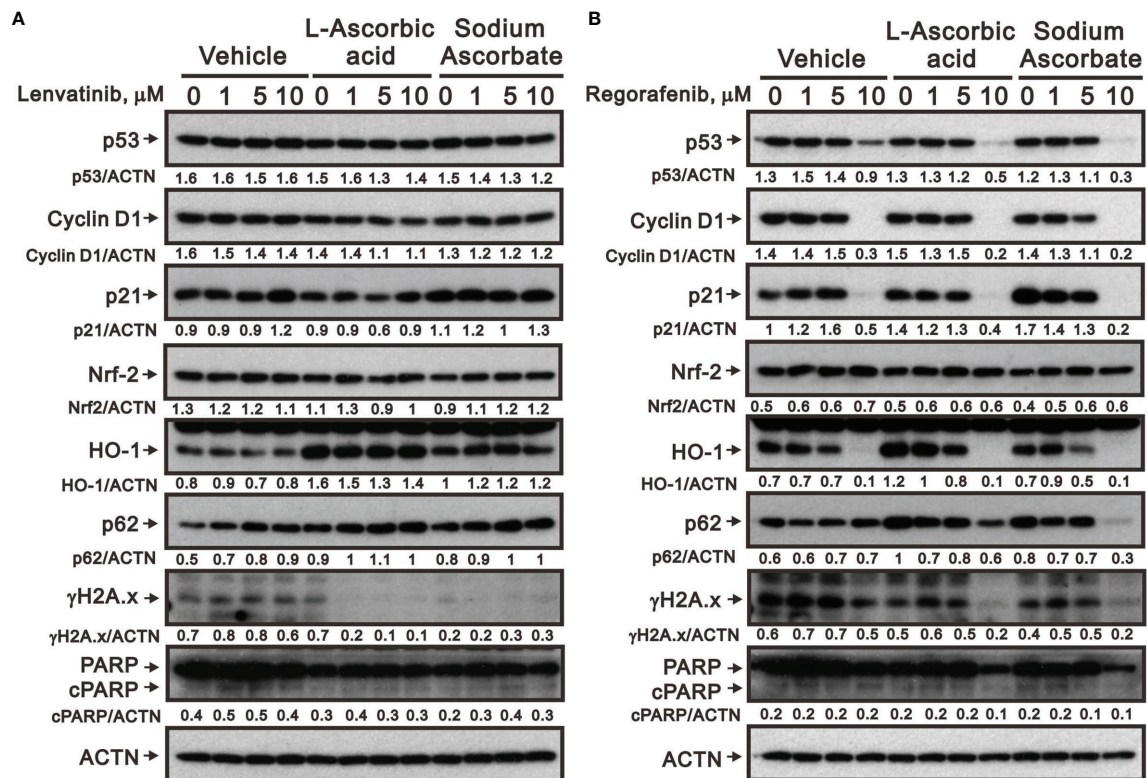


FIGURE 5 | Effects of ascorbate combined with TKIs on specific protein expressions in HepG2 cells. HepG2 cells (4×10^5) were treated for 24 h with the indicated concentrations of (A) lenvatinib or (B) regorafenib in the absence or presence of 5-mM L-AA or sodium ascorbate. Cell lysates were subjected to Western blot analysis using antibodies against the indicated proteins. ACTN was the protein loading control. Protein bands were quantified through pixel density scanning and evaluated using ImageJ, version 1.44a (<http://imagej.nih.gov/ij/>). We show one representative result.

regorafenib and L-AA in HepG2 and Hep3B cells (Figure 7). The therapeutic concentration of 60 μM lenvatinib was decreased to 5.5 μM (at 5.5 mM L-AA) in HepG2 cells, while the therapeutic concentration of 117 μM lenvatinib was decreased to 19.5 μM (at 4.9 mM L-AA) in Hep3B cells (Figures 7A, B). The therapeutic concentration of 5 μM regorafenib was decreased to 3.3 μM (at 1.7 mM L-AA) in HepG2 cells, while the therapeutic concentration of 588 μM regorafenib was decreased to 25 μM (at 13 mM L-AA) in Hep3B cells (Figures 7C, D). These findings suggest the benefit of the clinical application of lenvatinib or regorafenib plus L-AA as a potential adjuvant to overcome the current resistance to VEGFR-targeted TKI therapy in HCC.

DISCUSSION

In the present study, our TCGA LIHC analysis implied that the ROS-related pathway might correlate with the efficacy of TKI therapy in HCC treatment. Hence, we investigated the cytotoxic effects of pharmacological concentrations of ascorbate (sodium ascorbate or L-AA), which is a well-known redox reagent, alone or combined with TKI therapy on HepG2 and Hep3B cells to figure out the role of ROS in the treatment of HCC. Our study

examined the potential functional impact of pharmacological concentrations of ascorbate on the cell-cycle profiles, mitochondrial membrane potential, oxidative response, the synergistic effects of TKIs (lenvatinib and regorafenib), and the differential responsiveness between HepG2 and Hep3B cells. Our study data suggest that the relative level of cell density is an important determinant for ascorbate cytotoxicity in HCC. Our data also revealed that the cytotoxic effect of pharmacological concentrations of ascorbate might not be mediated through our proposed elevation of ROS generation. γH2AX is a well-known biomarker for cellular DNA damage. In our current case, the treatments of either lenvatinib and regorafenib or combined with ascorbate increased the cytotoxicity in a γH2AX -independent manner. Our data uncovered that cellular DNA damage is not the primary cause of cytotoxicity. Other possibilities might lead to these effects, including the induction of DNA repair systems through regulating ROS homeostasis.

There are substantial differences in biochemistry, biology, ethnic origins, and genetics between the HepG2 and Hep3B liver cancer cell lines. HepG2 maintains characteristics more closely related to hepatocytes, whereas Hep3B exhibits more fibroblast-related characteristics and more mesenchymal proteins, indicating an epithelial-to-mesenchymal transition (22, 23, 25).

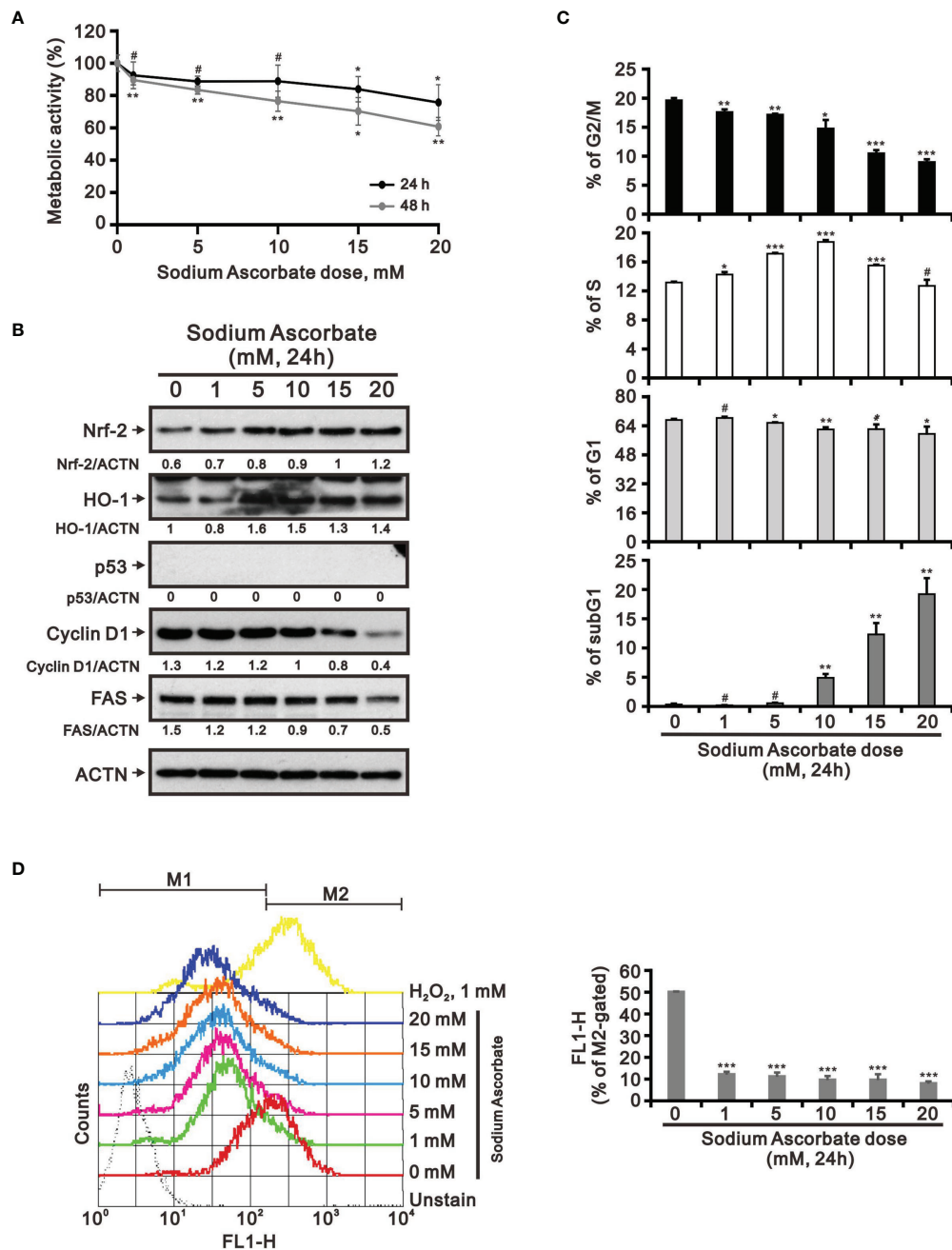


FIGURE 6 | Effects of sodium ascorbate on cell metabolic activity in Hep3B cells. **(A)** Hep3B cells were treated for 24 h or 48 h with the indicated concentrations of sodium ascorbate. Cell metabolic activity was measured using the MTT assay. Hep3B cells were treated with the indicated concentrations of sodium ascorbate for 24 h, after which their cell lysates were subjected to **(B)** Western blot analysis using antibodies against the indicated proteins (ACTN was the protein loading control), **(C)** cell-cycle profiling using flow cytometry analysis, and **(D)** ROS status determination using 10 μ M DCFH-DA. The cell volume gating strategy involved FSC-H and SSC-H, and the median fluorescence intensity of the vehicle was used as the starting point for M2 gating. Protein bands were quantified through pixel density scanning and evaluated using ImageJ, version 1.44a (<http://imagej.nih.gov/ij/>). We show one representative result. Bars depict the mean \pm SD of three independent experiments. # $p > 0.05$, * $p < 0.05$, ** $p < 0.01$, and *** $p < 0.001$ compared with the vehicle (Student's t -tests).

A difference in cell-cycle profiles between HepG2 and Hep3B cells was observed in this study. According to the current literature, instead of a single protein such as p53 or HBx being the crucial factor governing the differences between the HepG2

and Hep3B cell lines, the different origins of biopsy specimens and multiple related factors may be significant. These differences are likely to result in various responses to pharmacological medicines in these two cell lines and lead to opposite

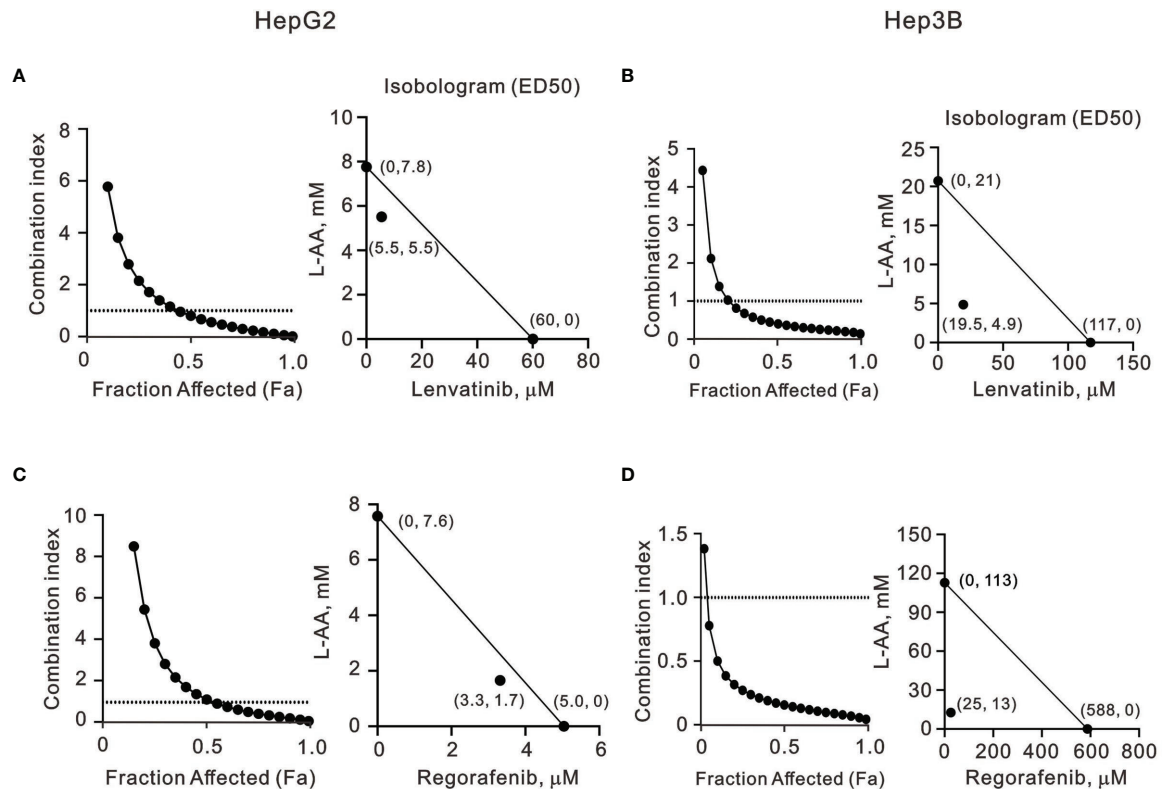


FIGURE 7 | The combination index of TKIs with L-AA in HepG2 and Hep3B cells. **(A, C)** HepG2 and **(B, D)** Hep3B cells were treated with various L-AA doses (0, 0.156, 0.3125, 0.625, 1.25, 2.5, 5, or 10 mM) combined with various lenvatinib doses (0, 0.3125, 0.625, 1.25, 2.5, 5, 10, 20, 40, or 80 μ M) or regorafenib doses (0, 0.07813, 0.15625, 0.3125, 0.625, 1.25, 2.5, 5, 10, or 20 μ M). Metabolic activity was measured using the MTT method. The combination index of L-AA plus lenvatinib or regorafenib in **(A, C)** HepG2 and **(B, D)** Hep3B cells. Isobolograms (ED₅₀) of lenvatinib or regorafenib were calculated using CalcuSyn software.

outcomes. Other HCCs, such as Huh6 and Huh7 cell lines, and one human normal hepatic cell line Lo2 cell line, were also analyzed in this study, though the effects varied a lot (data not shown). Our combinatory index analysis demonstrated that L-AA combined with lenvatinib and regorafenib expressed synergistic effects in the HepG2 and Hep3B cell lines. Hence, our data suggest that might be a potential candidate for combinatory therapy with VEGFR-targeted TKIs for treating different types of HCC.

A hallmark of HCC is the upregulation of FAS and FAS-related lipogenesis (45). FAS can also affect cell proliferation and anti-apoptotic pathways in a lipogenic-independent manner (46). Our Western blotting analysis demonstrated that sodium ascorbate downregulated the expression of G1 phase, cyclin D1, and FAS proteins, whereas it slightly increased the amount of cleaved PARP in both HepG2 and Hep3B cell lines. However, an increased population in the subG1 was only observed in Hep3B cells. The exact role of FAS in regulating HCC cell proliferation and inhibiting apoptosis needs to be further investigated.

The impact of sorafenib on the oxidative homeostasis of cancer cells occurs through increasing oxidative stress and reducing cellular antioxidant defenses (47, 48). The development of resistance is a primary problem for the antitumor effect of

sorafenib or other VEGFR-targeted TKIs in HCC (8, 9). According to our results, ascorbate might be a possible sensitizer for VEGFR-targeted TKIs to overcome the current challenge of clinical resistance. This possibility could further be determined by using TKI-resistant HCC cell lines. In this study, we hypothesized that, since pharmacological concentrations of ascorbate increase ROS production, its combination with VEGFR-targeted TKIs, lenvatinib and regorafenib, would increase intracellular ROS, leading to significant cancer cell death. However, although the combination of ascorbate with lenvatinib and regorafenib exhibited synergistic cytotoxicity in HCC, ROS generation was suppressed by the pharmacological concentrations of ascorbate alone in HepG2 and Hep3B cell lines. Two recent publications demonstrated that pharmacological concentrations of ascorbate might induce or suppress the generation of ROS depending on the type of liver cancer cell lines (49, 50). Compared with the hint from our TCGA LIHC analysis, the ROS issue for the responsiveness of TKI therapy is still puzzling. The efficacy of current combination therapy between TKIs also supports that the downregulation of ROS generation or the upregulation of reductive stress might be involved in the redox homeostasis in HepG2 and Hep3B cells. The potential mechanism remains to be further studied.

The cleavage of histone H3 by sodium ascorbate was observed in HepG2 and Hep3B cells, suggesting other possibilities by ascorbate. Cathepsin L, a lysosomal protease, has been shown to localize in the nucleus, where it participates in the proteolysis of transcription factor CDP/Cux and histone H3 (51). The cleavage site of the histone H3 N-tail targeted by cathepsin L was identified between amino acids 21 and 28, suggesting that N-terminal epigenetic modifications, such as H3K4, H3K9, H3S10, and H3K27, may be disrupted (52). Hence, to better elucidate the cytotoxicity of L-AA in HCC, the involved protease(s) and cleaved site(s) of histone H3 require further investigation.

Recycling of endogenous ascorbate enables continuous production of hydrogen peroxide, which can initiate Fenton's reactions and cause oxidative damage to cellular macromolecules (53–55). Many studies demonstrated that ascorbate at pharmacologic concentrations might serve as a possible anti-cancer drug acting *via* inducing hydrogen peroxide formation (14–17). However, the hydrogen peroxide production and initiation of Fenton's reactions through ascorbate oxidation might not be involved in the cytotoxic effect of pharmacological concentrations of ascorbate in HepG2 and Hep3B cells. Hence, the relationships between ascorbate, the formation of hydrogen peroxide and hydroxyl radicals, and the precise equilibria of Fenton's reaction in HCC remain to be investigated.

CONCLUSIONS

Our findings revealed that the relative level of cell density is an important determinant for the cytotoxicity of HCC due to ascorbate. The cytotoxic effect of pharmacological concentrations of ascorbate might not be mediated through our proposed elevation

of ROS generation. Ascorbate might be involved in redox homeostasis to enhance the efficacy of TKIs in HepG2 and Hep3B cells. However, the synergistic effects of ascorbate with TKIs (lenvatinib and regorafenib) support their potential as sensitizers for HCC targeted therapy.

DATA AVAILABILITY STATEMENT

The original contributions presented in the study are included in the article/supplementary material. Further inquiries can be directed to the corresponding author.

AUTHOR CONTRIBUTIONS

Conceptualization, H-LF, Y-LC(hang), S-MH, and T-WC; data curation, H-LF and S-TL; formal analysis, H-LF, S-TL, Y-LC(hang), and Y-LC(hiu); funding acquisition, T-WC; methodology, Y-LC(hang), Y-LC(hiu), and S-MH; project administration, S-MH; supervision, S-MH and T-WC; validation, H-LF and S-TL; writing—original draft, H-LF and T-WC; writing—review and editing, T-WC. All authors read and approved the final manuscript.

FUNDING

This work was supported by grants from the Ministry of Science and Technology [MOST-107-2314-B-016-056-MY3 to T-WC] and the Tri-Service General Hospital [TSGH-E-110209 to T-WC], Taiwan, Republic of China.

REFERENCES

- Bray F, Ferlay J, Soerjomataram I, Siegel RL, Torre LA, Jemal A. Global Cancer Statistics 2018: GLOBOCAN Estimates of Incidence and Mortality Worldwide for 36 Cancers in 185 Countries. *CA Cancer J Clin* (2018) 68 (6):394–424. doi: 10.3322/caac.21492
- Yang JD, Hainaut P, Gores GJ, Amadou A, Plymth A, Roberts LR. A Global View of Hepatocellular Carcinoma: Trends, Risk, Prevention and Management. *Nat Rev Gastroenterol Hepatol* (2019) 16(10):589–604. doi: 10.1038/s41575-019-0186-y
- Craig AJ, von Felden J, Garcia-Lezana T, Sarcognato S, Villanueva A. Tumour Evolution in Hepatocellular Carcinoma. *Nat Rev Gastroenterol Hepatol* (2020) 17(3):139–52. doi: 10.1038/s41575-019-0229-4
- Prieto J, Melero I, Sangro B. Immunological Landscape and Immunotherapy of Hepatocellular Carcinoma. *Nat Rev Gastroenterol Hepatol* (2015) 12 (12):681–700. doi: 10.1038/nrgastro.2015.173
- Bruix J, da Fonseca LG, Reig M. Insights Into the Success and Failure of Systemic Therapy for Hepatocellular Carcinoma. *Nat Rev Gastroenterol Hepatol* (2019) 16(10):617–30. doi: 10.1038/s41575-019-0179-x
- Huang A, Yang XR, Chung WY, Dennison AR, Zhou J. Targeted Therapy for Hepatocellular Carcinoma. *Signal Transduct Target Ther* (2020) 5(1):146. doi: 10.1038/s41392-020-00264-x
- Tella SH, Kommalapati A, Mahipal A. Systemic Therapy for Advanced Hepatocellular Carcinoma: Targeted Therapies. *Chin Clin Oncol* (2021) 10 (1):10. doi: 10.21037/cco-20-117
- Niu L, Liu L, Yang S, Ren J, Lai PBS, Chen GG. New Insights Into Sorafenib Resistance in Hepatocellular Carcinoma: Responsible Mechanisms and Promising Strategies. *Biochim Biophys Acta Rev Cancer* (2017) 1868 (2):564–70. doi: 10.1016/j.bbcan.2017.10.002
- Zhu YJ, Zheng B, Wang HY, Chen L. New Knowledge of the Mechanisms of Sorafenib Resistance in Liver Cancer. *Acta Pharmacol Sin* (2017) 38(5):614–22. doi: 10.1038/aps.2017.5
- Hernandez JJ, Pryszlak M, Smith L, Yanchus C, Kurji N, Shahani VM, et al. Giving Drugs a Second Chance: Overcoming Regulatory and Financial Hurdles in Repurposing Approved Drugs As Cancer Therapeutics. *Front Oncol* (2017) 7:273. doi: 10.3389/fonc.2017.00273
- Winterbourn CC. Reconciling the Chemistry and Biology of Reactive Oxygen Species. *Nat Chem Biol* (2008) 4(5):278–86. doi: 10.1038/nchembio.85
- Bakalova R, Zhelev Z, Miller T, Aoki I, Higashi T. New Potential Biomarker for Stratification of Patients for Pharmacological Vitamin C in Adjuvant Settings of Cancer Therapy. *Redox Biol* (2020) 28:101357. doi: 10.1016/j.redox.2019.101357
- Chen Q, Espey MG, Sun AY, Lee JH, Krishna MC, Shacter E, et al. Ascorbate in Pharmacologic Concentrations Selectively Generates Ascorbate Radical and Hydrogen Peroxide in Extracellular Fluid *In Vivo*. *Proc Natl Acad Sci U.S.A.* (2007) 104(21):8749–54. doi: 10.1073/pnas.0702854104
- Du J, Cullen JJ, Buettner GR. Ascorbic Acid: Chemistry, Biology and the Treatment of Cancer. *Biochim Biophys Acta* (2012) 1826(2):443–57. doi: 10.1016/j.bbcan.2012.06.003
- Venturelli S, Sinnberg TW, Niessner H, Busch C. Molecular Mechanisms of Pharmacological Doses of Ascorbate on Cancer Cells. *Wien Med Wochenschr* (2015) 165(11–12):251–7. doi: 10.1007/s10354-015-0356-7
- El Halabi I, Bejjany R, Nasr R, Mukherji D, Temraz S, Nassar FJ, et al. Ascorbic Acid in Colon Cancer: From the Basic to the Clinical

- Applications. *Int J Mol Sci* (2018) 19(9):2752. doi: 10.3390/ijms19092752
17. Wu TM, Liu ST, Chen SY, Chen GS, Wu CC, Huang SM. Mechanisms and Applications of the Anti-Cancer Effect of Pharmacological Ascorbic Acid in Cervical Cancer Cells. *Front Oncol* (2020) 10:1483. doi: 10.3389/fonc.2020.01483
 18. Kuiper C, Vissers MC. Ascorbate as a Co-Factor for Fe- and 2-Oxoglutarate Dependent Dioxygenases: Physiological Activity in Tumor Growth and Progression. *Front Oncol* (2014) 4:359. doi: 10.3389/fonc.2014.00359
 19. Chen P, Yu J, Chalmers B, Drisko J, Yang J, Li B, et al. Pharmacological Ascorbate Induces Cytotoxicity in Prostate Cancer Cells Through ATP Depletion and Induction of Autophagy. *Anticancer Drugs* (2012) 23(4):437–44. doi: 10.1097/CAD.0b013e32834fd01f
 20. Ma E, Chen P, Wilkins HM, Wang T, Swerdlow RH, Chen Q. Pharmacologic Ascorbate Induces Neuroblastoma Cell Death by Hydrogen Peroxide Mediated DNA Damage and Reduction in Cancer Cell Glycolysis. *Free Radic Biol Med* (2017) 113:36–47. doi: 10.1016/j.freeradbiomed.2017.09.008
 21. Szarka A, Kapuy O, Lorincz T, Banhegyi G. Vitamin C and Cell Death. *Antioxid Redox Signal* (2021) 34(11):831–44. doi: 10.1089/ars.2019.7897
 22. Slany A, Haudek VJ, Zwickl H, Gundacker NC, Grusch M, Weiss TS, et al. Cell Characterization by Proteome Profiling Applied to Primary Hepatocytes and Hepatocyte Cell Lines Hep-G2 and Hep-3b. *J Proteome Res* (2010) 9(1):6–21. doi: 10.1021/pr900057t
 23. Qiu GH, Xie X, Xu F, Shi X, Wang Y, Deng L. Distinctive Pharmacological Differences Between Liver Cancer Cell Lines HepG2 and Hep3B. *Cytotechnology* (2015) 67(1):1–12. doi: 10.1007/s10616-014-9761-9
 24. Khoury L, Zalko D, Audebert M. Evaluation of Four Human Cell Lines With Distinct Biotransformation Properties for Genotoxic Screening. *Mutagenesis* (2016) 31(1):83–96. doi: 10.1093/mutage/gev058
 25. Waldherr M, Misik M, Ferk F, Tomc J, Zegura B, Filipic M, et al. Use of HuH6 and Other Human-Derived Hepatoma Lines for the Detection of Genotoxins: A New Hope for Laboratory Animals? *Arch Toxicol* (2018) 92(2):921–34. doi: 10.1007/s00204-017-2109-4
 26. Misik M, Nersesyan A, Ropek N, Huber WW, Haslinger E, Knasmueller S. Use of Human Derived Liver Cells for the Detection of Genotoxins in Comet Assays. *Mutat Res* (2019) 845:402995. doi: 10.1016/j.mrgentox.2018.12.003
 27. Yoo M, Shin J, Kim J, Ryall KA, Lee K, Lee S, et al. DSignDB: Drug Signatures Database for Gene Set Analysis. *Bioinformatics* (2015) 31(18):3069–71. doi: 10.1093/bioinformatics/btv313
 28. Harris MA, Clark J, Ireland A, Lomax J, Ashburner M, Foulger R, et al. The Gene Ontology (GO) Database and Informatics Resource. *Nucleic Acids Res* (2004) 32:D258–261. doi: 10.1093/nar/gkh036
 29. Goldman MJ, Craft B, Hastie M, Repecka K, McDade F, Kamath A, et al. Visualizing and Interpreting Cancer Genomics Data via the Xena Platform. *Nat Biotechnol* (2020) 38(6):675–8. doi: 10.1038/s41587-020-0546-8
 30. Hanzelmann S, Castelo R, Guinney J. GSVA: Gene Set Variation Analysis for Microarray and RNA-Seq Data. *BMC Bioinf* (2013) 14:7. doi: 10.1186/1471-2105-14-7
 31. Ogłuszka M, Orzechowska M, Jedroszka D, Witas P, Bednarek AK. Evaluate Cutpoints: Adaptable Continuous Data Distribution System for Determining Survival in Kaplan-Meier Estimator. *Comput Methods Programs BioMed* (2019) 177:133–9. doi: 10.1016/j.cmpb.2019.05.023
 32. Chen CL, Meng E, Wu ST, Lai HF, Lu YS, Yang MH, et al. Targeting S1PR1 May Result in Enhanced Migration of Cancer Cells in Bladder Carcinoma. *Cancers (Basel)* (2021) 13(17):4474. doi: 10.3390/cancers13174474
 33. Wu YY, Lai HF, Huang TC, Chen YG, Ye RH, Chang PY, et al. Aberrantly Reduced Expression of miR-342-5p Contributes to CCND1-Associated Chronic Myeloid Leukemia Progression and Imatinib Resistance. *Cell Death Dis* (2021) 12(10):908. doi: 10.1038/s41419-021-04209-2
 34. Chakrabarti R, Kundu S, Kumar S, Chakrabarti R. Vitamin A as an Enzyme That Catalyzes the Reduction of MTT to Formazan by Vitamin C. *J Cell Biochem* (2000) 80(1):133–8. doi: 10.1002/1097-4644(20010101)80:1<133::aid-jcb120>3.0.co;2-t
 35. Chou TC. Theoretical Basis, Experimental Design, and Computerized Simulation of Synergism and Antagonism in Drug Combination Studies. *Pharmacol Rev* (2006) 58(3):621–81. doi: 10.1124/pr.58.3.10
 36. Verrax J, Calderon PB. Pharmacologic Concentrations of Ascorbate Are Achieved by Parenteral Administration and Exhibit Antitumoral Effects. *Free Radic Biol Med* (2009) 47(1):32–40. doi: 10.1016/j.freeradbiomed.2009.02.016
 37. Kuiper C, Molenaar IG, Dachs GU, Currie MJ, Sykes PH, Vissers MC. Low Ascorbate Levels are Associated With Increased Hypoxia-Inducible Factor-1 Activity and an Aggressive Tumor Phenotype in Endometrial Cancer. *Cancer Res* (2010) 70(14):5749–58. doi: 10.1158/0008-5472.CAN-10-0263
 38. Yun J, Mullarky E, Lu C, Bosch KN, Kavalier A, Rivera K, et al. Vitamin C Selectively Kills KRAS and BRAF Mutant Colorectal Cancer Cells by Targeting GAPDH. *Science* (2015) 350(6266):1391–6. doi: 10.1126/science.aaa5004
 39. Karaczyn A, Ivanov S, Reynolds M, Zhitkovich A, Kasprzak KS, Salnikow K. Ascorbate Depletion Mediates Up-Regulation of Hypoxia-Associated Proteins by Cell Density and Nickel. *J Cell Biochem* (2006) 97(5):1025–35. doi: 10.1002/jcb.20705
 40. Ghanem A, Melzer AM, Zaal E, Neises L, Baltissen D, Matar O, et al. Ascorbate Kills Breast Cancer Cells by Rewiring Metabolism via Redox Imbalance and Energy Crisis. *Free Radic Biol Med* (2021) 163:196–209. doi: 10.1016/j.freeradbiomed.2020.12.012
 41. Stotz M, Gerger A, Haybaeck J, Kiesslich T, Bullock MD, Pichler M. Molecular Targeted Therapies in Hepatocellular Carcinoma: Past, Present and Future. *Anticancer Res* (2015) 35(11):5737–44.
 42. Girardi DM, Pacifico JPM, Guedes de Amorim FPL, Dos Santos Fernandes G, Teixeira MC, Pereira AAL. Immunotherapy and Targeted Therapy for Hepatocellular Carcinoma: A Literature Review and Treatment Perspectives. *Pharm (Basel)* (2020) 14(1):28. doi: 10.3390/ph14010028
 43. Matsuki M, Hoshi T, Yamamoto Y, Ikemori-Kawada M, Minoshima Y, Funahashi Y, et al. Lenvatinib Inhibits Angiogenesis and Tumor Fibroblast Growth Factor Signaling Pathways in Human Hepatocellular Carcinoma Models. *Cancer Med* (2018) 7(6):2641–53. doi: 10.1002/cam4.1517
 44. Arai H, Battaglin F, Wang J, Lo JH, Soni S, Zhang W, et al. Molecular Insight of Regorafenib Treatment for Colorectal Cancer. *Cancer Treat Rev* (2019) 81:101912. doi: 10.1016/j.ctrv.2019.101912
 45. Koundouros N, Poulogiannis G. Reprogramming of Fatty Acid Metabolism in Cancer. *Br J Cancer* (2020) 122(1):4–22. doi: 10.1038/s41416-019-0650-z
 46. Che L, Pilo MG, Cigliano A, Latte G, Simile MM, Ribback S, et al. Oncogene Dependent Requirement of Fatty Acid Synthase in Hepatocellular Carcinoma. *Cell Cycle* (2017) 16(6):499–507. doi: 10.1080/15384101.2017.1282586
 47. Wilhelm S, Carter C, Lynch M, Lowinger T, Dumas J, Smith RA, et al. Discovery and Development of Sorafenib: A Multikinase Inhibitor for Treating Cancer. *Nat Rev Drug Discovery* (2006) 5(10):835–44. doi: 10.1038/nrd2130
 48. Llovet JM, Ricci S, Mazzaferro V, Hilgard P, Gane E, Blanc JF, et al. Sorafenib in Advanced Hepatocellular Carcinoma. *N Engl J Med* (2008) 359(4):378–90. doi: 10.1056/NEJMoa0708857
 49. Gao X, Wei K, Hu B, Xu K, Tang B. Ascorbic Acid Induced HepG2 Cells' Apoptosis via Intracellular Reductive Stress. *Theranostics* (2019) 9(14):4233–40. doi: 10.7150/thno.33783
 50. Zhang X, Liu T, Li Z, Feng Y, Corpe C, Liu S, et al. Hepatomas are Exquisitely Sensitive to Pharmacologic Ascorbate (P-AsCH(-)). *Theranostics* (2019) 9(26):8109–26. doi: 10.7150/thno.35378
 51. Duncan EM, Muratore-Schroeder TL, Cook RG, Garcia BA, Shabanowitz J, Hunt DF, et al. Cathepsin L Proteolytically Processes Histone H3 During Mouse Embryonic Stem Cell Differentiation. *Cell* (2008) 135(2):284–94. doi: 10.1016/j.cell.2008.09.055
 52. Adams-Cioaba MA, Krupa JC, Xu C, Mort JS, Min J. Structural Basis for the Recognition and Cleavage of Histone H3 by Cathepsin L. *Nat Commun* (2011) 2:197. doi: 10.1038/ncomms1204
 53. Suh J, Zhu BZ, Frei B. Ascorbate Does Not Act as a Pro-Oxidant Towards Lipids and Proteins in Human Plasma Exposed to Redox-Active Transition Metal Ions and Hydrogen Peroxide. *Free Radic Biol Med* (2003) 34(10):1306–14. doi: 10.1016/S0891-5849(03)00147-3
 54. Lane DJ, Chikhani S, Richardson V, Richardson DR. Transferrin Iron Uptake is Stimulated by Ascorbate via an Intracellular Reductive Mechanism. *Biochim Biophys Acta* (2013) 1833(6):1527–41. doi: 10.1016/j.bbamer.2013.02.010

55. Lane DJ, Richardson DR. The Active Role of Vitamin C in Mammalian Iron Metabolism: Much More Than Just Enhanced Iron Absorption! *Free Radic Biol Med* (2014) 75:69–83. doi: 10.1016/j.freeradbiomed.2014.07.007

Conflict of Interest: The authors declare that the research was conducted in the absence of any commercial or financial relationships that could be construed as a potential conflict of interest.

Publisher's Note: All claims expressed in this article are solely those of the authors and do not necessarily represent those of their affiliated organizations, or those of

the publisher, the editors and the reviewers. Any product that may be evaluated in this article, or claim that may be made by its manufacturer, is not guaranteed or endorsed by the publisher.

Copyright © 2022 Fan, Liu, Chang, Chiu, Huang and Chen. This is an open-access article distributed under the terms of the Creative Commons Attribution License (CC BY). The use, distribution or reproduction in other forums is permitted, provided the original author(s) and the copyright owner(s) are credited and that the original publication in this journal is cited, in accordance with accepted academic practice. No use, distribution or reproduction is permitted which does not comply with these terms.



OPEN ACCESS

EDITED BY

Benyi Li,
University of Kansas Medical Center,
United States

REVIEWED BY

Xiaoji Luo,
Chongqing Medical University, China
Qi Ma,
Ningbo First Hospital, China

*CORRESPONDENCE

Xia Ren
1989renxia@163.com
Xian-Jun Fu
xianxiu@hotmail.com

SPECIALTY SECTION

This article was submitted to
Pharmacology of Anti-Cancer Drugs,
a section of the journal
Frontiers in Oncology

RECEIVED 28 March 2022

ACCEPTED 28 October 2022

PUBLISHED 15 November 2022

CITATION

Song P, Li H, Xu K, Li Z-W, Ren X and
Fu X-J (2022) A bibliometric and
visualization-based analysis of
temozolomide research hotspots and
frontier evolution.
Front. Oncol. 12:905868.
doi: 10.3389/fonc.2022.905868

COPYRIGHT

© 2022 Song, Li, Xu, Li, Ren and Fu. This
is an open-access article distributed
under the terms of the [Creative
Commons Attribution License \(CC BY\)](#).
The use, distribution or reproduction
in other forums is permitted, provided
the original author(s) and the
copyright owner(s) are credited and
that the original publication in this
journal is cited, in accordance with
accepted academic practice. No use,
distribution or reproduction is
permitted which does not comply with
these terms.

A bibliometric and visualization-based analysis of temozolomide research hotspots and frontier evolution

Peng Song^{1,2}, Hui Li^{2,3}, Kuo Xu^{2,3}, Zi-Wei Li^{2,3}, Xia Ren^{2,3*}
and Xian-Jun Fu^{1,2,3*}

¹College of Pharmacy, Shandong University of Traditional Chinese Medicine, Jinan, China,

²Traditional Chinese Medicine Research Center, Qingdao Academy Shandong University of
Traditional Chinese Medicine, Qingdao, China, ³Shandong Engineering and Technology Research
Center of Traditional Chinese Medicine, Jinan, China

The literature related to TMZ research in the Web of Science (WOS) database was analyzed using bibliometrics and visualization by Citespace and VOSviewer. The publication status (number of publications, institutions, and frequency of citations), collaborations, and research focus was analyzed to clarify the current situation of TMZ research. And the recent research on TMZ provides a detailed summary. Based on objective data analysis, this study provides a complete analysis portraying the progression of historical milestones in TMZ development and future research directions from various TMZ research domains.

KEYWORDS

temozolomide, glioblastoma, bibliometrics, web of science, development process

Introduction

Temozolomide (TMZ) is a novel imidazole-tetrazine alkylating agent ([Figure 1](#)). It has a low molecular weight, a broad antitumor range, is lipophilic, and crosses the blood-brain barrier, among other properties. It is rapidly absorbed after oral administration and has no toxicity when combined with other medications ([1, 2](#)). On August 11, 1999, the FDA approved TMZ to treat adult recurrent glioblastoma ([3](#)), and it has since become the first-line chemotherapeutic medication for malignant glioma and other intracranial tumors ([4](#)). TMZ causes tumor cells to die by causing alkylation of the oxygen and nitrogen atoms at position 7 of DNA guanine, resulting in a base mismatch ([5](#)).

Most of the research literature on TMZ focuses on studies of resistance mechanisms and clinical trials, and the review literature on TMZ focuses on some specific aspects. It is relatively limited, and there are few overall analyses of TMZ.

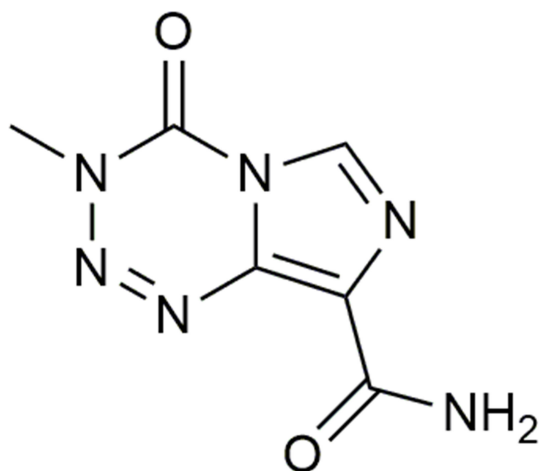


FIGURE 1
Structural formula of TMZ. Chemical name: 3,4-dihydro-3-methyl-4-oxoimidazo[5,1-d]-as-tetrazine-8-carboxamide.

Bibliometrics, which combines mathematics, statistics, and bibliography, uses quantitative analysis to investigate the discipline's structural features and hot trends and evaluate and predict outcomes (6). Publications, authors, keywords, and literature citations are the statistical objects. Using bibliometric software to visualize and analyze relevant literature, as opposed to textual descriptions of traditional theoretical reviews, can present the interrelationships among the literature of a discipline or a research field as a scientific knowledge map, which can not only sort out past research trajectories but also better grasp future research trends and directions (7). Thanks to computer tools, the topic has gotten more attention in terms of theory and practice. Scientific knowledge mapping, which compiles the literature, is commonly employed on this premise. CiteSpace and VOSviewer are two knowledge mapping-focused information visualization and analysis programs.

Only a few cases of knowledge mapping being used to assess the overall state of TMZ research have been reported so far. Based on this, we hope to present the development process and research hotspots in TMZ research in scientific knowledge mapping more intuitively and effectively by using software to data-mine, integrate, and analyze related research literature, and provide a reference for drug development.

Materials and methods

The Web of Science (Wos) core collection database was selected, indexed by Science Citation Index Expanded (SCI-E), Current Chemical reaction (CCR-E), and Index Chemicus (IC), and “Temozolomide” was used as the subject to search the relevant literature between 1994 and 2021, and articles and

reviews were used as the type of literature, and Citespace was used to de-duplicate and refine the search results, resulting in 12,910 publications. The records were exported as plain text files with the content of “Full records and cited references” for subsequent analysis.

CiteSpace, VOSviewer, and HistCite bibliometric software applications were used to examine the data collected. The data exported from the WOS database were analyzed in this paper using the citation analysis tool HistCite (HistCite Pro version 2.1 recompiled; Dr. Eugene Garfield) to obtain detailed information (including country, institution, journal, Category, and so on) on publications in the field of TMZ; and the bibliometric software VOSviewer (VOSviewer version 1.6.17; Centre for Science and Technology Studies, Leiden University, Netherlands) to construct. The global disparities in TMZ research by country can be better visualized using the geographic heat map. Using the Geographic Heat Map add-in in a spreadsheet, a geographic heat map of TMZ articles was constructed in this paper (Microsoft Office 2021 Excel; Microsoft Corp.). The Journal Citation Reports 2020 (JCR) included each journal's impact factors (IF) and H-indexes. Impact factor (IF) has become an internationally accepted index for journal evaluation. It is not only a measure of the usefulness and display of a journal, but also an important indicator of the academic level of a journal, and even the quality of a paper (8). The H-index is a method of evaluating academic achievement, which can accurately reflect a person's academic achievement (9).

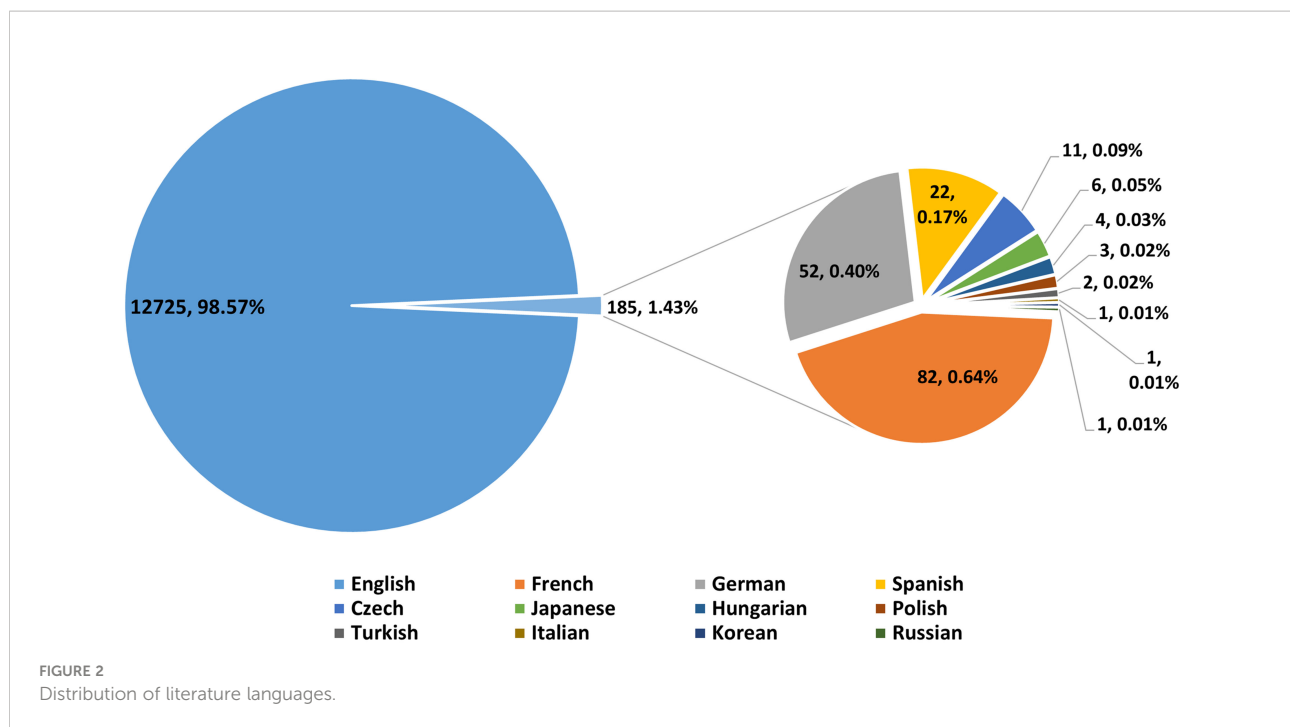
Results

General statistics

From 1994 to 2021, the Web of Science (WOS) core collection database yielded 12,910 research publications on the topic of TMZ. According to the pooled study, these 12,910 papers came from 104 nations, 9949 institutions, 49,458 authors, 1,485 journals, and 9,432 grant-funded institutions. They are written in 12 languages and contain 24,929 keywords. With 12,725 papers (98.57%), English-language articles are the most common, followed by French, German, and Spanish, with 82, 52, and 22 articles, respectively (Figure 2). The types of literature were separated into two categories: research-based literature (86.18%) and review-based literature (13.82%) (Table 1). This shows that the range of temozolomide-related studies mapped (countries, institutions, authors, etc.) is wide and the depth of research is deep.

Publication time statistics

The quantity of literature and its patterns reflect this topic's current study state (10). Malcolm F. G. Stevens et al. published



the first TMZ literature in 1994, indicating several different synthetic techniques employed for the overall synthesis of TMZ. This study shows the annual number of publications in the field of temozolomide about the total literature records (Recs) and global citation score (TGCS) from 1994–2021 (Figure 3). In terms of total literature records (Recs), the publications increased slowly from 1994 to 1998. They increased quickly from 1999 to 2021, with an average of 615 publications per year, and the maximum number was 1328 in 2020. TGCS increased rapidly from 1994 to 2015 before gradually decreasing from 2016 to 2021. The rapid growth of TGCS in 2000, 2005, and 2009 and the peak of TGCS in 2013 (highest value of 32919) indicate breakthroughs or significant discoveries in TMZ research may have occurred during these four years.

Country characteristics

It's critical to examine TMZ at the country level to assess its academic impact and choose nations to focus on. Between 1994 and 2021, teams from 104 countries published articles on TMZ. Figure 4A depicts the global distribution of all publications, whereas Figure 4B depicts the 15 nations with the highest Recs

and TGCSs productivity. The United States, China, Germany, and Italy were the countries with >1000 publications out of the 12910 total, with the United States having the most (4470, 34.6%), followed by China (2572, 19.9%) and Germany (1399, 10.8%). In terms of TGCS, the United States ranked first (192812, 47.1%), followed by Germany (81323, 20.1%), and the Switzerland (57165, 14.1%). In the field of TMZ, we discovered that the United States dominated both the number of publications and the overall global citation score, indicating that the United States may have the most comprehensive and in-depth research in this sector. Although China is second only to the United States in the Recs ranking, it is ranked seventh in the TGCS, indicating that China has a significant role in TMZ research. Still, its academic impact on the subject needs to be strengthened to improve its international significance.

Academic collaboration

Academic collaboration among countries, institutions, and authors is progressively becoming the standard scientific research approach as the breadth of scientific study extends and the depth of research deepens (11). To evaluate TMZ's academic influence and determine its research force, it's vital to look at it from three perspectives: countries, institutions, and authors. We investigated the academic collaboration between countries, institutions, and authors in the TMZ research area (Figure 5) and the evolution of collaborative networks between different research forces over a period of 28 years (Figure 6). Each node represents a different country/institution/author. The

TABLE 1 Distribution of literature types.

Type of Literature	Number	Percentage (%)
Research-based Literature	11126	86.18
Review-based Literature	1784	13.82

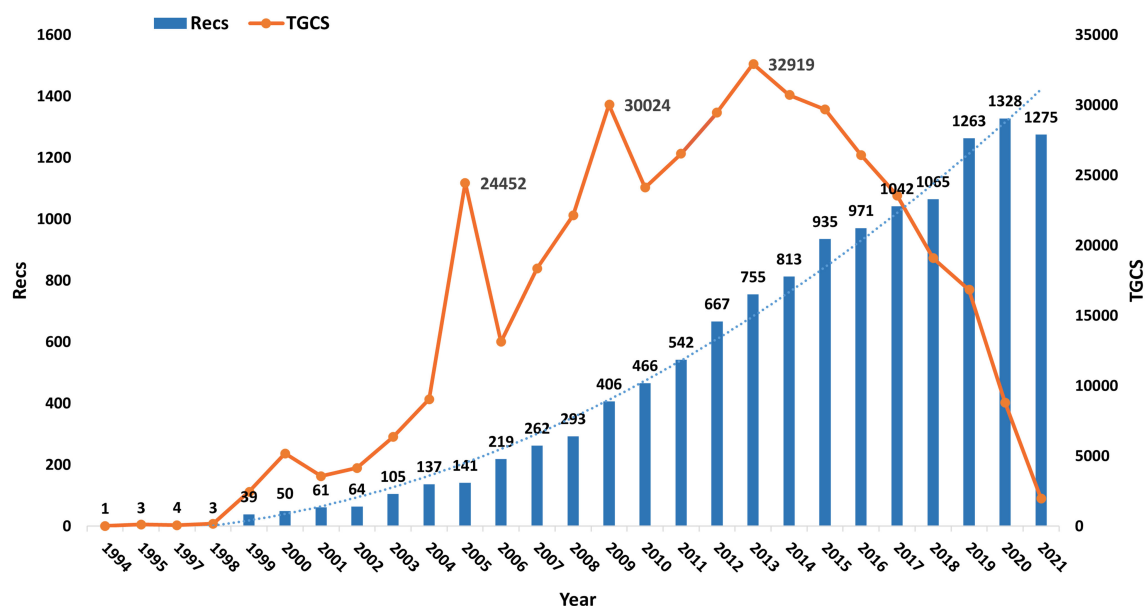


FIGURE 3
Timeline of publications and TGCS on TMZ.

node's size represents the number of articles. The thickness of the connecting lines represents the power of collaboration. Each group in the collaborative network with similar attributes represents a cluster colored differently.

With a threshold of at least 25 publications, the co-occurrence analysis of countries using VOSviewer software produced a network diagram of country co-occurrence (Figure 5A). 51 countries have crossed the cooperation threshold. There are closer collaboration links among nations, as evidenced by the intricate overlapping linkages, and the United States, in particular, plays a crucial role in international exchange. China-USA, Germany-Switzerland, and France-Canada have the highest total collaboration intensity among the six clusters of the national cooperation network. From the evolution of the country collaboration network (Figure 6A), it can be observed that initially (1994–2000), the major countries researching TMZ were all located in the United States and Europe, and the closest collaboration was between the United States and the United Kingdom. Over time, Asian countries, represented by China, Japan, and Korea, joined the collaborative network of TMZ research. The United States dominated throughout the 28-year period, but in the last 7 years, China's share of the national collaborative network has grown and has approached that of the United States. In the next 15 years, the United States may be overtaken by China.

A co-occurrence research of institutions revealed a graph of institutional co-occurrence networks with a threshold of at least 35 publications (Figure 5B). In Figure 5B, we see that 174 institutions were organized into eight distinct clusters. The

University of Texas MD Anderson Cancer Center, a world-class center for cancer research, diagnosis, and treatment, was the most prolific research institution (literature = 315) and the institution with the highest collaboration intensity (total collaboration intensity = 696), according to a closer look at the top 10 collaborating institutions (Table 2). Second and third places, respectively, went to the German Cancer Research Center (GRC) and the University of California, San Francisco (Univ California San Francisco). In addition to the German Cancer Research Center and the University Hospital Zurich, eight of the top 10 partnering institutions are from the United States, showing that TMZ research in the United States is high. Furthermore, seven of the top ten institutions are top oncology research institutes, while the remaining three universities are among the world's leading oncology research and treatment institutions. This shows that basic TMZ research is intimately tied to clinical applications. From the evolution of the institutional collaboration network (Figure 6B), it can be observed that during the period 1994–2007, the inter-institutional collaborations were not strong and the research strengths of the institutions varied widely, with Christie Hospital and University Texas being the most prominent. 2008–2014, compared to the other institutions in the institutional collaboration network The strength of the collaboration between Massachusetts General Hospital and Harvard University, German Cancer Research Center and University Zurich Hospital is outstanding compared to other institutions in the institutional collaboration network. In the last seven years, the strength of the collaboration between Massachusetts General

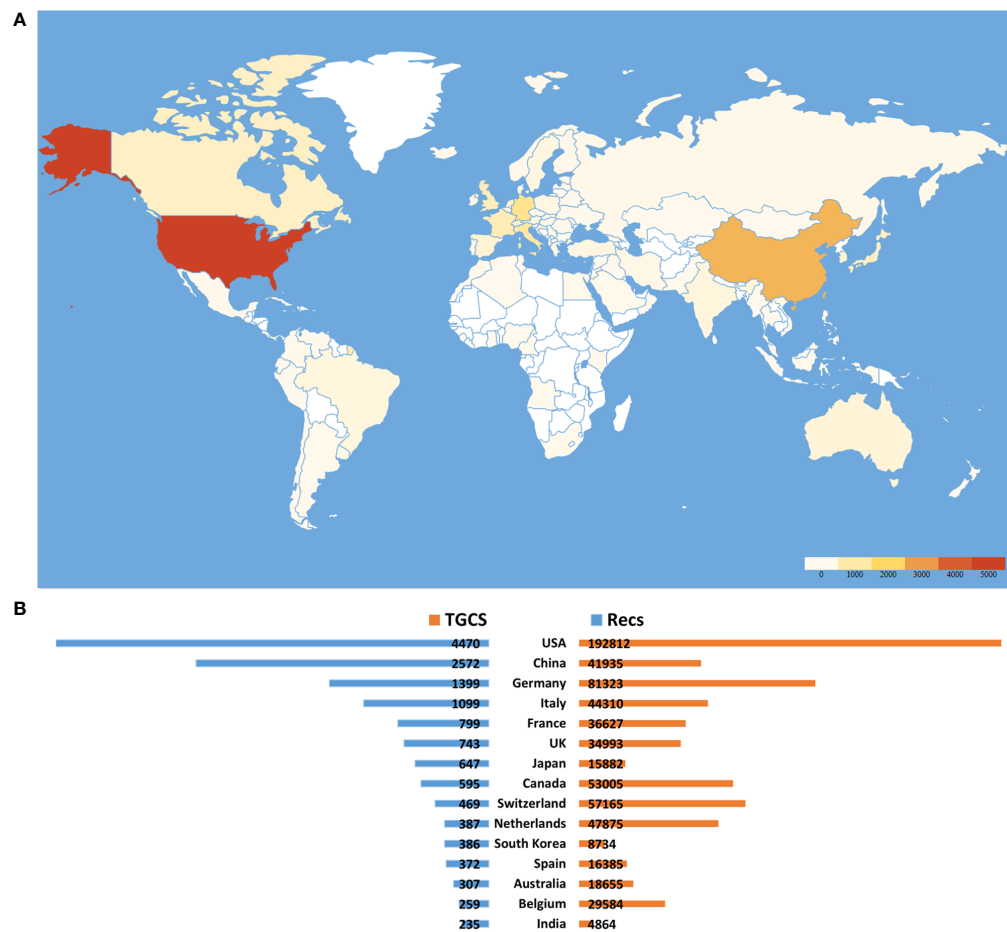


FIGURE 4

Main countries distribution on TMZ publications. (A) Geographical distribution of TMZ. (B) The top 15 most productive countries in the publication of TMZ and their corresponding TGCS.

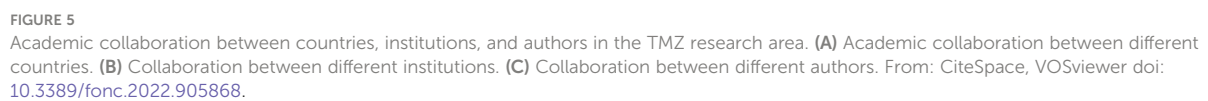
Hospital and Harvard University was stronger than the other institutions.

VOSviewer software was used to do a co-occurrence analysis of research authors. A threshold of at least 37 publications was employed to generate an author co-occurrence network graph, as shown in Figure 5C. The 50 writers are organized into six clusters, independent of the others. The strong ties that bind these six author clusters point to a global network of scholars working together. Michael Weller and Wolfgang Wick are the two nodes in the collaborative network with the most prominent publication volume and collaboration intensity. The core nodes of the six collaborative network clusters are Weller Michael, Reardon David A., Stupp Roger, Wen Patrick Y., Brandes Alba A., and Park chuckle. From the evolution of the author collaboration network (Figure 6C), it can be observed that in the first 14 years (1994–2007), the inter-institutional collaborations were in a relatively simple stage of development and did not form mature networks, but only chains of

collaboration. In the last 14 years, institutional collaborations have been further developed. between 2008-2014, compared to other authors in the author collaborative network, Weller Michael-Stupp Roger-Wick Wolfgang and Reardon David A.-Friedman Henry S.- Vredenburg James J. The two author clusters are the most prominent in the author collaboration network. In the last 7 years, two author groups, Weller Michael-Wick Wolfgang and Wen Patrick Y.-Cloughesy Timothy F., have replaced other authors as the core author groups in the author collaborative network.

Funding agency distribution

The research direction and content in TMZ are reflected in the distribution of funding agencies (12). The top ten institutions that funded TMZ-related research the most from 1994 to 2021, accounting for 65.41% of the total number of publications



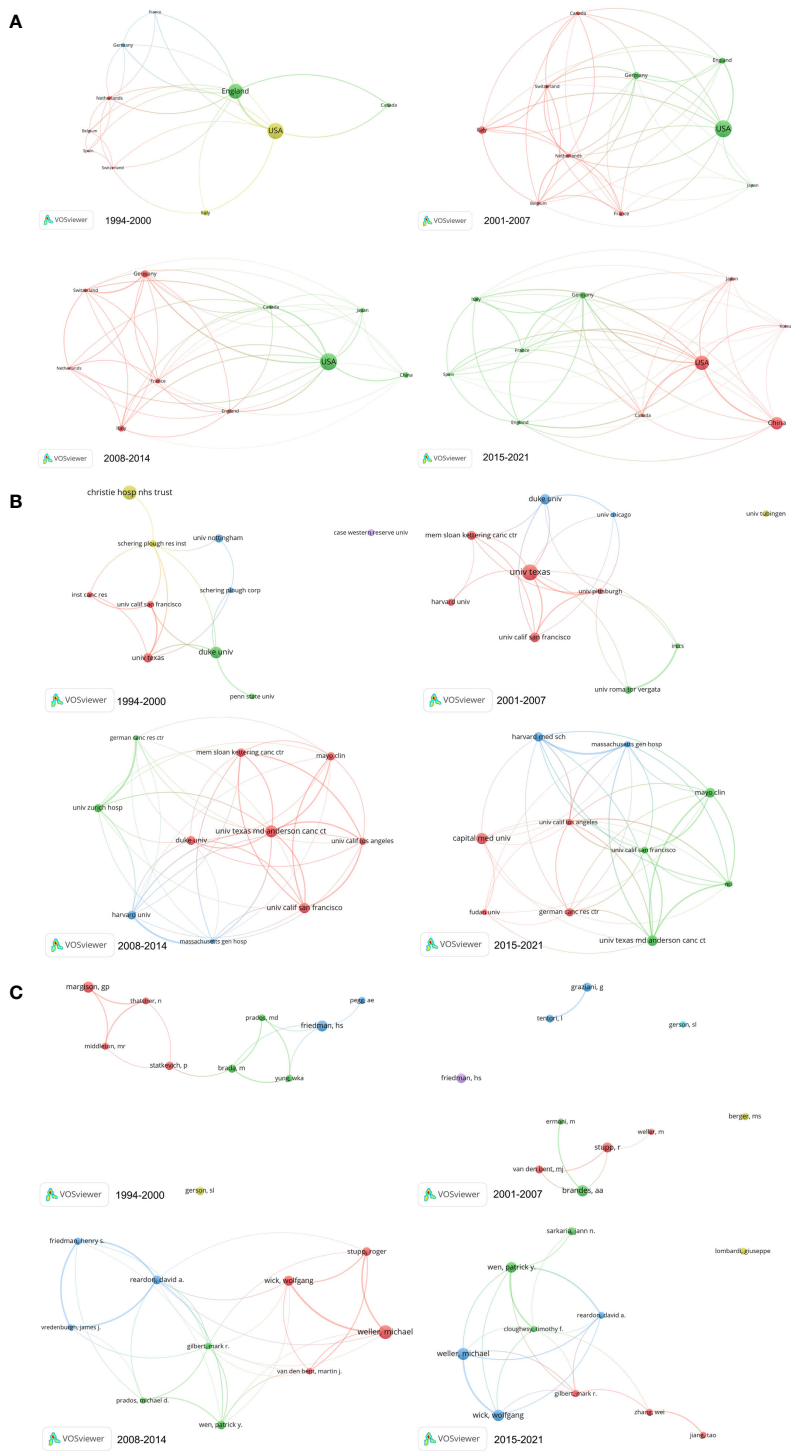


FIGURE 6
The evolution of collaborative networks among different research forces. **(A)** The evolution of collaboration networks of top 10 prolific countries. **(B)** The evolution of collaboration networks of top 10 prolific institutions. **(C)** The evolution of collaboration networks of top 10 prolific authors. From: CiteSpace, VOSviewer doi: 10.3389/fonc.2022.905868.

TABLE 2 The top 10 most collaborative institutions.

Organization	Document	Citation	Total collaborative strength
Univ Texas MD Anderson Canc Ctr	315	18245	696
German Canc Res Ctr	203	11231	588
Univ Calif San Francisco	268	19182	553
Massachusetts Gen Hosp	175	9343	533
Dana Farber Canc Inst	156	9236	508
Univ Calif Los Angeles	201	14848	487
Mayo Clin	262	12078	482
Mem Sloan Kettering Canc Ctr	213	15737	403
Univ Zurich Hosp	125	11730	389
Univ Pittsburgh	131	8232	373

(Figure 7). The top four funding agencies, including the USA Department of Health and Human Services, the National Institutes of Health (NIH) USA, the Nih National Cancer Institute (NCI), and the National Natural Science Foundation of China (NSFC), with 6,882 articles funded, accounting for more than half (53.31%) of the total number of publications. The top three research funding agencies are all from the United States, accounting for 44.72% of all publications, consistent with the high number of publications, high citations, and high level of collaboration, reflecting the United States' leading position in the field of TMZ research. The National Natural Science Foundation of China (NSFC) ranks fourth behind the three USA research funding organizations, with 1109 publications financed, demonstrating China's contribution to TMZ research. Two pharmaceutical corporations (Merck Company and Roche Holding) are in the top ten research funding organizations, indicating that basic and clinical TMZ research are closely linked.

Institution and author contributions

Authors and research institutions are vital forces driving academic development and innovation in a particular field, so this study is important to analyze the main institutions and essential authors in TMZ (13). This study presents the top 15 productive institutions in the Recs and TGCS (Figure 8). According to Recs and TGCS, the 15 research institutions can be divided into three categories: a) Institutions represented by University Texas MD Anderson Cancer Center, University Calif San Francisco, Duke University, and Mem Sloan Kettering Cancer Center are characterized by high TGCS and high Recs of publications. b) Institutions represented by University Tubingen, University Calgary, and the Medical University of Vienna are characterized by high TGCS and low Recs of publications. c) Institutions represented by Mayo Clinic, Capital Medical University, and The institutions represented by Mayo Clinic, Capital Medical University, and German Cancer

Research Center are characterized by low TGCS and high Recs of publications.

All authors are rated according to their number of publications and h-index in this study to investigate the most influential specialists in TMZ research for 1994-2021 (Figure 9). The H-index predicts future scientific accomplishment outperforms other measures (total citation count, citations per paper, and total paper count) (9). Weller Michael of the University Hospital Zurich is not only the most influential author (Recs=184) but also the author with the highest h-index (H-index=123), multiple highly referenced works, and the most significant overall TGCS score (TGCS=50816). With an h-index of 105 and a Recs rating of 85, Friedman Henry S. of Duke University, USA, has the second-highest h-index. Tao Jiang of the Beijing Neurosurgical Institute, the sole Chinese among the top ten specialists, has made significant contributions, with 72 and h-index of 45, respectively.

Journal performance

The research of journals identifies the specific directions and disciplines involved in a field and identifies the critical journals in that field, which provide a reference for researchers (14). Impact factor (IF) is a key indicator of the academic level of journals and even the quality of papers and a measure of their utility and display (8), which was proposed by Eugene Garfield in 1972 (15). This research lists the details of the journals involved in the top ten TMZ publications in terms of the number of publications (Table 3), six of which are from the United States, two from Switzerland, and one from the United Kingdom and Greece. It is worth noting that the top ten journals in terms of the number of publications account for 22.2% of the total number of publications, which indicates that the selected journals are representative and of research significance. The Journal of Neuro-Oncology has the most publications (Recs=879), but it also has the highest TGCS score (TGCS=23102). Seven of the top ten journals in terms of

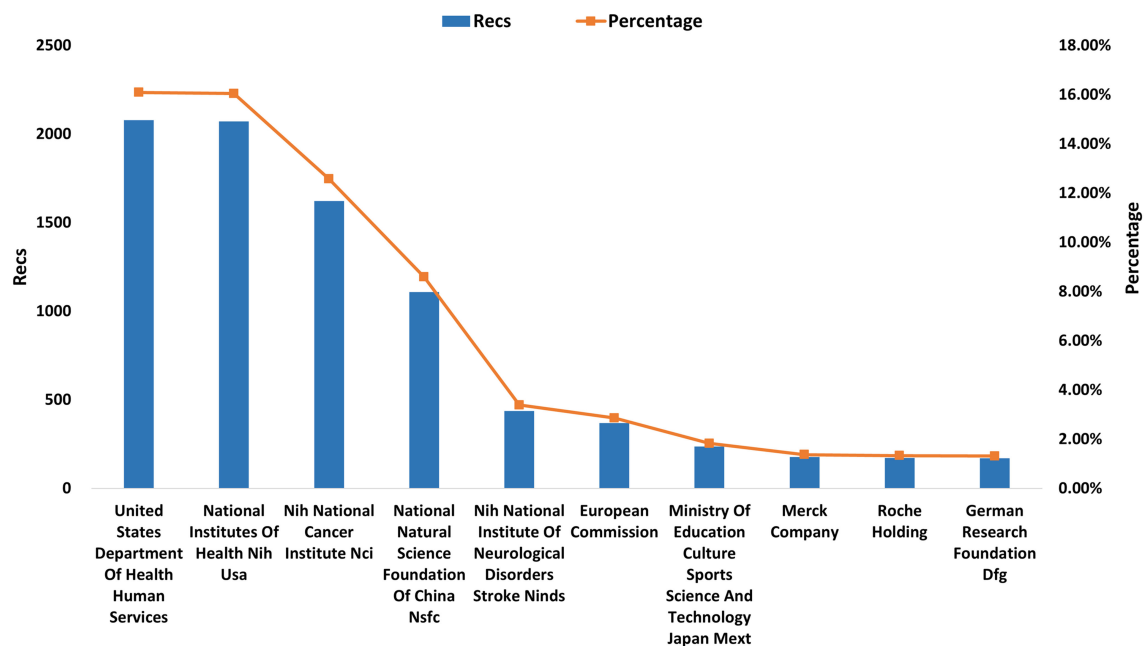


FIGURE 7
The top 10 productive funding agencies in the TMZ area.

articles are dedicated to oncology research. In contrast, two are dedicated to neuro-oncology, reflecting the focus of TMZ research in cranial cancers.

Category analysis

Research on the categories involved in a field can identify the field's development direction and research hotspots (16). This study conducted a sectoral percentage analysis (Figure 10A) and category co-occurrence chart analysis (Figure 10B) for the 10 most involved topics in the TMZ field.

According to Figure 10A, Oncology (3668 records, 28.41%), clinical neurology (3469 recordings, 26.87%), and pharmacology/pharmacy (1441 records, 11.16%) make up the top three categories, accounting for 66.44% of all articles. In addition, the bottom ten research categories, such as cell biology, surgery, and neurosciences, may be developing research areas and thus equally informative.

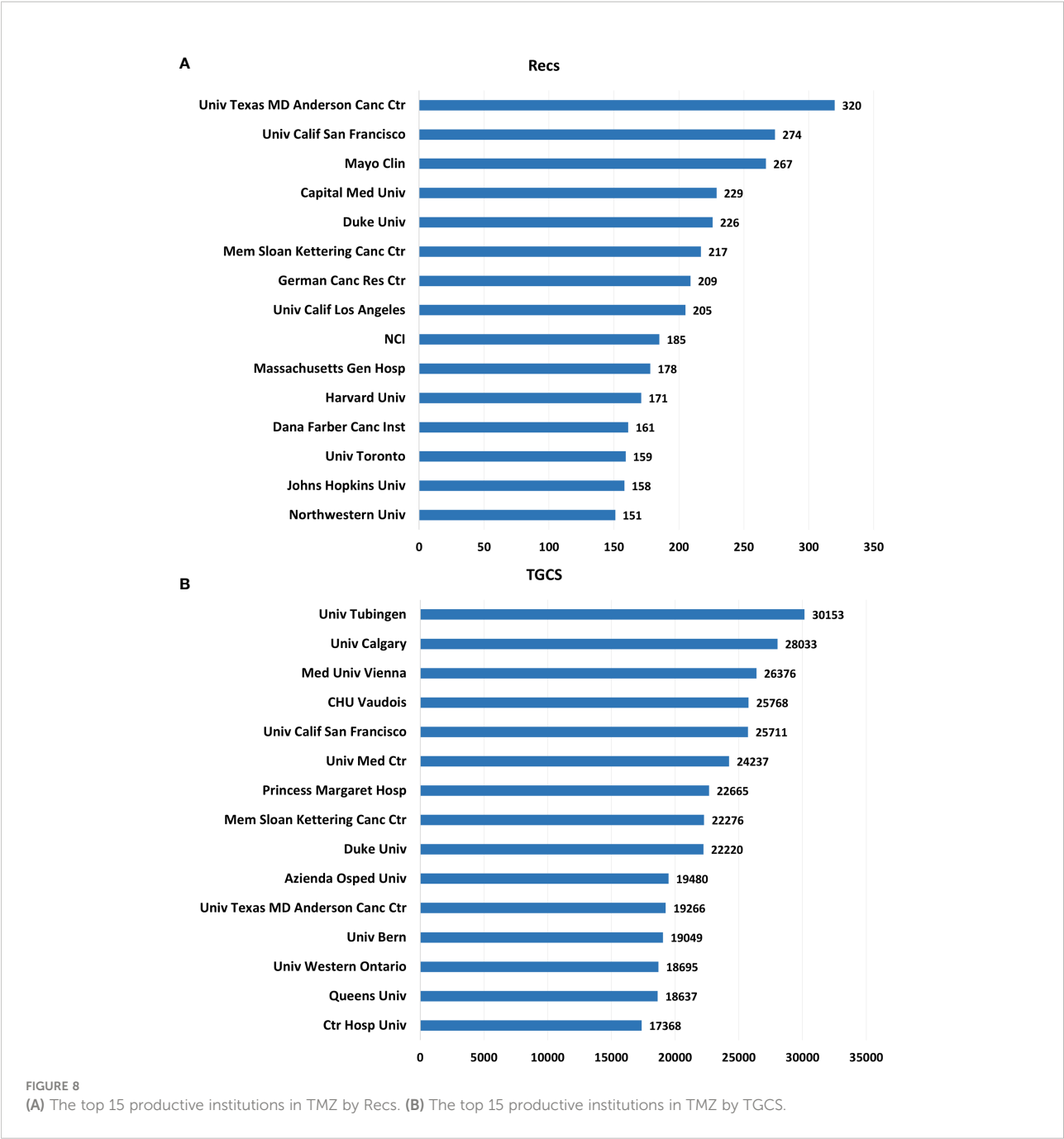
Figure 10B depicts the visual analysis of the TMZ research categories from 1994 to 2021. The 10 most cited articles' categories were reviewed to find more than 512 times cited. According to the Co-occurrence network, the most crucial research categories in TMZ are oncology, clinical neurology, and pharmacology/pharmacy. In contrast, biochemistry/molecular biology, radiology, nuclear medicine/medical imaging have a high citation frequency and a newer year of cited literature, indicating a possible emerging research hotspot.

Keyword detection and burst analysis

Keywords can express the primary content of a piece of writing. High-frequency keywords can reveal new research trends, whereas emergent keywords can reveal new research hotspots (17). After de-duplication and synonyms, 24928 keywords were extracted from 12910 texts. With 118 as the minimum number of keyword occurrences, 176 were eventually chosen, and the co-occurrence cluster analysis yielded three clusters.

The top ten most frequent keywords were TMZ (7434), glioblastoma (4873), radiotherapy (2966), survival (2266), adjuvant TMZ (2247), glioma (2095), chemotherapy (1928), cancer (1831), expression (1697), and malignant glioma (1398) (Figure 11A). Each node in Figure 11B represents one of the 176 keywords, with the node's size indicating the frequency of occurrence. The number of times two keywords appear simultaneously is represented by the connecting line between the nodes, and its thickness denotes the frequency of appearance. The three clusters represented by different colors are as follows: 1) Mechanism in red: glioblastoma, expression, MGMT, proliferation, and o-6-methylguanine-DNA methyltransferase; 2) Clinic treatment in yellow: TMZ, chemotherapy, therapy, immunotherapy, and combination; 3) Drug design in blue: radiotherapy, adjuvant TMZ, bevacizumab, and survival.

In addition, we have analyzed the burst keywords (Figure 12). The results showed that burst keywords lasting



more than 5 years are: antitumor imidazole-tetrazine, O6-alkylguanine-DNA alkyltransferase, trial, alkylating agent, mismatch repair, phase II trial, chemotherapy, dacarbazine, recurrent, glioblastoma multiforme, radiation therapy, procarbazine, malignant melanoma, anaplastic astrocytoma, malignant glioma, randomized trial, brain metastase, prognostic factor, recursive partitioning analysis and emergent terms that persist to the present are classification, TMZ resistance.

Co-citation analysis and roadmap of TMZ development

A co-citation relationship is defined as two or more papers simultaneously cited by one or more later articles. The core literature that plays a crucial role in the evolution of claims in a subject is displayed in literature co-citation analysis and the shifting trends in research focus. In this research, we do a co-citation analysis of 12,910 documents, setting the time slice

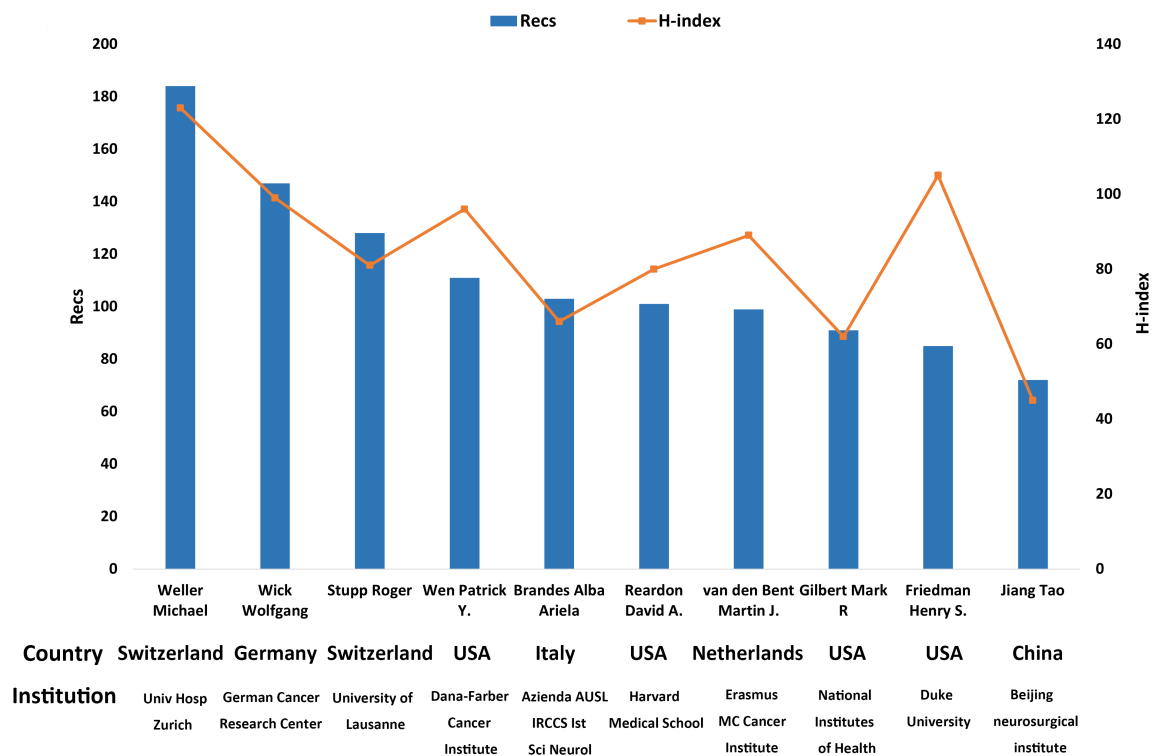


FIGURE 9
The top 10 most productive authors in the TMZ research area.

length to one year, the period to 1994–2021, showing the number of clusters to 11 (clusters are listed in numerical order by tag), and creating a timeline diagram to show the significant clusters of co-citations of references (Figure 13). The parameters of this timeline graph are $N = 721$, $E = 778$, totaling 721 nodes and 778 linkages; The network's density is 0.003, and its modularity is $Q = 0.9214$. The degree of modularity Q reflects the network's modularity, and modularity Q of 0.4 to 1 usually satisfies or approaches the clustering requirements (18). Thus the network

meets the standard requirements for clustering. The silhouette value is used to quantify the homogeneity of the network, and a silhouette value greater than 0.7 is considered a convincing clustering. Therefore, all of our clusters meet this criterion (Table 4). The timeline diagram shows 139 nodes, and the lines connecting these nodes represent co-referential relationships. Larger nodes reflect more frequent citations, while the lighter nodes/lines represent later publication dates along the dotted lines connecting each cluster label. The red

TABLE 3 The top 10 journals ranked by their Recs in the TMZ area.

Journal	Country	Recs	TLCS	TGCS	IF(2020)	H-Index	ISSN
Journal Of Neuro-Oncology	United States	879	7851	23102	4.130	105	0167-594X
Neuro-Oncology	United States	432	6952	22493	12.300	105	1522-8517
Oncotarget	United States	256	1527	7405	0	91	1949-2553
Clinical Cancer Research	United States	253	6715	20173	12.531	292	1078-0432
Plos One	United States	250	0	7345	3.240	268	1932-6203
Cancers	Switzerland	171	26	1220	6.639	53	2072-6694
Scientific Reports	England	171	0	2629	4.379	149	2045-2322
Frontiers In Oncology	Switzerland	166	0	1304	6.244	60	2234-943X
Anticancer Research	Greece	149	700	2280	2.480	110	0250-7005
World Neurosurgery	United States	142	370	1469	2.104	85	1878-8750

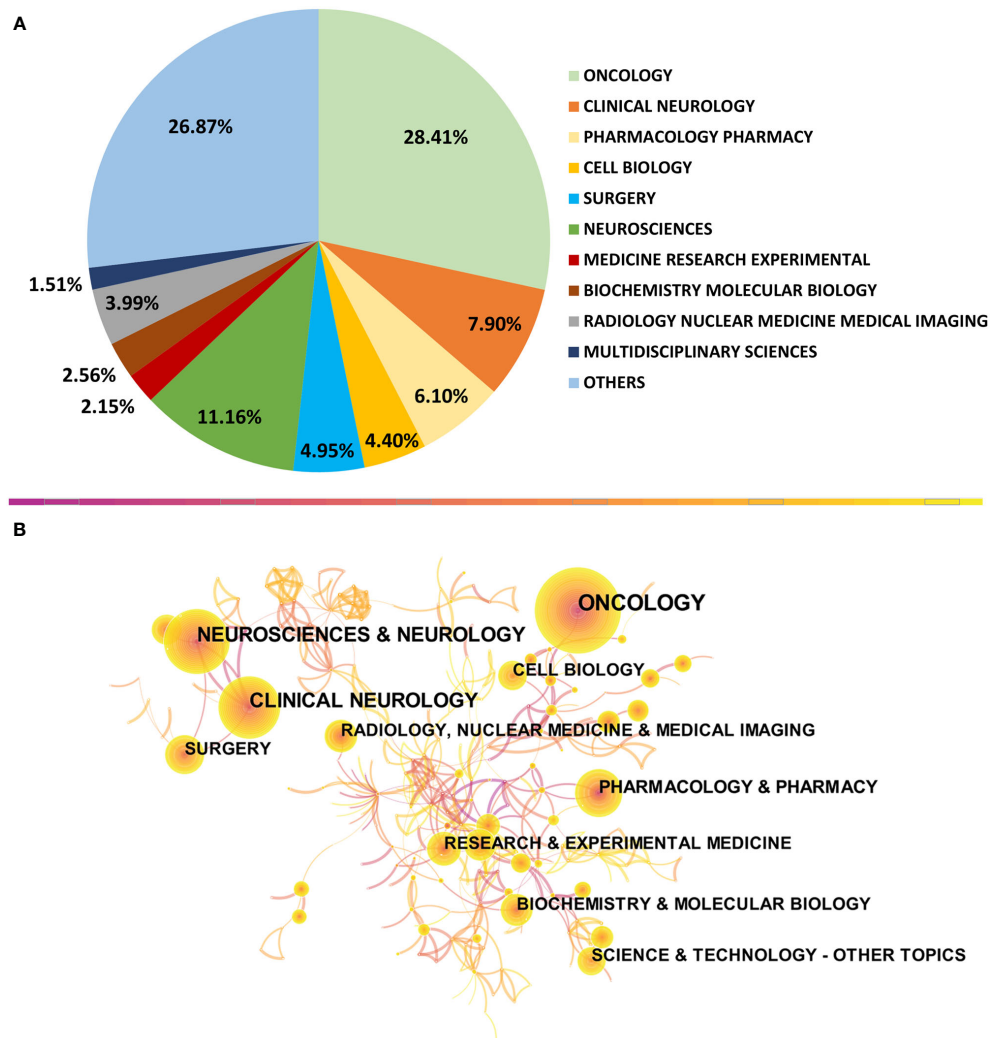


FIGURE 10

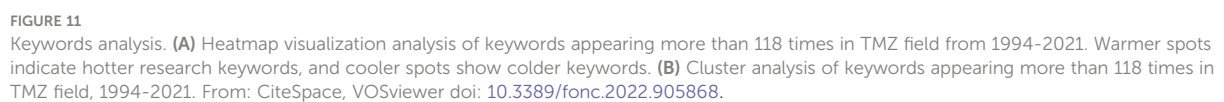
Analysis of categories. (A) The top 10 most published subjects within the TMZ area. (B) A category visualization of TMZ research. Each node represents a category, with the node's size representing the frequency of occurrence and the color shade representing the year's distance. The connecting line's thickness between the nodes represents the strength of their interactions, while the connecting lines between the nodes represent their interrelationships.

circles in the nodes indicate sudden co-citations, alluding to a spike in the frequency of mentions of a publication at a particular time, indicating a research trend on the subject.

Based on the timeline diagram, we can obtain the main popular themes of TMZ research during the period 1994–2021. The evolution of the main research themes during these 28 years is as follows, from 1987 to 1997, cluster #1 antitumor drug TMZ received attention from researchers as the earliest hot topic in TMZ research. There was overlap between the different research hotspots in the subsequent period. From 1996 to 2012, cluster #10 phase II study, cluster #7 presentation management, and cluster #8 methylguanine-DNA methyltransferase emerged sequentially as major popular themes, with cluster #8 having a high

concentration of nodes and citation bursts in the timeline graph and being an important theme in TMZ research. cluster #0 metastatic melanoma, cluster #2 world health organization classification, cluster #3 recurrent glioblastoma, cluster #4 treating field, cluster #5 pancreatic neuroendocrine tumor, cluster #6 elderly patient, cluster #9 brain glioma are the hot topics of TMZ research from 2005 to 2020.

In addition, we collect the first 15 articles of the TGCS, as shown in Table 5, to gain a more thorough understanding of critical events in the history of the TMZ sector. These publications cover several pivotal moments in the development of TMZ. The FDA approved TMZ capsules in 1999 for treating adult patients with refractory mesenchymal astrocytoma, and by the EU in the



glioblastoma who had a methylated MGMT (O 6-methylguanine -DNA methyltransferase) promoter benefited from TMZ. Still, those who did not have a methylated MGMT promoter did not (21). The addition of TMZ to radiation for newly diagnosed glioblastoma resulted in clinically relevant, and statistically, significant survival increases with minimal additional damage, according to Stupp, R. et al. in 2005 (22). This treatment regimen for glioblastoma has now become the gold standard.

Top 25 Keywords with the Strongest Citation Bursts

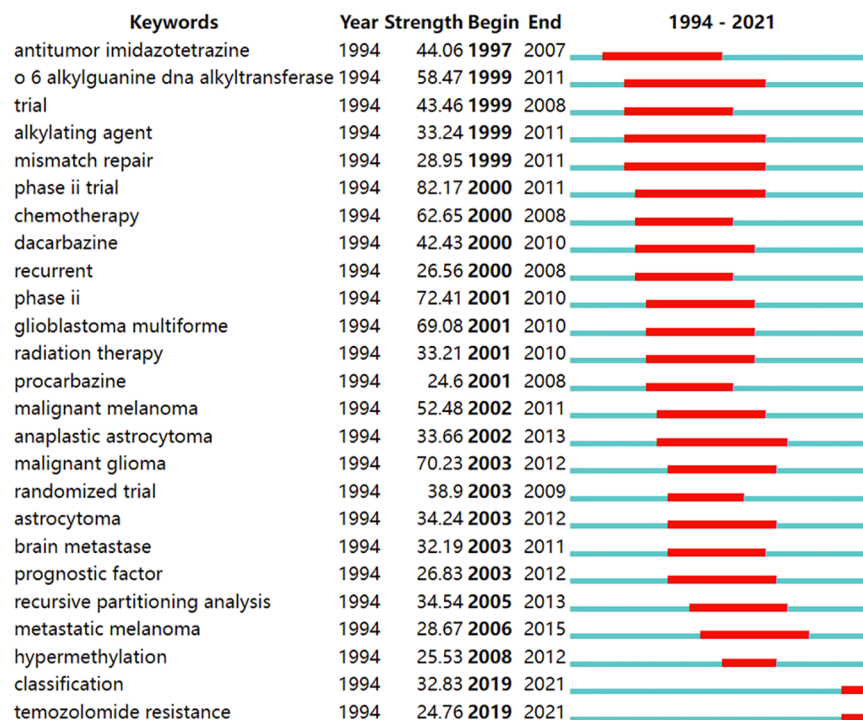


FIGURE 12

The burst detection of keywords of TMZ area in chronological order, 1994–2021.

Gentoo Liu et al. discovered in 2006 that CD133-positive tumor stem cells were highly resistant to chemotherapy treatments (led by TMZ). CD133-positive cells with high expression of BCRP1 and MGMT and anti-apoptotic proteins and inhibitors of the apoptotic protein family may be linked to this resistance (23). In conjunction with irinotecan, Bevacizumab effectively treated recurrent glioblastoma multiforme with mild toxicity by Vredenburgh, James J., et al. in 2007 (24). This study paved the way for bevacizumab to be added to the future treatment options for recurrent glioblastoma. Chin, L. et al. discovered common mutations in the phosphatidylinositol-3-OH kinase regulatory subunit gene PIK3R1 in 2008 and provided a network perspective of the pathways affected in glioblastoma growth (25). In a randomized phase III study published in 2009, Stupp, Roger discovered that glioblastoma patients treated with TMZ and radiation improved median and 2-year survival rates. MGMT promoter methylation was the strongest predictor of outcome and benefit of TMZ chemotherapy (26). Two studies published in 2014 by Chinot, Olivier L., et al., and Gilbert, Mark R., et al., found that using bevacizumab as a first-line treatment did not enhance overall survival in patients with newly diagnosed glioblastoma. Although progression-free survival was extended, the anticipated

goal of improvement was not met. This shows that bevacizumab isn't a perfect replacement for TMZ as the recommended glioblastoma treatment (27, 28). Ribas, Antoni, and colleagues established pembrolizumab as a new standard of care for ipilimumab-refractory melanoma in 2015 (29).

Emerging new research frontiers

The concentration and difficulty of scientific study are on research frontiers (30). The government, institutions, and researchers benefit from a current and accurate understanding of research frontiers. Because new papers take time to gain traction, this study examined articles published in the last five years (2017–2021) in eight TMZ-related journals with high impact factors and H-indexes and ranked publications in these journals by TGCS, selecting those with high TGCS, resulting in 35 articles. The eight selected journals include CA-A Cancer Journal for Clinicians (IF=508.702, H-index=144), New England Journal of Medicine (IF=91.245, H-index=933), JAMA- Journal of The American Medical Association (IF=56.272, H-index=622), Nature (IF=49.962, H-index=1096), The Lancet

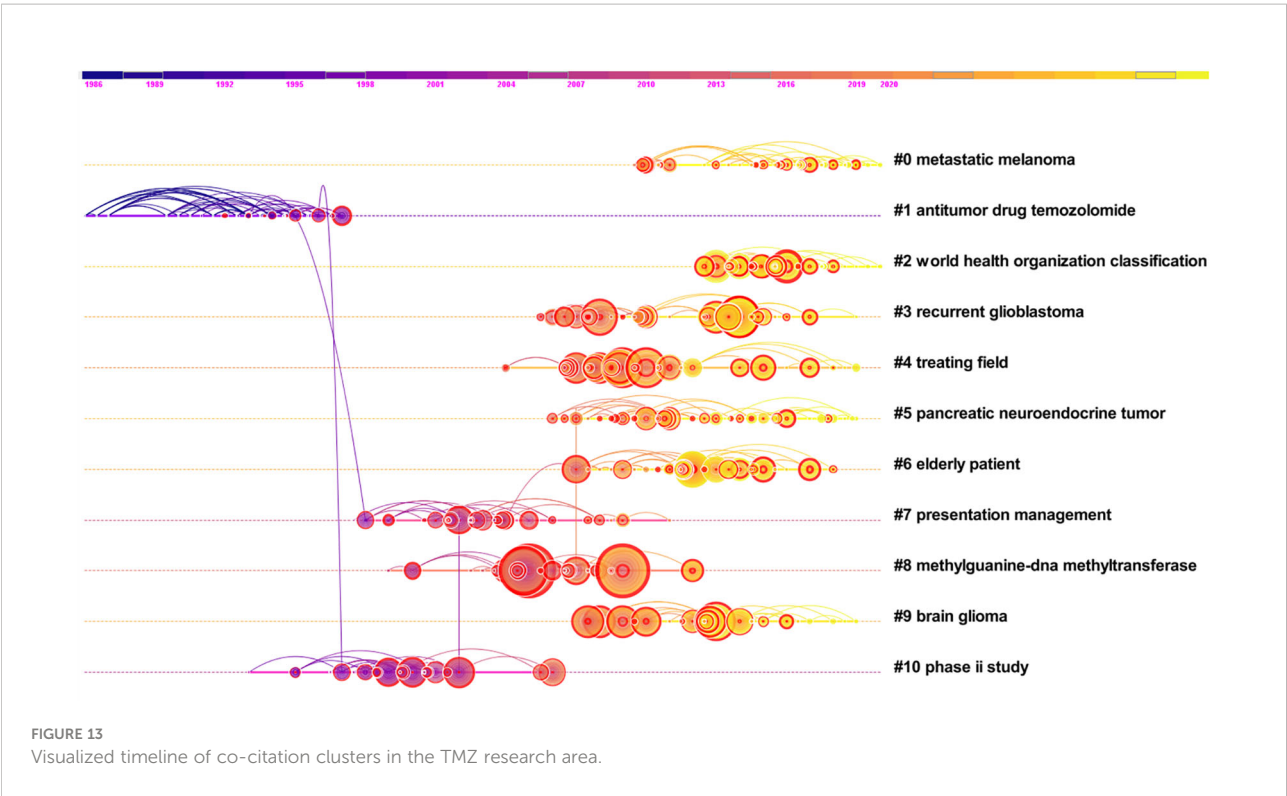


TABLE 4 The detailed information of the 11 clusters in Figure.

Cluster-ID	Cluster label	Size	Silhouette	Mean(Year)
0	Metastatic Melanoma	44	1	2015
2	World Health Organization Classification	33	1	2016
3	Recurrent Glioblastoma	33	1	2011
4	Treating Field	33	0.987	2010
5	Pancreatic Neuroendocrine Tumor	33	1	2012
1	Antitumor Drug TMZ	30	0.979	1993
6	Elderly Patient	30	1	2012
8	Methylguanine-DNA Methyltransferase	30	1	2006
7	Presentation Management	28	0.949	2003
10	Phase II Study	27	1	1999
9	Brain Glioma	26	0.986	2013

Oncology (IF=41.316,H- index=274), Science (IF=47.728,H-index=1058), Molecular Cancer (IF=27.401,H-index=103), Journal of Clinical Oncology (IF=44.544,H- index=494).

These 35 publications were grouped into the five categories below (with some overlap between them) and were partially compatible with the previous category, co-citation, and keyword analyses. 1) Immunotherapy for cancer (31–34). In recent years, tumor immunotherapy has developed rapidly, and FDA has approved several for clinical application. Immunotherapy against glioblastoma occupies a significant portion of the TMZ literature. EGFRvIII-positive glioblastoma patients were treated with Rindopepimut (a vaccination targeting the EGFR deletion

mutation EGFRvIII) in addition to standard chemotherapy in 2017 randomized, double-blind, phase III trial (ClinicalTrials.gov, NCT01480479). Rindopepimut did not improve survival in patients with newly diagnosed glioblastoma, according to the findings (31). To demonstrate the effect of immunotherapy in glioblastoma, combination medications, including Rindopepimut, may be required. 2) Resistant to drugs (35–39). Acquired drug resistance is a major challenge in the clinical treatment of glioblastoma, and long noncoding RNAs have been shown to play a role in chemotherapy resistance. In 2020, researchers concluded from ex vivo experiments that SNHG12 could serve as a promising therapeutic target to surmount TMZ resistance,

TABLE 5 The top 15 most cited articles.

Authors	Journal	IF (2020)	H-Index	Title	TGCS	TLCs
Stupp R et al.	New Engl J Med	91.245	933	Radiotherapy plus concomitant and adjuvant TMZ for glioblastoma	12496	5994
Chin L et al.	Nature	49.962	1096	Comprehensive genomic characterization defines human glioblastoma genes and core pathways	5061	702
Stupp R et al.	Lancet Oncol	41.316	274	Effects of radiotherapy with concomitant and adjuvant TMZ versus radiotherapy alone on survival in glioblastoma in a randomized phase III study: 5-year analysis of the EORTC-NCIC trial	4700	2702
Hegi ME et al.	New Engl J Med	91.245	933	MGMT gene silencing and benefit from TMZ in glioblastoma	4462	2502
Friedman HS et al.	J Clin Oncol	44.544	494	Bevacizumab Alone and in Combination With Irinotecan in Recurrent Glioblastoma	1683	641
Gilbert MR et al.	New Engl J Med	91.245	933	A Randomized Trial of Bevacizumab for Newly Diagnosed Glioblastoma	1494	651
Chinot OL et al.	New Engl J Med	91.245	933	Bevacizumab plus Radiotherapy-TMZ for Newly Diagnosed Glioblastoma	1400	706
Chen J et al.	Nature	49.962	1096	A restricted cell population propagates glioblastoma growth after chemotherapy	1350	221
Liu GT et al.	Mol Cancer	27.401	103	Analysis of gene expression and chemoresistance of CD133(+) cancer stem cells in glioblastoma	1313	0
Omuro A et al.	Jama-J Am Med Assoc	56.272	622	Glioblastoma and Other Malignant Gliomas A Clinical Review	1221	268
Vredenburg JJ et al.	J Clin Oncol	44.544	494	Bevacizumab plus irinotecan in recurrent glioblastoma multiforme	1074	425
Ribas A et al.	Lancet Oncol	41.316	274	Pembrolizumab versus investigator-choice chemotherapy for ipilimumab-refractory melanoma (KEYNOTE-002): a randomized, controlled, phase 2 trial	1038	5
Van Meir EG et al.	Ca-Cancer J Clin	508.702	144	Exciting New Advances in Neuro-Oncology The Avenue to a Cure for Malignant Glioma	972	1
Middleton MR et al.	J Clin Oncol	44.544	494	Randomized phase III study of TMZ versus dacarbazine in the treatment of patients with advanced metastatic malignant melanoma	908	304
Sanai N et al.	J Neurosurg	5.115	189	An extent of resection threshold for newly diagnosed glioblastomas	868	214

thereby improving the clinical efficacy of TMZ chemotherapy (35). 3) Tumor-treatment fields (40–42). Tumor electric field therapy is a novel oncology treatment technique that has shown significant prognostic results in combination with temozolomide to treat neoplastic glioblastoma and is now included in cancer treatment protocols in several countries. In 2017, researchers discovered that adding maintenance TMZ chemotherapy to Tumor-treating fields resulted in statistically significant improvements in progression-free survival and overall survival compared to maintenance TMZ alone in a randomized clinical trial in patients with glioblastoma (40). 4) Trials of novel anticancer drug combinations (32, 43–45). The emergence of TMZ resistance has increased the need for novel anticancer drugs. As a result, there is an increasing number of clinical studies on the combination of antitumor drugs today. In a randomized European phase II experiment published in 2021 (ClinicalTrials.gov, NCT01355445), researchers discovered that adding TMZ to Vincristine-Irinotecan increased chemotherapeutic efficacy in patients with recurrent rhabdomyosarcoma while increasing toxicity to an acceptable level (43). 5) Studies involving older and young patients (46–49). The specificity research of elderly cancer patients is different from that of young children cancer patients and is of great

significance. Researchers discovered that adding bevacizumab to radiation therapy + TMZ did not benefit newly diagnosed high-grade gliomas in a randomized, parallel-group, multicenter trial published in 2017 (ClinicalTrials.gov identifier: NCT01390948) (47). Researchers determined in 2018 that short-term radiation therapy combined with TMZ resulted in longer life in older individuals with glioblastoma than a short course of radiation therapy alone (ClinicalTrials.gov number, NCT00482677) (46).

Discussion

We used several visual analysis applications to undertake a bibliometric study of 12,910 TMZ papers in the Web of Science core database from 1994 to 2021.

The number of TMZ publications has increased annually between 1994 and 2021, demonstrating the excellent growth rate and promising future of the field. In terms of the country, the United States holds a commanding lead, with the most significant number of publications and the best academic reputation. This is attributed to the help of major medical research institutions such as the University of Texas M. D. Anderson Cancer Center, the University of California, San

Francisco, Memorial Sloan-Kettering Cancer Center, and the Mayo Clinic. It's worth noting that the University of Texas MD Anderson Cancer Center in the United States ranks first in both Recs and TGCS among all research institutes, indicating that this institution has had a significant impact on TMZ research. Among the top ten most influential authors, Wen Patrick Y., Reardon David A., Gilbert Mark R., and Friedman Henry S., are also linked with USA research institutes. Other countries, such as China, Germany, Italy, and France, are similarly crucial research forces, albeit with slightly different Recs and TGCS than the United States. China has recently rated second only to the United States in terms of publications but seventh in terms of TGCS, indicating that China's academic influence in this sector needs to be reinforced to boost its global impact. The United States leads by a wide margin in several industries in terms of academic collaborations. Among research institutions, the University of Texas MD Anderson Cancer Center, the German Cancer Research Center, and the University of California, San Francisco had the most; among authors, Weller Michael had the collaborative network with the highest total intensity of collaboration. The top three most influential writers, according to the author h-index, are Michael Weller from University Hospital Zurich in Switzerland, Henry S. Friedman from Duke University in the United States, and Wolfgang Wick from German Cancer Research Center in Germany. According to the author's collaboration network, the most active collaboration between Weller Michael and Wick Wolfgang has also taken place, maximizing their strengths and strengthening their academic influence.

The results of the annual co-citation timeline chart, the historical evolution of TMZ, and the research hotspots in different periods are analyzed. The discovery of TMZ (50), which has excellent anti-cancer activity, by Stevens' group at Aston University in the UK, funded by the charity Cancer Research Campaign (CRC) in 1987, was the beginning of TMZ research. This led to the rapid development of research on TMZ in the fields of drug synthesis and oncology, and gradually began to spread to other fields such as neurology and clinical surgery. TMZ was transferred to Schering-Plough for development and was approved by the FDA (51) and the EU (2) in 1999 for the treatment of recurrent glioblastoma in adults, and began to be used in medical institutions under the label of an anti-tumor drug. This led to a global spread of TMZ research efforts, with the number of countries studying TMZ spreading from the United Kingdom and the United States at the beginning to other countries around the world; the number of scientists working closely together on TMZ, represented by Weller Michael of the University Hospital of Zurich in Switzerland and Wick Wolfgang of the German Cancer Research Center, began to increase; TMZ's research disciplines began to spread to molecular biology, cell biology, radiology, immunology and other disciplines. After numerous clinical trial studies (52, 53) and cancer management

studies (54, 55), it was found that MGMT (O6-methylguanine-DNA-methyltransferase), a DNA damage repair protein, was a key factor in TMZ chemoresistance. It was shown that overexpression of MGMT and promoter methylation made tumor cells more effective in resisting TMZ drug toxicity, suggesting a close relationship between MGMT and tumor drug chemoresistance and a direct relationship with patient prognosis (21, 56–58). TMZ clinical treatment of oncological diseases (metastatic melanoma (59), recurrent glioblastoma (60), pancreatic neuroendocrine tumor (61), brain glioma (62)), the clinical trials in elderly oncology patients (48, 49), and the World Health Organization classification of TMZ-treated diseases (63) became popular topics for TMZ between 2007 and 2020. The above analysis is consistent with the statistical results of TMZ keywords and TMZ study categories, reflecting in general that the current research hotspot of TMZ is how to better utilize TMZ (with overcoming drug resistance of TMZ as the main challenge) to better treat cancer (mainly glioma). In terms of future research directions, combining the results of this study we can conclude that the diagnosis and treatment of cancer (mainly glioma, supplemented by melanoma, refractory rhabdomyosarcoma, small cell lung cancer and other diseases), including immunotherapy (31), overcoming drug resistance (35), trials of new combinations of antitumor drugs (43), clinical trials in young and elderly tumor patients (46, 47) and electric field treatment of tumors (40), will further advance the field of TMZ in the next 20 years.

Notably, in the current state of the COVID-19 pandemic, there is a considerable amount of literature addressing TMZ and COVID-19. According to studies, TMZ-associated immunosuppression increased mortality from severe acute respiratory syndrome coronavirus 2 (SARS-CoV-2) virus infection significantly during the COVID-19 outbreak (64–66). This study demonstrates the neurophilic potential of the SARS-CoV-2 virus and may also guide the clinical management of glioblastoma patients during the new coronary pneumonia pandemic.

The following recommendations are made based on the findings of this study: To begin, this section requires a significant amount of basic research and clinical trials in the combination of TMZ with other drugs, and although there are many challenges, they cannot be ignored. Second, researchers must identify the particular research value of antineoplastic medications (including TMZ) acting in young children and elderly cancer patients. Therefore, future drug studies targeting TMZ need to be conducted in adult cancer patients aged 18–60 years and young children and elderly cancer patients as an integral part of the research. Third, to encourage the invention of new therapies such as tumor electric field therapy to facilitate the association between new therapies and TMZ, there is a need to enhance multidisciplinary and multidisciplinary communication and integration for the treatment and diagnosis of refractory oncologic diseases.

Conclusion

This review uses bibliometric methods to provide a systematic overview of the research process, research hotspots, and research development directions of TMZ during 1994–2021. This research will help researchers better understand the current research status and development trend of TMZ worldwide.

Author contributions

XR and X-JF conceived and designed the article; XR, PS, KX, HL, and Z-WL collected data; XR and PS wrote the original draft; X-JF and XR edited and reviewed the paper. All authors contributed to the article and approved the submitted version.

Funding

This study was funded by the National Natural Science Foundation of China (Grant Nos. 41806191 and 81473369).

References

- Baker SD, Wirth M, Statkevich P, Reidenberg P, Alton K, Sartorius SE, et al. Absorption, metabolism, and excretion of c-14-Temozolomide following oral administration to patients with advanced cancer. *Clin Cancer Res* (1999) 5(2):309–17.
- Brada M, Judson I, Beale P, Moore S, Reidenberg P, Statkevich P, et al. Phase I dose-escalation and pharmacokinetic study of temozolomide (Sch 52365) for refractory or relapsing malignancies. *Br J Cancer* (1999) 81(6):1022–30. doi: 10.1038/sj.bjcr.6690802
- Cohen MH, Shen YL, Keegan P, Pazdur R. FDA drug approval summary: Bevacizumab (Avastin (R)) as treatment of recurrent glioblastoma multiforme. *Oncologist* (2009) 14(11):1131–8. doi: 10.1634/theoncologist.2009-0121
- Paz MF, Yaya-Tur R, Rojas-Marcos I, Reynes G, Pollan M, Aguirre-Cruz L, et al. CpG island hypermethylation of the DNA repair enzyme methyltransferase predicts response to temozolomide in primary gliomas. *Clin Cancer Res* (2004) 10(15):4933–8. doi: 10.1158/1078-0432.Ccr-04-0392
- Clark AS, Deans B, Stevens MFG, Tisdale MJ, Wheelhouse RT, Denny BJ, et al. Antitumor Imidazotetrazines.32. synthesis of novel imidazotetrazinones and related bicyclic heterocycles to probe the mode of action of the antitumor drug temozolomide. *J Medicinal Chem* (1995) 38(9):1493–504. doi: 10.1021/jm00009a010
- Chen CM, Song M. Visualizing a field of research: A methodology of systematic scientometric reviews. *PLoS One* (2019) 14(10):25. doi: 10.1371/journal.pone.0223994
- Hou JH, Yang XC, Chen CM. Emerging trends and new developments in information science: A document Co-citation analysis (2009–2016). *Scientometrics* (2018) 115(2):869–92. doi: 10.1007/s11192-018-2695-9
- Garfield E. The history and meaning of the journal impact factor. *JAMA-J Am Med Assoc* (2006) 295(1):90–3. doi: 10.1001/jama.295.1.90
- Egghe L. Theory and practise of the G-index. *Scientometrics* (2006) 69(1):131–52. doi: 10.1007/s11192-006-0144-7
- Radicchi F, Fortunato S, Castellano C. Universality of citation distributions: Toward an objective measure of scientific impact. *Proc Natl Acad Sci USA* (2008) 105(45):17268–72. doi: 10.1073/pnas.0806977105
- Waltman L, Calero-Medina C, Kosten J, Noyons ECM, Tijssen RJW, van Eck NJ, et al. The Leiden ranking 2011/2012: Data collection, indicators, and interpretation. *J Am Soc Inf Sci Technol* (2012) 63(12):2419–32. doi: 10.1002/asi.22708
- Mayernik MS, Hart DL, Maull KE, Weber NM. Assessing and tracing the outcomes and impact of research infrastructures. *J Assoc Inf Sci Technol* (2017) 68(6):1341–59. doi: 10.1002/asi.23721
- Glaser J, Glanzel W, Scharnhorst A. Same data-different results? towards a comparative approach to the identification of thematic structures in science. *Scientometrics* (2017) 111(2):981–98. doi: 10.1007/s11192-017-2296-z
- Mongeon P, Paul-Hus A. The journal coverage of web of science and scopus: A comparative analysis. *Scientometrics* (2016) 106(1):213–28. doi: 10.1007/s11192-015-1765-5
- Glanzel W, Moed HF. Journal impact measures in bibliometric research. *Scientometrics* (2002) 53(2):171–93. doi: 10.1023/a:1014848323806
- Ellegaard O, Wallin JA. The bibliometric analysis of scholarly production: How great is the impact? *Scientometrics* (2015) 105(3):1809–31. doi: 10.1007/s11192-015-1645-z
- Chen G, Xiao L. Selecting publication keywords for domain analysis in bibliometrics: A comparison of three methods. *J Informetrics* (2016) 10(1):212–23. doi: 10.1016/j.joi.2016.01.006
- Chen CM. Searching for intellectual turning points: Progressive knowledge domain visualization. *Proc Natl Acad Sci USA* (2004) 101:5303–10. doi: 10.1073/pnas.0307513100
- Stupp R, van den Bent MJ, Hegi ME. Optimal role of temozolomide in the treatment of malignant gliomas. *Curr Neurol Neurosci Rep* (2005) 5(3):198–206. doi: 10.1007/s11910-005-0047-7
- Middleton MR, Grob JJ, Aaronson N, Fierlbeck G, Tilgen W, Seiter S, et al. Randomized phase iii study of temozolomide versus dacarbazine in the treatment of patients with advanced metastatic malignant melanoma. *J Clin Oncol* (2000) 18(1):158–66. doi: 10.1200/jco.2000.18.1.158
- Hegi ME, Diserens A, Gorlia T, Hamou M, de Tribolet N, Weller M, et al. Mgmt gene silencing and benefit from temozolomide in glioblastoma. *N Engl J Med* (2005) 352(10):997–1003. doi: 10.1056/NEJMoa043331
- Stupp R, Mason WP, van den Bent MJ, Weller M, Fisher B, Taphoorn MJB, et al. Radiotherapy plus concomitant and adjuvant temozolomide for glioblastoma. *N Engl J Med* (2005) 352(10):987–96. doi: 10.1056/NEJMoa043330
- Liu GT, Yuan XP, Zeng ZH, Tunici P, Ng HS, Abdulkadir IR, et al. Analysis of gene expression and chemoresistance of Cdi33(+) cancer stem cells in glioblastoma. *Mol Cancer* (2006) 5:12. doi: 10.1186/1476-4598-5-67
- Vredenburg JJ, Desjardins A, Herndon JE, Marcello J, Reardon DA, Quinn JA, et al. Bevacizumab plus irinotecan in recurrent glioblastoma multiforme. *J Clin Oncol* (2007) 25(30):4722–9. doi: 10.1200/jco.2007.12.2440
- Chin L, Meyerson M, Aldape K, Bigner D, Mikkelsen T, VandenBerg S, et al. Comprehensive genomic characterization defines human glioblastoma genes and core pathways. *Nature* (2008) 455(7216):1061–8. doi: 10.1038/nature07385

and Key R & D project of Shandong Province (Grant No. 2016CYJS08A01-1).

Conflict of interest

The authors declare that the research was conducted in the absence of any commercial or financial relationships that could be construed as a potential conflict of interest.

Publisher's note

All claims expressed in this article are solely those of the authors and do not necessarily represent those of their affiliated organizations, or those of the publisher, the editors and the reviewers. Any product that may be evaluated in this article, or claim that may be made by its manufacturer, is not guaranteed or endorsed by the publisher.

26. Stupp R, Hegi ME, Mason WP, van den Bent MJ, Taphoorn MJB, Janzer RC, et al. Effects of radiotherapy with concomitant and adjuvant temozolomide versus radiotherapy alone on survival in glioblastoma in a randomised phase iii study: 5-year analysis of the eortc-ncic trial. *Lancet Oncol* (2009) 10(5):459–66. doi: 10.1016/s1470-2045(09)70025-7
27. Chinot OL, Wick W, Mason W, Henriksson R, Saran F, Nishikawa R, et al. Bevacizumab plus radiotherapy-temozolomide for newly diagnosed glioblastoma. *N Engl J Med* (2014) 370(8):709–22. doi: 10.1056/NEJMoa1308345
28. Gilbert MR, Dignam JJ, Armstrong TS, Wefel JS, Blumenthal DT, Vogelbaum MA, et al. A randomized trial of bevacizumab for newly diagnosed glioblastoma. *N Engl J Med* (2014) 370(8):699–708. doi: 10.1056/NEJMoa1308573
29. Ribas A, Puzanov I, Dummer R, Schadendorf D, Hamid O, Robert C, et al. Pembrolizumab versus investigator-choice chemotherapy for ipilimumab-refractory melanoma (Keynote-002): A randomised, controlled, phase 2 trial. *Lancet Oncol* (2015) 16(8):908–18. doi: 10.1016/s1470-2045(15)00083-2
30. Li MN, Chu YQ. Explore the research front of a specific research theme based on a novel technique of enhanced Co-word analysis. *J Inf Sci* (2017) 43(6):725–41. doi: 10.1177/0165551516661914
31. Weller M, Butowski N, Tran DD, Recht LD, Lim M, Hirte H, et al. Rindopemut with temozolomide for patients with newly diagnosed, egfrviii-expressing glioblastoma (Act iv): A randomised, double-blind, international phase 3 trial. *Lancet Oncol* (2017) 18(10):1373–85. doi: 10.1016/s1470-2045(17)30517-x
32. Mody R, Naranjo A, Van Ryn C, Yu AL, London WB, Shulkin BL, et al. Irinotecan-temozolomide with temsirolimus or dinutuximab crosstafak in children with refractory or relapsed neuroblastoma (Cog Anbl1221): An open-label, randomised, phase 2 trial. *Lancet Oncol* (2017) 18(7):946–57. doi: 10.1016/s1470-2045(17)30355-8
33. Mody R, Yu AL, Naranjo A, Zhang FF, London WB, Shulkin BL, et al. Irinotecan, temozolomide, and dinutuximab with gm-csf in children with refractory or relapsed neuroblastoma: A report from the children's oncology group. *J Clin Oncol* (2020) 38(19):2160–+. doi: 10.1200/jco.20.00203
34. van den Bent MJ, Tesileanu CMS, Wick W, Sanson M, Brandes AA, Clement PM, et al. Adjuvant and concurrent temozolomide for 1p/19q non-Co-Deleted anaplastic glioma (Catnon; eortc study 26053-22054): Second interim analysis of a randomised, open-label, phase 3 study. *Lancet Oncol* (2021) 22(6):813–23. doi: 10.1016/s1470-2045(21)00090-5
35. Lu CF, Wei YT, Wang XF, Zhang ZR, Yin JX, Li WT, et al. DNA-Methylation-Mediated Activating of Incrna Snhg12 promotes temozolomide resistance in glioblastoma. *Mol Cancer* (2020) 19(1):19. doi: 10.1186/s12943-020-1137-5
36. Tian T, Li AM, Lu H, Luo R, Zhang MZ, Li ZM. Taz promotes temozolomide resistance by upregulating mcl-1 in human glioma cells. *Biochem Biophys Res Commun* (2015) 463(4):638–43. doi: 10.1016/j.bbrc.2015.05.115
37. Qian ZR, Zhou SH, Zhou ZY, Yang X, Que SL, Lan J, et al. Mir-146b-5p suppresses glioblastoma cell resistance to temozolomide through targeting Traf6. *Oncol Rep* (2017) 38(5):2941–50. doi: 10.3892/or.2017.5970
38. Luo H, Chen ZX, Wang S, Zhang R, Qiu WJ, Zhao L, et al. C-Myc-Mir-29c-Rev3l signalling pathway drives the acquisition of temozolomide resistance in glioblastoma. *Brain* (2015) 138:3654–72. doi: 10.1093/brain/aww287
39. Hiddingh L, Tannous BA, Teng J, Tops B, Jeuken J, Hulleman E, et al. Efem1 induces gamma-Secretase/Notch-Mediated temozolomide resistance in glioblastoma. *Oncotarget* (2014) 5(2):363–74. doi: 10.18632/oncotarget.1620
40. Stupp R, Taillibert S, Kanner A, Read W, Steinberg DM, Lhermitte B, et al. Effect of tumor-treating fields plus maintenance temozolomide vs maintenance temozolomide alone on survival in patients with glioblastoma a randomized clinical trial. *JAMA-J Am Med Assoc* (2017) 318(23):2306–16. doi: 10.1001/jama.2017.18718
41. Stupp R, Taillibert S, Kanner AA, Kesari S, Steinberg DM, Toms SA, et al. Maintenance therapy with tumor-treating fields plus temozolomide vs temozolomide alone for glioblastoma a randomized clinical trial. *JAMA-J Am Med Assoc* (2015) 314(23):2535–43. doi: 10.1001/jama.2015.16669
42. Hottinger AF, Pacheco P, Stupp R. Tumor treating fields: A novel treatment modality and its use in brain tumors. *Neuro-oncology* (2016) 18(10):1338–49. doi: 10.1093/neuonc/now182
43. Defachelles AS, Bogart E, Casanova M, Merks JHM, Bisogno G, Calareso G, et al. Randomized phase ii trial of vincristine-irinotecan with or without temozolomide, in children and adults with relapsed or refractory rhabdomyosarcoma: A European paediatric soft tissue sarcoma study group and innovative therapies for children with cancer trial. *J Clin Oncol* (2021) 39(27):2979–+. doi: 10.1200/jco.21.00124
44. Weller J, Tzaridis T, Mack F, Steinbach JP, Schlegel U, Hau P, et al. Health-related quality of life and neurocognitive functioning with lomustine-temozolomide versus temozolomide in patients with newly diagnosed, mgmt-methylated glioblastoma (Ceteg/Noa-09): A randomised, multicentre, open-label, phase 3 trial. *Lancet Oncol* (2019) 20(10):1444–53. doi: 10.1016/s1470-2045(19)30502-9
45. Omuro A, Beal K, McNeill K, Young RJ, Thomas A, Lin XL, et al. Multicenter phase ib trial of carboxyamidotriazole orotate and temozolomide for recurrent and newly diagnosed glioblastoma and other anaplastic gliomas. *J Clin Oncol* (2018) 36(17):1702–+. doi: 10.1200/jco.2017.76.9992
46. Perry JR, Laperriere N, O'Callaghan CJ, Brandes AA, Menten J, Phillips C, et al. Short-course radiation plus temozolomide in elderly patients with glioblastoma. *N Engl J Med* (2017) 376(11):1027–37. doi: 10.1056/NEJMoa1611977
47. Grill J, Massimino M, Bouffet E, Azizi AA, McCowage G, Canete A, et al. Phase ii, open-label, randomized, multicenter trial (Herby) of bevacizumab in pediatric patients with newly diagnosed high-grade glioma. *J Clin Oncol* (2018) 36(10):951–+. doi: 10.1200/jco.2017.76.0611
48. Wick W, Platten M, Meisner C, Felsberg J, Tabatabai G, Simon M, et al. Temozolomide chemotherapy alone versus radiotherapy alone for malignant astrocytoma in the elderly: The noa-08 randomised, phase 3 trial. *Lancet Oncol* (2012) 13(7):707–15. doi: 10.1016/s1470-2045(12)70164-x
49. Malmstrom A, Gronberg BH, Marosi C, Stupp R, Frappaz D, Schultz H, et al. Temozolomide versus standard 6-week radiotherapy versus hypofractionated radiotherapy in patients older than 60 years with glioblastoma: The Nordic randomised, phase 3 trial. *Lancet Oncol* (2012) 13(9):916–26. doi: 10.1016/s1470-2045(12)70265-6
50. Stevens MFG, Hickman JA, Langdon SP, Chubb D, Vickers L, Stone R, et al. Antitumor activity and pharmacokinetics in mice of 8-Carbamoyl-3-Methyl-Imidazo[5,1-D]-1,2,3,5-Tetrazin-4(3h)-One (Ccrq 81045; m & b 39831), a novel drug with potential as an alternative to Dacarbazine. *Cancer Res* (1987) 47(22):5846–52.
51. Cohen MH, Johnson JR, Pazdur R. Food and drug administration drug approval summary: Temozolomide plus radiation therapy for the treatment of newly diagnosed glioblastoma multiforme. *Clin Cancer Res* (2005) 11(19):6767–71. doi: 10.1158/1078-0432.Ccr-05-0722
52. van den Bent MJ, Brandes AA, Rampling R, Kouwenhoven MCM, Kros JM, Carpentier AF, et al. Randomized phase ii trial of erlotinib versus temozolomide or carmustine in recurrent glioblastoma: Eortc brain tumor group study 26034. *J Clin Oncol* (2009) 27(8):1268–74. doi: 10.1200/jco.2008.17.5984
53. Lai A, Tran A, Nghiemphu PL, Pope WB, Solis OE, Selch M, et al. Phase ii study of bevacizumab plus temozolomide during and after radiation therapy for patients with newly diagnosed glioblastoma multiforme. *J Clin Oncol* (2011) 29(2):142–8. doi: 10.1200/jco.2010.30.2729
54. Preusser M, de Ribaupierre S, Wohrer A, Erridge SC, Hegi M, Weller M, et al. Current concepts and management of glioblastoma. *Ann Neurol* (2011) 70(1):9–21. doi: 10.1002/ana.22425
55. Brandsma D, Stalpers L, Taal W, Sminia P, van den Bent M. Clinical features, mechanisms, and management of pseudoprogression in malignant gliomas. *Lancet Oncol* (2008) 9(5):453–61. doi: 10.1016/s1470-2045(08)70125-6
56. Hegi ME, Liu LL, Herman JG, Stupp R, Wick W, Weller M, et al. Correlation of O-6-Methylguanine methyltransferase (Mgmt) promoter methylation with clinical outcomes in glioblastoma and clinical strategies to modulate mgmt activity. *J Clin Oncol* (2008) 26(25):4189–99. doi: 10.1200/jco.2007.11.5964
57. Brandes AA, Franceschi E, Tosoni A, Blatt V, Pession A, Tallini G, et al. Mgmt promoter methylation status can predict the incidence and outcome of pseudoprogression after concomitant radiochemotherapy in newly diagnosed glioblastoma patients. *J Clin Oncol* (2008) 26(13):2192–7. doi: 10.1200/jco.2007.14.8163
58. Cen L, Carlson BL, Pokorny JL, Mladek AC, Grogan PT, Schroeder MA, et al. Efficacy of protracted temozolomide dosing is limited in mgmt unmethylated gbm xenograft models. *Neuro-oncology* (2013) 15(6):735–46. doi: 10.1093/neuonc/nt010
59. Rangwala R, Leone R, Chang YYC, Fecher L, Schuchter LM, Kramer A, et al. Phase I trial of hydroxychloroquine with dose-intense temozolomide in patients with advanced solid tumors and melanoma. *Autophagy* (2014) 10(8):1369–79. doi: 10.4161/auto.29118
60. Stupp R, Hegi ME, Gorlia T, Erridge SC, Perry J, Hong YK, et al. Cilengitide combined with standard treatment for patients with newly diagnosed glioblastoma with methylated mgmt promoter (Centric eortc 26071-22072 study): A multicentre, randomised, open-label, phase 3 trial. *Lancet Oncol* (2014) 15(10):1100–8. doi: 10.1016/s1470-2045(14)70379-1
61. Cives M, Strosberg JR. Gastroenteropancreatic neuroendocrine tumors. *CA-Cancer J Clin* (2018) 68(6):471–87. doi: 10.3322/caac.21493
62. Weller M, Wick W, Aldape K, Brada M, Berger M, Pfister SM, et al. Glioma. *Nat Rev Dis Primers* (2015) 1(1):15017. doi: 10.1038/nrdp.2015.17
63. Villa C, Miquel C, Mosses D, Bernier M, Di Stefano AL. The 2016 world health organization classification of tumours of the central nervous system. *Presse Medicale* (2018) 47(11-12):E187–200. doi: 10.1016/j.lpm.2018.04.015

64. Kamson DO, Grossman SA. The role of temozolomide in patients with newly diagnosed wild-type idh, unmethylated mgmt glioblastoma during the covid-19 pandemic. *JAMA Oncol* (2021) 7(5):675–6. doi: 10.1001/jamaoncol.2020.6732
65. Tanriverdi O. Lymphopenia that may develop in patients treated with temozolomide and immune control check-point inhibitor may be a high risk for mortality during the covid-19 outbreak. *Med Oncol* (2020) 37(6):2. doi: 10.1007/s12032-020-01376-8
66. Wu BS, Wang WH, Wang HP, Zou QL, Hu BX, Ye L, et al. Single-cell sequencing of glioblastoma reveals central nervous system susceptibility to sars-Cov-2. *Front Oncol* (2020) 10:566599. doi: 10.3389/fonc.2020.566599

Frontiers in Oncology

Advances knowledge of carcinogenesis and tumor progression for better treatment and management

The third most-cited oncology journal, which highlights research in carcinogenesis and tumor progression, bridging the gap between basic research and applications to improve diagnosis, therapeutics and management strategies.

Discover the latest Research Topics

See more →

Frontiers

Avenue du Tribunal-Fédéral 34
1005 Lausanne, Switzerland
frontiersin.org

Contact us

+41 (0)21 510 17 00
frontiersin.org/about/contact

